Impact Assessment of the Upcoming Irrigation Projects and Climate Change on the Droughts and Desertification Scenario for Chambal Basin in Western Madhya Pradesh (NIH-5_2016_6)

National Hydrology Project
Department of Water Resources, River Development and Ganga Rejuvenation, Ministry of Jal Shakti, New Delhi

Water Resources Department
Govt. of Madhya Pradesh

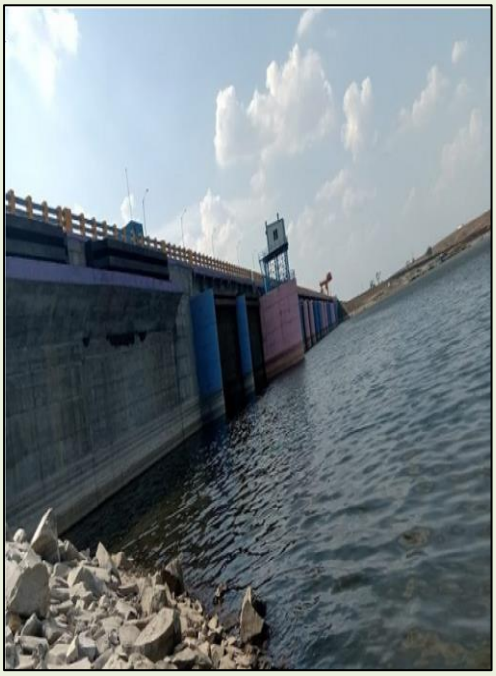

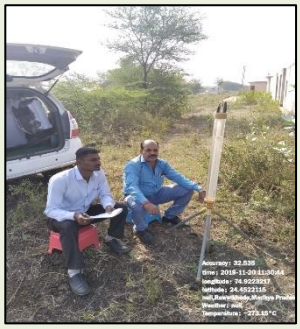

National Institute of Hydrology
Central India Hydrology Regional Centre, Bhopal

September, 2023

Dr. T. Thomas
Scientist 'F'

National Institute of Hydrology, Central India Hydrology Regional Centre, WALMI Campus, Kolar Road, Bhopal – 462016, M.P

PREFACE

Management of water resources in the arid and semiarid areas is a challenging task as large number of hydrologic, environmental and management factors have to be considered, in order to satisfy the ever-increasing demands. The challenge becomes more complex as most of the river systems have now become ephemeral. The adverse effects of climate change open up new challenges with higher frequency of extreme events viz., droughts, floods, heat waves; increased variability of rainfall; resulting in an uncertain future water availability scenario. Drought is one of the extreme events which can be expected to be more widespread in its spatial coverage. Also, the over-exploitation of the land and forest resources and changing climate has resulted in the complex issues of land degradation and possible desertification. As such, drought, desertification and climate change are closely interlinked and it is important to understand how these extreme phenomena will unfold in future. The occurrence of extreme events cannot be avoided but their impacts can be minimized to a great extent, by proper planning and preparedness. The development of an integrated framework for vulnerability assessment is rather a very multifaceted task.

The western Madhya Pradesh region has been under limelight due to frequent droughts, water shortages and large-scale depletion of groundwater. Most of the tributaries of the Chambal River system have ceased to perennial. The management of water on scientific lines and adoption of appropriate management strategies is therefore important for the well-being of the people in the Chambal region. It is in this context that two major projects viz., Mohanpura dam and Kundaliya dam have come up based on pressurized irrigation systems. This study helped to gain useful insights from historical events for studying various aspects of drought and desertification and carry forward from thereon to study the impacts of climate change and irrigation projects on these aspects into the future. An integrated vulnerability assessment framework comprising of drought vulnerability, desertification vulnerability and extreme climate vulnerability has been developed. The study has been carried out by Dr. T. Thomas, Scientist-F & PI; Dr. N.C. Ghosh, Ex-Scientist-G; Dr. P. C. Nayak, Scientist-F; Dr. Surjeet Singh, Scientist-G; Dr. B. Venkatesh, Scientist-G; Dr. R.V. Galkate, Scientist-F, Dr. R. K. Jaiswal, Scientist-F, Ms. Shashi P. Indwar, Scientist-D and Er. Gaurav Sharma, JRF from NIH and Director, Hydrometeorology; Sh. M. K. Paliwal, Dy. Director, Sr. Geo-hydrologist and Er. Sanjiv Das, Dy. Director & DBA (retd); Dr. Bijendra Baghel, Dy. Director & DBA; Sh. Sunil Vyas, Dy. Director and Sh. Girish Sharma, SDO under the able guidance of Dr. A. K. Lohani, Scientist ‘G’ & Coordinator and Er. G. P. Soni, Chief Engineer, BODHI, Water Resources Department, Bhopal.

Roorkee
15.09.2023

(M. K. Goel)
Director

Project Team	
National Institute of Hydrology Central India Hydrology Regional Centre, Bhopal	Dr. T. Thomas, Scientist 'F' (PI) Dr. N. C. Ghosh, Ex-Scientist 'G' (Co-PI) upto March 2019 Dr. P. C. Nayak, Scientist 'F' (Co-PI) Dr. Surjeet Singh, Scientist 'G' (Co-PI) Dr. B. Venkatesh, Scientist 'G' (Co-PI) Dr. R. V. Galkate, Scientist 'F' (Co-PI) Dr. R. K. Jaiswal, Scientist 'F' (Co-PI) Ms. Shashi P. Indwar, Scientist 'D' (Co-PI) Er. Gaurav Sharma, JRF National Institute of Hydrology, Central India Hydrology Regional Centre, WALMI Campus, Kolar Road, Bhopal.
Water Resources Department, Govt. of Madhya Pradesh	Director Hydrometeorology (PI) Sh. M. K. Paliwal, Dy. Director (Co-PI) Sh. Sanjiv Das, Dy. Director & DBA (Co-PI upto 30.09.2020) Sh. Bijendra Baghel, Dy. Director & DBA (Co-PI) Sh. Sunil Vyas, Dy. Director (Co-PI) Sh. Girish Sharma, SDO (Co-PI) Water Resources Department, Govt. of Madhya Pradesh, Jal Sansadhan Bhawan, Tulsi Nagar, Bhopal.
Consultant/s, if any (enter each consultant in a separate row)	None

Document control sheet

Title	Impact Assessment of the Upcoming Irrigation Projects and Climate Change on the Droughts and Desertification Scenario for Chambal Basin in Western Madhya Pradesh
PDS number	NIH-5_2016_6
Date of approval	04.12.2017
Budget in time of original approval (For Partner and for Lead)	Rs. 44.40 lakhs (NIH - Rs. 37.57 lakhs, WRD-MP - 6.83 lakhs)
Revised Budget (For Partner and for Lead)	No revision
Date of commencement	04.12.2017
Date of completion	03.10.2022
Number of pages	316
Number of figures and tables	Figures: 238 & Tables: 70

Abstract

The report highlights the key findings from assessments of drought, desertification and climate change perspective for Chambal basin in western Madhya Pradesh. The study devised a new approach to assess the integrated vulnerability to drought, climate change and desertification after the separate assessments of drought vulnerability, desertification vulnerability and extreme climate vulnerability using appropriate indicators. The vulnerability to drought, desertification and extreme climate was assessed using the spatial and spatio-temporal indicators based on their capability to quantify these aspects. An indicator-based approach has been used to evaluate the drought characteristics in the historical and future time periods. Only those indicators have been selected that can easily project the drought and desertification into the future with the available future climate data, so that the impacts of climate change can be easily assessed. Scenario based analysis has been carried out to study the impacts of the upcoming projects on the water availability and command that can be irrigated during drought periods of varying drought severities. The overall aim of the study has been to develop an integrated vulnerability assessment framework comprising of drought desertification and extreme climate change based on the indicator-based evaluation of the various characteristics of all these aspects.

The average annual rainfall in the study area is 944.2 mm and it has been

decreasing steadily during the last few decades. The extreme events including the extreme rainfall (>200mm/day), very heavy rainfall (>100mm/day) heavy rainfall (>50mm/day) have increased substantially during the present period (1991-2015). The 1-day maximum rainfall varied between 104.0 mm to 520.0 mm, but not significant trends have been detected. In general, there are 50 rainy days in a year which varies between 30 and 83 days. There has been a decrease in the number of rainy days during the present period. The heat waves have increased with significant increase in 1-day maximum temperature and 1-day minimum temperature. The average increase in maximum temperature is at the rate of 1.05^{o}C/100 years, which is significant and in tune with IPCC projections. The very hot days (MaxT>40^{o}C) and hot days (MaxT>35^{o}C) have increased whereas the number of cold nights (MinT<10^{o}C) has decreased during the present period. The severity of drought varied between moderate to severe. Five drought years occurred during the baseline period whereas only two droughts occurred during the present period. More than 50% of the blocks are drought prone based on the probability analysis of annual rainfall.

The assessment of the impacts of climate change on the future water availability, high flows, low flows, droughts and desertification has been assessed using the CMIP6 high resolution bias-corrected future climate data at 0.25 ^{o} x 0.25^{o} resolutions of 13 Global Climate Models (GCMs) for two future climate scenarios SSP245 and SSP585. The study period has been divided into five time horizons viz., baseline period (1961-1990), present period (1991-2015), near-term (2021-2040); mid-term (2041-2070) and end-term (2071-2100). The analysis pertaining to climate change indicated that the average maximum temperature and the average minimum temperature are increasing continuously in all future time periods. The extreme heat events represented by the 1-day maximum temperature is projected to increase in future also that may lead to more frequent occurrences of heat waves. The 1-day minimum temperature is also projected to increase in future which may have significant implications on the crop growth as well as crop yields in the study area. The frequency of very hot day events, hot day events, very hot night events (MinT > 25^{o}C) and tropical night events (MinT > 20^{o}C) are all projected to increase substantially in future whereas the number of cold nights

is projected to decrease significantly in the basin. This clearly indicates the warming of the basin in future as a consequence of the climate change.

The dry spell analysis has been carried out for all the five time periods. Generally, two critical dry spells (CDS) are observed in most of the years for which planning and provision of supplemental irrigation is necessary to prevent the crops from water stress during the crop growth period. The total CDS events, as are projected to increase substantially during mid-term and end-term under both scenarios. The CDS length is projected to increase during the near-term, mid-term and end-term under SSP245 and SSP585 scenarios. The average net supplemental irrigation requirement at Dhar for soyabean during the baseline period is 44.75 mm which is projected to decrease to 36.98 mm during the near- term period, 38.53 mm during the mid-term period and 35.62 mm during the end-term period under SSP245 scenario. A similar decrease in net supplemental irrigation requirement is observed under SSP585 scenario too. The average net supplemental irrigation requirement at for maize, cotton etc., and the principal kharif crops is projected to decrease under both future climate scenarios.

The drought characteristics have been evaluated using various indicators viz., departure for identification of drought years, probability analysis for identification of drought prone blocks, Standardized Precipitation Index (SPI) for evaluation of soil moisture drought characteristics, Surface water Drought Index (SDI) for evaluation of surface water drought characteristics, and Groundwater Drought Index (GDI) for evaluation of groundwater drought characteristics. The total soil moisture drought events comprising of extreme, severe and moderate events is projected to increase in all future time zones, the highest being during the mid-term. The soil moisture drought severity is also projected to increase both during the mid-term and end-term periods and it is projected to be higher under the SSP585 scenario. The total surface water drought events comprising of extreme, severe and moderate events is projected to decrease in all future time zones, the highest decrease being during the mid-term under both scenarios. As compared to the baseline period, the number of groundwater droughts is expected to decrease during the near-term and thereafter increase during the mid-term and end-term

time periods. The groundwater drought severity is projected to increase both during the mid-term and end-term periods as compared to the baseline period. The groundwater drought severity is projected to be higher under the SSP585 scenario.

The future streamflow has been simulated using the hydrological modeling approach using SWAT which has been calibrated and validated with the streamflow available at various gauging sites on river tributaries during the historical time period. The average annual stream flow is projected to increase substantially under all future time periods for all the major rivers including R. Chambal, R. Chambal, R. Shipra, R. Kalisindh, and R. Parwan. The high flows and low flows are both projected to increase substantially under all future time periods for all the major rivers in the study area, with the largest high flows during end-term. However, highest low flows are projected during the mid-term.

Drought vulnerability assessment comprised of spatially varying indicators and spatio-temporally varying indicators. The spatially varying indicators considered for the drought vulnerability assessment include elevation bands representing the topography, land-use and land cover, and soil types. The spatio-temporal indicators vary during each drought event and include rainfall departure; soil moisture drought, surface water drought and groundwater drought events and severities The areas vulnerable to drought have been identified based on the drought vulnerability index (DVI) after integrating these indicators by assigning appropriate weights to their sub-classes. The study area has been under moderate drought vulnerability during the baseline and present periods and is projected to continue to remain under the moderate vulnerability.

Desertification vulnerability assessment has been a challenging task as such indicators need to be selected that can be easily used for the future analysis as well. The spatio-temporal indicators used for the desertification vulnerability assessment other than the spatial indicators include aridity index, average annual air temperature, and rainfall erosivity. The desertification vulnerability assessment was carried out based on the (DSVI). The areas vulnerable to desertification have been identified based on the desertification vulnerability index (DSVI) after integrating these indicators by assigning appropriate weights to their sub-classes.

The desertification vulnerability is projected to increase substantially in future time periods progressively, with more areas falling under moderate vulnerability class. However, during the end-term, most of the area is under moderate vulnerability class with large patches under severe vulnerability in the districts of Neemuch and Mandsaur.

Extreme climate vulnerability assessment has been carried out using those climate indicators that may be responsible for extreme events including droughts and floods that may be responsible for soil erosion and desertification in the study area. The indicators used for the extreme climate vulnerability include 1-day maximum rainfall, daily rainfall intensity, number of rainy days, annual rainfall, 1-day maximum of MaxT, 1-day maximum of MinT, very hot days and very hot nights. The areas vulnerable to climate extremes have been identified based on extreme climate vulnerability index (ECVI) after integrating these indicators by assigning appropriate weights to their sub-classes. The extreme climate vulnerability in the study area was under mild, moderate and severe vulnerability classes during the baseline, present and near-term periods. However, the extreme climate vulnerability is projected to increase with considerable area falling under the extreme vulnerability class particularly during the end-term.

The integrated vulnerability based on the integration of the drought, desertification and extreme climate vulnerabilities is projected to increase substantially during the mid-term and end-term under both future climate scenarios. Suitable climate change adaptation and mitigation strategies have been suggested separately for the water sector and agricultural sector which will increase the climate resilience and make communities adapt to these unavoidable changes. Looking into the scenario of higher projected vulnerabilities in future, it is prudent to implement the suggested measures going forward, which will help in enhancing the water security and food security in the study area.

Originating unit	National Institute of Hydrology
Key words	climate change, drought, desertification, climate change, Chambal
Security classification	Restricted
Distribution	Restricted

Contents

List of Figures

List of Tables

1.0 INTRODUCTION

Climate change has emerged as one of the most-significant global environmental issue and has attracted the attention of scientists, policy planners, governments and politicians worldwide. The projected climatic changes are likely to affect adversely the key economic sectors and therefore, the sustainable development. Climate change has two components viz., the natural component and the anthropogenic influences. The various scientific assessment and special reports brought out by the Intergovernmental Panel on Climate Change (2001, 2007, 2014) reveal that there is discernible human impact on climate system. The anthropogenic influences have led to the increase in the global atmospheric concentrations of the major greenhouse gases (GHG's) such as carbon dioxide and methane, which have increased markedly as a result of human activities since the industrial revolution and now far exceed the pre-industrial values determined from ice cores spanning many thousand years. The increasing concentrations of the GHGs have been the most important drivers for increase in global temperatures. Climate change also shows its impact on the biodiversity, the very basis of existence of mankind. The warming is projected to increase for the next few decades and more the climate is disrupted, more are the chances of extreme risks and irreversible impacts. IPCC (2014) suggests that the human influence on the climate system is clear and it is extremely likely that the anthropogenic influences are the dominant cause of warming since the mid-20th century. Moreover, it has been reported that each of the past three decades have been successively warmer than the preceding decades since 1850.

Various climatic phenomena get affected due to climate change and it has the potential to induce unprecedented changes in the natural process. Climate related changes can cause increase in the frequency, intensity, duration and magnitude of disasters. The extreme events are expected to increase under this warming scenario of the climate system, leading to intensification in the amount of precipitation as well as increase in the frequency and intensity of droughts. Some of the changes in the extreme weather and climate events observed since 1950s have been linked to human influence. The extreme events such as floods and droughts are expected to increase causing serious implications for the water

sector. The rainfall intensity is expected to increase manifold leading to flash floods in cities and river systems. It is also expected that both floods and droughts may also occur in the same water year. The erratic pattern of the rainfall and its distribution will enhance the occurrence of dry spells. The drought affected areas are expected to likely increase in its extent. It is also very likely that hot extremes, heat waves and heavy precipitation events will continue to become more frequent. The extreme events will have a direct bearing on the water availability scenario. There may be sharp decline in the water availability in some regions whereas other regions may get more water. The groundwater recharge and availability shall also be affected due to the climate change. Climate change and drought in semi-arid and arid regions may also lead to desertification as the risk is significantly increased due to future rise in temperature as reported by Inter-governmental Panel on Climate change (IPCC).

Drought is a natural phenomenon which occurs due to deficit in rainfall and causes tremendous loss to the farmer's income and dents the region's economy. Due to its slow onset and long-lasting effects, it is one of the most devastating disasters as compared to other disasters. According to World Meteorological Organization (Monacelli, Galluccio, and Abbafati 2005) defined drought as a sustained, extended deficiency in precipitation. The UN Convention to Combat Drought and Desertification (UNCCD, 1994) defined drought as a naturally occurring phenomenon that exists when precipitation has been significantly below normal recorded levels, causing serious hydrological imbalances that adversely affect land resource production systems. There are different definitions for drought that are defined by taking into consideration various aspects which are influenced by drought. Also, drought definitions vary depending on the variable used to describe the drought. Among the extreme meteorological events, droughts are possibly the most slowly developing ones, that often have the longest duration, and at the moment the least predictability among all atmospheric hazards. Agriculture sector and those allied sectors which are largely dependent on raw materials produced from farm activities, are the worst affected and face tremendous loss of income which also dents the economy to a great extent.

Drought characteristics are directly influenced by the impacts of climate change and therefore it is of prime importance to evaluate the drought characteristics under a changing climate. However, unlike floods analyses, the changes in drought characteristics due to climate change impacts have not been explored fully. Amongst recent studies on understanding drought impacts, (Szép, Mika, and Dunkel 2005) have found that local soil moisture conditions in East Hungary became drier in the 20th century, parallel to the hemispherical changes. Mishra and Singh (2009) highlighted the changes in drought severity-area-frequency due to climate change scenarios and compared with historical droughts for Kansabati River basin in India. In the Indian context, it is most relevant to understand the climate change impact from drought perspective, due to large dependency of Indian agriculture on monsoon season which may see substantial changes due to climate change.

Desertification as defined by United Nations Convention to Combat Desertification (UNCCD) is 'land degradation in arid, semi-arid and dry sub-humid regions resulting from various factors, including climatic variations and human activities. Although desertification may have several definitions, it is pertinent to say that desertification is degradation of land to a level that it is no longer useful for human activities, which may the consequence of anthropogenic or natural climate change effects. Desertification includes a wide range of long term physical and biological processes. Desertification is a serious threat to the environment, and human welfare (Mainguet, 1994; Williams and Balling, 1996; Reynolds and Stafford Smith, 2002). Desertification could be seen as a process whereby the productivity of arid or semi-arid land falls by 10% or more (Miller, 1999). Basically, desertification is an advanced stage of land degradation where soil has lost part of its capability to support human communities and ecosystem. Land degradation is one of the processes, which is associated with the long-term effect of problems associated with climate change.

Desertification and climate change remain inextricably linked because of feedbacks between land degradation and precipitation, whereas the water resources are also intricately linked with climate. Climate change may therefore exacerbate desertification through the alteration of spatial and temporal patterns of

temperature, rainfall, solar radiation and winds. Based on the various projections of future climate change, there may be higher land degradation owing to regular droughts and greater soil erosion owing to high intensity rainfall events. The impacts of climate change, drought and desertification are all closely interlinked, and are most acutely experienced by the population whose livelihoods depend principally on natural resources. The relationships between climate change, drought and desertification have begun to be unpacked through the analysis of a number of climate-related and biological feedback loops (Sivakumar and Ndiangui, 2007; Sitch et al., 2007; Cox et al., 2000), while the nature of the linkages have led the IPCC (2007a, 2007b) to predict, that the extent of arid and semi-arid areas will expand between 5% and 8% under a range of future climatic scenarios. Moreover, the impacts of the climate change on the water resources sector in the future including the water availability scenario and occurrence of extreme events like droughts and floods is necessary, as these may directly and indirectly contribute to the process of land degradation and desertification in the study area. Despite the uncertainties involved, the combined evidence of current trends of increased rainfall variability and intensity of extreme events including droughts, along with global climate model predictions of warming, add significantly to concerns that climate change will exacerbate land degradation and desertification.

The droughts have increased in the areas falling in the Chambal basin, especially located in western Madhya Pradesh (MP). Many of the districts in the Chambal basin in MP have been hit by regular drought and water scarcity. As per the report of Madhya Pradesh State Pollution Control Board, considerable parts of western Madhya Pradesh have been perennially prone to droughts. As the years have progressed, the report suggests the drought prone area has been increasing continuously. Although irrigated area has increased, still almost 70% of the agricultural area remains dependent on rainfall. The Western Madhya Pradesh region located in the Malwa Plateau also known as Malwa region, is facing many hydrological problems, including recurrent droughts, soil erosion and perceived desertification to some extent in the districts adjoining Rajasthan. Some of the prominent districts falling in this region include Indore, Ujjain, Rajgarh, Mandsaur, Neemuch, Ratlam, Rajgarh, Agar, Shajapur, Sehore, Dewas, Dhar and

Guna. Most of these districts are partly or fully located in Chambal basin. There may be a possibility of enhanced desertification looking into the increasing intensity of droughts as well as the proximity of the MP districts in Chambal basin bordering Rajasthan to desert areas. The region has a semi-arid climate, with extended droughts, depletion of groundwater resources, coupled with uncontrolled developmental activities. These factors together with the threat of the impending climate change may lead to aggravation of droughts and desertification in the area.

The developmental aspects of this region therefore need to address the degradation of the ecosystem, mainstreaming the sustainable natural resources management, and building upon the existing adaptive capacities of communities and institutions under climate change scenario. Moreover, few major irrigation projects viz., Mohanpura Dam and Kundaliya Dam, both being irrigations projects have already come up very recently and few more projects are being planned on the Parbati river. It is in this background, the comprehensive analysis has been taken up for the assessment of the impacts of climate change and the impacts of the upcoming irrigation projects on the droughts and desertification in the future with the following objectives.

1. Assessment of climate change signals in Chambal basin.
2. Evaluation of drought characteristics and desertification investigation.
3. Hydrologic modelling for simulation of the hydrological processes.
4. Assessment the impact of climate change under projected climate scenarios on the future water availability, drought and desertification.
5. Evaluation of the impacts of upcoming irrigation projects.
6. Integrated assessment of vulnerability to drought, desertification and climate change.

2.0 REVIEW OF LITERATURE

2.1 Climate change

Climate change refers to the process in which a significant deviation from the mean climatic state is observed, for a significantly long period of time due to both

natural and/or anthropogenic influences (Solomon, 2007). Over the past century, a noticeable shift in the climate has been observed, as global temperatures have continued to rise steadily, which has been more pronounced over the last few decades. The rapid warming of the Earth's climate system has taken place since the 1950s, and these changes are unlike any, that have occurred in the past (Pachauri et al., 2014). Furthermore, each of the past three decades has been successively warmer at the Earth's surface than all the previous decades.

Climate change has occurred due to anthropogenic activities which have altered the pattern of much of the climatic phenomenon resulting in devastating impact to the environment. The human activities, particularly the burning of the fossil fuels have resulted in the drastic increase in the greenhouse gas (GHGs) emissions. According to the Fifth Assessment Report of the Intergovernmental Panel on Climate Change (IPCC AR5), the rate of the global average surface temperature increased by 0.197°C ± 0.031°C per decade over 1951-2012 (IPCC, 2014). Generally, the smaller climatic shifts are due to the results of the natural climatic variability but the unprecedented warming can largely be attributed to anthropogenic activities resulting in the large-scale emission of greenhouse gases (GHG's). The human activities, particularly the burning of the fossil fuels have resulted in the drastic increase in the greenhouse gas (GHGs) emissions. These drastic climate shifts will have a wide array of impacts, including increased temperatures, shifting precipitation amounts, rising sea levels, and higher variability in cyclonic events.

Rainfall and temperature trend analysis in India vis-a-vis climate change have been carried out extensively (Thapliyal and Kulshrestha 1991; Mehrotra and Mehrotra 1995; Kothyari and Singh 1996; Naidu et al. 1999; Stephenson et al. 2001; Lal and Singh 2001; De 2001; Wilk and Hughes 2002; Kumar et al. 2006, 2010; Dash and Hunt 2007; Dash et al. 2007; Krishnamurthy et al. 2009; Pal and Al-Tabbaa 2009, 2010; Krishnakumar et al. 2009; Bhan 2010; Guhathakurta et al. 2011; Aufhammer et al. 2012, Ghosh et al. 2012; Patra, 2012; Rai et al. 2014; Mondal et al. 2015; Thomas et al. 2015; Radhakrishnan et al. 2017). An increase in frequency and intensity of extreme rainfall events have been observed in several sub-divisions in India while the trend is decreasing in a few (Guhathakurta

and Rajeevan 2008). The increase in the number and intensity of extreme point rainfall events are reported for India (Khaladkar et al. 2009), notably for peninsular, east, and north east India (Guhathakurta et al. 2011). Jain and Kumar (2012) performed the trend analysis of rainfall and temperature for India using the MK test and SS estimator. The basin-wise trend analysis indicated that 15 basins depicted decreasing trend in annual rainfall but only one basin showed significant decreasing trend at 95% confidence level. Among the six basins showing increasing trend only one basin showed significant decreasing trend at 95% confidence level. All the basins had the same trend in rainfall and rainy days at the annual and seasonal scale.

Seneviratne et al. 2012 reported a statistically significant increase in the number of warm nights and a statistically significant reduction in the numbers of cold nights for 70 to 75% of the land regions. The changes in the number of warm days and cold days also showed warming, with about 40 to 50% of the area showing statistically significant changes consistent with warming. The research on the climate change extremes has progressed enormously, largely due to international coordinated efforts to simulate the future climate projections with collated, quality-controlled climate models, which serve as a basis to analyze parameters of interests and associated extreme events that may occur in the future. However, it is imperative to have an understanding about the various aspects involved in the climate change science including the climate change scenarios, Representative Concentration Pathways (RCPs) and General Circulation Models or Global Climate Models (GCMs), which are described briefly in the following sections.

The impact of climate change on the precipitation and intensity–duration–frequency relationship for Roorkee, India, was analyzed using an observed and ensemble of five general circulation models, revealing increasing rainfall intensities (Singh et al. 2016). Analyses of 100-year data (1901–2000) for rainfall for 236 districts in Ganga basin revealed that 39 districts displayed a significant negative trend, attributable to climate change (Bera 2017). Another study with 111-year rainfall data (1901–2011) for Madhya Pradesh reported decreasing rainfall trends for all seasons, particularly monsoon (Kundu et al. 2017).

Mahmood et. al. (2019) used the non-parametric Mann-Kendall test (MK Test) and Sen's Slope (SS) to identify statistically significant trends in temperature and precipitation after application of pre-whitening for Lake Chad basin. The precipitation in the study area depicted strong decreasing trend (38%) and very strong decreasing trend (9%) whereas the remaining 53% showed no signals or weak decreasing signals and suggested that if the present situation continues to prevail, then the basin will receive approximately 20-25% less rainfall in future. About 84% of the time series related to temperature show an extremely strong increasing trend and the average rate of increase in temperature was estimated to be 0.022^{o}C/year.

Panda and Sahu (2019) examined the long-term changes and short-term fluctuations in monsoonal rainfall and temperature over Kalahandi, Bolangir and Koraput (KBK) districts in the state of Odisha using Mann–Kendall test and Sen's slope estimator and concluded that the annual maximum temperature and annual minimum temperature have shown an increasing trend, whereas the monsoon's maximum and minimum temperatures have shown a decreasing trend. The annual rainfall depicted a quite strong increasing trend. Khan et. al. (2022) used the MK test and other statistical tests to assess the changes in temperature and precipitation over Pakistan from 1962-1990. The MK test demonstrated increasing precipitation (DJF) and decreasing maximum and minimum temperatures (JJA) at the meteorological stations located in the Karakoram region. These changes are highly significant at 5% level of significance at most of the stations.

The adverse effects of climate change on agriculture in India have been highlighted (Bhardwaj et al. 2022; Baig et al. 2022; Kulanthaivelu et al. 2022). The effects of climate change on groundwater hydrology have been investigated (Swain et al. 2022). The negative impact of deforestation and climate change on the biodiversity in North-Eastern India has been identified and remedial measures have been suggested (Gogoi and Lahon 2022).

2.1.1 Climate Change Scenarios

Climate change scenarios or socioeconomic scenarios are projections of future greenhouse gas (GHG) emissions used by analysts to assess future vulnerability to climate change. Future greenhouse gas (GHG) emissions are the product of very complex dynamic systems, determined by driving forces such as demographic development, socio-economic development, and technological change. However, the future evolution of GHGs is highly uncertain. Scenarios are alternative images of how the future might unfold and are an appropriate tool with which to analyze how driving forces may influence future emission outcomes and to assess the associated uncertainties. The possibility that any single emissions path will occur as described in scenarios is highly uncertain.

The depiction of the plausible scenario of the changing climatic conditions expected in future is rather crucial for understanding and evaluating the impacts of climate change on the various vital sectors including water, health, forests, urban, agriculture etc., so as to develop the planning frameworks for devising appropriate adaptation strategies. The projection of climate change scenarios using the integrated model simulation approaches can help to achieve these desired objectives. The Intergovernmental Panel on Climate Change (IPCC) is an international body for studying the science related to climate change. IPCC has been regularly releasing the Assessment Reports, which tries to portray as to how the climate will behave in the future and the likely consequences of the changing climate on the various vital sectors. One of the main commissions of the IPCC is to approve sets of scenarios for climate research, as well as to provide guidance for producing these scenarios. Previously, the scenario exercises were developed by the climate change research community and applied sequentially, that extended from the socio-economic factors that influence GHG emissions to the atmospheric and climatic processes and then to the impacts. Initially, the detailed socio-economic scenarios were developed and subsequently used to prepare the emission scenarios, which were later used in climate model experiments, which formed the basis of climate change projections (IPCC, 2007). The lags in the development process led to many years of waiting until climate and socio-

economic scenarios were available for its application in studies related to assessment of impacts, adaptation, and vulnerability.

In the IPCC-AR5, the emissions and socio-economic scenarios have been developed in parallel, building on different trajectories of radiative forcing over time. The RCPs are not associated with unique socio-economic assumptions or emissions scenarios but can result from different combinations of economic, technological, demographic, policy, and institutional futures. RCPs are four greenhouse gas concentration trajectories adopted by IPCC for its Fifth Assessment Report in 2014 and supersedes Special Report on Emissions Scenarios (SRES) projections published in 2000 (Nakicenovic et al., 2000). The four RCPs are named after a possible range of radiative forcing values in the year 2100 relative to pre-industrial values (i.e., +2.6, +4.5, +6.0, and +8.5 W/m^2) viz., i) RCP 2.6 (Rising radiative forcing pathway leading to 2.6 W/m^2 in 2100), ii) RCP 4.5 (Stabilization without overshoot pathway to 4.5 W/m^2 at stabilization after 2100), iii) RCP 6 (Stabilization without overshoot pathway to 6 W/m^2 at stabilization after 2100) and iv) RCP 8.5 (Peak in radiative forcing at 8.5 W/m^2 before 2100 and decline. RCP2.6 assumes that global annual GHG emissions peak during 2010-2020 with emissions declining substantially thereafter whereas the emissions in RCP4.5 are assumed to peak around 2040 and then decline. However, RCP6 assumes the emissions to peak around 2080 and then decline thereafter whereas the emissions in RCP8.5 are assumed to continue to rise throughout the 21^{st} century (Figure 2.1).

In IPCC-AR6, a new range of scenarios viz., Shared Socio-economic Pathways (SSPs) have been used in the Coupled Model Intercomparison Project Phase 6 (CMIP6). Five SSP scenarios have been suggested which includes SSP1-1.9, SSP1-2.6, SSP2-4.5, SSP3-7.0, and SSP5-8.5. In the SSP labels, the first number refers to the assumed shared socio-economic pathway, and the second refers to the approximate global effective radiative forcing (ERF) in 2100 (IPCC 2021). Compared to the previously used RCPs, the new SSP scenarios have been improved in many ways. Five narratives describing different development paths of society were designed and form the basis of the so-called SSP scenarios viz.

SSP1 (sustainable and green pathway), SSP2 (middle of the road or medium pathway), SSP3 (regional rivalry), SSP (inequality) and SSP5 (fossil-fuelled

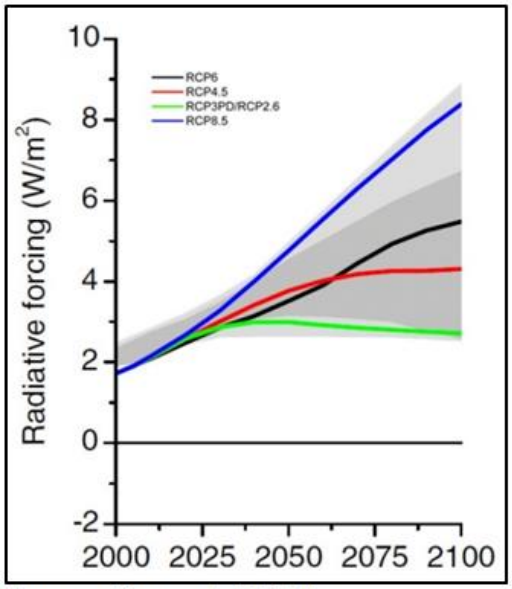

From van Vuuren et al (2011)

Figure 2.1: Representative Concentration Pathways (RCPs)

development). The classes of climate effects (radiative forcings) employed roughly correspond to RCP scenarios RCP2.6, RCP4.5, RCP6.0 and RCP8.5, complemented by a few additional classes. Combining the five pathways with the different climate forcings yields a scenario matrix (Figure 2.2).

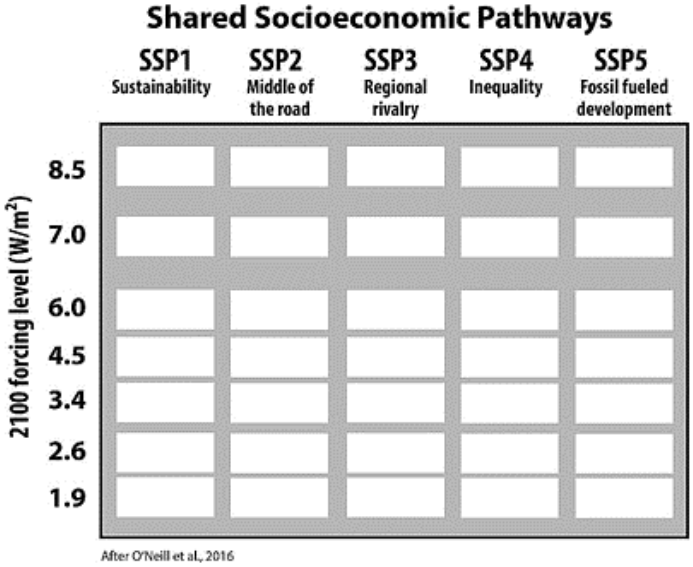

Figure 2.2: Shared Socio-economic Pathways (SSPs)

The four standard SSP scenarios based on the global agreement include i) SSP126 (scenario with 2.6 W/m² by the year 2100 is a remake of the optimistic scenario RCP2.6 and was designed with the aim of simulating a development that is compatible with the 2°C target), ii) SSP245 (radiative forcing of 4.5 W/m² by the year 2100 represents the medium pathway of future greenhouse gas emissions), iii) SSP370 (radiative forcing of 7 W/m² by the year 2100, this scenario is in the upper-middle part of the full range of scenarios), and iv) SSP585 (radiative forcing of 8.5 W/m² by the year 2100, this scenario represents the upper boundary of the range of scenarios). The standard SSP scenarios are given in Figure 2.3.

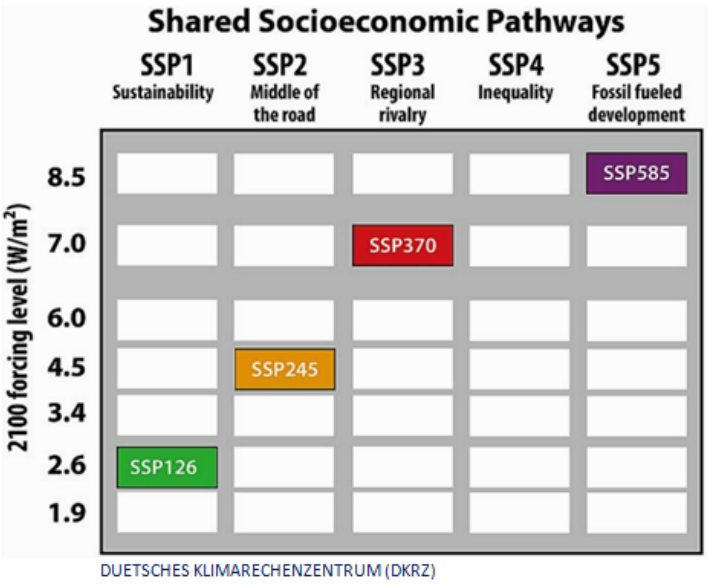

Figure 2.3: Four standard Shared Socio-economic Pathway Scenarios

2.1.2 General Circulation Models (GCMs)

Global climate results from the complex interactions between the atmosphere, cryosphere, hydrosphere, lithosphere and biosphere (Stute et al. 2001). Climate modelling is pursued by means of mathematical models of varying complexity ranging from simple energy-balance models to complex three-dimensional coupled global models. GCMs (general circulation models/global climate models) are the fundamental research tool used for understanding climate and climate change impacts. The climate system in a GCM is represented by a 3D grid, with horizontal coarse resolution of 100 to 600 km over the world, and 10 to 20 vertical layer in the atmosphere and about 30 layers in the ocean.

GCMs follow conservation laws (momentum, mass, energy, moisture), fluid dynamics, equation of state and more. Some of the parameters and boundary conditions considered include rotation speed of the Earth, thermodynamic and radiation constants of atmospheric gases and clouds, surface elevation, total mass of the atmosphere and its composition, soil type and surface albedo (Schmidt et al. 2006). The causes of uncertainties include different physical parameterizations, initializations, and model structures, approximations during numerical modeling, different feedback mechanisms, lack of complete information about atmospheric and oceanic processes among various other factors, which results in different outcomes from different GCMs for the same model inputs (forcing) (Sood & Smakhtin, 2015; Jain et al. 2019).

These models which represent physical processes in the atmosphere, ocean, cryosphere and land surface are the most advanced tools currently available for simulating the response of global climate system to increasing greenhouse gas concentrations. GCMs, possibly in conjunction with regional models, have the potential to provide geographically and physically consistent estimates of regional climate change which are required in impact analysis. The results from GCMs are a set of global datasets that describes future changes of climate forcing under different socio-economic and RCP scenarios. The cause of inherent errors and uncertainties occurring due to simplification of highly complex atmospheric physics in GCMs was discussed (Hughes et al. 2014). They found multi-model ensemble (MME) was a good fit for such situations in comparison to individual GCMs mainly due to compensation of individual errors. Several other researchers (Tebaldi & Knutti, 2007; Hughes et al. 2011); Basharin et al. 2016; Ahmed et al. 2020) have advocated the use of MME.

2.1.3 Dynamical and Statistical Downscaling

The spatial resolution of GCMs is too coarse (typically in the order 100-600 km) to adequately represent extreme events (Fowler et al., 2007; Maraun et al., 2010). There is a need to mitigate this issue by using downscaling approaches via regional modelling or statistical methods (Sylwia Trzaska, 2014). Thus, dynamical and statistical downscaling techniques are required to obtain climate

projections at the local scale (Fowler et al., 2007). In dynamical downscaling, a Regional Climate Model (RCM) is set up for a region of interest. In the statistical downscaling, statistical relationships are developed between large resolution climate variables and local variable of interest.

RCMs are physically based models, which use GCM outputs as the boundary conditions and are a means to downscale results from the GCMs, to obtain a higher spatial resolution (typically in the order 10-50 km). The finer resolution from RCM outputs, helps to obtain a better description of the local topography, land-sea distribution, vegetation and other land surface properties. Also, the finer resolution allows for a better simulation of such regional-scale features compared to coarser-scale models. RCMs are often biased and their spatial resolution might still be too coarse for assessing extreme precipitation at the local scale. Further statistical downscaling of RCM outputs may be necessary to obtain bias corrected higher spatial resolution projections. Statistical downscaling models (SDMs) are based on the idea that it is possible to define a relationship between the large-scale variables of the GCMs (or RCMs) and the local scale variables. The outputs from RCMs/SDMs are then used in impact models such as hydrological models to quantify the impact of climate change (Kjellstrom et al., 2016). Previous regional climate modeling studies showed useful results at the levels of homogenous zones and cities (Dash et al. 2013, 2015). (Dash et al. 2013, 2015; Pattnayak et al. 2013) inferred that some of the dynamically downscaled climate products are useful even at the city level.

Mishra et al. 2020 developed the bias corrected data of rainfall, maximum and minimum temperatures at 0.25o spatial resolution for South Asia using using Empirical Quantile Mapping (EQM) for the historic (1951–2014) and projected (2015–2100) climate for the four scenarios (SSP126, SSP245, SSP370, SSP585) using output from 13 General Circulation Models (GCMs) from Coupled Model Intercomparison Project-6 (CMIP6). Tabari et al. 2021 compared four statistical downscaling methods of bias correction, i) change factor of mean (CFM), ii) quantile perturbation (QP) and iii) event-based weather generator (WG) to assess climate change impact on drought by the end of the 21st century (2071–2100) relative to a baseline period of 1971–2000 for the weather station of Uccle located

in Belgium. The downscaling is applied to a 28-member ensemble of CMIP6) GCMs, for four future scenarios of SSP126, SSP245, SSP370 and SSP585. QP method outperformed the others in reproducing the magnitude and monthly pattern of the observed indicators. While all methods show a good agreement on downscaling total precipitation, their results differ quite largely for the frequency and length of dry spells.

Misra et al. 2022 used the Regional Spectral Model-Regional Ocean Model (RSM-ROMS) for dynamical downscaling of the South Asian Summer Monsoon. The RSM-ROMS simulation showed a more realistic alignment of the simulated rainfall along the orographic features of the domain. The regional climate model simulated the observed unique feature of intra-seasonal variations of the monsoon low pressure systems. Salunke et al. (2023) evaluated ninety climate models from CMIP5, CMIP6, NEX-GDPP and CORDEX for the simulation of seasonal precipitation and temperature over India. NEX-GDPP was found to be the best performer for the simulation of surface air temperature, whereas for the simulation of precipitation, CMIP performs the best in DJF and MAM seasons and NEX-GDPP performs best in JJAS and ON seasons. Misra et al. 2023 used the novel statistical downscaling model based on Convolutional Long Short-Term Memory (ConvLSTM) Network to obtain future projection of rainfall at 0.25° spatial resolution over entire Indian sub-continental region. The ConvLSTM methodology performed superior as compared to the LSTM and Kernel Regression based methodologies previously applied for Indian sub continental region.

2.1.4 Climate change indices

Various indices have been developed to categorize the climate change trends being observed around the world. These indices help to form a consistent framework for analyzing climate change. In the late 1990s, several meetings across the world took place on the topic of climate change in preparation for the IPCC Third Assessment Report. The WMO/CLIVAR Joint Working Group on Climate Change Detection held a meeting in 1999 and agreed to establish 10 simple climate indices for use in climate change analysis (Frich et al., 2002).

These climate indices were intended to be simple and independent enough to effectively describe temperature and precipitation patterns on a regional basis.

The climate indices not only create a framework for understanding climate patterns (Easterling et al., 2003). Climate change analysis generally focuses on the change of mean values and deviations for normal variability. This can easily be accomplished utilizing monthly global data sets that provide strong coverage across the world (Alexander et al., 2006). When trying to analyze extreme changes and more detailed patterns, a complete daily data set is required. The Expert Team on Climate Change Detection and Indices (ETCCDI) worked to address this problem by bringing together climate scientists from the various regions of the world with limited data (Alexander et al., 2006). The ETCCDI formed 27 indices to better detect climate change and create methods for explaining trends in extreme events of both temperature and precipitation. Increasing extremes in agriculture dependent countries will lead to various challenges in stabilizing the future food security (Singh 2012). The extreme events have been rising at an escalating rate at many parts of India and the extreme events are getting intensified over time (Pichuka et al. 2017; Roxy et al. 2017). The escalation of extreme events is due to global warming since the water holding capacity of the atmosphere increases by about 6–7% per 1°C temperature rise (Trenberth 2011; Muluneh et al. 2017).

Dash and Maity (2019) evaluated the spatio-temporal variation of eleven precipitation-based climate change indices over three 35-year epochs, viz., 1906–1940, 1941–1975, and 1976–2010 for annual and monsoon season daily precipitation data separately. The regions with significant changes are identified across the country, reflecting different characteristics (magnitude, frequency, intensity, and duration) of precipitation-based climate change indices. Significant trends over the country were more prominent for the indices derived with annual daily precipitation. Yaduvanshi et al. (2021) explored the changes in the ETCCDI of rainfall and temperature from CMIP5 over different climatic zones of India under RCP4.5 and RCP8.5. Hot temperature extremes are expected to increase while cold temperature extremes decrease with hot days projected to increase by 44% and 52%, warm nights projected to increase by 23% and 13%; cold days

projected to decrease by 10% and 9%, and cold nights projected to decrease by 13% and 12% relative to pre-industrial levels. Rehana et al. (2022) investigated the relationship between precipitation and temperature extremes as recommended by ETCCDI and large-scale climatological phenomenon indices viz., Indian Summer Monsoon Index (ISMI), Arctic Oscillation (AO), and North Atlantic Oscillation (NAO) for India and reported that the extreme warm indices were negatively related to ISMI and positively related to extreme cold indices. The extreme precipitation indices had a significant positive relationship with AO. Also, India witnessed increase in warm extremes over western, central and peninsular India, while cold indices increased over north-west India.

The trend analysis on the climate variables have been carried out by various researchers using various trend detection techniques. To identify trend in the climatic variables with reference to climate change, the Mann-Kendall test has been employed by a number of researchers with temperature, precipitation and stream flow data series (Taylor and Loftis, 1989; McLeod et al. 1991; Yu et al. 1993; Burn, 1994; Douglas et al. 2000; Yue et al. 2002; Burn et al. 2004; Lindström & Bergström, 2004; Xiong & Guo, 2004). Mekis and Hogg (1999) reported a significant rise in total annual precipitation in almost all regions of Canada over the past century. Stone et al. (2000) showed that the total annual precipitation increased in southern Canada during the twentieth century (record lengths range from 34 to 102 years within the 1895–1996 period), partly due to an increase in intermediate and heavy precipitation events. Zhang et al., (2000) showed that the total annual precipitation increased by 5% to 35% between 1900 and 1998 over southern Canada. Some of those trends are not significant, but they are positive and significant during the winter season for the Gaspésie and Côte-Nord regions located in the province of Québec as well as in New Brunswick. Shabbar and Bonsal (2003) performed trend analysis using the slope estimator proposed by Sen (1968) to verify if frequency, intensity and duration of winter cold and warm spells in Canada changed significantly during the second half of the twentieth century. Kundzewicz & Robson (2004) provide general guidance to the methodology of change detection in time series of hydrological records.

2.2 Drought

Drought is universally regarded as a natural hazard of considerable severity that can occur under any climatic condition. It is differentiated from the other natural disasters because its implications lack structure and it may involve vast geographical regions (Wilhite and Glantz, 1985). Furthermore, the phenomenon of drought is characterized by its slow development and thereafter may spread through the full hydrological cycle. Generally, its consequences are often shown after its completion. Drought is frequently described as a creeping phenomenon (Vogt et al., 2011) as opposed to other natural hazards, and it is challenging to determine both the onset and the termination of a drought event. Droughts are of great importance in the planning and management of water resources (Mishra & Singh, 2010).

The society, environment and economy are sectors that are severely afflicted by the impacts of droughts. Firstly, the social sector has suffered great losses and according to findings of the UN Global Assessment Report, (UNISDR, 2011) more than 2 billion people have been affected by droughts and these numbers exceed than those of any other natural hazard. The droughts that were reported in Sub-Saharan Africa in the early to mid-1980s have had adverse effects in the lives of more than 40 million people (OFDA, 2012). Amazon River was hit by a drought in 2005 which seriously affected both the transportation and the total crop yield (Marengo et al., 2007). As far as the economic sector is concerned, Australia suffered huge losses of about 20% in the income owing to the severe drought of 2002-2003 (Horridge et al., 2005).

Furthermore, the lack of an accurate and globally accepted definition of drought leads to confusions about the existence and the severity of the phenomenon. In addition, the definition of drought is modified depending on the objectives of each scientific field. More specifically, the meteorological drought is defined as the precipitation deficit as compared to the normal precipitation derived for a considerably longer period of time; the agricultural drought refers to low crop production due to inadequate soil moisture to meet the transpiration needs of the plants in their crucial stages of development; the hydrological drought refers to

drop in the water level of lakes, rivers and groundwater table below a certain limit for a specified length of time; whereas the social-economic drought, refers to the vulnerability of society to water shortage. All the above explain the vast number of definitions that have been recorded during the recent years [World Meteorological Organization (WMO), 2006; Wilhite and Glantz, 1985]. Wilhite and Glantz (1985) reported that more than 150 definitions have been used to explain the phenomenon of drought.

The major drought characteristics include drought severity, drought duration and drought intensity Wilhite (1992, 2000) and Wilhite and Pulwart (2005). The spatio-temporal distribution of the drought is another important characteristic. In USA, on an average, 14% of the country is affected by severe to extreme drought every year (Wilhite and Pulwart, 2005). Droughts impacts both surface and groundwater resources and can lead to reduced water supply, deteriorated water quality, crop failure, reduced range productivity, diminished power generation, disturbed riparian habitats, and suspended recreation activities, as well as affect a host of economic and social activities. Droughts also affect water quality of reservoirs, as the low water levels and its related hydrology leads to changes in the lake chemistry or water chemistry of reservoirs. Also, the pathway of transport of sediment, nutrients and organic matter gets interrupted and severely impacts the water quality. The period between extreme events seems to have become shorter in most of the regions.

2.2.1 Drought Indices

Drought indices have an important role for the monitoring and assessment of droughts. A drought index is acceptable when it presents a clear, simple and qualitative analysis of the main drought characteristics viz., intensity, duration and spatial extent (Hayes, 2000). Drought indices may incorporate several variables related to drought, (precipitation, temperature, potential evapotranspiration, soil moisture, snowpack) into a single number, the use of which is more efficient in the decision-making process than raw data (Hayes et al., 2007). Several meteorological drought indices have been developed based on precipitation. The precipitation has been commonly used for meteorological drought analysis

(Benitez & Domecq, 2014; Hatmoko, Radhika, Raharja, Tollenaar, & Vernimmen, 2015; Levina, Hatmoko, Seizarwati, & Vernimmen, 2016).

Standardized Precipitation Index (McKee et al., 1993) have been used by an increasing number of scientists around the world and has been recommended by the World Meteorological Organization (WMO) as the primary tool for monitoring meteorological droughts. McKee et al., (1993) estimated the SPI for the time scales of 3, 6, 12, 24, and 48 months. The multi-temporal approach of SPI provides a larger insight of the impacts of drought on the availability of water resources (Angelidis et al., 2012). The long-term monthly rainfall record is fitted to a probability distribution, which is then transformed to a normal distribution. The positive SPI values signify greater than median precipitation, and negative values signify less than median precipitation (Edwards and McKee, 1997). A detailed description of the SPI calculation can be found in Lloyd-Hughes & Saunders (2002). Guttman, (1998) and Hayes et al., (1999) compared SPI with Palmer Drought Severity Index (PDSI) and found that the SPI has advantages of statistical consistency, and the ability to describe both short-term and long-term drought impacts through the different time scales than the PDSI.

Hayes et al., 1999 explained the advantages of SPI. Due to its intrinsic probabilistic nature, the SPI is an ideal candidate for carrying out drought risk analysis (Guttman, 1999). Vicente-Serrano (2006) performed spatial and temporal analysis of droughts using Standardized Precipitation Index (SPI) on the Iberian Peninsula for 1910–2000, and identified the principal drought episodes. Patel et al. (2007) analyzed the spatial patterns of meteorological drought using SPI and quantified the effects of drought on food grain productivity. Different researchers have used SPI in different areas for real-time monitoring or retrospective analysis of droughts viz., Turkey (Komuscu 1999), Argentina (Seiler et al. 2002), Canada (Anctil et al. 2002), Spain (Lana et al. 2001), Korea (Min et al. 2003), Hungary (Domonkos 2003), China (Wu et al. 2005), Europe (Lloyd- Hughes and Saunders 2002) and India (Chaudhari and Dadhwal 2004). Many other investigators (Sonmez et al., 2005; Burke and Brown 2008; Owrangi et al., 2011; Golian et al., 2014) used the SPI to study the spatial variation in drought events at multiple time steps. Short time scales (no more than 3 months) are appropriate to reflect the impact of drought on soil moisture, snowpack, and stream flows of small rivers;

medium term aggregated values (3–12 months) are suitable to assess the drought on stream flow and reservoir storage whereas long time scales (12–24 months) can be used for long-term processes i.e. for groundwater recharge (Spinoni et al., 2013).

Swetalina and Thomas (2016) carried out drought vulnerability assessment for Bearma Basin using temporally varying indicators which include standardized precipitation index (SPI), surface water drought index and groundwater drought index. The SPI was applied to quantify monthly precipitation deficit anomalies on multiple time scales (1, 3, 6 and 12 months). It was observed that highly vulnerable areas are located in the southern and northern regions and more than 26 % of the basin lies in the highly and critically vulnerable classes and had high drought related negative impacts. Basamma et al. (2017) carried out the assessment of drought situation using SPI in the Mewar district of Rajasthan. Rahman et. al. (2018) studied the spatial rainfall variability and drought assessment in Khyber Pakhtunkhwa province of Pakistan using Standardized Precipitation Index (SPI) and the results based on the 12-month SPI depicted two distinct dry periods, i.e., 1984 to 1989 and 1998 to 2002.

Saini et al. (2020) attempted to investigate the dry and wet conditions over the state of Rajasthan based on standardized precipitation index (SPI) for which diurnal rainfall data of 33 stations was procured and used for the period 1961–2017 Mann-Kendall test was applied to examine the trends in rainfall and SPI. The analysis revealed an increasing trend in annual SPI over majority of stations (23 stations), with significant increasing trend at 5 stations (significant at 95% confidence level). There was severe drought in almost all the stations except Banswara, Barmer, Nagaur and Sirohi stations during dry years. Bhunia et al. (2020) investigated drought phenomena in pre-monsoon, monsoon, post-monsoon and monthly time steps in three relatively drought prone districts (Purulia, Bankura, Midnapore) of West Bengal in India using rainfall data of 117 years (1901–2017) using SPI and found that occurrence of drought was frequent in these districts with increasing dry events and decreasing wet and normal events.

The Reconnaissance Drought Index (RDI) (Tsakiris et al. 2007) was developed using the precipitation and potential evapotranspiration (PET) which is a temperature component, to provide an effective index for monitoring droughts. On the same grounds, Vicente-Serrano et al. (2010) suggested Standardized Precipitation Evapotranspiration Index (SPEI), in order to examine the effect of temperature on drought analysis using a water balance concept. This SPEI can be used for climate change related drought characteristics Mavromatis (2007), which is capable of including the regularly increasing temperature in the recent years.

Zehtabian et al. (2013) investigated similarities/differences of SPI and RDI utilizing precipitation and ratio of precipitation over potential evapotranspiration (ETo). The results indicated the frequency of high severity droughts in this area. Shah et al. (2013) carried out an analysis for operational drought assessment to identify three parameters i.e. the beginning, the end and the degree of severity of drought using RDI for Bhavnagar. Kousari et al. 2014 investigated drought severity trend in Iran using RDI for assessment of drought severities. The non-parametric Mann-Kendall test and Sen's slope estimator were applied for investigating trends in different time series of RDI (3, 6, 9, 12, 18 and 24 monthly time series). Decreasing trends in RDI time series particularly for long-term time series (12, 18 and 24 monthly time series) were observed suggesting an increasing trend in drought severities. Mutafa et al. (2017) used the SPI and RDI to quantify the aggregated deficit between precipitation and the evaporative demand of the atmosphere. The results showed that evapotranspiration and rainfall deficits are determining the meteorological drought, and is directly related with groundwater recharge deficits.

The Palmer Drought Severity Index (PDSI) (Palmer, 1965), is calculated based on precipitation, temperature and Available Water Content (AWC), and its original purpose was to identify droughts in crop-producing regions of the United States. The index has been used to illustrate the areal extent and severity of various drought episodes and to investigate the spatial and temporal drought characteristics (Senatore et al., 2018; Yang et al., 2018; Zhu et al., 2018). The PDSI is highly sensitive to temperature and precipitation anomaly. PDSI is perhaps the most widely used regional drought index for monitoring droughts but

it still has some limitations. The limitations of PDSI have been documented in several studies (McKee et al., 1995; Guttman, 1998). The limitations of PDSI include, i) an inherent time scale making PDSI more suitable for agricultural impacts and not so much for hydrologic droughts; ii) assumptions that all precipitation is rain, thus making values during winter months and at high elevations often questionable; iii) can be slow to respond to developing and diminishing droughts (Hayes et al., 1999).

Liu and Kogan (1996) used Vegetation Condition Index (VCI) derived from the weekly Normalized Difference Vegetation Index (NDVI) data for the period of July 1985 to June 1992, to monitor large scale drought patterns and their climatic impact on vegetation for Brazil. The areas under agricultural drought were delineated with separate threshold values of the NDVI and VCI. The seasonal and inter-annual comparisons of drought delineated by VCI provided a useful tool to analyse the temporal and spatial evolution of regional drought as well as to estimate crop production qualitatively. Jain et al. (2010) carried out drought monitoring for three districts namely, Bhilwara, Kota and Udaipur in Rajasthan, India using SPI, NDVI, Water Supply Vegetation Index (WSVI) and VCI derived from the Advanced Very High-Resolution Radiometer (AVHRR). Integrated analysis of ground measured data and satellite data has a great potential in drought monitoring. Dutta et al. (2015) studied the efficiency of remote sensing and GIS techniques for monitoring the spatio-temporal extent of agricultural drought. VCI was calculated for whole Rajasthan using the long term NDVI images which reveals the occurrence of drought related crop stress during the year 2002. Rimkus et al. (2017) examined the effect of drought on vegetation using the NDVI and VCI in the eastern Baltic Sea region. The positive correlation between 3- and 6-month SPI and VCI was observed. The precipitation deficit is only one of the vegetation condition drivers and NDVI can be used to identify effects of droughts.

The deficit in precipitation alone cannot be considered as the factors responsible for drought, but also below-average water level in surface water, reservoirs, and groundwater are important factors that contributes to drought (Tsakiris et al. 2013; Kumar et al. 2016). Hydrological drought is the consequence of the propagation of a meteorological drought in the hydrological system. Its assessment based on

hydrological variables including stream flow, lake levels, reservoir levels and groundwater levels is very important for the comprehensive planning of water resources management at the basin scale. A surface water drought event can be related to stream flow deficit with respect to the normal conditions which can be characterized by its severity, its time of onset and its duration, its areal extent, and its frequency of occurrence.

The Surface Water Drought Index (SDI) developed by Nalbantis and Tsakiris (2009) is an index analogous to SPI, and is used for characterizing the severity of hydrological droughts. A hydrological drought index analogous to SPI is helpful in obtaining a meaningful relationship between SPI and SDI. The hydrological drought analysis has been carried out in several regions across the globe such as the Northern Peloponnese in the Achaia and Korinthia Prefectures in Greece (Tigkas et al. 2012), the northwest of Iran (Tabari et al. 2013) , the Sefid-Rud basin in the Iran plateau (Arabzadeh et al. 2016), the junction of the upper Yangtze River and the middle Yangtze River in China (Zhang et al. 2019), the Neman river basin in Europe (Rimkus et al. 2013), the Diyala river basin shared between Iraq and Iran (Al-Faraj et al. 2014), and the Kucuk Menderes Basin in Turkey (Kermen et al., 2018).

Guttman (1991) examined the sensitivity of Palmer Hydrological Drought Index (PHDI) to departure from average temperature and precipitation conditions. Independent series were calculated for temperature anomalies plus and minus 1, 3, 5 and 100^{o}F and for precipitation anomalies of 25, 50, 75,125,150 and 200% of normal, for each calendar month for Colorado, Indiana, Nevada, New York, Oklahoma, South Dakota, Washington and Wisconsin. The Surface Water Supply Index (Shafer and Dezman, 1982) was developed from the Palmer Index to take into account the mountain snowpack. It represents surface water supply conditions, and includes water management combining the hydrological and climatic features. The Surface Water Supply Index (SWSI) considers reservoir storage management dependent and unique to each basin, which limits inter-basin comparisons.

Shukla and Wood, (2008) derived Standardized Runoff Index (SRI) which incorporates hydrologic processes that determine the seasonal loss in stream flow due to the influence of climate. As a result, monthly to seasonal time scales of SRI is a useful complement to SPI for depicting hydrological aspects of droughts. In the subsection below, special emphasis will be laid some meteorological drought indices SPI and PDSI because they have been extensively used all over the world. Prajapati et al. (2021) studied drought characteristics in the Marathwada region of Maharashtra, which experiences recurring droughts, using SPI, SDI and VCI, wherein SPI and SDI was computed at 1, 3, 6, 9 and 12-month time scales using precipitation and stream flow data, respectively whereas the VCI was computed using MODIS satellite data at 500 m resolution for 1, 3 and 5-month time scales. The severity and the areal extent of droughts observed by these indices are varied both spatially and temporally.

Groundwater drought is another important consideration that needs to be assessed as during droughts, the groundwater is in most utilized source to meet the various water demands. The most well-known methods used in groundwater drought analysis based on the long-term groundwater level data are the Threshold Level approach and the Sequent Peak Algorithm (Tallaksen and van Lanen 2004). In a comprehensive overview of the 1988-1992 droughts in the UK (Marsh et al., 1994), the effect of the drought on groundwater levels is discussed, but no definition of a groundwater drought is given. A conceptual definition as given by (Calow et al., 1999) states that groundwater drought describes a situation where groundwater sources fail as a direct consequence of drought. This definition of a groundwater drought apparently also incorporates human demand of water. Van Lanen & Peters, 2000, defined that a groundwater drought occurs if in an aquifer the groundwater heads have fallen below a critical level over a certain period of time, which results in adverse effects that are noticeable. In most of the cases, groundwater levels are monitored to detect groundwater droughts (Hatmoko et al., 2015; Shahid & Hazarika, 2010).

As groundwater level is a state variable and not a flux like recharge, rainfall and stream flow, the deficit volume calculated with the threshold level approach can identify groundwater droughts or scarcities better compared to other approaches

(Shahid & Hazarika, 2010; Thomas et al., 2014). Although the fixed threshold provides quite acceptable results, the cumulative deficit is preferred, as the major droughts can be identified more clearly (Adhikary, 2013; Van Lanen & Peters, 2000). Shahid & Hazarika 2010 investigated the groundwater scarcity and drought in three north western districts of Bangladesh and results indicated that groundwater scarcity prevailed in 42% area in every year. Thomas et al. (2014) evaluated stream flow drought characteristics using stream flow drought index (SDI), and groundwater drought characteristics using groundwater drought index (GDI). The maximum groundwater drought intensity was observed at Rehli (-0.44). The time step to be used in the analysis of a groundwater drought should necessarily be large, usually more than a week or a month (Shahid & Hazarika, 2010; Van Lanen & Peters, 2000).

2.3 Supplementary Irrigation

Dutta and Das (2001) estimated crop water requirement by Modified Penman and Pan Evaporation methods in Lunkaransar area of Indira Gandhi canal command. The values of ETc for kharif crops were estimated as, pigeon pea (503 mm), pearl millet (488 to 491 mm), groundnut (430 to 452 mm), and for rabi crops as gram (239 to 260 mm), wheat (213 to 227 mm), mustard (129 to 142 mm). Temesgen et al. (2005) compared four reference evapotranspiration (ET_o) equations (CIMIS Penman, FAO-56, ASCE-PM, and the Hargreaves equation) using weather data from 37 agricultural weather stations across the state of California, USA. Hourly and daily comparisons of ET_o and net radiation (R_n) were made using graphical and simple linear regression approach. Hargreaves equation performed well in most parts of the state, considering that it only requires air temperature measurement. ET_o values estimated by the CIMIS Penman and the Penman-Monteith (ASCE-PM and FAO-56 PM) equations correlated very well for both hourly and daily time steps.

Nandagiri and Kovoor (2006) evaluated the performance of several ETo methods (FAO-56 PM, FAO-24 Blaney-Criddle, FAO-24 Radiation, Priestly Taylors, Turc, Hargreaves and Pan Evaporation) in the four stations in arid (Jodhpur), semiarid (Hyderabad), sub-humid (Bangalore), and humid (Pattambi) climates of India.

Among the methods evaluated, the FAO-56 Hargreaves (temperature based) method, yielded ET_o estimates closest to the FAO-56 PM method for daily and monthly time steps, in all climates except the humid climate, where the Turc method (radiation based) was the best. Simpler equations yield much smaller errors when monthly computations were made. Factor analysis also indicated that wind speed appears to be an important variable in the arid climate, whereas sunshine hours appear to be more dominant in sub-humid and humid climates.

Bouraima et al. (2015) estimated the reference and actual evapotranspiration (ET_o and ET_c) respectively and the irrigation water requirement of rice (Oryza sativa L.) in Benin sub-basin of Niger river (BSBNR) of west Africa, using CROPWAT. The long records of climatic, crop and soil data (1942 to 2012) were used in CROPWAT and the Penman-Monteith method was used to estimate ET_o. Crop coefficients (K^c) from the phenomenological stages of rice were applied to estimate the actual evapotranspiration ET_c. The annual reference evapotranspiration of BSBNR was estimated at 1967.0 mm. The lowest monthly ET_o of 123.0 mm, was observed in August, i.e. during the middle of the rainy season while the highest value of 210.0 mm was observed in March, i.e. the dry season. The crop evapotranspiration ET_c and the crop irrigation requirements were estimated at 651 mm and 383 mm respectively for rainy season and 920 mm and 1148 mm respectively for the dry season.

Desta et al. (2015) determined the crop water requirement in Ethiopia for planning of supplemental irrigation for chickpea production using CROPWAT 8.1. The net irrigation requirement was 37.2 mm, 114.4 mm, 205.2 mm, and 79.8 mm during seedling, vegetation, development and late (maturity) stages respectively. Khandelwal et al. (2015) calculated the net irrigation water requirement for different crops in Limbasi branch canal command area of Mahi Right Bank Canal (MRBC) project located in Gujarat, India. The Hargreaves-Samani approach was used for estimation of ETo. The crop evapotranspiration (ETc) and net irrigation requirement (NIR) of kharif, rabi and summer season crops were estimated. The NIR for kharif paddy was 166.8 mm; rabi crops viz., jowar, tobacco and wheat were 404.3 mm, 504.2 mm and 564.7 mm respectively; and summer crops viz., paddy and bajra were 851.1 mm and 619 mm respectively.

Kar et al. (2016) compared ET_o estimated by eight different methods, viz., Penman-Monteith, Modified Penman-Monteith, Hargreaves-Samani, Irmak, Hargreaves, Valiantzas, ANN and FAO24 models for the dry sub-humid agro-ecological region (Varanasi). The feed forward ANN was used for prediction of ET_o using resilient back-propagation method and the architecture 2-2-1 (having parameters T_{mean} and solar radiation) was found to be the best one. The average annual evapotranspiration (Penman-Monteith method) for Varanasi was estimated as 1447.4 mm. As compared to Penman-Monteith method, the FAO-24 and Hargraves-Samani under-estimates ET_o, whereas the Modified-Penman-Monteith, Hargreaves-Samani, Irmak, Hargreaves, Valiantzas over-estimates ET_o, whereas ANN closely approximates the ET_o as estimated by the Penman-Monteith method.

Bhatt et al. (2017) estimated the optimal irrigation scheduling to increase crop yield under water scarcity conditions. The crop water requirement was estimated as 304 mm and irrigation requirement as 288.2 mm. Alternate cases studied included, i) refilling soil moisture to field capacity with irrigation at critical depletion; ii) irrigate at a given ET_c reduction per stage; and iii) irrigate at fixed interval per stage at 70% field efficiency; which resulted in the yield reduction of about 0%, 14.9%, 25.1% respectively. Therefore, it was advocated that the irrigation should be carried out at the critical depletion to achieve no (0%) reduction in crop yield of maize so as to achieve maximum efficiency.

2.4 Desertification

Desertification is defined as the degradation of the soil, landscape and bio-productive terrestrial system, in arid, semiarid and sub-humid areas resulting from several factors including climate change and human activities (UNCCD). Desertification is the end stage of the land degradation process which ultimately affects the economical and biological productivity of the land and leads to economic stress to the vulnerable population (Bisaro et al. 2014) by degrading soil fertility completely. Land degradation caused by the removal of vegetation is perceived as a consequence of soil degradation (Akhtar-Schuster et al. 2011). Once the physical, chemical and biological properties of the soils start degrading,

natural regeneration is not possible in a human lifespan (UNCCD), hence soil is termed as a non-renewable resource.

Desertification is generally perceived as a slow hazard in semi-arid regions, initially induced by climatic factors, which accelerates when combined with human actions (population pressure, intensive land use, improper land management etc.) in a longer time frame (Lin and Tang, 2002). Much of the concern is related to desertification that comes from the decline in the land productivity, especially in arid areas (UNCCD). According to available statistics, 10 to 20% of the arid regions of the world, suffers from some degree of damage (Rubio and Recatala, 2005). Dry lands cover about 30% of the earth's surface and over 250 million persons are thought to be directly affected by the desertification process (Reynolds et al. 2007). As a result, wide range of environmental, cultural, political and socio-economic impacts have emerged at local, national and global scales. This situation demonstrates that desertification is not only a global concern but also a local problem (Salvati et al. 2013) which has to be addressed in order to mitigate the desertification process (Fleskens and Stringer, 2014). Globally, this phenomenon affects about 1.9 billion hectares of land and 250 million people (Low, 2013).

Among many events which affect earth's environment and ecosystem, drought often has a direct association with desertification (Shewale and Shravan, 2005). Poor land management during periods of unusually dry weather can cause loss of vegetation, which in turn leads to desertification. Drought-induced desertification is aggravated due to the spatio-temporal variations in rainfall, temperature, wind and solar radiation (D'Odorico et al. 2013) and human-induced desertification is exacerbated due to the ever-increasing population, along with the food and fodder demand, which results in socio-economic pressure on the land resources (Wang et al. 2010). Despite of the importance of land degradation and desertification in arid regions of the world, there are limited studies and assessments (Lal, 1989).

2.4.1 Desertification indices

The Global Assessment of Human-induced Soil Degradation (Oldeman et al. 1992) was the first global evaluation of soil degradation and is still main global source of soil degradation data (FAO, 2000). Several methods have been used to understand the indicators that may lead to land degradation. Helen and Tobias, (1996) used a unique approach to assess desertification, through the ability of growth of various grassroots on land. The time taken by the plant grown on the land is compared with the time taken by the same plant to grow in a fertile land. Some of the other important models include GLASOD (Oldeman et al. 1992), ASSOD (Van Lynden and Oldeman, 1997) and recently (FAO, 2002).

Kharin et al. (2000) prepared the desertification map of West Asia by presenting several methods for desertification assessment. Zhu et al. (2007) and Sakcali et al. (2008) demonstrated that the vegetation cover condition after soil condition has maximum effect on desertification and intensity of desertification may increase with the decrease of vegetation cover. Salvatti et al. (2007) integrated economic and environmental indicators, stating that in complex ecosystems, human and social characteristics should also be included along with other geo-physical features. After integrating, a synthetic index was setup and compared to a standard desertification index and they concluded that human impact on environment contributes to desertification. Lavado et al. (2009) evaluated the land sensitivity to degradation by using ESA model in south-western of Spain and prepared the desertification map. Tavares, (2012) evaluated and prepared sensitivity to desertification map using MEDALUS model in Riberia Seca basin. Ahmadi et al., (2009) surveyed desertification condition of Fakhr Abad Region in Mehriz city using changed MEDALUS method and concluded that half of the region falls in lower category of desertification and about 41% of it located in medium desertification class.

Nikoo, (2011) applied the Iranian Model of Desertification Potential Assessment (IMDPA) to assess potential desertification, in a study to identify factors contributing to land degradation in Damghan, Iran and the results showed that the region was dominated by a high-intensity desertification. The most important

factors in desertification were identified as soil surface cover deficiency, indiscriminate withdrawal of groundwater, exploitation of irrigation and agriculture. Jafari et al. (2011) studied desertification in Segzi pediment by IMDPA model and developed a map which suggested that 1.5%, 20% and 78.5% of the study area can be considered under medium, high and very high desertification intensity class respectively. Shakerian et al. (2011) evaluated desertification intensity in Jarghooyeh region, based on IMDPA model and results indicated that the area falls under low class of desertification. Also, desertification intensity maps were developed using various indicators related to the socio-economic indices such as amenities index, economic development index, and biophysical indices such as soil index, climatic index and land utilization index which are finally integrated into a desertification vulnerability index.

Remote sensing and GIS techniques that can give various vegetation indices (Higginbottom and Symeonakis, 2014), the indices related to top soil, and land use and land cover maps of past several years (Natasha, 2011). The majority of the investigators have used the field related on various soil parameters, rainfall, agricultural, vegetation types, wildlife status, human census and many such socio-economic data and integrated these using GIS. Ladisa et al. (2012) used new environmental indicators and socio-economic parameters to evaluate the risk of desertification in the region of Apulia (southeast Italy). Many of the desertification related research have been carried out based on a model that basically comes under the framework of the MEDALUS (**Me**diterranean **D**esertification **A**nd **L**and **US**e), an European project, which identifies the desertification prone areas on the basis of the Environmentally Sensitive Areas (ESA) index. To develop an environmentally sensitive area index, the various parameters or sub-indices related to the four major indices namely climate, soil, vegetation and management are suitably integrated and processed using GIS. The parameters of soil texture (T), depth of the surface horizon (Dp), slope (S), drainage (Dr) and organic matter present in soil (OM) were used for desertification assessment. Each parameter was assigned a weighting and used to obtain soil quality index (SQI). Similarly, vegetation quality index (VQI), climate quality index (CQI) and management quality index (MQI) were obtained by assigning weightage to the parameters of fire risk (FR), protection against erosion

(PE), drought resistance (DR), coverage (C), rainfall (R), evapotranspiration (ETP), aridity (Ar), aspect (A), grazing (G), population density (PD) and conservation practices (CP). These indices are used and integrated into a single index named ESA Index or Desertification Sensitivity Index (DSI) thereafter used to develop an environmentally sensitive area map showing which regions are sensitive to land degradation or desertification (Kosmas et al. 2013).

Khosravi et al. (2014) assessed the hazard of desertification in Kashan region and demonstrated that water scarcity is the major problem of the study area. Moreover, groundwater decreases and water crisis and depth of soil were the most and least effective factors, respectively. Nasrollah et al. (2014) used climate based and vegetation-based indices in IMPDA model and integrated them using GIS by assigning weightage to each of the indices. IMDPA was calibrated for different climatic regions viz., arid, semi-arid and desert environments and has been successfully used in Iran (Ahmadi, 2014). 9 criteria and 130 indices were introduced in the form of quantitative and weighted values to determine the desertification intensity under all cases. Land use alteration which generally involves the processes of biologically and technically reshaping, converting and managing land for socio-economic benefits often triggers degradation of the environment and lead to a series of environmental problems such as soil and water erosion, wetland, desertification, land contamination (Xie et al. 2015).

Saleh et al. (2018) used a higher number of sub-indices for soil quality for the area of study in the part of Egypt, where the vegetation cover is less and lesser variability in soil cover. Similar to MEDALUS, other simpler models have been used to identify desertification prone areas. Some researchers have also used statistical methods to identify indicators that can be best suitable for desertification (Sarparast et al. 2018). Sarparast, (2018) developed a desertification hazard index which is calculated through a statistical algorithm that includes climate, soil, geology, agriculture, vegetation, socio-economic, erosion, technology development, and groundwater related indicators and integrates them through a regression analysis. Salunkhe et al. (2018) developed a comprehensive model for the assessment of desertification risk in the Jodhpur district of Rajasthan, India, using 23 desertification indicators. Indicators that are included to

investigate desertification are soil, climate, vegetation and socio-economic parameters and are integrated into a GIS environment to get environmental sensitive areas (ESAs) to desertification. Zolfaghari et al. (2019) proposed cluster analysis in different working units after determining the desertification intensity map to identify the units that require the same management decisions. Four desertification criteria (climate, soil, vegetation and wind erosion with different indices) were examined based on the MEDALUS model in the dry east region of Iran.

Huang et al. (2020) used the global desertification vulnerability index (GDVI) to project its future evolution and the results of the study indicated that the area with moderate, high and very high desertification risk accounted for 13%, 7% and 9% of the global area respectively. The areas where desertification risks are predicted to increase over time are mainly in Africa, North America, and the northern areas of China and India. Osman et al. (2023) carried out geospatial analysis to detect the changes in land use/land cover that may have led to major conversions from ecologically active land covers to sand dunes. The results of the analysis indicated that areas covered by sand dunes, which is a major indicator of desertification, have doubled over the 25 years under consideration (1990 to 2015). An overview of the land degradation, desertification and sustainable land management based on GIS and remote sensing applications have been given by Rahman (2023).

2.5 Soil and Water Assessment Tool (SWAT)

Jha (2004) used the Soil and Water Assessment Tool (SWAT) model to assess the climate change impacts on the hydrological variables using GCM downscaled future climate inputs and concluded 43% increase in groundwater recharge, 51% increase in annual stream flow and 50% increase in total water yield for Upper Mississippi river basin. Uniyal et al. (2015) modeled the impacts of climate change in Baitarni basin using SWAT model. The SWAT model was calibrated using the daily stream flow during 1998-03 and validated during 2004-05. The NSE during calibration was 0.88 and 0.95 for daily and monthly time-steps. The study reported a reduction in runoff to the extent of 4% to 40% for the temperature

increase of 1oC to 5^{o}C, whereas an increase of rainfall by 5% to 10% results in increase in surface runoff by 13.2% to 26.3%.

Priyanka and Patil, (2016) carried out the runoff modeling in Malaprabha basin in Karnataka, India using SWAT model and reported satisfactory results during calibration (1982-85) and validation (1986-89). Himanshu et al. (2017) applied SWAT model for modeling runoff, sediment and water balance for the Ken River basin in Central India and the water balance indicated that evapotranspiration accounted for more than 44% of the average annual precipitation and the average annual sediment yield was very high at 15.41 t/ha/yr. Many other studies on application of SWAT model have also been reported (Ghosh and Dutta, 2012; Diwakar, et al. 2014; Jain and Sharma, 2014; Shivhare et al. 2014; Khare et al. 2014; Swain et al. 2022; Sahu et al. 2016).

Nilawar and Waikar (2019), carried out the climate change impact assessment on stream flow and sediment for Purna river basin in India using SWAT and three RCMs for RCP4.5 and RCP8.5 scenarios. The precipitation and temperature are projected to increase significantly for both RCP scenarios as compared to the baseline period. Accordingly, the stream flow and sediment are also expected to increase significantly from June to September at the outlet of the basin. Pandey et al. (2021) proposed an integrated approach for simulating hydrological responses in the Upper Narmada Basin, India, under dynamic land use / land cover (LULC) and climate change scenarios. The calibrated SWAT model was combined with historical and projected land use scenarios to calculate hydrological sensitivity to land use change (1990, 2000, 2010 and 2030). The findings point to increased precipitation in the late twenty-first century, while annual mean temperature could rise by 1.79°C and 3.57°C by the end of the century under mid and high emission scenarios, respectively. During the 2050s (2041–2070) and 2080s (2071–2100), annual and monsoon flow in the basin is expected to grow.

Mengistu (2021) carried out the assessment of climate change impacts on water resources in the Upper Blue Nile (Abay) River Basin using a regional climate model (RCM), COSMO Climate Limited-area Model (CCLM), coupled with a hydrological model, Soil and Water Assessment Tool (SWAT). An increase in

mean annual temperature and a decrease in precipitation has been projected. A 27% rise in potential evapotranspiration (PET) by the end of the twenty-first century is projected under RCP8.5 scenario whereas the surface is expected to increase by 14%. Oliveira et al. (2021) studied the changes in land use and land cover (LULC) on local hydrology and sediment production for a basin in the Brazilian Amazon. The study looked at the effects of 40 years of LULC changes in an Amazonian basin on hydro-sedimentological variables, which can change the hydrological cycle. The SWAT model was found to be a good estimator of hydro-sedimentological processes in Amazonian basins and can be used by decision-makers in water and environmental resource management.

Satriagasa et al. 2023 studied the impact of climate change on future floods in Upper Nan watershed in Thailand using SWAT and HEC-RAS models using three GCMs under RCP4.5 and RCP8.5 scenarios. They reported that climate change will lead to increase in rainfall by 18% to 19% which will lead to wetter conditions in both wet and dry seasons. Nagireddy et al. (2023) evaluated the effects of climate change on water quantity and quality at a regional scale in Vamsadhara and Nagavalli watersheds using SWAT and bias-corrected statistically downscaled CMIP6 data under three SSP scenarios and concluded that higher rainfall in the future will lead to higher stream flow and sediment yield in both watersheds.

3.0 STUDY AREA AND DATA USED

3.1 Hydrology, Land use and Soils

The River Chambal is one of the most important tributaries of the Yamuna and was also known as Charmanvati in ancient times. It originates in the southern slopes of the Vindhyan ranges at Janapav village near Mhow in Indore district of Madhya Pradesh at an elevation of 854 m. The river flows north-northeast direction through Madhya Pradesh, running for a brief distance through Rajasthan, then forming the boundary between Rajasthan and Madhya Pradesh, before turning south-east to join the River Yamuna in Uttar Pradesh state. The River Chambal and its tributaries drain the Malwa region of north-western Madhya Pradesh, while its tributary, the Banas, which rises in the Aravalli range, drains southeastern Rajasthan. The catchment of River Chambal is rain-fed with a total

drainage area of 143219 sq. km. up to its confluence with the River Yamuna. The Chambal River basin lies between 22°27'N and 27°20'N latitudes and 73°20' E and 79°15' E longitudes. The basin is bounded by the Vindhyan mountain ranges on its south, east and west and by the Aravallis on its north-west. The present study caters to the river basin falling in Madhya Pradesh only and the index map of the study area is given in Figure 3.1.

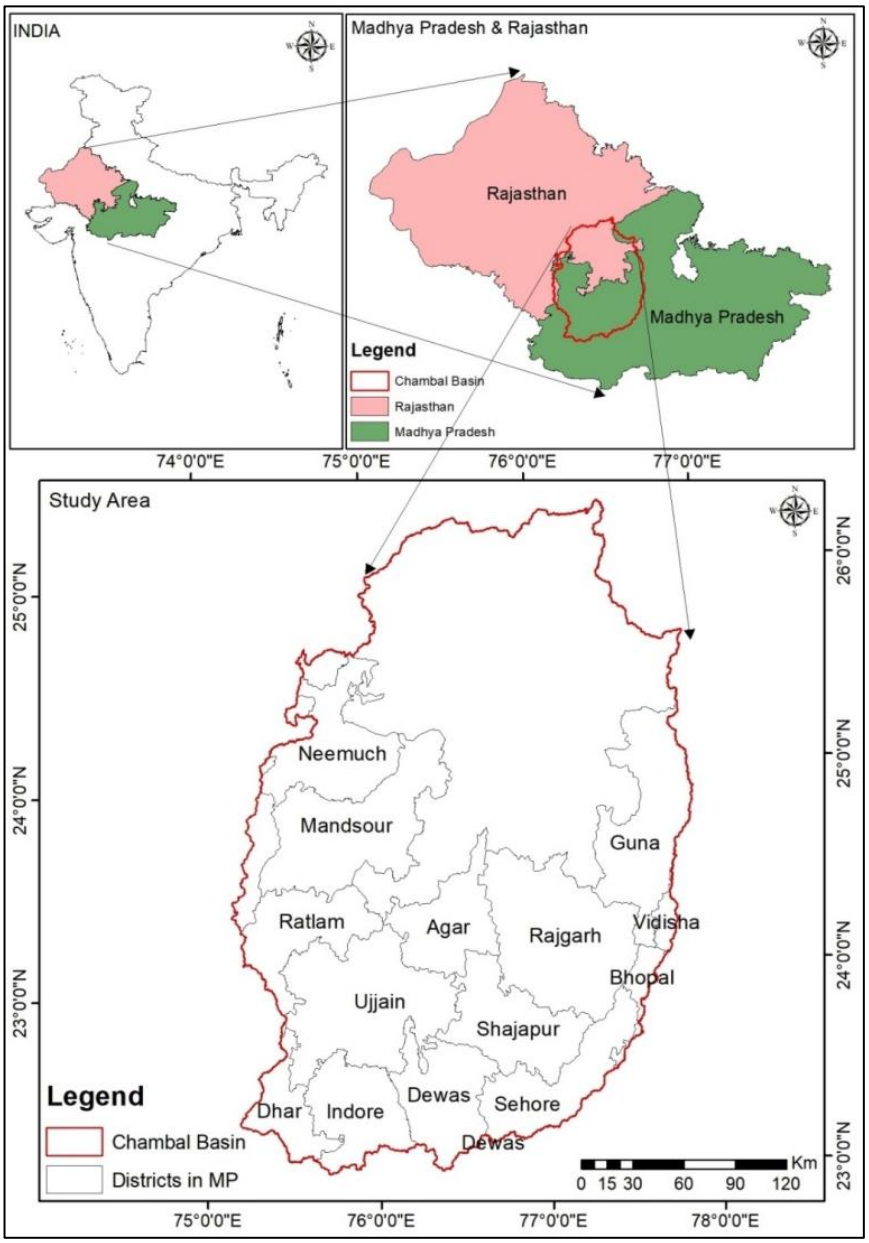

Figure 3.1: Index map of the study area

The catchment becomes narrower and elongated after the confluence of River Parvati and River Banas with it. Out of the total catchment area, about 76854 sq. km. lies in Madhya Pradesh, 65264 sq. km lies in Rajasthan and 1101 sq. km in

Uttar Pradesh. Among its many tributaries, River Chamla, River Siwana and River Retam join from the left whereas River Shipra and River Chhoti Kali Sindh join from the right. The drainage map of the Chambal basin up to Sawai Madhopur in Rajasthan is given in Figure 3.2. The River Kali Sindh which is one of its major tributary joins from the right near Laban village whereas River Kural joins from the left. River Banas is the major left bank tributary originating and flowing through Rajasthan and joins of River Chambal near Rameshwar village. The River Parbati is another major right bank tributary which joins River Chambal near Pali. Some of the other tributaries include Ansar, Seep, Kuwari, Kuno, Alnia, Mej, Chakan, Gambhir, Khan, Lakhunder, Bangeri, Kedal and Teelar.

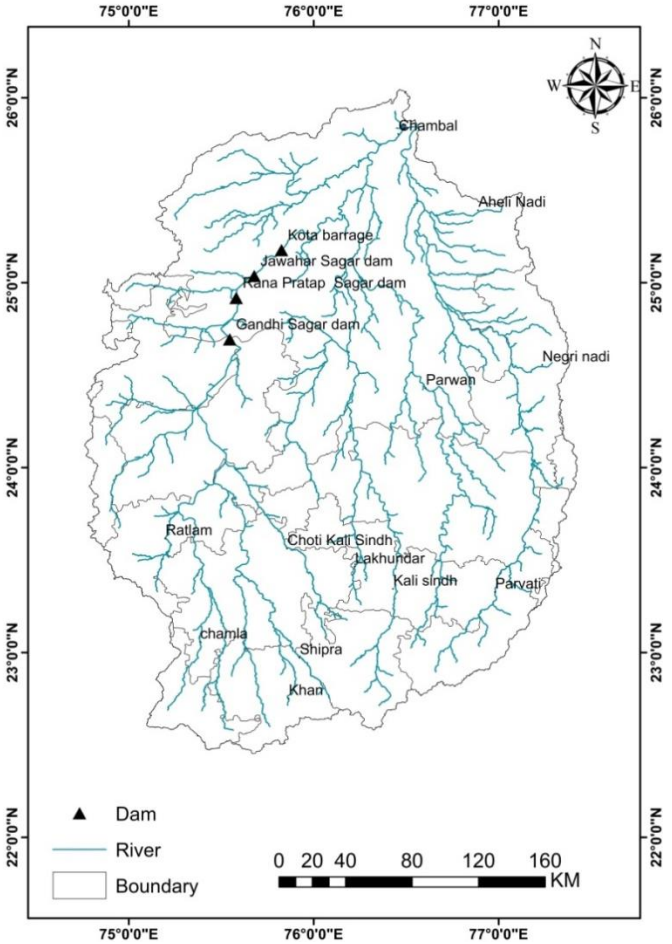

Figure 3.2: Drainage map of Chambal basin up to Sawai Madhopur

Four large dams, namely Gandhi Sagar in Madhya Pradesh, Rana Pratap Sagar, Jawahar Sagar and Kota Barrage in Rajasthan have been constructed on River Chambal and are being used for hydropower generation and irrigation in Madhya

Pradesh and Rajasthan. The river has a course of 965 km up to its confluence with the River Yamuna in the Etawah district of Uttar Pradesh. Two projects viz., Mohanpura dam and Kundaliya dam have been constructed recently on River Kali Sindh. Both are irrigation projects and envisage irrigation through pressurized irrigation systems only and are located in Rajgarh district in Madhya Pradesh.

The Chambal River valley is part of the Vindhyan system which comprises of massive sandstone, slate and limestone of pre-Cambrian age. The hillocks and plateaus are the major landforms of the Chambal valley. The Chambal basin is characterized by undulating flood plains, gullies and ravines. Badland topography is a characteristic feature of the Chambal valley, whereas kankar has extensively developed in the older alluvium. In a stretch of 96 km, River Chambal flows through a deep gorge, while there are wide plains in the downstream side. The predominant slope in the hilly region ranges between 15 to 40%. Erosion is one of the major issues in the catchment area which is quite intensive due to the undulating topography and degradation of forest and land. The Digital Elevation Model (DEM) of the river basin upto Sawai Madhopur is given in Figure 3.3.

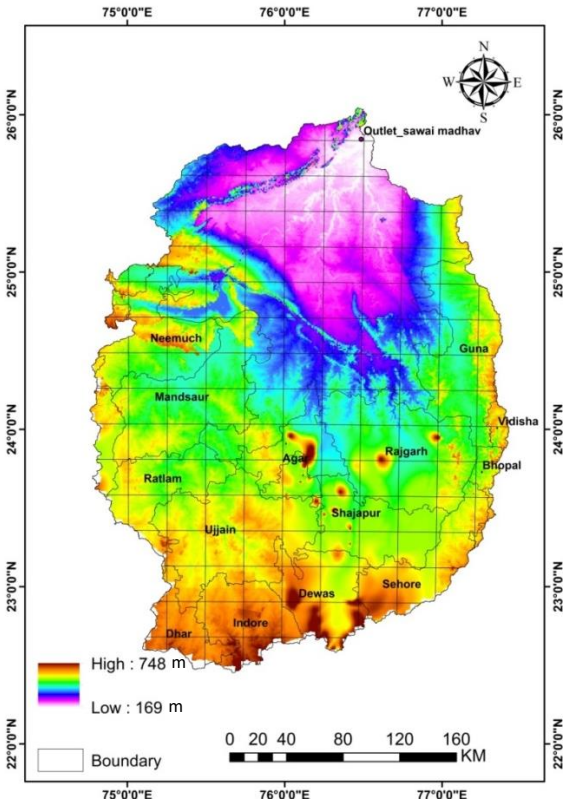

Figure 3.3: DEM of Chambal basin up to Sawai Madhopur

The Chambal basin lies within the semi-arid zone of north-western India. The vegetation consists of ravines and thorny forests, a sub-type of the Northern Tropical Forests (NTF) that typically occurs in lesser arid areas with rainfall of 600 to 700 mm. Also, saline/alkaline Babul Savannah, a type of Northern Tropical Dry Deciduous Forest (NTDDF) is also found in limited areas. The evergreen riparian vegetation is completely absent, with only sparse ground cover along the severely eroded river banks and adjacent ravine lands. The land use / land cover map of Chambal basin up to Sawai Madhopur in Rajasthan is given in Figure 3.4. Water, urban, agriculture, range grasses and arid zones are the dominant land use classes in the study area. However, majority of the area comprises of agricultural lands followed by range grasses and degraded forests in some patches. Indore and

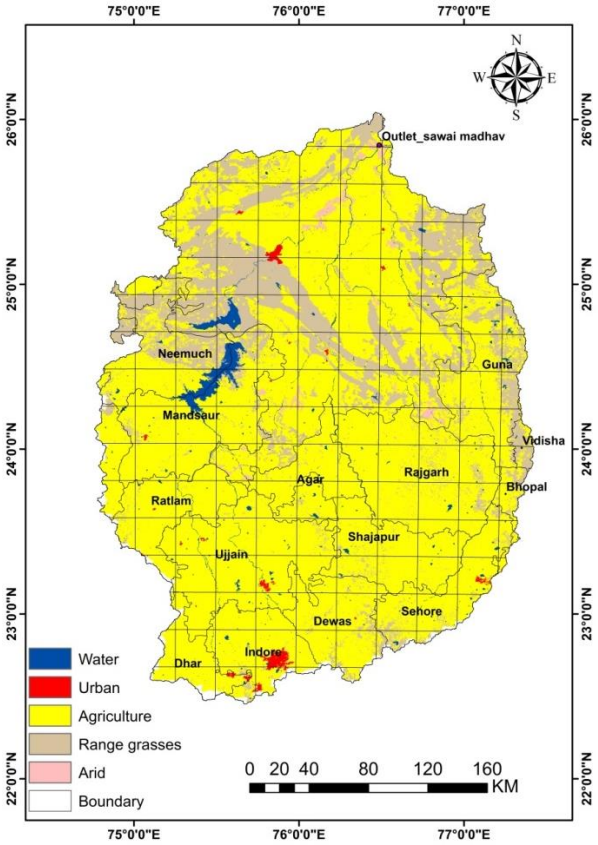

Figure 3.4: LULC of Chambal basin up to Sawai Madhopur

Kota is the two biggest urban centers in the Chambal basin in Madhya Pradesh and Rajasthan respectively. Majority of the area is dominated by clay loam followed by coarse sand clay found in the north-western parts and eastern parts of the basin. Loamy soils are also found in patches. The soil map of the basin is given in Figure 3.5.

The study area has been limited to the southern part of Chambal basin lying only in Western Madhya Pradesh covering an area of 48193 sq. km. The study area covers fully or partially 14 districts of Madhya Pradesh and comprises of 57 developmental blocks located in these districts. The districts bordering Rajasthan include Neemuch, Mandsaur, Ratlam, Agar, Rajgarh and Guna, whereas the other districts in the study area include Ujjain, Dhar, Indore, Dewas, Sehore, Shajapur and one block each of Bhopal and Vidisha districts. There is good road connectivity between the various cities and villages. The map showing the settlements is given in Figure 3.6. The list of the districts and blocks falling in the study area is given in Table 3.1.

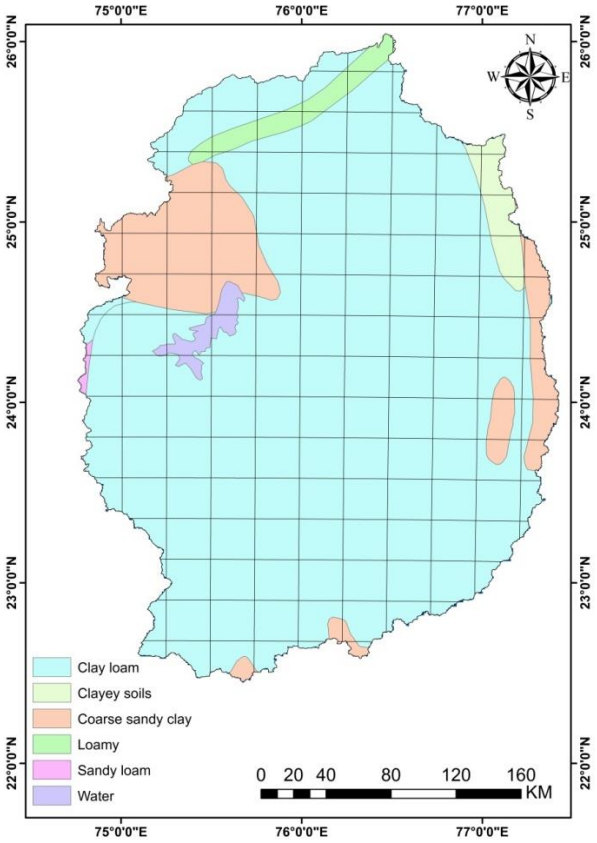

Figure 3.5: Soil map of Chambal basin up to Sawai Madhopur

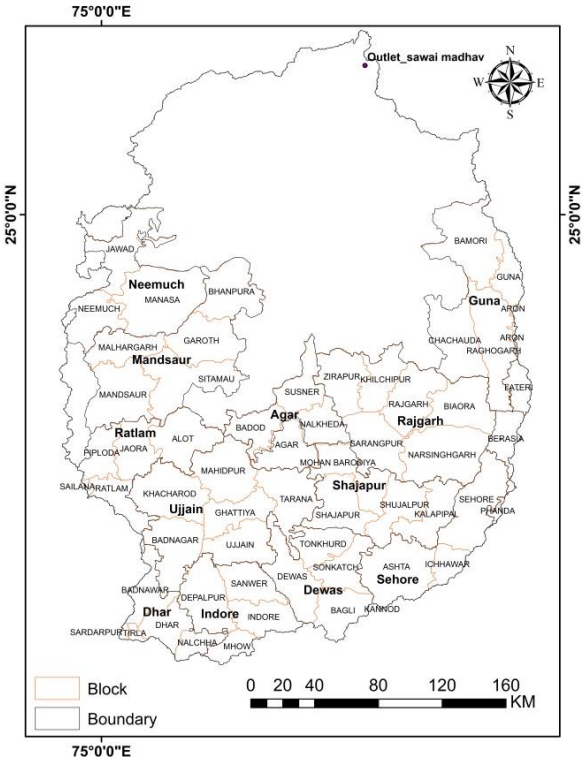

Figure 3.6: Map showing the settlements in the study area

Table 3.1: Districts and blocks in the study area

S. No.	District	Block		S. No.	District	Block
1	Agar	Barod		30	Neemuch	Neemuch
2		Agar		31		Manasa
3		Susner		32		Javad
4		Nalkheda		33	Rajgarh	Narsingarh
5	Bhopal	Berasia		34		Khilchipur
6	Dewas	Dewas		35		Biaora
7		Tonkkhurd		36		Rajgarh
8		Sonkatch		37		Sarangpur
9		Bagli		38		Zirapur
10		Kannod		39	Ratlam	Piploda
11	Dhar	Nalcha		40		Sailana
12		Badnawar		41		Jaora
13		Dhar		42		Alot
14		Sardarpur		43		Ratlam
15		Tirla		44	Sehore	Ashta
16	Guna	Bamhori		45		Ichhawar
17		Raghogarh		46		Sehore
18		Aron		47	Shajapur	Shajapur
19		Guna		48		Shujalpur
20		Chachouri		49		Kalapipal
21	Indore	Mhow		50		Mohan Barodiya

22		Depalpur		51		Badnagar
23		Indore		52		Ujjain
24		Sanwar		53	Ujjain	Tarana
25		Mandsaur		54		Khachrod
26		Sitamau		55		Mahidpur
27	Mandsaur	Malhargarh		56		Ghatia
28		Garoth		57	Vidisha	Lateri
29		Bhanpura				

3.2 Data used

The daily rainfall data at the various blocks in the 14 districts of Madhya Pradesh was collected from the State Water Data Centre, Govt. of Madhya Pradesh. The data pertaining to the daily discharge (classified) has been collected for few sites from Central Water Commission, Yamuna basin, New Delhi the details of which are given in Table 3.2. However, the high-resolution gridded rainfall data at 0.25˚ x 0.25˚ as well as the gridded maximum and minimum temperature at 1.0˚ x 1.0˚ was obtained from the India Meteorological Department (IMD), Govt. of India.

Table 3.2: Details of gauging sites on various tributaries of Chambal River system

Gauging site	District	Catchment (sq km)	River /Tributary	Latitude	Longitude
A. B. Road Crossing	Guna	5669	Parwati	24°21'57"	77°05'56"
Tal	Ratlam	4270	Chambal	23°43'24"	75°20'49"
Ujjain	Ujjain	2070	Shipra	23°10'06"	75°46'16"
Sarangpur	Rajgarh	2600	Kalisindh	23°33'00"	76°28'02"
Mahidpur	Ujjain	4430	Shipra	23°28'50"	75°38'11"
Salavad	Jhalawar	7450	Kalisindh	24°22'03"	76°12'21"
Aklera	Jhalawar	6050	Kalisindh/Parwan	24°25'47"	76°36'14"

The data pertaining to the crops and related information have been collected from Agriculture Department, Govt. of Madhya Pradesh whereas the District Statistical Handbooks have been collected from the State Planning Office, Govt. of Madhya Pradesh.

The land use information for the study area was extracted using remote sensing and GIS techniques from LANDSAT digital datasets. The land use information at 100 x 100 m resolution was also obtained from Decadal Land use and Land cover Map, Oak Ridge National Laboratory (ORNL), Distributed Active Archive Center

(DAAC). The groundwater levels being monitored in the observation wells and piezometers have been obtained from Central Groundwater Board, Bhopal and Groundwater Survey, Water Resources Department, Govt. of Madhya Pradesh. The information related to the major projects has been obtained from the Project Authorities at the various dam sites located in Madhya Pradesh.

To assess the future climate, hydrology, drought and desertification scenario over the study area, the bias-corrected daily precipitation, maximum and minimum temperature from 13 CMIP6 GCMs under two future emission scenarios SSP245 and SSP585 at 0.25˚ x 0.25˚ resolution was downloaded from CMIP sites (https://esgf-node.llnl.gov/projects/cmip6/). The projections used consisted of two time periods viz., historical period (1951–2014) and future period (2015–2100). The Empirical Quantile Mapping (EQM) approach was used for bias correction of the CMIP6 GCM outputs at a daily time scale against the historical reference period (1988–2014) period for Asian region (Mishra et al., 2020). The selection of scenario mainly encompasses the moderate scenario case (SSP245) and worst scenario case (SSP585). Table 3.3 gives the details of the 13 CMIP6 GCMs used in the study with all necessary details.

Table 3.3: CMIP6 GCMs utilized in the study

General Circulation Model (GCMs)	Abbreviation	Reference
ACCESS-CM2	Australian Com. Clim. and Earth Syss Simulator Clim. Mod. Version 2	Bi et al., (2013)
ACCESS -ESM1-5	Australian Com. Clim. and Earth Sys. Simulator Earth Sys. Model Ver 1.5	Ziehn et al., (2017), Bi et al. (2013)
EC-Earth3	European community Earth-System Model 3	N/A
EC-Earth-Veg	European community Earth-System Model 3 (Vegetation)	N/A
BCC_CSM2-MR	Beijing Climate Center climate system model version 2	Wu et al., (2019)
CanESM-5	The Canadian Earth System Model version 5	Swart et al., (2019)
INM-CM4-8	Institute for Numerical Mathematics	Song et al., (2020)
INM-CM5-0	Institute for Numerical Mathematics	Song et al., (2020)
MPI-ESM1-2-HR	Max Planck Institute for Meteorology Earth System Model version 1.2	Müller et al., (2018)

	(higher resolution version)	
MPI-ESM1-2-LR	Max Planck Institute for Meteorology Earth System Model version 1.2 (lower resolution version)	Mauritsen et al., (2019), Gutjahr et al. (2019)
MRI-ESM2-0	Meteorological Research Institute Earth System Model Version 2.0	Yukimoto et al., (2019)
NorESM2-LM	Norwegian Earth System Model version 2 Low Resolution	Seland et al., (2020)
NorESM2-MM	Norwegian Earth System Model version 2 Medium Resolution	Seland et al., (2020)

4.0 METHODOLOGY

4.1 Investigation of the Climate Change Signals

4.1.1 Correlation analysis

To assess the similarity of the high-resolution gridded rainfall data with the station rainfall data, the correlation analysis was carried out based on the monthly time series. The grid corresponding to each rain gauge station falling in the 53 blocks were identified for carrying out the correlation analysis. Multiple stations were not located in any of the grids. The correlation coefficient has been used to find the strength of the relationship between the station and gridded rainfall data. A correlation coefficient of +1 indicates a very strong positive relationship whereas -1 indicates a strong negative relationship and 0 indicates no relationship. The correlation coefficient is calculated using Equation 3.1 as given below:

$$r = \frac{n(\sum xy) - (\sum x)(\sum y)}{\sqrt{[n\sum x^2 - (\sum x)^2][n\sum y^2 - (\sum y)^2]}} \quad \ldots\ldots\ldots\ldots\ldots\ldots\ldots\ldots\ldots\ldots (4.1)$$

where, n is number of pairs of rainfall data being compared, *x* is the station rainfall and y is the gridded rainfall.

4.1.2 Climate change indices

The Expert Team on Climate Change Detection Indices (ETCCDI) formed by World Meteorological Organization (WMO) finalized 27 core indices for climate change detection based on daily precipitation and temperature. These indices provide data on change in the frequency or severity of extreme climate events. As per the suitability of the parameters to the study area, few important indices were

considered and the changes observed in daily, monthly, seasonal and annual patterns of the selected indices have been studied. The selected indices are although similar to the indices suggested by ETCCDI, but the thresholds may vary slightly according to the climatic conditions prevailing in the study area. The various indices evaluated for the study area are given below,

1. Very hot days: Annual count of days when daily maximum temperature is greater than 40^{o}C.
2. Hot days: Annual count of days when daily maximum temperature is greater than 35^{o}C.
3. Cold days: Annual count of days when daily maximum temperature is less than 15^{o}C.
4. Very cold days: Annual count of days when daily maximum temperature is less than 10^{o}C.
5. Highest maximum temperature: Highest value of 1-day maximum temperature observed in a year.
6. Very hot nights: Annual count of days when daily minimum temperature is greater than 25^{o}C.
7. Hot nights: Annual count of days when daily minimum temperature is greater than 20^{o}C.
8. Cold nights: Annual count of days when daily minimum temperature is less than 10^{o}C.
9. Very cold nights: Annual count of days when daily minimum temperature is less than 5^{o}C.
10. Highest minimum temperature: Highest 1-day minimum temperature observed in a year.
11. Lowest maximum temperature: Lowest value of minimum temperature observed in a year.
12. Rainy days: Annual count of days when daily precipitation is greater than 2.5 mm.
13. Heavy precipitation: Annual count of days when daily precipitation is greater than 50 mm.
14. Very heavy precipitation: Annual count of days when daily precipitation is greater than 100 mm.

15. Extreme precipitation: Annual count of days when daily precipitation is greater than 200 mm.
16. One-day maximum precipitation observed in a year.
17. Five-day maximum precipitation (AMC) observed in a year.
18. Annual total wet day precipitation: Annual precipitation observed on rainy days.
19. Daily rainfall intensity

The above indicators have been computed and changes that have taken place during the present time horizon (1991-2015) vis-à-vis baseline period (1961-1990) have been evaluated.

4.1.3 Mann-Kendal Test for identification of trend

The non-parametric Mann-Kendall test has been applied study to determine monotonic trends in different climatic variables and climate indices. Before applying the Mann-Kendall test, the data series have been tested for presence of serial correlation, if any. If the lag-1 auto-correlation (r_1) was found to be non-significant at 95% confidence level, then the Mann-Kendall test was applied to the original data series (x_1, x_2, …, x_n), otherwise the Mann-Kendall test was applied to 'pre-whitened' series obtained as ($x_2 - r_1x_1$, $x_3 - r_1x_2$, …, $x_n - r_1x_{n-1}$) (Von Storch and Navarra, 1995; Partal and Kahya, 2006). The Mann-Kendall statistic (S) is defined as (Salas, 1993):

$$S = \sum_{i=1}^{N-1} \sum_{j=i+1}^{N} \mathrm{sgn}\left(x_j - x_i\right) \qquad \ldots\ldots\ldots\ldots\ldots\ldots\ldots\ldots (4.2)$$

where,

$$\mathrm{sgn}\left(x_j - x_i\right) = \begin{bmatrix} 1 if \left(x_j - x_i\right) > 1 \\ 0 if \left(x_j - x_i\right) = 1 \\ -1 if \left(x_j - x_i\right) < 1 \end{bmatrix}$$

and N is the number of data points. This statistic represents the number of positive differences minus the number of negative differences for all the differences considered. For large samples (N > 10), the test is conducted using a normal distribution (Helsel & Hirsch, 1992) with the mean and the variance as follows,

$$E(S) = 0$$

…… (4.3)

$$\mathrm{var}(S) = \frac{N(N-1)(2N+5) - \sum_{k=1}^{n} t_k (t_k - 1)(2t_k + 5)}{18}$$

…… (4.4)

where n is the number of tied (zero difference between compared values) groups, and t_k is the number of data points in the k_{th} tied group. The standard normal deviate (Z statistic) is then computed as (Hirsch *et al*., 1984),

$$Z = \begin{cases} \dfrac{S-1}{\sqrt{\mathrm{var}(S)}}; S > 0 \\ 0; S = 0 \\ \dfrac{S+1}{\sqrt{\mathrm{var}(S)}}; S < 0 \end{cases}$$

…… (4.5)

If $Z > +1.96$ or $Z < -1.96$, the null hypothesis (Ho) is rejected at 95% significance level.

4.2 Desertification analysis

Various indices are available to assess the extent of land degradation and desertification. Generally, the remote sensing and GIS based analysis of the historical and present land use land cover gives an idea of the extent of the degradation in any area. However, to project the desertification scenario in future, only those indicators have been considered which can be projected into the future as well. The aridity index (AI) is one of the indicators used related to desertification, and have been to identify the changes as compared to the baseline period. This helps to identify whether the aridity has increased in certain areas/pockets in the study area as compared to the historical time horizon. The indicators of desertification include average annual air temperature and average annual PET. Air temperature in any particular region is one of the most critical environmental factors that influences desertification due to enhance water stresses, higher transpiration rate from the growing vegetation, more soil water evaporation, and also causing soil salinity and soil alkalinity (Agricultural

University of Athens 2010). Higher air temperature promotes desertification. Also, high rates of evapotranspiration with a lower amount of rainfall in arid and semi-arid climatic condition will significantly influence the water resources availability in the region. Inadequate soil moisture availability resulted to lower biomass production and thereby causing loss of the top soil which significantly promotes desertification in the region. Also, higher evapotranspiration and sodicity degrades soil properties by weakening the bond between soil particles and thereby encouraging desertification.

4.2.1 Aridity Index (AI)

The Aridity index (AI) is the ratio of annual precipitation (P) to annual potential evapotranspiration (PET) and is computed as given below,

$$AI = \frac{P}{PET} \qquad \text{…… (4.6)}$$

Potential evapotranspiration has been evaluated using Thornthwaite equation, which using the set of formulae given below,

Monthly heat index (i)

$$i = \left(\frac{t}{5}\right)^{1.514} \qquad \text{…… (4.7)}$$

Annual heat index (I)

$$I = \sum(i) \qquad \text{…… (4.8)}$$

$$PET_{(non\text{-}corrected)} = 16 \left(\frac{10\,t}{I}\right)^{\propto} \qquad \text{…… (4.9)}$$

The PET is computed for each month, considering a month which is 30 days long and 12 sunshine hours per day. $\propto$ is a regional thermic index calculated from the annual heat index as follows,

$$\propto = 675x10^{-9} \text{ x } I^3 - 771x10^{-7} \text{ x } I^2 + 0.49239 \qquad \text{……. (4.10)}$$

$$PET_{(corrected)} = PET_{(non\text{-}corrected)} \text{ x } \left(\frac{N\ d}{12 \text{ x } 30}\right) \qquad \text{…… (4.11)}$$

4.2.2 Analysis of agricultural data

The agricultural and other statistical data were analyzed for the years 2000, 2006, 2011 and 2015 district-wise compared to detect the changes during these time periods. Even though many variables have been analyzed, but distinct changes have been observed in the classes viz., 'agricultural area' and 'land not available for agriculture'. The changes in the 'cropping pattern' and the changes in the species of the livestock' also showed substantial changes which may be a pointer that indicates land degradation and species changes.

4.2.3 Land use and land cover classification

In order to detect changes in land use and land cover (LULC) over the Chambal River basin located in Madhya Pradesh region, the LULC classification have been carried out and broadly five classes have been identified viz., agriculture, settlements, forest, barren land and water bodies. The objective is to detect the changes in these LULC classes in the past few decades. The LANDSAT 5 (Thematic Mapper (TM) and LANDSAT 5 Multispectral Scanner (MSS) satellite data have been selected for LULC mapping, as it provides data from 1990 to 2011 (over Indian region). Its MSS has total 7 bands ranging from visible blue band (0.45 - 0.52 µm) to mid infrared (0.45 - 0.52 µm) at 30 m spatial resolution. The Google Earth Engine (GEE) has been used to perform the supervised classification of the multiple tiles of LANDSAT 5 covering the complete study area. GEE is a platform that provides cloud-based processing of remote sensing data and its archives also has LANDSAT 5 (atmospheric corrected) data and with machine learning based supervised classification technique.

Initially, the LANDSAT 5 satellite image is imported using GEE and the region of interest is specified along with the region for which the LULC classification is desired. Thereafter the several points on this image are sampled and divide these into training sets and testing sets. Thereafter, the clusterer algorithm is initiated and trained on the training set and then applied to the image. The resulting clusters are then visualised after which these clusters are used to train the classifier. Once the classifier is trained, the trained classifier is then applied to the image for its classification. The resulting classified map which is classified into various land use / land cover classes is then visualised and the script executed.

GEE clusters the images into various predominant land cover classes based on their spectral signatures.

The decadal supervised classification has been carried out for 2000, 2001 and 2010. The ground truth verification was carried out at several points including agricultural fields and few points in the forested areas. Since the study area is predominantly under agriculture, most of the ground truth verification points were located in agricultural areas. The ground truth verification was also carried out at soil sampling sites. The ground truth verification indicated that the satellite-based land use / land cover classification matched well with the actual field conditions. The statistical analysis has been performed for the complete study area including the districts bordering Rajasthan viz., Guna, Neemuch, Mandsaur, Rajgarh and Agar.

4.3 Drought Analysis

4.3.1 Identification of drought years

The departure analysis of annual rainfall has been carried out to identify the drought years and drought severity based on the rainfall deficit from normal rainfall. Generally, a year is considered to be a drought year, if the total amount of annual rainfall is deficient by more than 25% of its normal. In this study, the drought severity has been further classified on the basis of percentage deviations from the normal rainfall into three severity classes. A moderate drought occurs when the annual rainfall departure varies between -25% to -35%, whereas a severe drought occurs when the annual rainfall departure varies between -35% to -50%, and annual departure less than -50% is considered as extreme drought. The percentage departure (D%) of annual rainfall is calculated as,

$$D_i = \frac{(X_i - X_m)}{X_m} \times 100 \qquad \text{..... (4.12)}$$

where, X_m – mean annual rainfall and Xi is the annual rainfall time series (X_i).

4.3.2 Relative Departure Index

In order to assess the relative drought proneness of the various blocks in a district, a ranking scheme was designed wherein different weights were assigned based on

the drought severity. A mild drought was assigned a weight of 1, moderate drought assigned a weight of 2 and severe drought assigned a weight of 3. The total weights were arrived at by summing up individual weights for all the drought years in a block and a relative departure index for each block was computed by dividing the total weight of the block by the total number of years considered for the analysis in that particular block. The relative departure index gives an idea of the ranking of the occurrences of droughts of varying severities solely based on the departure analysis. Based on the ranking provided by this index, priorities can be assigned for initiation of drought mitigation strategies in the various blocks of each district.

$$RDI = \frac{\sum_{i=1}^{n} W_i}{N} \qquad \ldots\ldots\ldots\ldots\ldots\ldots\ldots\ldots (4.13)$$

where, W_i is the weight for the i^{th} drought year and N = total number of years under consideration.

4.3.3 Identification of Drought Prone Blocks

The probability analysis of annual rainfall is important to predict the relative frequency of occurrence in different group intervals of annual rainfall. The estimated probability of an event is taken as the relative frequency of occurrence of the event when the number of observations is very large. The average annual rainfall at the stations has been computed based on long-term rainfall records. The probability of occurrence of 75% of mean annual rainfall has been computed to delineate the drought proneness in various districts of study area. An area can be considered as drought prone if the probability of occurrence of 75% of normal rainfall is less than 80% (CWC, 1982).

$$P = \frac{m}{(N+1)} \times 100 \qquad \ldots\ldots\ldots\ldots\ldots\ldots\ldots\ldots (4.14)$$

where, P is the probability of exceedance of annual rainfall, m is the rank of a particular record and N is the total number of years under consideration

4.3.4 Evaluation of Meteorological Drought Characteristics

The meteorological drought characteristics have been evaluated based on SPI. SPI is based on an equiprobability transformation of aggregated monthly precipitation into a standard normal variable. In practice, computation of the index requires fitting a probability distribution to aggregated monthly precipitation series (k = 1, 3, 6, 12, 24 months); computing the non-exceedance probability related to such aggregated values; and defining the corresponding standard normal quantile as the SPI. McKee et al. (1993) assumed the aggregated precipitation to be gamma distributed and used a maximum likelihood method to estimate the parameters of the distribution. Although, McKee et al. (1993) originally proposed a classification restricted only to drought periods, it has become customary to use the index to classify the wet periods as well. This permits it use to compare both dry and wet periods at different locations. Moreover, since it is based on precipitation alone, a drought assessment is possible even if other meteoro-hydrological data are not available, which is generally the case in developing countries. The negative values of the standardized normal variable are compared with the boundaries of different classes of drought proposed by McKee et al. (1993) which helps to identify the severity level of the drought event. Among users, there is a general consensus about the fact that the SPI on shorter time scales (3 or 6 months) describes drought events affecting agricultural practices, while on the longer ones (12 or 24 months) it is more suitable for water resources management purposes. The computation of the SPI is accomplished as per the following equations,

$$\bar{X}_{ln} = \frac{\sum \ln X}{N} \qquad \text{..... (4.15)}$$

$$\beta = \frac{1}{4U}\left[1 + \sqrt{\frac{4U}{3}}\right] \qquad \text{..... (4.16)}$$

$$\alpha = \frac{\bar{X}}{\beta} \qquad \text{..... (4.17)}$$

where, U is the constant given by,

$$\text{U} = \ln(\overline{X}) - \bar{X}_{ln} \qquad \text{..... (4.18)}$$

The resulting parameters are then used to find the cumulative probability of an observed precipitation event for the given month and time scale for the station. The cumulative probability as given by Gamma distribution is given by,

$$G(x) = \frac{1}{\alpha^{\beta}\,\Gamma\beta}\int_0^x x^{\beta-1}e^{\frac{-x}{\alpha}}\,dx \qquad \text{……..……} \quad (4.19)$$

Letting t = $\frac{-x}{\alpha}$, this equation becomes the incomplete gamma function,

$$G(x) = \frac{1}{\Gamma\beta}\int_0^{t\alpha} t^{\beta-1}e^{-t}\,dt \qquad \text{……..….} \quad (4.20)$$

Since the gamma function is undefined for x = 0 and a precipitation distribution may contain zeros, the cumulative probability becomes,

$$H(x) = q + (1-q)G(x) \qquad \text{…….} \quad (4.21)$$

where, 'q' is the probability of a zero.

However, the three-parameter gamma distribution is considered to produce more robust values of SPI. If 'm' is the number of zeros in a precipitation time series, states that 'q' can be estimated by 'm/N' and used tables of incomplete gamma function to determine cumulative probability H(x). The cumulative probability is then transformed to the standard normal random variable Z with mean zero and variance one, which is the value of the SPI. The Z or SPI values are more easily obtained computationally using an approximation provided by Abramowitz & Stegun (1972) that converts cumulative probability to the standard normal random variable Z.

$$Z = SPI = -\left[t - \frac{c_0+c_1t+c_2t^2}{1+d_1t+d_2t^2+d_3t^3}\right] \quad \text{for } 0< H(x) \leq 0.5 \qquad \text{...….} \quad (4.22)$$

$$Z = SPI = +\left[t - \frac{c_0+c_1t+c_2t^2}{1+d_1t+d_2t^2+d_3t^3}\right] \quad \text{for } 0.5 < H(x) \leq 1.0 \qquad \text{……} \quad (4.23)$$

where, $t = \sqrt{ln\left\{\frac{1}{(H(x))^2}\right\}}$ for $0< H(x) \leq 0.5$ and

…… (4.243)

$$t = \sqrt{ln\left\{\frac{1}{(1.0-H(x))^2}\right\}} \quad \text{for } 0.5 < H(x) \leq 1.0$$

…….. (4.25)

$$c_0 = 2.515517\,, c_1 = 0.802853\ and\ c_2 = 0.010328$$

$$d_1 = 1.432788, d_2 = 0.189269\ and\ d_3 = 0.001308$$

A drought event continues during the period when SPI is continuously negative and reaches an intensity of -1.0 or less. The event ends when the SPI become positive. As the SPI is normally distributed it can also be helpful to find out the dry event as well as wet event. The frequency, duration and intensity (magnitude) of drought are the characteristics that can be calculated with SPI. The positive sum of the SPI for all the months within a drought event is termed as drought magnitude. The division of magnitude by its duration is the intensity of drought for that particular duration. In order to evaluate of drought severity in different areas using SPI, one of the most commonly used classification presented by (Hayes et al., 1999), at the National Drought Mitigation Center (NDMC) is given in Table 4.1.

Table 4.1: Standard ranges of SPI values and their classification

S. No.	SPI range	Classification	Occurrence probability (%)
1.	2.0 ≥	Extremely wet	2.3
2.	1.5 to 1.99	Very wet	4.4
3.	1.0 to 1.49	Moderately wet	9.2
4.	0.0 to 0.99	Mild wet	34.1
5.	0.0 to -0.99	Mild drought	34.1
6.	-1.0 to -1.49	Moderate drought	9.2
7.	-1.5 to-1.99	Severe drought	4.4
8.	-2.0 ≤	Extreme drought	2.3

In summary, the SPI allocates a single numeric value to the precipitation (-3 to 3), which can be compared across regions with different climates. Thus, an SPI of 2 or more happens about 2.3% of the time and a mild drought (SPI between 0 and -0.99) happens 34.1% of the time. The SPI was designed to state that it is possible to simultaneously experience wet conditions on one or more-time scales, and dry conditions at other time scales. Table 4.2 gives the SPI and its corresponding cumulative probability.

Table 4.2: SPI and corresponding cumulative probability

S. No.	SPI	Cumulative probability	S. No.	SPI	Cumulative probability
1.	-3.0	0.0014	7.	0.0	0.5000
2.	-2.5	0.0062	8.	+0.5	0.6915
3.	-2.0	0.0228	9.	+1.0	0.8413
4.	-1.5	0.0668	10.	+1.5	0.9332
5.	-1.0	0.1587	11.	+2.0	0.9772
6.	-0.5	0.3085	12.	+2.5	0.9938

The SPI for a month/year in the period of record is dependent upon the timescale. SPI can be evaluated for various time scales of 1, 3, 6 and 12 months. A 3-month SPI is used for a short-term or seasonal drought index and 12-month SPI is used for an intermediate-term drought index. 24-month and 48-month SPI is used as long-term drought index. The SPI has been favorably evaluated and compared with others indices (Keyantash and Dracup, 2004) and is now integrated in the set of indices used by the Drought Monitor in the USA (Svoboda et al., 2002). The SPI can be used on all stations having more than 30-year rainfall data (Hayes et al., 1999).

4.3.5 SDI-based hydrological drought evaluation

Surface water resources can be effectively expressed by stream flow and hydrological drought events can be related to stream flow deficit from its normal conditions. Severity, onset, duration, areal extent and frequency can be used to characterize the hydrological drought events. The stream flow provides an integrated measure of the spatially distributed runoff from the catchment at the basin outlet, and therefore the actual areal extent of a hydrological drought event cannot be known exactly. However, understanding the spatial variability of the hydrological drought characteristics is equally important for the development of effective drought mitigation actions and plans (Thomas et al. 2015).

The surface water drought index (SDI) developed by (Nalbantis and Tsakiris 2009) is an index analogous to SPI, used for characterizing severity of hydrological droughts. The comparison of hydrological drought index analogous

to SPI is helpful in obtaining a meaningful relationship between SPI and SDI. Time is treated in an overlapping zone with June 1, being considered as the beginning of the hydrological year and after every three months (August, November, February, May) a drought assessment is made regarding the time interval from the start of the hydrological year up to that time (Tsakiris et al. 2013; Nalbantis 2008; Thomas et al. 2015).The SDI calculation based on monthly observed stream flow volumes (Thomas et al. 2015) for a chosen reference period k of the i^{th} year is as follows:

$$SDI_{i,k} = \frac{y_{i,k} - \bar{y}_k}{\sigma_{y,k}}, \quad i = 1, 2, \ldots\ldots, \quad k = 1, 2, 3, 4 \qquad \ldots\ldots\ldots\ldots\ldots\ldots (4.26)$$

$$y_{i,k} = \ln(V_{i,k}), \quad i = 1, 2, \ldots\ldots, \quad k = 1, 2, 3, 4 \qquad \ldots\ldots\ldots\ldots\ldots\ldots (4.27)$$

$$V_{i,k} = \sum_{j=1}^{3k} Q_{i,j} \qquad i = 1, 2, \ldots\ldots, \quad j = 1, 2, 3 \qquad \ldots\ldots\ldots\ldots\ldots\ldots (4.28)$$

where, $\bar{y}_k$ is the average of all $y_{i,k}$ values, $\sigma_{y,k}$ is the standard deviation of all $y_{i,k}$values, $V_{i,k}$ is the cumulative streamflow volume for i^{th} hydrological year and k^{th} reference period.

In the analysis, k = 1 for June to August, k = 2 for June to November, k = 3 for June to February, and k = 4 for June to May (Thomas et al. 2015). While McKee et al. (1993) suggested that gamma distribution could be applied to streamflow, (Nalbantis and Tsakiris 2009) and (Shukla and Wood 2008) suggested log-normal distribution as a better choice for streamflow-based indices. The classification of the drought categories is based on the values of SDI viz., non-drought (SDI $\geq$ 0); mild drought (-1.0 $\leq$ SDI $\leq$ 0); moderate drought (-1.5 $\leq$ SDI $\leq$ -1.0); severe drought (-2.0 $\leq$ SDI $\leq$ -1.5) and extreme drought (SDI <-2.0).

4.3.6 GDI-based groundwater drought evaluation

The groundwater drought is defined as a natural decline in the groundwater levels that may result in dewatering of the aquifer completely or partly, or to a point where it could cause serious water supply problems. A drought sensitive aquifer, is an aquifer or a part of it, subject to groundwater droughts. The interesting aspect is to study how the droughts change as a result of their propagation through

groundwater systems and how this transformation depends on the characteristics of the climate and the groundwater system. The ground water level monitoring is carried out on a quarterly basis in Madhya Pradesh during August, November, January and May every year, whereas in Uttar Pradesh, it is carried out on a seasonal basis in November and May. In the present study, a groundwater level index (GDI) has been proposed to monitor the anomalies in groundwater levels.

The GDI is computed by normalizing quarterly/seasonal groundwater levels and dividing the difference between the quarterly/seasonal water level and its long-term seasonal mean by its standard deviation. For normalization, an incomplete gamma function was used for water level data before using them for calculating GDI. The GDI is an indicator of water-table decline and an indirect measure of groundwater discharge, and thus an indirect reference to drought. The GDI is computed as per the following equation given below,

$$GDI = \left\{\frac{GWL_{ij} - GWL_{im}}{\sigma}\right\} \quad \text{..... (4.29)}$$

where, GWL_{ij} is the seasonal water level for the i[th] well and j[th] observation, GWL_{im} is the seasonal mean and σ = is the standard deviation.

The negative anomalies correspond to 'water stress' while positive anomalies represent a 'no drought' condition. The summation of negative anomalies of groundwater levels below a threshold level for each drought event indicates the groundwater drought severity. In the present study, groundwater drought events are identified by calculating the cumulative deficit below a threshold groundwater level (Van Lanen and Peters 2000) as presented below:

$$CDI_i = CDI_{i-1} + \{\theta_D - \theta_i\};\ for\ \{\theta_D - \theta_i\}\ being\ negative \quad \text{..... (4.30)}$$

where θ_i is the groundwater level (m) in a particular month of the year and θ_D is the threshold groundwater level (m).

4.3.7 NDVI and VCI based agricultural drought evaluation

The Normalized Difference Vegetation Index (NDVI) is a measure of the 'greenness', or 'vigor' of the vegetation. NDVI is a good indicator of green biomass, leaf area index, and patterns of production because, when sunlight strikes on the surface of leaves, majority of radiation in Near-Infrared wavelength (0.7 – 1.1 mm) are reflected by cell structure of leaves, while most of the red wavelength in the visible portion of the spectrum (0.4 – 0.7 mm) are absorbed by chlorophyll in the leaves. In general, the vegetation is likely to be healthy (dense), if there is more reflected radiation in the NIR wavelength than in the visible wavelength whereas the vegetation is likely to be unhealthy (spare) or in a bad condition, if there is less reflected radiation in NIR wavelength. However, this can also result from partially or non-vegetated surfaces. It is derived based on the known radiometric properties of plants, using visible (Red) and near-infrared (NIR) radiation and computed as given below,

$$NDVI = \frac{(NIR-Red)}{(NIR+Red)} \quad \text{..……..…… (4.31)}$$

where, NIR and Red are the reflectance in the near-infrared and red bands.

NDVI values range from −1 to +1, with values near zero indicating no green vegetation and values near +1 indicating the highest possible density of vegetation. Areas of barren rock, sand, and snow produce NDVI values of < 0.1, while shrub and grassland typically produce NDVI values of 0.2 – 0.3, and temperate and tropical rainforests produce values in the 0.6 – 0.8 range.

The comparison of NDVI time series for a number of years at the same location provides information about the relative health of the vegetation in the respective years. Inter-annual variations in the magnitude and evolution of NDVI for a particular location are mainly governed by the meteorological variables such as precipitation, temperature, and relative humidity. However, changes in the land use and land cover can also cause inter-annual variations and trends in NDVI. It can be inferred that low productivity (lack of 'greenness' or 'vigor') is caused, in part, by poor weather conditions, and that high productivity is due, in part, by favorable weather conditions (Belal et al. 2014). It should be noted that the

interpretation of NDVI values is spatially dependent (Sahoo 2015). This is because more productive ecosystems have different radiometric properties than less productive ones due to differences in climate, soil, and topography (Quiring and Ganesh 2010).

The Vegetation Condition Index (VCI) id obtained when pixel-wise normalization of NDVI is done for making relative assessments of changes in the NDVI signal by filtering out the contribution of local geographic resources to the spatial variability of NDVI (Belal et al. 2014; Murthy 2010; Pettorelli et al. 2005; Townshend and Justice 1995; Quiring and Ganesh 2010). Jain et al. 2010 stated that VCI is an indicator of the status of vegetation cover as a function of NDVI minimum and maximum encountered for a given ecosystem over many years. It normalizes NDVI and allows for a comparison of different ecosystems (Belal et al. 2014). VCI is an attempt to separate the short-term climate signal from the long-term ecological signal, and therefore it gives a better signal for water stress condition than NDVI (Jain et al. 2010). The significance of VCI is strongly related to the relation between the vegetation index and the vitality of the vegetation cover under investigation.

VCI is computed as given below,

$$VCI = 100 \times \frac{(NDVI - NDVI_{min})}{(NDVI_{max} - NDVI_{min})} \quad \text{..... (4.32)}$$

VCI varies between 0 and 100 corresponding to the changes in vegetation condition from extremely unfavorable to optimal (Singh, Roy, and Kogan 2003). In the case of an extremely dry month and the vegetation condition being poor, the VCI is close to zero. A VCI of 50 reflects fair vegetation conditions whereas at optimal condition of the vegetation, VCI is close to 100. The VCI values also indicate to what extent, the vegetation has improved or deteriorated in response to the prevailing weather conditions (Gidey et al. 2018). Many researchers have concluded that VCI provides a reasonably good assessment of the spatial characteristics of agricultural drought, its duration and severity, which are generally in good agreement with precipitation patterns (Dutta et al. 2015; Gebrehiwot et al. 2011).

4.4 Supplemental Irrigation Planning for critical dry spells

4.4.1 Onset of effective monsoon

The selection of crop varieties and time for seedbed preparation is governed by the onset, termination of rainfall and length of the monsoon season, which plays a very significant role in the successful growth and yield of agricultural crops. The date of onset of effective monsoon can be defined as the date of commencement of a wet spell satisfying the following criteria given as,

1. The first day's rain in a 7-day spell is not less than average daily evapotranspiration (ET).

2. At least four out of 7 days are rainy days with not less than 2.5 mm of rain each day.

3. The total rain during the 7-day spell is not less than (5ET+10) mm.

4.4.2 Dry spell analysis

The distribution of rainfall during the monsoon season is not uniform and the occurrence of dry spells is a regular phenomenon. After the onset of the monsoon, a dry spell is determined as the intervening period of dry days between any two consecutive wet spells. Dry days are days with rainfall less than 2.5 mm rain. A wet spell can be defined based on the following criteria given as,

1. A rainy day with rainfall equal to or more than 5ET or

2. A spell of two consecutive rainy days with rainfall totaling at least 5ET or

3. A 7-day period having at least 3 or 4 rainy days with a total rainfall not less than 5ET

On the basis of crop-soil combination in the study area, the minimum length of critical dry spell has been considered as ten days. It has been observed that a dry spell with a spell length of 10 days or more is critical for the major crops grown in the study area.

4.4.3 Computation of reference evapotranspiration

The evapotranspiration estimates are required for identification of the onset of monsoon, determination of wet spells, and computation of water requirement of

crops and subsequent estimation of irrigation water requirement of various crops. The FAO Penman-Monteith equation (FAO 1998) has been used for computation of reference evapotranspiration, using weather data such as solar radiation, air temperature, air humidity, temperature and wind speed as given by,

$$ET_0 = \frac{0.408\Delta(R_n - G) + \gamma \frac{900}{T+273} u_2 (e_s - e_a)}{\Delta + \gamma(1 + 0.34u_2)} \quad \text{..... (4.32)}$$

where, ET_o is the reference evapotranspiration (mm/day), R^n is the net radiation at the crop surface (MJm-2/day), G is the soil heat flux density (MJ/m^2/day), T is the mean of daily air temperature (°C), u_2 is the wind speed at 2 m height (m/s), e_s is the saturation vapor pressure (kPa), e_a is the actual vapor pressure (kPa), Δ = slope of the vapor pressure curve (kPa/°C], and γ is the psychometric constant (kPa/°C).

4.4.4 Crop water requirement

The quantum of water needs to compensate the evapotranspiration loss from the cropped area is defined as crop water requirement. The crop water requirement has been calculated for each crop based on its crop coefficient applicable for different developmental/growth stages. The crop evapotranspiration (ET_{crop}) has been computed by,

$$ET_c = K_c \times ET_o \quad \text{..... (4.32)}$$

where, ET_c is the crop evapotranspiration (mm/day), ET_o is the reference evapotranspiration (mm/day), K_c is the crop coefficient.

The spectral signature of different crops have been taken from different sites based on which the crop map has been prepared. The area under various crops has been computed for different districts, and thereafter the crop water requirement has been calculated by multiplying the area under a particular crop with its ET_c.

4.5 Hydrologic Modelling using SWAT

The Soil and Water Assessment Tool (SWAT) is a semi-distributed watershed model capable of performing simulations on a daily time scale for very long continuous periods (Arnold et al., 1999). It can be used to assess the impacts of alternate management practices, land use change and climate change on the water

resources, sediment, and non-point pollution in large river basins. The model was developed with an objective to assess the impacts of alternate management practices on the water resources and non-point pollution in large river basins, by the United States Department of Agriculture (USDA) in the early 1990's and has been updated regularly. SWAT can be used in ungauged watersheds also to predict the effect of land use changes and water resources management on the water, sediment, and agricultural chemical yields. The input database for the setup of SWAT model comprised of the following.

For system characterization

i) Base map of watershed

ii) Drainage network map

iii) Topographic map

iv) DEM

v) Slope map

vi) Soil Map

vii) Land use and Land cover map

Input forcing data

i) Daily rainfall data

ii) Daily weather data including minimum and maximum temperature, relative humidity, wind speed and solar radiation

iii) Crop data and cropping pattern

iv) River flow data

v) Reservoir properties

In SWAT, the spatial variability within the watershed is represented by dividing the basin into multiple sub-basins, which are then further sub-divided into hydrologic response units (HRUs). The HRUs comprise of homogeneous land use, topography, soil characteristics, and management practice (Neitsch et al., 2002). The water balance is the basic principle behind all the processes in SWAT and as it impacts the plant growth, movement of sediments, nutrients, pesticides

and pathogens. The forcing variables used to run SWAT include daily precipitation, maximum and minimum temperature, solar radiation, relative humidity, and wind speed all which directly control the water balance, which is simulated separately for each HRU including canopy interception of precipitation, partitioning of precipitation, snowmelt water, and irrigation water, redistribution of water within the soil profile, evapotranspiration (ET), lateral subsurface flow from the soil profile, and return flow from shallow aquifers. These weather variables and/or the missing weather variables can also be generated using the weather generator available within the model.

The watershed simulation is separated into i) land phase, which controls the amount of water, sediments, pesticide loadings and nutrients coming into the main channel in each sub-basin, and ii) the in-stream or routing phase which is the movement of water, sediments, nutrients and pesticides through the channel network of the watershed to the outlet. SWAT takes into account a range of hydrologic processes such as canopy storage, surface runoff, infiltration, evapotranspiration, lateral flow, snow accumulation and melt, consumptive use through pumping, return flow, recharge by seepage from surface water bodies, pond and tributaries. The surface runoff from daily rainfall is estimated using the modified Soil Conservation Service Curve Number (SCS-CN) model, whereas the land cover is simulated using plant growth models. The Manning's roughness coefficient is used for the overland and channel flow analysis and sediment yield is simulated using the Modified Universal Soil Loss Equation (MUSLE). The potential evapotranspiration (PET) is computed by any one of the three methods viz., (Penman-Monteith, 1948, 1965; Priestly Taylor, 1972; or Hargreaves, 1982). The Richard's equation is used for flow calculations in the unsaturated zone, whereas the Darcy's law and the mass conservation of 2D laminar flow are used for groundwater flow through saturated zone. The SWAT operates on a daily time scale and mathematically, the water balance equation as conceived in SWAT is given by,

$$\sum Input - \sum Output = Change\ in\ storage \quad \text{..... (4.33)}$$

The detailed components representing the major hydrologic processes in SWAT is given by,

$$\sum_{i=1}^{t}(P + W_{ia}) - \sum_{i=1}^{t}(Q_{surf} + E_t + Q_{lf} + W_{seep} + Q_{rf.sh}) = (SW_t - SW_o) \quad \text{..... (4.34)}$$

where, SW_t is the final soil water content on any day i (mm); SW_o is the initial soil water content on day i (mm); P is the precipitation amount on day i (mm); $Q_{surf}$is the surface runoff consequent to the precipitation in mm; $E_t$is the evapotranspiration on day i (mm), $Q_{lf}$is the lateral flow or interflow component (mm); W_{seep} is the amount of water entering the vadose zone from the soil profile on day i (mm); W_{ia} is the irrigation application amount on day i (mm); and $Q_{rf.sh}$ is the return flow or base flow component (mm). The representation of the various flow processes and their interactions in SWAT model is illustrated in Figure 4.1. The surface runoff Q_{surf}has been estimated using the SCS Curve Number (SCS-CN) (SCS, 1972) procedure and is given by,

$$Q_{surf} = \frac{(P-I_a)^2}{(P-I_a+S)} \quad \text{for} \quad P > I_a$$

$$\text{else} \quad Q_{surf} = 0.0$$

..... (4.35)

where, I_a is the initial abstraction, which includes the surface storage, interception and infiltration prior to runoff (mm); S is the soil moisture retention parameter (mm), which generally varies spatially due to changes in the soil type, land use pattern and management practices and temporally due to changes in water content. The parameter S is related to the curve number (CN) by the SCS equation (USDA, 1972) given by,

$$\frac{25400}{CN} - 254 \quad \text{..... (4.36)}$$

The CN here represents the curve number used for Antecedent Moisture Condition-II (AMC-II). The CN suitable for the different soil-crop combinations have been used for Indian conditions for the AMC-II condition. The retention parameter varies according to the variation in the soil water content in the soil

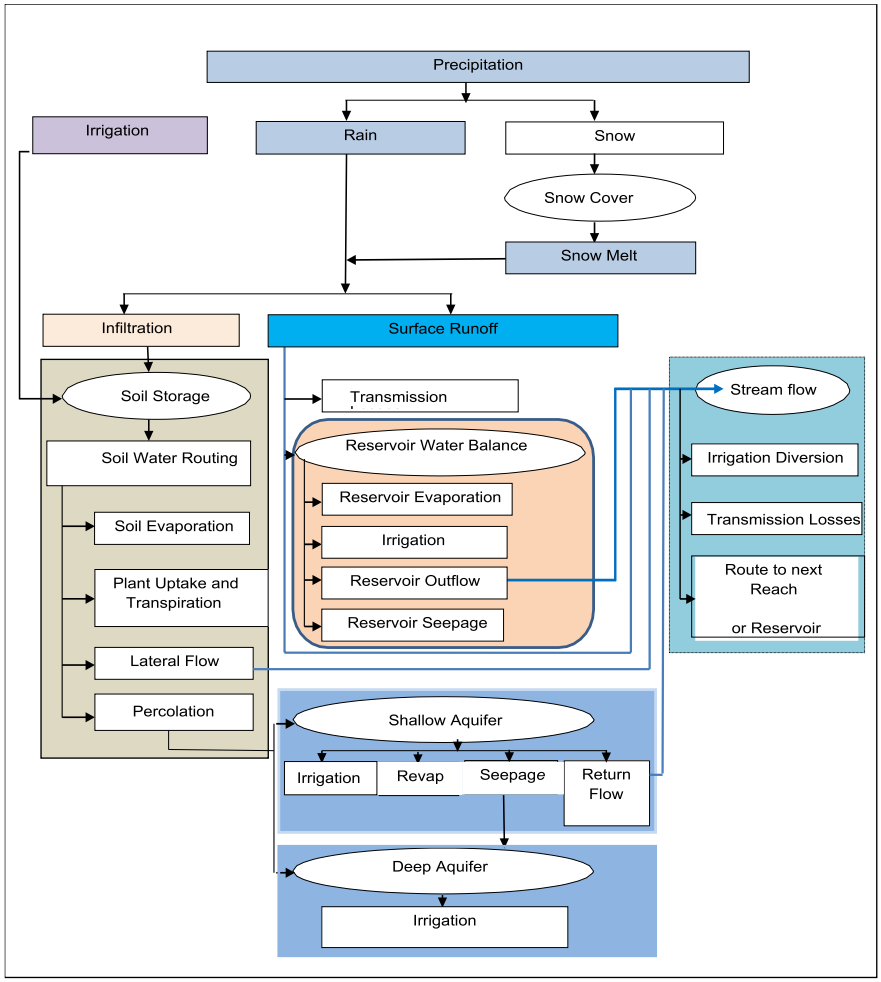

Figure 4.1: Computational workflow of SWAT (Source: Uhlenbrook, 2008)

profile. The retention parameter S can also be assumed to vary with the accumulated plant evapotranspiration. The irrigation application component W_{ia} can be computed externally using the expression given by,

$$W_{ia} = \{(Q_{si} + F_1 Q_{w,sh} + F_2 Q_{w,dp})/A_{ia}\} \quad \text{..... (4.37)}$$

where, F_1 and F_2 are the fractions of the shallow and deep groundwater withdrawals used for irrigation; $A_{ia}$is the area of irrigation water application. The water seep component W_{seep} is computed implicitly from the analysis of vadose zone soil water profile and shallow aquifer water profile.

The potential evapotranspiration (PET) can be computed by any of the three available methods including Penman Monteith method, Priestly Taylor method or the Hargreaves method depending on the availability of data in the basin. The Penman-Monteith method has been used to estimate the potential

evapotranspiration (PET) in the study area. The lateral flow in the soil profile takes place for soils with high hydraulic conductivities in the surface layers and an impermeable or semi-impermeable layer at a shallow depth. The lateral flow taking place in each soil layer once the soil in that zone becomes saturated is given by,

$$Q_{lat} = 0.024.\left(\frac{2.SW_{ly,excess}.K_{sat}.slp}{\emptyset_d.L_{hill}}\right) \quad \text{..... (4.38)}$$

In the above equation, K_{sat} is the saturated hydraulic conductivity (mm/hour); $SW_{ly,excess}$ is the drainable water stored (mm) in the saturated layer when the water content exceeds the layer's field capacity and is the difference between the soil water content on a given day minus the soil layer field capacity; L_{hill} is the hill slope length (m); $\emptyset_d$ is the drainable porosity of the soil layer (mm/mm); slp is the slope.SWAT simulates two aquifers in each sub-basin viz., the shallow aquifer (unconfined aquifer) $Q_{rf.sh}$which contributes to the main channel or reach, based on the Darcy's equation. However, the deep aquifer (confined aquifer) is assumed to contribute to the stream flow outside the watershed (Arnold et al., 1993). The water balance of the shallow aquifer is given by,

$$aq_{sh,j} = aq_{sh,j-1} + w_{rchr,sh} - Q_{rf.sh} - w_{revap} - w_{pump,sh} \quad \text{..... (4.39)}$$

where, $aq_{sh,j}$is the amount of water stored in shallow aquifer on day i (mm); $aq_{sh,j-1}$ is the amount of water stored in shallow aquifer on day i-1 (mm); $w_{rchr,sh}$ is the amount of recharge entering the shallow aquifer on day i (mm); $Q_{rf.sh}$ is the groundwater flow or base flow into the main channel on day i (mm); w_{revap} is the amount of water moving into soil zone in response to water deficiencies on day i (mm); $w_{pump,sh}$ is the amount of water removed from the shallow aquifer by pumping on day i (mm).

The amount of recharge entering the shallow aquifer is given by,

$$w_{rchrg,sh} = w_{rchrg} - w_{deep} \quad \text{..... (4.40)}$$

where, w_{rchrg} is the total daily recharge in both aquifers in mm and w_{deep} is the amount of recharge entering the deep aquifer on day i (mm)and is given by,

$$w_{rchrg,sh} = w_{rchrg} - w_{deep}$$

..…….…… (4.41)

where, β_{deep} is the aquifer percolation coefficient.

4.5.1 SWAT multisite calibration, validation and uncertainty assessment

The model calibration is one of the most important procedures in any hydrologic modeling study, the basic aim of which is to reduce the model simulation uncertainty (Engel et al., 2007). It typically involves the sensitivity analysis followed by manual or automatic calibration. Sensitivity analysis is the process of determining the rate of change in model output with respect to rate of change of model parameters (Arnold et al., 2012). The sensitivity analysis helps to determine the most sensitive parameters for the given basin and sub-basins and the parameter precision required for calibration. Generally, two types of sensitivity analysis are available viz., i) local sensitivity analysis or one at a time (OAT) sensitivity analysis in which only one parameter is allowed to change while keeping all other parameters at the fixed values, and ii) global sensitivity analysis in which all parameter values are allowed to change simultaneously, but this technique requires very large number of simulations.

During the calibration process, the model is parameterized based on the given set of data and local conditions so as to reduce the simulation uncertainty. Care should be taken to select the model parameter values within their respective uncertainty ranges by comparing the simulated flows with the observed flows at the gauging site of interest. The calibration can be accomplished manually or by using the calibration tools in SWAT (van Griensven and Bauwens, 2003; Van Liew et al., 2005) or SWAT Calibration and Uncertainty Programs (SWAT-CUP) (Abbaspour et al., 2007). The water balance components should be checked during the calibration process to make sure that the simulations are reasonable for the basin. After the calibration process has been completed, the model needs to be validated by running calibrated model using the independent dataset (not used in calibration) and comparing the simulated and observed flows during the validation period, so as to develop confidence in the model developed for the basin. SWAT-

CUP has been used for the calibration and uncertainty analysis and validation of the SWAT model setup for the study area.

4.6 Vulnerability Assessment

The vulnerability assessments are based on three vulnerabilities based on i) vulnerability to drought, ii) vulnerability to desertification and iii) vulnerability to climate change. Therefore, separate vulnerability assessment has been carried out for indicators-based assessment of drought vulnerability, desertification vulnerability and climate change vulnerability. The indicators that can be projected into the future have been considered so that how the vulnerability is going to unfold in the future can be evaluated. The methodology for each of the vulnerability assessments are given in the following sub-sections.

4.6.1 Drought vulnerability

The drought vulnerability analysis is based on the multiple indicator approach to spatially identify the areas vulnerable to drought within the study area. Two types of indicators viz., i) spatial indicators which do not vary with every drought event and ii) spatio-temporal indicators which vary for every drought event have been used to evaluate the drought vulnerability. The spatial indicators may include a) elevation bands, b) land use / land cover and c) soil type. The spatio-temporal drought indicators can include a) soil moisture drought severity and events, b) surface water drought severity and events, c) groundwater drought severity and events and d) rainfall departure. Figure 4.2 depicts various indicators that have been used in the development of drought vulnerability map for the study area.

Drought Vulnerability Index (DVI) has been utilized to assess areas vulnerable to drought and the study area has been divided into four various classes viz., slightly vulnerable, moderately vulnerable, highly vulnerable and critically vulnerable. The DVI is a composite indicator that aims at integrating the various manifestations of drought and the concept of vulnerability into a single value. In the present study, drought vulnerability map comprises of three components which includes different indicators. To produce a drought vulnerability map for Chambal

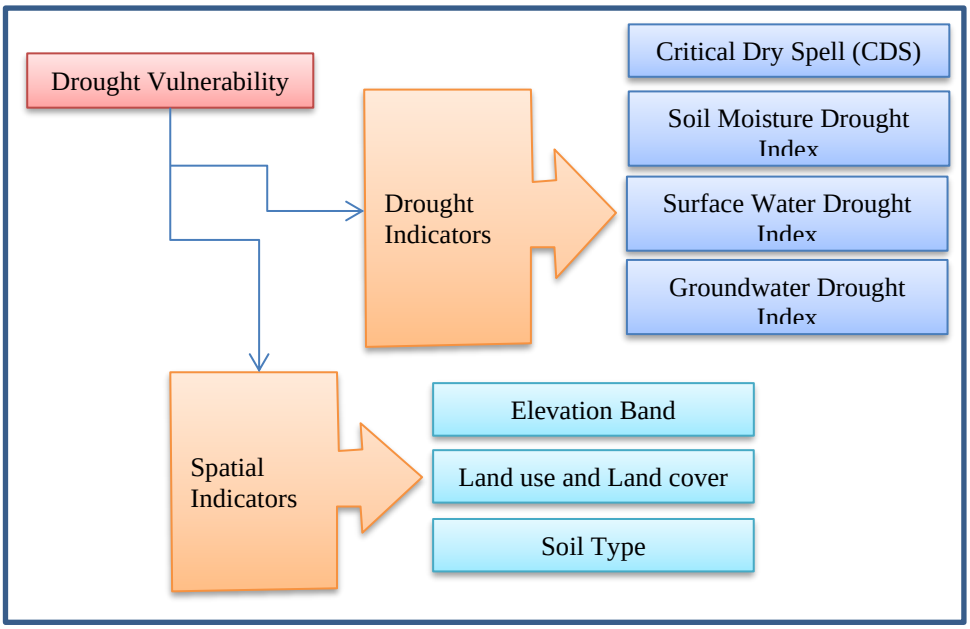

Figure 4.2: Flow chart depicting drought vulnerability assessment

River basin, various layers representing different factors were prepared using Arc-GIS software and weights are assigned based on their degree of vulnerability to drought. The weights have been assigned to the various sub-classes of each of these drought indicators. The weights assigned are added using a simple scheme of addition of weights. The composite weight score divided by the sum of maximum weights of each factor represents the DVI. Thus, the DVI is defined as the ratio of sum of assigned weight value of each factor to the sum of the maximum weights of all selected spatial and temporal factors. Consequently, the degree of vulnerability to drought has been mathematically estimated using following equation,

$$DVI = \frac{\sum_{i=1}^{n} Wdi}{\sum_{i=1}^{n} Wdimax} \quad \text{..... (4.42)}$$

where, DVI is the Drought Vulnerability Index; Wdi is the weight scored by an indicator; Wdi_{max} is the maximum weight of i^{th} indicator and n is the number of factors under consideration.

4.6.2 Desertification Vulnerability

Consistent land degradation over a period of time coupled with climate change and detrimental anthropogenic activities may lead to a situation of desertification.

Under such circumstances evaluation of vulnerability to desertification is essential. The vulnerability to desertification in the study area situated in semi-arid setting is based on the multiple indicator approach. The indicators considered for the assessment are the ones that are responsible for land degradation ultimately leading to desertification. Also, such indicators have been selected that can be used to forecast the future desertification scenario. The indicators can include a) aridity index, b) average annual temperature, and c) rainfall erosivity. The annual erosivity factor of rainfall (R) is a function of falling raindrop and the rainfall intensity, and is the product of kinetic energy of the raindrop and the 30-minute maximum rainfall intensity (Pandey et al., 2007). But as this type of detailed meteorological data is not available for the study area, the empirical equation of G. Singh (1981) has been used in estimating the rainfall erosivity factor. The annual rainfall erosivity factor has been computed using the equation given below.

$$R_a = 79 + 0.363 * P \qquad \text{..... (4.43)}$$

where, R_a is the average annual rainfall erosivity factor (mt ha-cm-1) and P is the rainfall in mm.

Figure 4.3 depicts various indicators that have been used in the development of desertification vulnerability map for the study area.

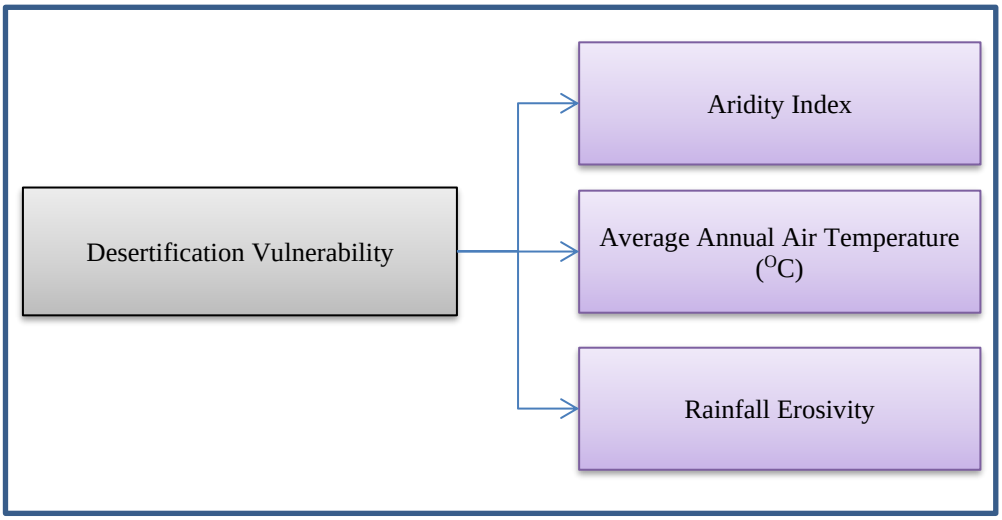

Figure 4.3: Flow chart depicting desertification vulnerability assessment

For the assessment of the desertification vulnerability for Chambal River basin, various layers representing different factors were prepared using Arc-GIS

software and weights have been assigned based on the relative significance of various factors on vulnerability to desertification. The weights have been assigned to the various sub- classes of each of these desertification indicators. The weights assigned are added using a simple scheme of addition of weights. The composite weight score divided by the sum of maximum weights of each factor represents the DSVI. Thus, the DSVI is defined as the ratio of sum of assigned weight value of each factor to the sum of the maximum weights of all selected factors. The degree of vulnerability to desertification has been estimated using following equation,

$$DSVI = \frac{\sum_{i=1}^{n} Wdsvi}{\sum_{i=1}^{n} Wdsvimax} \quad \text{..... (4.44)}$$

where, DSVI is the Drought Vulnerability Index; Wdsi is the weight scored by an indicator; $Wdsi_{max}$ is the maximum weight of i^{th} indicator and n is the number of factors under consideration.

4.6.3 Climate Vulnerability

Climate change is having its impacts on the land and water resources which are clearly visible off-late. The extreme climate events have rendered hardships to people, as many regions have become vulnerable to the extreme weather events like intense rainfall and heat waves, making many regions vulnerable to extreme climatic events. Therefore, looking into the increased frequency of extreme events, the evaluation of vulnerability to climate is essential. The vulnerability to extreme climate vis-à-vis drought and desertification has been carried out based on the multiple indicator approach. The extreme climate indicators used for rainfall include, a) one-day maximum rainfall, b) daily rainfall intensity, and c) number of rainy days and d) annual rainfall whereas the extreme climate indicators used for temperature include, a) one-day maximum of maximum temperature, b) one-day maximum of minimum temperature, c) number of very hot days and d) number of very hot nights. Figure 4.4 depicts various indicators that have been used in the development of climate vulnerability map for the study area.

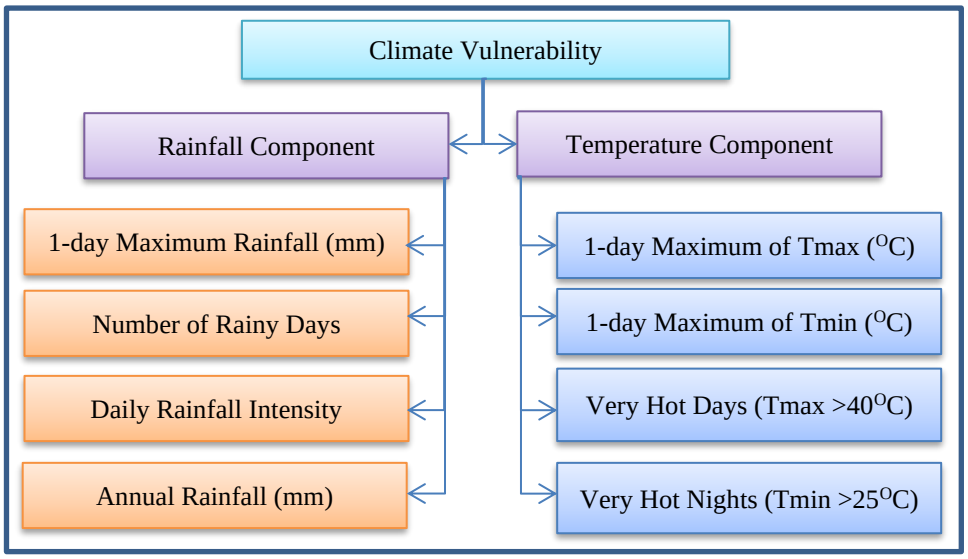

Figure 4.4: Flow chart depicting extreme climate vulnerability assessment

For the assessment of the climate vulnerability for Chambal River basin, various layers representing these factors were prepared using Arc-GIS software and weights have been assigned based on the relative significance of various factors on vulnerability to climate. The weights have been assigned to the various sub-classes of each of these extreme climate indicators. The weights have been designed based on the range of the variation of each of these indicators and their relative contribution to the extreme climate vulnerability. Thereafter the weights of each of the extreme climate indicators have been summed up. The composite weight score divided by the sum of maximum weights of each factor represents the ECVI. Thus, the ECVI is defined as the ratio of sum of assigned weight value of each factor to the sum of the maximum weights of all selected factors. The higher values of ECVI indicate higher vulnerability with respect to extreme climate in such areas. The degree of vulnerability to extreme climate has been estimated using following equation,

$$ECVI = \frac{\sum_{i=1}^{n} Wecvi}{\sum_{i=1}^{n} Wecvimax} \quad \text{..... (4.45)}$$

where, ECVI is the Extreme Climate Vulnerability Index; Wecvi is the weight scored by an indicator; $Wecvi_{max}$ is the maximum weight of i^{th} indicator and n is the number of factors under consideration.

4.6.4 Integrated Vulnerability

The integrated vulnerability map has been prepared by summing the weights of the various sub-classes of the indicators used for the assessment of drought vulnerability, desertification vulnerability and extreme climate vulnerability. The summation of the weights of all the indicators used in the analysis has been used to derive the integrated vulnerability index (INVI). The INVI is indicative of the combined vulnerability to droughts, desertification and extreme climate. The higher values of INVI indicate higher overall vulnerability with respect to drought, desertification and extreme climate in such areas. The INVI has been estimated as given,

$$INVI = \sum_{i=1}^{n} Weci + \sum_{i=1}^{n} Wdi + \sum_{i=1}^{n} Wdsi \quad \text{..... (4.46)}$$

where, INVI = Integrated Vulnerability Index

Figure 4.5 shows the methodology for integrated vulnerability assessment in the study area.

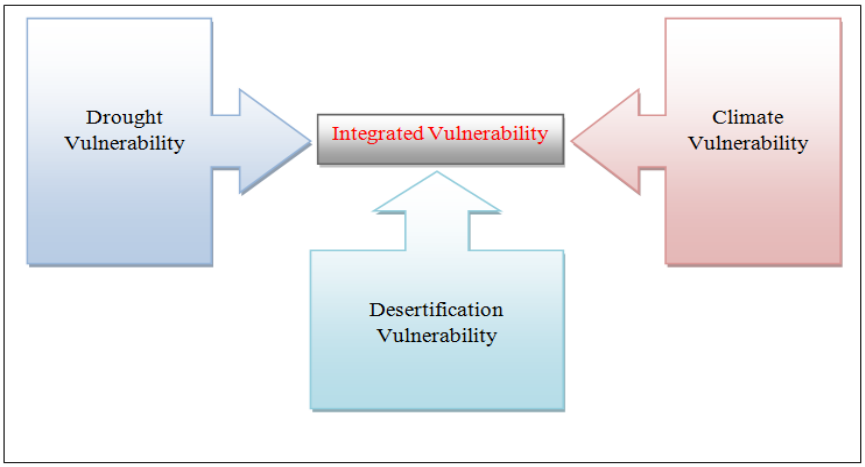

Figure 4.5: Methodology for integrated vulnerability assessment

5.0 RESULTS AND DISCUSSIONS

The study area comprises of 14 districts falling in MP viz., a) bordering districts namely Neemuch, Mandsaur, Ratlam, Agar, Rajgarh and Guna and b) other districts namely, Ujjain, Dhar, Indore, Dewas, Shajapur, Sehore, and parts of Bhopal and Vidisha districts. 57 blocks of these 14 districts fall in the study area.

The daily rainfall at these blocks was collected from the Water Resources Department, Govt. of Madhya Pradesh. There are large data gaps in these datasets. Therefore, the high resolution IMD gridded rainfall (0.25^o x 0.25^o) has been used for the analyses. The complete extent of the Chambal basin comprises of 399 grids. However, the grids pertaining to the location of these blocks have been selected from the gridded datasets. The data pertaining to these 53 grids have been selected as the four blocks were represented by the same grids. To test the applicability of the gridded precipitation datasets, the correlation analysis was carried out between the station rainfall and the gridded rainfall.

5.1 Investigation of the Climate Change Signals

5.1.1 Precipitation

5.1.1.1 Correlation analysis of monthly rainfall

The investigation of historical climate datasets of precipitation, maximum and minimum temperature is essential to detect the presence any relevant signals of climate change. This helps to assess the extent to which the variables responsible for climate change have already started impacting the vulnerable regions within the study area. The station rainfall and the gridded daily rainfall at the 53 blocks falling in Chambal basin were aggregated to arrive the monthly rainfall time series. The station rainfall data at the three blocks viz., Nalkheda, Moman Badodiya and Kalapipal blocks of Shajapur district were not available and the correlation analysis has been performed for the remaining 50 blocks only. The correlation coefficient between the station and gridded monthly rainfall was estimated along with the comparison of plots between them. The correlation coefficient varies between 0.85 at Lateri block of Vidisha district to 0.99 at Mahidpur block of Ujjain district except for 0.71 at Berasia block of Bhopal district. Table 5.1 gives the correlation coefficient for all the blocks in the study area. As most of the blocks have a correlation coefficient greater than 0.85 with very few exceptions, the gridded rainfall data is considered to be reliable and representative of the station rainfall data and has therefore been used for all further analysis.

Table 5.1: Correlation coefficient between gridded and station rainfall

S. No.	District	Block	Correlation coefficient
1.	Agar	Agar	0.96
2.	Agar	Barod	0.98
3.	Agar	Nalkheda	NA
4.	Agar	Susner	0.99
5.	Bhopal	Berasia	0.71
6.	Dewas	Bagli	0.93
7.	Dewas	Dewas	0.88
8.	Dewas	Sonkatch	0.89
9.	Dewas	Tonkkhurd 71	0.92
10.	Dhar	Badnawar	0.95
11.	Dhar	Dhar	0.95
12.	Dhar	Nalcha	0.92
13.	Guna	Aron	0.92
14.	Guna	Bamhori	0.93
15.	Guna	Guna	0.98
16.	Guna	Raghogarh	0.93
17.	Indore	Depalpur	0.86
18.	Indore	Indore	0.95
19.	Indore	Mhow	0.92
20.	Indore	Sanwar	0.96
21.	Mandsaur	Bhanpura	0.96
22.	Mandsaur	Garoth	0.96
23.	Mandsaur	Malhargarh	0.86
24.	Mandsaur	Mandsaur	0.95
25.	Mandsaur	Sitamau	0.95
26.	Neemuch	Jawad	0.95
27.	Neemuch	Manasa	0.98
28.	Neemuch	Neemuch	0.94
29.	Rajgarh	Biaora	0.97
30.	Rajgarh	Khilchipur	0.91
31.	Rajgarh	Narsingarh	0.99
32.	Rajgarh	Rajgarh	0.97
33.	Rajgarh	Sarangpur	0.86
34.	Rajgarh	Zirapur	0.90
35.	Ratlam	Alot	0.94
36.	Ratlam	Jaora	0.93
37.	Ratlam	Piploda	0.89
38.	Ratlam	Ratlam	0.88
39.	Ratlam	Sailana	0.92
40.	Sehore	Ashta	0.94
41.	Sehore	Ichhawar	0.89
42.	Sehore	Sehore	0.98
43.	Shajapur	Kalapipal	NA
44.	Shajapur	Moman Badodiya	NA
45.	Shajapur	Shajapur	0.94
46.	Shajapur	Sujalpur	0.97
47.	Ujjain	Badnagar	0.94
48.	Ujjain	Ghatia	0.95
49.	Ujjain	Khachrod	0.98
50.	Ujjain	Mahidpur	0.99
51.	Ujjain	Tarana	0.95
52.	Ujjain	Ujjain	0.98
53.	Vidisha	Lateri	0.85

The plots showing the comparison of the station and gridded rainfall at few blocks are given in Figure 5.1 to Figure 5.6.

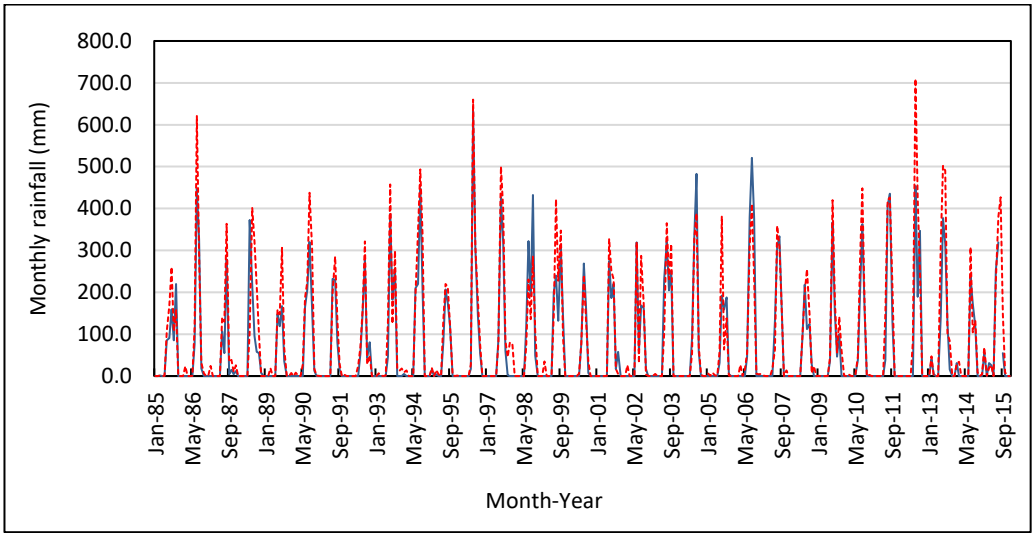

Figure 5.1: Comparison of station and gridded rainfall for Bagli block in Dewas district

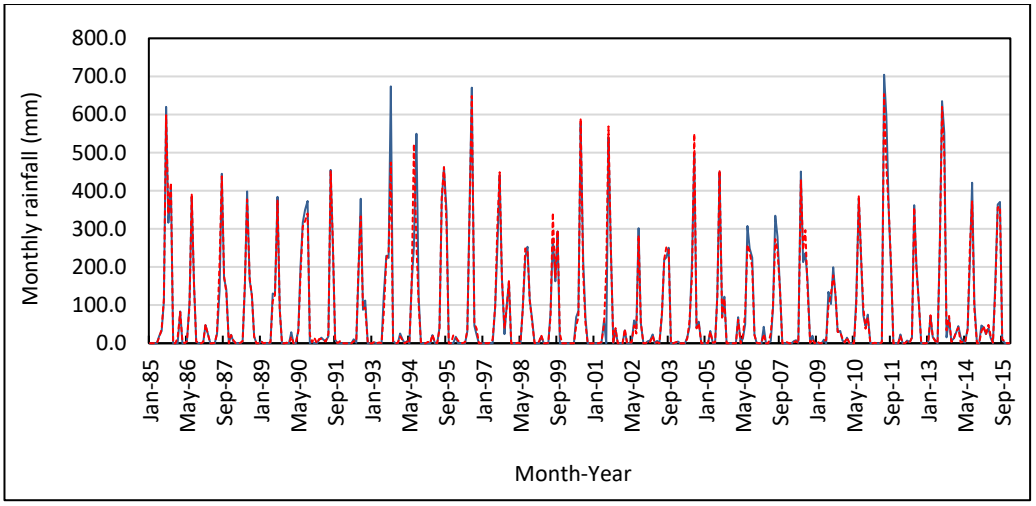

Figure 5.2: Comparison of station and gridded rainfall for Guna block

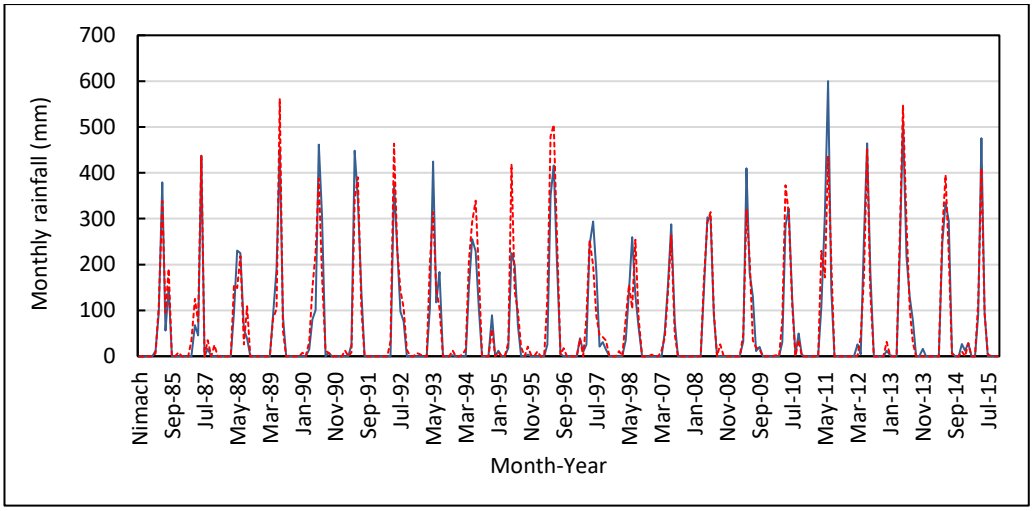

Figure 5.3: Comparison of station and gridded rainfall for Neemuch block

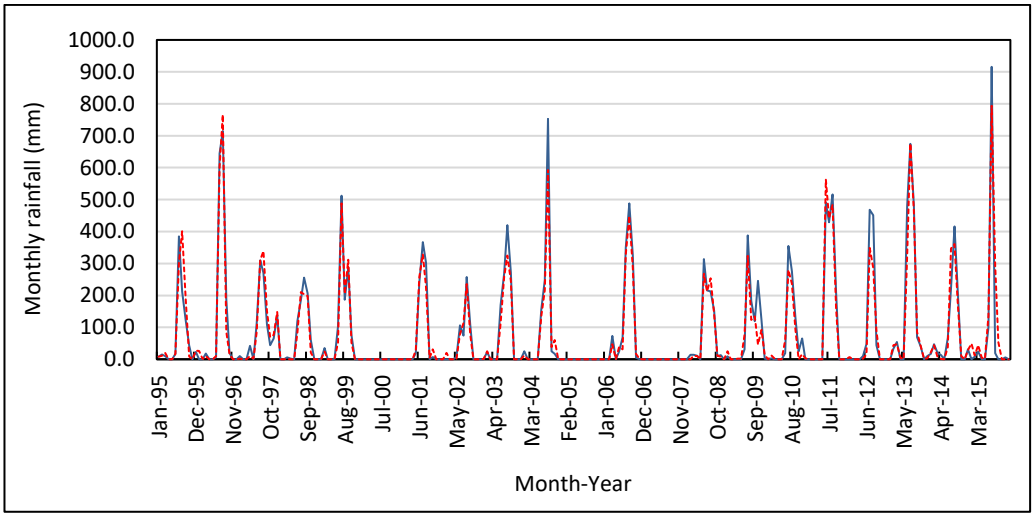

Figure 5.4: Comparison of station and gridded rainfall for Biaora block in Rajgarh district

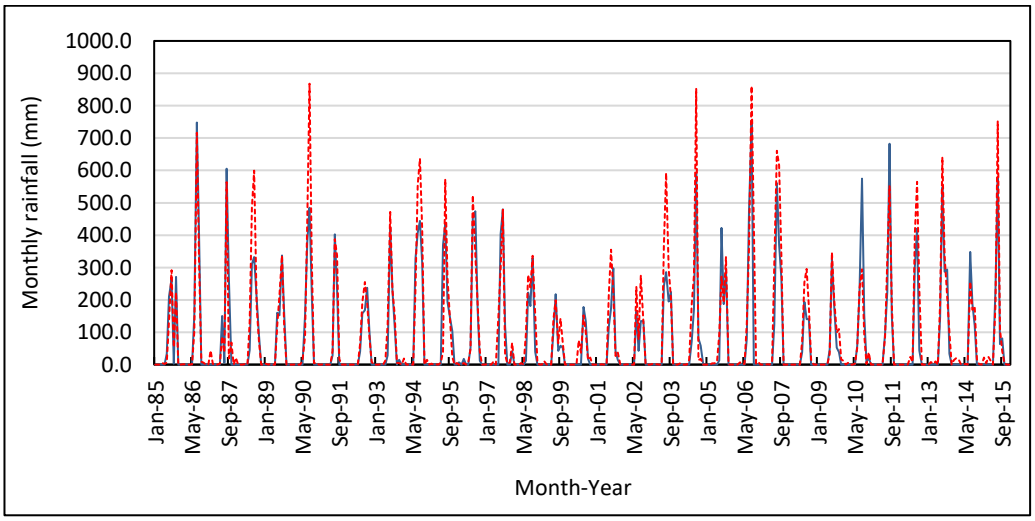

Figure 5.5: Comparison of station and gridded rainfall for Bajna block in Ratlam district

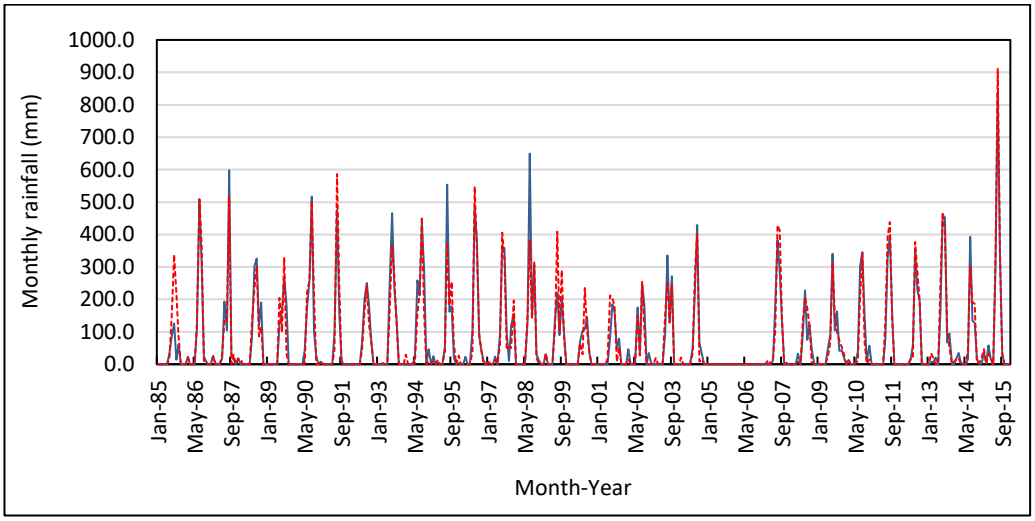

Figure 5.6: Comparison of station and gridded rainfall for Ghatia block in Ujjain district

5.1.1.2 Average annual rainfall

The daily rainfall data have been further aggregated to seasonal and annual rainfall. The analysis has been carried out for the period spanning 1901 to 2015 (115 years). The average annual rainfall over the study area has been estimated by taking the average values over the 53 grids falling in the study area. The temporal variation of the average annual rainfall over the study area is given in Figure 5.7. It can be observed that there is no trend in the average annual rainfall. The average annual rainfall over the study area during the period of analysis is 944.20 mm and it varies between 511.8 mm in 1965 and 1692.9 mm in 1973.

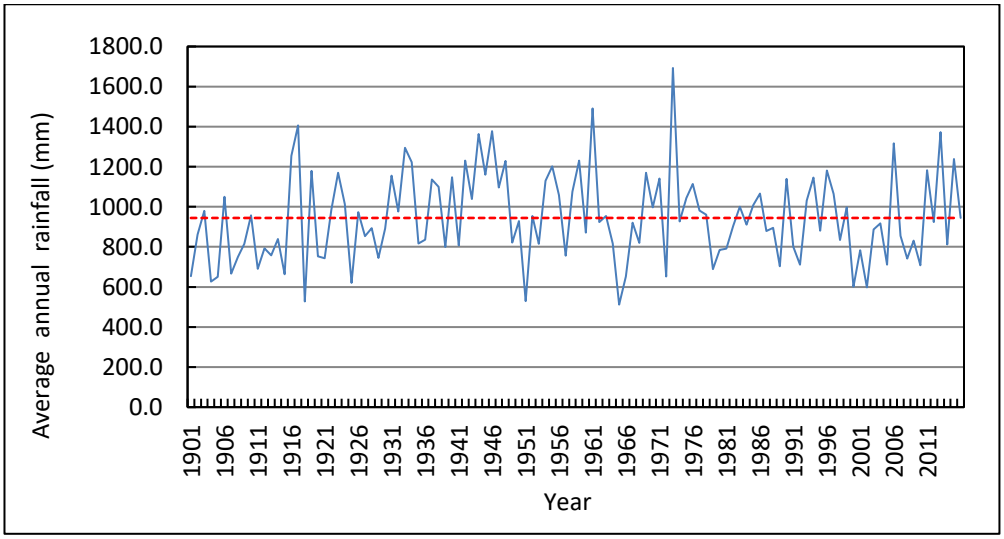

Figure 5.7: Temporal variation of the mean annual rainfall (1901-2015)

The spatial variation of the average annual rainfall is given in Figure 5.8. The average annual rainfall varies spatially between 789.2 mm at Mandsaur and 1193.80 mm at Sehore. It can be observed that the average annual rainfall increases from west to east with 800-900 mm in the districts of Neemuch, Mandsaur, Ratlam and parts of Ujjain and Dhar districts, which thereafter increases to 900-1000 mm in the districts of Agar, Indore, major parts of Ujjain and parts of Dhar, Dewas, Shajapur and Rajgarh districts. Further increases in the average annual rainfall are observed (1000-1100 mm) at Guna, parts of Rajgarh, Shajapur, Dewas, Vidisha and Sehore districts.

The average annual rainfall > 1100 mm is observed in the eastern parts of the study area falling partly in the districts of Bhopal, Rajgarh, Shajapur and Sehore. However, it is an interesting fact that the annual average rainfall in the districts bordering Rajasthan vary between 800 mm and 1100 mm. The analysis was thereafter extended to time slices of 30 years and the variation of the mean annual rainfall during these time horizons are given in Table 5.2. It can be observed that the average annual rainfall in the present time horizon (1991-2015) is limited to 925.1 mm. The baseline period for the comparison has been selected as 1961-1990. The comparison of the mean annual rainfall anomaly between the present time horizon (1991-2015) and the baseline period (1961-1990) shows 35 blocks out of 53 blocks depict a decreasing rainfall pattern, which is also depicted in the spatial plot of the rainfall anomaly as given in Figure 5.9. It can be observed that the mean annual rainfall during the latest time horizon is decreasing in most of the districts as compared to the baseline period. The comparison of the decadal annual average rainfall during the last few decades also depicts a similar pattern of decrease in the mean annual rainfall from 959.70 mm during 1951-60 to 832.20 mm during 2001-10 (Figure 5.10). The analysis of the seasonal rainfall and monthly rainfall did not reveal any significant trends as depicted in Figure 5.11.

Table 5.2: Mean annual rainfall during various 30-yr time horizons

S. No.	Time horizon	Mean annual rainfall (mm)
1.	1901-30	858.8
2.	1931-60	1038.5
3.	1961-90	951.4
4.	1991-15	925.1

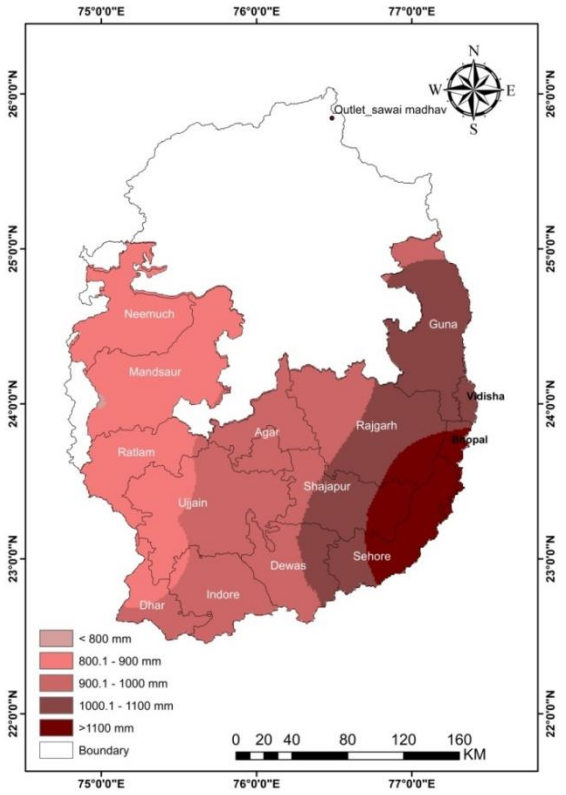

Figure 5.8: Spatial variation of the average annual rainfall

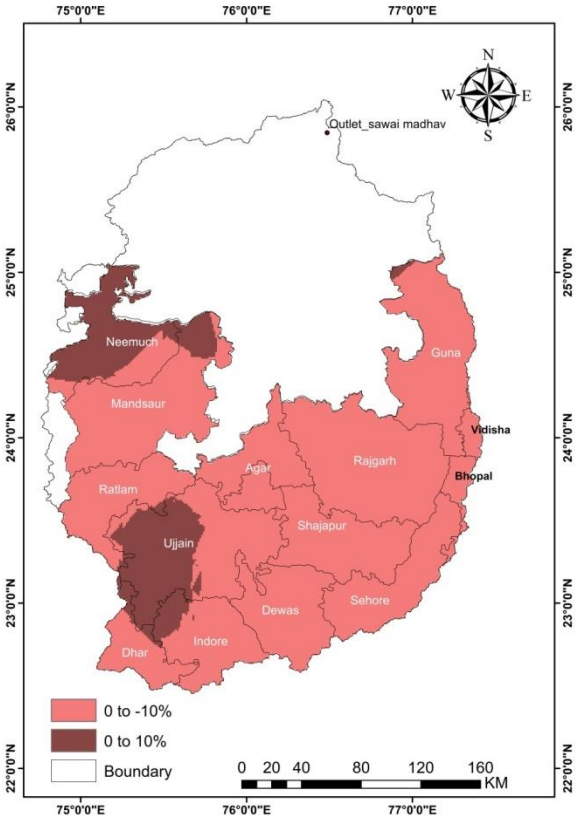

Figure 5.9: Annual rainfall anomaly between the present and baseline period

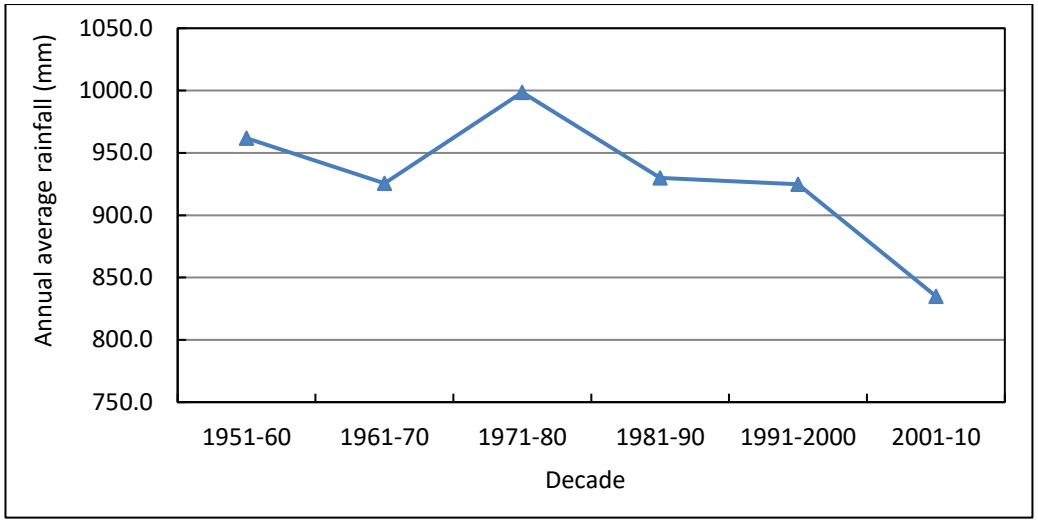

Figure 5.10: Decadal variation of average annual rainfall

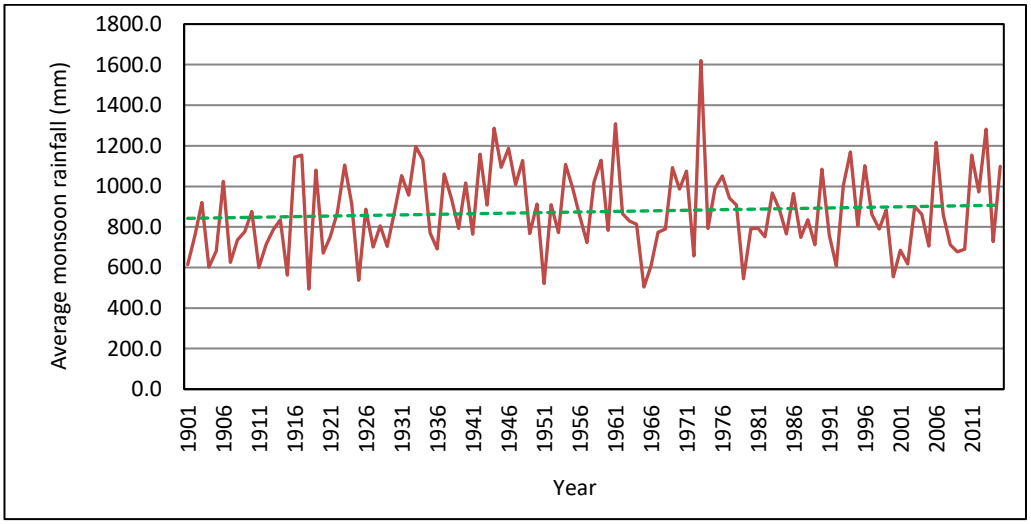

Figure 5.11: Temporal variation of the seasonal rainfall during 1901-2015

However, the variability of the seasonal rainfall is very high at 23.4% which may be responsible for the water scarcity and droughts in the study area. The average rainfall during the monsoon season is 874.8 mm.

5.1.1.3 Number of rainy days

A day which records a rainfall of 2.50 mm or more has been considered as a rainy day. The annual number of rainy days has been extracted from the daily rainfall time series spanning 1901-2015. The plot showing the temporal variation of the annual number of rainy days is given in Figure 5.12. There are 50 rainy days on an average in the study area and it varies between 30 days and 83 days. The comparison of the number of rainy days during the present time horizon (1991-

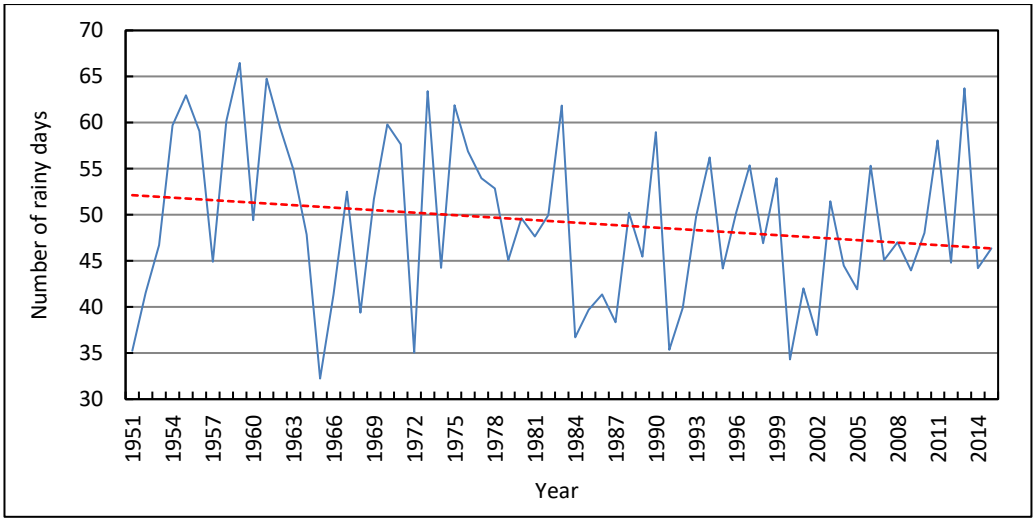

Figure 5.12: Annual number of rainy days in the study area

2015) and the baseline period (1961-1990) is given in Figure 5.13. It can be seen that number of rainy days have decreased in almost all the districts in the study area. 47 blocks depict a decreasing number of rainy days whereas only 6 blocks portray an increase in number of rainy days. The decrease in number of rainy days between present time horizon and baseline varies between 1 and 6 days.

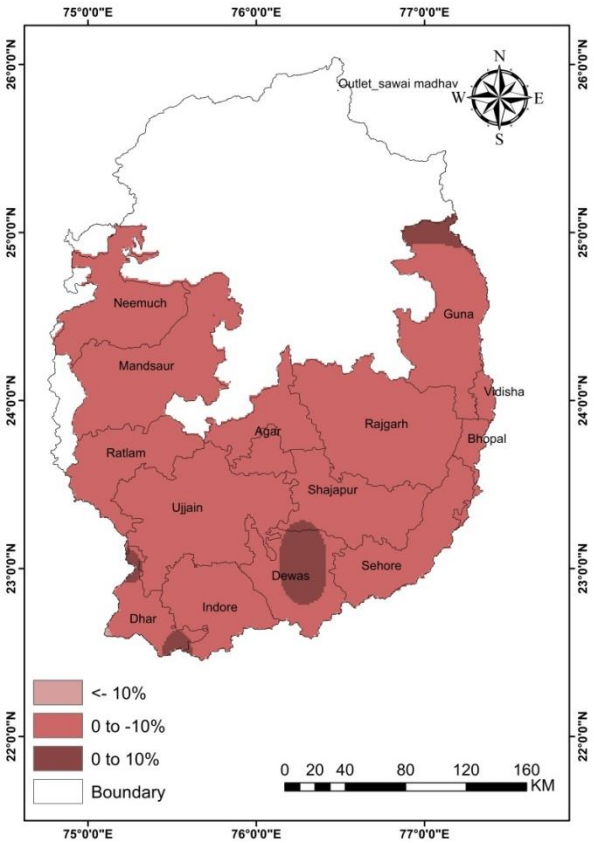

Figure 5.13: Comparison of changes in number of rainy days during present and baseline periods

5.1.1.4 Extreme rainfall analysis

5.1.1.4.1 Heavy rainfall events

To understand the historical pattern of the extreme rainfall events, the rainfall is categorized into three categories viz., heavy rainfall as daily rainfall > 50 mm/day, very heavy rainfall as daily rainfall > 100 mm/day and extreme rainfall as daily rainfall > 200 mm/ day. There was a maximum of 8 heavy rainfall events and the maximum rainfall obtained from these heavy rainfalls event was 808.6 mm in 1973. The minimum number heavy rainfall events are one and the minimum annual rainfall from the heavy rainfall events was 67.8 mm in 1901. On an average, the basin received 3 heavy rainfall events with the annual rainfall contribution of 275.6 mm from such heavy rainfall events. Figure 5.14 shows the annual rainfall from the heavy rainfall events. It can be observed that there is a

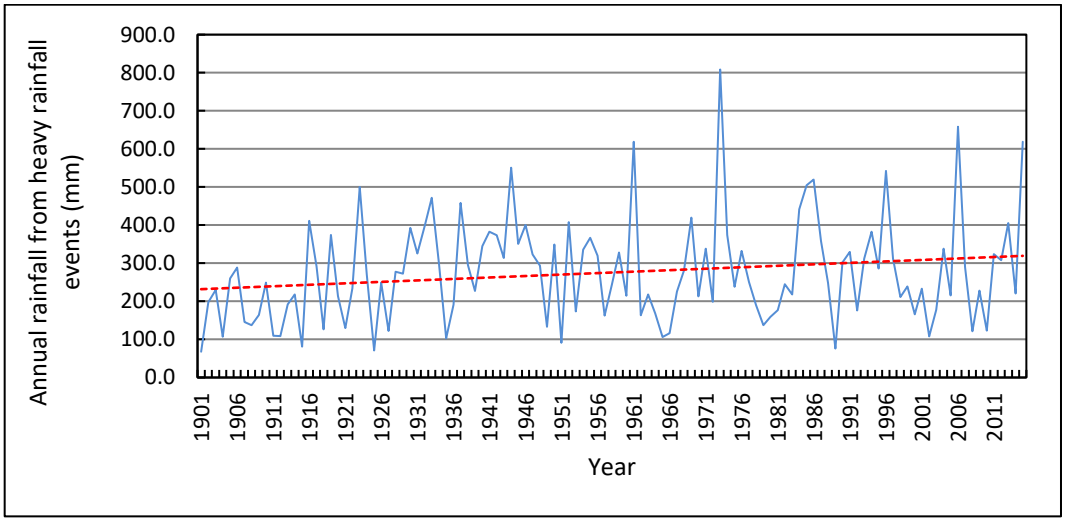

Figure 5.14: Annual rainfall contribution from heavy rainfall events

marginal increase in the annual rainfall contribution received from the heavy rainfall events. The comparison of the heavy rainfall events during baseline period and present time horizon is given Figure 5.15. A mixed pattern has been observed with increase in heavy rainfall events observed in the districts of Neemuch, Mandsaur, Ratlam and Ujjain, whereas a decrease in the heavy rainfall events have been seen in the remaining districts. A decrease of more than 25% in the heavy rainfall contribution has been noticed in some parts of Indore and Dewas districts. Number of heavy rainfall days showed an increase in 25 blocks and decrease in 28 blocks as compared to the baseline period (Figure 5.16). A mixed trend has been observed with an increase in the heavy rainfall events noticed in

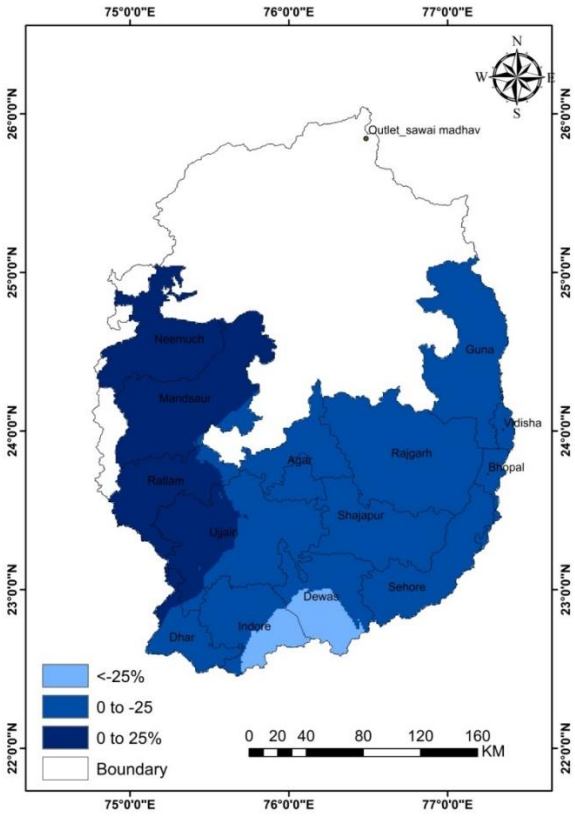

Figure 5.15: Changes in annual maximum heavy rainfall during present and baseline periods

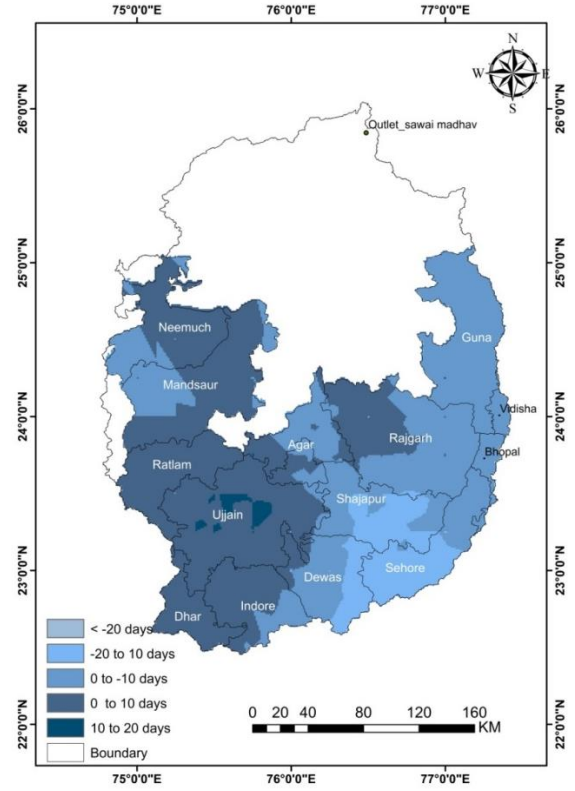

Figure 5.16: Changes in number of heavy rainfall events during present and baseline periods

the districts of Neemuch, Mandsaur, Ujjain, Dhar, Agar, Indore and Rajgarh whereas a reduction in the heavy rainfall events has been observed at Guna, Vidisha, Bhopal, Sehore, Agar, Shajapur and Dewas districts.

5.1.1.4.2 Very heavy rainfall events

Figure 5.17 shows the annual rainfall contribution from the very heavy rainfall events for the period 1951-2015. An increasing trend has been observed in the rainfall obtained from the very heavy rainfall events. The annual rainfall contribution from very heavy rainfall events is 97.6 mm. The spatial variation of

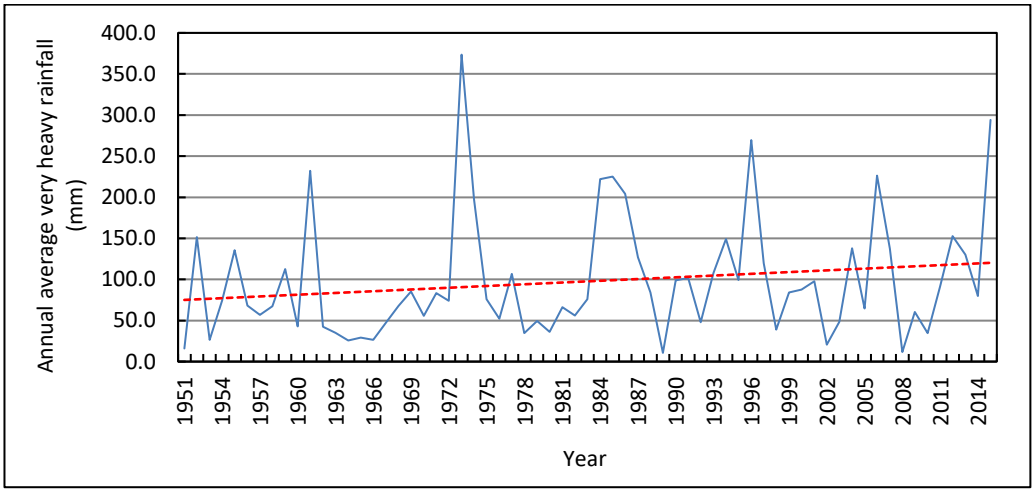

Figure 5.17: Annual rainfall contribution from very heavy rainfall events

the very heavy rainfall is given in Figure 5.18. It can be observed that the very heavy rainfall has also increased in Neemuch, Mandsaur, Ujjain, Indore and Dhar districts whereas it has decreased in the remaining districts. A decrease of more than 25% has been observed at the northern parts of Guna district. Out of the 53 blocks, 32 blocks show an increase in the very heavy rainfall events, the increase varying between 1 to 16 days, whereas 21 grids show a decrease in the heavy rainfall events, the decrease varying between 1 and 18 days. This shows that the occurrences of the very heavy rainfall events have increased in substantial parts of the study area.

5.1.1.4.3 Extreme Rainfall

The maximum of annual extreme rainfall events is given in Figure 5.19. An increasing pattern has been observed in the maximum extreme rainfall in the study

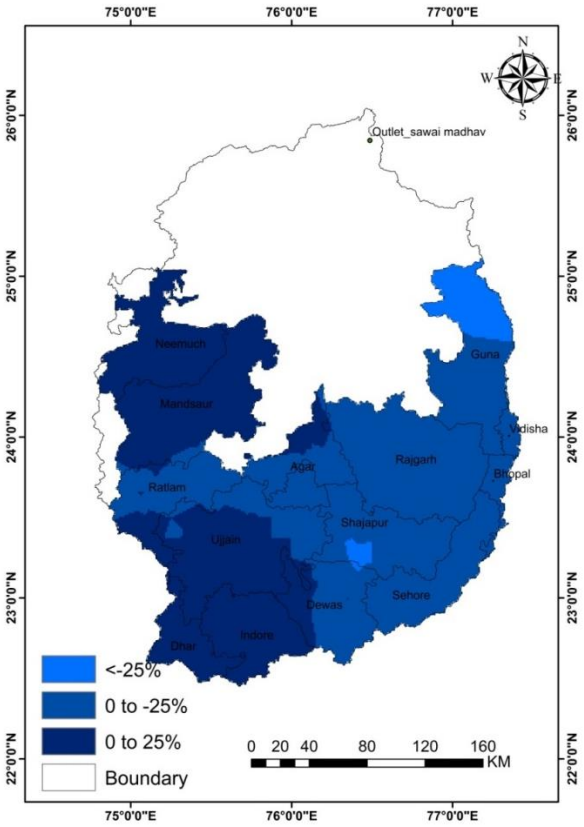

Figure 5.18: Comparison of changes in very heavy rainfall present and baseline periods

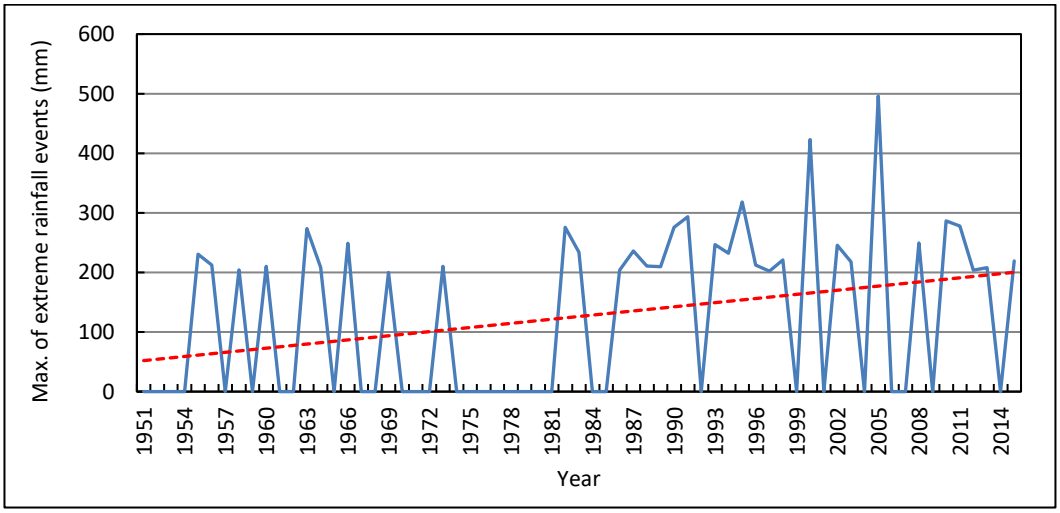

Figure 5.19: Maximum of the extreme rainfall events

area. The comparison of the annual maximum extreme rainfall during the present time horizon with reference to the baseline period is given in Figure 5.20. It can be observed that the maximum extreme rainfall events have increased almost for the entire study area. More than 25% increase has been observed in the districts of

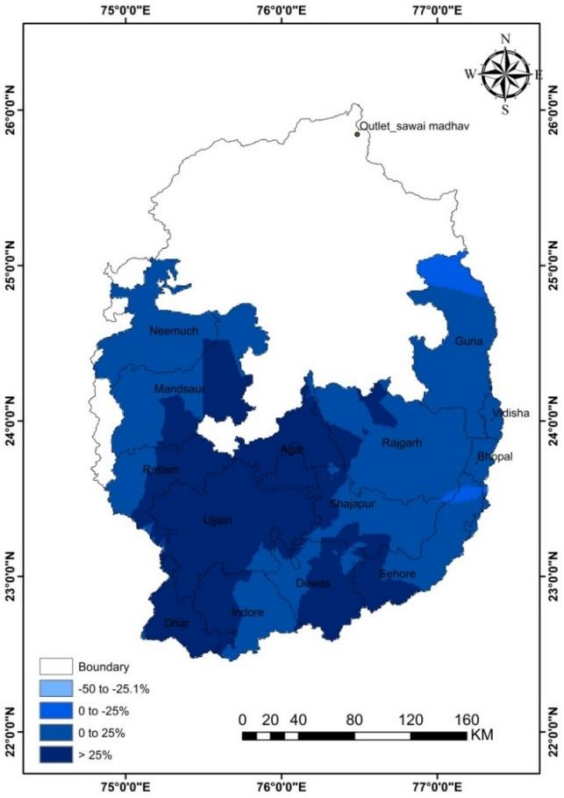

Figure 5.20: Comparison of changes in annual maximum extreme rainfall during present and baseline periods

Agar, Ujjain, Dhar, parts of Mandsaur, Ratlam, Shajapur, Indore, Damoh and Sehore. The extreme rainfall has decreased only in the northern parts of Guna district. The number of extreme rainfall events have increased in 35 blocks varying between 1 to 5 days, whereas the decrease of extreme rainfall events in the range of -1 to -5 days have been observed in 18 blocks.

5.1.1.4.4 1-day Maximum Rainfall

The 1-day maximum rainfall varied between 104.00 mm and 520.00 mm in the study area. The temporal variation of the 1-day maximum rainfall is given in Figure 5.21. No particular trend can be observed in the 1-day maximum rainfall. However, the 1-day maximum rainfall has increased in 29 grids and decreased in 24 grids. The comparison of the changes in 1-day maximum rainfall during the current period with reference to the baseline period is given in Figure 5.22. The1-day maximum rainfall has increased in the districts of Neemuch, Mandsaur, Ratlam, Ujjain, Dhar, Indore, Rajgarh, and parts of Sehore, Bhopal and Vidisha.

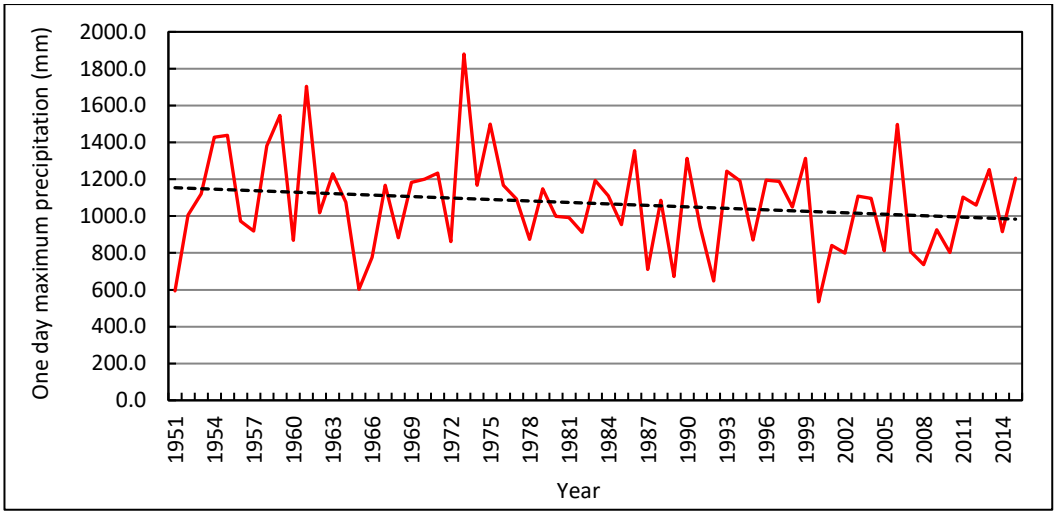

Figure 5.21: Temporal variation of 1-day maximum rainfall

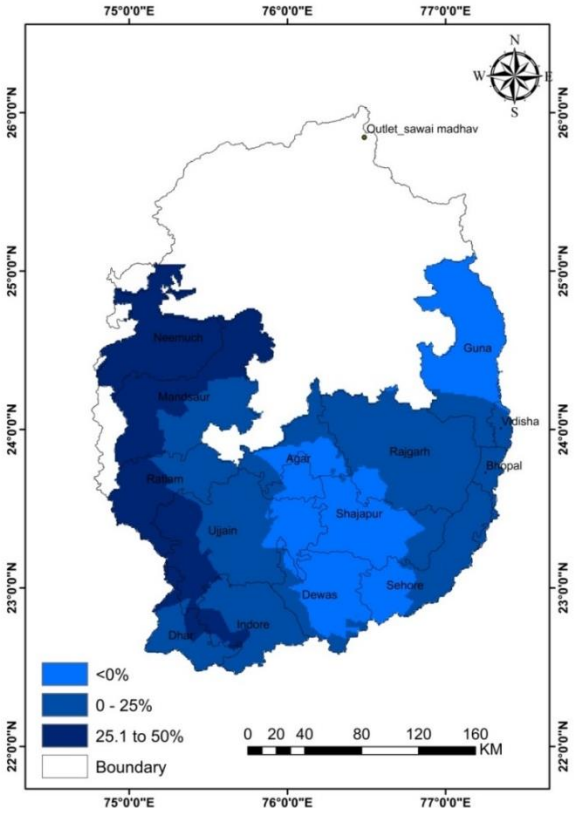

Figure 5.22: Changes in 1-day maximum rainfall during the current period with reference to the baseline period

5.1.1.4.5 Rainfall intensity

The average annual wet day rainfall is 935.0 mm, and the average annual rainfall from non-wet days is 9.20 mm. The temporal variation of the wet day rainfall is given in Figure 5.23 and no distinct trend has been observed. The spatial plot of

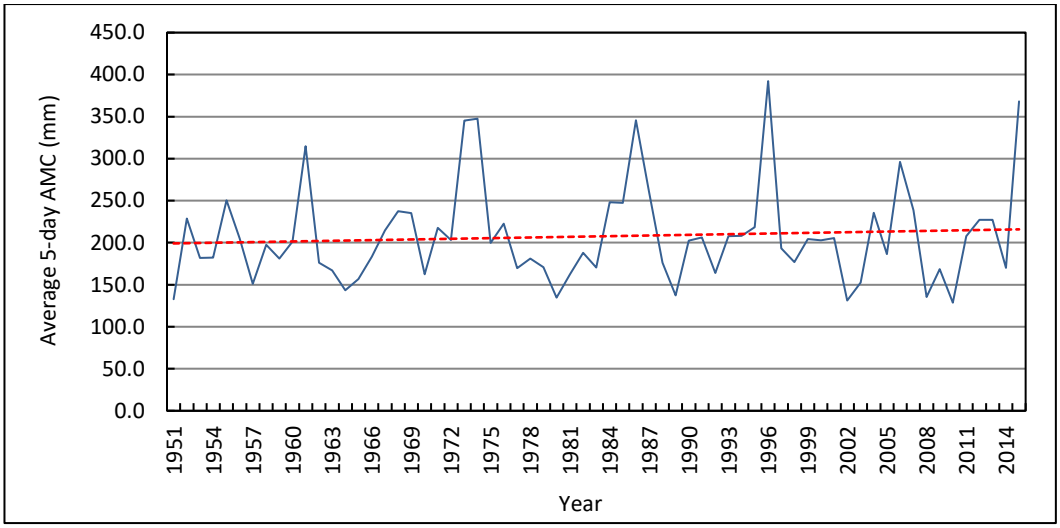

Figure 5.23: Temporal variation of average wet day rainfall

differences in wet day rainfall during present time horizon and the baseline period is given in Figure 5.24. Decrease in the wet day rainfall have been observed in the districts of Mandsaur, Ratlam, Agar, Shajapur, Guna, Sehore, Dewas, parts of Rajgarh, Bhopal and Vidisha whereas the wet day rainfall has increased at Neemuch, Ujjain, parts of Dhar, Rajgarh and Indore districts. There are 30 grids with decreasing wet day rainfall whereas there are 23 grids with increasing wet

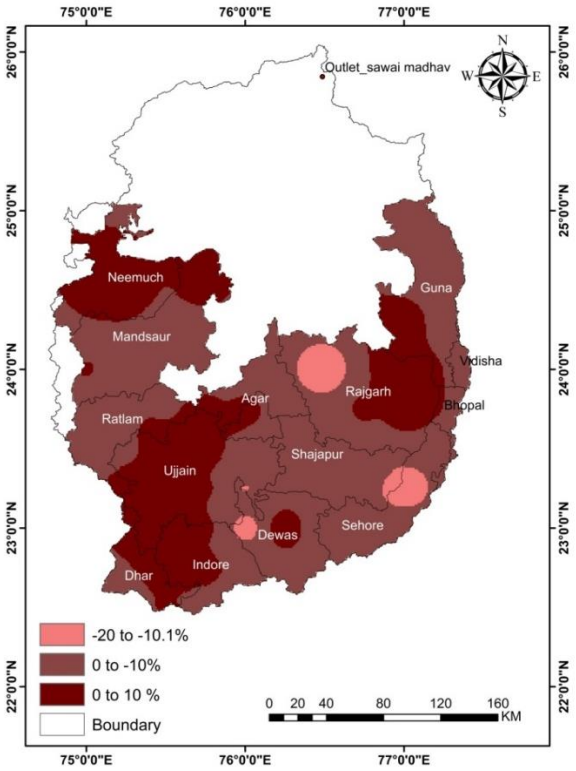

Figure 5.24: Changes in wet day rainfall during present and baseline periods

day rainfall in the study area. The rainfall intensity has been computed as the ratio of wet day rainfall to number of wet days. The average rainfall intensity is 18.82 mm/day. The maximum rainfall intensity varied between a minimum of 18.83 mm/day in 1951 and a maximum of 41.18 mm/day in 2015.in the average rainfall intensity in the present period whereas only 21 grids are showing reduced rainfall intensity. The districts of Neemuch, Mandsaur, Ratlam, Ujjain, Dhar, Indore, parts of Agar, Rajgarh, Guna, Bhopal and Vidisha are depicting an increasing rainfall intensity in the present time horizon. However, few districts have also recorded marginal decrease in rainfall intensity which include Dewas, Shajapur, Sehore, parts of Guna and Rajgarh (Figure 5.25).

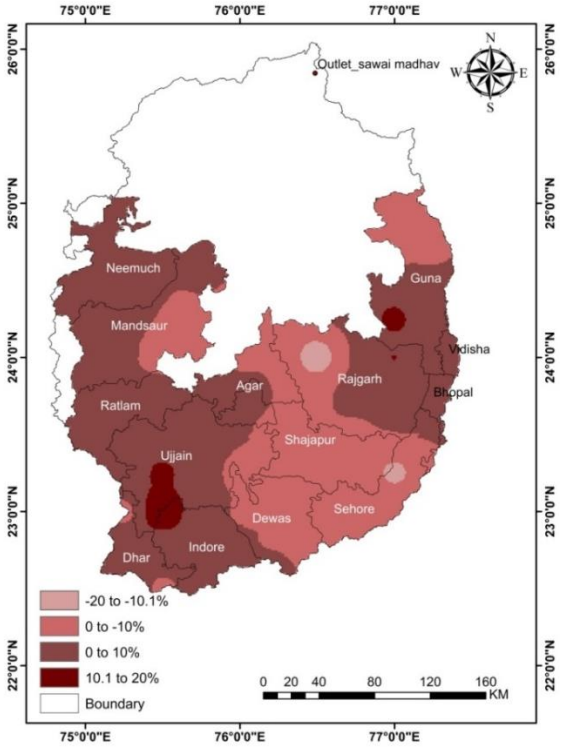

Figure 5.25: Changes in average rainfall intensity during present and baseline periods

5.1.1.4.6 Antecedent Moisture Conditions (AMC)

The 5-day antecedent moisture conditions (AMC) have been extracted from the daily rainfall time series. The spatial plot showing the comparison of the changes in the 5-day AMC during the present time horizon and baseline period is given in Figure 5.26. Majority of the study area comprising of Dhar, Indore, Dewas, Ujjain, Ratlam, Rajgarh, Bhopal, Vidisha, parts of Dewas, Agar, Mandsaur, Neemuch and Guna districts has seen an increase in the 5-day AMC whereas the

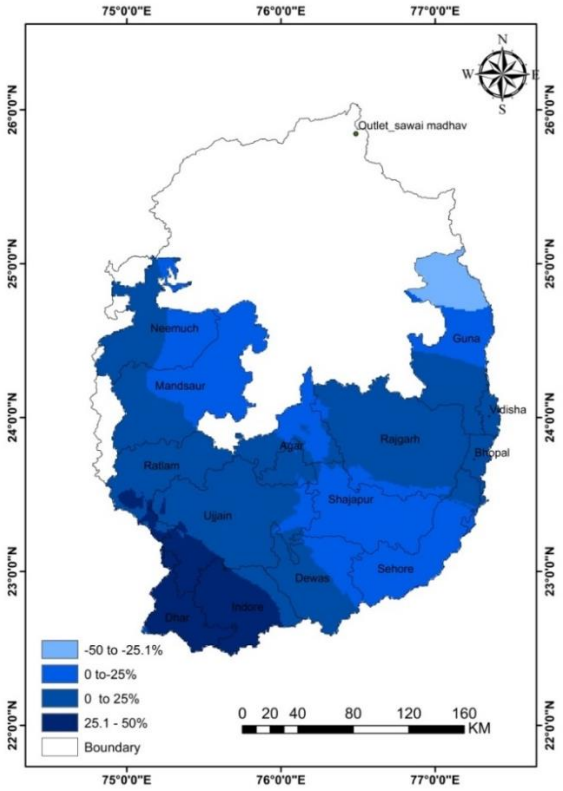

Figure 5.26: Changes in maximum 5-day precipitation during present and baseline periods

5-day AMC has decreased in Shajapur, Sehore, parts of Mandsaur, Neemuch, Guna and Agar districts.

5.1.2 Temperature

The high resolution gridded maximum and minimum temperature at 1^o x 1^o has been used for the evaluation of various temperature indices for the detection of climate change signals in the historical temperature datasets. The study area comprises of 12 grids of 1^o x 1^o resolution. The analysis pertaining to the historical temperature is given in the following sections. The analysis pertaining to the maximum temperature (MaxT) has been further divided into three indices viz., 1-day maximum temperature, very hot days (MaxT>40 ^{o}C) and hot days (MaxT>35 ^{o}C). The analysis pertaining to the minimum temperature (MinT) has been further divided into four indices viz., 1-day maximum of minimum temperature time series, very hot nights (MinT>25^{o}C) and hot nights (MinT>20 ^{o}C) and cold nights (MinT<10 ^{o}C).

5.1.2.1 1-day maximum of MaxT

The annual one-day maximum temperature has been extracted from the time series of the daily maximum temperature (MaxT) for the period 1951-2013 (63 years). The temporal variation of the 1-day maximum of the MaxT is given in Figure 5.27. It can be observed that there is a clear increasing trend in the 1-day maximum temperature in the study area. The spatial plot showing the comparison of the changes in 1-day maximum of MaxT is given in Figure 5.28. The entire study area has witnessed an increase in the 1-day maximum temperature. The average of maximum temperature during the baseline period was 43.40^{o}C which

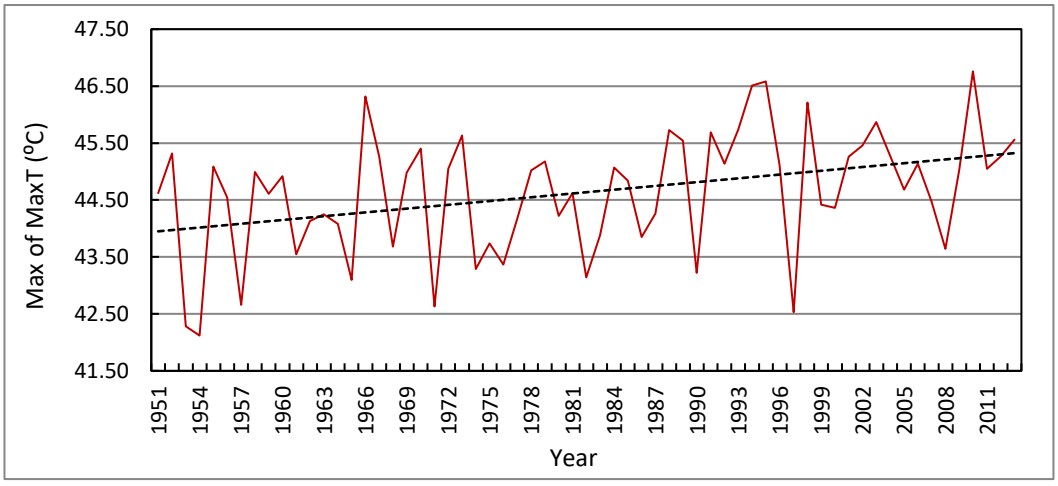

Figure 5.27: Temporal variation of the 1-day maximum of MaxT

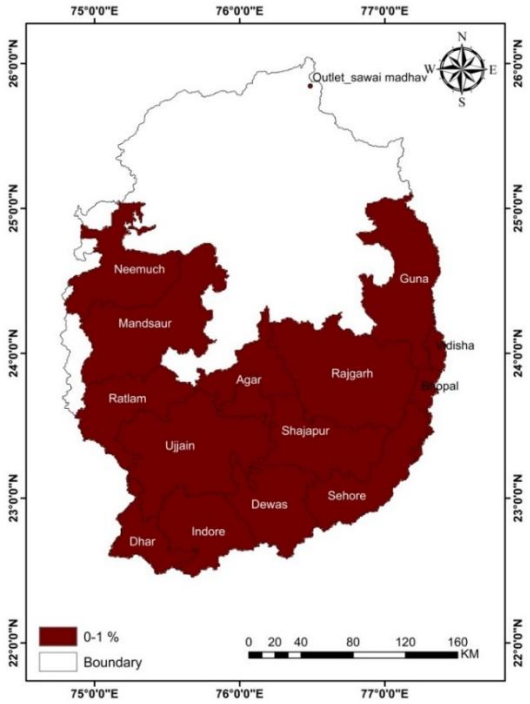

Figure 5.28: Changes in the 1-day maximum temperature

thereafter increased to 44.06°C during the present time horizon. The average increase in the MaxT is at the rate of 1.05°C/100 years, which is quite significant and in tune with the IPCC projections.

5.1.2.2 Very Hot Days

A very hot day has been classified as day during which the maximum temperature is greater than 40°C. The temporal variation of the maximum temperature on very hot days is given in Figure 5.29. It can be observed that the maximum temperature is increasing steadily during the very hot days and all the 12 grids have depicted an increasing trend in the maximum temperature during very hot days.

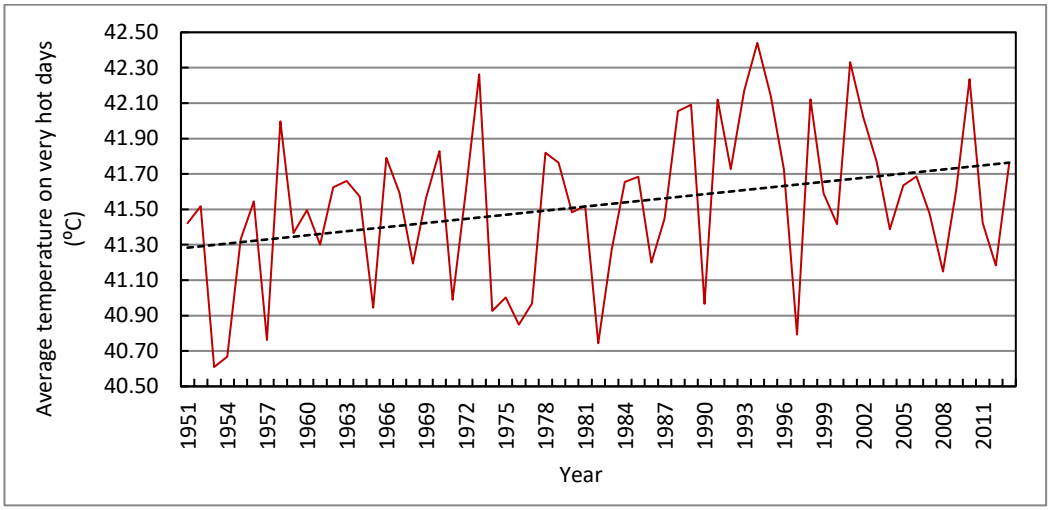

Figure 5.29: Maximum temperature variation on very hot days

Similarly, the variation in the average number of very hot days is given in Figure 5.30. The numbers of very hot days are also increasing steadily in the basin in line with the increase in the very hot day temperatures. On an average, there are 37 very hot days in the basin. The spatial plot showing the average number of days with very hot temperature is given in Figure 5.31. It has been observed that the number of very hot days are maximum in all the districts bordering Rajasthan viz., Neemuch, Mandsaur, Ratlam, Agar, Rajgarh and Guna (150-200 days) whereas the middle portions of the study area comprising of Ujjain, Shajapur, Rajgarh, Bhopal, Vidisha and Guna also has considerable number of very hot days (100-150 days).

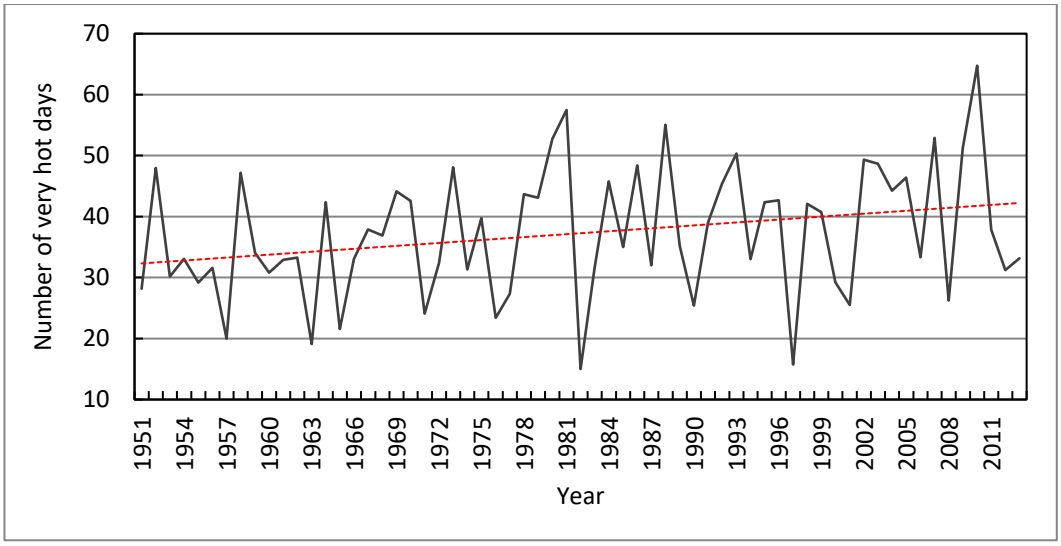

Figure 5.30: Number of very hot days

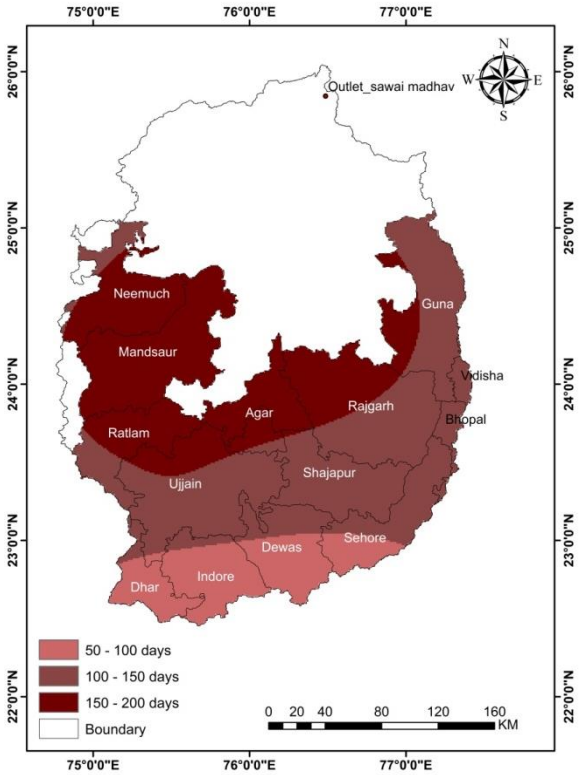

Figure 5.31: Average number of very hot days in the study area

5.1.2.3 Hot Days

A hot day has been classified as day during which the maximum temperature is greater than 35^{o}C. The temporal variation of the maximum temperature on hot days given in Figure 5.32. It can be observed that the maximum temperature is increasing steadily during the hot days and all the 12 grids have depicted an

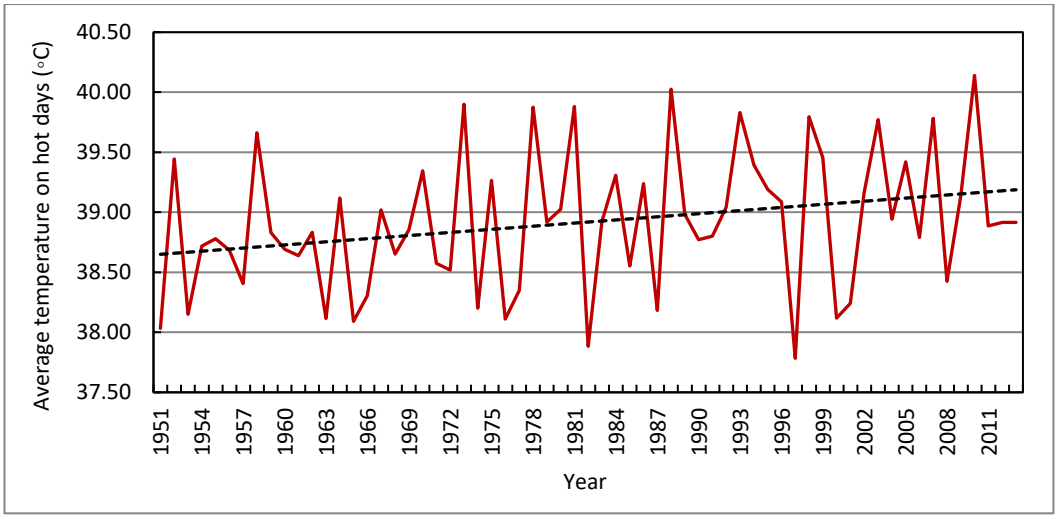

Figure 5.32: Temperature variation on hot days

increasing trend in the maximum temperature during hot days also. On an average, there are 107 hot days in the study area. The spatial plot showing the changes in the number of hot days during the present time horizon and baseline period is given in Figure 5.33. The average number of hot days is increasing in 10 grids and decreasing in 2 grids only. It can be observed that the number of hot days is increasing in major parts of the study area, the increase being maximum

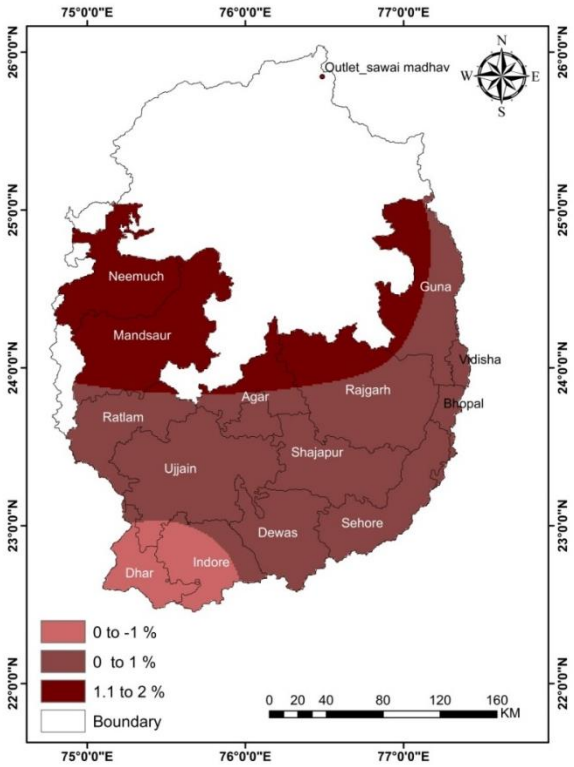

Figure 5.33: Changes in the number of hot days

in the bordering districts of Neemuch, Mandsaur, Agar, Rajgarh and Guna whereas hot days have also increased in Ratlam, Ujjain, Shajapur, Rajgarh Bhopal, Vidisha, Sehore and Dewas.

5.1.2.4 1-day maximum of MinT

The annual 1-day maximum of the minimum temperature time series has been extracted from the time series of the daily minimum temperature (MinT) available during the period 1951-2013 (63 years). The temporal variation of the 1-day maximum of the MinT is given in Figure 5.34. It can be observed that there is no trend in the 1-day maximum of the minimum temperature in the study area. The spatial plot showing the comparison of the changes in 1- day maximum of MinT during the present time horizon and baseline period is given in Figure 5.35.

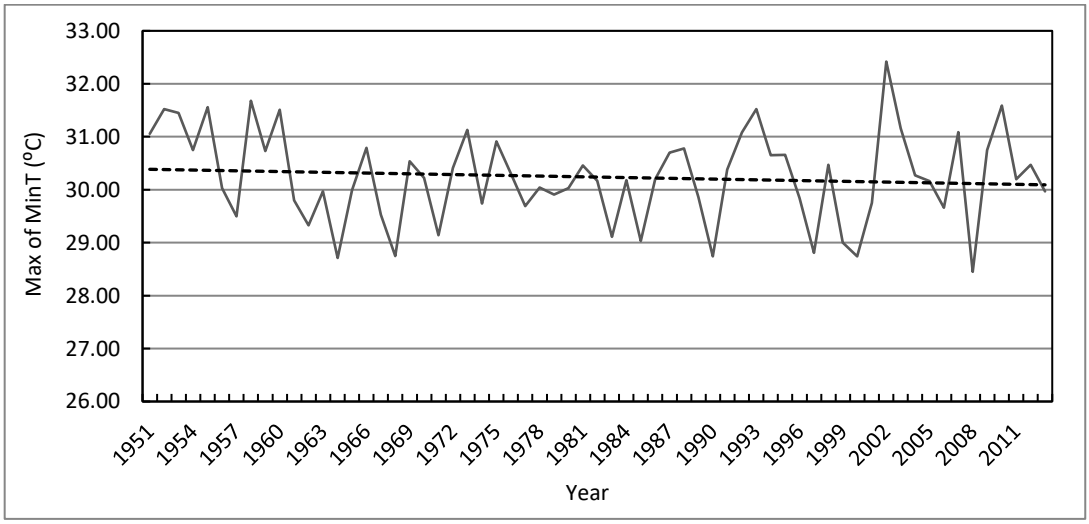

Figure 5.34: 1-day max of MinT

Major portions of the study area, particularly all districts bordering Rajasthan have witnessed increase in the minimum temperature. 11 grids have depicted an increase in the 1-day maximum of the minimum temperature. The bordering districts of Neemuch, Mandsaur, parts of Agar, Rajgarh and Guna have recorded the highest increase in the mean temperature in the rage of 4 to 6% as compared to the baseline period whereas the other districts located in the central portion of the study area viz., Ratlam, Shajapur, major portions of Rajgarh and Guna have seen an increase in the minimum temperature in the range of 2 to 4% as compared to the baseline period. The average MinT during baseline period is 28.67ºC whereas it has increased to 28.91ºC during the present time horizon. The average increase

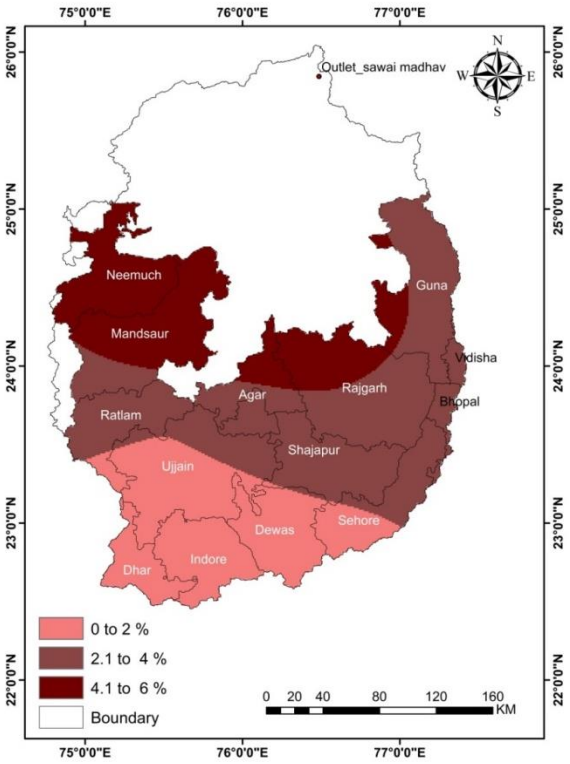

Figure 5.35: Changes in 1-day maximum of MinT

in the minimum temperature is at the rate of 0.38^{o}C/100 yr.

5.1.2.5 Very hot nights

A very hot night has been classified as day during which the minimum temperature is greater than 25^{o}C. The temporal variation of the minimum temperature on very hot days is given in Figure 5.36. It can be observed that there

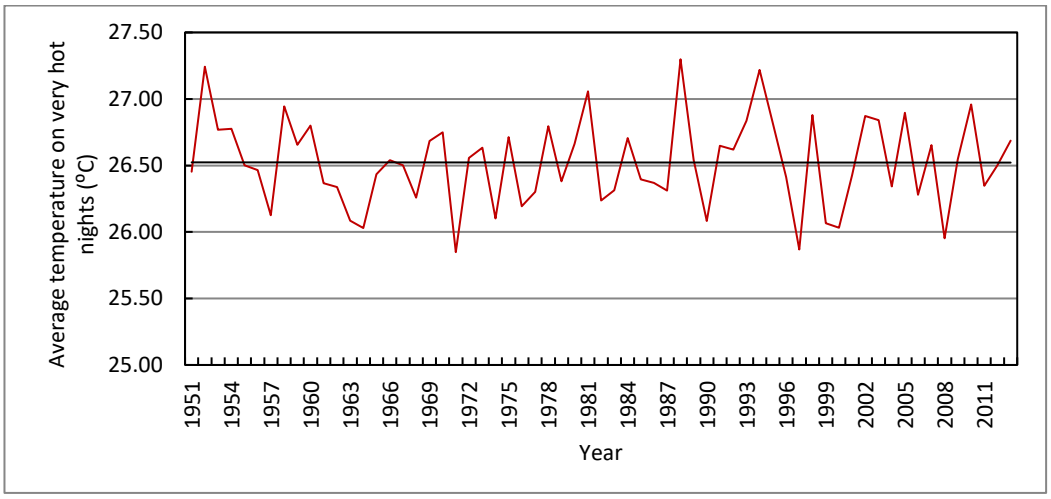

Figure 5.36: Average temperature on very hot nights

is no trend in the variation of the average minimum temperature during the very hot nights. However, the comparison of the average minimum temperature during the very hot nights, between present time horizon and baseline period, shows that all 12 grids depicted an increasing trend. Also, the number of very hot nights was extracted and there are 48 very hot nights on an average in the study area.

The spatial plot showing the comparison of the number of very hot nights during the present time horizon and baseline period is given in Figure 5.37. The number of very hot days has increased in all the 12 grids covering the study area. All the bordering districts have seen an increase in the number of very hot nights, with highest increase in Rajgarh district (>20%) followed by Neemuch, Mandsaur, Agar, Shajapur, Bhopal, Vidisha and Guna (15-20%). Ratlam, Ujjain, Dewas and Sehore districts have also recorded increase in the number of very hot days in the range of 10-15%.

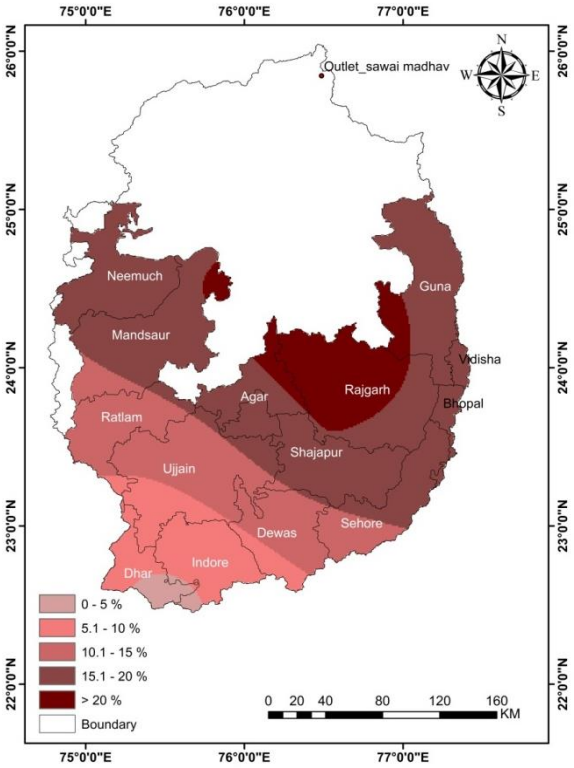

Figure 5.37: Changes in number of very hot nights

5.1.2.6 Hot nights

A hot night has been classified as day during which the minimum temperature is greater than 20^{o}C. The temporal variation of the minimum temperature on hot days in the study area is given in Figure 5.38. It can be observed that there is no

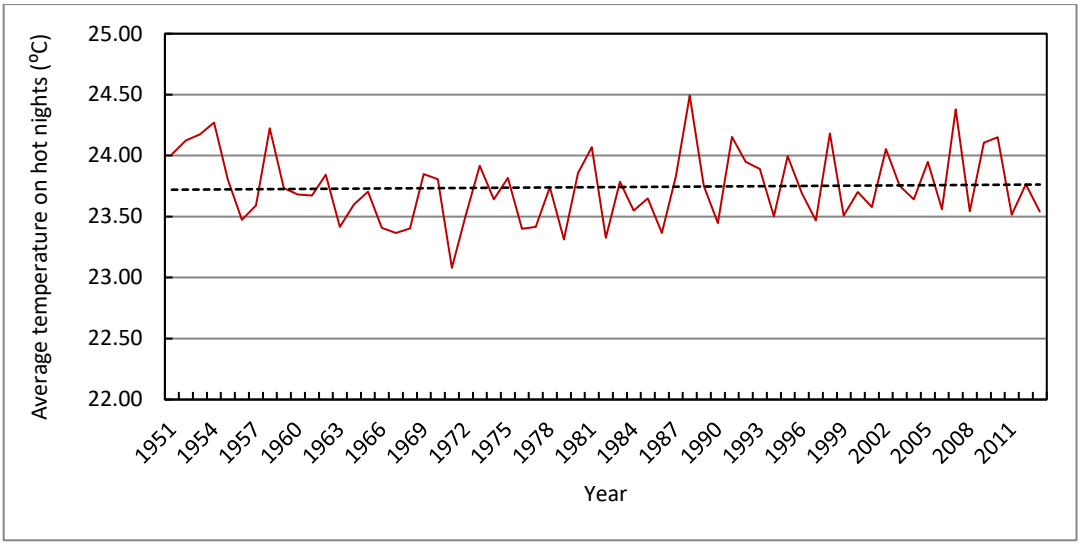

Figure 5.38: Average temperature on hot nights

trend in the variation of the average minimum temperature during the hot nights in the study area. All the 12 blocks have shown an increase in the minimum temperature during the hot nights during the present time horizon as compared to the baseline period. The number of hot nights have also been extracted from the time series of the minimum temperature**.** On an average there are 190 hot nights in the study area. The number of hot nights has also increased substantially in all the 12 grids covering the study area. The spatial plot showing the comparison of the number of hot nights during the present time horizon and baseline period is given in Figure 5.39. All the bordering districts have seen an increase in the number of very hot nights, with highest increase in Neemuch, Mandsaur, Ratlam, Agar, Rajgarh and Guna districts.

5.1.2.7 Cold nights

A cold night has been classified as day during which the minimum temperature is less than 10^{o}C. The temporal variation of the minimum temperature on cold nights in the study area is given in Figure 5.40. It can be observed that there is a small increasing trend in the average minimum temperature during the cold nights in the study area. 11 blocks have shown an increase in the minimum temperature during the cold nights during the present time horizon as compared to the baseline period. The number of cold nights has also been extracted. On an average there are 41 cold nights in the basin. The temporal variation of minimum temperature on cold nights in study area is given in Figure 5.41.

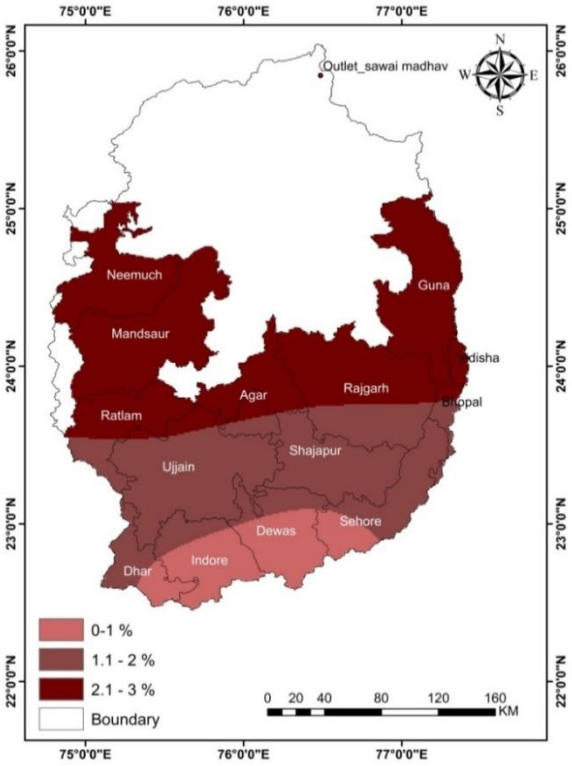

Figure 5.39: Changes in number of hot nights

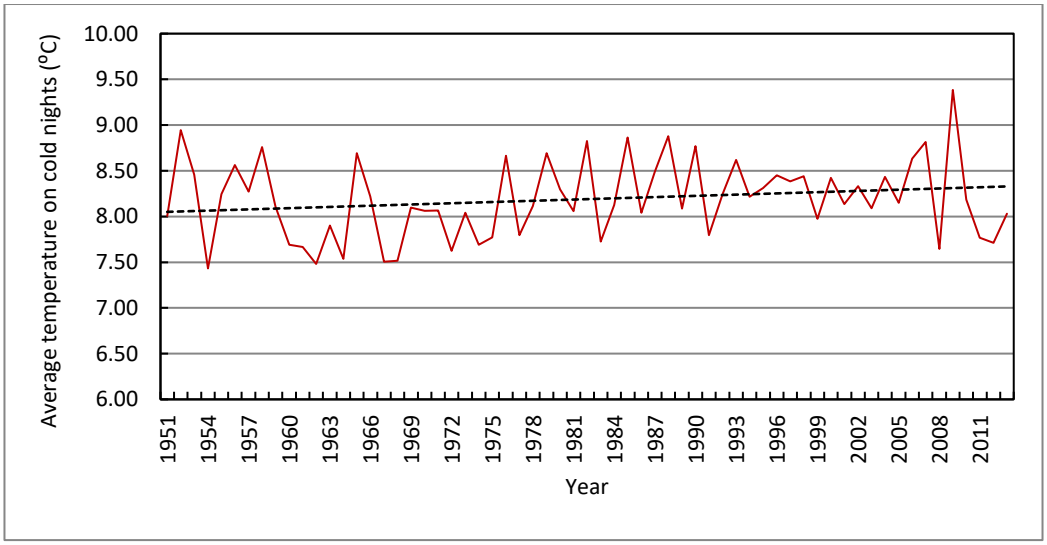

Figure 5.40: Average temperature on cold nights

It can be observed that there is a clear decreasing trend in the number of cold nights in the study area. This suggests that a a consequence of the warming, the cold nights have decreased in all the 12 grids in the study area. The comparison of the number of cold nights during the present time horizon and baseline period is given in Figure 5.42.

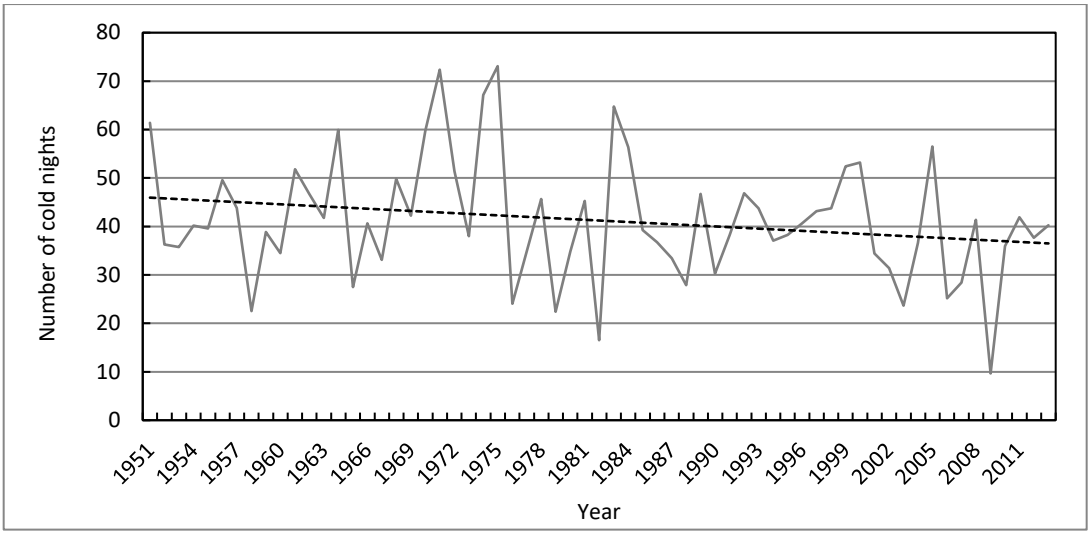

Figure 5.41: Number of cold nights

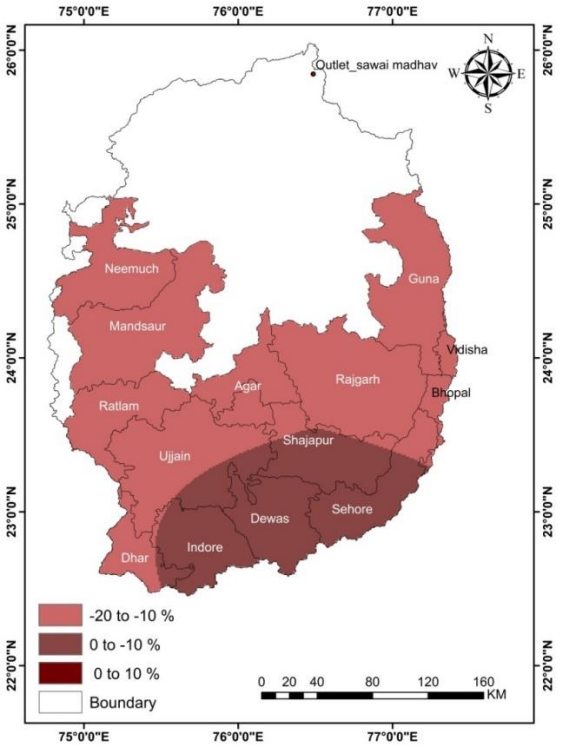

Figure 5.42: Changes in the number of cold nights

It shows that all the districts bordering Rajasthan have seen a decrease in the number of cold nights particularly in the districts of Neemuch, Mandsaur, Ratlam, Agar, Ujjain, Dhar, Rajgarh, Guna, Bhopal and Vidisha.

5.1.3 Detection of Trends

The various climate indices pertaining to the rainfall, maximum and minimum temperature have been evaluated and their spatial plots studied in detail to detect the changes and relate it to the climate change and its impacts as described in the previous section. The non-parametric Mann-Kendall test has been used to detect the trend in the climatic variables and various climate indices after checking for serial correlation and pre-whitening wherever found necessary.

5.1.3.1 Rainfall

The Mann-Kendall test was applied to the times series of the average annual rainfall at the 53 grids (blocks) covering the study area. A significant increasing trend at 95% confidence level has been observed at 6 grids only out of the 53 grids (Table 5.3). This indicates in major portion of the study area, there have been no significant trends in the annual average rainfall. However, there is a decreasing trend in the number of rainy days and significant falling trends have been noticed at Dahi, Bagh, Gandhwani, Badnagar, Sanwar, Dewas, Ashta, Kukshi, Malhargarh and Ranpur (Table 5.4). A significant increasing trend in the heavy rainfall was seen only at Manawar, Dhar, Kannod and Piploda (Table 5.5) whereas the number of days with heavy rainfall has increased only at Manawar (Table 5.6).

Table 5.3: Increasing trends in average annual rainfall

S. No.	Station name	Test statistic	Trend
1.	Badnawar	3.41	+
2.	Bajna	2.79	+
3.	Piploda	2.01	+
4.	Khachrod	2.72	+
5.	Neemuch	2.16	+
6.	Manasa	2.47	+

Table 5.4: Decreasing trends in annual number of rainy days

S. No.	Station name	Test statistic	Trend
1.	Dahi	-2.13	-
2.	Bagh	-2.40	-
3.	Gandhwani	-2.18	-
4.	Badnagar	-2.30	-

5.	Sanwar	-2.23	-
6.	Dewas	-2.60	-
7.	Ashta	-2.21	-
8.	Kukshi	-2.33	-
9.	Malhargarh	-1.96	-
10.	Ranpur	-2.53	-

Table 5.5: Increasing trends in annual average heavy rainfall

S No.	Station name	Test statistic	Trend
1.	Manawar	2.17	+
2.	Dhar	1.97	+
3.	Kannod	1.96	+
4.	Piploda	2.11	+

Table 5.6: Increasing trends in annual number of days with heavy rainfall

S. No.	Station name	Test statistic	Trend
1.	Manawar	2.16	+

The MK test has also been applied to the very heavy rainfall events. Table 5.7 gives the trend in the rainfall from very heavy rainfall events. Even though there is an overall increasing trend in the rainfall obtained from the heavy rainfall events, significant rising trends have been observed only at 8 rainfall grids in the study area. Similarly, Table 5.8 gives the trend in the number of days of heavy rainfall events. Significant rising trends were observed only at Gandhwani, Dhar, Mhow, Piploda and Khilchipur. In general, the 1-day maximum rainfall has increased in the basin, but significant rising trends have been observed only at Gandhwani, Nalcha, Depalpur, Badnagar, Rajgarh and Manasa blocks as given in Table 5.9. However, the wet day precipitation has increased only at Sehore and Zirapur as given in Table 5.10.

Table 5.7: Increasing trends in rainfall from very heavy rainfall events

S. No.	Station name	Test statistic	Trend
1.	Gandhwani	2.19	+
2.	Nalcha	2.15	+
3.	Depalpur	1.96	+
4.	Bajna	2.03	+
5.	Rajgarh	2.06	+
6.	Biaora	2.29	+
7.	Manasa	1.98	+
8.	Bhanpura	2.22	+

Table 5.8: Increase in annual number of days with very heavy rainfall events

S. No.	Station name	Test statistic	Trend
1.	Gandhwani	2.20	+
2.	Dhar	1.97	+
3.	Mhow	1.99	+
4.	Piploda	2.03	+
5.	Khilchipur	2.29	+

Table 5.9: Increasing trends in the annual 1-day maximum rainfall

S. No.	Station name	Test statistic	Trend
1.	Gandhwani	2.38	+
2.	Nalcha	2.46	+
3.	Depalpur	2.28	+
4.	Badnagar	2.37	+
5.	Rajgarh	2.02	+
6.	Manasa	2.59	+

Table 5.10: Decreasing trends in the annual wet day precipitation

S. No.	Station name	Test statistic	Trend
1.	Sehore	-2.30	-
2.	Zirapur	-1.97	-

Table 5.11 gives the trends in the rainfall intensity and it can be observed that significant rising trends have been observed in 14 rainfall grids located at Bagh, Gandhwani, Udainagar, Labaria, Budhni, Badnagar, Sanwar, Bajna, Sehore, Agar, Narsingarh, Ranpur, Bhanpura and Sarangpur blocks, The increase in the rainfall intensity is mainly due to the reduction in the number of the wet day events and may be one of the major reasons for the widespread soil erosion and land degradation in the study area.

Table 5.11: Increasing trends in the average rainfall intensity

S. No.	Station name	Test statistic	Trend
1.	Bagh	2.59	+
2.	Gandhwani	3.09	+
3.	Udainagar	2.07	+
4.	Labariya	2.12	+
5.	Budhni	3.18	+
6.	Badnagar	2.69	+
7.	Sanwar	2.14	+
8.	Bajna	2.29	+
9.	Sehore	-2.16	-

10.	Agar	2.24	+
11.	Narsingarh	2.26	+
12.	Ranpur	2.09	+
13.	Bhanpura	2.09	+
14.	Sarangpur	2.57	+

5.1.3.2 Maximum and Minimum Temperature

The MK test has been employed to detect the significant trends in the maximum and minimum temperature time series. A significant rising trend at 95% confidence level has been observed for the 1–day maximum of the maximum temperature (Z= +2.81). Significant rising trends have been observed for the maximum number of very hot nights (Z= +2.26) and the maximum number of hot nights have also shown significant rising trends in the study area (Z= +2.52). Also, the average number of cold nights have decreased in the study area (Z= -2.20). Another interesting finding is that the minimum temperature is increasing significantly at 95% confidence level (Z= +2.70). Table 5.12 gives the significant decreasing trends in number of cold nights at few (5) temperature grids whereas the minimum of MinT has shown significant rising trends at 5 grids as given in Table 5.13.

Table 5.12: Increasing trends in the number of cold nights

S. No.	Latitude	Longitude	Test statistics	Trend
1.	22.5	77.5	-2.25	-
2.	23.5	77.5	-2.39	-
3.	24.5	75.5	-1.97	-
4.	24.5	76.5	-2.48	-
5.	24.5	77.5	-2.81	-

Table 5.13: Increasing trend in the minimum of MinT

S. No.	Latitude	Longitude	Test statistics	Trend
1.	23.5	75.5	2.22	+
2.	23.5	76.5	1.96	+
3.	24.5	75.5	2.76	+
4.	24.5	76.5	2.88	+
5.	24.5	77.5	2.13	+

5.2 Desertification analysis

5.2.1 Aridity Index (AI)

The aridity index (AI) has been computed based on the annual rainfall and the annual potential evapotranspiration (PET). The PET has been estimated by the Thornthwaite method. The average aridity has increased in the basin as the aridity index has decreased from 0.60 during the baseline period to 0.57 during the current period (5%). The temporal variation of the aridity during 1951-2013 is given in Figure 5.43. The comparison of the AI during the present time horizon and baseline period indicated that the aridity in increasing in 11 out of the 12 grids covering the study area. The spatial plot showing the comparison of the AI is given in Figure 5.44.

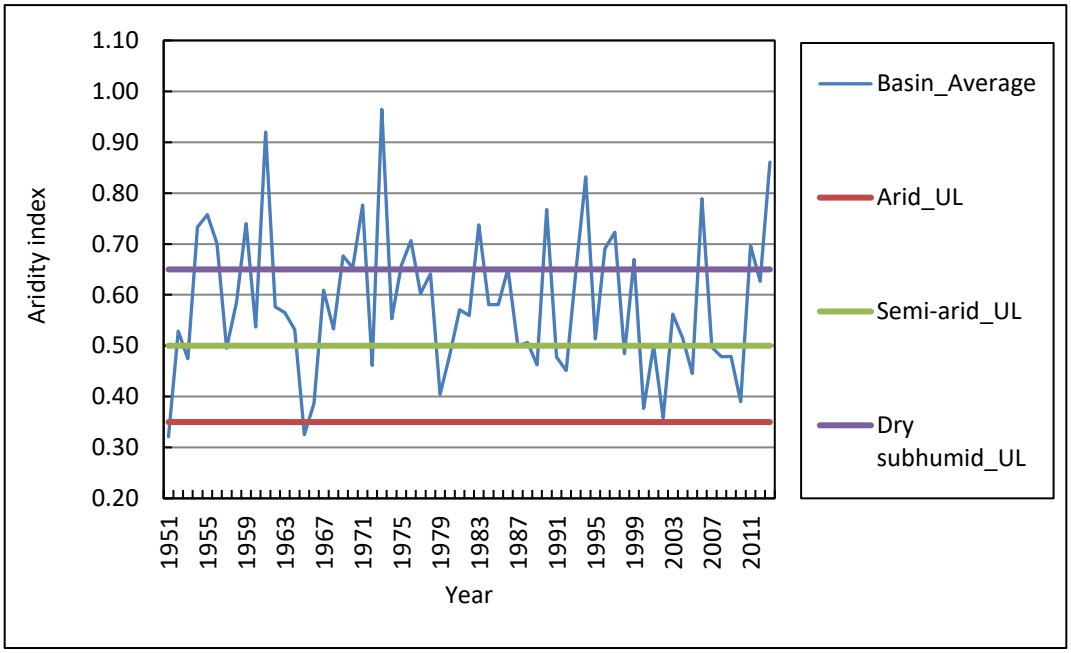

Figure 5.43: Temporal variation of the Aridity index in the study area

5.2.2 Agriculture Statistics based analysis

The district statistical handbooks for most of the districts in the study area containing the information about the various statistics of the districts and the blocks have been collected. As compared to year 2000, the agricultural area during year 2015 decreased substantially in the seven districts comprising of Dewas, Indore, Mandsaur, Neemuch, Sehore, Ratlam, Shajapur and Ujjain,

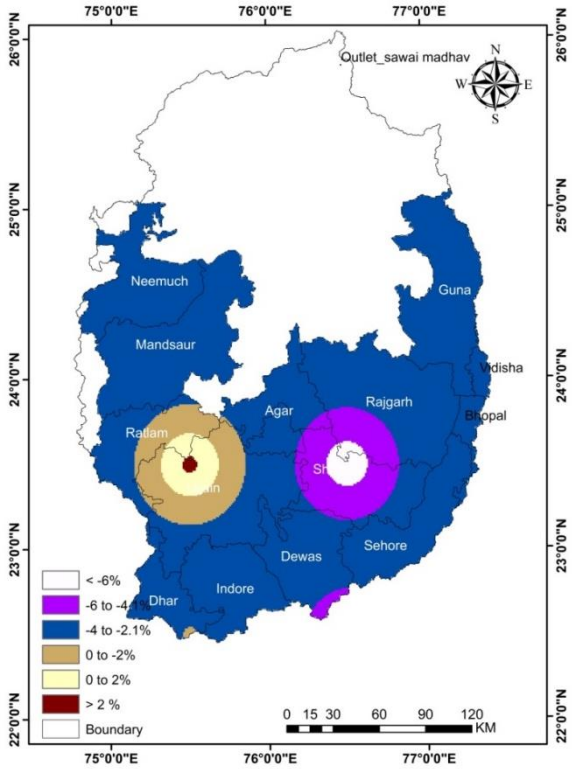

Figure 5.44: Comparison of changes in Aridity Index during present and baseline periods

whereas the agricultural area increased marginally in Rajgarh and Guna districts. On the basis of the years 2000, 2006, 2011 and 2015, it has been observed that the agricultural area has been decreasing steadily in most of the districts. The spatial plot of the decrease in the agricultural area during 2015 as compared to 2000 is given in Figure 5.45. It can be observed that the reduction in agricultural area is widespread in the study area, and may be attributed to many factors including reduced water availability and soil fertility with land degradation aspects.

Similarly, the 'land not available for agriculture' is increasing significantly in Indore, Mandsaur, Sehore, Ratlam, Shajapur, Dhar, Agar and marginally decreasing in Guna and Rajgarh. The comparison of the changes in 'land not available for agriculture' during 2015 and 2000 is given in Figure 5.46. It can be seen that lesser area is presently (2015) available for agriculture as compared to2000, with more and more land becoming unsuitable for agriculture due to the land degradation and other factors. The agriculture based statistical analysis considering the 'agricultural area' and 'land not suitable for agriculture' has indicated progressive decline in the land availability for agricultural operations.

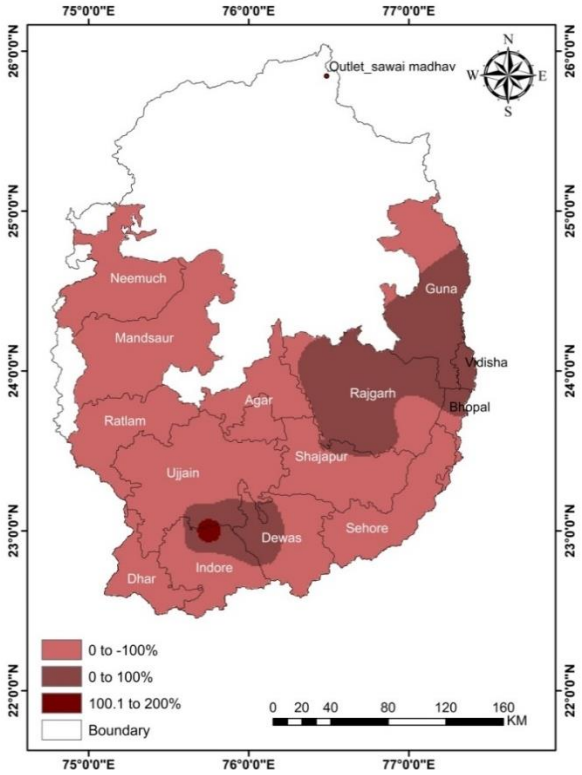

Figure 5.45: Changes in agricultural area during 2015 as compared to 2000

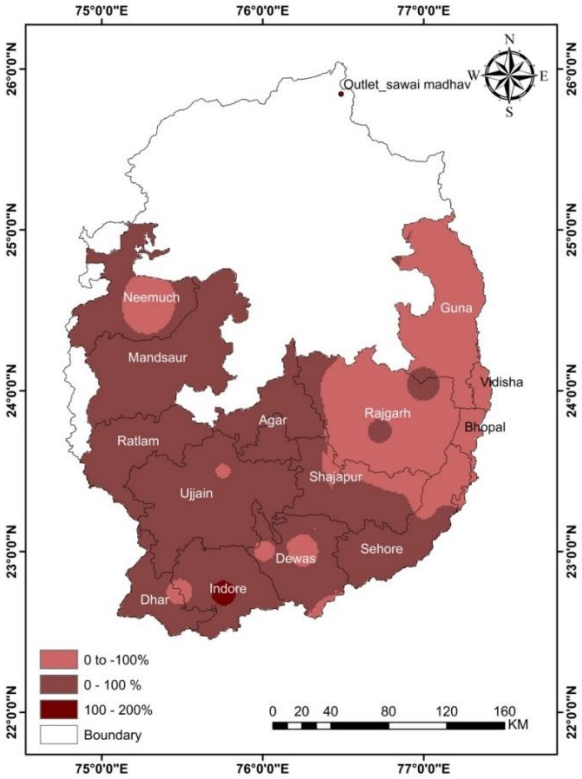

Figure 5.46: Changes in land not available for agriculture during 2015 as compared to 2000

This may also be an indication of the progression of the land degradation/desertification processes.

A comparison of the cropping pattern in the study area during 2015 and 2000 shows that area under paddy cultivation and pulses have decreased substantially in Mandsaur, Neemuch, Ratlam and Rajgarh districts. However, the area under oilseeds and non-fodder crops, which are less water intensive, have increased substantially in the study area. Wheat cultivation has increased in most of the major districts in the study area. The crop yields have decreased substantially in some of the districts bordering Rajasthan particularly Mandsaur, Neemuch, Rajgarh, and Ratlam. Significant reduction in the crop yield has been observed for soybean, tuar which are rain-fed crops in most of the districts. Also, the number of macro-farmers (land holding > 10 ha) and medium farmers (land holding of 4-10 ha) have decreased substantially in most districts. However, the number of marginal farmers (land holding < 1ha), small farmers (land holding of 1-2 ha) and semi-medium farmers (land holding of 2-4 ha) have increased considerably in the study area. The species distribution under the livestock population has changed considerably wherein the goat and sheep population has increased substantially in most of the districts. The goat and sheep often grazes the grasslands completely, making it exposed and barren, which subsequently leads to higher rates of soil erosion and loss of soil fertility and land degradation.

5.2.3 Land Use/Land Cover Classification

The land use / land cover (LULC) classification has been carried out for the study area using the LANDSAT TM satellite data available at 30 m resolution. The supervised classification (decadal) has been carried out for the years 2000, 2001 and 2010. The years have been selected based on the availability of cloud free satellite data for the complete study area. The major land use classes in the study area are agriculture, water, settlements, forest and barren lands.

The accuracy of the land cover classification was ascertained during the various stages of the classification process by removing the errors and miscalculations step-by-step from each classified image obtained at the end of each stage. This included selection of cloud free datasets to avoid missing pixels caused by

cloudiness as the cloud covered areas cannot be classified as they have no spectral values on which to apply the classifier. Cloud free datasets were available for the various years considered for the classification of land cover in the study area. If such an issue still exists for other areas of interest, then it better to expand the mosaic to include more years of data for image composting and re-extract the spectral values at various points and rebuild the classifier.

Apart from this, miscalculation errors can also occur wherein a particular land cover class is not classified correctly and made to fall in a separate class to which it does not belong. This occurs when a pixel of one class falls in the spectral data space that the classifier has assigned to a different class. This can be solved by providing more dimensionality to the spectral data space or by adding more training points in the regions where misclassification is taking place or by adopting a more flexible classifier to the same dataset (CART) or by applying a different supervised classifier like random forests machine learning etc.

After applying these checks and rectification of all errors, the final land cover classified map is also tested for accuracy by carrying out the ground truth verification exercise which has been discussed earlier in detail in Section 4.2.3. The ground truth verification was carried out for areas falling under agriculture, forests, barren, settlements and forests. Apart from this, extensive ground truth verification was also carried at all the soil sampling sites in the study area. Figure 5.57 to Figure 5.60 also shows the agriculture fields with crops which tallied with the LULC classified data.

The classified LULC map for the study area during 1990, 2001 and 2010 is given in Figure 5.47, Figure 5.48 and Figure 5.49 respectively. It can be observed that the barren areas have increased in Neemuch district along with barren patches in Mandsaur, Agar, Shajhapur and Rajgarh districts. The area under the various land use classes during 1990, 2001 and 2010 is given in Table 5.14 whereas the percentage area under various land use classes is given in Table 5.15. The changes in the LULC during the different decades are given in Table 5.16. It can be observed that there is a significant increase in the barren areas by 2010, by as much as 25% as compared to 1990. The agricultural area has also reduced marginally by 2.19%.

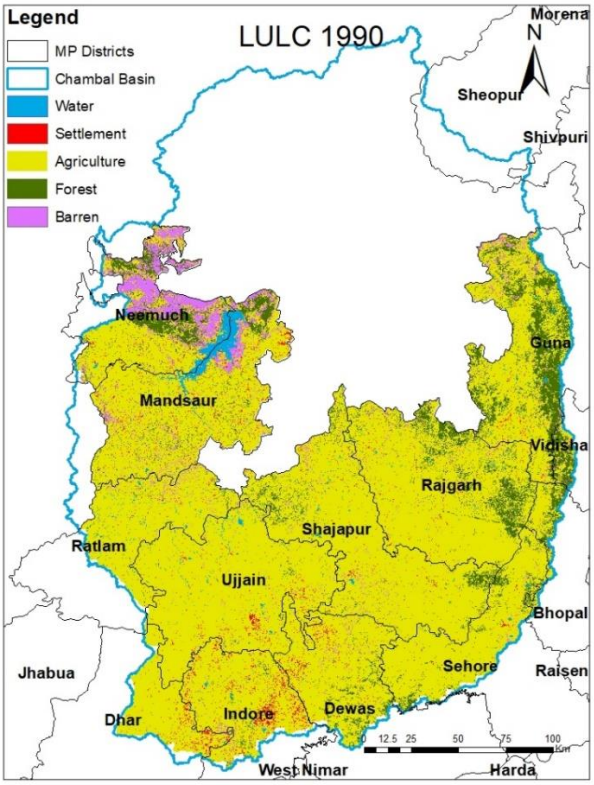

Figure 5.47: Land use land cover classification during 1990

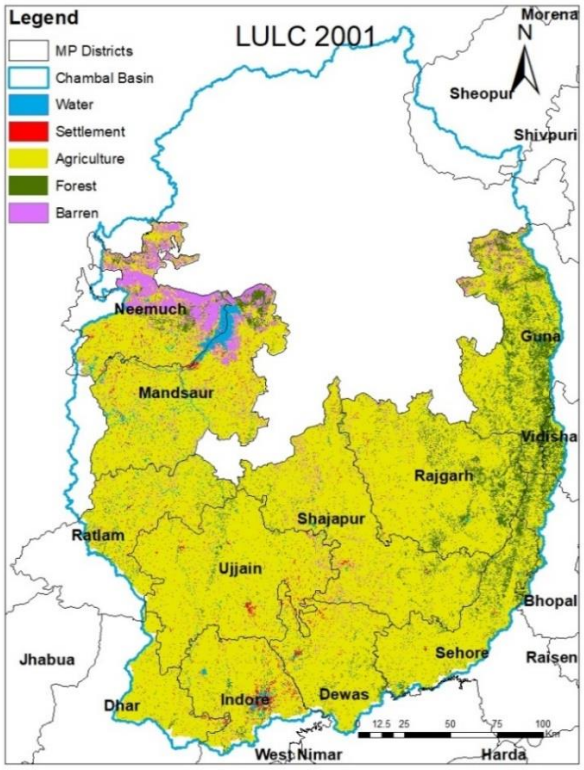

Figure 5.48: Land use land cover classification during 2001

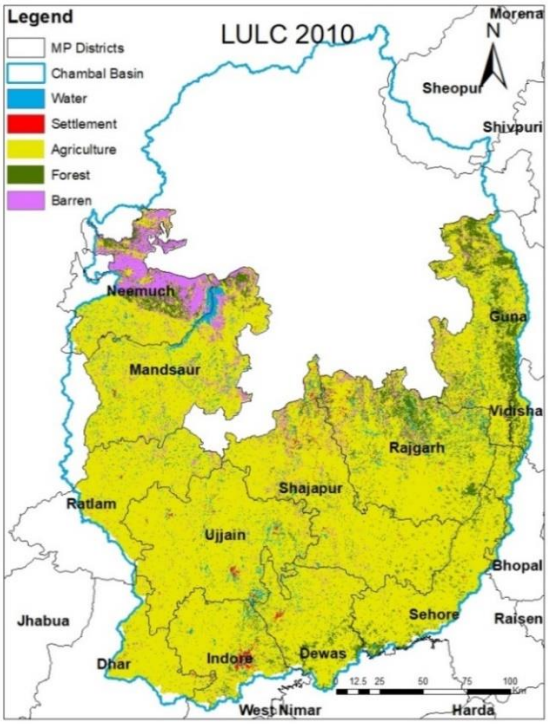

Figure 5.49: Land use land cover classification during 2010

Table 5.14: Land use classes

Land use classes	1990	2001	2010
	(area in sq. km)		
Water	827.74	900.60	1472.95
Urban	692.81	626.86	331.46
Agriculture	36090.08	35727.91	35300.53
Forest	3884.42	3615.39	3713.17
Barren	2564.79	3178.56	3222.61

Table 5.15: Area under various land use classes

Land use	1990	2001	2010
	(Percentage area)		
Water	1.88	2.04	3.34
Urban	1.57	1.42	0.75
Agriculture	81.91	81.11	80.15
Forest	8.82	8.21	8.43
Barren	5.82	7.22	7.32

Table 5.16: Changes in the LULC during different decades

Land use	Changes (%)		
	2001-1990	2010-2001	2010-1990
Water	8.80	63.55	77.95
Urban	-9.52	-47.12	-52.16

Agriculture	-1.00	-1.20	-2.19
Forest	-6.93	2.70	-4.41
Barren	23.93	1.39	25.65

The changes in the LULC have been evaluated for the districts bordering Rajasthan including Neemuch, Mandsaur, Ratlam, Agar, Rajgarh and Guna. The land use land cover for Neemuch district during 1990, 2001 and 2010 is given in Figure 5.50. It can be observed that there is a considerable decrease in the area under agriculture as well as the area under forest cover. However, there is a

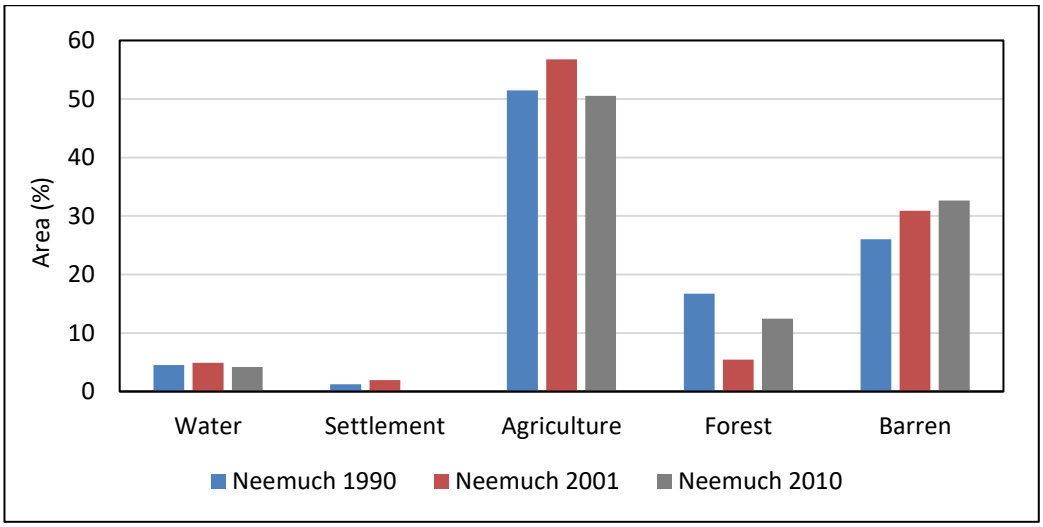

Figure 5.50: Neemuch district LULC during 1990, 2001 and 2010

considerable increase in the barren areas in the district. Similar pattern of increase in barren area coupled with the decrease in agricultural area is also observed at Agar district (Figure 5.51). However, there is an increase in the agricultural area as well as a marginal decrease in the barren area in Mandsaur district as observed in Figure 5.52. A considerable reduction in the agricultural area has been observed in Rajgarh district, whereas the barren area has witnessed marginal increase (Figure 5.53). However, it can be observed that the forested area has decreased in Guna district along with an increase in barren areas (Figure 5.54). In general, it can be seen that there is a marginal decrease in the agricultural areas but the barren areas have increased considerably in most of the districts bordering Rajasthan.

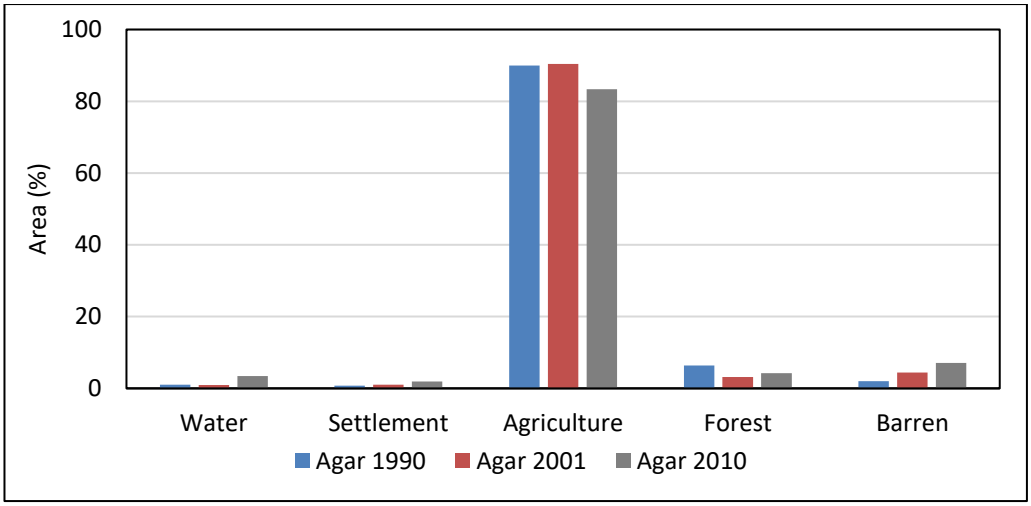

Figure 5.51: Agar district LULC during 1990, 2001 and 2010

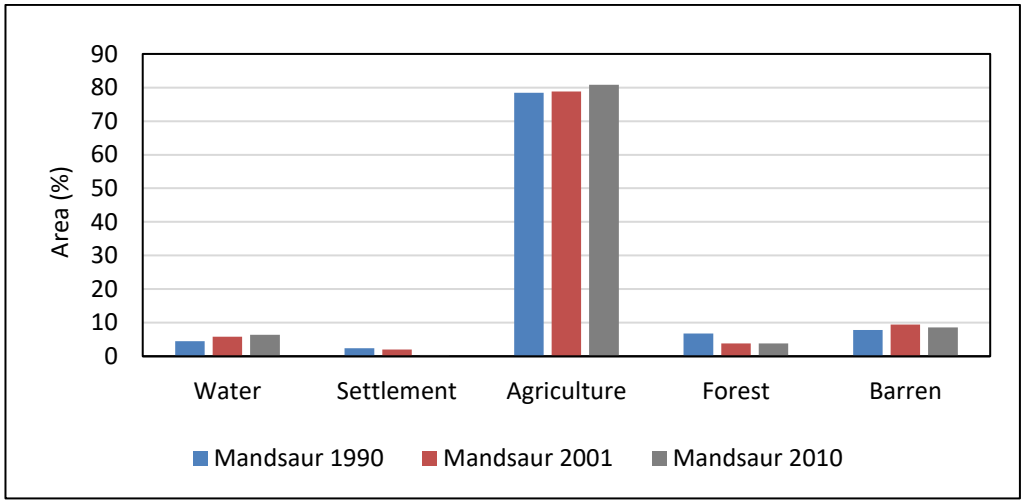

Figure 5.52: Mandsaur district LULC during 1990, 2001 and 2010

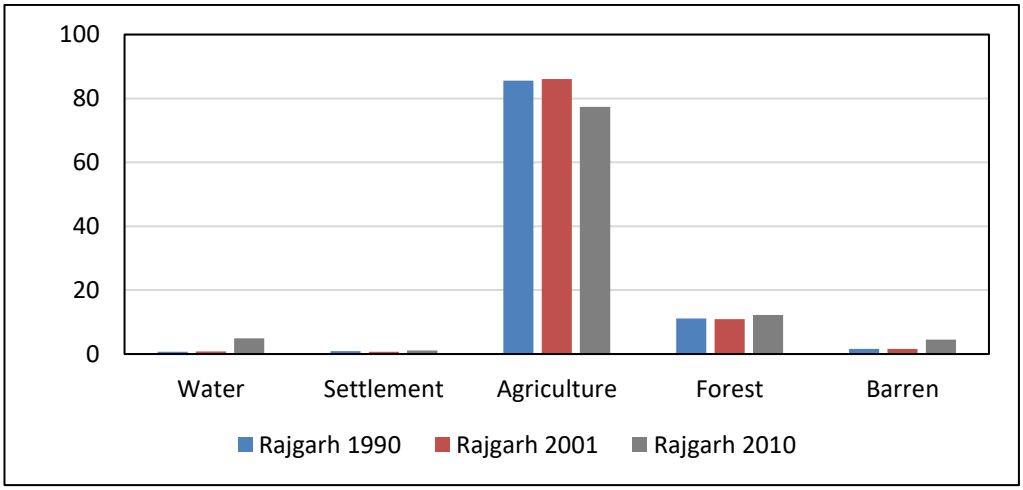

Figure 5.53: Rajgarh district LULC during 1990, 2001 and 2010

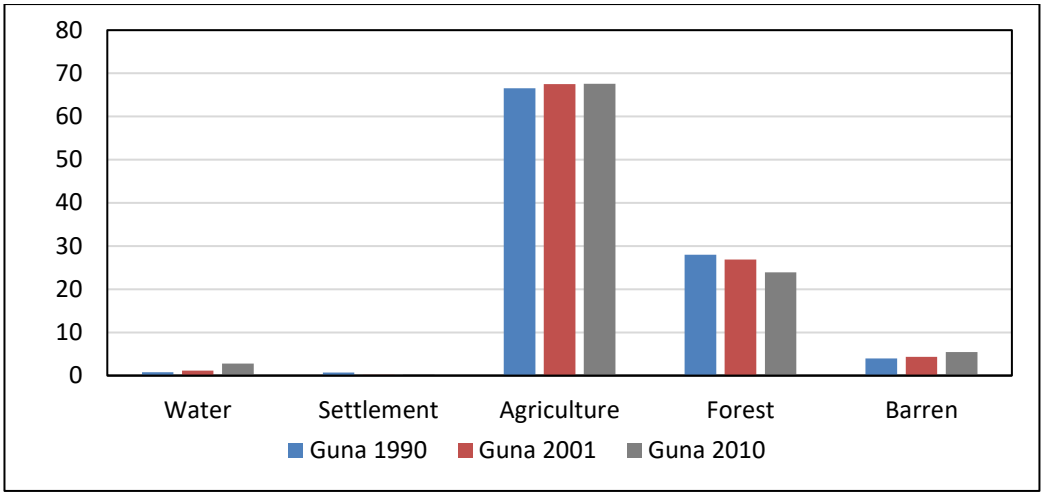

Figure 5.54: Guna district LULC during 1990, 2001 and 2010

5.3 Evaluation of Hydrologic Soil Properties

The infiltration capacity and saturated and unsaturated hydraulic conductivity were computed for different soil types-land use combinations in the study area through field experiments. The locations for field experiments were decided based on dominant soil type-land use combination. The infiltration capacity was measured using Double Ring Infiltrometer, whereas the saturated hydraulic conductivity was determined using Guelph Permeameter whereas the Minidisk Infiltrometer was used to compute unsaturated hydraulic conductivity of the soils at the test sites. The field inspection, ground truth verification and discussions were held with locals and farmers in various districts to understand the cropping pattern and other water related issues of the region. Table 5.17 enlists the results of field experiments for evaluation of infiltration capacity, saturated and unsaturated hydraulic conductivity. Figure 5.55 to Figure 5.60 shows the field photographs of the various field experiments, soil sample collection and discussion with farmers at different test sites.

Table 5.17: Infiltration capacity and hydraulic conductivity of soils

Soil testing sites	Infiltration capacity (cm/hr)	Unsaturated hydraulic conductivity (cm/s)	Saturated hydraulic conductivity (cm/s)
Awantipura (Sehore)	3.5	0.000354	0.000346
Narsingarh (Narsingarh)	2.3	0.000191	
Kamalpur, Rajgarh	5.2	0.001304	0.000842
Tapria Khedi, Rajgarh	2.5	0.000436	0.000388
Rawat Kheda (Neemuch)	2.7	0.000382	0.000006
Dewas (Dewas)	3.7	0.00034	0.000258
Mhow (Indore)	3.0	0.000355	0.000329

Figure 5.55: Double ring infiltrometer test at Kamalpura

Figure 5.56: Guelph Permeameter test at Neemuch

Figure 5.57: Minidisk Infiltrometer test at Neemuch

Figure 5.58: Soil sample collection at Narsingarh

Figure 5.59: Interactions with farmers in Rajgarh

Figure 5.60: Interactions with farmers at Singoli (M.P-Rajasthan border)

5.4 Drought analysis

5.4.1 Identification of Drought Years

The departure analysis of the annual rainfall has been used for the identification of the meteorological drought and drought years in the study area. The average annual rainfall has been estimated from the annual rainfall in the study area during the baseline period (1961-1990), present period (1991-2015), near-term (2021-2040), mid-term (2041-2070) and end-term (2071-2100). If the annual rainfall anomaly is less than 25%, then that year is considered as a drought year. The annual rainfall departure for the study area has then been computed and used for identification of drought years.

The average annual rainfall departure in the study area during the baseline period is given in Figure 5.61. Five drought years identified include 1965, 1966, 1972, 1979 and 1989 during which more than 50% of the area was under drought. The drought during the years 1965 and 1966 covered almost all the blocks in the study area. The departure analysis for the 53 blocks depicted that that there has been a maximum of 10 drought years at Mahidpur followed by 9 drought years at Khachrod and Garoth.

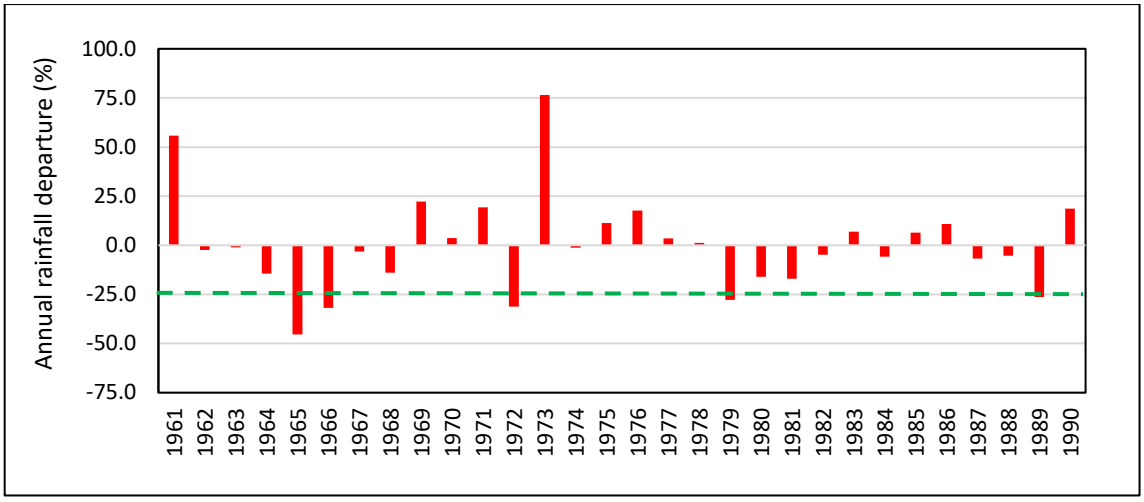

Figure 5.61: Annual rainfall departure (average) during baseline period

The annual rainfall departure at Mahidpur during the baseline period is given in Figure 5.62. 8 drought years have been observed at Garoth, Alot, Barod, Sitamau, Khilchipur, Lateri, and 7 drought years at Dewas, Tonkkalan, Sehore, Sailana, Jaora, Zirapur, Raghogarh and Guna. A minimum of 2 drought years was observed at Jawad. On an average there have been 6 drought years which indicates a drought frequency of 1 in 5 years during the baseline period. Table 5.18 gives the number of drought years observed at the various blocks during the baseline period.

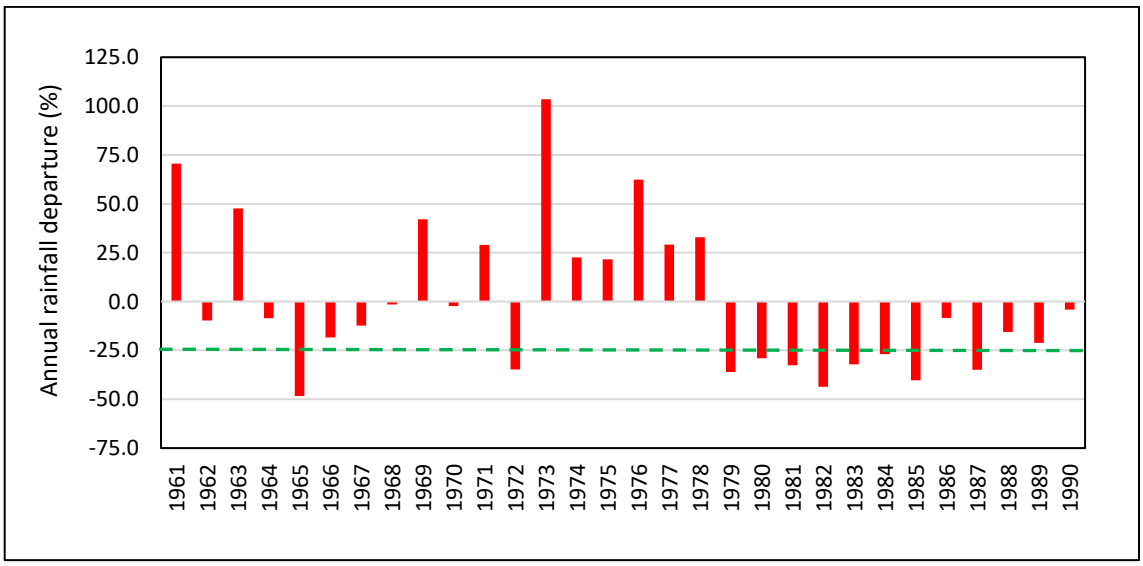

Figure 5.62: Annual rainfall departure at Mahidpur during baseline period

Table 5.18: Number of drought years during the baseline period

S. No.	Block name	Number of Drought Years
1	Mahidpur	10
2	Khachrod	9
3	Garoth	9
4	Alot	8
5	Barod	8
6	Sitamau	8
7	Khilchipur	8
8	Lateri	8
9	Dewas	7
10	Tonkkalan	7
11	Sehore	7
12	Sailana	7
13	Jaora	7
14	Zirapur	7
15	Raghogarh	7
16	Guna	7
17	Depalpur	6
18	Badnagar	6
19	Sonkatch	6
20	Ujjain	6
21	Ghatia	6
22	Shajapur	6
23	Mandsaur	6
24	Biaora	6
25	Malhargarh	6
26	Bhanpura	6
27	Badarwas	6
28	Dhar/Tirla	5
29	Ichhawar	5
30	Piploda	5
31	Tarana	5
32	Shujalpur	5
33	Agar	5
34	Rajgarh	5
35	Narsingarh	5
36	Susner	5
37	Sarangpur	5
38	Berasia	5
39	Javad	5
40	Nalkheda	5
41	Ratlam	5
42	Nalcha	4

43	Mhow	4
44	Bagli	4
45	Indore	4
46	Sanwar	4
47	Ashta	4
48	Chachora	4
49	Aron	4
50	Kalapipal	4
51	Mohan Barodia	4
52	Manasa	3
53	Jawad	2

It can be seen that severity of drought changes considerably during each drought year. However, extreme droughts and severe droughts are experienced in some parts of the basin during drought years.

The Relative Drought Index (RDI) has been estimated, which the ratio between the total weights of drought severity divided by the number of years used for the analysis. To arrive at the total weights of drought severity, weights have been assigned depending on the severity of drought in a particular drought year. The weights assigned are as follows: extreme drought = 3, severe drought = 2 and moderate drought = 1. The RDI has be used to identify the blocks that can in general, be accorded priority during drought years. The RDI varies between 0.10 at Jawad to 0.533 at Tonkkalan, 0.50. Table 5.19 gives the RDI of the priority blocks having RDI $\geq$ 0.40. Accordingly, Tonkkalan, Mahidpur, Lateri, Alot, Sitamau, Garoth, Badnagar, Jaora, and Barod have been the most drought prone blocks during the baseline period.

Table 5.19: RDI of the priority blocks during baseline period

S. No.	Block	RDI
1	Tonkkalan	0.533
2	Mahidpur	0.500
3	Lateri	0.500
4	Alot	0.433
5	Sitamau	0.433
6	Garoth	0.433
7	Badnagar	0.400
8	Jaora	0.400
9	Barod	0.400

The annual rainfall departure in the study area during the present period is given in Figure 5.63. Only two drought years identified viz., 2000 and 2002 during which more than 50% of the area was under drought. The drought during the years 2000 and 2002 covered almost 75% blocks in the study area. The departure analysis for the 53 blocks depicted that that there has been a maximum of 9 drought years at Sonkatch followed by 8 drought years at Raghogarh. The annual rainfall departure at Sonkatch during the baseline period is given in Figure 5.64.

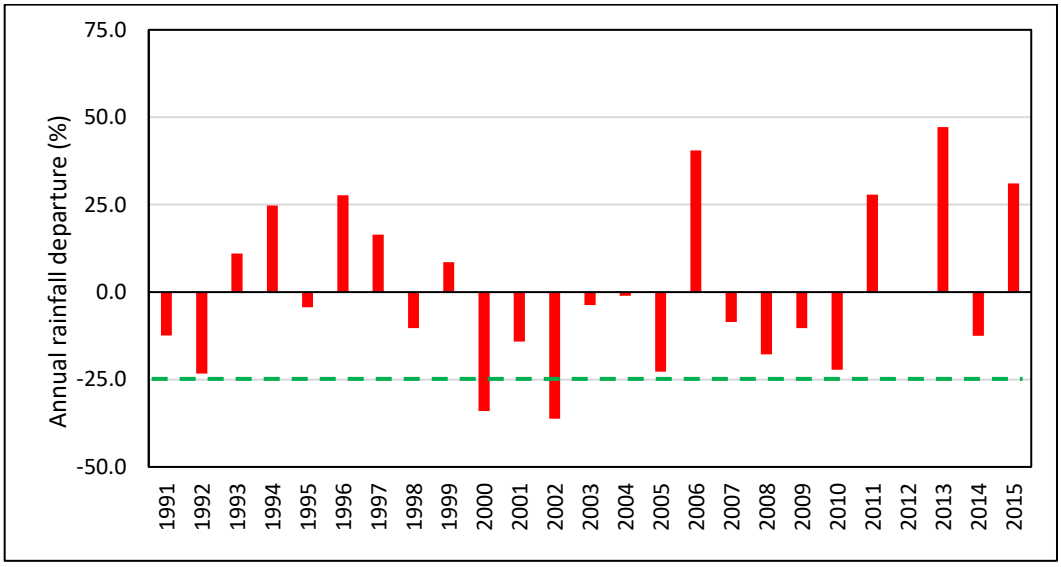

Figure 5.63: Annual rainfall departure (average) during present period

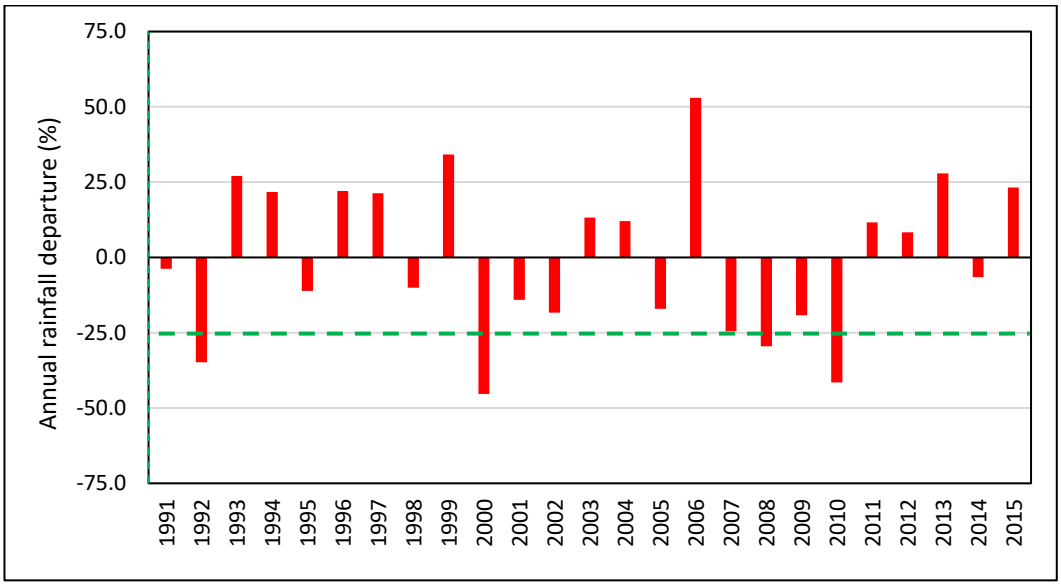

Figure 5.64: Annual rainfall departure at Sonkatch during present period

7 drought years have been observed at Alot, Zirapur, Badnagar, Ghatia, Malhargarh and Jawad. A minimum of 2 drought years was observed at Piploda.

On an average there have been 5 drought years which indicates a drought frequency of 1 in 5 years during the present period. Table 5.20 gives the number of drought years observed at the various blocks during the present period.

Table 5.20: Number of drought years during the present period

S. No.	Block name	Number of drought years
1	Sonkatch	9
2	Raghogarh	8
3	Alot	7
4	Zirapur	7
5	Badnagar	7
6	Ghatia	7
7	Malhargarh	7
8	Jawad	7
9	Sitamau	6
10	Khilchipur	6
11	Lateri	6
12	Dewas	6
13	Tonkkalan	6
14	Ujjain	6
15	Shajapur	6
16	Bhanpura	6
17	Tarana	6
18	Kalapipal	6
19	Garoth	5
20	Barod	5
21	Sailana	5
22	Guna	5
23	Biaora	5
24	Badarwas	5
25	Shujalpur	5
26	Agar	5
27	Rajgarh	5
28	Berasia	5
29	Sanwar	5
30	Manasa	5
31	Khachrod	4
32	Sehore	4
33	Depalpur	4
34	Mandsour	4
35	Javad	4
36	Ratlam	4

37	Nalcha	4
38	Bagli	4
39	Aron	4
40	Mohan Barodia	4
41	Mahidpur	3
42	Jaora	3
43	Dhar/Tirla	3
44	Ichhawar	3
45	Narsingarh	3
46	Susner	3
47	Sarangpur	3
48	Nalkheda	3
49	Mhow	3
50	Indore	3
51	Ashta	3
52	Chachora	3
53	Piploda	2

The spatial plots showing the variation of the annual rainfall departure during some of the widespread years during 2000 and 2002 is given in Figure 5.65 to Figure 5.66.

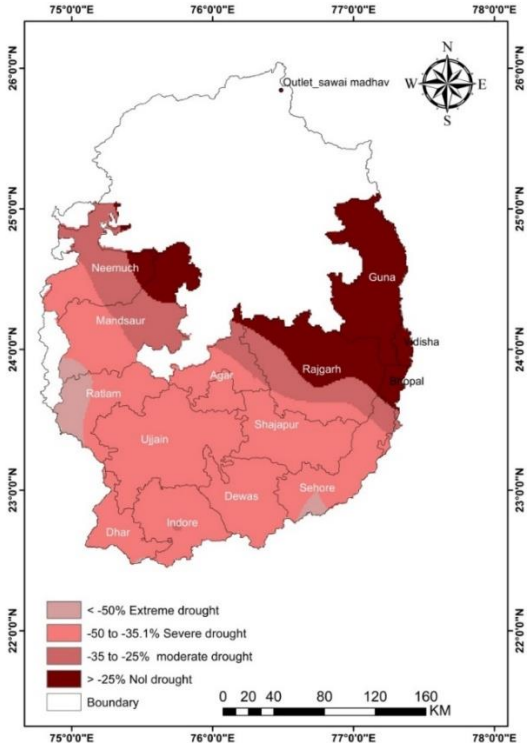

Figure 5.65: Drought categorization during the widespread drought of 2000

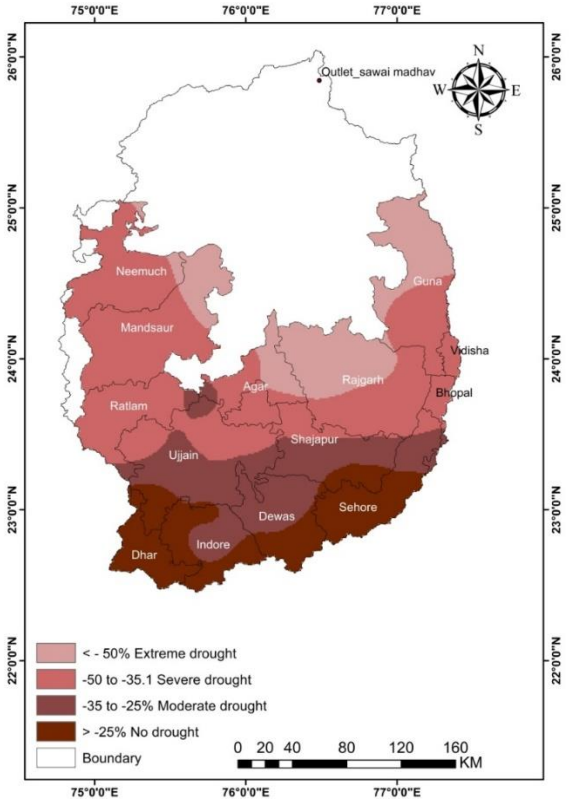

Figure 5.66: Drought categorization during the widespread drought of 2002

It can be seen that severity of drought changes considerably during each drought year. However, extreme droughts and severe droughts are experienced in some parts of the basin during drought years.

The RDI has been used to identify the blocks that can in general, be accorded priority during drought years. During the present period, RDI varies between 0.12 at Berasia to 0.560 at Khachrod. Table 5.21 gives the RDI of the priority blocks having RDI $\geq$ 0.40. Accordingly, Khachrod, Sailana, Ujjain, A lot, Ratlam, Bagli, Indore, Piploda, Mahidpur, Jaora, Barod and Badarwas have been the most drought prone blocks during the present period.

5.4.2 Identification of Drought Prone Blocks

The probability analysis of the annual rainfall has been used for identification of drought prone blocks in the study area. A block is considered as drought prone when the probability of the 75% mean annual rainfall is less than 80%. Weibull's plotting position has been used to compute the probability of exceedance.

Table 5.21: RDI of the priority blocks during present period

S. No.	Block	RDI
1	Khachrod	0.56
2	Sailana	0.48
3	Ujjain	0.44
4	Alot	0.44
5	Ratlam	0.44
6	Bagli	0.40
7	Indore	0.40
8	Piploda	0.40
9	Mahidpur	0.40
10	Jaora	0.40
11	Barod	0.40
12	Badarwas	0.40

Table 5.22 gives the probability of the drought prone blocks in the study area. It can be seen that 26 blocks out of the 53 selected blocks are drought prone in the study area which means that about 50% of the study area is drought prone. The plots showing the probability of exceedance with annual rainfall at Dewas and Kundanpur, both of which have been identified as drought prone blocks are given in Figure 5.67 and Figure 5.68.

Table 5.22: Drought prone blocks identified in the study area

S. No.	Station name	Normal rainfall	Probability of 75% mean rainfall
1	Sanwar	930.11	79.20
2	Dewas	979.45	75.28
3	Tonkkalan	979.65	77.86
4	Piploda	894.06	77.30
5	Ujjain	915.23	74.51
6	Sailana	858.54	75.66
7	Khachrod	858.50	75.42
8	Mahidpur	871.39	73.93
9	Ghatia	911.50	78.33
10	Shajapur	963.41	76.42
11	Jaora	809.06	76.38
12	Alot	876.16	74.13
13	Barod	920.14	74.21
14	Agar	921.04	77.32
15	Mandsaur	789.21	78.85
16	Sitamau	839.16	74.14
17	Susner	902.21	76.55

18	Garoth	887.63	76.89
19	Bamhori/Chachora	1040.75	77.34
20	Neemuch/Jawad	836.35	78.71
21	Bhanpura	870.20	77.07
22	Raghogarh	1037.97	77.04
23	Guna	1032.63	78.01
24	Ratlam	611.18	77.73
25	Sarangpur	720.53	79.12
26	Bagli	737.3	79.69

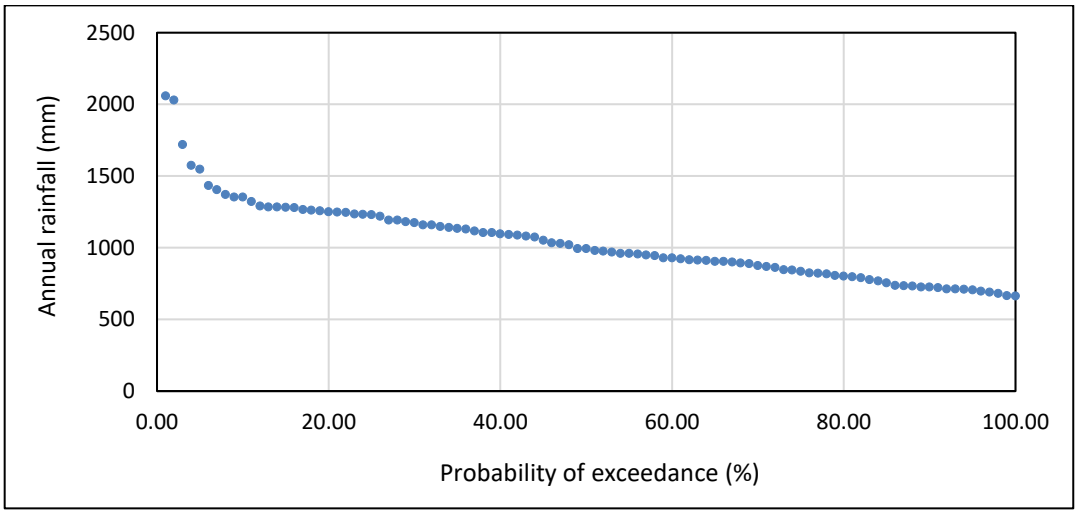

Figure 5.67: Probability of exceedance of annual rainfall at Dewas

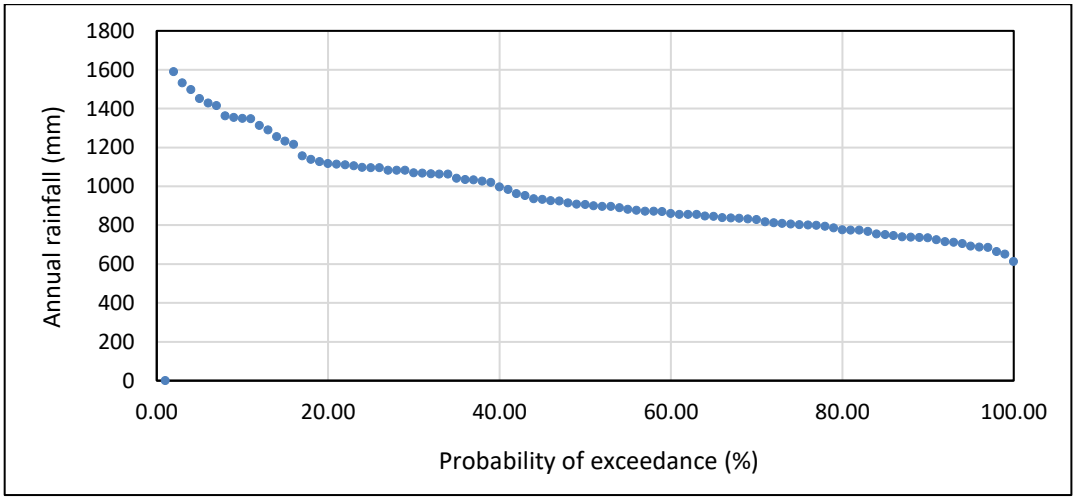

Figure 5.68: Probability of exceedance of annual rainfall at Dhar

5.4.3 Evaluation of 3m-SPI based Drought Characteristics

The drought characteristics (soil moisture) have been evaluated using Standardized Precipitation Index (SPI). The SPI has been evaluated at three

different time slices viz., 3-month SPI (3m-SPI), 6-month SPI (6m-SPI) and 12-month SPI (12m-SPI). It has been generally observed from several studies that the 3-m SPI provides a seasonal estimation of the precipitation and also represents the soil moisture availability (short-term moisture conditions), the 6-m SPI represents the surface water availability (medium-term moisture conditions) whereas the 12-m SPI represents the groundwater availability (long-term moisture conditions). Therefore, 3-m SPI has been used as an indicator to evaluate the seasonal precipitation availability and the short-term moisture conditions in the study area. The SPI at time scales of 3, 6 and 12 months have been evaluated for baseline period (1961-1990) and present time horizon (1991-2015). During the baseline period, temporal variation of the 3-m SPI at Mahidpur (Figure 5.69), 6-m SPI at Mahidpur (Figure 5.70) and 12-m SPI at Mahidpur is given in Figure 5.71.

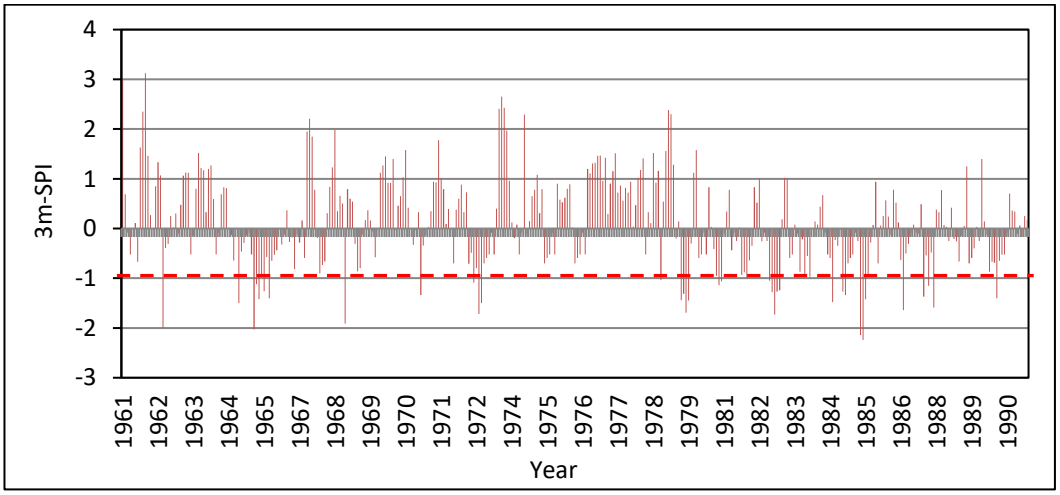

Figure 5.69: Temporal variation of 3m-SPI at Mahidpur

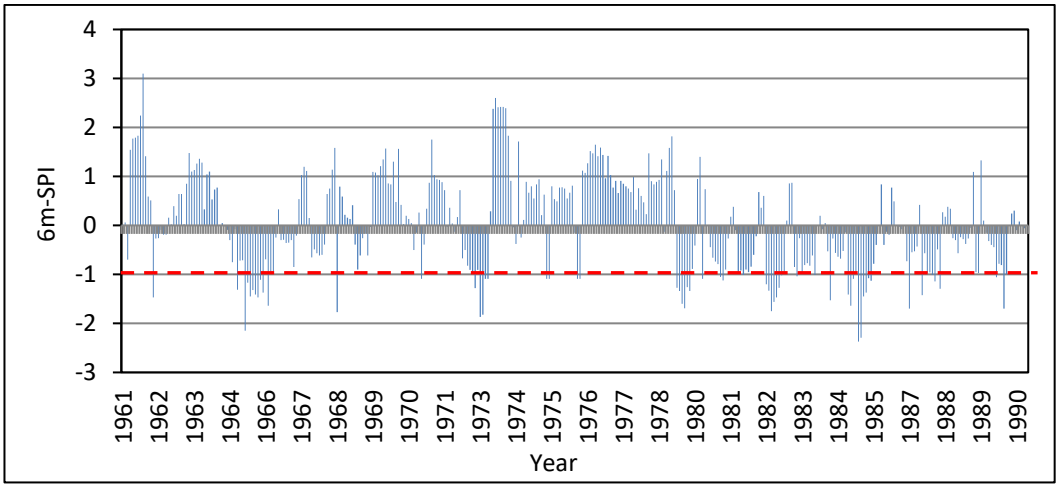

Figure 5.70: Temporal variation of 6m-SPI at Mahidpur

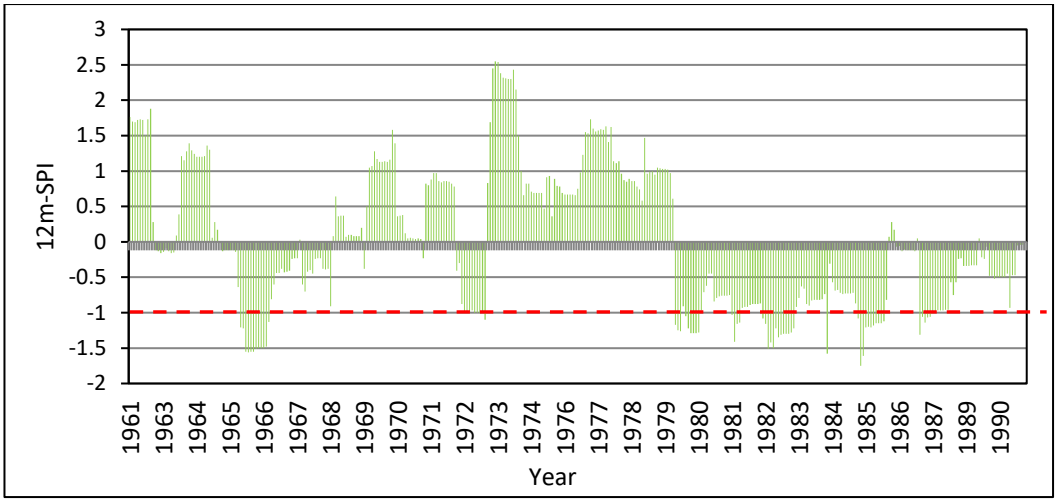

Figure 5.71: Temporal variation of 12m-SPI at Mahidpur

It can be observed that there are few occasions during which the 3-m SPI has been below -2.0 which indicates extreme drought, viz., Jun-1962, Jun-1965, Aug-1965, Nov-1986. The extreme drought has mostly been observed during the monsoon months particularly in June and August and in November on few occasions. Table 5.23 indicates the number of extreme, severe and moderate drought events that have occurred in the various blocks during baseline period. The number of extreme drought events varied between 9 events at Tonkkalan and 1 event at Narsingarh and Shujalpur. Similarly, the number of severe drought events varied between 20 events at Badarwas and 4 events at Alot, whereas the number of moderate drought events varied between 51 events at Sehore and 11 events at Nalcha and Neemuch.

Table 5.23: 3-month SPI based drought events during baseline period

S. No.	Station name	Extreme events	Severe events	Moderate events
1	Agar	4	8	35
2	Alot	4	4	26
3	Aron	6	10	21
4	Ashta	3	10	35
5	Badarwas	3	20	28
6	Badnagar	4	13	26
7	Bagli	2	10	27
8	Biaora	6	10	31
9	Bamhori/Chachora	7	8	16
10	Barod	3	6	32

11	Berasia	5	7	36
12	Bhanpura	1	11	21
13	Depalpur	5	14	15
14	Dewas	2	8	21
15	Dhar/Tirla	3	14	20
16	Garoth	2	11	17
17	Ghatia	4	8	34
18	Guna	6	9	43
19	Ichhawar	3	11	33
20	Indore	6	11	21
21	Jaora	5	9	24
22	Javad	5	12	22
23	Kalapipal	3	11	28
24	Khachrod	4	9	20
25	Khilchipur	5	6	28
26	Lateri	5	9	15
27	Mahidpur	4	8	23
28	Malhargarh	5	10	31
29	Manasa	4	11	18
30	Mandsaur	7	4	20
31	Mhow	5	13	21
32	Mohan Barodia	2	9	32
33	Nalcha	6	9	11
34	Nalkheda	3	6	35
35	Narsingarh	1	14	31
36	Neemuch/Jawad	5	7	11
37	Piploda	4	8	34
38	Raghogarh	5	10	39
39	Rajgarh	2	11	44
40	Ratlam	4	6	23
41	Sailana	4	9	21
42	Sanwar	4	11	33
43	Sarangpur	5	8	19
44	Sehore	5	10	51
45	Shajapur	2	13	24
46	Shujalpur	1	12	47
47	Sitamau	4	7	14
48	Sonkatch	5	5	23
49	Susner	3	9	14
50	Tarana	2	8	34

51	Tonkkalan	9	12	13
52	Ujjain	3	8	35
53	Zirapur	2	13	35

The number of occurrences and severity during the identified drought events has been used for the computation of the total drought severity and drought intensity in the study area. The severity for the various types of droughts [i.e., extreme drought (SPI < -2.0), severe drought (-2.0 < SPI < -1.5), moderate drought (-1.5 < SPI < -1.0)] during the drought years, have been summed to compute the total drought severity. The total drought severity divided by the number of drought events gives the drought intensity. The meteorological drought characteristics including the drought duration, drought severity and drought intensity based on the 3-m SPI during the baseline period is given in Table 5.24.

The total drought duration varied between 64 months at Sehore and 23 months at Neemuch whereas the drought intensity varied between and -1.84 at Nalcha and -1.33 at Rajgarh. The ten blocks with highest drought duration are given in Table 5.25, whereas the ten blocks with the highest drought intensity is given in Table 5.26. The highest drought duration with more than 46 months occurred at Sehore, Shujalpur, Guna, Rajgarh, Raghogarh, Zirapur, Badarwas, Berasia, Alot and Ashta. The highest drought intensity with less than -1.52 was observed at Nalcha, Tonkkalan, Bamhori, Depalpur, Aron, Lateri, Sitamau, Indore, Jaora, and Manasa. The spatial variation of the 3-m SPI during the months of June to October 1966 is given in Figure 5.72 to Figure 5.76.

Table 5.24: 3m-SPI based drought characteristics during baseline period

S. No.	Station name	Total duration	Total drought magnitude	Drought intensity
1	Agar	47	-64.28	-1.37
2	Alot	34	-46.67	-1.37
3	Aron	36	-56.53	-1.57
4	Ashta	47	-63.85	-1.36
5	Badarwas	49	-73.4	-1.5
6	Badnagar	42	-61.87	-1.47
7	Bagli	39	-54.86	-1.41

8	Biaora	47	-66.29	-1.41
9	Bamhori/Chachora	31	-50.77	-1.64
10	Barod	40	-54.26	-1.36
11	Berasia	48	-67.68	-1.41
12	Bhanpura	33	-46.79	-1.42
13	Depalpur	34	-55.5	-1.63
14	Dewas	31	-43.99	-1.42
15	Dhar/Tirla	37	-55.39	-1.5
16	Garoth	29	-42.82	-1.48
17	Ghatia	45	-60.67	-1.35
18	Guna	57	-81.78	-1.43
19	Ichhawar	45	-64.29	-1.43
20	Indore	37	-57.08	-1.54
21	Jaora	38	-57.86	-1.52
22	Javad	37	-54.04	-1.46
23	Kalapipal	42	-58.01	-1.38
24	Khachrod	33	-49.48	-1.5
25	Khilchipur	39	-55.54	-1.42
26	Lateri	29	-45.32	-1.56
27	Mahidpur	35	-51.02	-1.46
28	Malhargarh	45	-64.22	-1.43
29	Manasa	33	-50.02	-1.52
30	Mandsaur	31	-46.09	-1.49
31	Mhow	37	-56.27	-1.52
32	Mohan Barodia	41	-55.46	-1.35
33	Nalcha	26	-47.91	-1.84
34	Nalkheda	42	-58.83	-1.4
35	Narsingarh	46	-65.72	-1.43
36	Neemuch/Jawad	23	-37.19	-1.62
37	Piploda	46	-64.39	-1.4
38	Raghogarh	54	-78.29	-1.45
39	Rajgarh	57	-75.65	-1.33
40	Ratlam	32	-45.31	-1.42
41	Sailana	34	-52.03	-1.53
42	Sanwar	46	-65.28	-1.42
43	Sarangpur	32	-48.28	-1.51
44	Sehore	64	-90.05	-1.41
45	Shajapur	37	-53.88	-1.46
46	Shujalpur	60	-80.12	-1.34
47	Sitamau	24	-37.1	-1.55

48	Sonkatch	32	-47.01	-1.47
49	Susner	26	-39.12	-1.5
50	Tarana	44	-59.75	-1.36
51	Tonkkalan	33	-55.35	-1.68
52	Ujjain	45	-61.87	-1.37
53	Zirapur	50	-68.27	-1.37

Table 5.25: Blocks with maximum drought duration during baseline period

S. No.	Station name	Total duration
1.	Sehore	64
2.	Shujalpur	60
3.	Guna	57
4.	Rajgarh	57
5.	Raghogarh	54
6.	Zirapur	50
7.	Badarwas	49
8.	Berasia	48
9.	Alot	47
10.	Ashta	47

Table 5.26: Blocks with maximum drought intensity during baseline period

S. No.	Station name	Total duration
1.	Nalcha	-1.84
2.	Tonkkalan	-1.68
3.	Bamhori	-1.64
4.	Depalpur	-1.63
5.	Aron	-1.57
6.	Lateri	-1.56
7.	Sitamau	-1.55
8.	Indore	-1.54
9.	Jaora	-1.52
10.	Manasa	-1.52

It can be seen that in June 1966 only a small portion of Dewas and Sehore blocks faced extreme drought condition whereas the moderate drought condition existed only in the southern portion of the basin. Due to sufficient rainfall in July, most of the region was under mild drought and some small patches in different region across the basin faces moderate drought. In August, small region in Guna block faced extreme drought which expanded to a larger area in successive months due to insufficient rainfall in large parts of Guna, Rajgarh and Bhopal blocks and

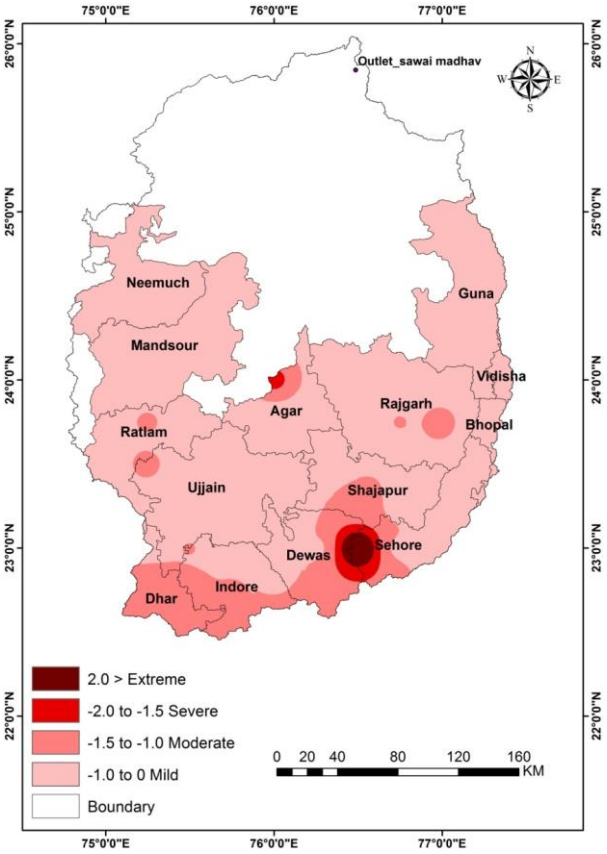

Figure 5.72: Spatial variation of 3m-SPI during June 1966

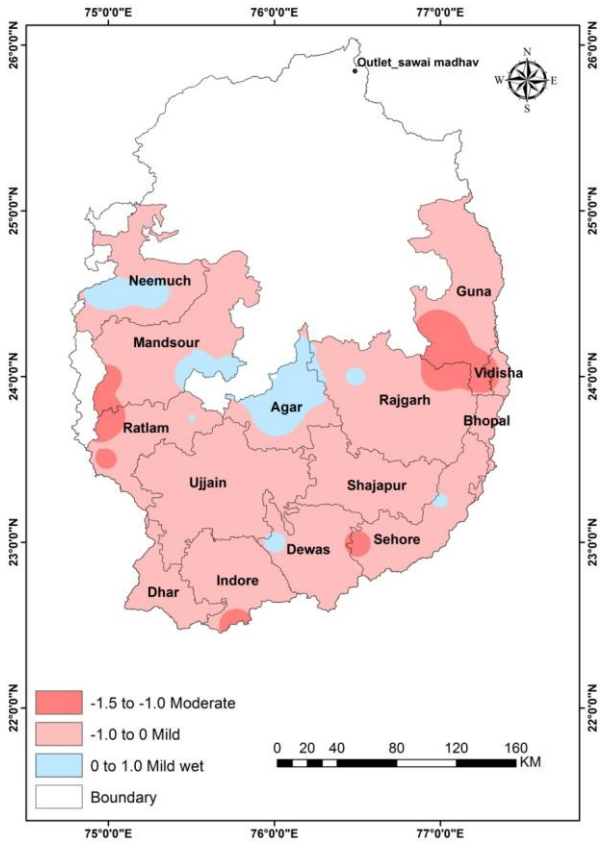

Figure 5.73: Spatial variation of 3m-SPI during July 1966

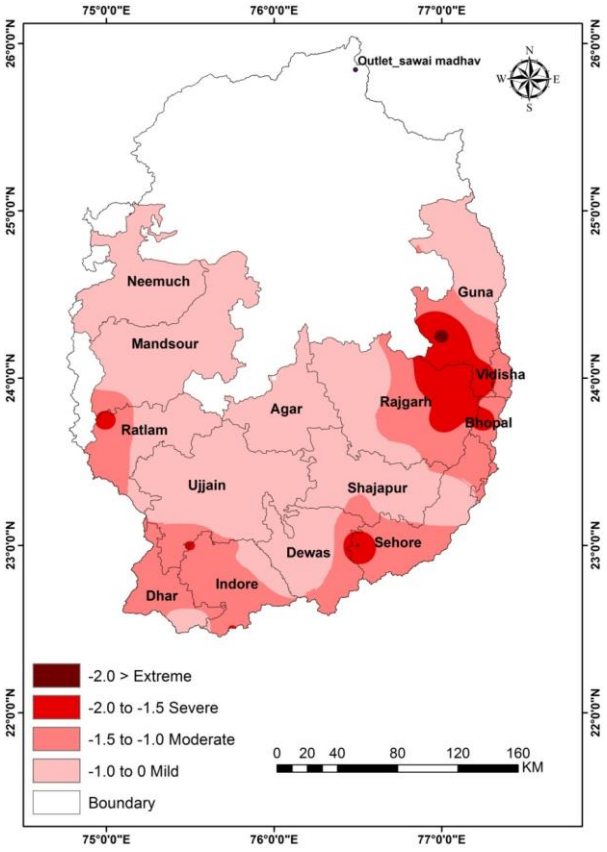

Figure 5.74: Spatial variation of 3m-SPI during August 1966

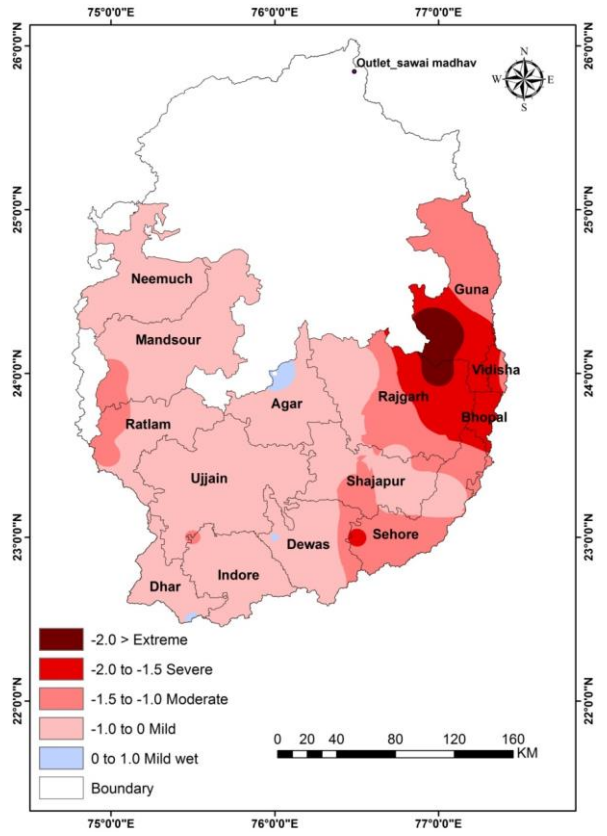

Figure 5.75: Spatial variation of 3m-SPI during September 1966

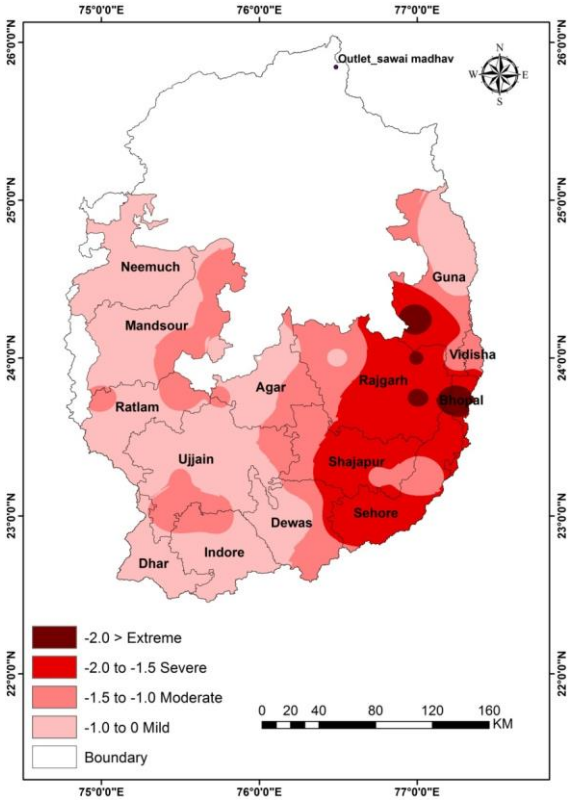

Figure 5.76: Spatial variation of 3m-SPI during October 1966

severe drought occurred in October month in Rajgarh, Shajapur, Sehore and Bhopal blocks.

A similar evaluation using SPI was conducted for present time horizon (1991-2015). Table 5.27 indicates the number of extreme, severe and moderate drought events that have occurred in the various blocks during the present time horizon. The temporal variation of 3-m SPI, 6-m SPI and 12-m SPI for Nalcha block is shown in Figure 5.77 to Figure 5.79. It can be observed that there are few occasions of 3-m SPI being below -2.0 which indicates extreme drought, which was observed during Nov-1991, Jun-1995, Oct-2000, Sep-2002 and Jun-2010. The drought condition generally prevails during the month of June and August. The number of extreme drought events varied between 7 events at Nalcha and 1 event at Ratlam. Similarly, the number of severe droughts varied between 10 at Tarana and 2 at Narsingarh whereas the number of moderate drought events varied between 27 at Raghogarh and 6 at Kalapipal.

Table 5.27: 3m-SPI based drought events during present period

S. No.	Station name	Extreme events	Severe events	Moderate events
1	Agar	5	5	10
2	Alot	3	8	14
3	Aron	2	7	13
4	Ashta	5	6	10
5	Badarwas	3	7	19
6	Badnagar	3	5	13
7	Bagli	3	6	14
8	Biaora	3	7	16
9	Bamhori/Chachora	2	4	23
10	Barod	4	7	9
11	Berasia	5	3	10
12	Bhanpura	5	4	10
13	Depalpur	5	6	8
14	Dewas	3	6	13
15	Dhar/Tirla	6	8	9
16	Garoth	4	5	14
17	Ghatia	3	7	14
18	Guna	4	6	24
19	Ichhawar	5	3	16
20	Indore	5	5	18
21	Jaora	3	5	12
22	Javad	3	6	10
23	Kalapipal	4	8	6
24	Khachrod	2	9	10
25	Khilchipur	2	8	12
26	Lateri	3	7	15
27	Mahidpur	3	9	8
28	Malhargarh	3	5	10
29	Manasa	4	3	16
30	Mandsaur	4	3	14
31	Mhow	6	4	17
32	Mohan Barodia	3	8	9
33	Nalcha	7	3	11
34	Nalkheda	2	9	15
35	Narsingarh	5	2	9
36	Neemuch/Jawad	3	7	10
37	Piploda	3	8	12

38	Raghogarh	3	6	27
39	Rajgarh	5	3	15
40	Ratlam	1	8	14
41	Sailana	2	6	12
42	Sanwar	4	6	12
43	Sarangpur	5	5	13
44	Sehore	3	9	25
45	Shajapur	3	5	16
46	Shujalpur	3	8	7
47	Sitamau	2	8	19
48	Sonkatch	4	5	11
49	Susner	2	7	11
50	Tarana	2	10	18
51	Tonkkalan	6	4	8
52	Ujjain	3	8	13
53	Zirapur	5	5	17

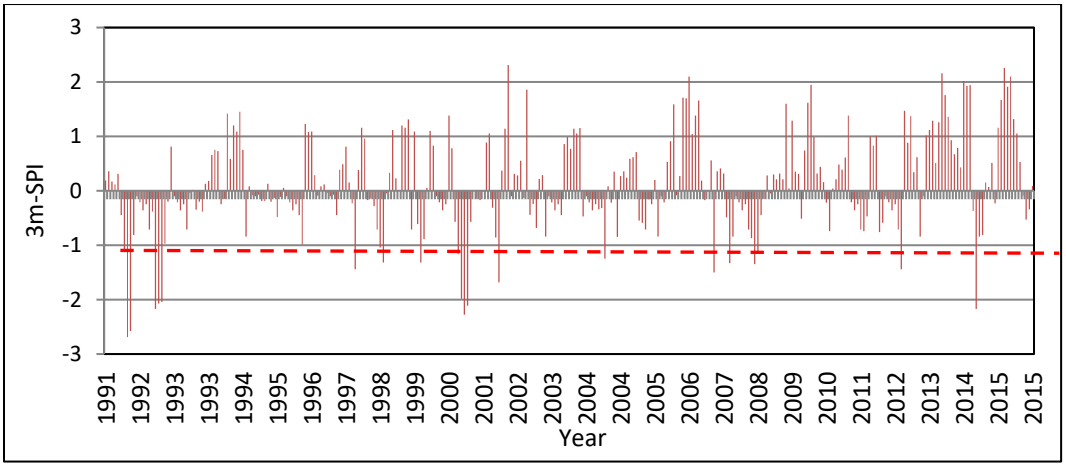

Figure 5.77: Temporal variation of 3-m SPI at Nalcha during present period

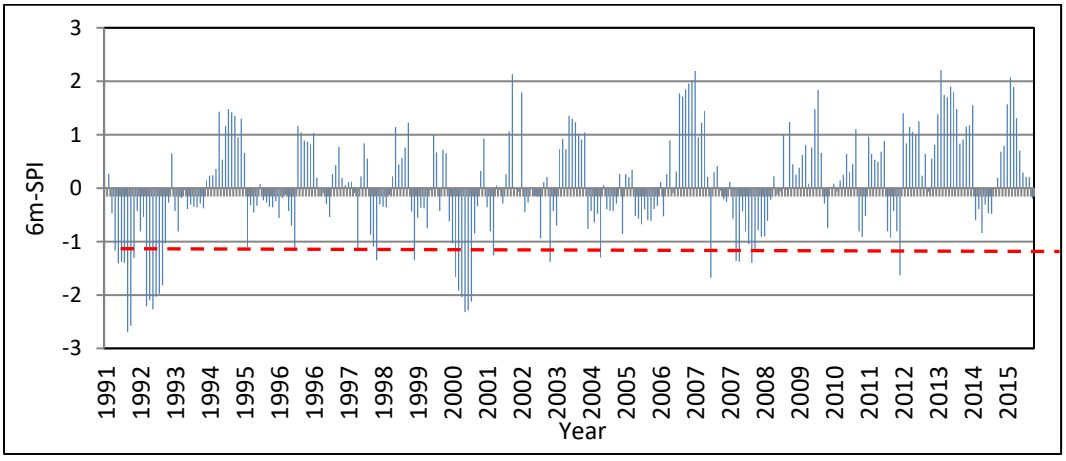

Figure 5.78: Temporal variation of 6-m SPI at Nalcha during present period

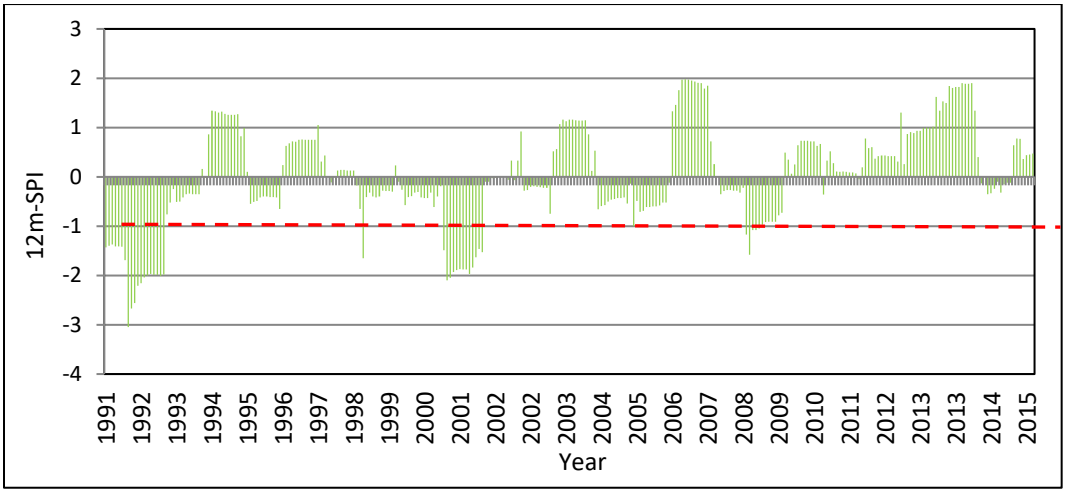

Figure 5.79: Temporal variation of 12-m SPI at Nalcha during present period

The drought characteristics including the drought duration, drought severity and drought intensity based on the 3-m SPI during the present time period is given in Table 5.28. The total drought duration varies between 36 months at Sehore and 16 months at Narsingarh whereas the drought intensity varies between and -1.74 at Tonkkalan and -1.38 at Sitamau.

Table 5.28: 3 month-SPI based drought characteristics during present period

S. No.	Station name	Total duration	Total drought magnitude	Drought intensity
1.	Agar	20	-32.89	-1.64
2.	Alot	25	-37.68	-1.51
3.	Aron	22	-33.85	-1.54
4.	Ashta	21	-33.93	-1.62
5.	Badarwas	29	-42.18	-1.45
6	Badnagar	20	-31.35	-1.57
7	Bagli	23	-33.88	-1.47
8	Biaora	26	-38.14	-1.47
9	Bamhori/Chachora	28	-38.96	-1.39
10	Barod	20	-32.14	-1.61
11	Berasia	18	-29.97	-1.67
12	Bhanpura	19	-30.83	-1.62
13	Depalpur	18	-30.83	-1.71
14	Dewas	22	-33.81	-1.54
15	Dhar/Tirla	23	-38.4	-1.67
16.	Garoth	22	-34.41	-1.56

17.	Ghatia	24	-36.27	-1.51
18.	Guna	32	-46.51	-1.45
19	Ichhawar	24	-37.44	-1.56
20	Indore	28	-41.76	-1.49
21	Jaora	20	-29.91	-1.5
22	Javad	19	-31.39	-1.65
23	Kalapipal	18	-30.72	-1.71
24	Khachrod	20	-31.48	-1.57
25	Khilchipur	22	-33.07	-1.5
26	Lateri	25	-36.53	-1.46
27	Mahidpur	20	-33.55	-1.68
28	Malhargarh	18	-29.41	-1.63
29	Manasa	22	-31.54	-1.43
30	Mandsaur	21	-31.4	-1.5
31	Mhow	27	-41.26	-1.53
32	Mohan Barodia	20	-32.52	-1.63
33	Nalcha	21	-35	-1.67
34	Nalkheda	26	-38.52	-1.48
35	Narsingarh	16	-25.9	-1.62
36	Neemuch/Jawad	20	-30.45	-1.52
37	Piploda	22	-34.46	-1.57
38	Raghogarh	36	-49.57	-1.38
39	Rajgarh	22	-33.07	-1.5
40	Ratlam	22	-33.14	-1.51
41	Sailana	19	-27.69	-1.46
42	Sanwar	22	-33.24	-1.51
43	Sarangpur	23	-35.85	-1.56
44	Sehore	36	-51.91	-1.44
45	Shajapur	24	-35.57	-1.48
46	Shujalpur	18	-30.08	-1.67
47	Sitamau	29	-40.02	-1.38
48	Sonkatch	20	-31.81	-1.59
49	Susner	19	-29.93	-1.58
50	Tarana	29	-42.73	-1.47
51	Tonkkalan	18	-31.36	-1.74
52	Ujjain	23	-35.61	-1.55
53	Zirapur	27	-39.72	-1.47

The ten blocks with the highest drought duration are given in Table 5.29, whereas the ten blocks with the highest drought intensity is given in Table 5.30. The highest drought duration with more than 25 months occurred at Sehore, Raghogarh, Guna, Badarwas, Sitamau, Tarana, Bamhori, Indore, Mhow, and Biaora. The highest drought intensity with less than -1.63 was observed at Depalpur, Kalapipal, Mahidpur, Berasia, Dhar, Nalcha, Shujalpur, Javad, Agar, and Mohan Barodia.

Table 5.29: Blocks with maximum drought duration present period

S. No.	Station name	Total duration
1	Sehore	36
2	Raghogarh	36
3	Guna	32
4	Badarwas	29
5	Sitamau	29
6	Tarana	29
7	Bamhori	28
8	Indore	28
9	Mhow	27
10	Biaora	26

Table 5.30: Blocks with maximum drought intensity present period

S. No.	Station name	Total duration
1	Depalpur	-1.71
2	Kalapipal	-1.71
3	Mahidpur	-1.68
4	Berasia	-1.67
5	Dhar	-1.67
6	Nalcha	-1.67
7	Shujalpur	-1.67
8	Javad	-1.65
9	Agar	-1.64
10	Mohan Barodia	-1.63

Based on the 3-m SPI at various blocks, the spatial variation of the 3-m SPI during the months of June to October 2002, a drought year during the present time

horizon is given in Figure 5.80 to Figure 5.84. In June 2002, extreme drought occurred in limited areas of Agar, Ujjain and Shajapur blocks. The areas close to Dewas, Sehore, Rajgarh, Bhopal Ratlam and Mandsaur blocks were under severe drought condition and the areas in their near vicinity were under moderate drought condition. In July, the severe drought prevailed in Shajapur, and Sehore blocks whereas moderate drought prevailed in the southern portion of the study area. In August, the extent of severe drought extended further and covered most of Shajapur and Sehore blocks. Due to availability of abundant rainfall in September, the extent of severe drought reduced, and except for Dhar and limited areas in Indore and Neemuch, most of the study area was under mild drought. In October, the extent of moderate and mild drought reduced mostly and reasonably favorable conditions prevailed in the study area.

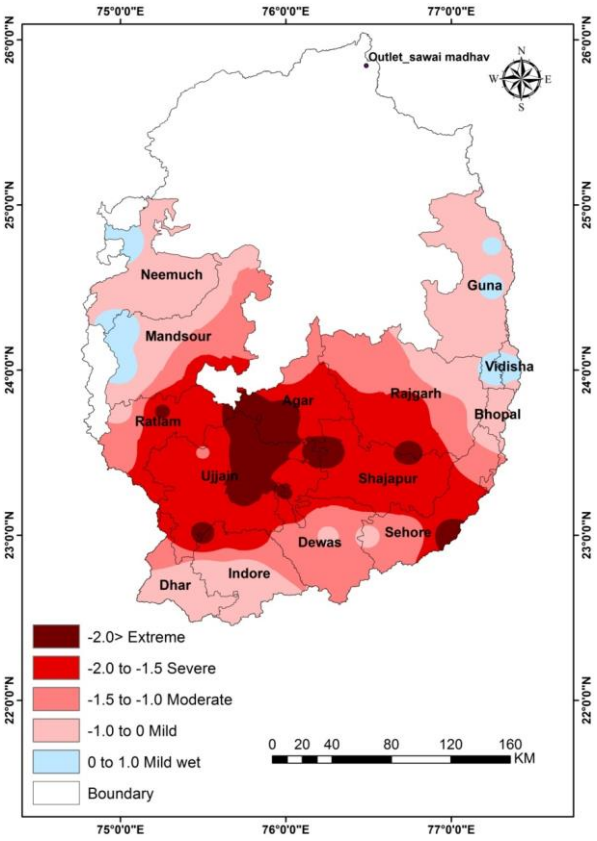

Figure 5.80: Spatial variation of 3m-SPI during June 2002

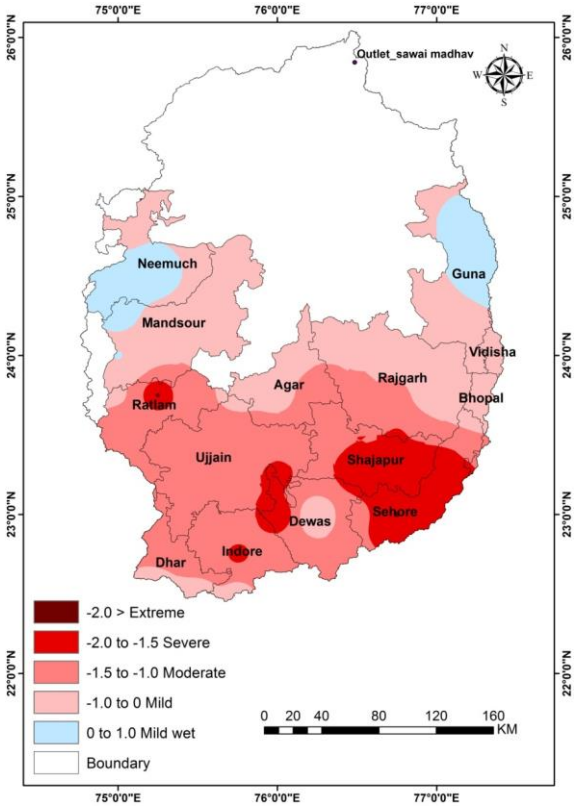

Figure 5.81: Spatial variation of 3m-SPI during July 2002

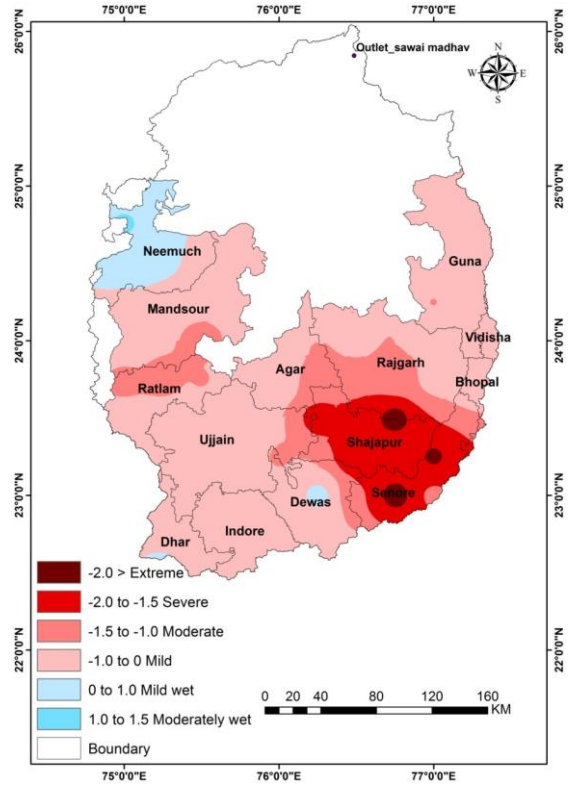

Figure 5.82: Spatial variation of 3m-SPI during August 2002

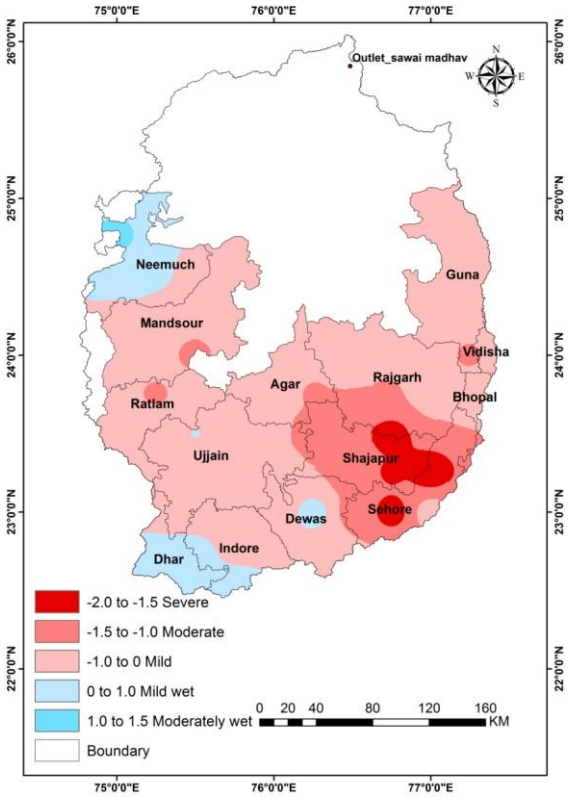

Figure 5.83: Spatial variation of 3m-SPI during September 2002

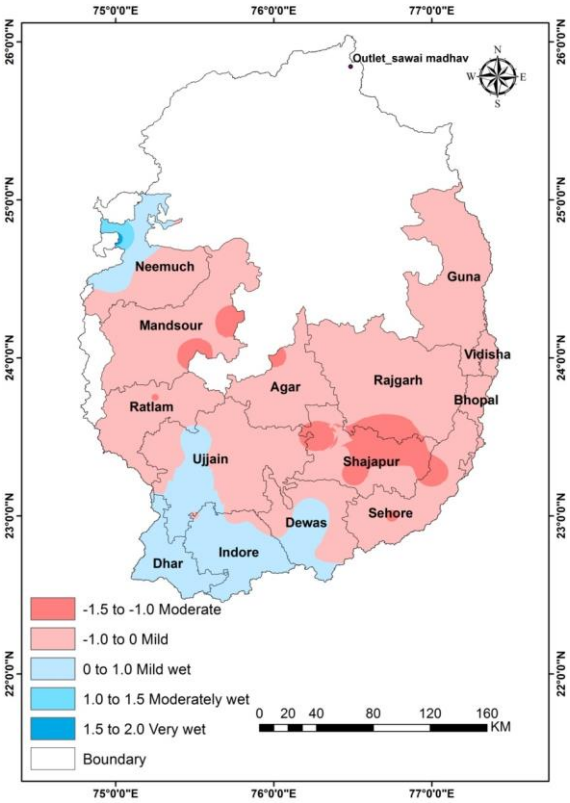

Figure 5.84: Spatial variation of 3m-SPI during October 2002

The 3m-SPI has been evaluated for the future time periods as well, i.e. near-term (2021-2040), mid-term (2041-2070) and end-term (2071-2100). Table 5.31 indicates the average number of extreme, severe and moderate drought events projected in the complete study area during the near-term period. In the near-term, the number of moderate events under SSP245 scenario is projected to vary between 13 events for MPI-ESM-2-LR GCM and 30 events for INM-CM4-8 GCM, with the ensemble mean projection of 20 moderate drought events. Similarly, under SSP585 scenario, the number of moderate events is projected to vary between 9 events for MPI-ESM-2-HR and MPI-ESM-2-LR GCMs and 30 events for ACCESS-CM2 and ACCESS-ESM1-5 GCMs, with the ensemble mean projection of 21 moderate drought events in the near-term.

Table 5.31: Drought events projected during near-term (2021-2040)

S. No.	GCMs	Moderate SSP245	Moderate SSP585	Severe SSP245	Severe SSP585	Extreme SSP245	Extreme SSP585
1	ACCESS-CM2	22	30	11	11	6	3
2	ACCESS-ESM1-5	22	30	11	11	6	3
3	BCC-CSM2-MR	16	20	7	9	4	3
4	CanESM5	23	19	9	10	4	4
5	EC-Earth3	22	17	8	7	4	5
6	EC-Earth3-Veg	15	19	9	8	4	4
7	INM-CM4-8	22	23	7	5	3	2
8	INM-CM5-0	30	24	7	8	2	3
9	MPI-ESM1-2-HR	16	9	7	6	3	6
10	MPI-ESM1-2-LR	13	9	7	8	3	3
11	MRI-ESM2-0	20	23	6	12	4	5
12	NorESM2-LM	19	25	14	10	5	3
13	NorESM2-MM	21	21	8	9	6	7
Ensemble mean		**20**	**21**	**9**	**9**	**4**	**4**

In the near term, the number of severe drought events under SSP245 scenario is projected to vary between 7 events for MPI-ESM-2-LR and 19 events for NorESM2-MM, with the ensemble mean projection of 12 severe drought events. Similarly, under SSP585 scenario, the number of severe drought events is projected to vary between 7 events for MPI-ESM-2-LR and INM-CM4-8 GCMs and 21 events for CanESM5, with the ensemble mean projection of 13 severe drought events in the near-term. Also, the number of extreme drought events under SSP245 scenario is projected to vary between 3 events (MPI-ESM-2-LR and MPI-ESM-2-LR) and 6 events (ACCESS-CM2, ACCESS-ESM1-5, NorESM2-MM), with the ensemble mean projection of 4 severe drought events.

Similarly, under SSP585 scenario, the number of extreme drought events is projected to vary between 3 events for six GCMs and 7 events for NorESM2-MM, with the ensemble mean projection of 4 extreme drought events in the near-term. The number of drought events of varying severities during the near-term is given in Figure 5.85.

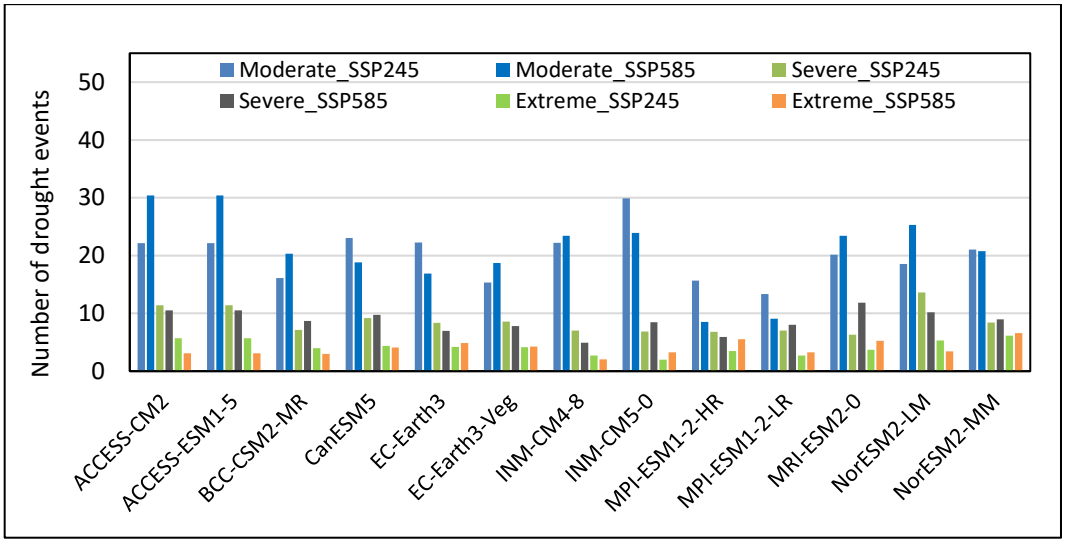

Figure 5.85: Drought events projected during near-term (2021-2040)

Table 5.32 indicates the average number of extreme, severe and moderate drought events projected in the complete study area during the mid-term period. In the mid-term, the number of moderate events under SSP245 scenario is projected to vary between 16 events for MPI-ESM-2-HR and 35 events for CanESM5, with the

Table 5.32: Drought events projected during mid-term (2041-2070)

S. No.	GCMs	Moderate SSP245	Moderate SSP585	Severe SSP245	Severe SSP585	Extreme SSP245	Extreme SSP585
1	ACCESS-CM2	33	35	12	16	9	5
2	ACCESS-ESM1-5	33	35	12	16	9	5
3	BCC-CSM2-MR	35	27	10	13	5	5
4	CanESM5	35	26	18	21	5	10
5	EC-Earth3	33	31	13	9	4	7
6	EC-Earth3-Veg	29	21	10	8	5	9
7	INM-CM4-8	38	36	8	7	4	1
8	INM-CM5-0	36	39	12	12	5	4
9	MPI-ESM1-2-HR	16	19	10	8	8	7
10	MPI-ESM1-2-LR	15	17	7	7	6	7
11	MRI-ESM2-0	33	33	10	20	4	5
12	NorESM2-LM	26	29	17	15	9	9
13	NorESM2-MM	32	37	19	15	5	6
Ensemble mean		**30**	**30**	**12**	**13**	**6**	**6**

ensemble mean projection of 30 moderate drought events. However, under SSP585 scenario, the number of moderate events is projected to vary between 17 events for MPI-ESM1-2-LR and 39 events for INM-CM5-0, with the ensemble mean projection of 30 moderate drought events in the mid-term.

In the mid-term, the number of severe drought events under SSP245 scenario is projected to vary between 8 events for INM-CM4-8 and 19 events for NorESM2-MM, with the ensemble mean projection of 12 severe drought events. Similarly, under SSP585 scenario, the number of severe drought events is projected to vary between 8 events (MPI-ESM-2-HR and EC-Earth3-Veg) and 21 events for CanESM5, with the ensemble mean projection of 13 severe drought events in the mid-term. Also, the number of extreme drought events under SSP245 scenario is projected to vary between 5 events (NorESM2-MM) and 9 events (ACCESS-CM2, ACCESS-ESM1-5) with the ensemble mean projection of 6 events. Similarly, under SSP585 scenario, the number of extreme drought events is projected to vary between 1 event for EC-Earth3-Veg and 10 events for CanESM5, with the ensemble mean projection of 6 extreme drought events in the mid-term. The number of drought events of varying severities during the mid-term is given in Figure 5.86.

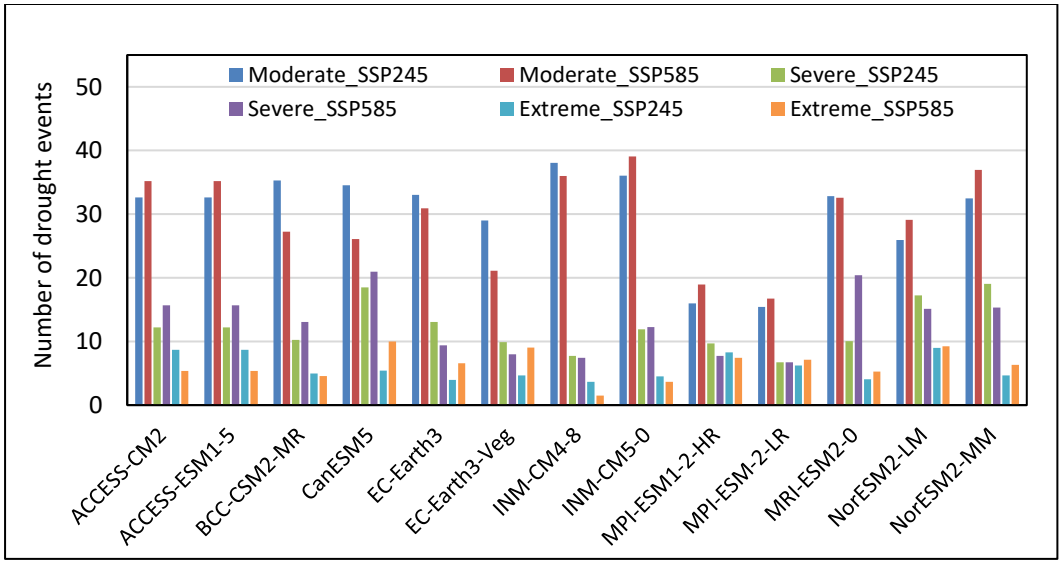

Figure 5.86: Drought events projected during mid-term (2041-2070)

Table 5.33 gives the average number of extreme, severe and moderate drought events projected in the complete study area during the end-term period. In the end-

term, the number of moderate events under SSP245 scenario is projected to vary between 19 events (MPI-ESM1-2-HR, MPI-ESM1-2-LR) and 33 events (ACCESS-CM2, ACCESS-ESM1-5), with the ensemble mean projection of 30 moderate drought events. However, under SSP585 scenario, the number of moderate events is projected to vary between 19 events for MPI-ESM1-2-HR and 37 events (ACCESS-CM2, ACCESS-ESM1-5), with the ensemble mean projection of 30 moderate drought events in the end-term.

Table 5.33: Drought events projected during end-term (2071-2100)

S. No.	GCMs	Moderate SSP245	Moderate SSP585	Severe SSP245	Severe SSP585	Extreme SSP245	Extreme SSP585
1	ACCESS-CM2	33	37	18	16	7	6
2	ACCESS-ESM1-5	33	37	18	16	7	6
3	BCC-CSM2-MR	29	33	9	12	5	6
4	CanESM5	29	33	17	18	7	10
5	EC-Earth3	27	24	10	12	7	6
6	EC-Earth3-Veg	34	23	9	9	4	6
7	INM-CM4-8	36	34	12	10	2	2
8	INM-CM5-0	33	35	13	14	4	6
9	MPI-ESM1-2-HR	19	19	10	8	7	8
10	MPI-ESM1-2-LR	19	20	7	8	5	5
11	MRI-ESM2-0	33	28	10	15	4	7
12	NorESM2-LM	26	35	9	17	6	8
13	NorESM2-MM	35	31	15	13	7	7
Ensemble mean		**30**	**30**	**12**	**13**	**6**	**6**

In the end-term, the number of severe drought events under SSP245 scenario is projected to vary between 7 events for MPI-ESM-2-LR and 18 events (ACCESS-CM2, ACCESS-ESM1-5), with the ensemble mean projection of 13 severe drought events. Similarly, under SSP585 scenario, the number of severe drought events is projected to vary between 8 events (MPI-ESM1-2-HR, MPI-ESM1-2-LR) and 17 events for NorESM2-LM, with the ensemble mean projection of 6 severe drought events in the end -term. Also, the number of extreme drought events under SSP245 scenario is projected to vary between 5 events (NorESM2-MM) and 9 events (ACCESS-CM2, ACCESS-ESM1-5) with the ensemble mean projection of 6 events. Similarly, under SSP585 scenario, the number of extreme drought events is projected to vary between 4 events (EC-Earth3-Veg, MRI-ESM2-0) and 7 events for six GCMs, with the ensemble mean projection of 6 extreme drought events in the end-term. The number of drought events of varying severities during the mid-term is given in Figure 5.87.

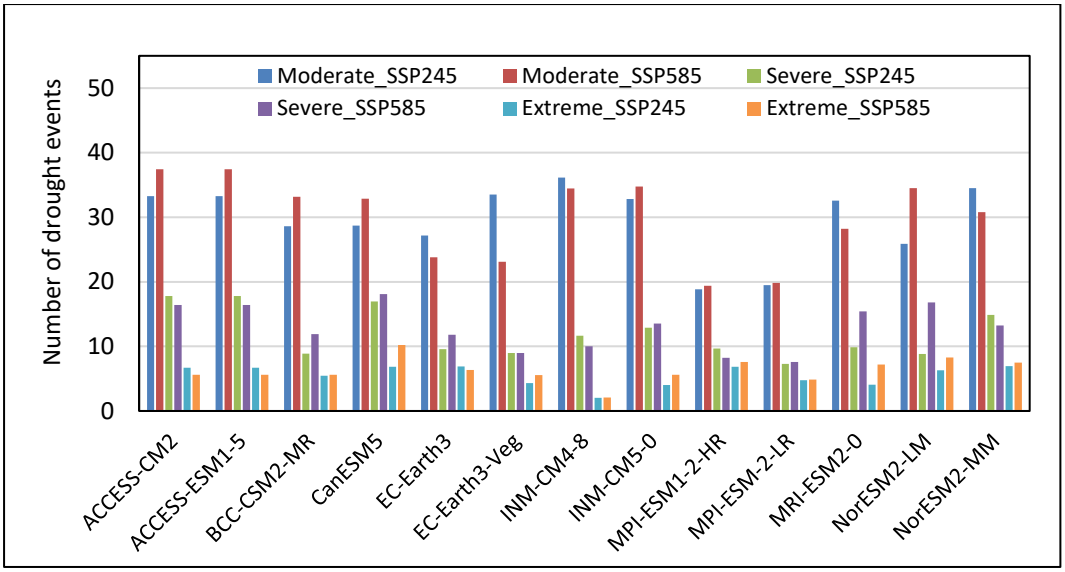

Figure 5.87: Drought events projected during end-term (2071-2100)

It can be observed that there is a considerable variability in the number of moderate events predicted by various GCMs as compared to the variability in the projections in the severe and extreme drought events. However, the moderate events are projected to increase in the mid-term and end-term as compared to the near-term. The comparison of the ensemble means of the total drought events, which includes the summation of moderate, severe and extreme events during the baseline, present and all future time periods is given in Figure 5.88.

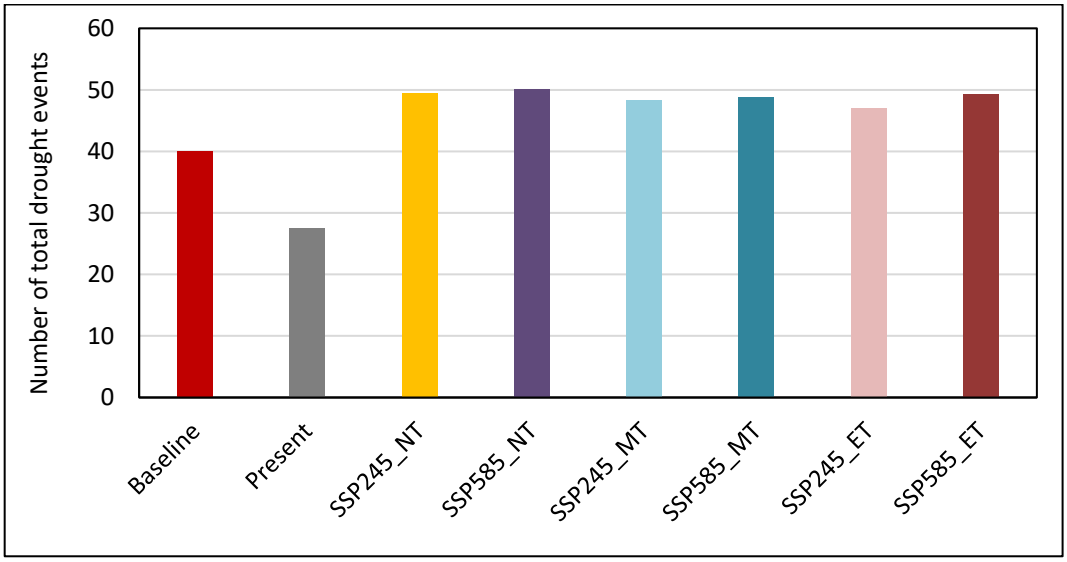

Figure 5.88: Comparison of drought events during different time periods

As compared to the baseline period, the total number of drought events have depicted a substantial decline during the present period (23 events i.e. 28 events

on pro-rata basis for 30-yr period) from 40 events during the baseline period, which is thereafter projected to increase to 33 events (50 events on pro-rata basis for 30-yr period) during the near-term under both scenarios, and further expected to marginally vary between 48 and 47 events during mid-term and end-term respectively under SSP245 scenario, whereas it is expected to be at 49 events during mid-term and end-term under SSP585 scenario. Even though variability was observed in the results from individual GCMs, but the ensemble means give a clear direction of the drought events that are expected to increase in future.

The drought severity has also been compared during the various time periods. The projected drought severity during the near-term by various GCMs under both scenarios is given in Table 5.34. During the near-term, the severity of the extreme and severe drought events is higher under SSP585 scenario as compared to the SSP245 scenario, whereas the severity of the moderate drought events is higher under the SSP245 scenario. There is considerable inter-model variability which also shows the underlying uncertainty in the future projections. The comparison of the projected drought severity during the near-term is given in Figure 5.89. The projected drought severity during the mid-term is given in Table 5.35. During the mid-term, the severity of the extreme drought events is higher under SSP585 scenario as compared to the SSP245 scenario, whereas the severities of the severe and moderate drought events are higher under the SSP245 scenario. There is considerable inter-model variability which also shows the underlying uncertainty

Table 5.34: Drought severity projected during near-term (2021-2040)

S. No.	GCMs	Moderate SSP245	Moderate SSP585	Severe SSP245	Severe SSP585	Extreme SSP245	Extreme SSP585
1	ACCESS-CM2	-33.21	-24.52	-13.66	-18.36	-7.83	-13.53
2	ACCESS-ESM1-5	-27.03	-37.06	-19.55	-17.91	-12.75	-7.02
3	BCC-CSM2-MR	-19.72	-24.70	-12.27	-15.00	-8.85	-6.62
4	CanESM5	-28.58	-22.91	-15.64	-16.35	-10.31	-9.94
5	EC-Earth3	-26.53	-20.32	-14.47	-11.98	-9.14	-12.14
6	EC-Earth3-Veg	-18.52	-22.59	-14.68	-13.17	-9.32	-10.04
7	INM-CM4-8	-26.91	-28.15	-11.94	-8.19	-6.25	-4.84
8	INM-CM5-0	-36.88	-29.40	-11.52	-14.59	-4.57	-7.72
9	MPI-ESM1-2-HR	-18.85	-10.47	-11.60	-10.35	-8.03	-13.85
10	MPI-ESM1-2-LR	-16.23	-11.04	-12.16	-13.91	-6.26	-7.23
11	MRI-ESM2-0	-23.97	-28.62	-10.85	-20.33	-8.75	-12.26
12	NorESM2-LM	-22.75	-25.11	-23.34	-15.25	-12.01	-17.19
13	NorESM2-MM	-25.87	-25.11	-14.08	-15.25	-15.70	-17.19
Ensemble mean		**-25.00**	**-23.84**	**-14.29**	**-14.67**	**-9.21**	**10.73**

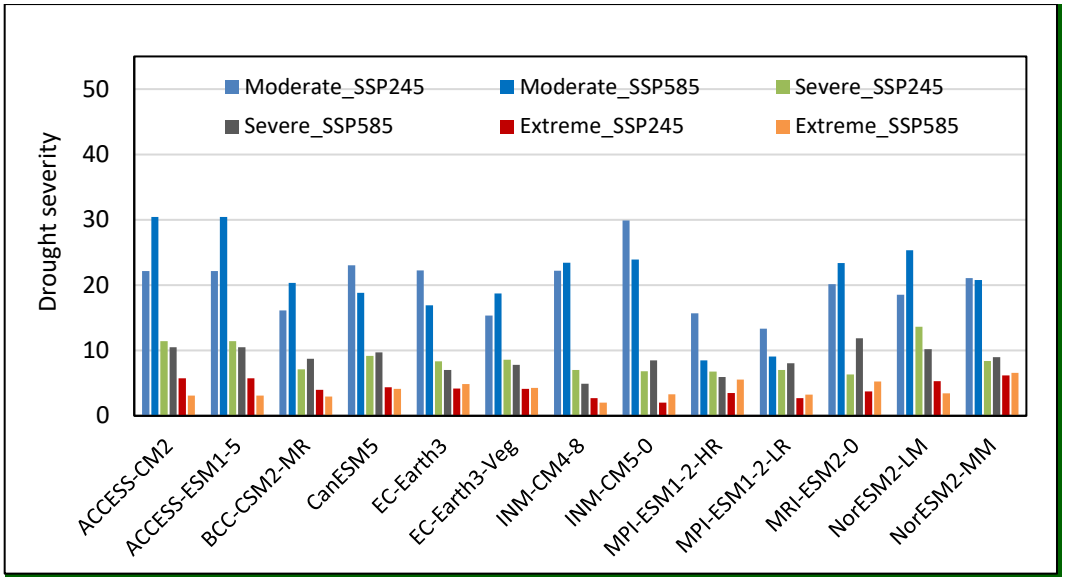

Figure 5.89: Drought severity projected during near-term (2021-2040)

Table 5.35: Drought severity projected during mid-term (2041-2070)

S. No.	GCMs	Moderate SSP245	Moderate SSP585	Severe SSP245	Severe SSP585	Extreme SSP245	Extreme SSP585
1	ACCESS-CM2	-36.14	-35.52	-36.46	-25.24	-16.88	-21.62
2	ACCESS-ESM1-5	-40.14	-43.08	-20.83	-26.93	-22.22	-12.57
3	BCC-CSM2-MR	-42.64	-33.12	-18.07	-22.66	-11.43	-10.09
4	CanESM5	-42.31	-31.38	-31.70	-35.83	-11.85	-23.29
5	EC-Earth3	-40.81	-37.26	-22.41	-16.48	-9.60	-17.57
6	EC-Earth3-Veg	-35.52	-25.56	-17.09	-13.86	-12.39	-22.67
7	INM-CM4-8	-45.59	-44.06	-13.50	-12.64	-8.17	-3.69
8	INM-CM5-0	-43.83	-47.84	-20.21	-21.03	-10.07	-7.95
9	MPI-ESM1-2-HR	-19.35	-23.10	-16.86	-13.44	-20.25	-19.94
10	MPI-ESM1-2-LR	-19.02	-20.40	-11.71	-11.54	-15.52	-17.57
11	MRI-ESM2-0	-39.94	-40.65	-17.24	-35.08	-9.51	-12.02
12	NorESM2-LM	-32.18	-35.65	-29.83	-25.94	-21.40	-22.68
13	NorESM2-MM	-40.49	-45.06	-33.19	-26.52	-10.14	-14.95
Ensemble mean		**-36.77**	**-35.59**	**-22.24**	**-22.09**	**-13.80**	**-15.89**

in the future projections. During the end-term, the severity of the extreme, severe and moderate drought events is higher under SSP585 scenario as compared to the SSP245 scenario. There is again a considerable inter-model variability which also shows the underlying uncertainty in the future projections. The comparison of the projected drought severity during the end-term is given in Table 5.36.

However, it can be seen that the accumulated severity of the extreme drought events is projected to be much lesser in comparison to the severe and moderate

Table 5.36: Drought severity projected during end-term (2071-2100)

S. No.	GCMs	Moderate SSP245	Moderate SSP585	Severe SSP245	Severe SSP585	Extreme SSP245	Extreme SSP585
1	ACCESS-CM2	-33.37	-34.99	-36.97	-32.24	-15.30	-15.78
2	ACCESS-ESM1-5	-40.70	-45.98	-31.05	-27.87	-15.72	-12.95
3	BCC-CSM2-MR	-35.19	-40.84	-15.03	-20.44	-13.13	-12.86
4	CanESM5	-35.26	-40.40	-29.07	-30.90	-16.16	-24.38
5	EC-Earth3	-33.38	-28.58	-16.23	-20.31	-18.10	-15.33
6	EC-Earth3-Veg	-40.42	-27.69	-15.43	-15.43	-10.42	-14.27
7	INM-CM4-8	-43.54	-41.87	-20.06	-17.21	-4.58	-4.70
8	INM-CM5-0	-40.36	-42.60	-22.14	-23.55	-9.33	-12.46
9	MPI-ESM1-2-HR	-22.77	-23.94	-16.89	-14.00	-19.46	-21.00
10	MPI-ESM1-2-LR	-23.24	-23.92	-12.67	-12.93	-11.09	-11.54
11	MRI-ESM2-0	-39.67	-34.50	-16.99	-26.40	-9.52	-17.14
12	NorESM2-LM	-31.28	-42.47	-15.47	-29.20	-16.05	-19.22
13	NorESM2-MM	-41.86	-37.44	-25.83	-22.93	-17.95	-19.12
Ensemble mean		**-35.46**	**-35.79**	**-21.06**	**-22.57**	**-13.60**	**-15.44**

drought events in all future time periods. The comparison of the ensemble mean of the drought severity under both scenarios with that during the baseline and present periods is given in Figure 5.90. It can be observed that the drought severity is projected to increase during the near-term, mid-term and end-term periods and the drought severity is projected to be higher under the SSP585 scenario as compared to the SSP245 scenario.

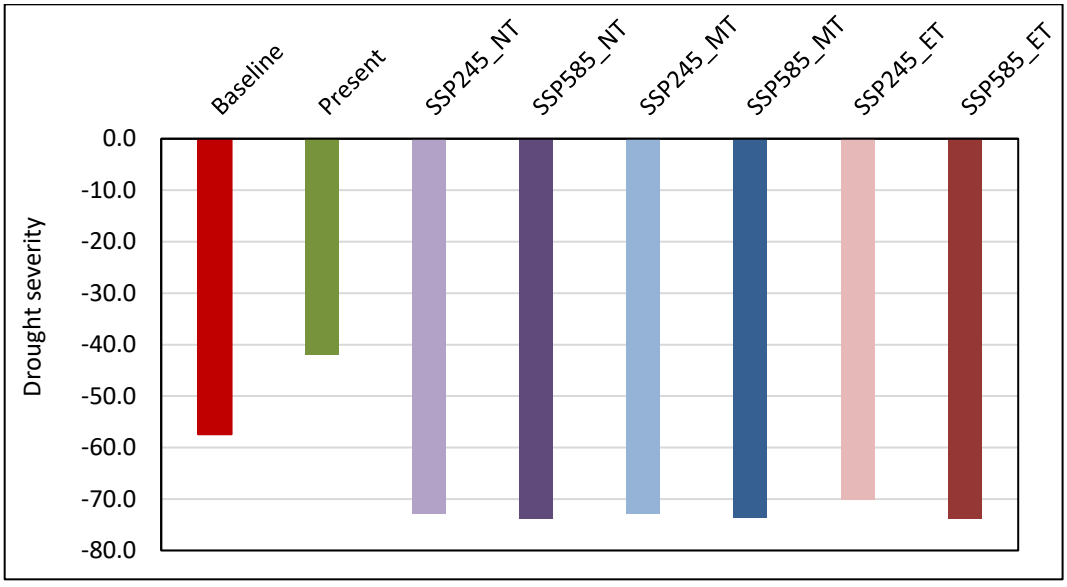

Figure 5.90: Comparison of drought severity during different time periods

5.4.4 Evaluation of agricultural drought

5.4.4.1 Evaluation of agricultural drought using VCI and 3m-SPI

The 3m-SPI has been invariably used as a short-term drought indicator, particularly to represent the agricultural drought. The same approach has been used in this study. As the monsoon season is effectively spread over the study area from mid-June to mid-September, which is three months, the 3m-SPI is an indicator of the soil moisture build-up during the various monsoon months. More than 90% of the annual rainfall is received during the monsoon season in the study area. However, an investigation has been carried out for the assessment of the normalized difference vegetation index (NDVI) based vegetation condition index (VCI) for the baseline and present periods. The evaluation of future VCI involves difficulties and large uncertainties. As such, the 3m-SPI has been used as an indicator for the soil moisture availability/deficit for the future time periods viz., near-term, mid-term, end-term along with the baseline and present time periods.

The normalized difference vegetation index (NDVI) is one of the most widely used indices for assessing the crop health. Healthy vegetation means higher chlorophyll concentration which is equal to its degree of greenness. Most of the healthy plant absorbs red light and reflects infrared radiation due to water-filled leaf. It implies that plants are under no stress and adequate water is available to fulfill their demand. In the present study, NDVI has been used to examine the changes in vegetation growth rate and to detect the production of vegetation. NDVI values range from -1 to +1. The lower values of NDVI indicate lesser vegetation and the NDVI goes on increasing with healthier vegetation condition. The NDVI was computed for the various months of drought years during the present period (1991-2015) i.e., 2000 and 2002 using MODIS NDVI product. The variation in vegetation condition during June to October 2000 is given in Figure 5.91 to Figure 5.94.

As the health of the vegetation gets affected due to reduction in soil-water availability due to water deficit, NDVI value also decreases accordingly. From Figure 5.91 it can be observed that the vegetation remains green (high NDVI values) in small parts of eastern and southern regions, mainly due to availability of

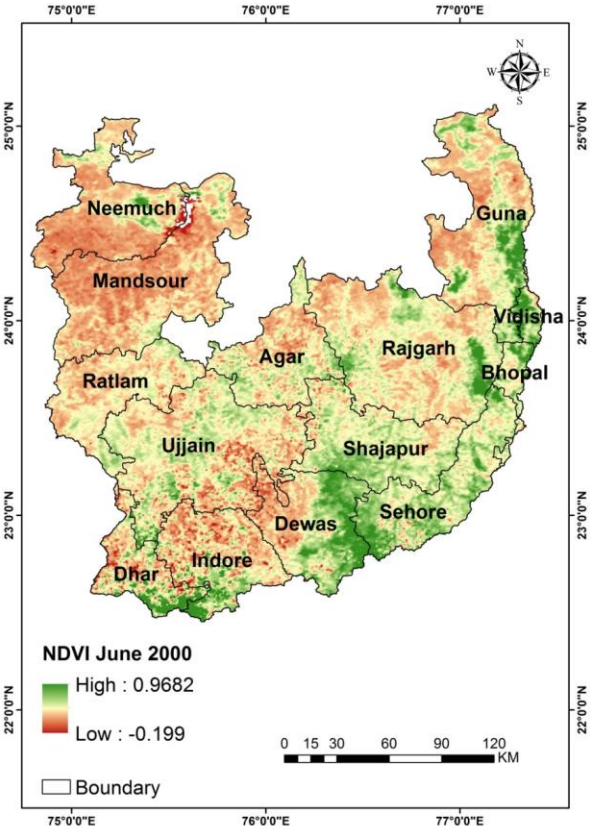

Figure 5.91: NDVI for June 2000

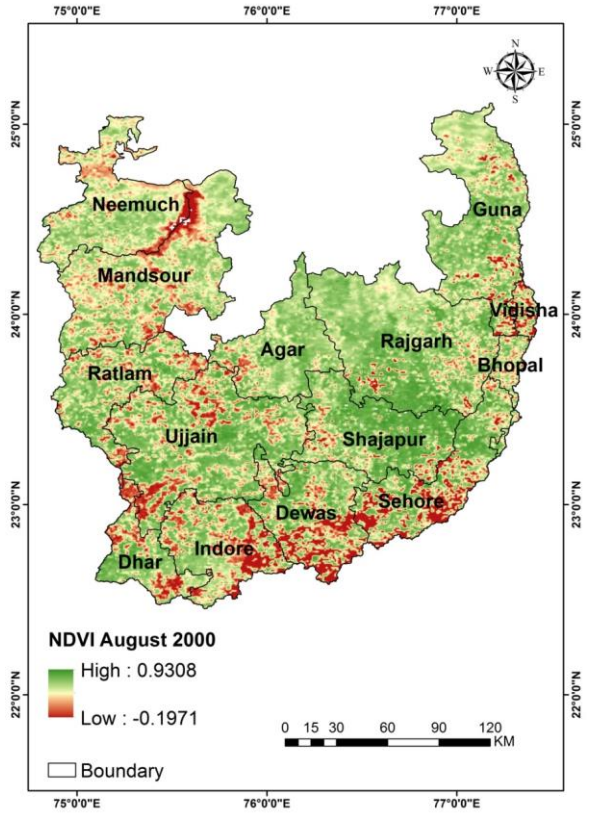

Figure 5.92: NDVI for July 2000

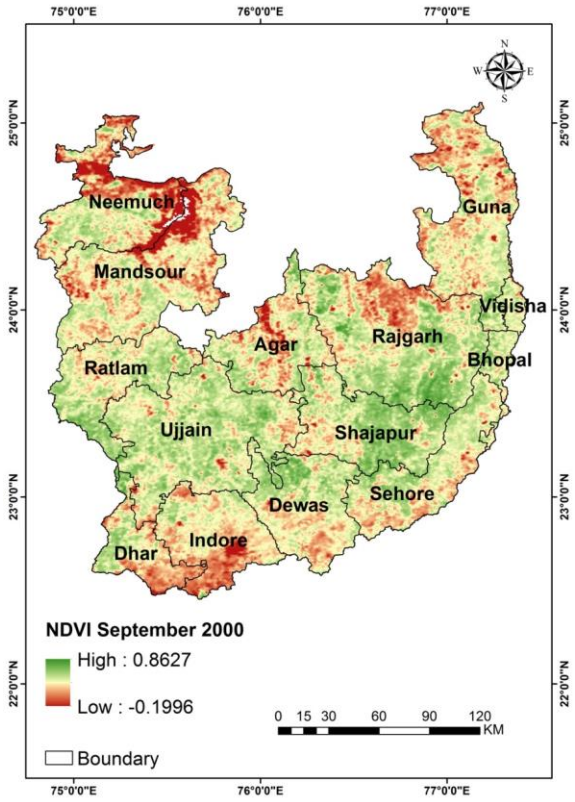

Figure 5.93: NDVI for September 2000

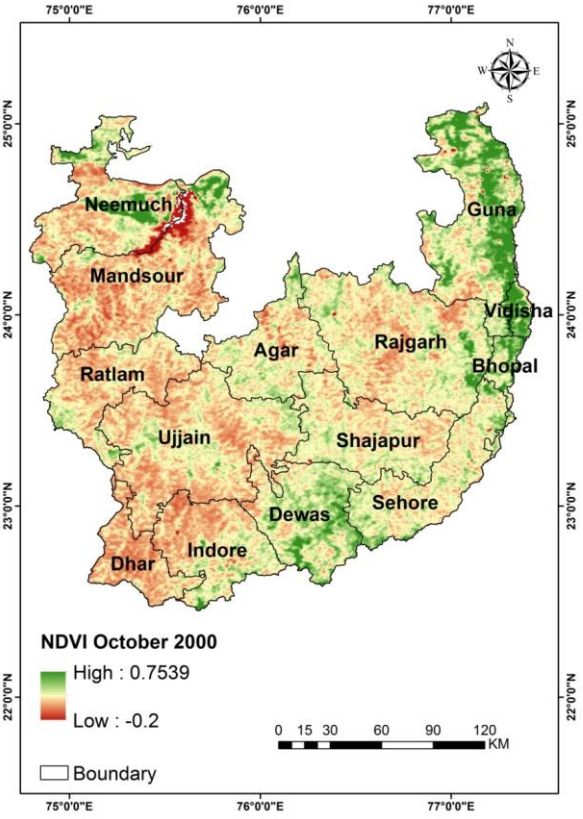

Figure 5.94: NDVI for October 2000

sufficient water in the soil. Most of the kharif crops are sown in June. Figure 5.92 depicts that that the extent of vegetation has increased in the region in July 2000 and only some parts in southern region had no vegetation. The extent of vegetation in September 2000 decreased and healthy vegetation could only be seen in some parts of Shajapur and Rajgarh blocks. This is due to the high variability in rainfall and subsequent drought conditions that prevailed, resulting in lower NDVI vales and poor crop conditions in the study area. The NDVI image shows high temporal variation in vegetation condition within the study area during October 2000. The NDVI method gives superior results for identification of the vegetation health which can be correlated to the prevailing drought/water stress conditions at that point of time.

5.4.4.2 Vegetation Condition Index (VCI)

VCI, a NDVI derived drought index, was used to quantify drought in the region. The onset and extent of drought can be clearly seen from the VCI maps for drought year of 2000. Figure 5.95 to Figure 5.98 shows the VCI based drought conditions in the study area from June to October 2000. Figure 5.94 shows the vegetation condition during June 2000 and it has can be seen that severe drought condition prevailed in Mandsaur, Neemuch, and in the small areas of Agar, Ratlam, Guna and Rajgarh blocks, whereas the remaining area was under moderate drought to a very large extent. Some parts of Dewas and Guna districts were under mild drought condition. Acute water stress was evident all over the study area due to existence of severe drought condition. The vegetation health improved during August and September 2000 due to favorable rainfall conditions and sufficient soil moisture build-up due to which there was and healthy crop growth. However, mild drought condition prevailed in the region in October 2000. The agricultural drought characteristics have been evaluated similarly during 2002 which was the other drought year witnessed in the study area. The agricultural sector is one of the most important sectors that drive the India economy and the occurrence of the drought has its maximum and widespread impact on this sector. The VCI is a comprehensive remote sensing-based indicator which can be effectively used to monitor the agricultural drought and evaluate the agricultural drought characteristics. The progression and withdrawal of the agricultural

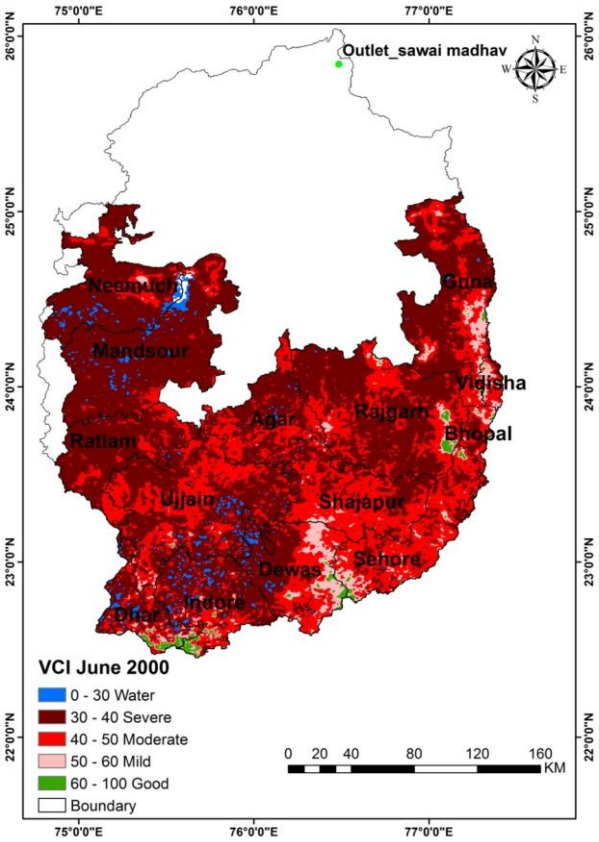

Figure 5.95: VCI for June 2000

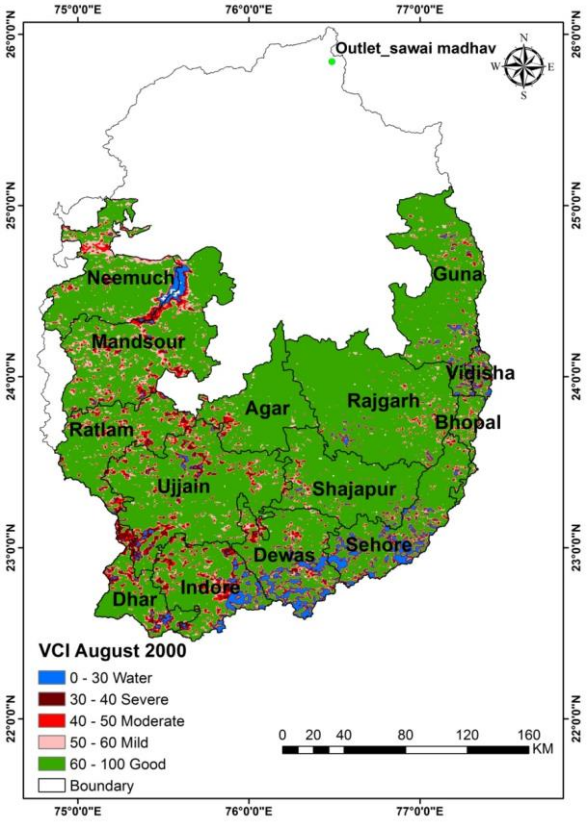

Figure 5.96: VCI for August 2000

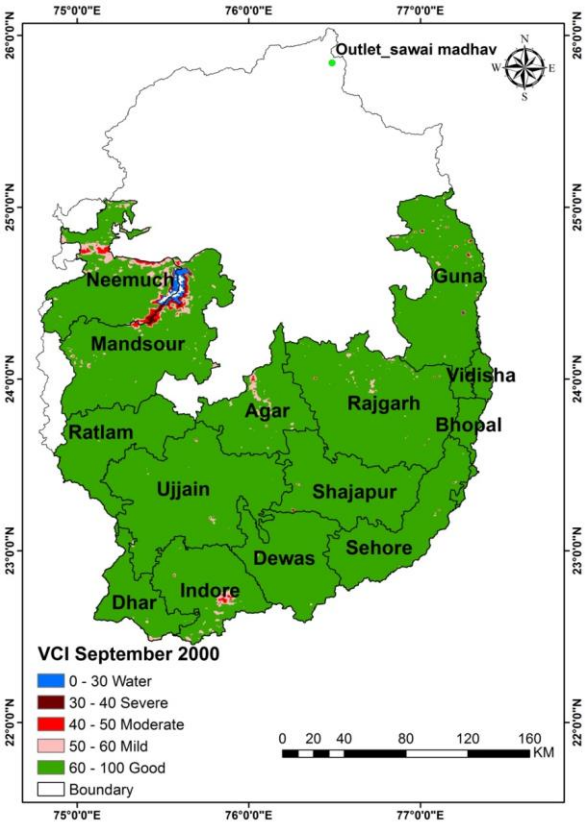

Figure 5.97: VCI for September 2000

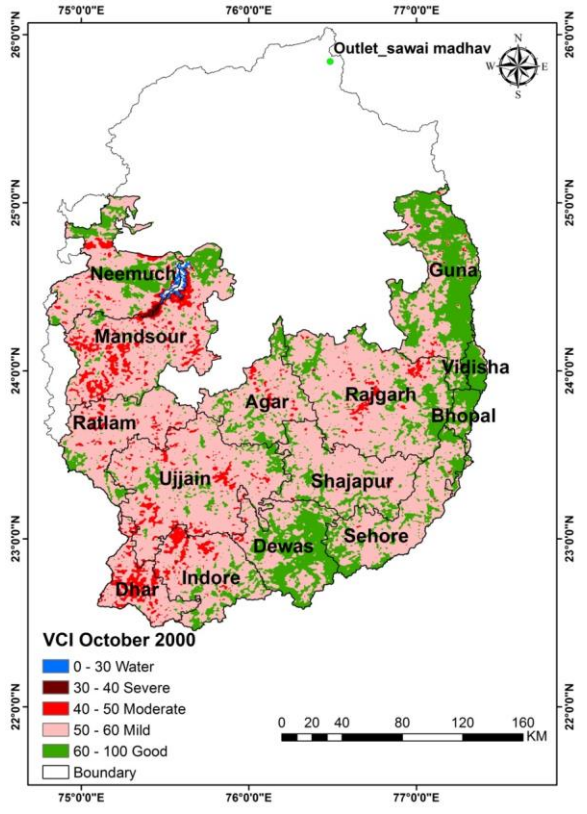

Figure 5.98: VCI for October 2000

drought can be understood using the VCI which can be used for development of drought management plans which can help to mitigate the hardships for the farming community.

As the projection of land use into future time horizons, that too, for very long durations may involve large uncertainties, the agricultural drought conditions have therefore been evaluated based on the 3m-SPI, which has been largely used by the research community as an indicator of the short-term drought viz., soil moisture drought. Moreover, the monsoon season prevails over the study area during mid-June to mid-September which is effectively three months. Therefore, the 3m-SPI can be used effectively to assess the short-term soil moisture drought conditions in the study area for all future time horizons. Also, in order to maintain similarity in computations in short-term drought conditions during all time horizons, the 3m-SPI has been used as well for the baseline and present time horizons.

5.4.5 Evaluation of Groundwater Drought Characteristics

The groundwater drought characteristics have been evaluated based on the Groundwater Drought Index (GDI) derived from the groundwater levels of the monitoring wells in the various districts. The long-term groundwater levels are available on a quarterly basis at the groundwater monitoring wells located in various blocks of the 14 districts of the study area during 1985 to 2017. The temporal variation of GDI at Nalwa in Ujjain district, Malikheri in Agar district, Bhuniyakhedi in Mandsaur district, Jawad in Neemuch district, and Kalakheda in Rajgarh district is given in Figure 5.99 to Figure 5.103. The observation wells located in the Agar, Indore, Mandsaur, Rajgarh and Ujjain districts depict falling trends which indicates that the groundwater drought are increasing in these locations. However, few observation wells located in Dewas, Neemuch, Ratlam and Shajapur districts show that the GDI is increasing which indicates that there is no situation of groundwater drought at these places. The years of groundwater drought including their severity and duration are highlighted in each of these graphs. Mixed trends of groundwater drought as evaluated by the GDI can be seen in the study area. However, it can be observed that in most of these selected observation wells there has been a groundwater drought situation during the last

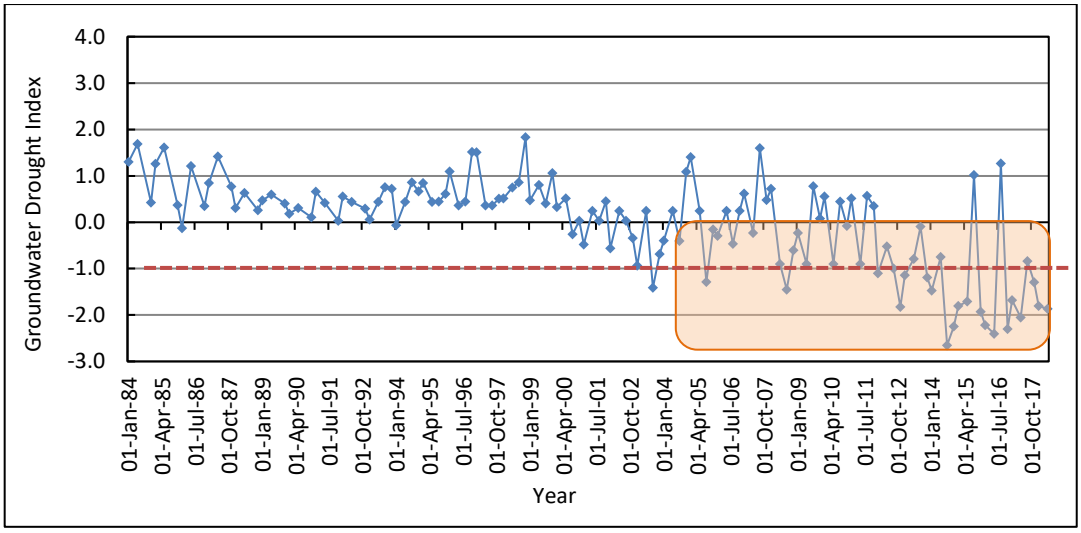

Figure 5.99: Temporal variation of GDI at Nalwa in Ujjain district

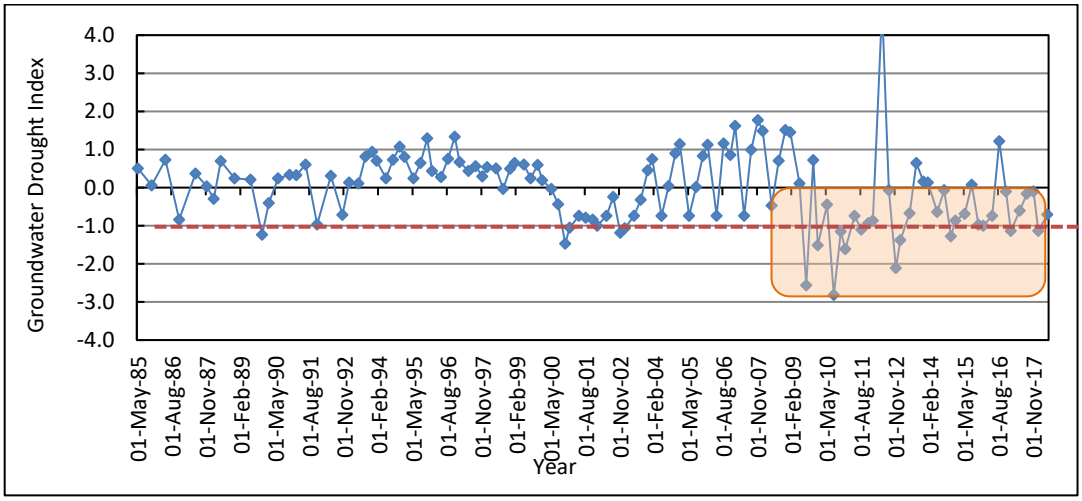

Figure 5.100: Temporal variation of GDI at Malikheri in Agar district

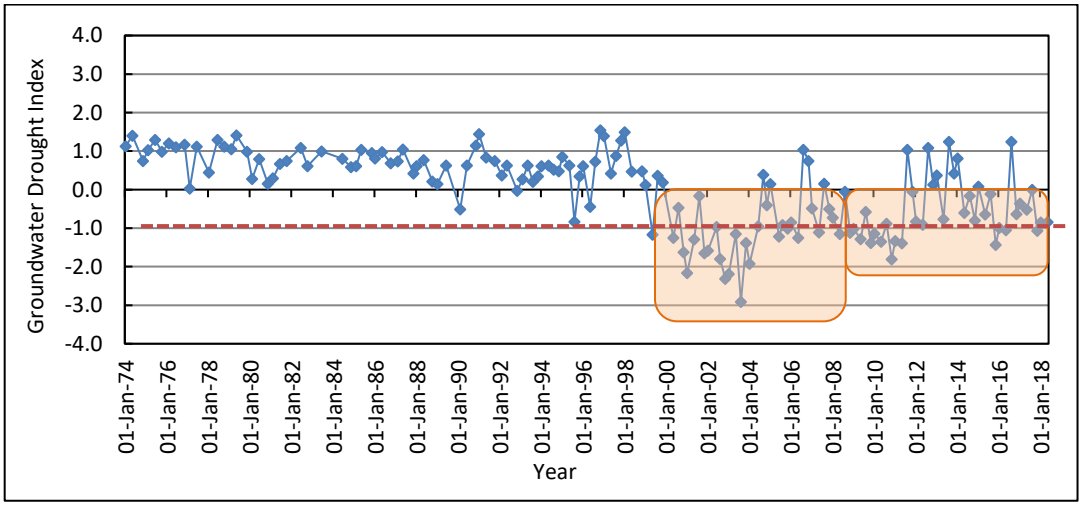

Figure 5.101: Temporal variation of GDI at Bhuniyakhedi in Mandsaur district

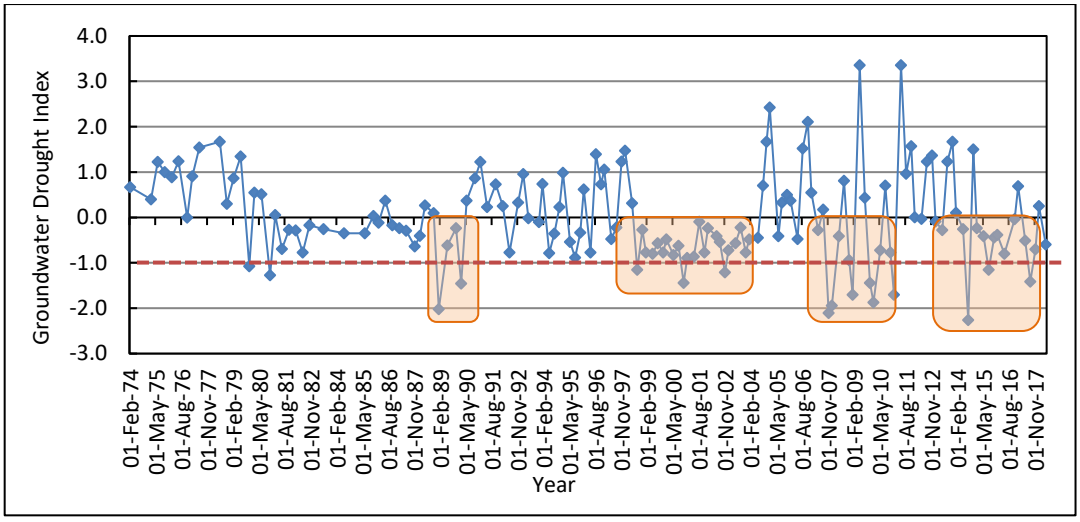

Figure 5.102: Temporal variation of GDI at Jawad in Neemuch district

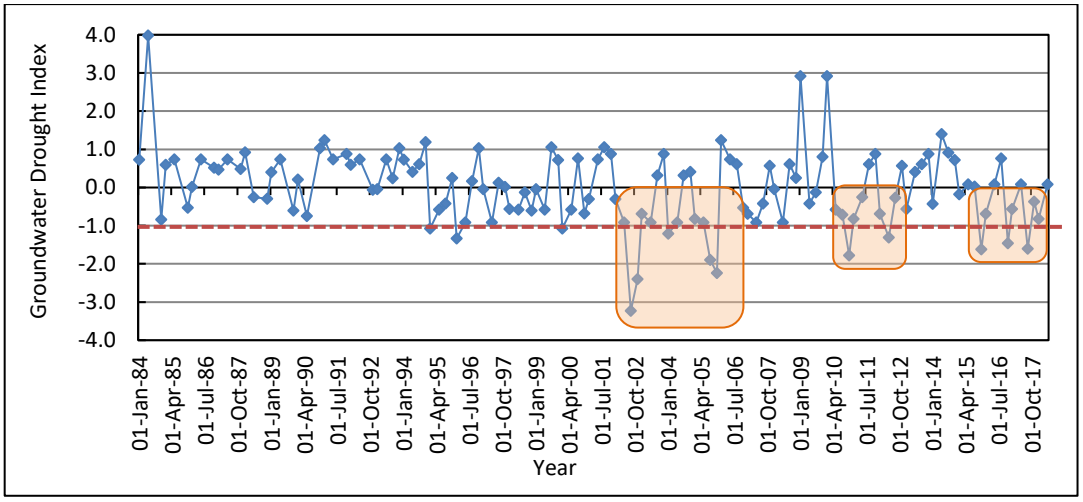

Figure 5.103: Temporal variation of GDI at Kalakheda in Rajgarh district

few years. Moreover, it can be seen that it takes few months/years for the situation to recover from a groundwater drought condition to a normal condition. The groundwater characteristics including its severity, duration and intensity have been evaluated. The locations indicating the increase in groundwater droughts can be demarcated for planning of artificial recharge measures to arrest the declining trend of groundwater levels in such regions/locations within the study area.

Table 5.37 indicates the number of occurrences of extreme, severe and moderate groundwater drought events during 1985-2017 in the various blocks of the 14 districts falling in the study area. The drought severity classes were computed based on GDI classification i.e., extreme drought event (GDI < -2.0), severe drought event (-2.0 < GDI < -1.5), moderate drought event (-1.5 < GDI < -1.0).

Table 5.37: GDI based groundwater drought events in the study area

S. No.	Village	Moderate	Severe	Extreme	Total
1	Badgonda	5	2	8	15
2	Bagankheda	20	2	2	24
3	Bahadri	15	5	5	25
4	Baodi kheda	8	2	4	14
5	Baraoda	14	8	4	26
6	Barkheda	12	5	5	22
7	Barod	21	8	0	29
8	Barvai	9	3	5	17
9	Bhainsoda	10	5	0	15
10	Bhodwamata	16	5	10	31
11	Bhutiya	11	7	2	20
12	Biaora	17	10	3	30
13	Boliya	15	10	2	27
14	Bond piplia	16	5	4	25
15	Budhaniya	12	5	2	19
16	Chhawani- zodia	20	5	2	27
17	Dhangoon	5	7	4	16
18	Dhannod	10	6	2	18
19	Dhantalab	10	8	0	18
20	Dhurla	17	1	4	22
21	Dolaj	8	6	2	16
22	Dudhakhedi	19	1	1	21
23	Dupara	10	5	0	15
24	Gandhi hall	17	3	4	24
25	Gandhi-garm	5	11	4	20
26	Ghatiya/Lovekhedi	21	7	3	31
27	Gudrawan	14	7	0	21
28	Jamoniya	16	9	3	28
29	Jannod	19	5	4	28
30	Jathal	14	1	5	20
31	Jawad	9	4	3	16
32	Jetpur kala	10	3	4	17
33	Jhonta	13	2	2	17
34	Kalapipal	11	8	2	21
35	Kalisindh	12	2	4	18
36	Kalpatha	10	9	1	20
37	Kamthana	27	9	1	37
38	Kangani kheda	11	8	1	20
39	Khajrana	13	4	4	21
40	Khajuriya	15	3	4	22

41	Kherwa khurd	5	4	4	13
42	Khilchipur	14	5	3	22
43	Khodawda	13	6	2	21
44	Khonkra kalan	6	3	7	16
45	Kundanpur	8	7	3	18
46	Lodkiya	9	2	8	19
47	Madkota	18	6	3	27
48	Makodi	16	4	0	20
49	Malagaon	18	3	3	24
50	Malikhedi	10	9	0	19
51	Manankhedo	10	6	2	18
52	Manasa	7	7	3	17
53	Maxi	13	3	0	16
54	Melkheda	21	6	4	31
55	Molana	20	5	1	26
56	Moman barodia	18	3	0	21
57	Morwon	16	6	2	24
58	Mundla dostdak	7	7	8	22
59	Nalwa	9	7	6	22
60	Nayan	13	9	2	24
61	Neal Kanth	11	6	5	22
62	Neemach	12	6	7	25
63	Osara	12	5	4	21
64	Patalpani	23	3	1	27
65	Patan	12	5	0	17
66	Pipalda	14	6	3	23
67	Pipaliya mohmod	4	9	3	16
68	Pipalpati	10	5	5	20
69	Pipri	14	10	2	26
70	Pirjhalar	17	5	3	25
71	Punjapura	8	3	6	17
72	Ragbel	16	3	3	22
73	Rajapura	23	4	2	29
74	Rajgarh	15	2	1	18
75	Rojana	15	7	3	25
76	Runija	5	6	8	19
77	Shajapur	6	7	5	18
78	Shamgarh	8	5	5	18
79	Singoda	19	1	0	20
80	Singoli	10	5	1	16
81	Siya gram	13	2	0	15
82	Suigaon	6	5	0	11

83	Tal	16	5	3	24
84	Tinchha	6	8	5	19
85	Todi	15	5	3	23
86	Ujjaina	18	8	3	29
87	Unhel / Dauparawada	20	1	3	24
88	Yashwant Nagar	10	3	1	14

The total groundwater drought events varied between a maximum of 37 events at Kamthana in Ujjain district to minimum of 11 events at Suigaon in Agar district. The number of extreme drought events varied between 10 events at Bhodwamata and 1 event at Rajgarh, Singoli, Patalpani and Yashwant Nagar. Similarly, the number of severe drought varied between 11 events at Gandhi-gram and 1 event at Singoda, Dhurla, Dudhakhedi and Unhel / Dauparawada. The number of moderate groundwater drought occurrences varied between 27 events at Kamthana and 4 events at Pipaliya Mohmod.

The total groundwater drought severity was computed during the period of analysis. The severity of various types of droughts during drought years have been added to compute the total groundwater drought severity and divided by the number of groundwater drought events to compute the average groundwater drought intensity. The groundwater drought characteristics including the groundwater drought severity and intensity are given in Table 5.38.

Table 5.38: GDI based groundwater drought severity and drought intensity

S. No.	Village	Drought severity	Drought intensity
1	Badgonda	-29.71	-1.98
2	Bagankheda	-32.25	-1.34
3	Bahadri	-39.81	-1.59
4	Baodi kheda	-24.07	-1.72
5	Baraoda	-38.71	-1.49
6	Barkheda	-36.01	-1.64
7	Barod	-38.07	-1.31
8	Barvai	-28.85	-1.70
9	Bhainsoda	-21.04	-1.40
10	Bhodwamata	-60.04	-1.94
11	Bhutiya	-29.72	-1.49
12	Biaora	-43.17	-1.44
13	Boliya	-40.27	-1.49

14	Bond piplia	-38.2	-1.53
15	Budhaniya	-30.36	-1.60
16	Chhawani- zodia	-38.49	-1.43
17	Dhangoon	-25.77	-1.61
18	Dhannod	-25.64	-1.42
19	Dhantalab	-25.91	-1.44
20	Dhurla	-31.88	-1.45
21	Dolaj	-26.15	-1.63
22	Dudhakhedi	-25.86	-1.23
23	Dupara	-21.83	-1.46
24	Gandhi hall	-34.16	-1.42
25	Gandhi-garm	-34.54	-1.73
26	Ghatiya/Lovekhedi	-43.98	-1.42
27	Gudrawan	-27.87	-1.33
28	Jamoniya	-42.88	-1.53
29	Jannod	-39.49	-1.41
30	Jathal	-28.85	-1.44
31	Jawad	-25.21	-1.58
32	Jetpur kala	-27.96	-1.64
33	Jhonta	-23.66	-1.39
34	Kalapipal	-32.61	-1.55
35	Kalisindh	-26.62	-1.48
36	Kalpatha	-29.94	-1.50
37	Kamthana	-51.21	-1.38
38	Kangani kheda	-29.95	-1.50
39	Khajrana	-31.60	-1.50
40	Khajuriya	-34.40	-1.56
41	Kherwa khurd	-22.85	-1.76
42	Khilchipur	-33.42	-1.52
43	Khodawda	-31.00	-1.48
44	Khonkra kalan	-28.4	-1.78
45	Kundanpur	-29.89	-1.66
46	Lodkiya	-35.26	-1.86
47	Madkota	-38.17	-1.41
48	Makodi	-26.92	-1.35
49	Malagaon	-35.71	-1.49
50	Malikhedi	-28.59	-1.50
51	Manankhedo	-26.31	-1.46
52	Manasa	-28.86	-1.70
53	Maxi	-21.88	-1.37
54	Melkheda	-47.13	-1.52
55	Molana	-34.51	-1.33

56	Moman Barodia	-26.85	-1.28
57	Morwon	-36.42	-1.52
58	Mundla Dostdak	-39.95	-1.82
59	Nalwa	-37.83	-1.72
60	Nayan	-36.74	-1.53
61	Neal Kanth	-36.5	-1.66
62	Neemach	-42.85	-1.71
63	Osara	-32.62	-1.55
64	Patalpani	-34.52	-1.28
65	Patan	-22.68	-1.33
66	Pipalda	-33.48	-1.46
67	Pipaliya Mohmod	-27.73	-1.73
68	Pipalpati	-32.40	-1.62
69	Pipri	-38.17	-1.47
70	Pirjhalar	-35.98	-1.44
71	Punjapura	-29.28	-1.72
72	Ragbel	-30.43	-1.38
73	Rajapura	-39.2	-1.35
74	Rajgarh	-23.79	-1.32
75	Rojana	-37.18	-1.49
76	Runija	-34.75	-1.83
77	Shajapur	-30.29	-1.68
78	Shamgarh	-30.59	-1.7
79	Singoda	-24.12	-1.21
80	Singoli	-24.73	-1.55
81	Siya gram	-19.38	-1.29
82	Suigaon	-15.48	-1.41
83	Tal	-35.00	-1.46
84	Tinchha	-32.11	-1.69
85	Todi	-33.36	-1.45
86	Ujjaina	-44.38	-1.53
87	Unhel / Dauparawada	-33.86	-1.41
88	Yashwant Nagar	-22.40	-1.60

The drought of maximum severity occurred at Bhodwamata in Neemuch block (-60.04) whereas the drought of minimum severity occurred at Suigaon in Agar block (-15.48). Drought intensity in the region varies between a maximum of -1.98 at Badgonda block in Indore district to a minimum of -1.21 at Singoda block in Dewas district.

The groundwater drought characteristics during one of the drought years 2002, during May-2002, Aug-2002 and Nov-2002 is given in Figure 5.104 to Figure 5.106 respectively. Figure 5.103 indicates that during May 2002, moderate groundwater drought conditions were seen only small patches in Rajgarh district whereas during August 2002, the situation worsened to extreme groundwater drought in major parts of Rajgarh, Guna and Neemuch districts. The moderate groundwater drought was widespread in the districts of Mandsaur, Ratlam, Agar, Dhar, Indore, Shajapur, Bhopal and Vidisha districts. The situation further aggravated in November 2002 and almost all district's bordering Rajasthan was under extreme groundwater drought conditions, particularly in the districts of Guna, Rajgarh, Mandsaur and Neemuch followed by moderate drought in the areas adjoining these districts.

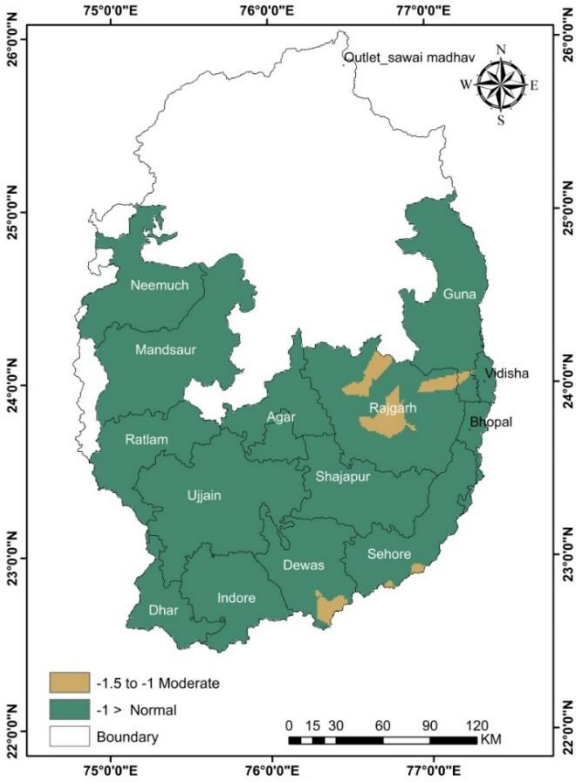

Figure 5.104: Spatial variation of GDI during May 2002

Normal conditions prevailed elsewhere in the southern portion of the basin. These plots showing the spatial variation of the groundwater severity helps in understanding the progression and withdrawal of groundwater droughts in the region.

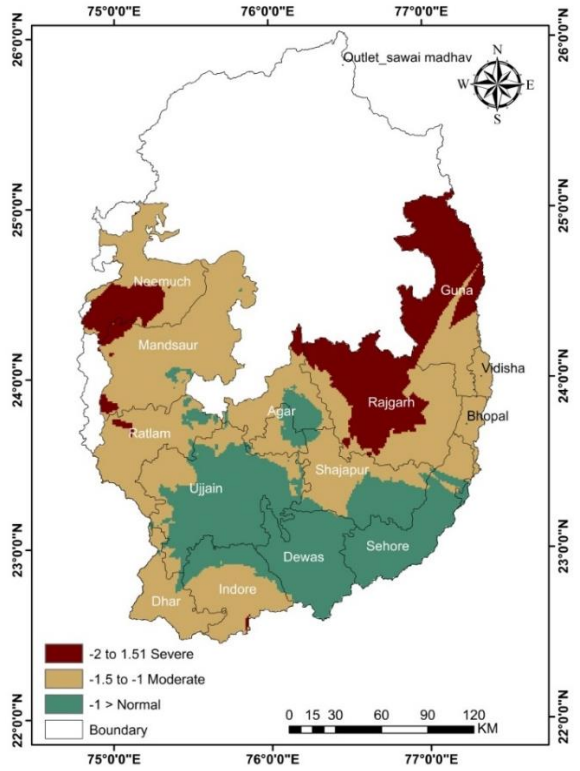

Figure 5.105: Spatial variation of GDI during August 2002

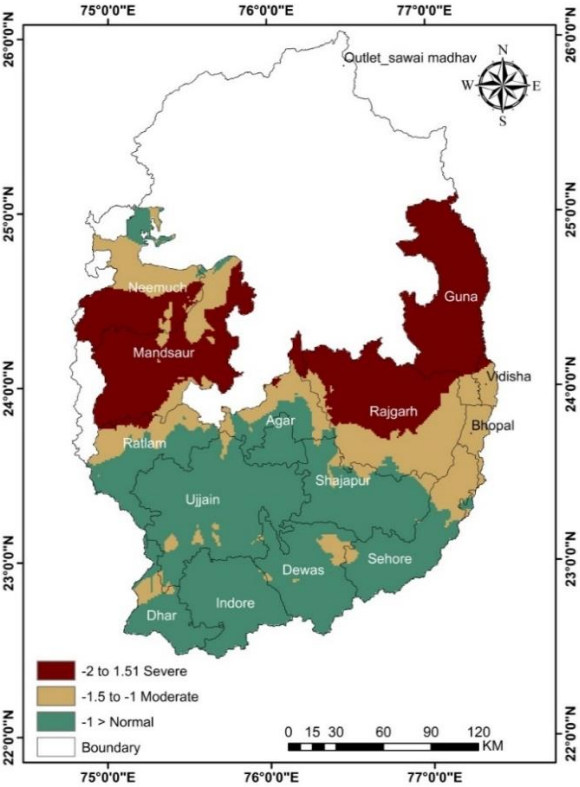

Figure 5.106: Spatial variation of GDI during November 2002

The future groundwater droughts during the near-term, mid-term and end-term have been evaluated and are given in Table 5.39 to Table 5.41. The number of extreme groundwater drought events is lowest as compared to the moderate and severe groundwater drought events during all future time periods. During the near-term, extreme groundwater drought events are projected to be 10 events under SSP245 scenario and only 5 events under SSP585 scenario. Similarly, the severe groundwater drought events are projected to be 20 events under SSP245 scenario and only 11 events under SSP585 scenario. However, 20 moderate groundwater drought events are projected under both SSP245 and SSP585 scenarios during the near-term

Table 5.39: Groundwater drought events during near-term (2021-2040)

S. No.	GCMs	Moderate SSP245	Moderate SSP585	Severe SSP245	Severe SSP585	Extreme SSP245	Extreme SSP585
1	ACCESS-CM2	23	15	12	10	1	7
2	ACCESS-ESM1-5	23	15	12	10	1	7
3	BCC-CSM2-MR	26	22	10	12	1	3
4	CanESM5	23	22	12	9	1	1
5	EC-Earth3	15	20	14	10	7	3
6	EC-Earth3-Veg	13	18	2	13	13	7
7	INM-CM4-8	11	30	10	9	9	1
8	INM-CM5-0	26	20	14	9	3	6
9	MPI-ESM1-2-HR	27	9	15	10	2	12
10	MPI-ESM-2-LR	16	18	13	10	9	8
11	MRI-ESM2-0	20	21	8	14	7	2
12	NorESM2-LM	18	31	12	17	8	0
13	NorESM2-MM	20	18	13	4	5	11
Ensemble mean		**20**	**20**	**20**	**11**	**10**	**5**

During the mid-term, extreme groundwater drought events are projected to be 14 events under SSP245 scenario and only 9 events under SSP585 scenario. However, the extreme drought events are projected to be more during the mid-term under both SSP scenarios. Similarly, the severe groundwater drought events are projected to be 28 events under SSP245 scenario and only 17 events under SSP585 scenario, which are much higher than that projected during the near-term. However, 20 moderate groundwater drought events are projected under SSP245 whereas higher number of drought events (32) is projected under the SSP585 scenario during the mid-term.

The comparison of the groundwater drought events during the various time period

Table 5.40: Groundwater drought events during mid-term

S. No.	GCMs	Moderate SSP245	Moderate SSP585	Severe SSP245	Severe SSP585	Extreme SSP245	Extreme SSP585
1	ACCESS-CM2	22	25	17	10	4	11
2	ACCESS-ESM1-5	22	25	17	10	4	11
3	BCC-CSM2-MR	41	35	19	24	4	4
4	CanESM5	37	31	12	21	8	4
5	EC-Earth3	40	11	17	7	9	18
6	EC-Earth3-Veg	32	16	28	16	4	21
7	INM-CM4-8	28	33	10	19	12	4
8	INM-CM5-0	40	37	16	17	7	2
9	MPI-ESM1-2-HR	38	21	17	10	14	15
10	MPI-ESM-2-LR	26	18	8	10	17	18
11	MRI-ESM2-0	30	37	16	11	7	9
12	NorESM2-LM	35	46	9	19	13	3
13	NorESM2-MM	26	32	30	12	9	11
Ensemble mean		**20**	**32**	**28**	**17**	**14**	**9**

Table 5.41: Groundwater drought events during end-term

S. No.	GCMs	Moderate SSP245	Moderate SSP585	Severe SSP245	Severe SSP585	Extreme SSP245	Extreme SSP585
1	ACCESS-CM2	33	36	19	27	1	1
2	ACCESS-ESM1-5	33	36	19	27	1	1
3	BCC-CSM2-MR	37	29	16	18	7	9
4	CanESM5	40	32	13	12	5	12
5	EC-Earth3	29	21	12	14	11	17
6	EC-Earth3-Veg	41	38	21	13	1	12
7	INM-CM4-8	28	30	12	8	5	1
8	INM-CM5-0	19	29	18	16	13	15
9	MPI-ESM1-2-HR	28	14	9	8	13	16
10	MPI-ESM-2-LR	33	46	19	7	10	6
11	MRI-ESM2-0	30	23	16	7	7	15
12	NorESM2-LM	27	22	21	23	1	5
13	NorESM2-MM	19	26	16	19	15	14
Ensemble mean		**30**	**29**	**16**	**15**	**7**	**9**

is given in Figure 5.107 to 5.109. The ensemble mean of the number of groundwater drought events during various time periods is given in Table 5.42 and Figure 5.110. It can be observed that as compared to the baseline period, the number of groundwater droughts is expected to decrease during the near-term both under SSP245 and SSP585 scenarios (54 events on pro-rata basis for 30 years) whereas during the mid-term it is projected to increase 57 events under SSP245 scenario and 53 events under SSP585 scenario. During the end-term, the number of 54 groundwater drought events are projected during the end-term which is only marginally lower as compared to the baseline period (55 events).

The groundwater drought severity has also been compared during the various time periods. The projected groundwater drought severity during the near-term by various GCMs under both scenarios is given in Table 5.43. During the near-term,

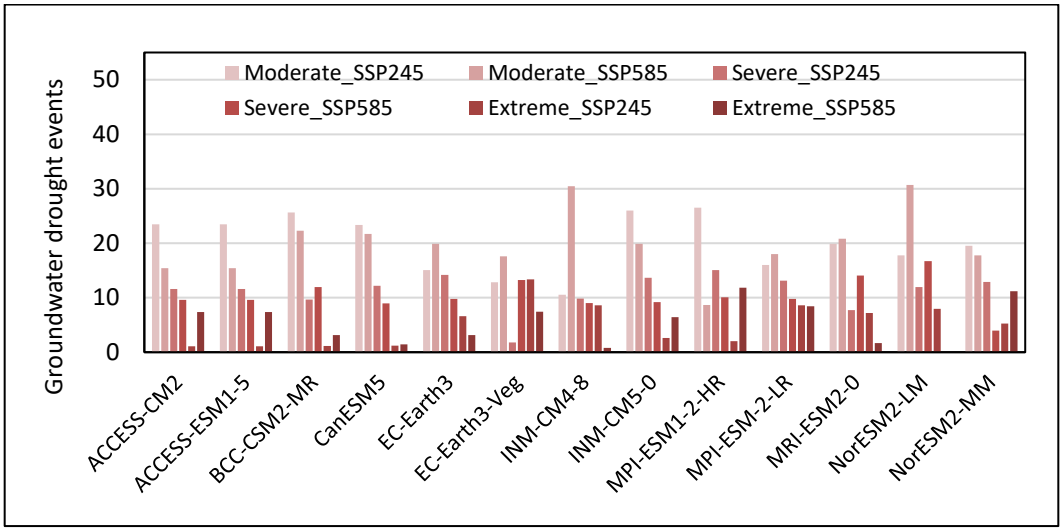

Figure 5.107: Number of groundwater droughts in the near-term

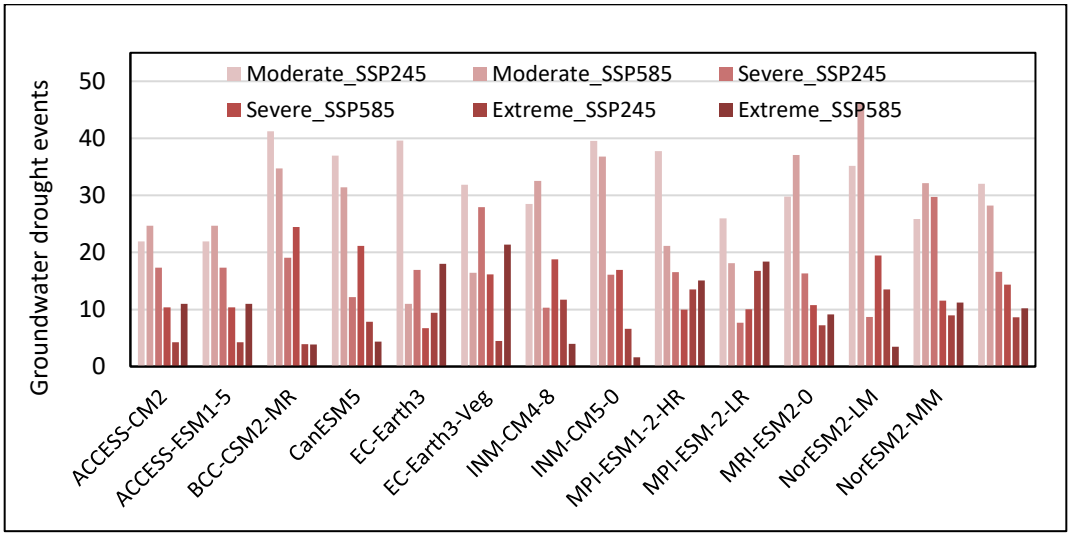

Figure 5.108: Number of groundwater droughts during the mid-term

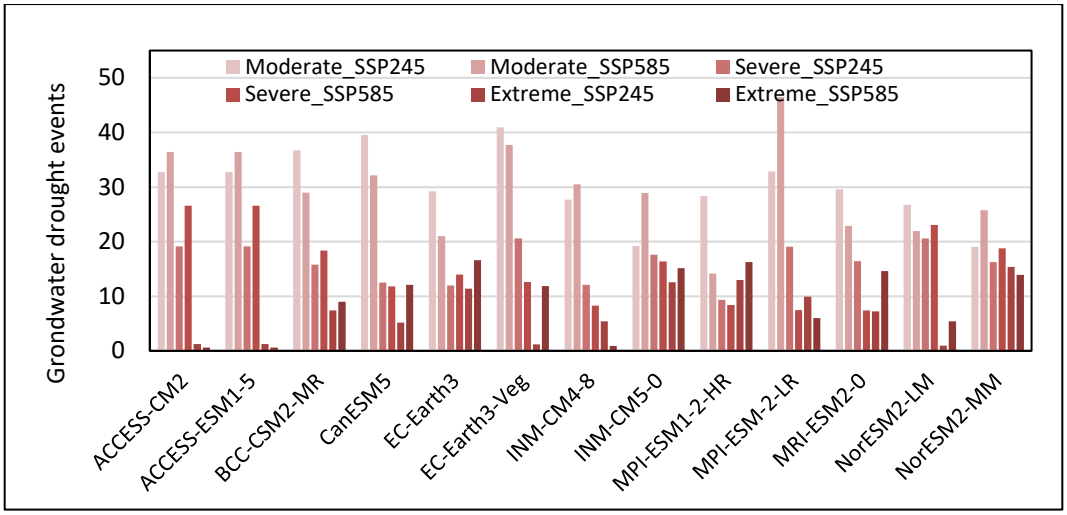

Figure 5.109: Number of groundwater droughts during the end-term

Table 5.42: Groundwater drought events during different time periods

S. No.	Time period	Total drought events
1	Baseline	55
2	Present	46
3	Near-term SSP245	36
4	Near-term SSP585	36
5	Mid-term SSP245	57
6	Mid-term SSP585	53
7	End-term SSP245	54
8	End-term SSP585	54

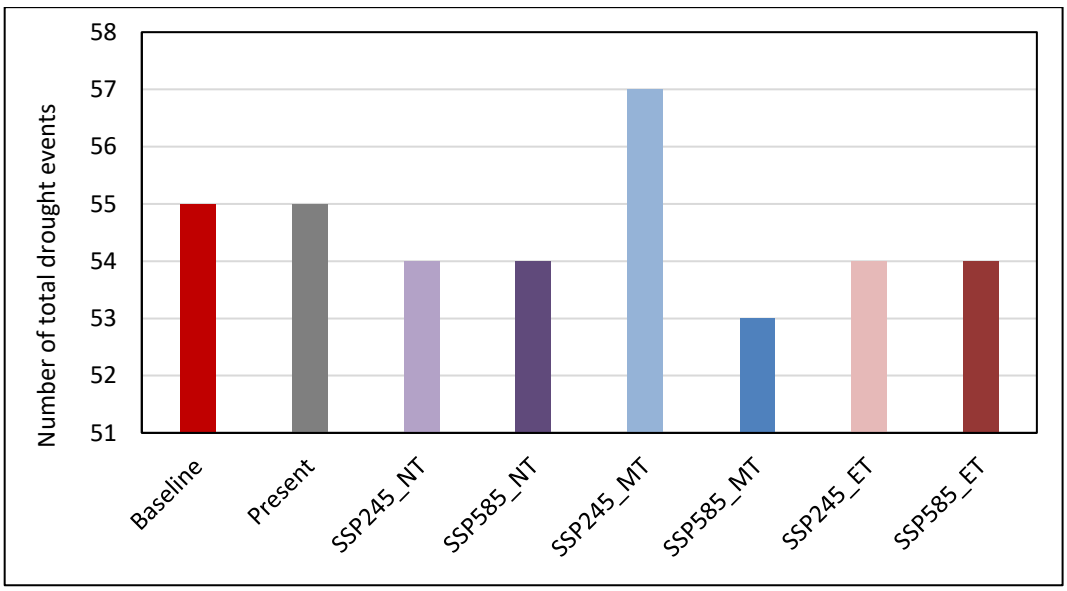

Figure 5.110: Comparison of groundwater drought events during various time periods

the severity of the extreme drought events is higher under SSP585 scenario as compared to the SSP245 scenario, whereas the severity of the moderate and severe drought events is higher under the SSP245 scenario. There is considerable inter-model variability which also shows the underlying uncertainty in the future projections. The comparison of the projected groundwater drought severity during the near-term is given in Figure 5.111.

Table 5.43: Groundwater drought severity during near-term (2021-2040)

S. No.	GCMs	Moderate SSP245	Moderate SSP585	Severe SSP245	Severe SSP585	Extreme SSP245	Extreme SSP585
1	ACCESS-CM2	-26.59	-18.58	-21.55	-28.12	-3.89	-4.48
2	ACCESS-ESM1-5	-28.95	-19.48	-19.83	-16.36	-2.31	-17.10
3	BCC-CSM2-MR	-31.98	-27.53	-16.28	-20.52	-2.47	-6.87
4	CanESM5	-29.55	-26.10	-20.68	-15.00	-2.43	-3.25
5	EC-Earth3	-19.08	-24.54	-24.43	-16.19	-14.66	-7.38
6	EC-Earth3-Veg	-14.62	-21.73	-3.26	-23.09	-32.32	-16.82
7	INM-CM4-8	-12.23	-37.34	-17.44	-14.48	-18.94	-1.73
8	INM-CM5-0	-32.35	-23.76	-23.15	-16.01	-5.74	-14.39
9	MPI-ESM1-2-HR	-31.89	-10.65	-25.62	-17.76	-4.41	-29.42
10	MPI-ESM-2-LR	-19.67	-22.20	-23.13	-16.77	-18.89	-19.69
11	MRI-ESM2-0	-24.19	-25.16	-13.47	-24.30	-16.80	-3.58
12	NorESM2-LM	-22.17	-21.99	-20.62	-6.58	-17.97	-29.53
13	NorESM2-MM	-23.53	-21.99	-22.68	-6.58	-11.90	-29.53
Ensemble mean		**-24.37**	**-23.16**	**-19.40**	**-17.06**	**-11.75**	**-14.14**

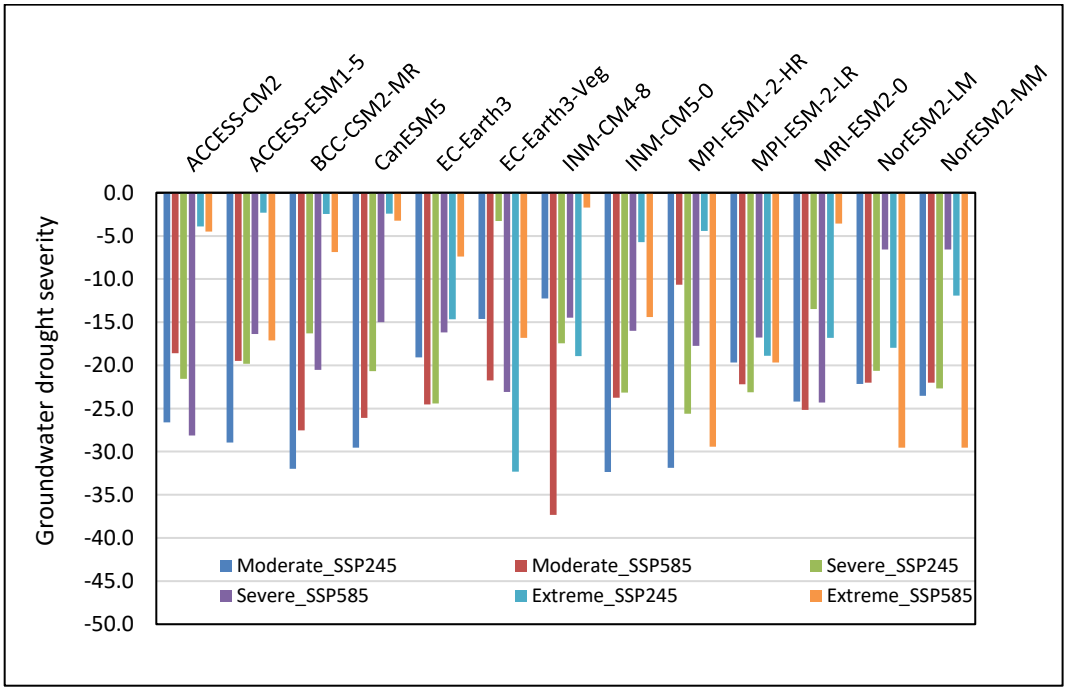

Figure 5.111: Groundwater droughts severity during the near-term

The projected groundwater drought severity during the mid-term is given in Table 5.44. During the mid-term, the severity of the extreme groundwater drought events is higher under SSP585 scenario as compared to the SSP245 scenario, whereas the severities of the severe and moderate drought events are higher under the SSP245 scenario. The comparison of the projected drought severity during the near-term is given in Figure 5.112. The comparison of the projected drought severity during the end-term is given in Table 5.45. During the end-term, the severity of the extreme groundwater drought severity is higher under SSP585 scenario as compared to the SSP245 scenario, whereas the severe and moderate groundwater drought severity is higher under SSP245 scenario. There is again a considerable inter-model variability which also shows the underlying uncertainty in the future projections. The comparison of the projected drought severity during

Table 5.44: Groundwater drought severity during mid-term (2041-2070)

S. No.	GCMs	Moderate SSP245	Moderate SSP585	Severe SSP245	Severe SSP585	Extreme SSP245	Extreme SSP585
1	ACCESS-CM2	22	25	17	10	4	11
2	ACCESS-ESM1-5	22	25	17	10	4	11
3	BCC-CSM2-MR	41	35	19	24	4	4
4	CanESM5	37	31	12	21	8	4
5	EC-Earth3	40	11	17	7	9	18
6	EC-Earth3-Veg	32	16	28	16	4	21
7	INM-CM4-8	28	33	10	19	12	4
8	INM-CM5-0	40	37	16	17	7	2
9	MPI-ESM1-2-HR	38	21	17	10	14	15
10	MPI-ESM-2-LR	26	18	8	10	17	18
11	MRI-ESM2-0	30	37	16	11	7	9
12	NorESM2-LM	35	46	9	19	13	3
13	NorESM2-MM	26	32	30	12	9	11
Ensemble mean		**20**	**32**	**28**	**17**	**14**	**9**

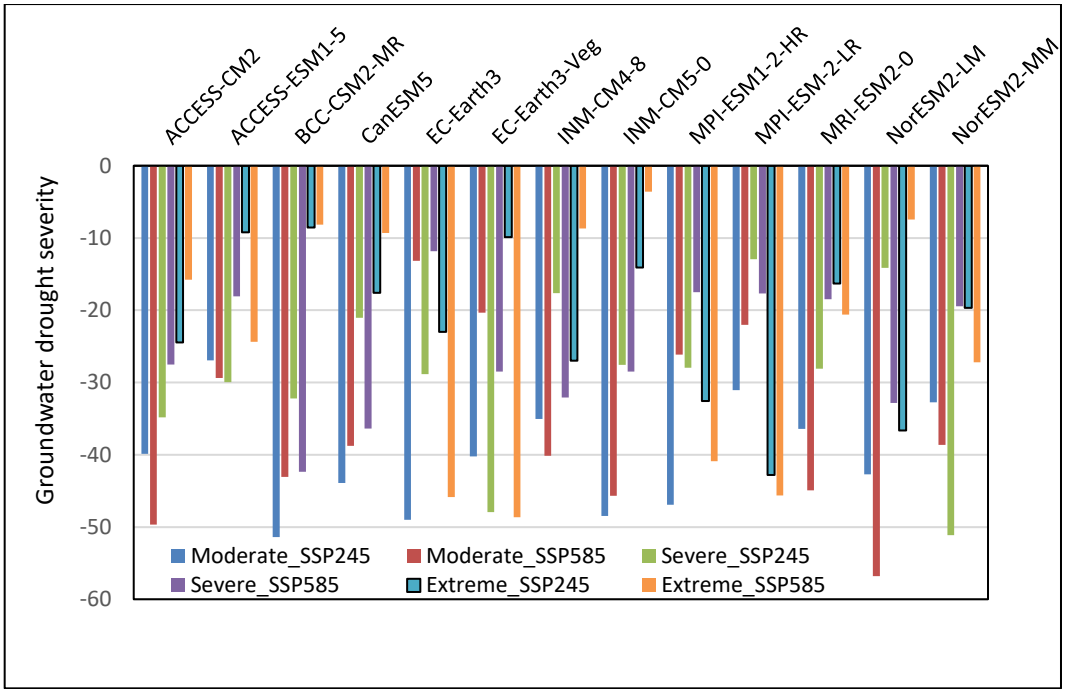

Figure 5.112: Groundwater droughts severity during the mid-term

the near-term is given in Figure 5.113. It can be seen that the accumulated severity of the extreme drought events is projected to be much lesser in comparison to the severe and moderate drought events in all future time periods. The comparison of the ensemble mean of the groundwater drought severity under both scenarios with that during the baseline and present periods is given in Figure 5.114. It can be observed that the groundwater drought severity is projected to increase both during the mid-term and end-term periods and the drought severity is projected to

Table 5.45: Groundwater drought severity during end-term (2071-2100)

S. No.	GCMs	Moderate SSP245	Moderate SSP585	Severe SSP245	Severe SSP585	Extreme SSP245	Extreme SSP585
1	ACCESS-CM2	-47.94	-33.50	-17.87	-29.26	-19.59	-27.26
2	ACCESS-ESM1-5	-39.34	-45.97	-32.50	-43.83	-2.68	-1.25
3	BCC-CSM2-MR	-45.01	-35.73	-26.94	-31.15	-17.36	-20.11
4	CanESM5	-48.57	-39.68	-21.22	-19.79	-11.57	-30.42
5	EC-Earth3	-34.85	-25.70	-20.75	-24.54	-27.79	-37.81
6	EC-Earth3-Veg	-50.40	-47.14	-34.43	-21.40	-2.42	-27.37
7	INM-CM4-8	-34.33	-36.55	-20.72	-14.14	-12.68	-1.96
8	INM-CM5-0	-23.71	-35.91	-30.77	-28.02	-28.30	-33.80
9	MPI-ESM1-2-HR	-34.05	-17.29	-15.47	-14.64	-38.83	-48.17
10	MPI-ESM-2-LR	-40.23	-56.81	-32.77	-12.39	-21.97	-15.02
11	MRI-ESM2-0	-36.21	-26.98	-28.26	-12.96	-16.29	-33.13
12	NorESM2-LM	-32.85	-26.01	-35.87	-39.35	-2.16	-12.36
13	NorESM2-MM	-23.61	-31.54	-28.07	-31.64	-36.82	-35.46
Ensemble mean		**-37.78**	**-35.29**	**-26.59**	**-24.86**	**-18.34**	**-24.93**

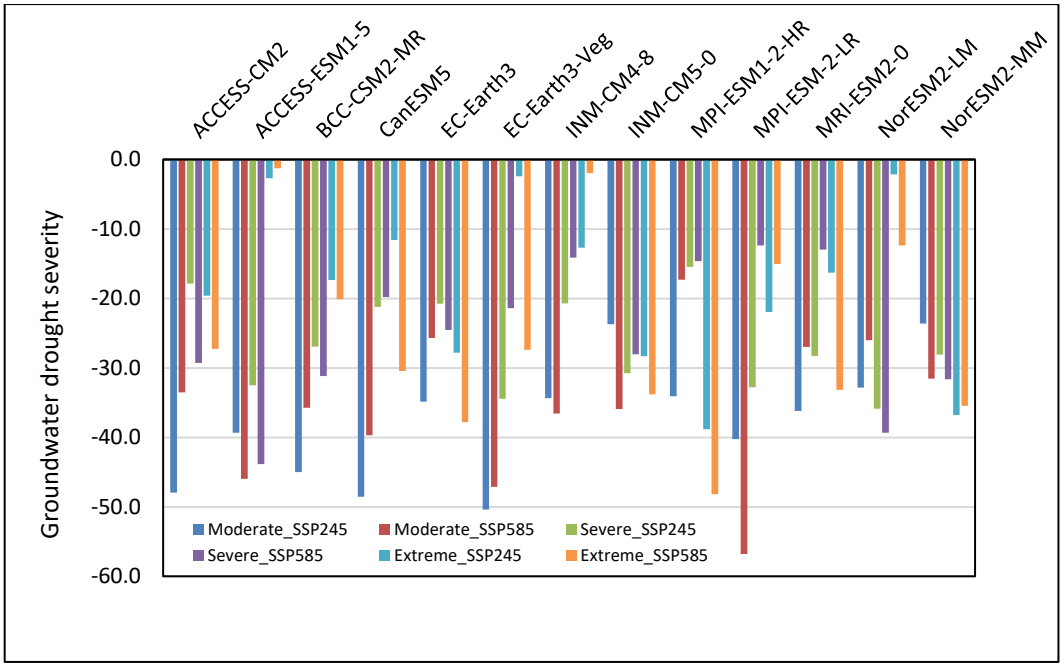

Figure 5.113: Groundwater droughts severity during the end-term

be higher under the SSP585 scenario. The maximum groundwater drought severity is projected during the mid-term under SSP245 scenario.

5.4.6 Evaluation of Critical Dry Spells

5.4.6.1 Baseline and Present periods

The distribution of rainfall during the monsoon season is not uniform and the

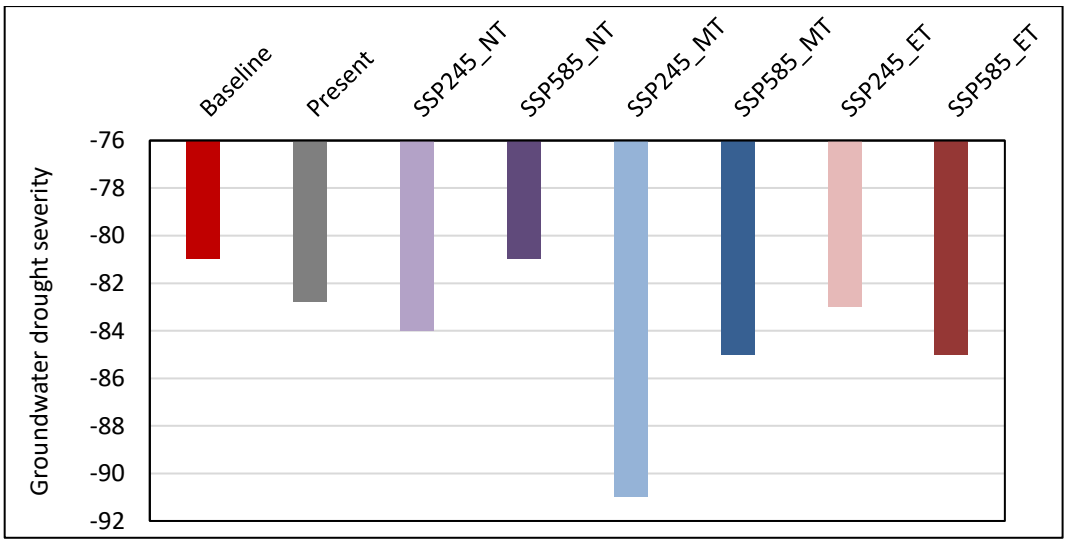

Figure 5.114: Comparison of groundwater drought severity during various time periods

occurrence of regular dry spells is a common phenomenon in the study area. After the onset of the monsoon, a dry spell is determined as the intervening period of dry days between any two consecutive wet spells. Dry days are considered as days having rainfall less than 2.5 mm. It has been observed that a dry spell with a spell length of 10 days or more is critical for the major crops grown in the region. The Critical Dry Spell (CDS) have been determined for the various blocks in Chambal basin in Madhya Pradesh. Generally, two CDS are observed in most of the years for which supplemental irrigation is necessary to prevent the crops from water stress during the crop growth period, which otherwise may lead to reduced crop yields. The dry spell analysis indicated that generally two critical dry spells occur during most of the years under study.

The evaluation of the CDS has been carried out for the baseline period (1961-1990) as well as the present period (1991-2015). The comparison of the CDS during the baseline period and present period helps to get an idea about the changes in the duration and timing of the CDS. The spatial plot of the first CDS length during the baseline period in June 1972 is given in Figure 5.115. The maximum first CDS length of 24 days occurred in Sehore district, followed by 23 days in Guna district. The first CDS length of 22 days occurred at Vidisha, Sehore, Guna and Rajgarh districts. The length of the first CDS during the baseline period varied between 10 and 24 days in the study area and is given in Figure 5.116. The maximum second CDS length of 26 days occurred in Indore district followed by 23 days in Rajgarh district. The maximum second CDS length of 22 days occurred at many districts including Agar, Vidisha, Sehore, Shajapur, and Ratlam districts. The length of CDS varied between 10 and 24 days during the baseline period. The combined duration during first and second CDS during the baseline period is given in Figure 5.116. The total CDS events during baseline period were 44 events.

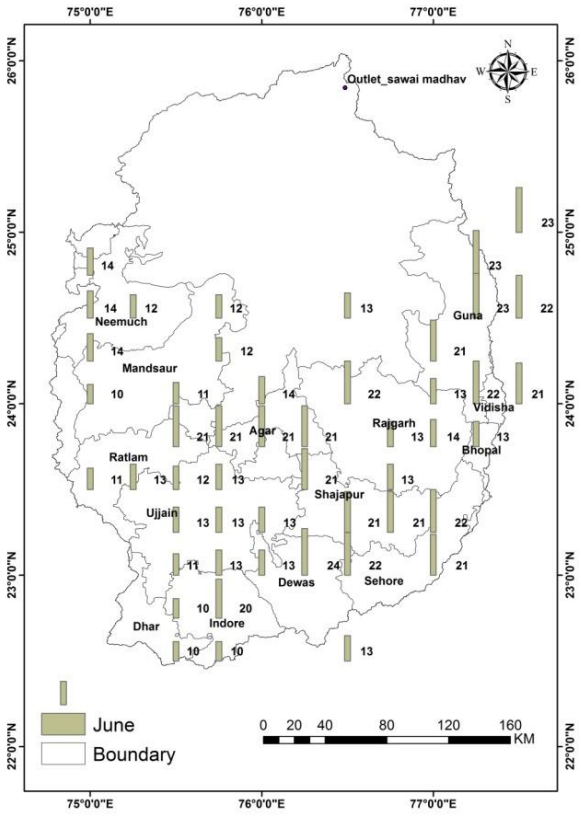

Figure 5.115: Spatial variation of first CDS in June 1972

During the present period, the first CDS occurred during the second to third week of July for duration of 14–18 days, whereas the second CDS occurred during the third week of August for duration of 16–18 days. In few blocks of Mandsaur, Sehore and Dhar, the third CDS of 18-20 days also occurred in some of the years under consideration during the present period. The dry spell analysis and the identification of the dry spell length and its timing helps to plan and design for the supplemental irrigation requirements to tide over the water stress during CDS. The spatial plot showing the length of first CDS that occurred during July 2002 is given in Figure 5.117. The maximum length of first CDS of 19 days occurred in Ratlam and Ujjain districts whereas first CDS length of 18 days have been observed at Mandsaur, Agar, Dewas and Indore districts. The length of first CDS varied between 10 and 19 days in the study area. The variation of second CDS length that occurred during August 2002 in the study area is given in Figure 5.118. The maximum second CDS length of 14 days occurred in Mandsaur district whereas second CDS length of 13 days occurred at Agar district. The length of the

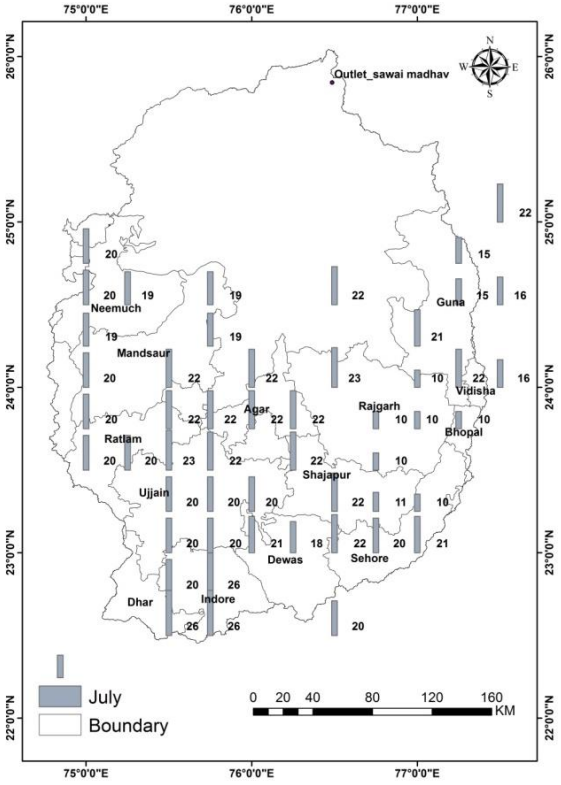

Figure 5.116: Spatial variation of second CDS in July 1972

second critical dry spell varied between 10 and 14 days in the study area during the present period. The total CDS events during present period were 40 events.

5.4.6.2 Future time periods

The evaluation of the CDS has been carried out for the near-term, mid-term and end-term and compared with the CDS during the baseline and present periods. The number of CDS events projected during the future time periods at Dhar under SSP245 scenario along with its comparison during the baseline and present periods are given in Table 5.46. During the near-term, the CDS events at Dhar are projected to vary between 32 and 51 events with an ensemble mean of 37 CDS events, which is much lower as compared to CDS events that occurred during the baseline (44) and present (40) periods. However, the CDS events at Dhar during the mid-term (51) and end-term periods (51) are projected to increase as compared to the near-term period (37). However, significant difference is observed between the CDS events at Dhar during baseline (44) with the CDS events at Dhar during

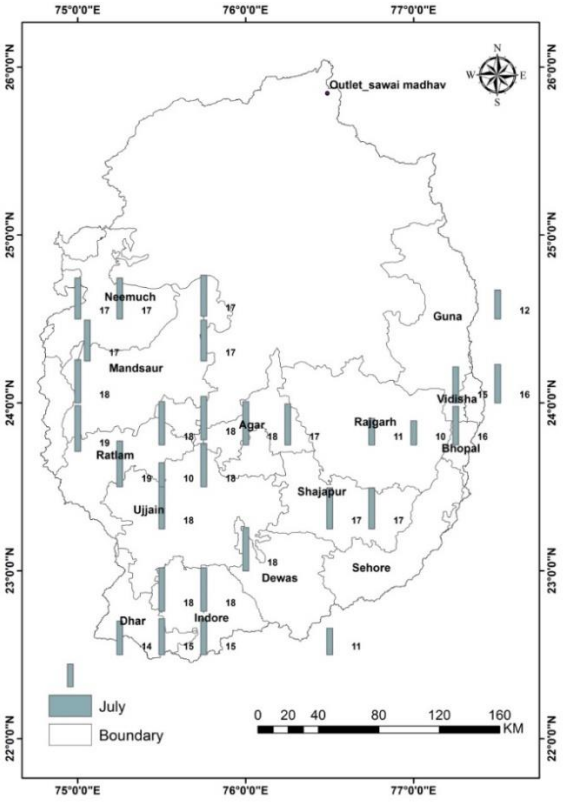

Figure 5.117: Spatial variation of first CDS during July 2002

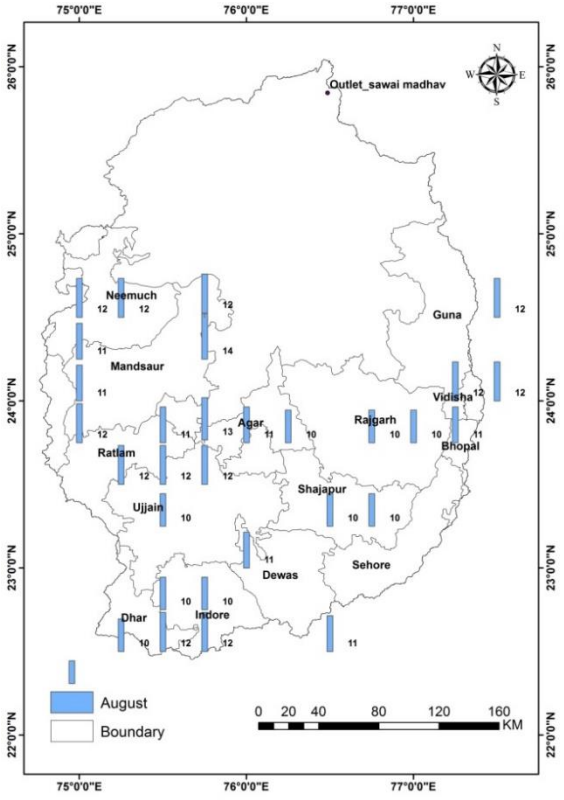

Figure 5.118: Spatial variation of second CDS during August 2002

Table 5.46: Average number of CDS events at Dhar under SSP245 scenario

GCMs	Baseline	Present	Near-term	Mid-term	End-term
ACCESS-CM2	44	40	48	65	63
ACCESS-ESM1-5			38	57	51
BCC-CSM2-MR			35	42	44
CanESM5			51	65	69
EC-Earth3			36	48	49
EC-Earth3-Veg			35	53	47
INM-CM4-8			30	37	36
INM-CM5-0			29	40	48
MPI-ESM1-2-HR			32	42	39
MPI-ESM1-2-LR			36	48	45
MRI-ESM2-0			32	48	48
NorESM2-LM			40	59	63
NorESM2-MM			38	60	57
Ensemble Mean	**44**	**40**	**37**	**51**	**51**

the mid-term and end-term (51) CDS events. The comparison of the future CDS events at Dhar under SSP245 scenario is given in Figure 5.119.

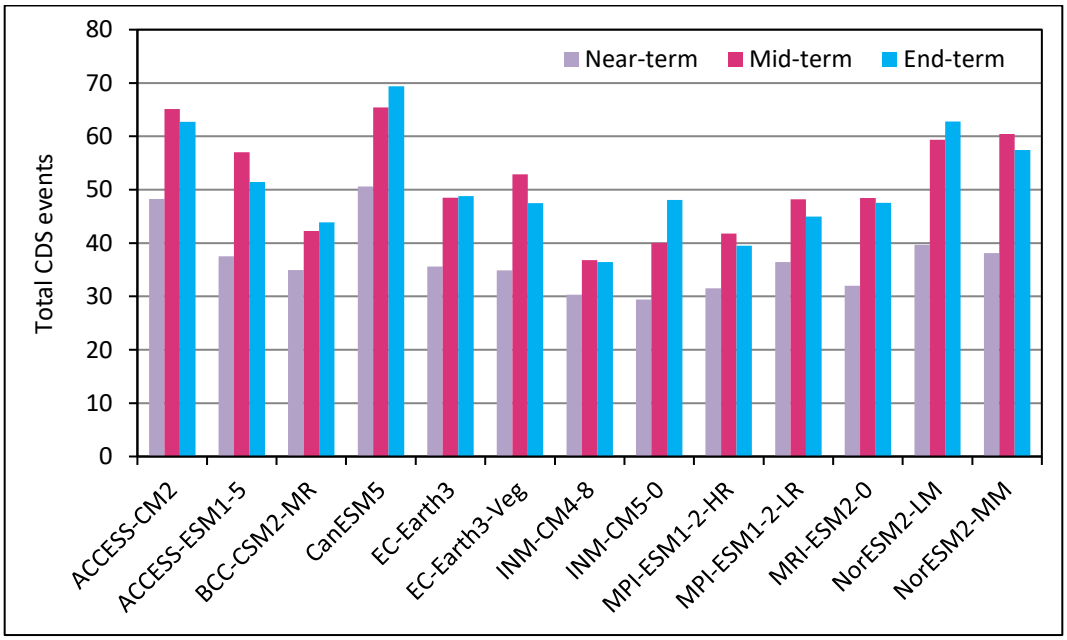

Figure 5.119: Total CDS events at Dhar under SSP245 scenario

Similarly, the total CDS events at Dhar under SSP585 scenario and its comparison with CDS events during baseline and present time periods are given in Table 5.47. During the near-term, CDS events at Dhar are projected to vary between 32 and 49 events with an ensemble mean of 38 CDS events, which is marginally lower as compared to the CDS events that occurred during the baseline (44) and present (40) periods. However, the CDS events at Dhar during the mid-term and end-term

Table 5.47: Average number of CDS events at Dhar SSP585 scenario

GCMs	Baseline	Present	Near-term	Mid-term	End-term
ACCESS-CM2	44	40	49	70	63
ACCESS-ESM1-5			40	58	56
BCC-CSM2-MR			37	48	52
CanESM5			49	67	54
EC-Earth3			32	43	51
EC-Earth3-Veg			36	55	49
INM-CM4-8			28	39	42
INM-CM5-0			30	41	39
MPI-ESM1-2-HR			36	48	36
MPI-ESM1-2-LR			35	44	32
MRI-ESM2-0			37	55	54
NorESM2-LM			45	57	62
NorESM2-MM			43	65	56
Ensemble Mean	**44**	**40**	**38**	**53**	**50**

periods are projected to increase as compared to the near-term period. However, significant differences have been observed between the CDS events during baseline (44) with the CDS events during mid-term (53) and end-term (50). The number of CDS events at Dhar is projected to be only marginally higher under SSP585 scenario as compared to the SSP245 scenario. The comparison of the total CDS events at Dhar under SSP585 scenario is given in Figure 5.120.

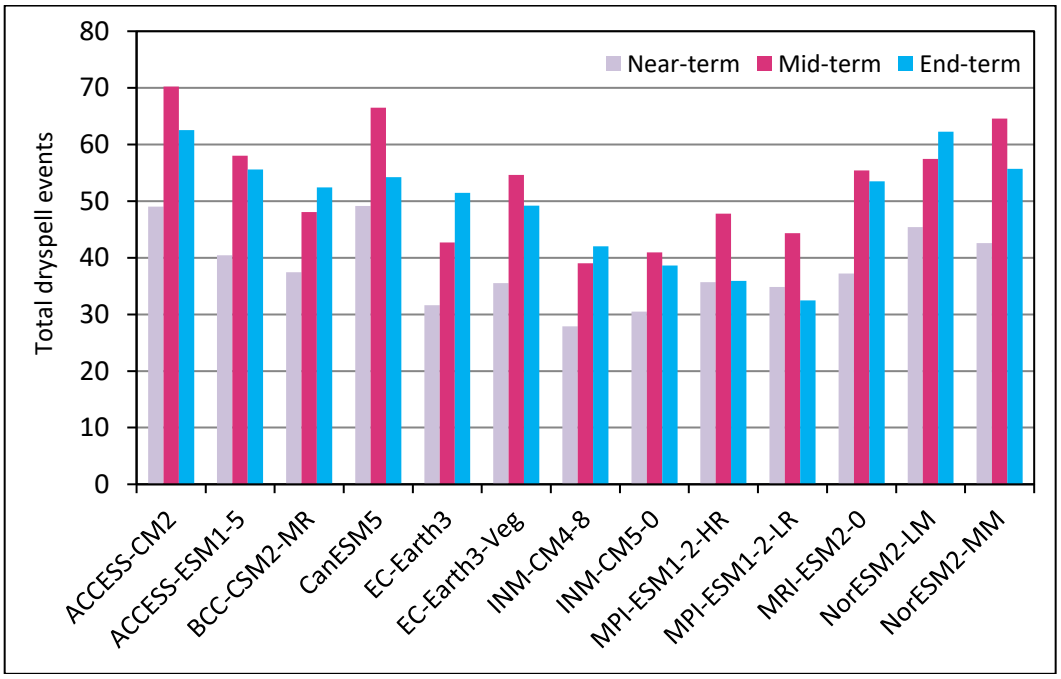

Figure 5.120: Total CDS events at Dhar under SSP585 scenario

The comparison of the ensemble means of the CDS events at Dhar during all time periods is given in Figure 5.121. It can be seen that the number of CDS events at Dhar are projected to increase in the near-term under both scenarios (SSP245 & SSP585) as compared to the baseline (44). Also, the CDS events at Dhar during mid-term and end-term are also projected to increase as compared to the present period (48 CDS events on a pro-rata basis of 30 years for the present period).

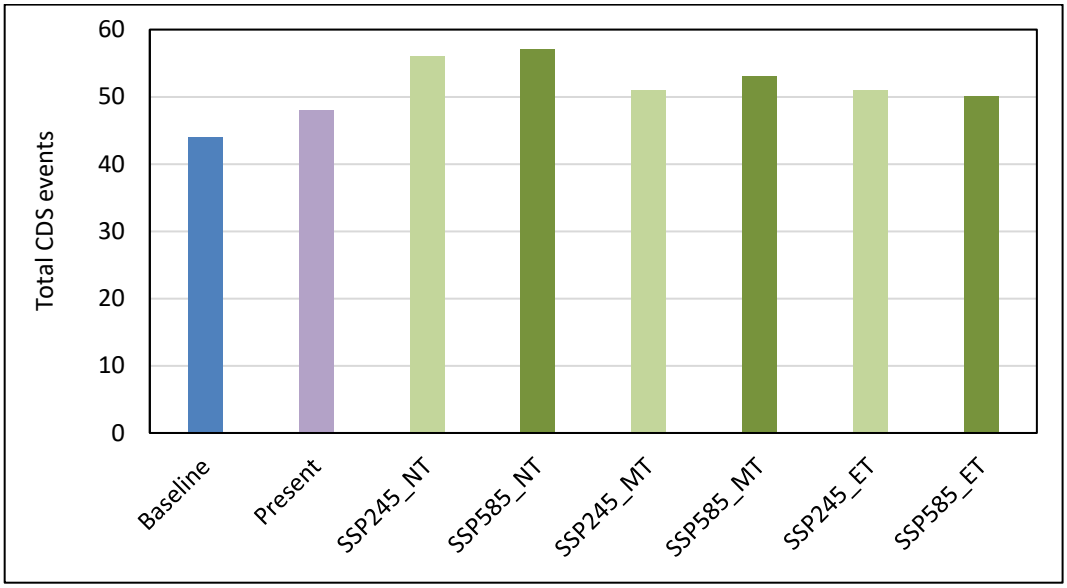

Figure 5.121: Comparison of CDS events at Dhar during various time periods

The mean duration of future CDS events at Dhar under SSP245 scenario and its comparison with the CDS duration during baseline and present periods are given in Table 5.48. During the near-term, under SSP245 scenario, the duration of CDS

Table 5.48: Mean duration of CDS at Dhar under SSP245 scenario

GCMs	Baseline	Present	Near-term	Mid-term	End-term
ACCESS-CM2	17	16	19	19	19
ACCESS-ESM1-5			29	27	28
BCC-CSM2-MR			18	19	18
CanESM5			30	29	26
EC-Earth3			24	25	26
EC-Earth3-Veg			28	25	26
INM-CM4-8			29	30	31
INM-CM5-0			32	36	28
MPI-ESM1-2-HR			23	26	25
MPI-ESM1-2-LR			22	23	22

MRI-ESM2-0			17	17	17
NorESM2-LM			26	26	25
NorESM2-MM			22	22	23
Ensemble mean	**17**	**16**	**25**	**25**	**24**

are projected to be 38 days (ensemble mean) on a pro-rata basis for 30-year period, which is higher as compared to the duration of CDS during the baseline (17) and present (16) days. However, the CDS duration during the mid-term and end-term periods is projected to remain at 25 and 24 days respectively, which is much lower as compared to the near-term but higher than the CDS during the baseline and present time periods.

The comparison of the mean duration of CDS events at Dhar, under SSP585 scenario with that during the baseline and present time periods are given in Table 5.49. During the near-term, the CDS duration are projected to be 39 days (ensemble mean) on a pro-rata basis for 30-year period under SSP585 scenario, which is considerably higher as compared to the CDS duration during the baseline (17) and present (16) time periods. However, under SSP585 scenario, the CDS duration at Dhar during the mid-term and end-term periods (25 days) is projected to remain the same (25 days).

Table 5.49: Mean duration of CDS at Dhar under SSP585 scenario

GCMs	Baseline	Present	Near-term	Mid-term	End-term
ACCESS-CM2	17	16	20	19	19
ACCESS-ESM1-5			28	26	25
BCC-CSM2-MR			19	18	18
CanESM5			26	26	25
EC-Earth3			27	26	26
EC-Earth3-Veg			29	25	27
INM-CM4-8			30	30	27
INM-CM5-0			31	30	33
MPI-ESM1-2-HR			24	24	22
MPI-ESM1-2-LR			23	22	20
MRI-ESM2-0			30	34	35
NorESM2-LM			26	28	25
NorESM2-MM			23	24	25
Ensemble mean	**17**	**16**	**26**	**25**	**25**

The comparison of the ensemble means of the CDS duration at Dhar during the future time periods is given in Figure 5.122. It can be seen that the CDS duration

during all future time periods are projected to increase under both scenarios as compared to the baseline and present time periods, but the projected increase in the mean duration of CDS is highest during the near-term under both future climate scenarios.

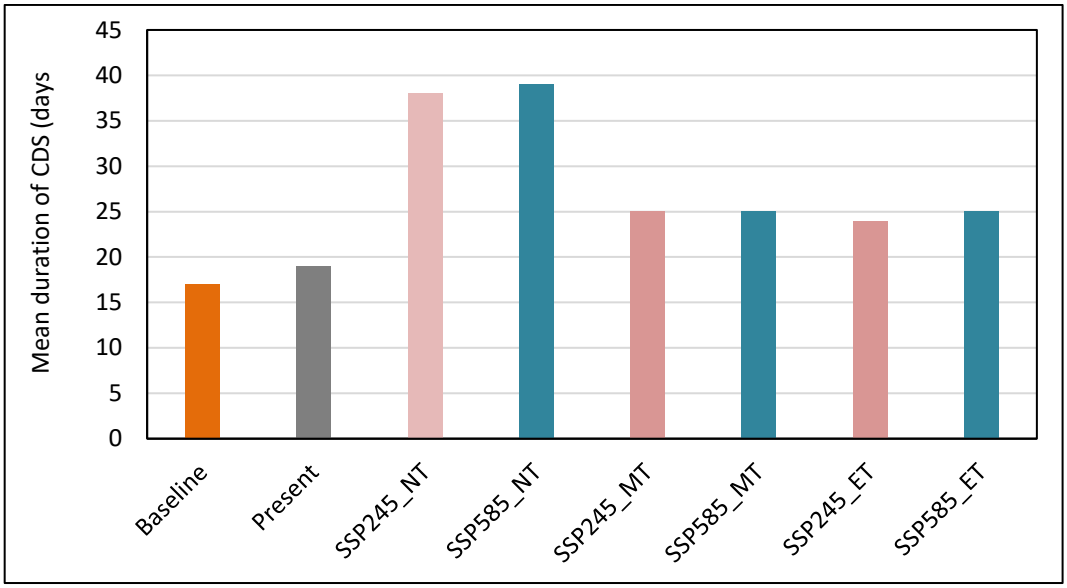

Figure 5.122: Mean duration of CDS events at Dhar during various time periods

5.5 Supplemental Irrigation Planning for Critical Dry Spells

The supplemental irrigation planning has to be carried out to account for the water deficit that occurs during the critical dry spells. In order to accomplish this, the reference evapotranspiration has been estimated and thereafter the crop water requirement computed on the basis of the effective rainfall, reference evapotranspiration and crop coefficients during the different stages of the crop growth period. The net irrigation water requirement has been thereafter computed considering the crop water requirement and effective rainfall. The Hargreaves method has been used for computation of reference evapotranspiration. The crop water requirement has been calculated considering the major crops based on the crop coefficient during different developmental stages of the crop growth. Soybean is one of the important kharif crops in the study area. The crop water requirements and irrigation requirements were computed for the baseline period (1961-1990) and other time periods in the various blocks and thereafter supplementary irrigation requirement needed during each of the critical dry spell

periods has been calculated based on the duration and timing of occurrences of CDS.

Table 5.50 gives the comparison of the CDS events, CDS events requiring irrigation and the supplementary (net) irrigation requirement during the various time periods at Dhar for soyabean with ACCESS-CM2 GCM, under SSP245 and SSP585 scenarios. All the details pertaining to the future time periods are based on the ensemble means of the 13 GCMs for SSP245 and SSP585 scenarios. Based on ACCESS-CM2 projections, it can be observed that the average number of CDS at Dhar is projected to increase during the all-future time periods as compared to the baseline and present periods.

Table 5.50: Comparison of net supplementary irrigation requirement for soyabean at Dhar under ACCESS-CM2 GCM

S. No.	Particular	BL	PR	Near-term		Mid-term		End-term	
				SSP245	SSP585	SSP245	SSP585	SSP245	SSP585
1	No of CDS	44	40	46	46	57	57	53	53
2	Average duration (days)	18	16	17.1	17.1	14.3	14.3	18.4	18.4
3	CDS requiring irrigation	40	37	44	44	52	53	52	51
4	Average NIR (mm)	44.8	32.1	47.0	33.52	57.86	43.52	56.57	45.15
5	Maximum NIR (mm)	129.8	93.5	166.2	87.84	153.7	123.58	180.82	104.4

However, the CDS events at Dhar requiring irrigation is similar during the mid-term (52 & 53 under SSP245 & SSP585 respectively) and end-term (52 & 51 under SSP245 & SSP585 respectively), but still much higher than the baseline period (40). The comparison of the CDS events and CDS events that require irrigation at Dhar for soyabean based on ACCESS-CM2 projections is given in Figure 5.123. It can be observed that the highest number of CDS and CDS requiring irrigation is maximum during the near-term period (on a pro-rata basis for 30-year period) as compared to other time periods. The number of CDS and the CDS requiring supplementary irrigation is projected to be much higher than

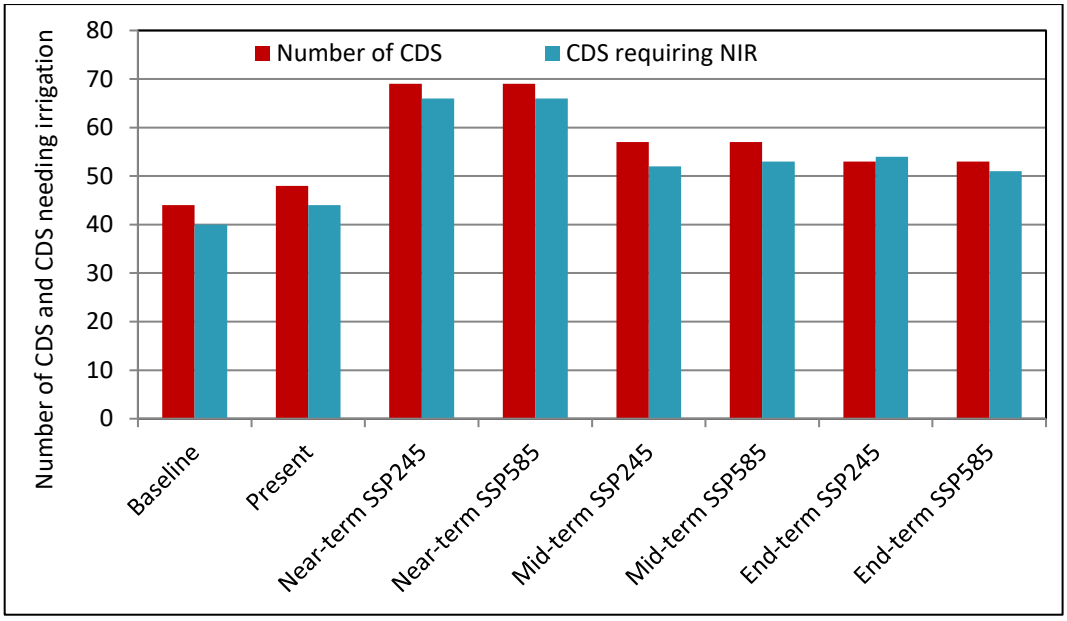

Figure 5.123: Number of CDS and CDS requiring irrigation at Dhar with ACCESS-CM2 GCM

the baseline and present period during all future time periods. The comparison of the average duration of CDS at Dhar with ACCESS-CM2 is given in Figure 5.124.

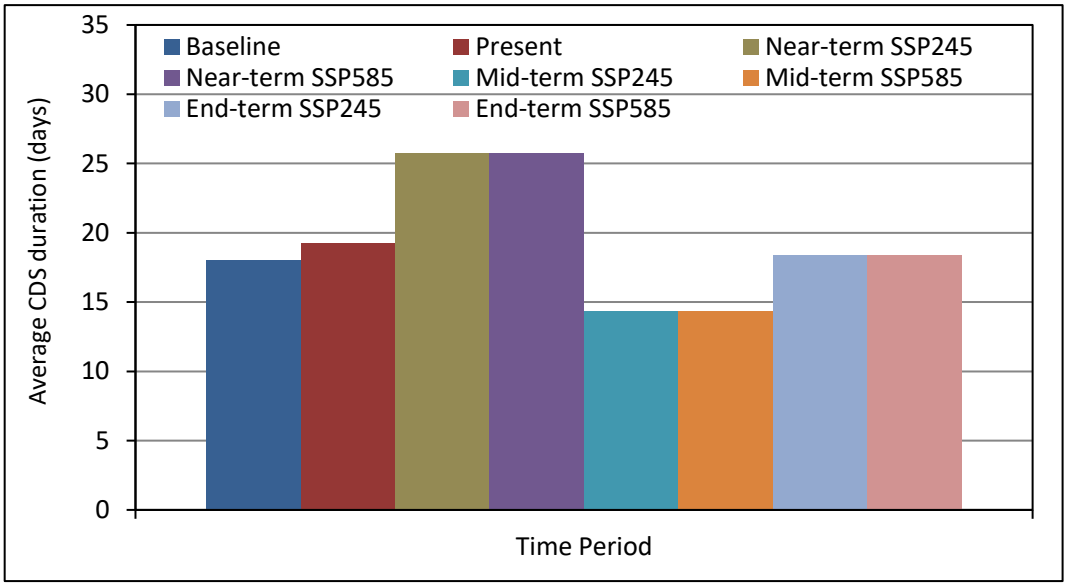

Figure 5.124: Average duration of CDS at Dhar with ACCESS-CM2

The average net supplemental irrigation requirement at Dhar for soyabean during the baseline period is 44.75 mm which is projected to increase to 71.0 mm during the near-term period (on pro-rata basis for 30-year period), 57.86 mm during the mid-term period and 56.57 mm during the end-term period under SSP245 scenario, based on ACCESS-CM2 projections. Similarly, based on ACCESS-CM2

projections, the average net supplemental irrigation requirement at Dhar for soyabean is projected to as 51.00 mm during the near-term period (on pro-rata basis for 30-year period), and thereafter projected at 43.52 mm during the mid-term period and marginally increase again during the end-term period (45.15 mm). It can also be observed that with ACCESS-CM2, the net supplementary irrigation at Dhar for the soyabean crop is much higher under the SSP245 scenario as compared to the SSP585 scenario. The comparison of the net supplemental irrigation requirement during the CDS for soyabean at Dhar with ACCESS-CM2 is given in Figure 5.125.

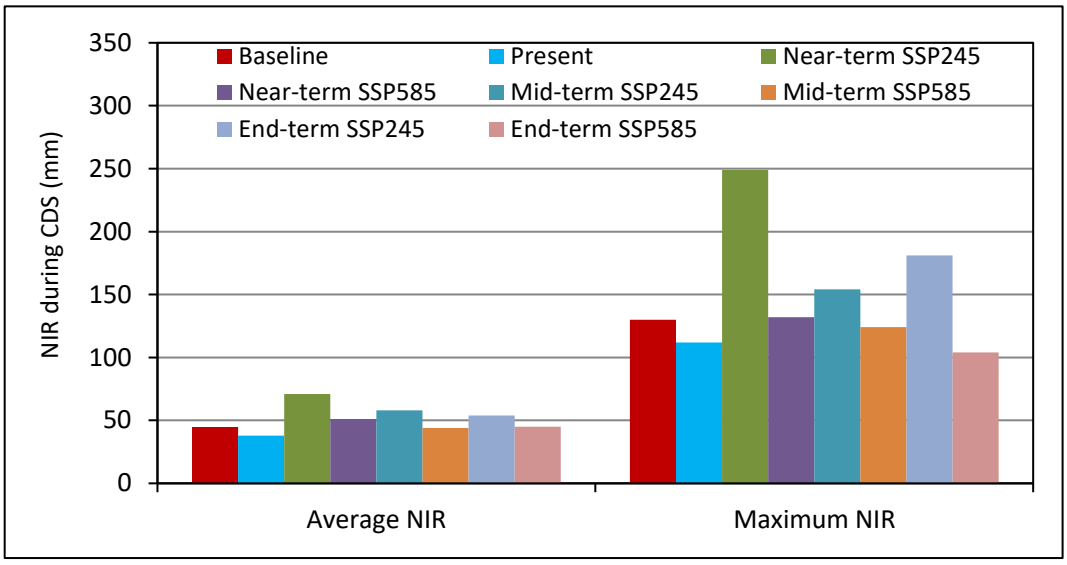

Figure 5.125: Net Irrigation Requirement (NIR) for soyabean at Dhar with ACCESS-CM2

The comparison of the net supplemental irrigation requirement during the CDS for soyabean at Dhar as evaluated by few GCMs is given in Figure 5.126. The comparison of net supplemental irrigation requirement during CDS for soyabean at Dhar, as evaluated by ensemble mean of GCMs, along with that during the baseline and present periods is given in Figure 5.127. The average net supplemental irrigation requirement at Dhar for soyabean during the baseline period is 44.75 mm which is projected to increase to 55.47 mm during the near-term period, 38.53 mm during the mid-term period and 35.62 mm during the end-term period under SSP245 scenario, based on ensemble mean of the GCMs projections. Similarly, the average net supplemental irrigation requirement at Dhar

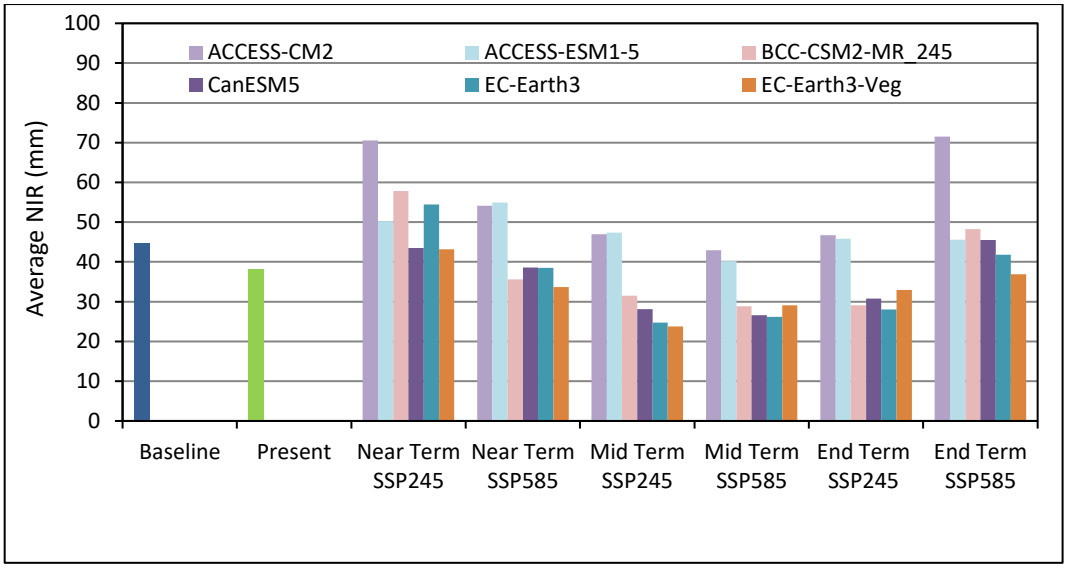

Figure 5.126: Net Irrigation Requirement (NIR) for soyabean at Dhar with various GCMs

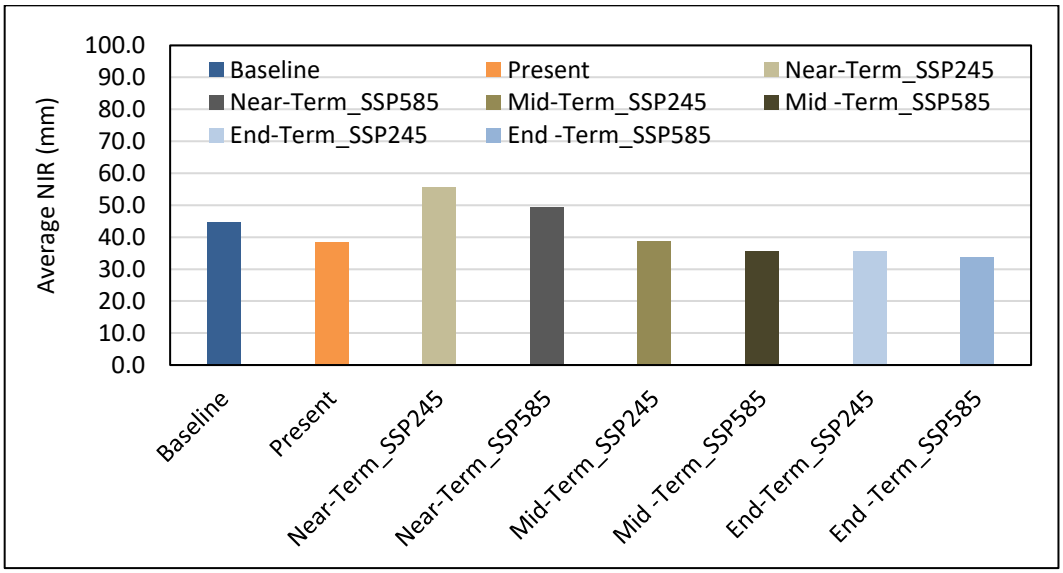

Figure 5.127: Comparison of Net Irrigation Requirement (NIR) for soyabean at Dhar (ensemble mean of GCMs)

for soyabean is projected to further increase to 49.20 mm during the near-term period, 35.52 mm during the mid-term period and 33.59 mm during the end-term period under SSP585 scenario, based on ensemble mean of the GCMs projections. It can be observed that the supplemental irrigation requirement for soyabean at Dhar is higher under SSP245 scenario as compared to SSP585 scenario. Similar analysis has been carried out for estimation of supplemental irrigation for soyabean for all the 53 blocks in the study area.

Table 5.51 gives the comparison of the CDS events, CDS events requiring irrigation and the supplementary (net) irrigation requirement during the various time periods at Ujjain for maize with EC-Earth3 GCM, under SSP245 and SSP585 scenarios. All the details pertaining to the future time periods are based on the ensemble means of the 13 GCMs for SSP245 and SSP585 scenarios. Based on

Table 5.51: Comparison of net supplementary irrigation requirement for maize at Ujjain with EC-Earth3

S. No.	Particular	BL	PR	Near-term		Mid-term		End-term	
				SSP245	SSP585	SSP245	SSP585	SSP245	SSP585
1	No of CDS	44	40	46	46	57	57	53	53
2	Average duration (days)	18	16	17.13	17.13	17.86	17.86	18.38	18.38
3	CDS requiring irrigation	38	31	44	43	52	53	51	51
4	Average NIR (mm)	53.88	41.84	30.74	29.07	30.74	28.47	29.43	32.40
5	Maximum NIR (mm)	182.1	120. 9	107.36	76.81	94.55	111.1	101.3	99.61

EC-Earth3 projections, it can be observed that the average number of CDS at Ujjain is projected to increase during the all-future time periods as compared to the baseline and present periods. However, the increase in CDS events at Ujjain is highest during the mid-term period (57) under both scenarios. However, the CDS events at Ujjain requiring irrigation are similar during the mid-term under both scenarios (52 & 53) and end-term (51) under SSP245 & SSP585, but substantially higher than the baseline period (38). The comparison of the CDS events and CDS events that require irrigation at Ujjain based on EC-Earth3 projections is given in Figure 5.128. Also, based on EC-Earth3 projections, the average duration of the CDS at Ujjain for maize is substantially higher during the near-term (25.70 days) on pro-rata basis for 30-year period whereas it is 17.86 days during the mid-term under both scenarios as compared to the baseline period (18 days), whereas it is only marginally higher during the end-term under both scenarios (18.38). The comparison of the average duration of CDS at Ujjain with EC-Earth3 is given in Figure 5.129.

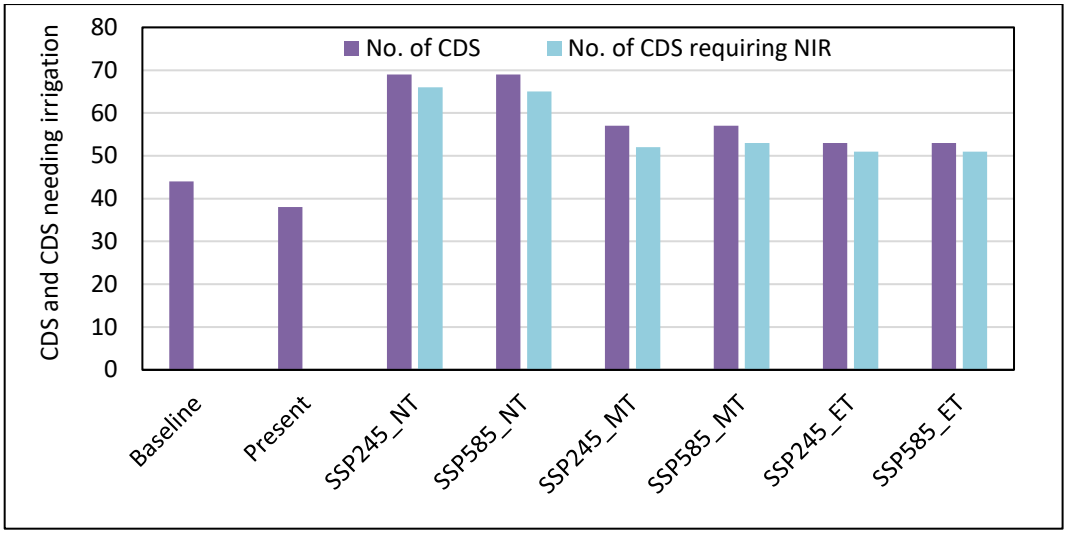

Figure 5.128: Number of CDS and CDS requiring irrigation at Ujjain with EC-Earth3

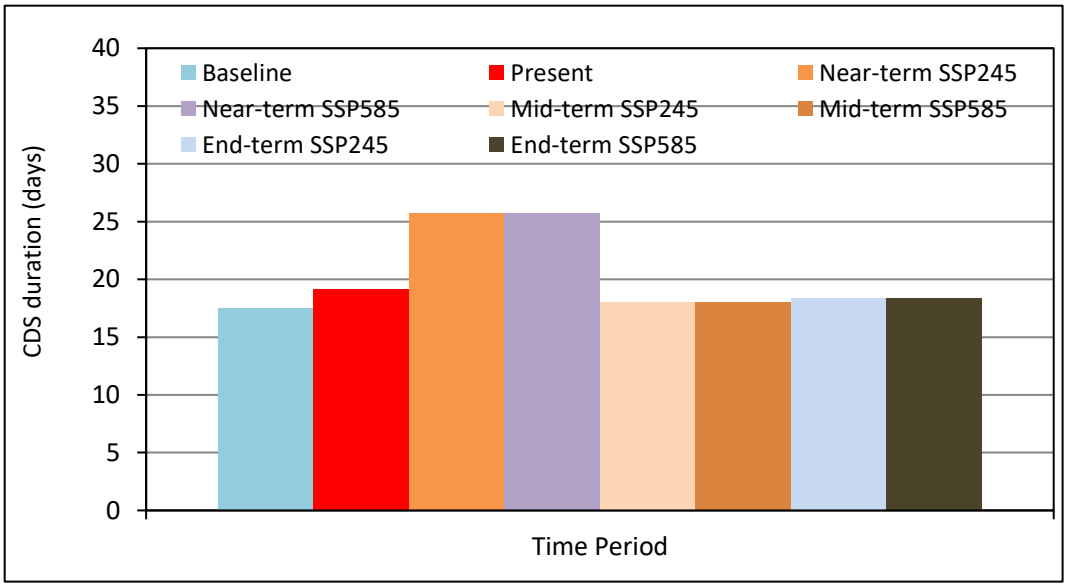

Figure 5.129: Average duration of CDS at Ujjain with EC-Earth3

The average net supplemental irrigation requirement at Ujjain for maize during the baseline period is 53.88 mm which is projected to decrease to 46.11 mm on pro-rata basis for 30-year period during the near-term period, 30.79 mm during the mid-term period and 29.43 mm during the end-term period under SSP245 scenario, based on EC-Earth3 projections.

The comparison of the net supplemental irrigation requirement during the CDS for maize at Ujjain with EC-Earth3 is given in Figure 5.130. Based on EC-Earth3 projections under SSP245 scenario, the average net supplemental irrigation

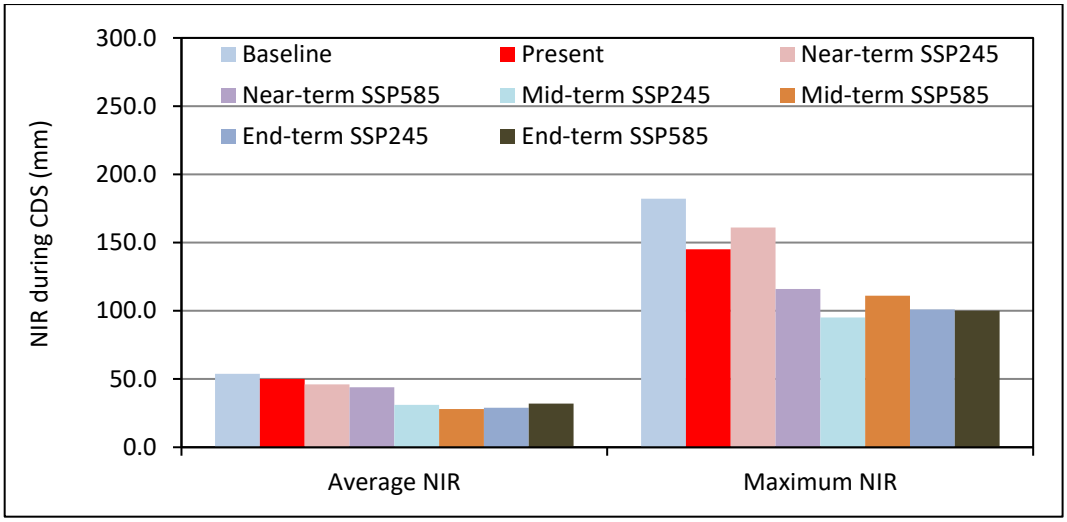

Figure 5.130: Net Irrigation Requirement (NIR) for maize at Ujjain with EC-Earth3

requirement at Ujjain for maize is projected to decrease (46.11 mm) during the near-term period on pro-rata basis for 30-year period from 53.88 mm during the baseline period, and further decrease to 30.74 mm during the mid-term period and marginally decrease again during the end-term period (29.43 mm). It can also be observed that with EC-Earth3, the net supplementary irrigation at Ujjain for maize crop differs marginally only under the SSP585 scenario as compared to the SSP245 scenario. The comparison of the net supplemental irrigation requirement during the CDS for maize at Ujjain as evaluated by few GCMs is given in Figure 5.131.

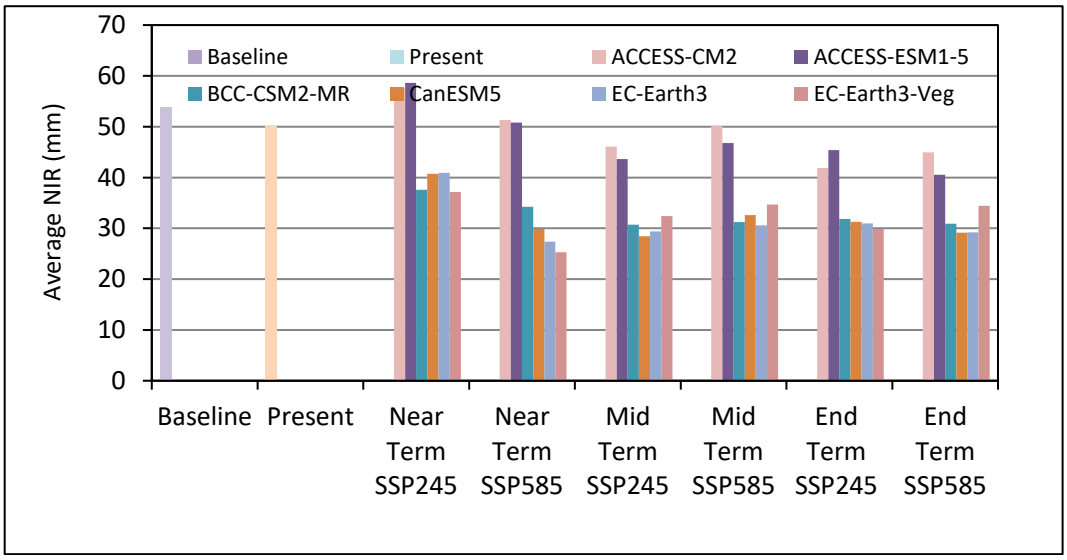

Figure 5.131: Net Irrigation Requirement (NIR) for maize at Ujjain with various GCMs

The comparison of net supplemental irrigation requirement during CDS for maize at Ujjain, as evaluated by ensemble mean of GCMs, along with that during the baseline and present periods is given in Figure 5.132. The average net supplemental irrigation requirement at Ujjain for maize during the baseline period is 53.88 mm which is projected to decrease to 49.40 mm during the near-term period on pro-rata basis for 30-year period, 33.77 mm during the mid-term period and 31.42 mm during the end-term period under SSP245 scenario, based on ensemble mean of the GCMs projections.

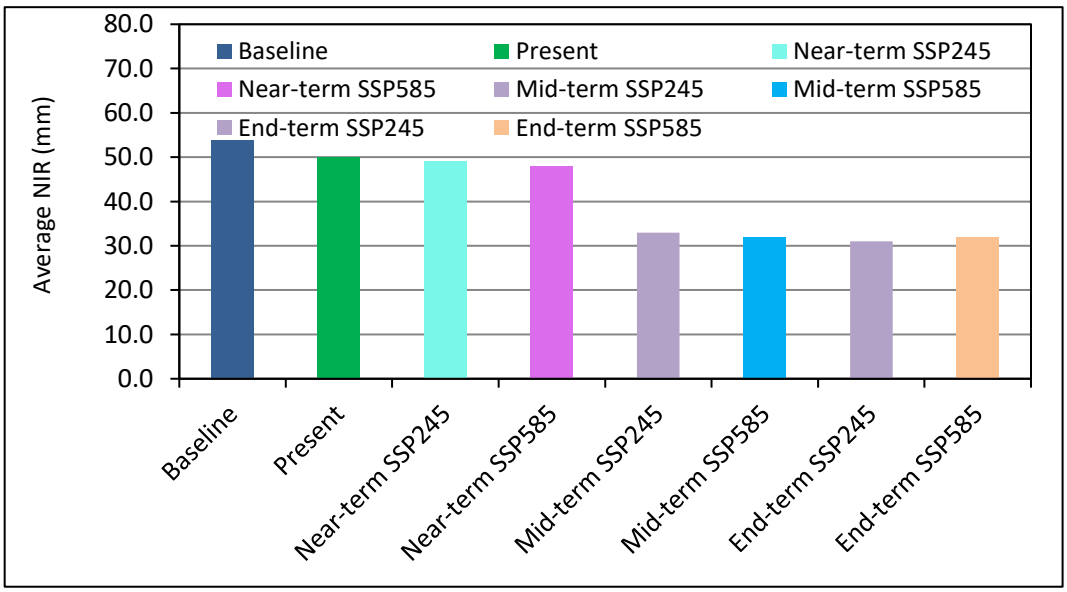

Figure 5.132: Comparison of Net Irrigation Requirement (NIR) for maize at Ujjain (ensemble mean of GCMs)

Similarly, the average net supplemental irrigation requirement at Ujjain for maize is projected to further decrease marginally to 48.00 mm during the near-term period on pro-rata basis for 30-year period, 32.03 mm during the mid-term period and 32.30 mm during the end-term period under SSP585 scenario, based on ensemble mean of the GCMs projections. It can be observed that the supplemental irrigation requirement for maize at Ujjain is marginally higher under SSP245 scenario as compared to SSP585 scenario except during the end-term. Similar analysis has been carried out for estimation of supplemental irrigation for maize for all the 53 blocks in the study area.

Table 5.52 gives the comparison of the CDS events, CDS events requiring irrigation and the supplementary (net) irrigation requirement for cotton during the various time periods at Ujjain with INM-CM5-0 GCM, under SSP245 and SSP585 scenarios. All the final results pertaining to the future time periods are based on the ensemble means of the 13 GCMs for SSP245 and SSP585 scenarios. Based on INM-CM5-0 projections, it can be observed that the average number of CDS at Ujjain is projected to increase during the all-future time periods as

Table 5.52: Comparison of net supplementary irrigation requirement for cotton at Ujjain with INM-CM5-0

S. No.	Particular	BL	PR	Near-term		Mid-term		End-term	
				SSP245	SSP585	SSP245	SSP585	SSP245	SSP585
1	No of CDS	44	40	46	46	57	57	53	53
2	Average duration (days)	18	16	17.13	17.13	17.86	17.86	18.38	18.38
3	CDS requiring irrigation	42	36	43	40	53	50	51	46
4	Average NIR (mm)	53.29	42.22	51.78	28.91	61.54	29.74	62.60	36.06
5	Maximum NIR (mm)	185.9	141.6	226.1	91.32	216.2	72.08	236.5	74.00

compared to the baseline and present periods. However, the increase in CDS events at Ujjain is highest during the near-term period (69) under both scenarios on pro-rata basis for 30-year period. However, the CDS events at Ujjain requiring irrigation for cotton are only substantially different during the near-term under both scenarios (65 & 70) on pro-rata basis for 30-year period, 53 & 30 events during the mid-term and 51 & 46 events during the end-term under SSP245 & SSP585 respectively, but substantially higher than the baseline period (42) except during mid-term under SSP585 scenario (30). The comparison of the CDS events and CDS events that require irrigation at Ujjain for cotton based on INM-CM5-0 projections is given in Figure 5.133.

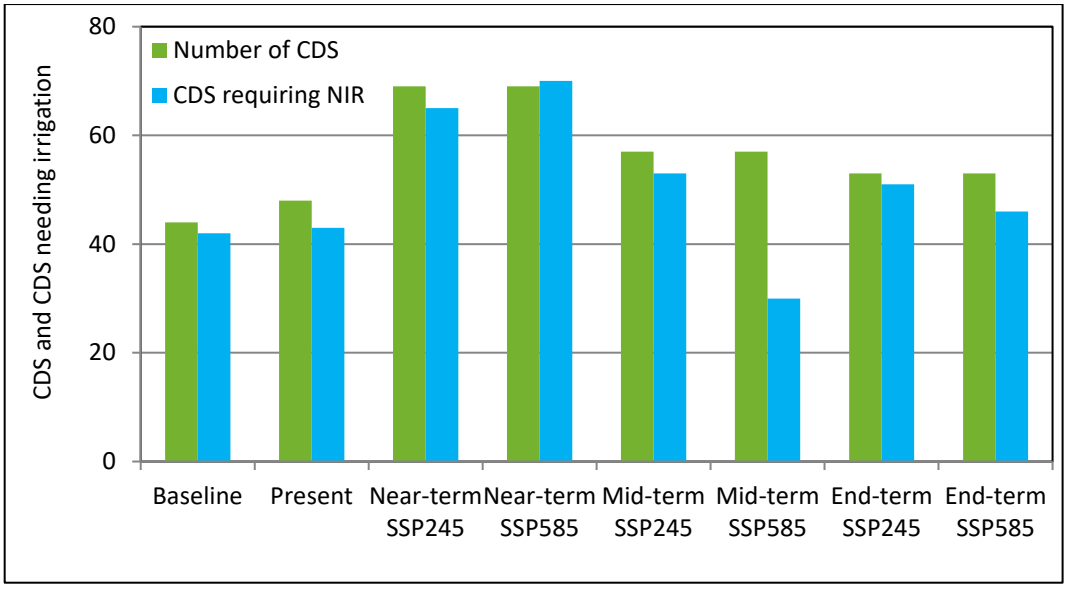

Figure 5.133: Number of CDS and CDS requiring irrigation at Ujjain with INM-CM5-0

Also, based on INM-CM5-0 projections, the average duration of the CDS at Ujjain for cotton is marginally higher during the near-term (25.69 days) on pro-rata basis for 30-year period and mid-term (17.86 days) under both scenarios as compared to the baseline period (18 days), whereas it is marginally higher during the end-term under both scenarios (18.38). The comparison of the average duration of CDS at Ujjain with INM-CM5-0 is given in Figure 5.134.

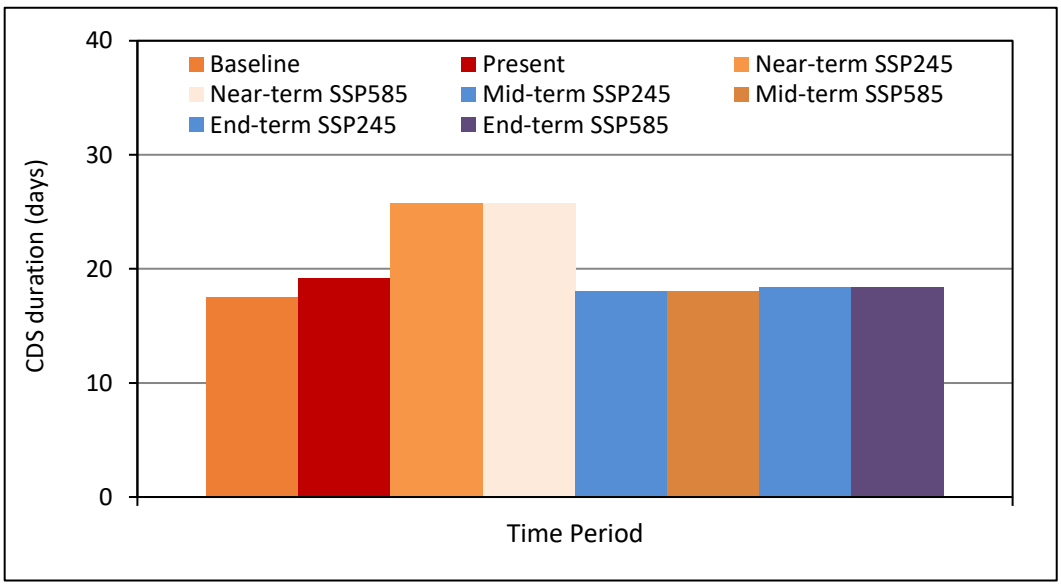

Figure 5.134: Average duration of CDS at Ujjain with INM-CM5-0

The average net supplemental irrigation requirement at Ujjain for maize during the baseline period is 53.29 mm which is projected to increase marginally to 78.00 mm during the near-term period on pro-rata basis for 30-year period, and thereafter increase to 61.54 mm during the mid-term period and 62.60 mm during the end-term period under SSP245scenario, based on INM-CM5-0 projections. Similarly, based on INM-CM5-0 projections, under SSP585 scenario, the average net supplemental irrigation requirement at Ujjain for cotton is projected to marginally decrease to 44.00 mm during the near-term period on pro-rata basis for 30-year period, 29.74 mm during the mid-term period and marginally increase again during the end-term period (36.06 mm). It can also be observed that with INM-CM5-0, the net supplementary irrigation at Ujjain for cotton crop is substantially higher all future time periods under SSP245 scenario. The comparison of the net supplemental irrigation requirement during the CDS for cotton at Ujjain with INM-CM5-0 is given in Figure 5.135. The comparison of the net supplemental irrigation requirement during the CDS for cotton at Ujjain as evaluated by few GCMs is given in Figure 5.136.

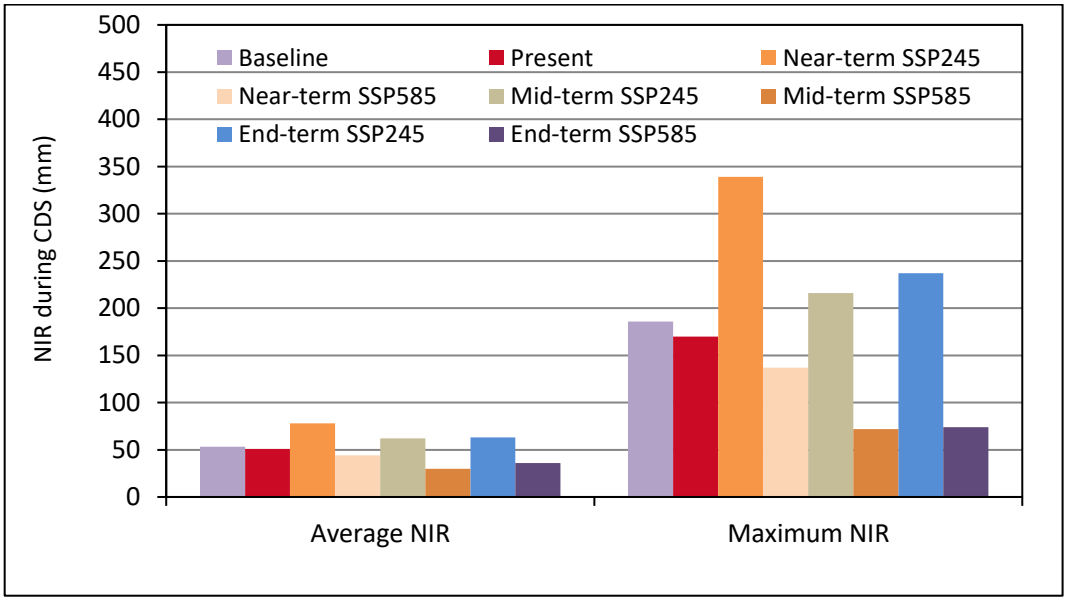

Figure 5.135: Net Irrigation Requirement (NIR) for cotton at Ujjain with INM-CM5-0

The comparison of net supplemental irrigation requirement during CDS for cotton at Ujjain, as evaluated by ensemble mean of GCMs, along with that during the baseline and present periods is given in Figure 5.137. The average net supplemental irrigation requirement at Ujjain for cotton during the baseline period

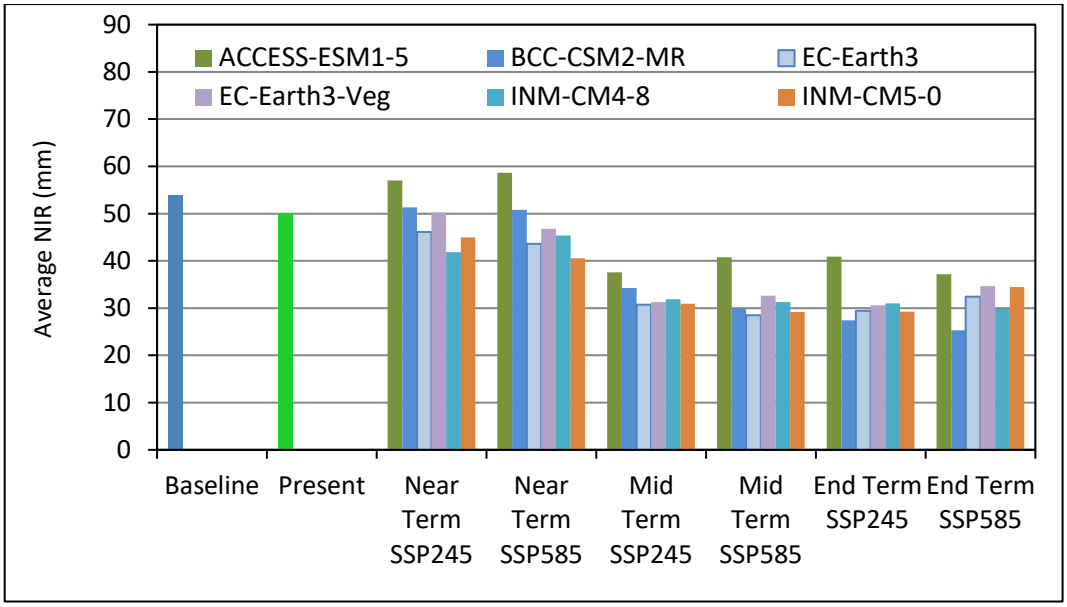

Figure 5.136: Net Irrigation Requirement (NIR) for cotton at Ujjain with various GCMs

is 53.29 mm which is projected to increase to 72.62 mm during the near-term period on pro-rata basis for 30-year period, 52.35 mm during the mid-term period and 53.76 mm during the end-term period under SSP245 scenario, based on ensemble mean of the GCMs projections.

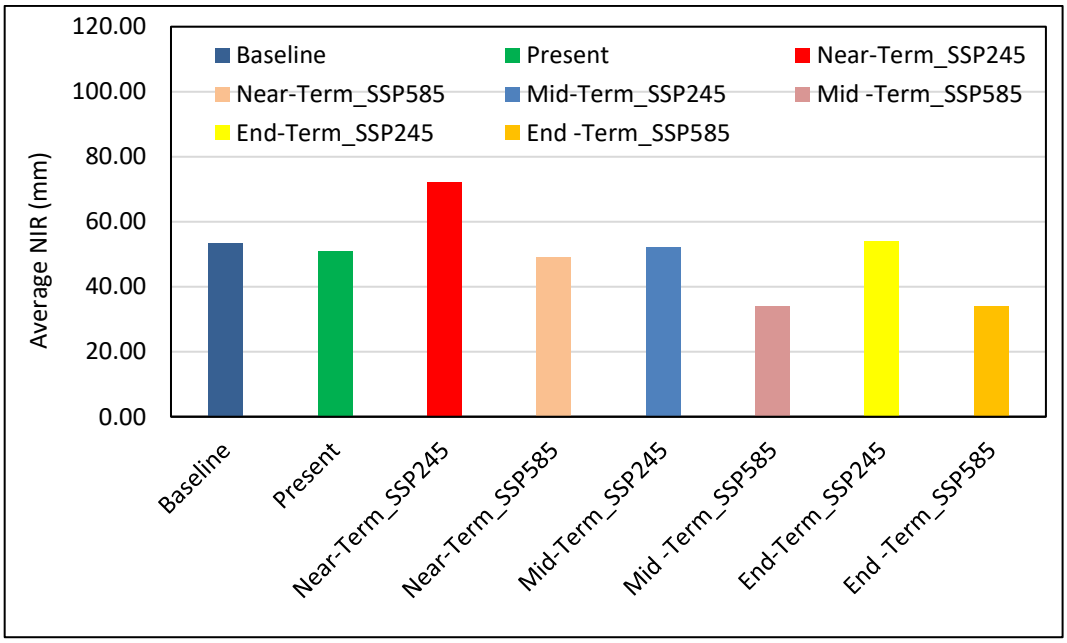

Figure 5.137: Comparison of Net Irrigation Requirement (NIR) for cotton at Ujjain (ensemble mean of GCMs)

Similarly, the average net supplemental irrigation requirement at Ujjain for cotton is projected to further increase substantially to 49.00 mm during the near-term period on pro-rata basis for 30-year period, 33.99 mm during the mid-term period and 33.98 mm during the end-term period under SSP585 scenario, based on ensemble mean of the GCMs projections. It can be observed that the supplemental irrigation requirement for cotton at Ujjain is substantially higher under SSP245 scenario as compared to SSP585 scenario except during all future time periods. Similar analysis has been carried out for estimation of supplemental irrigation for all major crops for the 53 blocks located in the study area.

5.6 Impact of Climate Change on Water Resources

5.6.1 Hydrologic Modeling

The ArcSWAT extension for ArcGIS10.4 has been used for simulating the hydrology in Chambal basin. The study, analysis and results have been carried out for the Chambal basin and its various tributaries falling in Madhya Pradesh. Most of proposed watershed interventions in the form of proposed/recently built dams are planned in this region of the basin. Moreover, the rainfall and base flow from the upper regions is responsible for sustaining the flows in the Chambal River in Central India, a major tributary of the Yamuna River system which is a major tributary of the Ganga River system. The Gandhi Sagar Dam (GS) is one of the major dams existing on Chambal River in MP, whereas Rana Pratap Sagar Dam (RPS), Jawahar Sagar Dam (JS) and Kota barrage is located on the Chambal River on the downstream of GS dam in Rajasthan. Figure 5.1 shows the location of the existing major dams in the Chambal basin.

The SRTM DEM of 90 m resolution downloaded from CGIAR consortium for spatial information (CGIAR-CSI) website (http://srtm.csi.cgiar.org/); land use/land cover map prepared from the multispectral satellite data from National Remote Sensing Centre (NRSC) LISS IV satellite data; soil characteristics based on the Food and Agricultural Organization's (FAO) Harmonized World Soil Database (HWSD) prepared by International Institute for Applied Systems Analysis (IIASA) have been used to represent the spatial distribution of the topography, land use and soil properties respectively, in the study area. The maps

showing the study area with the location of existing major dam sites and gauging sites DEM, land use and soil type, and dams incorporated in SWAT are given in Figure 5.138 to Figure 5.141.

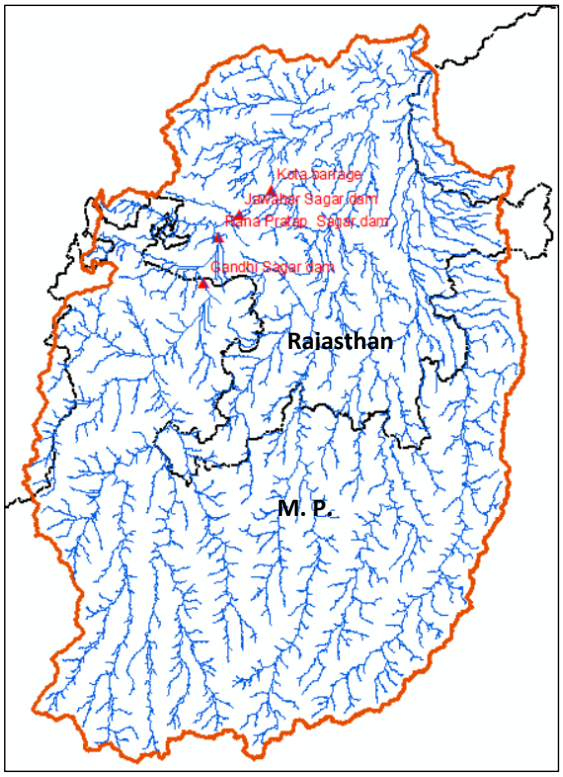

Figure 5.138: Location of major dams in MP and Rajasthan

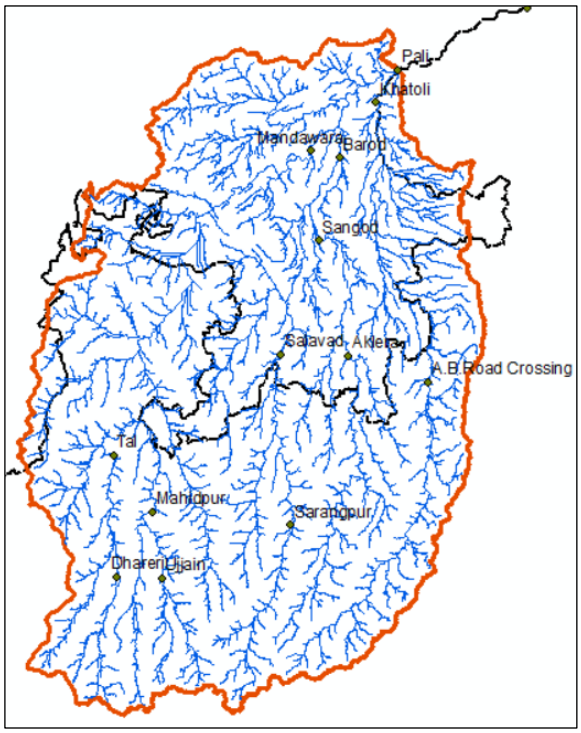

Figure 5.139: Drainage pattern of Chambal basin with CWC gauging sites

Based on the ten SWAT land use classes, nine SWAT soil classes and two slope classes, the sub-basins and HRUs have been derived with threshold values for the

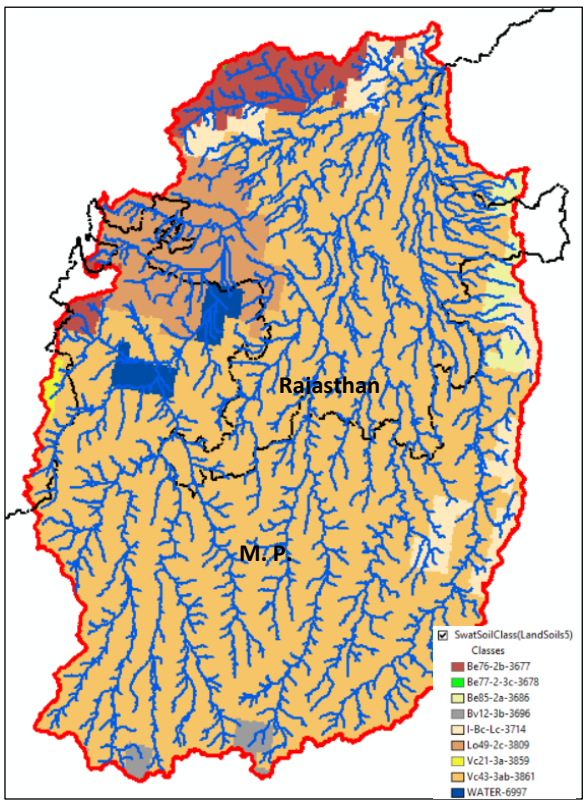

Figure 5.140: Soil types in Chambal basin

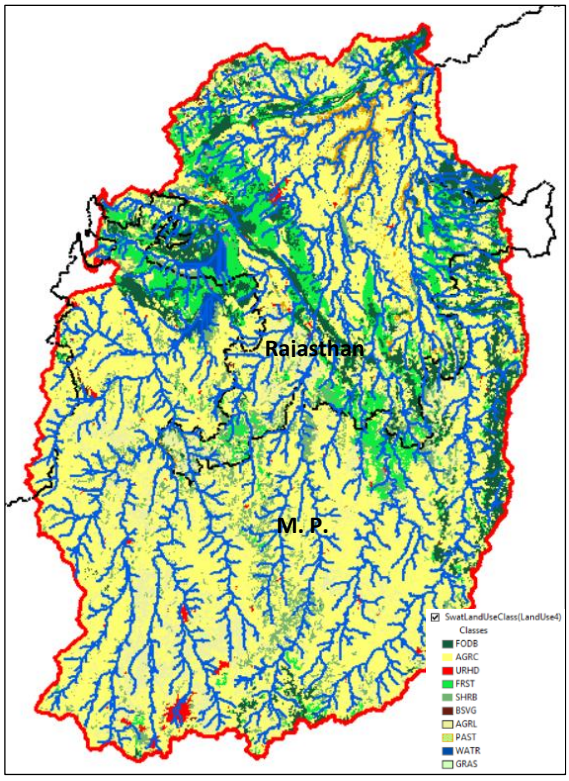

Figure 5.141: Land use / Land cover in Chambal basin

sub-basins as 20%, which resulted in 2343 subbasins and 3776 HRUs. The total catchment area of Chambal basin upto Pali GD site is 76693.04 sq. km. Close grown agricultural land (AGRC) is the predominant land use type (70.49%) whereas the predominant soil type is Vc43-3ab-3861 (79.55%).

The high resolution ($0.25^o \times 0.25^o$) daily gridded rainfall data (Rajeevan et al., 2005), and the ($1^o \times 1^o$) gridded minimum and maximum temperature (Srivastava et al., 2005) prepared by IMD have been imported into the model framework. The remaining weather data for running SWAT viz., wind speed, relative humidity, solar radiation and sunshine hours have been generated using the weather generator available in SWAT at daily time steps. Thus, the input database for the setup of SWAT model comprised of the following:

For system characterization

i) DEM
ii) Slope map
iii) Soil Map
iv) Land use / Land cover map

Input forcing data

i) Daily gridded rainfall at 0.25^o resolution
ii) Daily climate data including minimum and maximum temperature at 1.0^o resolution
iii) Daily wind speed, relative humidity, solar radiation from SWAT weather generator
iv) Daily discharge at the gauging sites on the tributaries and main river
v) Hydraulic properties of reservoirs

The basic model setup with the high-resolution climate data, DEM, soil, and land use/land cover along with the manual insertion of additional nodes at gauging sites and dam sites have been used for simulation of the hydrology pertaining to the virgin condition of the basin. The default run assumes the basin to be virgin with no watershed interventions. Subsequently, the management operations including irrigation by reservoirs, groundwater etc., have been input into the model depending on the actual field conditions. The daily discharge data at Dhareri, Ujjain, Tal, Mahidpur, Sarangpur, AB Road Crossing GD sites in Madhya Pradesh

and Salavad and Aklera GD sites in Rajasthan provided by the Central Water Commission (CWC) has been used to compare the SWAT simulated discharge with the observed discharge. The details of the gauging sites are given in Table 5.53.

Table 5.53: Gauging sites on River Chambal and its tributaries

Gauging site	District	Catchment (sq km)	River /Tributary	Latitude	Longitude
A. B. Road Crossing	Guna	5669	Parwati	24°21'57"	77°05'56"
Tal	Ratlam	4270	Chambal	23°43'24"	75°20'49"
Ujjain	Ujjain	2070	Shipra	23°10'06"	75°46'16"
Sarangpur	Rajgarh	2600	Kalisindh	23°33'00"	76°28'02"
Mahidpur	Ujjain	4430	Shipra	23°28'50"	75°38'11"
Salavad	Jhalawar	7450	Kalisindh	24°22'03"	76°12'21"
Aklera	Jhalawar	6050	Kalisindh/Parwan	24°25'47"	76°36'14"

The workflow of the setup and modeling process is given in Figure 5.142. The reservoir properties including the full supply level, gross storage capacity, emergency spillway level, dead storage level, dead storage capacity, water spread area at full supply level, etc., has been used to set up the model and was extracted from the detailed project reports of the respective dams, provided by Water Resources Department (WRD), Govt. of Madhya Pradesh. The management operations viz., irrigation from reservoir, shallow aquifer and deep aquifer have been added and model runs performed at the daily and monthly time steps, with warm-up period of 4 years.

5.6.2 Multisite calibration, validation and uncertainty assessment

The multi-site calibration of SWAT model has been carried using the SUFI-2 algorithm using SWAT-CUP, which combines parameter calibration and uncertainty predictions. The input parameter uncertainty is represented by uniform distributions whereas the model output uncertainty is quantified by the 95 Percent Prediction Uncertainty (95PPU). The multi-site calibration has been performed using the daily stream flow data at AB Road Crossing (R. Parvati), Tal (R. Chambal), Ujjain (R. Shipra), Sarangpur (R. Kalisindh), Mahidpur (R. Shipra), Salavad (R. Kalisindh), and Aklera (R. Kalisindh/Parwan) during various time durations based on data availability.

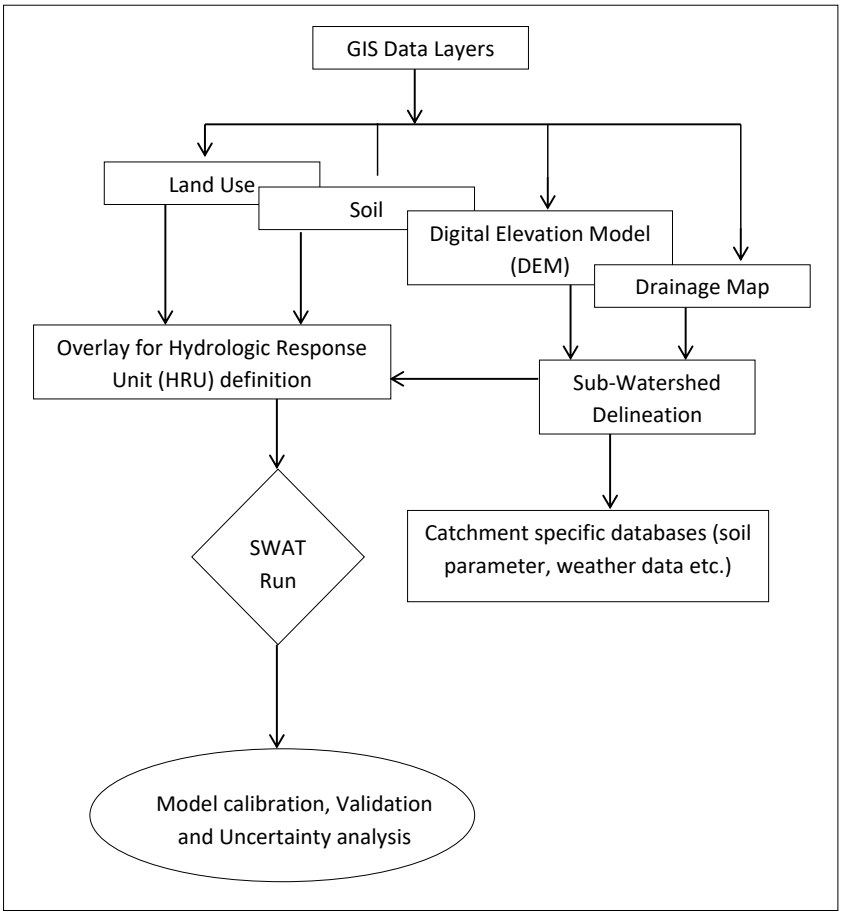

Figure 5.142: Workflow of the SWAT setup

The initial uncertainty ranges were assigned to each parameter globally and the model runs were made with 1000 simulations. The global sensitivity analysis and one at a time sensitivity analysis was used to identify the most sensitive parameters and the non-sensitive parameters were then eliminated based on the p-values and t-statistic. The model parameter and input data uncertainty are represented by the 95PPU band and quantified by the P-factor and R-factor. The 95PPU band ideally gets smaller with subsequent iteration during the calibration process. A balance is maintained between the P-factor and R-factor such that the P-factor does not become too small while the R-factor remains high. The desired parameter ranges are obtained when the P-factor and the R-factor does not change in the subsequent iterations.

The curve number (CN2) is the most sensitive parameter followed by groundwater delay (GWDELAY), groundwater revap coefficient (GW_REVAP) and threshold depth of water in the shallow aquifer required for return flow to

occur (GWQMN). The other important parameters are available water capacity of the soil layer (SOL_AWC), base flow alpha factor (ALPHA_BF) and soil evaporation compensation factor (ESCO). The validation has been carried out with the independent data at the various gauging sites. The model evaluation statistics during the calibration for all the gauging sites are given in Table 5.54.

Table 5.54: Model evaluation statistics during calibration and validation

S. No.	Gauging site	Calibration			Validation		
		NSE	RMSE	RSR	NSE	RMSE	RSR
1.	A. B. Road Crossing	0.86	58.53	0.37	0.75	70.62	0.48
2.	Tal	0.61	53.15	0.53	0.86	50.45	0.38
3.	Ujjain	0.69	18.08	0.51	0.80	18.69	0.44
4.	Sarangpur	0.70	61.09	0.54	0.76	39.95	0.49
5.	Mahidpur	0.83	48.82	0.42	0.76	48.36	0.49
6.	Salavad	0.85	58.52	0.38	0.85	76.53	0.39
7.	Aklera	0.62	58.72	0.51	0.65	56.47	0.55

The comparison of the observed and simulated monthly discharges at A. B. Road Crossing GD site on River Parvati during calibration and validation is given in Figure 5.143 and Figure 5.144 respectively. The NSE during calibration was 0.86 and 0.75 during validation whereas the RSR was 0.37 and 0.50 during calibration and validation respectively. As such, the model is able to simulate the flows reasonably well during both calibration and validation.

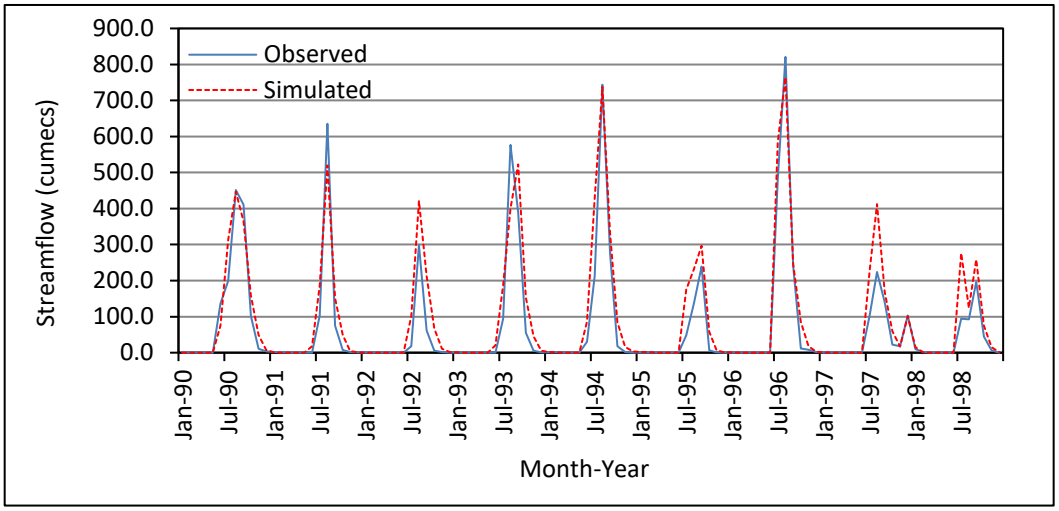

Figure 5.143: Comparison of observed and simulated flows at AB Road Crossing during calibration

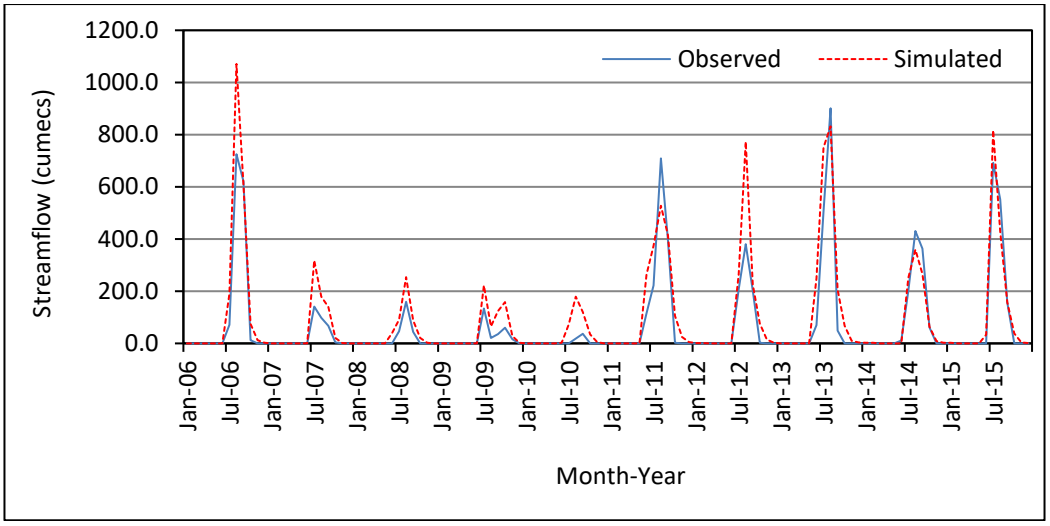

Figure 5.144: Comparison of observed and simulated flows at AB Road Crossing during validation

The comparison of the observed and simulated monthly discharges at Tal GD site during calibration and validation is given in Figure 5.145 and 5.146 respectively. The NSE during calibration was 0.61 and 0.86 during validation whereas the RSR was 0.53 and 0.38 during calibration and validation respectively. Therefore, the model is able to simulate the flows reasonably well during both calibration and validation, even though few flow peaks have been overestimated particularly during the calibration period. However, the peaks have been better simulated during the validation.

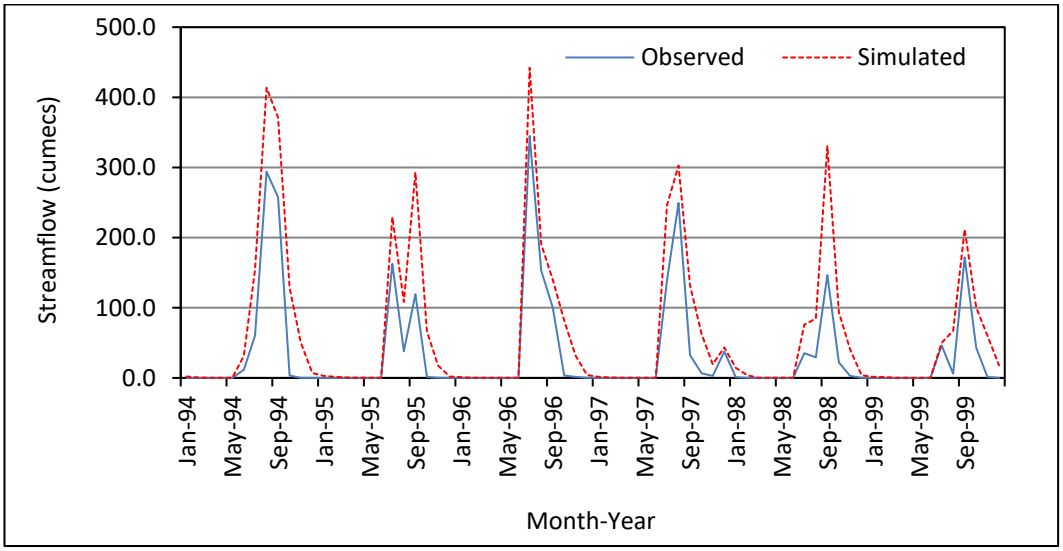

Figure 5.145: Comparison of observed and simulated flows at Tal during calibration

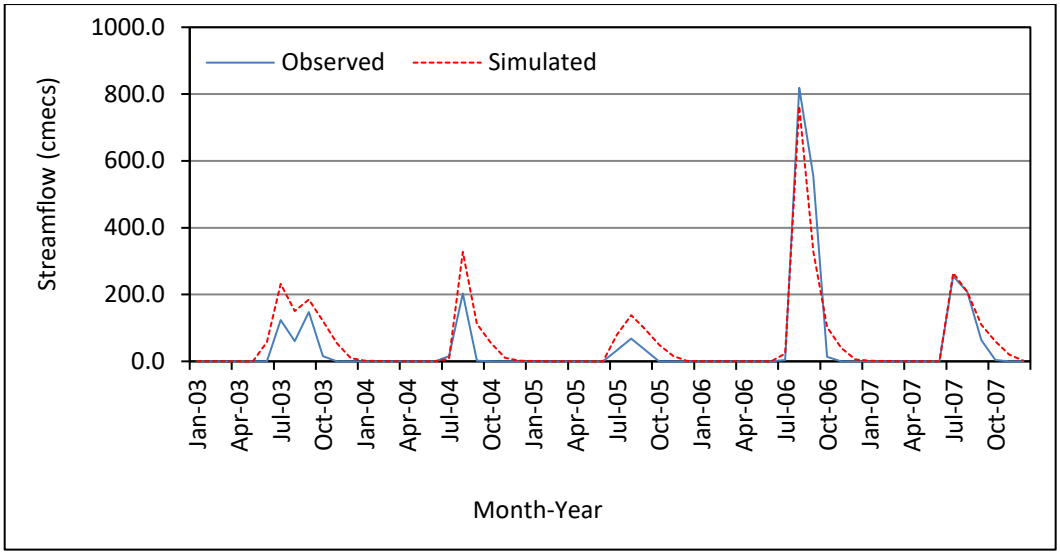

Figure 5.146: Comparison of observed and simulated flows at Tal during validation

The comparison of the observed and simulated monthly discharges at Ujjain GD site during calibration and validation is given in Figure 5.147 and 5.148 respectively. The NSE during calibration was 0.69 and 0.80 during validation whereas the RSR was 0.56 and 0.44 during calibration and validation respectively. It can be observed that the model is able to simulate the peak flows and the lean flows reasonably well during both calibration and validation.

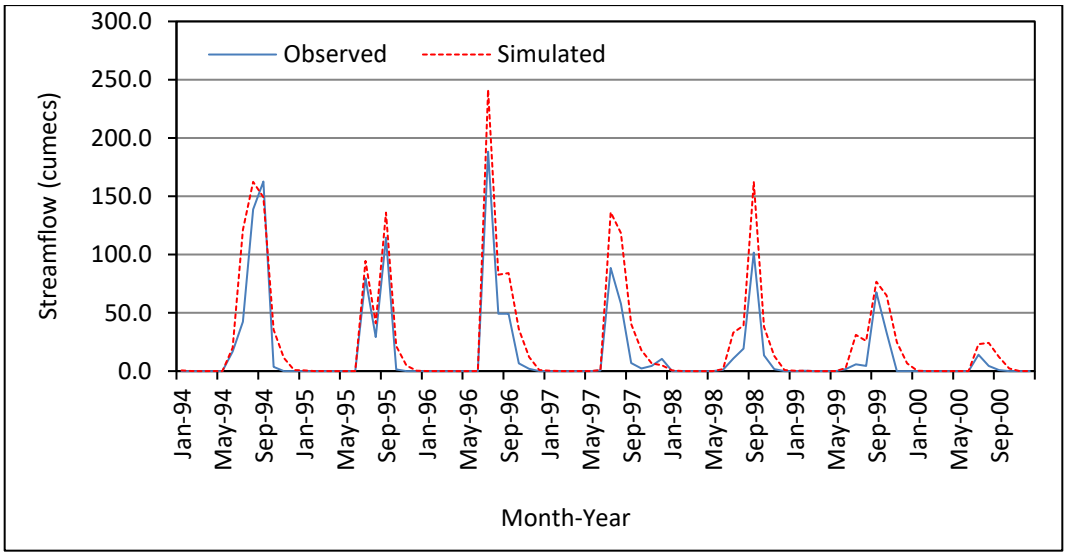

Figure 5.147: Comparison of observed and simulated flows at Ujjain during calibration

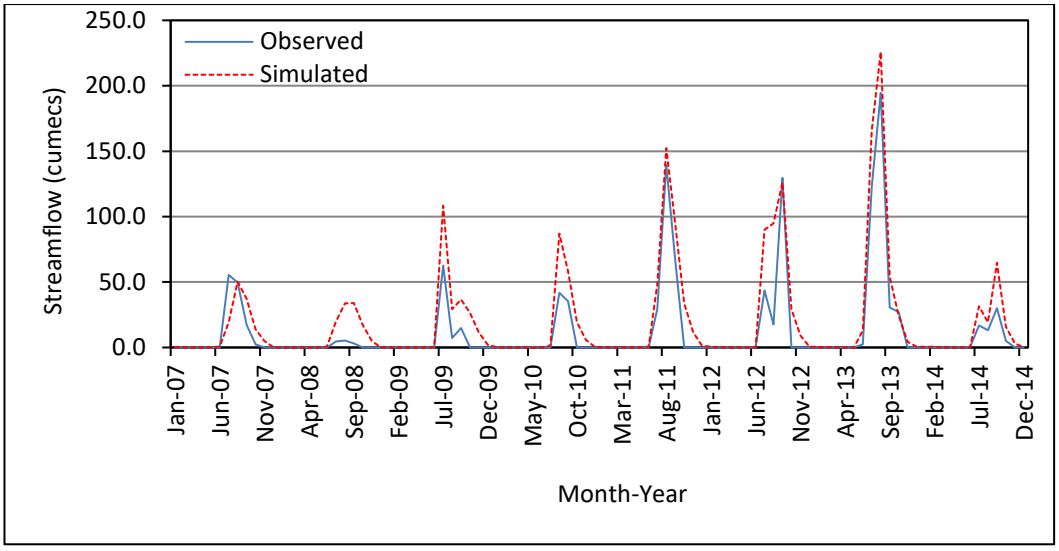

Figure 5.148: Comparison of observed and simulated flows at Ujjain during validation

The comparison of the observed and simulated monthly discharges at Sarangpur GD site during calibration and validation is given in Figure 5.149 and 5.150 respectively. The NSE during calibration was 0.70 and 0.76 during validation whereas the RSR was 0.54 and 0.49 during calibration and validation respectively. As such, the model is able to simulate the flows reasonably well during both calibration and validation. During the calibration period one peak flow during August 2006 was underestimated. However, the simulation during the validation period performed well.

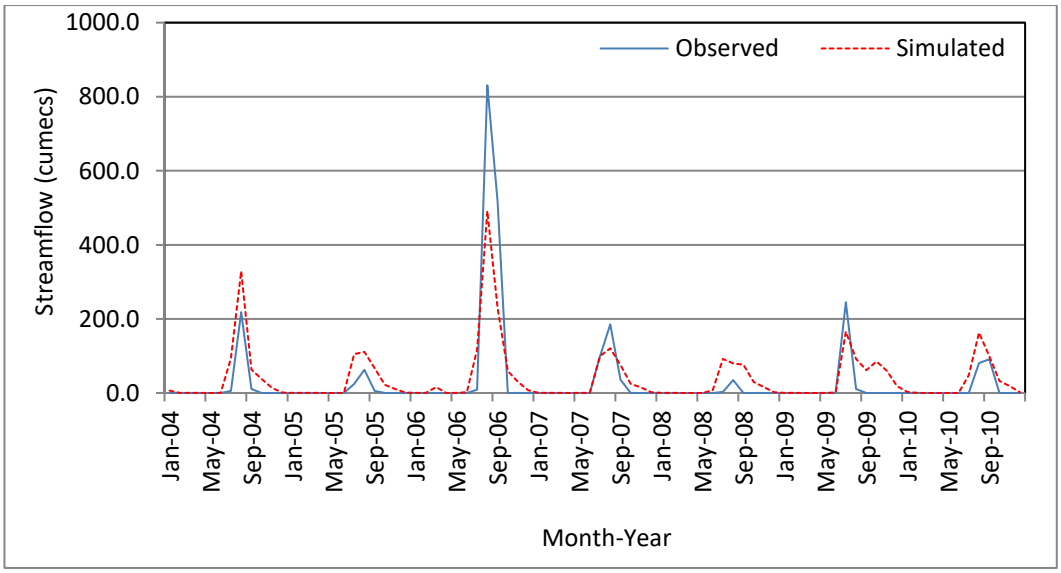

Figure 5.149: Comparison of observed and simulated flows at Sarangpur during calibration

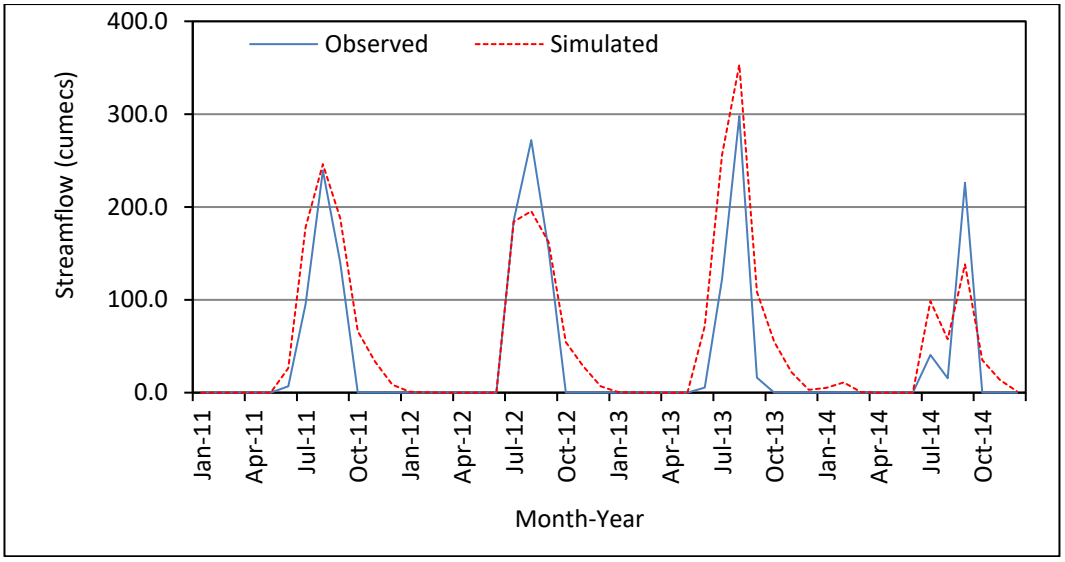

Figure 5.150: Comparison of observed and simulated flows at Sarangpur during validation

Similarly, the comparison of the observed and simulated monthly discharges at Mahidpur GD site during calibration and validation is given in Figure 5.151 and 5.152 respectively. The NSE during calibration was 0.83 and 0.76 during

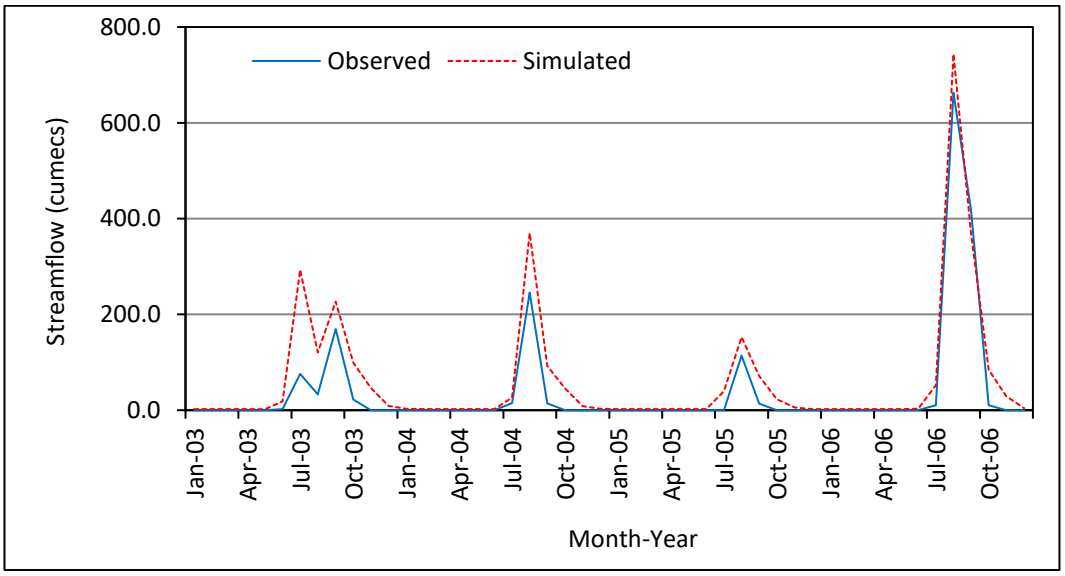

Figure 5.151: Comparison of observed and simulated flows at Mahidpur during calibration

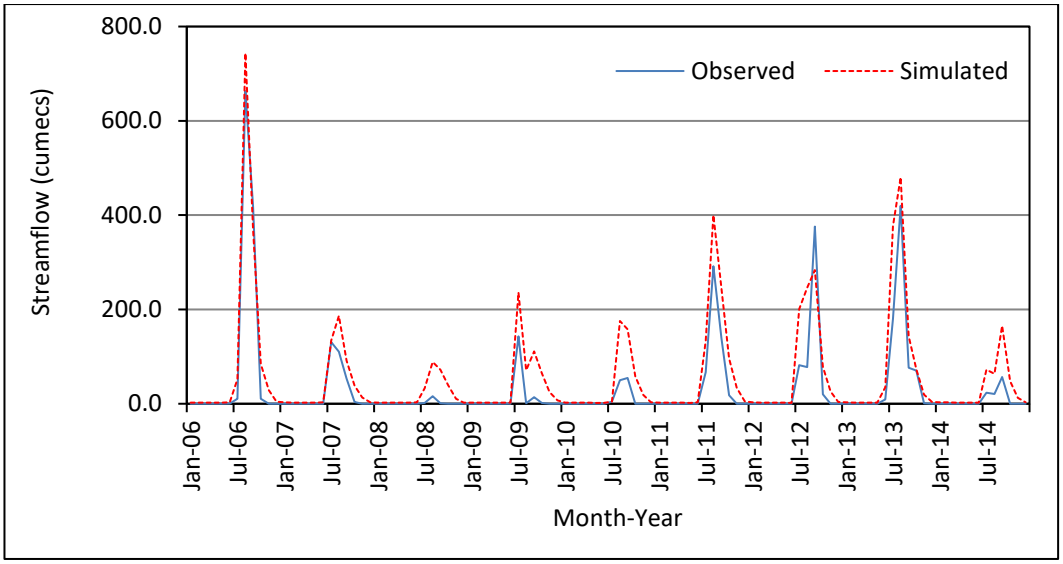

Figure 5.152: Comparison of observed and simulated flows at Mahidpur during validation

validation whereas the RSR was 0.42 and 0.49 during calibration and validation respectively. The model is therefore able to simulate the flows reasonably well during both calibration and validation.

The comparison of the observed and simulated monthly discharges at Salavad GD site during calibration and validation is given in Figure 5.153 and 5.154 respectively. NSE during calibration was 0.85 and 0.85 during validation whereas the RSR was 0.38 and 0.38 during calibration and validation respectively. The

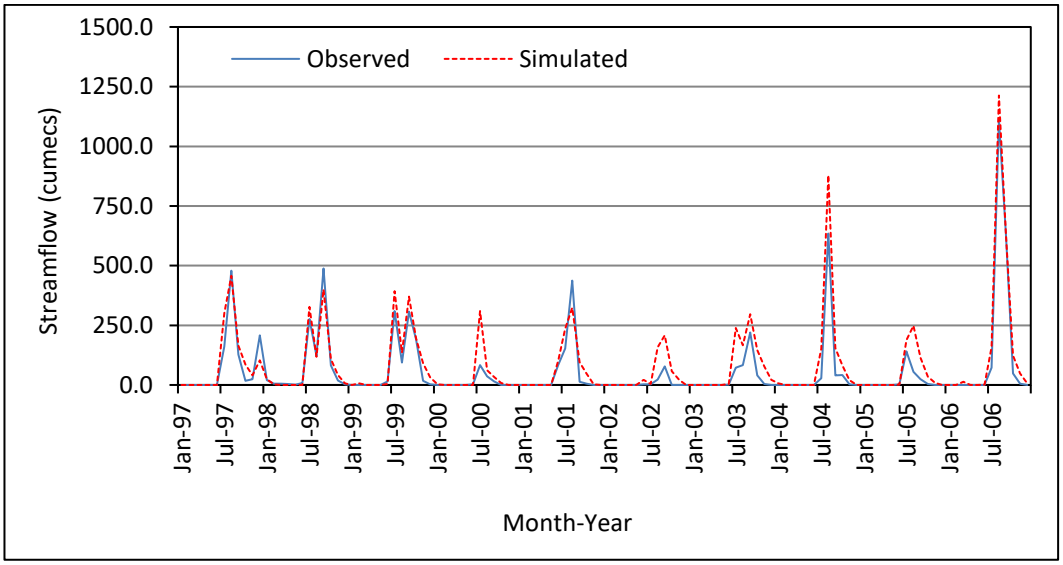

Figure 5.153: Comparison of observed and simulated flows at Salavad during calibration

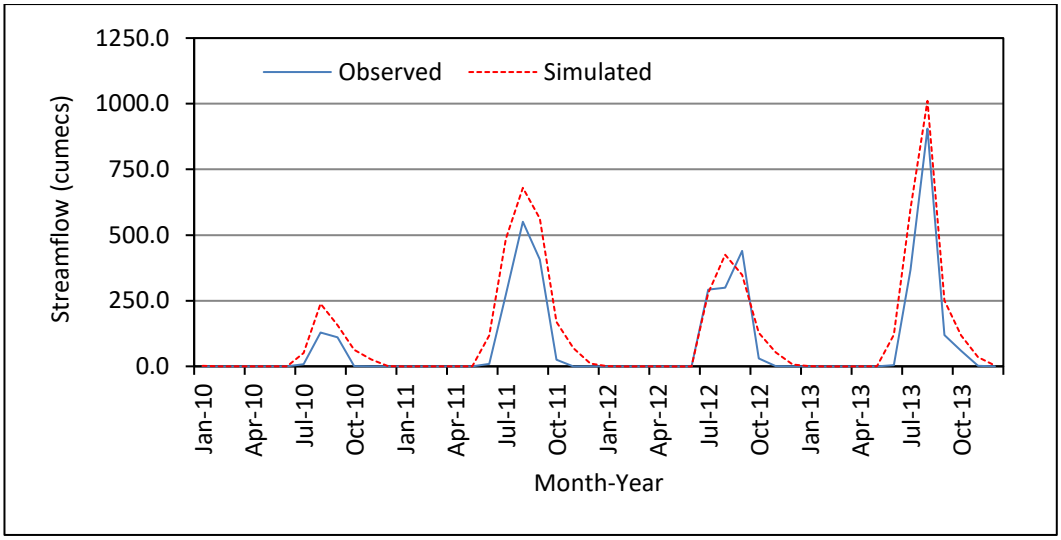

Figure 5.154: Comparison of observed and simulated flows at Salavad during validation

model is able to simulate the peak flows and the lean flows reasonably well during both calibration and validation.

Similarly, the comparison of the observed and simulated monthly discharges at Aklera GD site during calibration and validation is given in Figure 5.155 and 5.156 respectively. NSE during calibration was 0.62 and 0.65 during validation whereas the RSR was 0.51 and 0.50 during calibration and validation respectively. The model is able to simulate the peak flows and low flows reasonably well during both calibration and validation. During calibration period flow peak during

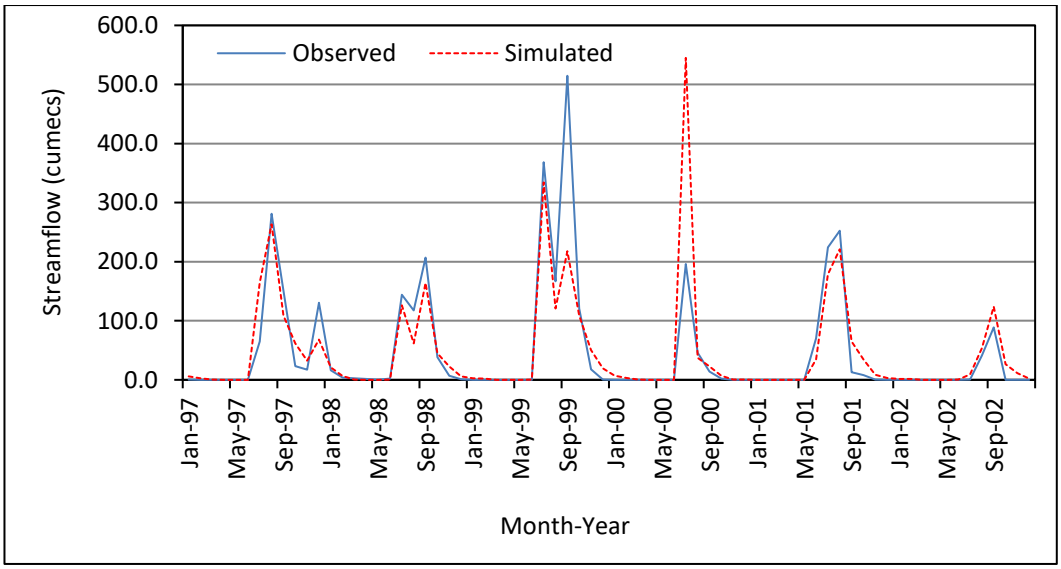

Figure 5.155: Comparison of observed and simulated flows at Aklera during calibration

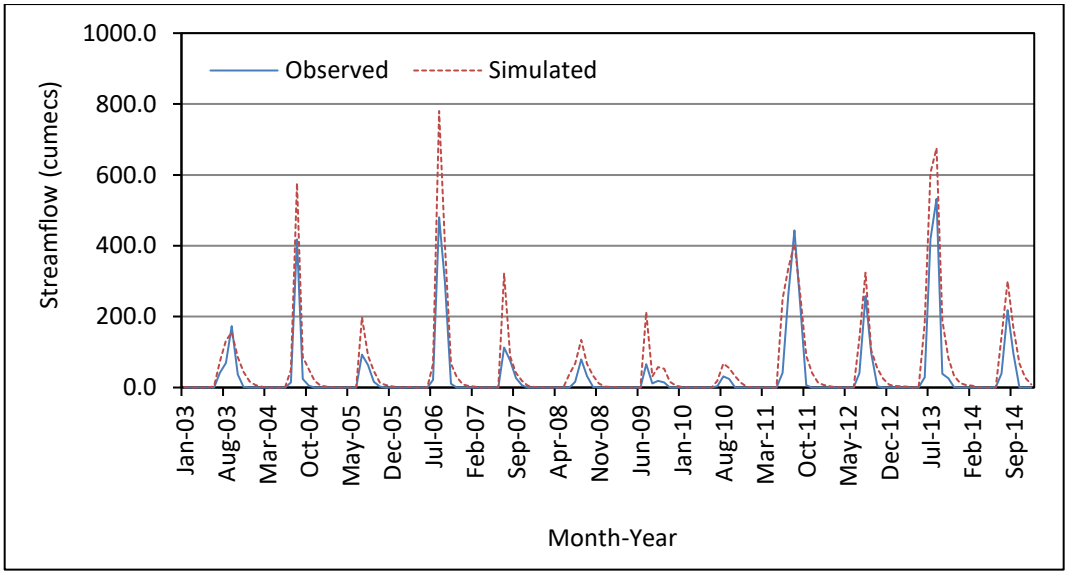

Figure 5.156: Comparison of observed and simulated flows at Aklera during validation

September 1999 was underestimated whereas flow peak during August 2000 was overestimated. However, the simulation performed well during validation period except during August 2006 and July 2013 during which the peak flow was slightly overestimated.

5.6.3 Impact of Climate Change on Mean Flows

The climate change impact assessment on the stream flow in the various sub-basins of Chambal River system falling in the study area has been carried out using the SWAT simulated runoff during the baseline, present, near-term, mid-term and end-term time periods. The impact assessment on the water resources includes assessment of the changes in the mean flow during various time periods. The changes in the high flows and low flows (water availability) have also been carried out by the dependable flow analysis of the SWAT simulated runoff. The dependable flow analysis has been carried out on an annual basis and on a monthly basis for all the months.

The comparison of the average annual stream flow derived by simulation based on future climate data of 13 GCMs under both future climate scenarios viz., SSP245 and SSP585 during various time periods at AB Road Crossing on River Parvati is given in Figure 5.157. The inter-model variability is clearly depicted here as the projections by CANESM5 are relatively very high as compared to simulations derived from other GCMs. The mean flow during the baseline and present periods

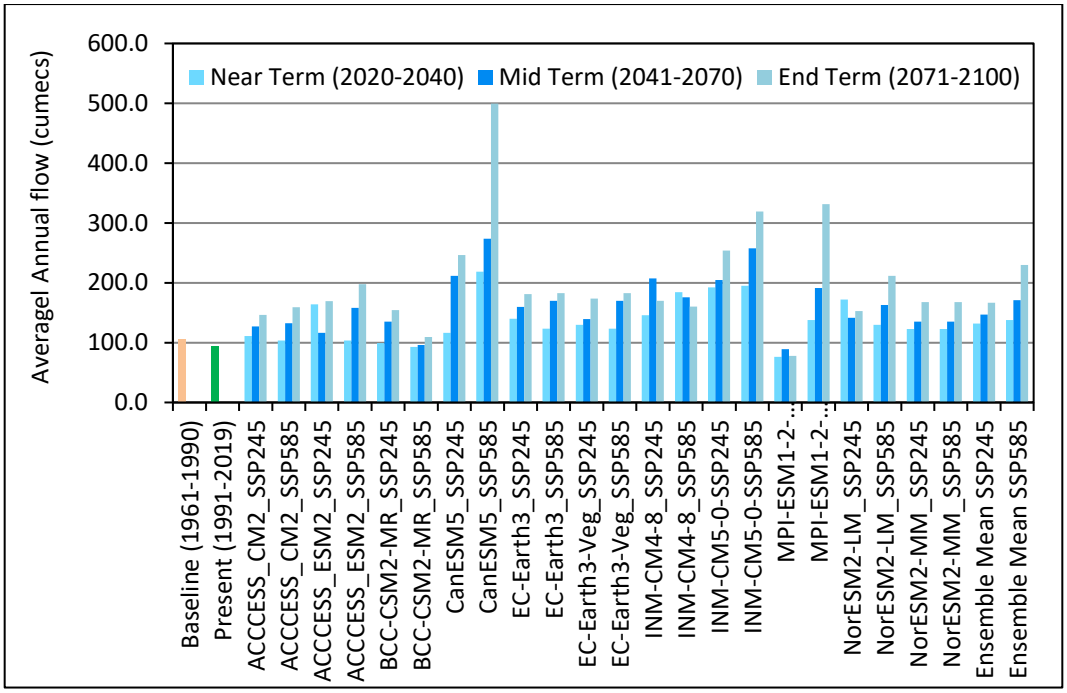

Figure 5.157: Comparison of average annual stream flow at AB Road on R. Parvati

was 47.33 cumecs and 45.12 cumecs respectively. It can be observed that the mean flows are projected to increase with all the GCMs under both future climate scenarios except for MPI-ESM1-2-HR under SSP245.

The ranges of the projections by the various models under both scenarios vary between higher projection of 105.77 cumecs during the near-term, 130.20 cumecs during the mid-term and 229.70 cumecs during the end-term by CANESM5 under SSP585 scenario to a low of viz., 35.71 cumecs during the near-term, 41.91 cumecs during the mid-term and 37.89 cumecs during the end-term by MPI-ESM1-2-HR under SSP245 scenario. However, the ensemble mean of all the GCMS are comparable with the average annual stream flow during the baseline and present periods. The ensemble mean average annual stream flow under SSP245 scenario varies between 59.45 cumecs during the near-term, 66.02 cumecs during the mid-term and 73.30 cumecs during the end-term. Similarly, the ensembles means average annual stream flow is relatively higher under SSP585 scenario and varies between 61.50 cumecs during the near-term, 75.46 cumecs during the mid-term and 102.45 cumecs during the end-term. It can be observed that the average annual stream flow projections are relatively much higher under the SSP585 scenario for all future time periods and difference is highest during

the end-term. As compared to the baseline period, the average annual stream flow is projected to increase by 25.6%, 39.5% and 54.9% during near-term, mid-term and end-term under SSP245 scenario. Much higher increase is projected under SSP585 scenario as compared to the baseline period, with an increase of 36.3%, 67.3% and 127.1% under SSP585 scenario.

The comparison of the average annual stream flow under both future climate scenarios viz., SSP245 and SSP585 at Tal on River Chambal is given in Figure 5.158. The inter-model variability is clearly depicted here as the projections by CANESM5 are comparatively very high as compared to simulations derived from other GCMs. The mean flow during the baseline and present periods was 94.66 cumecs and 94.42 cumecs respectively. It can be observed that as compared to the baseline period, the mean flows are projected to decrease with few GCMs viz., ACCESS-CM2 under both scenarios, ACCESS-ESM2 under SSP245 scenario, BCC-CSM2-MR under both scenarios, MPI-ESM1-2-HR under both scenarios and NorESM2-MM under both scenarios for all future time periods. However,

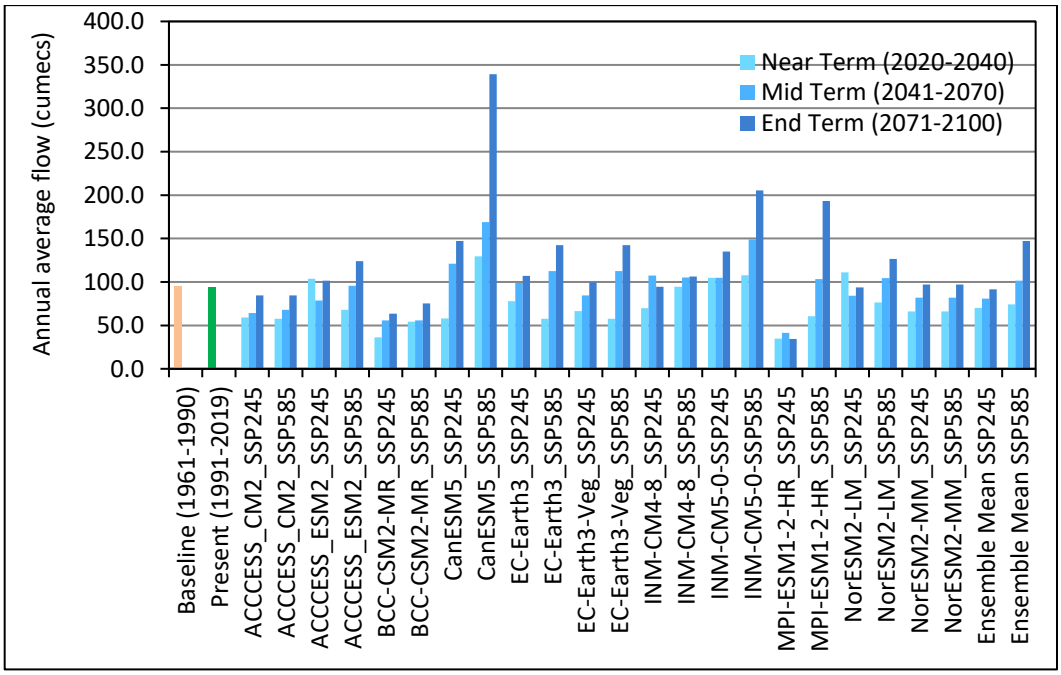

Figure 5.158: Comparison of average annual stream flow at Tal on R. Chambal

few GCMs project higher average annual stream flow viz., ACCESS-ESM2 under SSP585 scenario, CANESM5 under both scenarios, EC-Earth3 under both scenarios, EC-Earth3-Veg under both scenarios, INM-CM4-8 under both

scenarios, INM-CM5-0 under both scenarios and NorESM2-LM under both scenarios.

The ensemble mean of average annual stream flow from all GCMS are comparable with the average annual stream flow during the baseline and present periods. The ensemble mean average annual stream flow under SSP245 scenario is marginally lower than the baseline period and varies between 70.00 cumecs during the near-term, 88.03 cumecs during the mid-term and 91.60 cumecs during the end-term. Similarly, the ensemble means average annual stream flow is relatively higher under SSP585 scenario and varies between 74.01 cumecs during the near-term, 101.58 cumecs during the mid-term and 147.28 cumecs during the end-term. It can be observed that the average annual stream flow projections are relatively much higher under the SSP585 scenario for all future time periods and difference is highest during the end-term. As compared to the baseline period, the average annual stream flow is projected to decrease during near-term, mid-term and end-term under SSP245 scenario. However, under SSP585 scenario, the average annual stream flow is projected to decrease during the near term (-21.6%), whereas higher increase is projected as compared to the baseline period, with an increase of 7.60% and 56.0% during the mid-term and end-term respectively.

The comparison of the average annual stream flow under both future climate scenarios viz., SSP245 and SSP585 at Ujjain on River Shipra is given in Figure 5.159. The inter-model variability is clearly depicted here as the projections by CANESM5 under SSP585 scenario are relatively excessive as compared to simulations derived from other GCMs. The mean flow during the baseline and present periods was 28.98 cumecs and 23.14 cumecs respectively. It can be observed that as compared to the baseline period, the mean flows are projected to increase under both scenarios, for all the GCMs except for MPI-ESM21-2-HR under SSP245 scenario. It can be observed that the average annual stream flow projections are relatively much higher under the SSP585 scenario for all future time periods and difference is highest during the end-term. As compared to the baseline period, the average annual stream flow is projected to increase by 29.1%, 47.8% and 66.1% during near-term, mid-term and end-term respectively, under

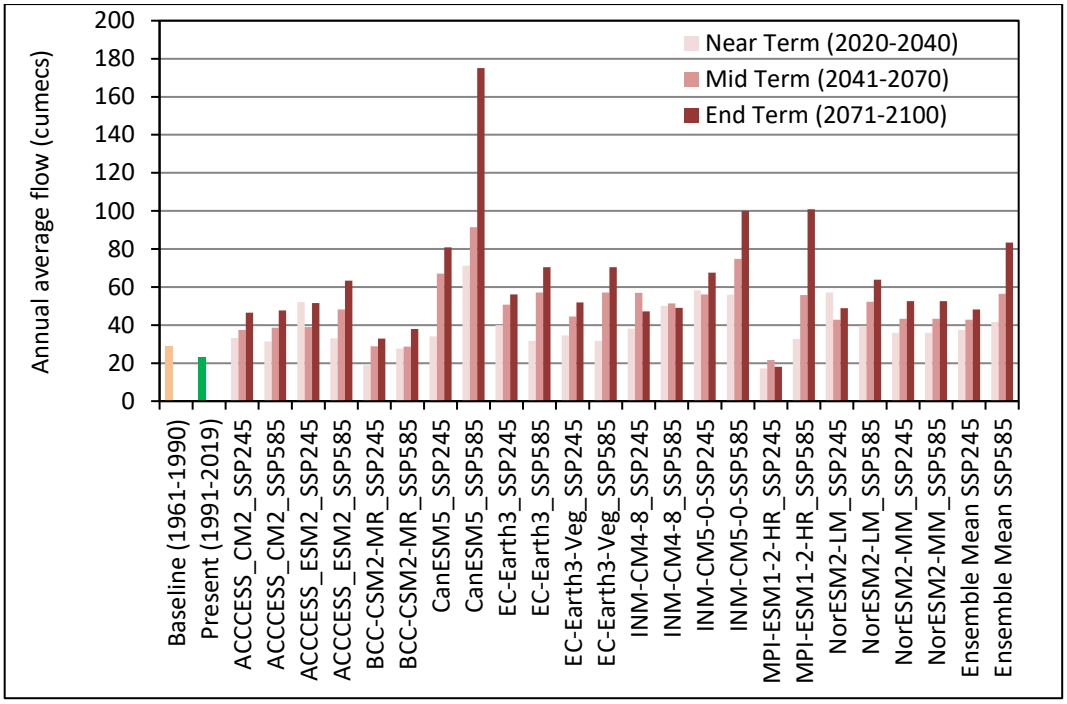

Figure 5.159: Comparison of average annual stream flow at Ujjain on R. Shipra

SSP245 scenario. However, under SSP585 scenario, the average annual stream flow is projected to further increase during the near term (80.0%), mid-term (143.9%) and end-term (260.5%).

The comparison of the average annual stream flow under both future climate scenarios viz., SSP245 and SSP585 at Ujjain on River Shipra is given in Figure 5.160. The mean flow during the baseline and present periods was 47.33 cumecs and 45.12 cumecs respectively. It can be observed that as compared to the baseline period, the mean flows are projected to increase under both scenarios, for all the GCMs except for MPI-ESM21-2-HR under SSP245 scenario. The ensemble mean average annual stream flow under SSP245 scenario is higher than the baseline period and varies between 59.45 cumecs during the near-term, 66.02 cumecs during the mid-term and 73.30 cumecs during the end-term.

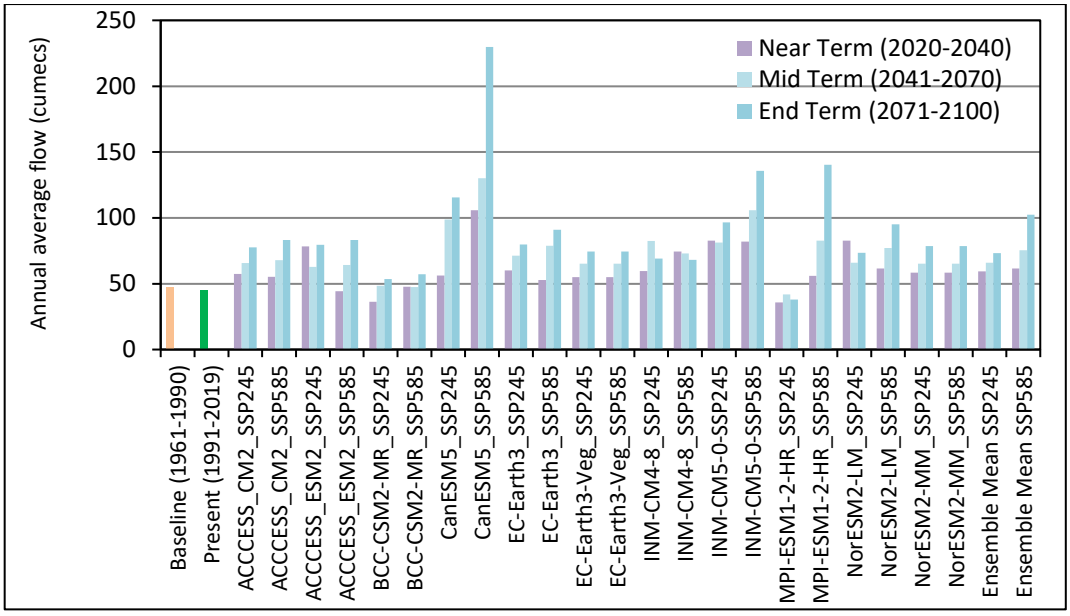

Figure 5.160: Comparison of average annual stream flow at Sarangpur on R. Kalisindh

Similarly, the ensemble mean average annual stream flow is reasonably higher under SSP585 scenario and varies between 61.50 cumecs during the near-term, 75.46 cumecs during the mid-term and 102.45 cumecs during the end-term. It can be observed that the average annual stream flow projections are relatively much higher under the SSP585 scenario for all future time periods and difference is highest during the end-term. As compared to the baseline period, the average annual stream flow is projected to increase by 25.6%, 39.5% and 54.9% during near-term, mid-term and end-term respectively, under SSP245 scenario. However, under SSP585 scenario, the average annual stream flow is projected to further increase during the near term (36.3%), mid-term (67.30%) and end-term (127.1%).

The comparison of the average annual stream flow under both future climate scenarios viz., SSP245 and SSP585 at Mahidpur on River Shipra is given in Figure 5.161. The mean flow during the baseline and present periods was 62.13 cumecs and 57.14 cumecs respectively. It can be observed that as compared to the baseline period, the mean flows are projected to increase under both scenarios, for all the GCMs except for MPI-ESM21-2-HR under SSP245 scenario. The ensemble mean average annual stream flow under SSP245 scenario is higher than the baseline period and varies between 80.85 cumecs during the near-term, 92.33 cumecs during the mid-term and 103.80 cumecs during the end-term. Similarly,

the ensemble mean average annual stream flow is reasonably higher under SSP585 scenario and varies between 85.30 cumecs during the near-term, 114.50 cumecs during the mid-term and 161.87 cumecs during the end-term. It can be observed that the average annual stream flow projections are relatively much higher under the SSP585 scenario for all future time periods and difference is highest during the end-term. As compared to the baseline period, the average annual stream flow is projected to increase by 30.1%, 48.6% and 67.1% during

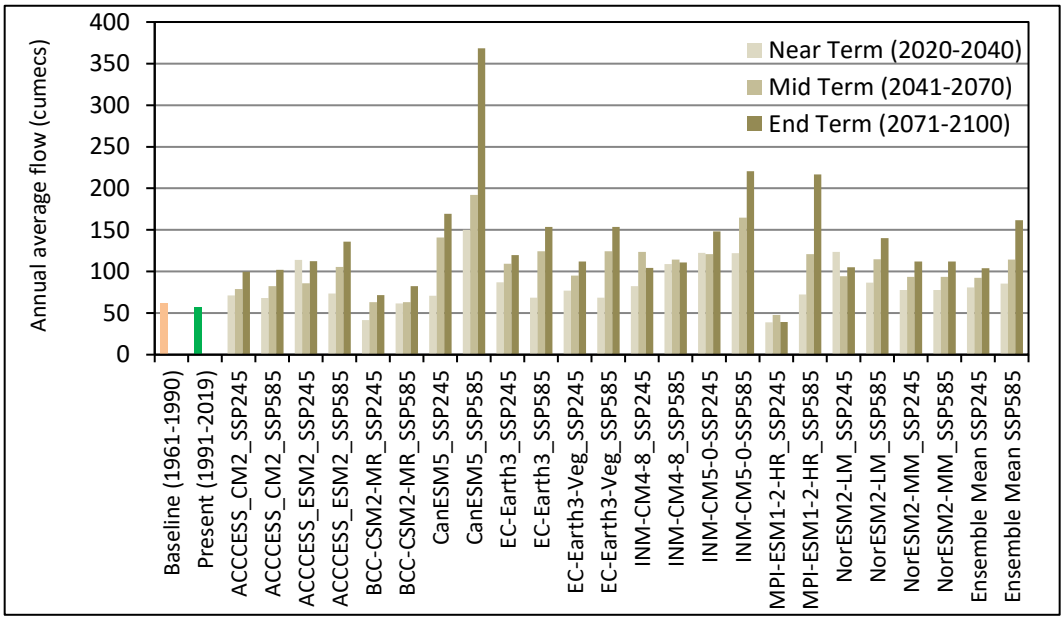

Figure 5.161: Comparison of average annual stream flow at Mahidpur on R. Shipra

near-term, mid-term and end-term respectively, under SSP245 scenario. Similarly, under SSP585 scenario, the average annual stream flow is projected to further increase during the near term (49.3%), mid-term (99.8%) and end-term (183.3%).

The comparison of the average annual stream flow under both future climate scenarios viz., SSP245 and SSP585 at Salavad on River Kalisindh is given in Figure 5.162. The mean flow during the baseline and present periods was 105.02 cumecs and 98.97 cumecs respectively. It can be observed that as compared to the baseline period, the mean flows are projected to increase under both scenarios, for all the GCMs except for MPI-ESM21-2-HR under SSP245 scenario.

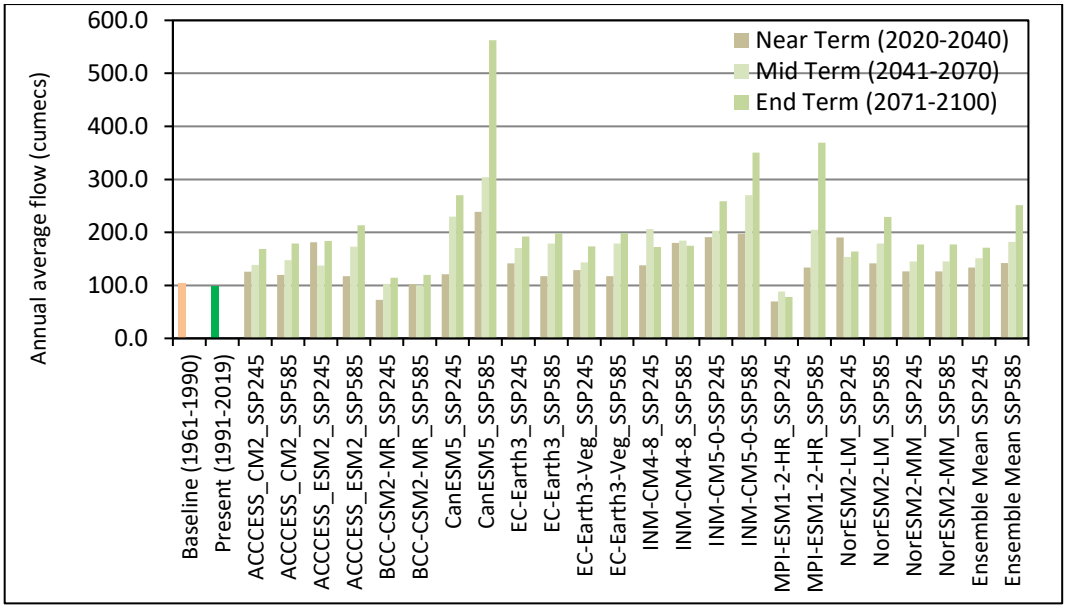

Figure 5.162: Comparison of average annual stream flow at Salavad on R. Kalisindh

The ensemble mean average annual stream flow under SSP245 scenario is higher than the baseline period and varies between 133.33 cumecs during the near-term, 150.91 cumecs during the mid-term and 170.91 cumecs during the end-term. Similarly, the ensemble mean average annual stream flow is reasonably higher under SSP585 scenario and varies between 142.14 cumecs during the near-term, 182.21 cumecs during the mid-term and 251.35 cumecs during the end-term. It can be observed that the average annual stream flow projections are relatively much higher under the SSP585 scenario for all future time periods and difference is highest during the end-term. As compared to the baseline period, the average annual stream flow is projected to increase by 27.0%, 43.70% and 62.7% during near-term, mid-term and end-term respectively, under SSP245 scenario. Similarly, under SSP585 scenario, average annual stream flow is projected to further increase during the near term (43.6%), mid-term (84.1%) and end-term (154.0%). The comparison of average annual stream flow under both future climate scenarios viz., SSP245 and SSP585 at Aklera on River Parwan is given in Figure 5.163. The mean flow in baseline and present periods was 69.55 cumecs and 68.57 cumecs respectively. It can be observed that as compared to the baseline period, the mean flows are projected to increase under both scenarios, for all the GCMs except for MPI-ESM21-2-HR under SSP245 scenario. The ensemble mean

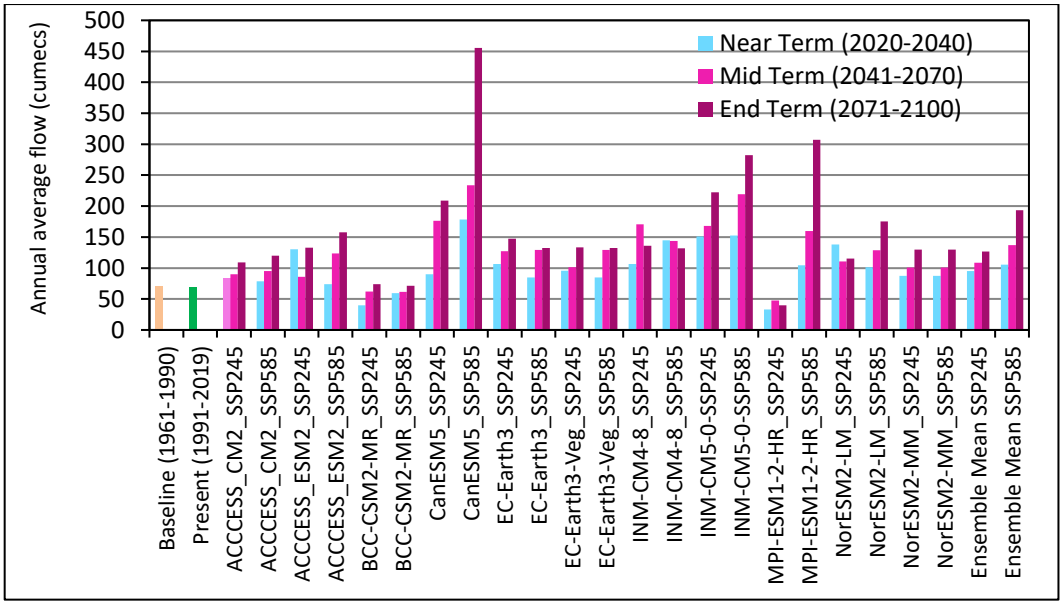

Figure 5.163: Comparison of average annual stream flow at Aklera on R. Parwan

average annual stream flow under SSP245 scenario is higher than the baseline period and varies between 95.16 cumecs during the near-term, 108.61 cumecs during the mid-term and 126.89 cumecs during the end-term. Similarly, the ensemble mean average annual stream flow is reasonably higher under SSP585 scenario and varies between 105.58 cumecs during the near-term, 136.97 cumecs during the mid-term and 193.52 cumecs during the end-term.

It can be observed that the average annual stream flow projections are relatively much higher under the SSP585 scenario for all future time periods and difference is highest during the end-term. As compared to the baseline period, the average annual stream flow is projected to increase by 36.8%, 56.2% and 82.4% during near-term, mid-term and end-term respectively, under SSP245 scenario. Similarly, under SSP585 scenario, the average annual stream flow is projected to further increase during the near term (54.0%), mid-term (99.8%) and end-term (182.2%).

5.6.4 Impact of Climate Change on High Flows

The climate change impacts may also include changes in the high flows due to the increase in the frequency of the extreme weather events. The high intensity rainfall events including the extreme, very heavy and heavy rainfall events has the potential to generate much larger high flows as compared to the baseline period.

The high flows are determined by the 5% and 10% dependable flows, which have been derived from the dependable flow analysis. The dependable flow analysis has been carried out for the baseline, present and all future time periods based on the SWAT simulated flows derived by driving the SWAT model with the bias-corrected future weather data. Thereafter the ensemble mean from the GCMs have been computed and compared with the dependable flow during the baseline and present periods.

The comparison of the high flow represented by the 5% dependable flows at A. B. Road Crossing on River Parvati is given in Figure 5.164. As compared to the baseline period, the high flows have increased substantially in the present period

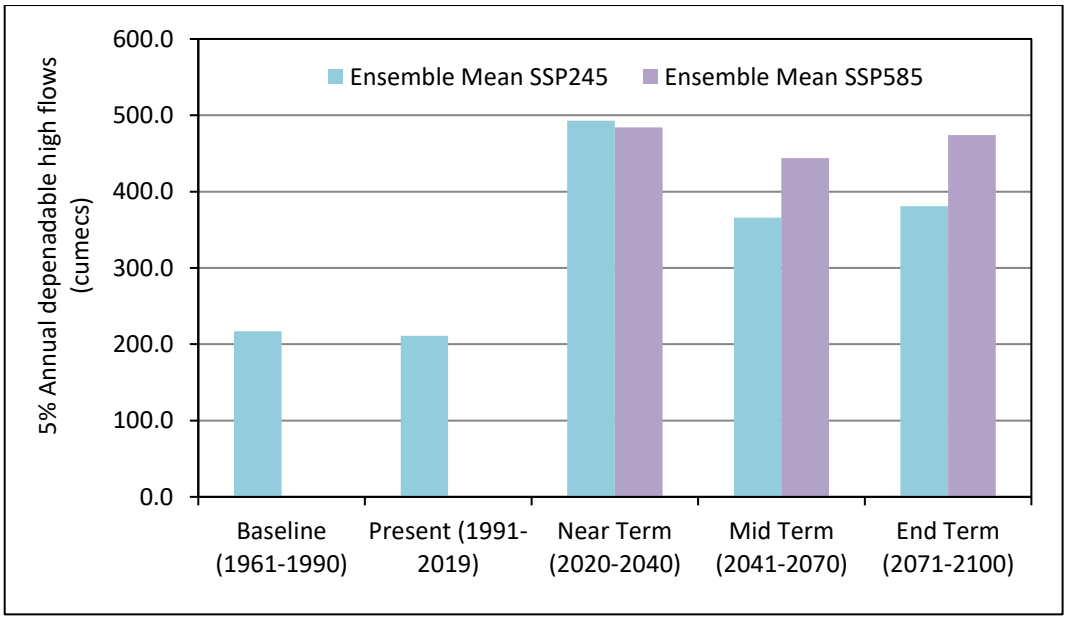

Figure 5.164: Comparison of 5% dependable flows at A.B. Road Crossing on R. Parvati

whereas it is projected to increase considerably during all future time periods under both future climate scenarios. The 5% dependable flow during the baseline period was 217.04 cumecs which is projected to increase substantially in the near-term to 493.83 cumecs under SSP245 scenario and 484.36 cumecs under SSP585 scenario on pro-rata basis for 30-year period. It is projected to decrease thereafter to 366.25 cumecs and 380.66 cumecs under SSP245 scenario during the mid-term and end-term respectively, whereas it is projected to again increase to 443.55 cumecs and 474.34 cumecs under SSP585 scenario during the mid-term and end-term respectively.

The comparison of the high flow represented by the 5% dependable flows at Tal on River Chambal is given in Figure 5.165. The high flows have decreased marginally in the present period as compared to the baseline period, whereas it is projected to increase marginally during the near-term under both scenarios but thereafter increase marginally during the mid-term and again vary marginally during the end-term under both future climate scenarios. The 5% dependable flow during the baseline period was 228.56 cumecs which is projected to increase in the near-term to 294.54 cumecs under SSP245 scenario and 301.38 cumecs under SSP585 scenario on pro-rata basis for 30-year period. It is projected to increase further to 241.72 cumecs and 231.24 cumecs under SSP245 scenario during the mid-term and end-term respectively, whereas it is projected to again increase to 288.24 cumecs and 315.16 cumecs under SSP585 scenario during the mid-term and end-term respectively.

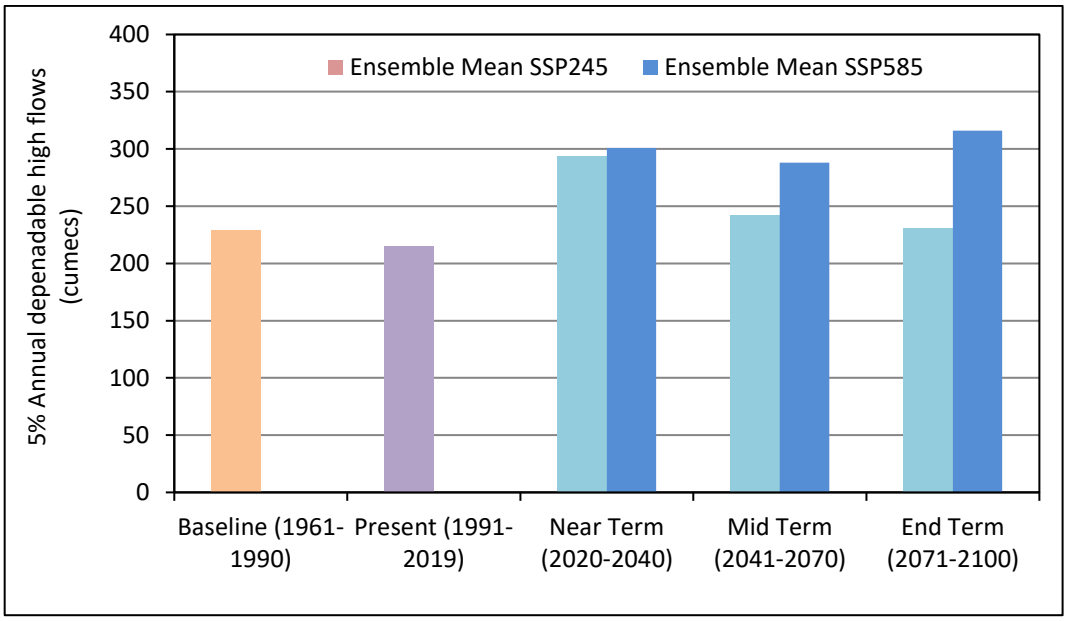

Figure 5.165: Comparison of 5% dependable flows at Tal on R. Chambal

The comparison of the high flow represented by the 5% dependable flows at Ujjain on River Shipra is given in Figure 5.166. As compared to the baseline period, the high flows have increased considerably in the present period whereas it is projected to vary considerably during all future time periods under both future climate scenarios.

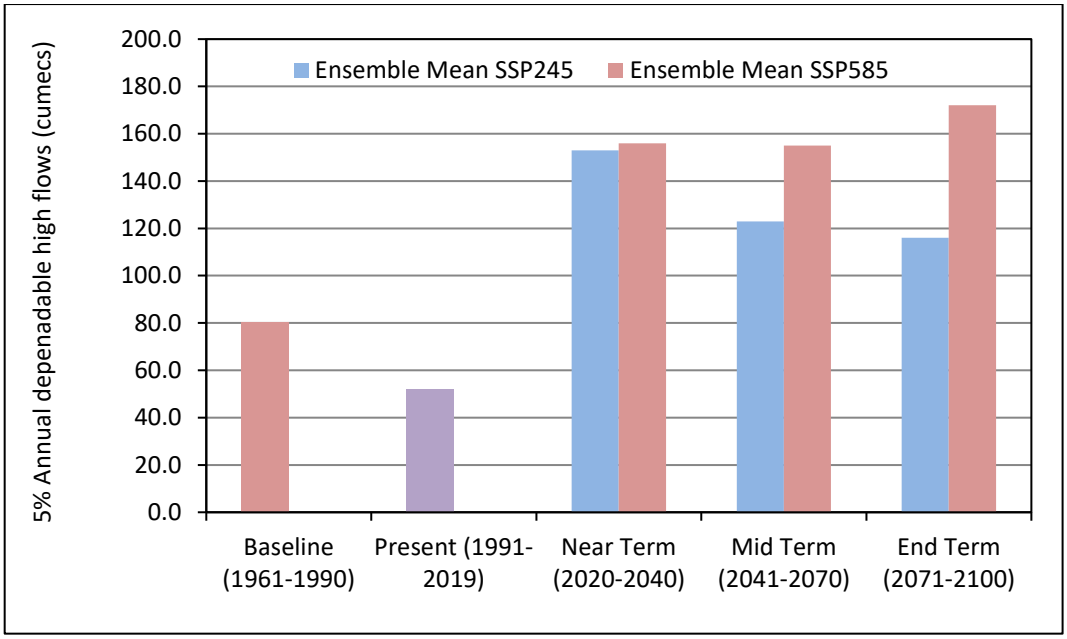

Figure 5.166: Comparison of 5% dependable flows at Ujjain on R. Shipra

The 5% dependable flow during the baseline period was 80.36 cumecs which is projected to increase in the near-term to 153.08 cumecs under SSP245 scenario and 156.51 cumecs under SSP585 scenario on pro-rata basis for 30-year period. It is projected to further vary between 122.80 cumecs and 116.33 cumecs under SSP245 scenario during the mid-term and end-term respectively, whereas it is projected to again vary between 155.03 cumecs and 172.46 cumecs under SSP585 scenario during the mid-term and end-term respectively.

The comparison of the high flow represented by the 5% dependable flows at Sarangpur on River Kalisindh is given in Figure 5.167. As compared to the baseline period, the high flows have decreased marginally in the present period whereas it is projected to increase considerably during all future time periods under both future climate scenarios. The 5% dependable flow during the baseline period was 103.24 cumecs which is projected to increase in the near-term to 211.08 cumecs under SSP245 scenario and 213.32 cumecs under SSP585 scenario on pro-rata basis for 30-year period. It is projected to further vary between 162.72 cumecs and 157.3 cumecs under SSP245 scenario during the mid-term and end-term respectively, whereas it is projected to vary between 157.30 cumecs and201.37 cumecs under SSP585 scenario during the mid-term and end-term respectively.

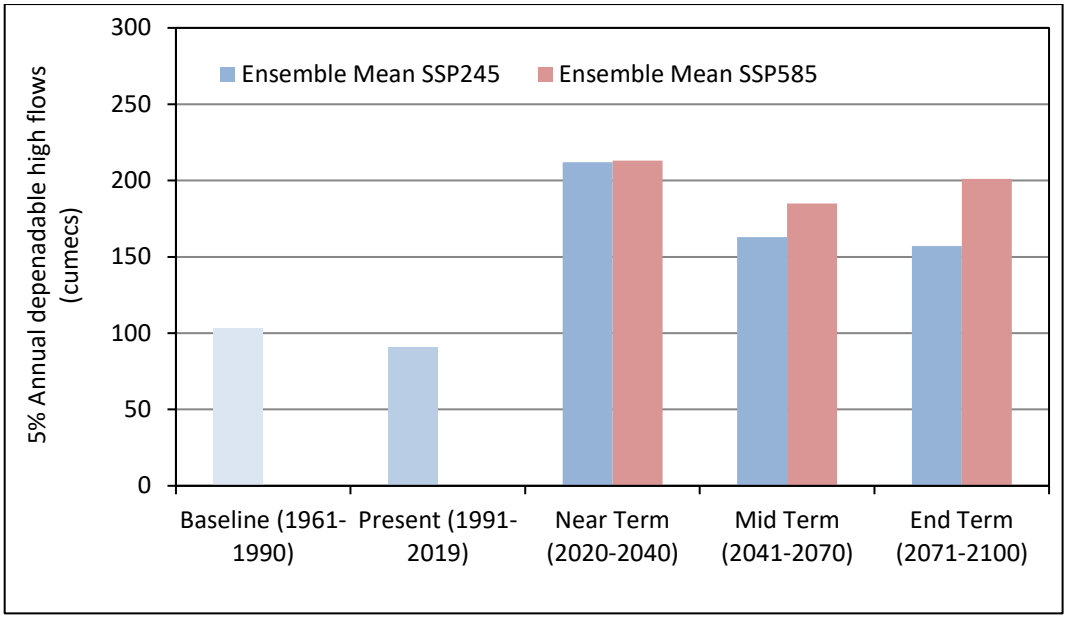

Figure 5.167: Comparison of 5% dependable flows at Sarangpur on R. Kalisindh

The comparison of the high flow represented by the 5% dependable flows at Mahidpur on River Shipra is given in Figure 5.168. As compared to the baseline period, the high flows have increased marginally in the present period whereas it is projected to increase considerably during all future time periods under both future climate scenarios. The 5% dependable flow during the baseline period was 166.54 cumecs which is projected to increase in the near-term to 328.89 cumecs under SSP245 scenario and 324.21 cumecs under SSP585 scenario on pro-rata basis for 30-year period. It is projected to decrease thereafter to 264.89 cumecs and 251.31 cumecs under SSP245 scenario during the mid-term and end-term respectively, whereas it is projected to again vary between 308.29 cumecs and 339.52 cumecs under SSP585 scenario during the mid-term and end-term respectively.

The comparison of the high flow represented by the 5% dependable flows at Salavad on River Kalisindh is given in Figure 5.169. As compared to the baseline period, the high flows are projected to decrease marginally in the present period whereas it is projected to increase considerably during all future time periods under both future climate scenarios. The 5% dependable flow during the baseline period was 244.61 cumecs which is projected to increase in the near-term to 520.05 cumecs under SSP245 scenario and 523.01 cumecs under SSP585 scenario

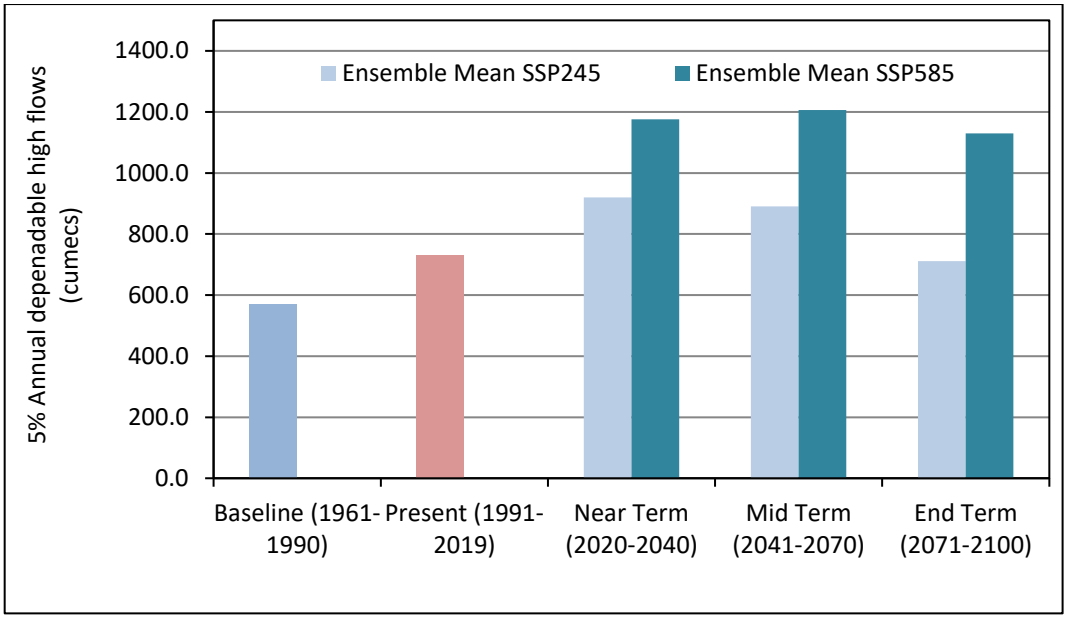

Figure 5.168: Comparison of 5% dependable flows at Mahidpur on R. Shipra

on pro-rata basis for 30-year period. It is projected to decrease further to 399.40 cumecs and 395.09 cumecs under SSP245 scenario during the mid-term and end-term respectively, whereas it is projected to again vary between 476.61 cumecs and 515.59 cumecs under SSP585 scenario during the mid-term and end-term respectively.

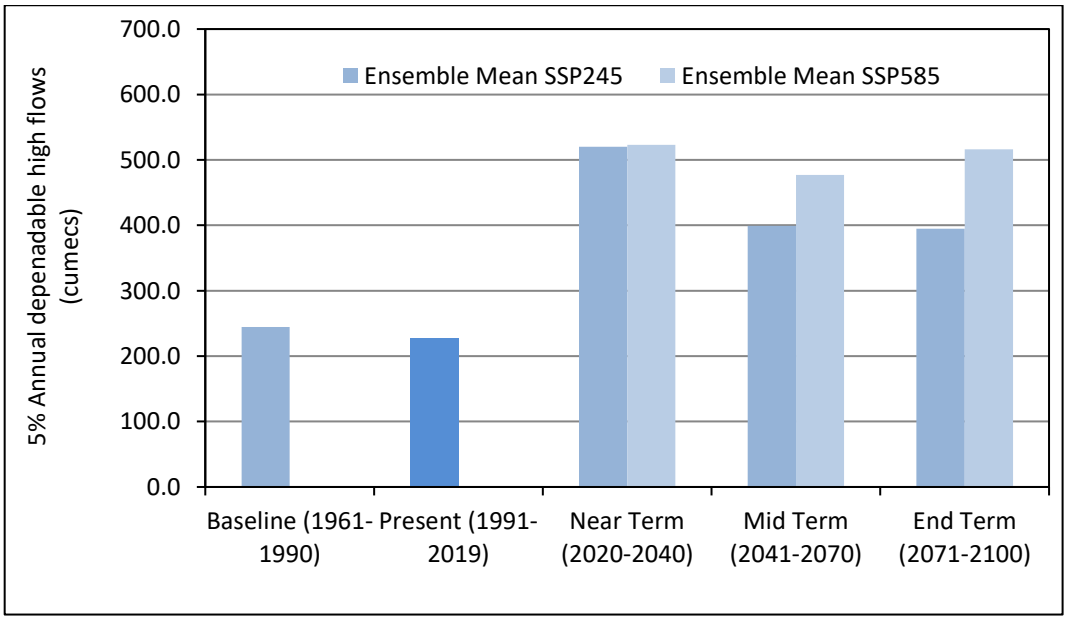

Figure 5.169: Comparison of low flows at Salavad on R. Kalisindh

The comparison of the high flow represented by 5% dependable flows at Aklera on River Parwan is given in Figure 5.170. As compared to the baseline period, the

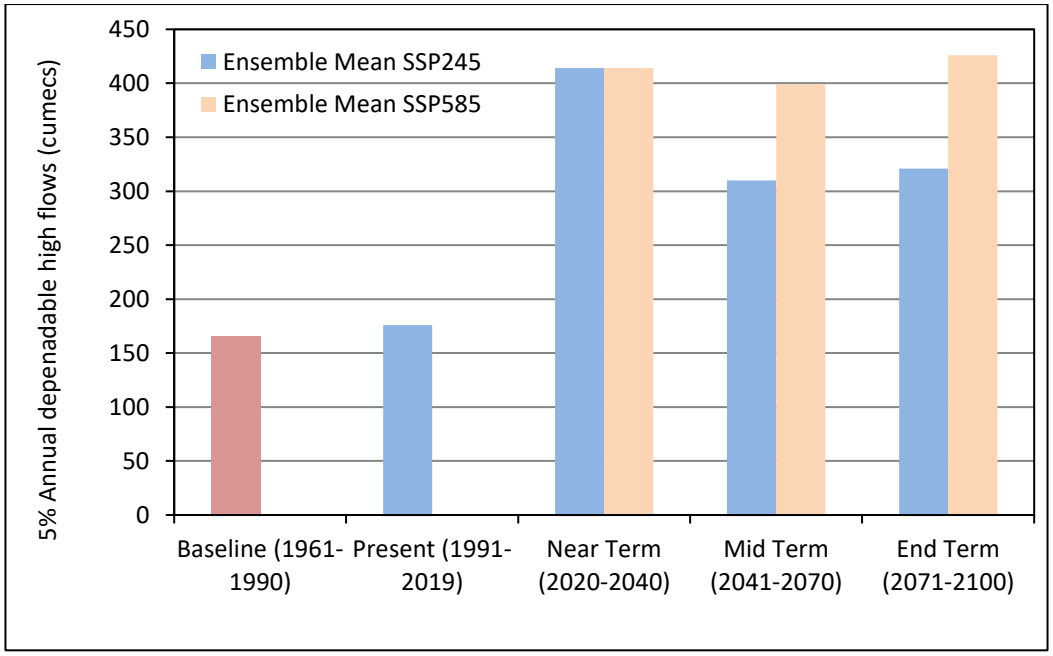

Figure 5.170: Comparison of high flows at Aklera on R. Parwan

high flows have increased marginally in the present period whereas it is projected to increase considerably during all future time periods under both future climate scenarios. The 5% dependable flow during the baseline period was 165.33 cumecs which is projected to increase in the near-term to 413.91 cumecs under SSP245 scenario and 414.24 cumecs under SSP585 scenario on pro-rata basis for 30-year period. Further it is projected to vary between to 310.24 cumecs and 321.03 cumecs under SSP245 scenario during the mid-term and end-term respectively, whereas it is projected to vary between 399.38 cumecs and 425.80 cumecs under SSP585 scenario during the mid-term and end-term respectively.

5.6.5 Impact of Climate Change on Low Flows

The climate change impacts may also include changes in the low flows. The increase in the drought events and the number of dry spells with possible increase in the duration of dry spell lengths will also impact the lean flows or the sustained water availability in the study area. The low flows have been determined based on the 90% and 95% dependable flow. The 50% dependable flows are indicative of the average water availability in the basin. The dependable flow analysis has been carried out for the baseline, present and all future time periods based on the SWAT simulated flows Thereafter the ensemble mean from the GCMs have been

computed and compared with the dependable flow during the baseline and present periods.

The comparison of the low flows represented by the 90% dependable flows at A. B. Road Crossing on River Parvati is given in Figure 5.171. As compared to the baseline period, the low flows have increased marginally during the present period whereas it is projected to again increase marginally only during the near-term and thereafter increase considerably during the mid-term and end-term under both future climate scenarios. The 90% dependable flow during the baseline period was 34.62 cumecs which is projected to decrease in the near-term to 42.87 cumecs

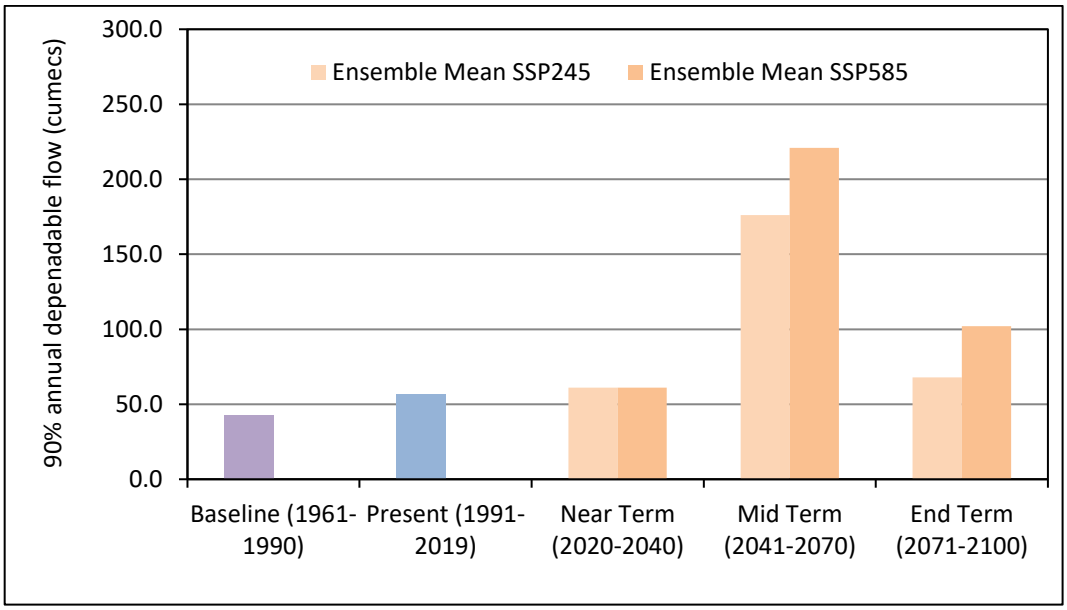

Figure 5.171: Comparison of low flows at A.B. Road on R. Parvati

under SSP245 scenario and 45.63 cumecs under SSP585 scenario on pro-rata basis for 30-year period. It is projected to increase further to 170.65 cumecs and 51.51 cumecs under SSP245 scenario during the mid-term and end-term respectively, whereas it is projected to again increase to 214.88 cumecs and 79.64 cumecs during the mid-term and end-term respectively under SSP585 scenario. It can be observed that the projected low flows are maximum during the mid-term as compared to the baseline, present and all future time periods.

The comparison of the low flows represented by the 90% dependable flows at Tal on River Chambal is given in Figure 5.172. As compared to the baseline period,

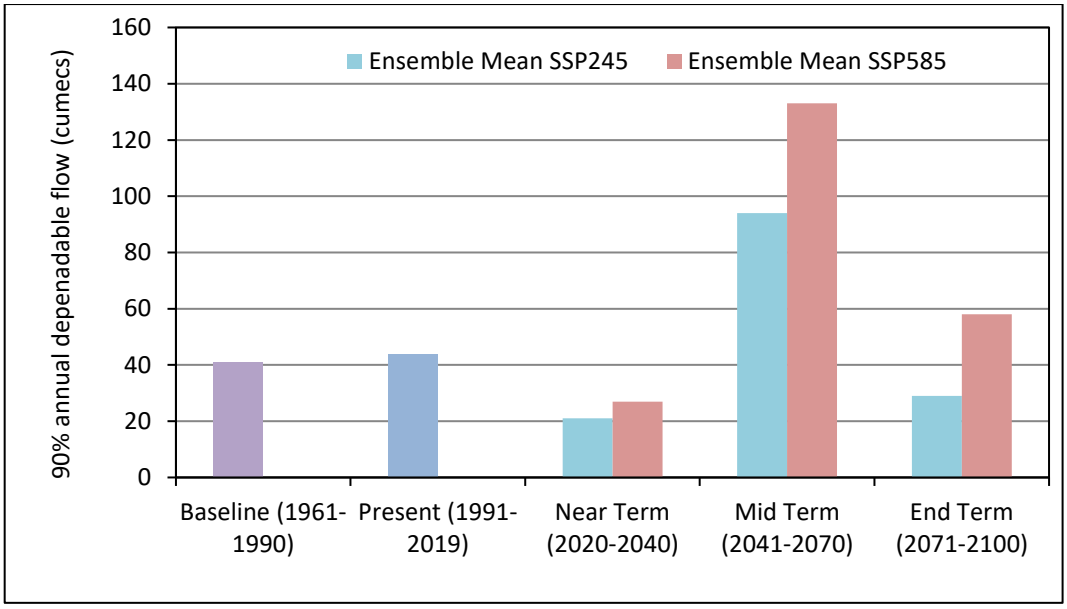

Figure 5.172: Comparison of low flows at Tal on R. Chambal

the low flows have increased marginally during the present period whereas it is projected to decrease substantially during the near-term and thereafter increase considerably during the mid-term and end-term under both future climate scenarios.

The 90% dependable flow during the baseline period was 40.62 cumecs which is projected to decrease in the near-term to 20.55 cumecs under SSP245 scenario and 27.33 cumecs under SSP585 scenario on pro-rata basis for 30-year period. It is projected to increase further to 94.22 cumecs and then decrease to 29.17 cumecs under SSP245 scenario during the mid-term and end-term respectively, whereas it is projected to again increase to 132.72 cumecs and then decrease to 58.18 cumecs during the mid-term and end-term respectively under SSP585 scenario. It can be observed that the low flows are projected to be maximum during the mid-term as compared to the baseline, present and all future time periods.

The comparison of the low flows represented by the 90% dependable flows at Ujjain on River Shipra is given in Figure 5.173. As compared to the baseline period, the low flows have decreased marginally during the present period whereas it is projected to again increase marginally during the near-term and thereafter increase considerably during the mid-term and end-term under both future climate scenarios. The 90% dependable flow during the baseline period was

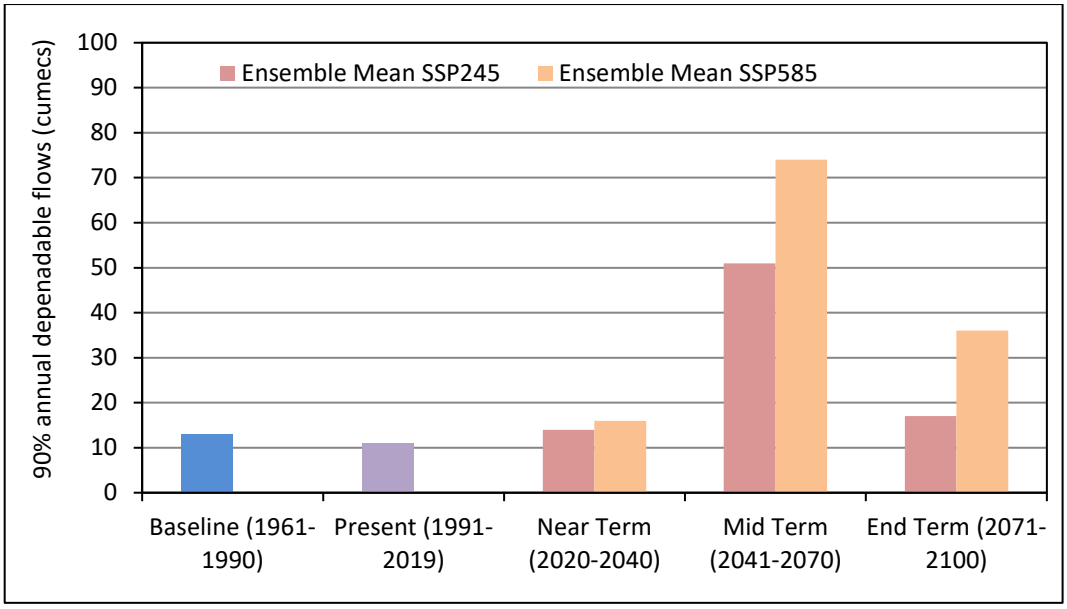

Figure 5.173: Comparison of low flows at Ujjain on R. Shipra

12.57 cumecs which is projected to decrease in the near-term to 13.73 cumecs under SSP245 scenario and 15.86 cumecs under SSP585 scenario on pro-rata basis for 30-year period. It is projected to increase further to 50.89 cumecs and thereafter decrease to 17.41 cumecs under SSP245 scenario during the mid-term and end-term respectively, whereas it is projected to again increase to 74.40 cumecs and thereafter decrease to 35.66 cumecs during the mid-term and end-term respectively under SSP585 scenario. It can be observed that the low flows are projected to be maximum during the mid-term as compared to the baseline, present and all future time periods.

The comparison of the low flows represented by the 90% dependable flows at Sarangpur on River Kalisindh is given in Figure 5.174. As compared to the baseline period, the low flows have decreased marginally during the present period whereas it is projected to again decrease marginally during the near-term and thereafter increase considerably during the mid-term and end-term under both future climate scenarios. The 90% dependable flow during the baseline period was 26.53 cumecs which is projected to increase marginally in the near-term to 32.25 cumecs under SSP245 scenario and 30.36 cumecs under SSP585 scenario on pro-rata basis for 30-year period. It is projected to increase further to 77.73 cumecs and thereafter decrease to 34.23 cumecs during the mid-term and end-term respectively under SSP245 scenario whereas it is projected to increase to 96.12

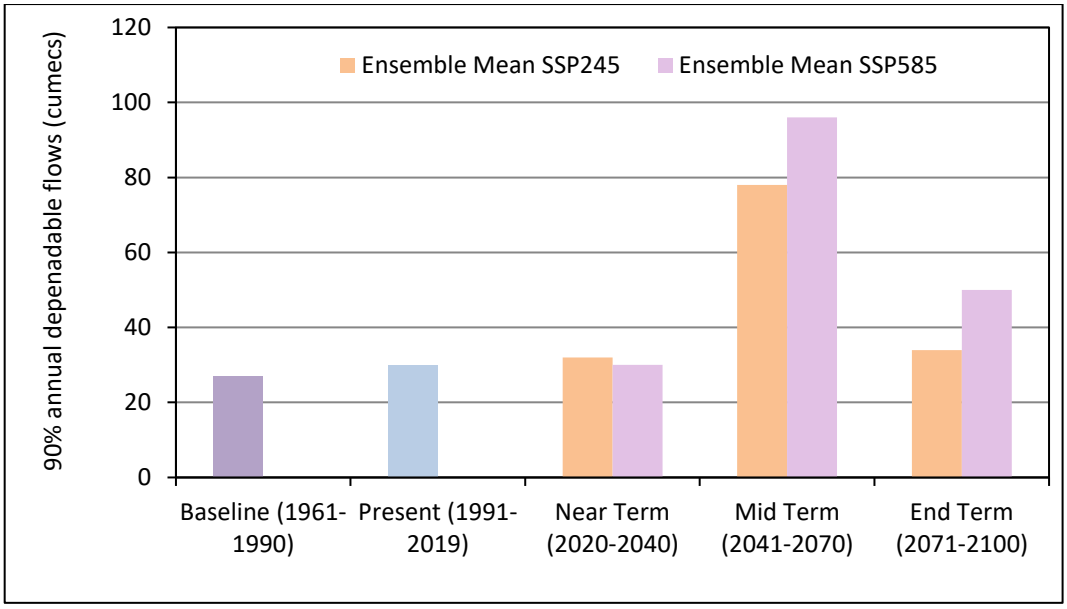

Figure 5.174: Comparison of low flows at Sarangpur on R. Kalisindh

cumecs and thereafter decrease to 50.13 cumecs during the mid-term and end-term respectively under SSP585 scenario. It can be observed that the low flows are projected to be maximum during the mid-term as compared to the baseline, present and all future time periods.

The comparison of the low flows represented by the 90% dependable flows at Mahidpur on River Shipra is given in Figure 5.175. As compared to the baseline period, the low flows have decreased marginally during the present period whereas it is projected to again decrease marginally during the near-term and thereafter increase considerably during the mid-term and end-term under both future climate scenarios. The 90% dependable flow during the baseline period was 32.62 cumecs which is projected to decrease marginally in the near-term to 29.16 cumecs under SSP245 scenario and increase marginally to 34.88 cumecs under SSP585 scenario on pro-rata basis for 30-year period. It is projected to increase further to 109.51 cumecs and thereafter decrease to 36.83 cumecs during the mid-term and end-term respectively under SSP245 scenario whereas it is projected to increase to 147.50 cumecs and thereafter decrease to 68.19 cumecs during the mid-term and end-term respectively, under SSP585 scenario. It can be observed that the low flows are projected to be maximum during the mid-term as compared to the baseline, present and all future time periods.

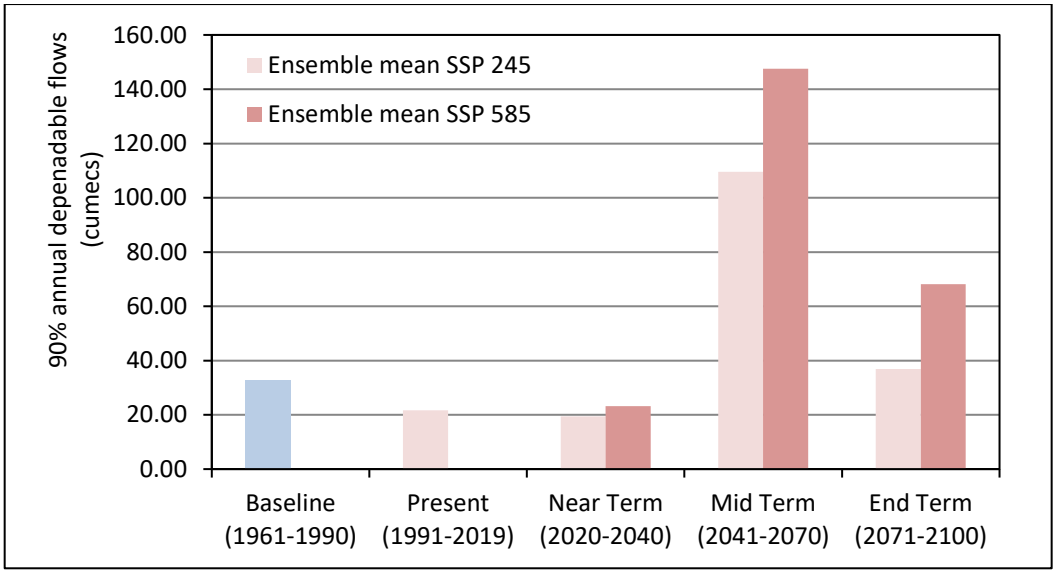

Figure 5.175: Comparison of low flows at Mahidpur on R. Shipra

The comparison of the low flows represented by the 90% dependable flows at Salavad on River Kalisindh is given in Figure 5.176. As compared to the baseline period, the low flows have decreased marginally during the present period whereas it is projected to again decrease marginally during the near-term and thereafter increase considerably during the mid-term and end-term under both future climate scenarios. The 90% dependable flow during the baseline period was 53.01 cumecs which is projected to increase marginally in the near-term to 56.51 cumecs under SSP245 scenario and 59.36 cumecs under SSP585 scenario on pro-rata basis for 30-year period. It is projected to increase further to 178.21 cumecs

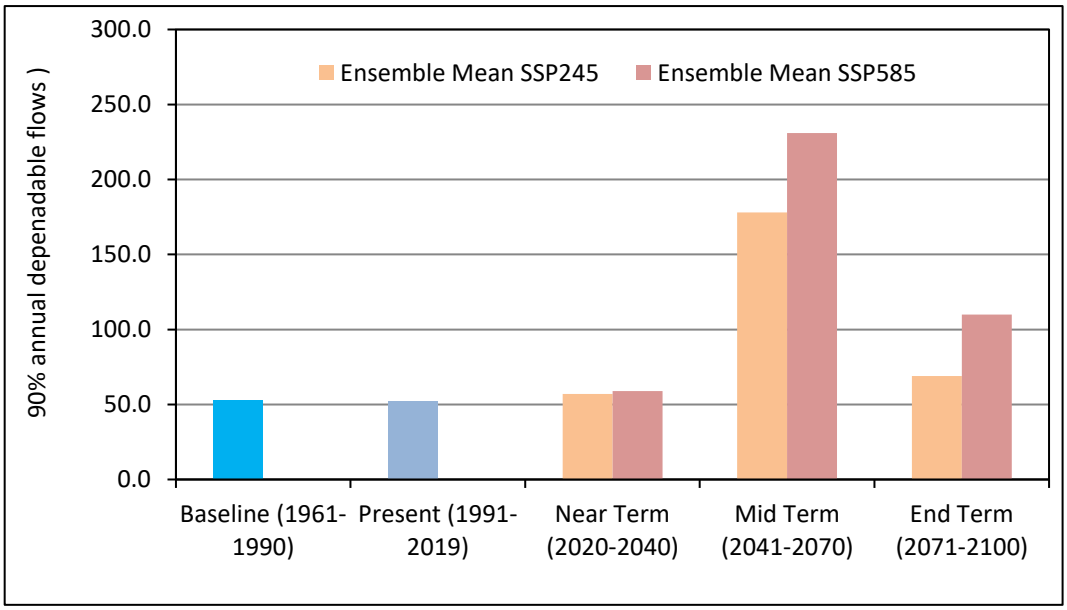

Figure 5.176: Comparison of low flows at Salavad on R. Kalisindh

and thereafter decrease to 68.77 cumecs during the mid-term and end-term respectively under SSP245 scenario, whereas it is projected to increase to 231.39 cumecs and thereafter decrease to 110.47 cumecs during the mid-term and end-term respectively under SSP585 scenario. It can be observed that the low flows are projected to be maximum during the mid-term as compared to the baseline, present and all future time periods.

The comparison of the low flows represented by the 90% dependable flows at Aklera on River Parwan is given in Figure 5.177. As compared to the baseline period, the low flows have increased marginally during the present period whereas it is projected to again decrease marginally during the near-term and thereafter increase considerably during the mid-term and end-term under both future climate scenarios. The 90% dependable flow during the baseline period was 25.10 cumecs which is projected to decrease marginally in the near-term to 32.16 cumecs under SSP245 scenario and 36.90 cumecs under SSP585 scenario on pro-rata basis for 30-year period. It is projected to increase further to 131.15 cumecs and thereafter decrease to 40.18 cumecs during the mid-term and end-term respectively under SSP245 scenario, whereas it is projected to increase to 180.48 cumecs and thereafter decrease to 79.02 cumecs during the mid-term and end-term respectively under SSP585 scenario. It can be observed that the low flows are projected to be maximum during the mid-term as compared to the baseline, present and other future time periods.

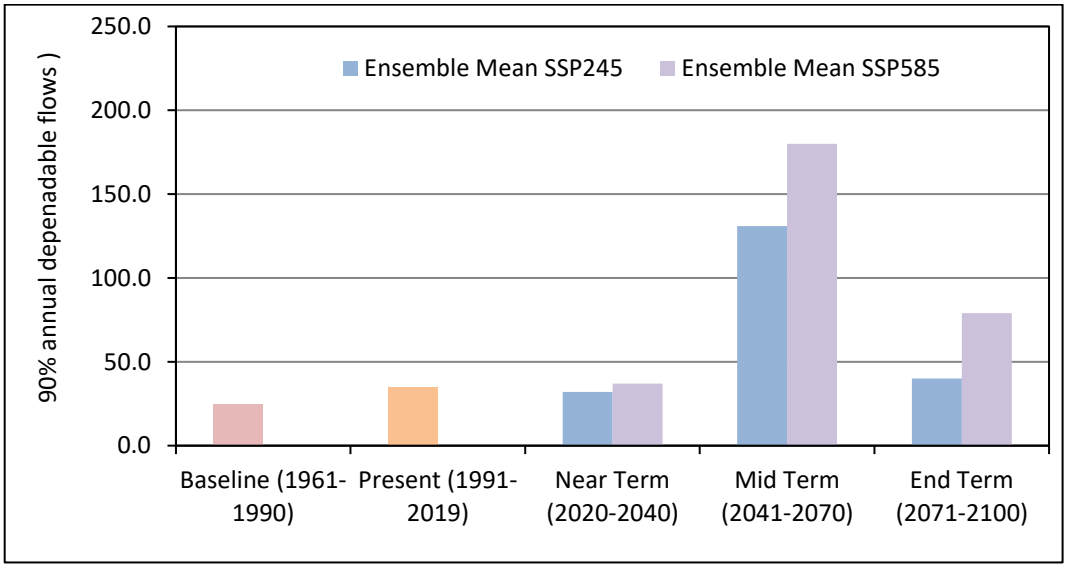

Figure 5.177: Comparison of low flows at Aklera on R. Parwan

5.7 Surface Water Drought Characteristics

The surface water drought characteristics for the baseline and present periods along with that for the future time periods have been evaluated based on the SWAT simulated runoff at the various gauging sites located in the study area. The surface water drought characteristics have been evaluated using the SDI based on the SWAT model outputs derived by driving the model with historical and future climate data during various time periods under consideration. The hydrological drought characteristics including the number of events, have severity have been evaluated for various time periods

The comparison of the moderate hydrological drought events by various GCMs under SSP245 scenario at Tal on River Chambal is given in Figure 5.178. The moderate hydrological drought events have increased in the present term (29) from 27 events during the baseline period. The number of hydrological drought events is projected to decrease in the near-term with most of the GCMs except for INM-CM5-0 (28), but generally more than 10 moderate hydrological drought events have been projected by most of the GCMs under SSP245 scenario.

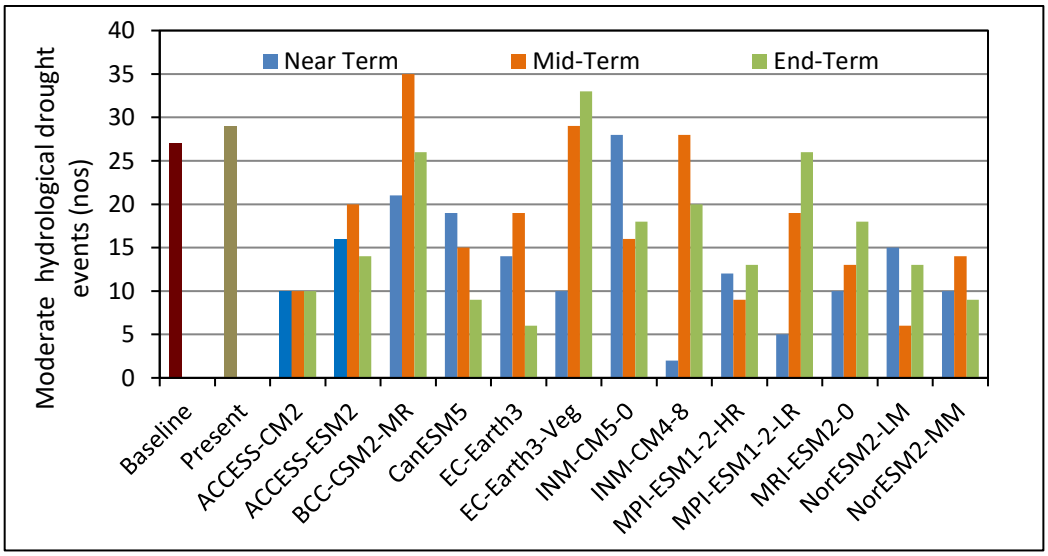

Figure 5.178: Moderate hydrological drought events at Tal on R. Chambal under SSP245 scenario

However, during the mid-term, considerable variability is observed wherein most of GCMs project lower than baseline period hydrological drought events but few GCMs viz., BCC-CSM-MR (35), EC-Earth3-Veg (29) and INM-CM4-8 (28) project higher hydrological drought events during the mid-term. Similarly, during

the end-term, most of the GCMs project fewer number of hydrological drought events except for EC-Earth3-Veg (33).

The comparison of the moderate hydrological drought events by various GCMs under SSP585 scenario at Tal on River Chambal is given in Figure 5.179. The number of moderate hydrological drought events is projected to decrease in the near-term with most of the GCMs except for INM-CM5-0 (29). Generally, more

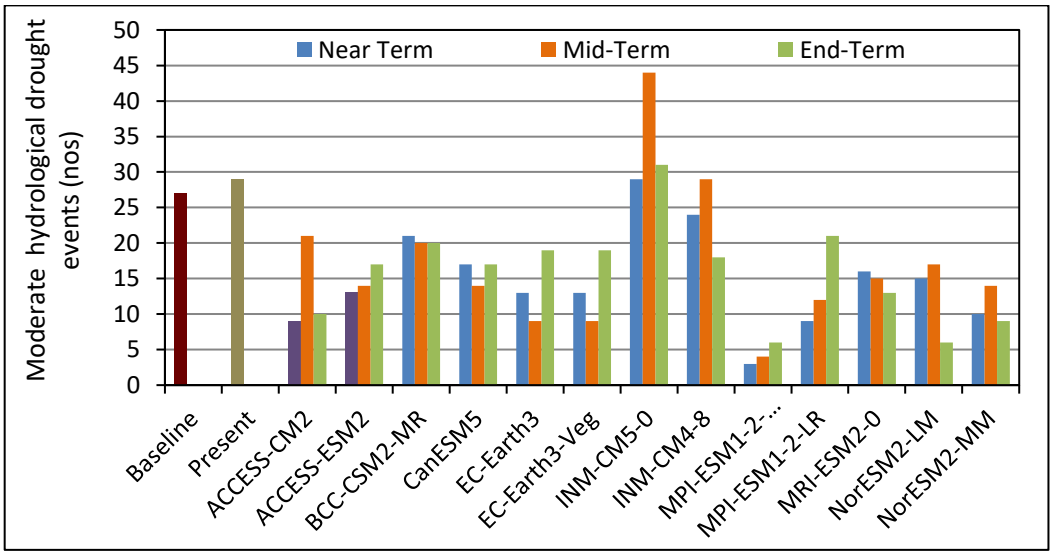

Figure 5.179: Moderate hydrological drought events at Tal on R. Chambal under SSP585 scenario

than 10 moderate hydrological drought events have been projected by most of the GCMs under SSP585 scenario. However, during the mid-term, considerable variability is observed wherein most of GCMs project lower than baseline period moderate hydrological drought events but few GCMs viz., INM-CM5-0 (44) and INM-CM4-8 (29) project higher moderate hydrological drought events during the mid-term. Similarly, during the end-term, most of the GCMs project fewer number of hydrological drought events except for INM-CM5-0 (31).

The comparison of the ensemble mean of the mild hydrological droughts at Tal on River Chambal during the future time periods with that during the baseline and present periods is given in Figure 5.180. It can be observed that the mild hydrological droughts are projected to decrease in all future time periods. The comparison of the ensemble mean of the moderate hydrological droughts at Tal on River Chambal during the future time periods with that during the baseline and present periods is given in Figure 5.181. It can be observed that the moderate

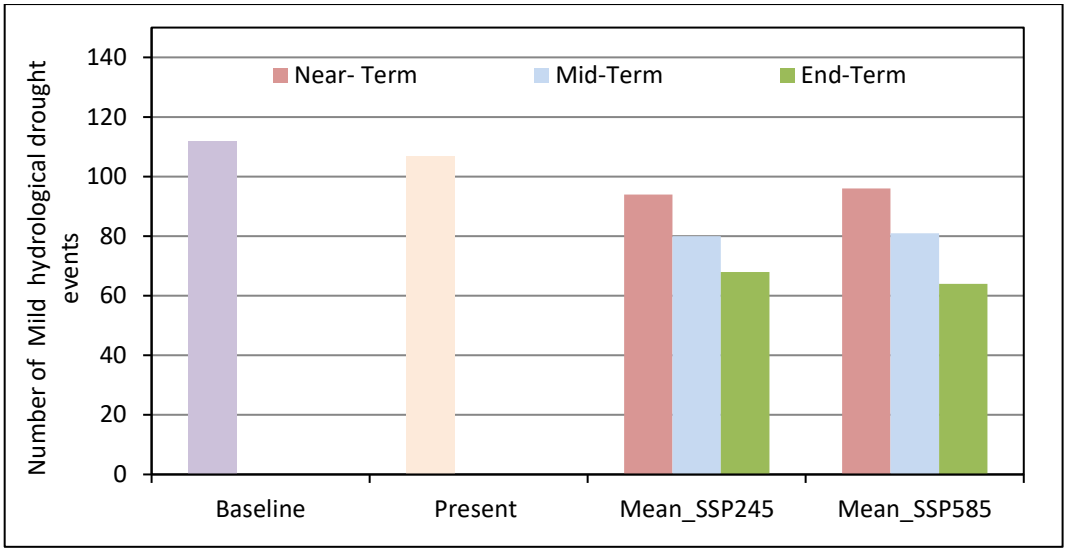

Figure 5.180: Comparison of Mild hydrological drought events at Tal on R. Chambal under future climate scenarios

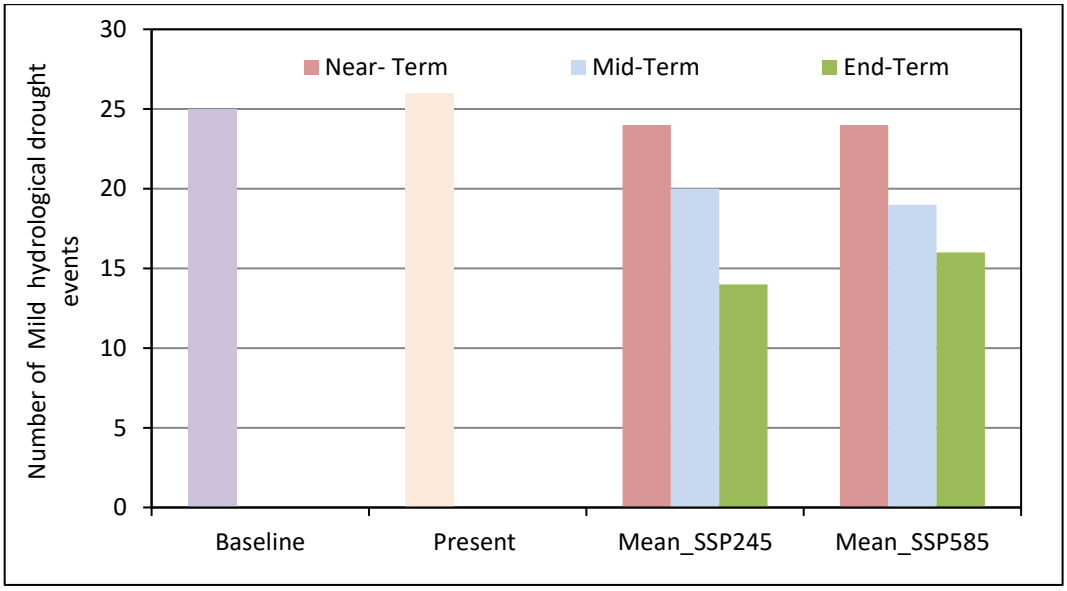

Figure 5.181: Comparison of Moderate hydrological drought events at Tal on R. Chambal under future climate scenarios

hydrological droughts are projected to decrease during all future time periods. The comparison of the ensemble mean of the severe hydrological droughts at Tal on River Chambal during the future time periods with that during the baseline and present periods is given in Figure 5.182. It can be observed that the severe hydrological droughts are also projected to decrease during all future time periods.

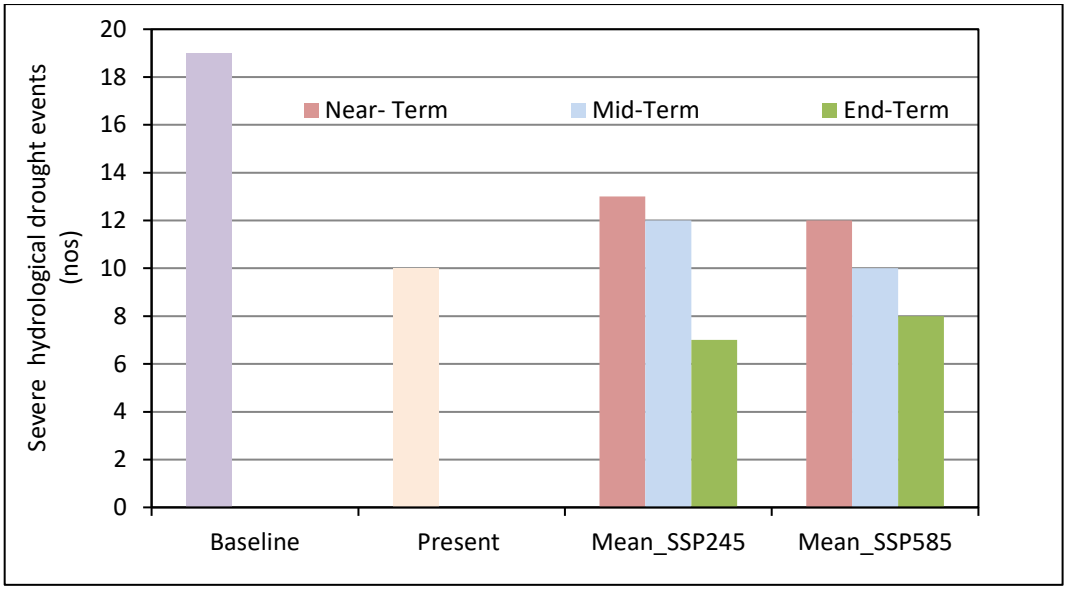

Figure 5.182: Comparison of Severe hydrological drought events at Tal on R. Chambal under future climate scenarios

The comparison of the ensemble mean of the extreme hydrological droughts at Tal on River Chambal during the future time periods with that during the baseline and present periods is given in Figure 5.183. It can be observed that the extreme hydrological droughts are also projected to increase during all future time periods, whereas the mild moderate and severe hydrological drought events were projected

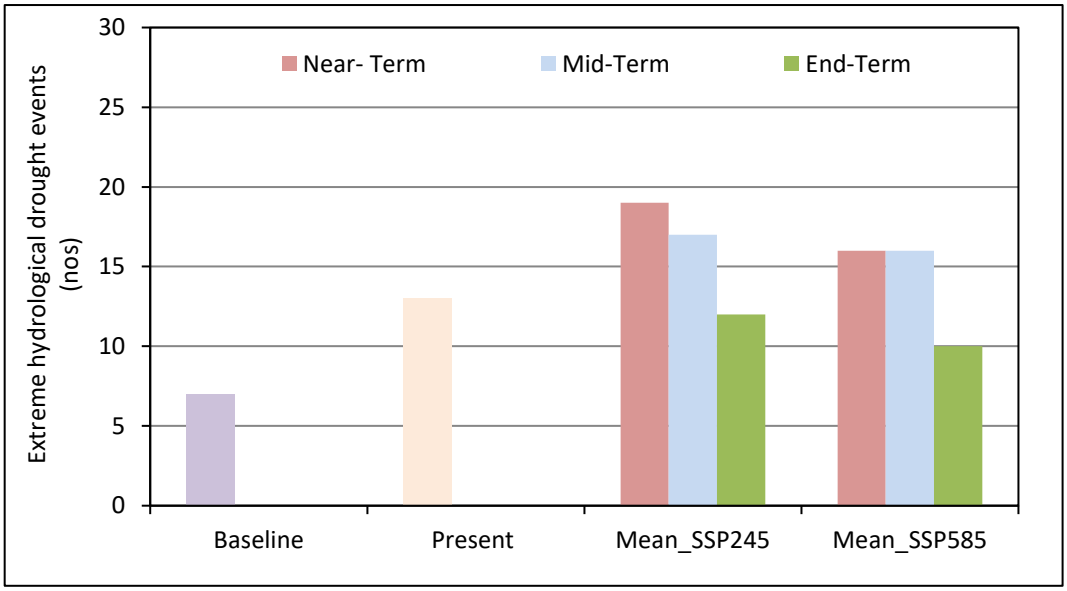

Figure 5.183: Comparison of Extreme hydrological drought events at Tal on R. Chambal under future climate scenarios

to decrease in future. The extreme hydrological drought events have increased in the present time (13) as compared to that during the baseline period (7). It is projected to increase further in the near-term on pro-rata basis for 30-year period

to 18 and 15 events under SSP245 and SSP585 scenario respectively. However, it is projected to decrease marginally during the mid-term to 17 and 15 events under SSP245 and SSP585 scenario respectively. Thereafter it is projected to decrease marginally during the end-term as compared to the mid-term to 12 and 10 events under SSP245 and SSP585 scenario respectively.

The comparison of the ensemble mean of the extreme and severe hydrological droughts at A. B. Road Crossing on River Parvati during the future time periods with that during the baseline and present periods is given in Figure 5.184 and Figure 5.185 respectively. The extreme hydrological drought events as compared to that during the baseline period (10) have decreased in the present period (7) but are projected to decrease to 15 and 13 events during the near-term, on pro-rata basis for 30-year period under SSP245 and SSP585 scenarios respectively; and thereafter increase to 14 events during the mid-term under both scenarios; and thereafter decrease marginally to 12 and 10 events during the end-term under SSP245 and SSP585 scenarios respectively. However, the severe hydrological drought events are projected to decrease substantially during all future time periods under both future climate scenarios.

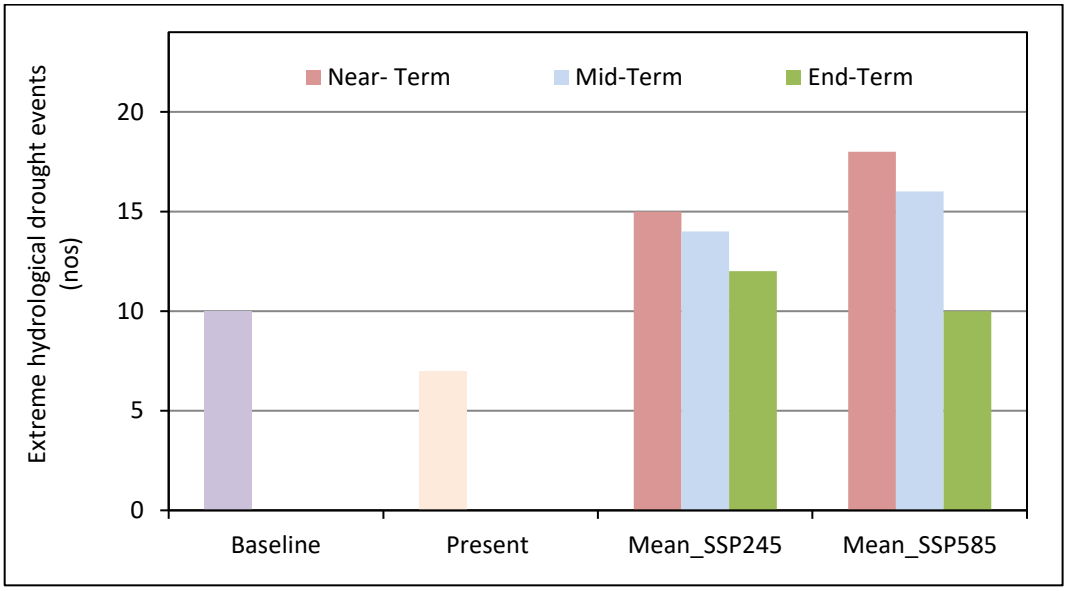

Figure 5.184: Comparison of extreme hydrological drought events at A. B. Road Crossing on R. Parvati under future climate scenarios

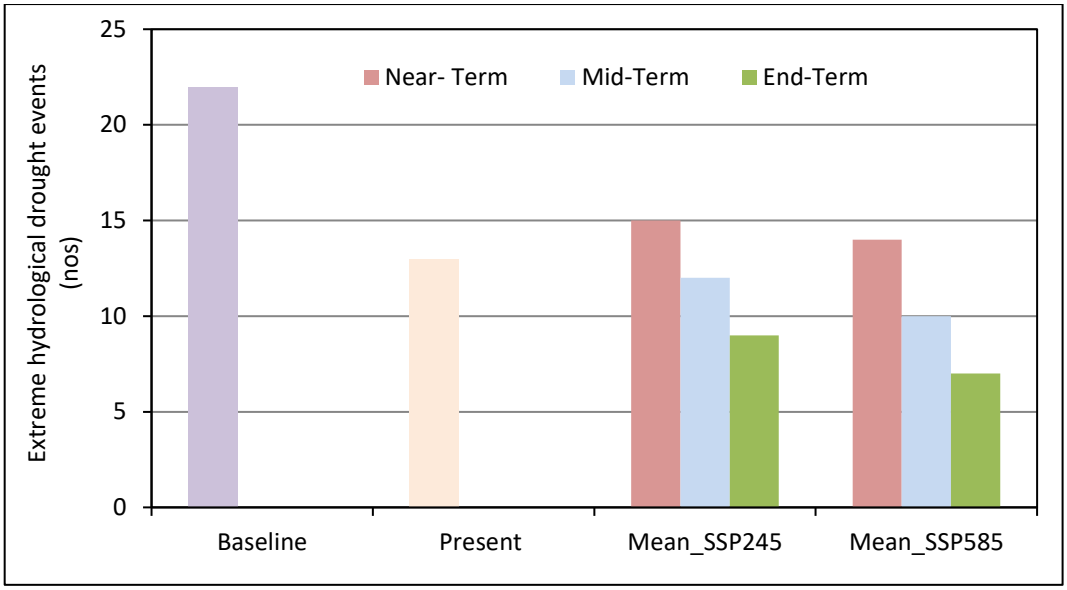

Figure 5.185: Comparison of severe hydrological drought events at A. B. Road Crossing on R. Parvati under future climate scenarios

The comparison of the ensemble mean of the extreme and severe hydrological droughts at Mahidpur on River Shipra during the future time periods with that during the baseline and present periods is given in Figure 5.186 and Figure 5.187 respectively. The extreme hydrological drought events as compared to that during the baseline period (8) have decreased in the present period (7) but are projected

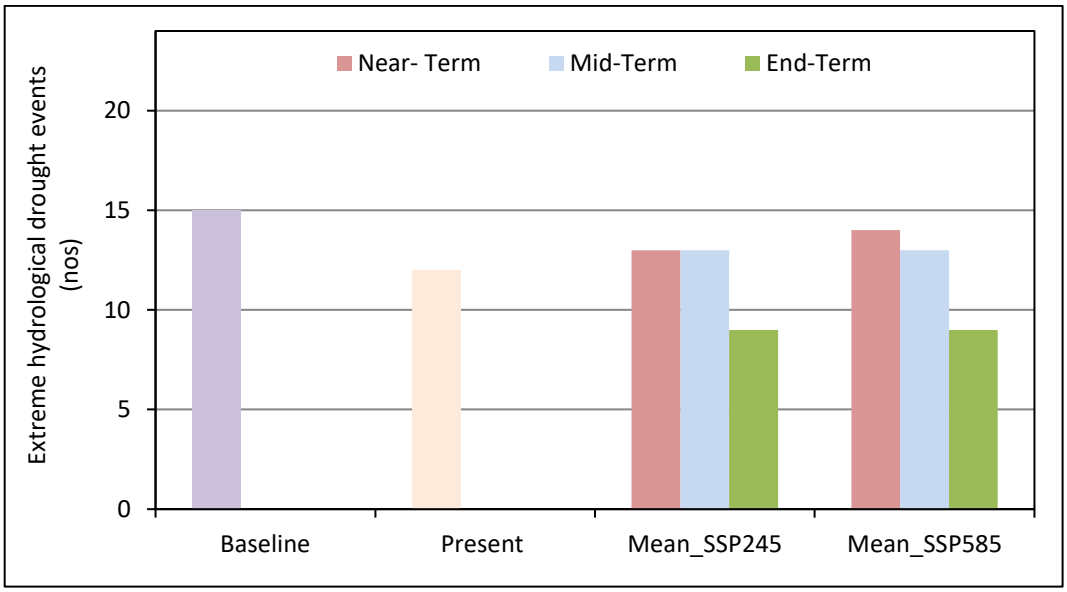

Figure 5.186: Comparison of extreme hydrological drought events at Mahidpur on R. Shipra under future climate scenarios

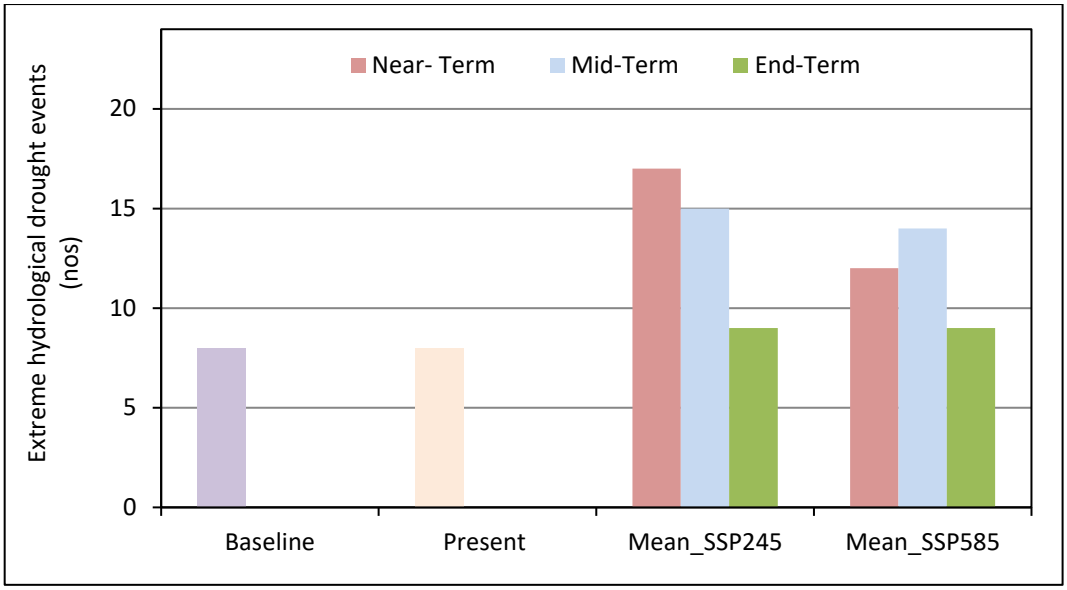

Figure 5.187: Comparison of severe hydrological drought events at Mahidpur on R. Shipra under future climate scenarios

to increase to 17 and 12 events during the near-term on pro-rata basis for 30-year period under SSP245 and SSP585 scenarios respectively; and thereafter increase to 14 events during the under SSP245 and SSP585 scenarios respectively; and to 9 and 10 events during the mid-term under SSP245 and SSP585 scenarios respectively; and to 9 events during the end-term under SSP245 and SSP585 scenarios respectively. However, in contrast the severe hydrological drought events are projected to increase substantially to 11 and 8 events during the near-term under SSP245 and SSP585 scenarios respectively; and to 15 and 14 events during the mid-term under SSP245 and SSP585 scenarios respectively; and to 9 events under SSP245 and SSP585 scenarios respectively.

The comparison of the ensemble mean of the extreme and severe hydrological droughts at Salavad on River Kalisindh during the future time periods with that during the baseline and present periods is given in Figure 5.188 and Figure 5.189 respectively. The extreme hydrological drought events as compared to that during the baseline period (12) have increased marginally in the present period (13) but are projected to increase to 21 and 20 events during the near-term on pro-rata basis for 30-year period under SSP245 and SSP585 scenarios respectively; and thereafter increase to 14 events during the under SSP245 and SSP585 scenarios respectively; and to 16 events during the mid-term under both future climate scenarios; and to 12 and 10 events during the end-term under SSP245 and SSP585

scenarios respectively. However, in contrast, the severe hydrological drought events are projected to decrease substantially to 8 and 11 events during the near-term on pro-rata basis for 30-year period under SSP245 and SSP585 scenarios respectively; and to 10 and 13 events during the mid-term under SSP245 and SSP585 scenarios respectively; and to 8 events under both future climate scenarios.

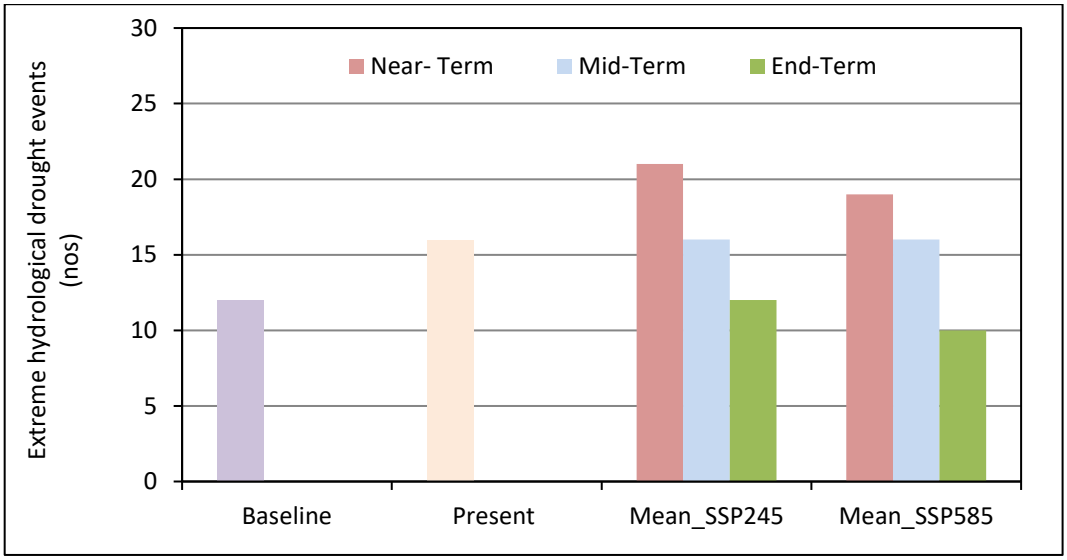

Figure 5.188: Comparison of extreme hydrological drought events at Salavad on R. Kalisindh under future climate scenarios

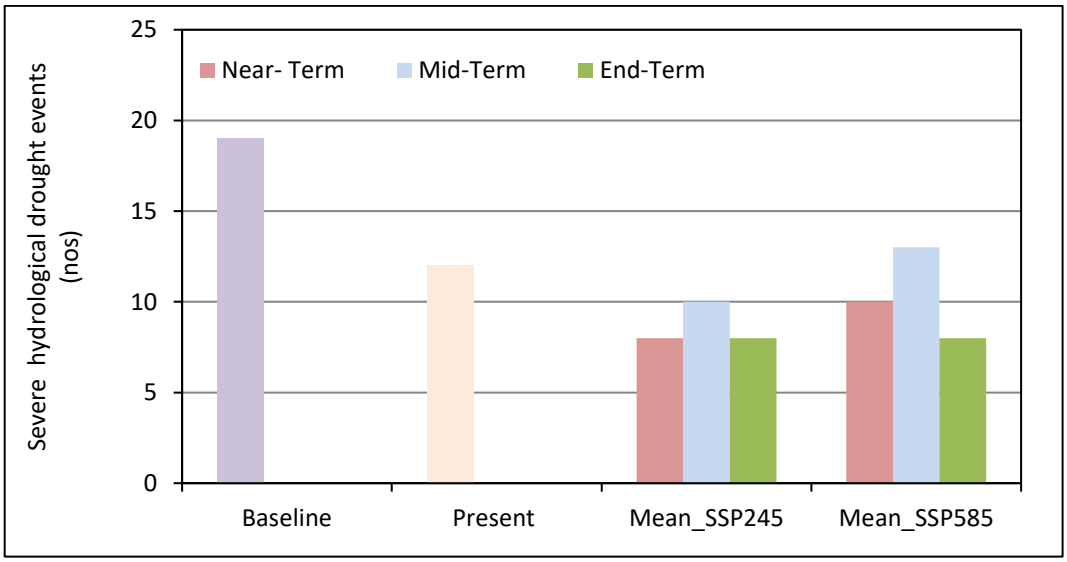

Figure 5.189: Comparison of severe hydrological drought events at Salavad on R. Kalisindh under future climate scenarios

The comparison of hydrological drought events of various severities viz., extreme, severe, moderate and mild at Tal on River Chambal during various time periods are given in Table 5.55 and Figure 5.190. It can be observed that the extreme hydrological events are projected to increase in the near-term, mid-term and end-term under both future climate scenarios whereas the severe and moderate hydrological events are projected to decrease in the near-term, mid-term and end-term under both future climate scenarios. Similarly, the mild drought events are also projected to decrease substantially during all future time periods under both future climate scenarios.

Table 5.55: Comparison of hydrological drought events at Tal on R. Chambal

Drought Events	BL	PR	NT_SSP245	NT_SSP585	MT_SSP245	MT_SSP585	ET_SSP245	ET_SSP585
Extreme	7	11	12.38	10.85	17.38	15.62	11.77	9.77
Severe	19	8	8.38	8.31	12.00	10.15	6.54	8.23
Moderate	27	29	13.23	14.77	17.92	17.08	16.54	15.85
Mild	112	89	62.46	64.00	80.00	80.92	67.69	64.15

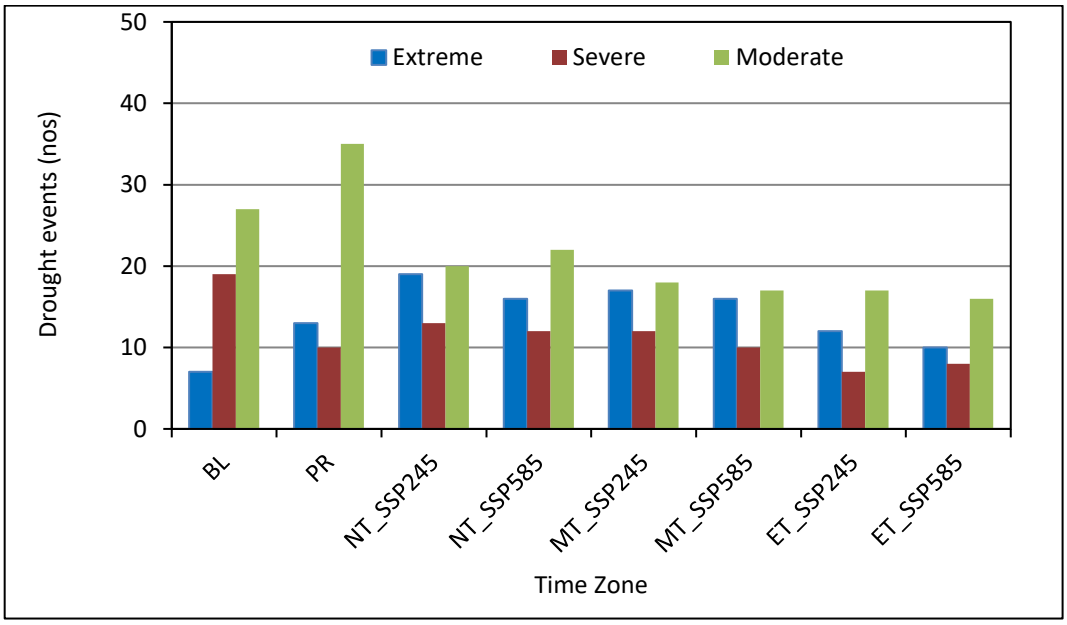

Figure 5.190: Comparison of all types of hydrological drought events at Tal on R. Chambal under future climate scenarios

The comparison of hydrological drought events viz., extreme, severe, moderate and mild at A. B. Road Crossing on River Parvati during various time periods are given in Table 5.56 and Figure 5.191. It is observed that extreme hydrological events are projected to increase in near-term, mid-term and end-term under both

future climate scenarios whereas the severe and moderate hydrological events are projected to decrease in near-term, mid-term and end-term under both future climate scenarios. Similarly, mild drought events are also projected to decrease considerably during all future time periods under both future climate scenarios.

Table 5.56: Comparison of hydrological drought events at A. B. Road Crossing on R. Parvati

Drought Events	BL	PR	NT_ SSP245	NT_ SSP585	MT_ SSP245	MT_ SSP585	ET_ SSP245	ET_ SSP585
Extreme	10	6	10.31	11.85	14.08	16.46	11.77	10.15
Severe	22	11	10.31	9.31	12.00	10.38	8.85	7.31
Moderat	27	31	14.23	16.54	23.85	19.46	13.69	19.77
Mild	103	107	72.23	68.00	88.85	87.15	72.54	65.54

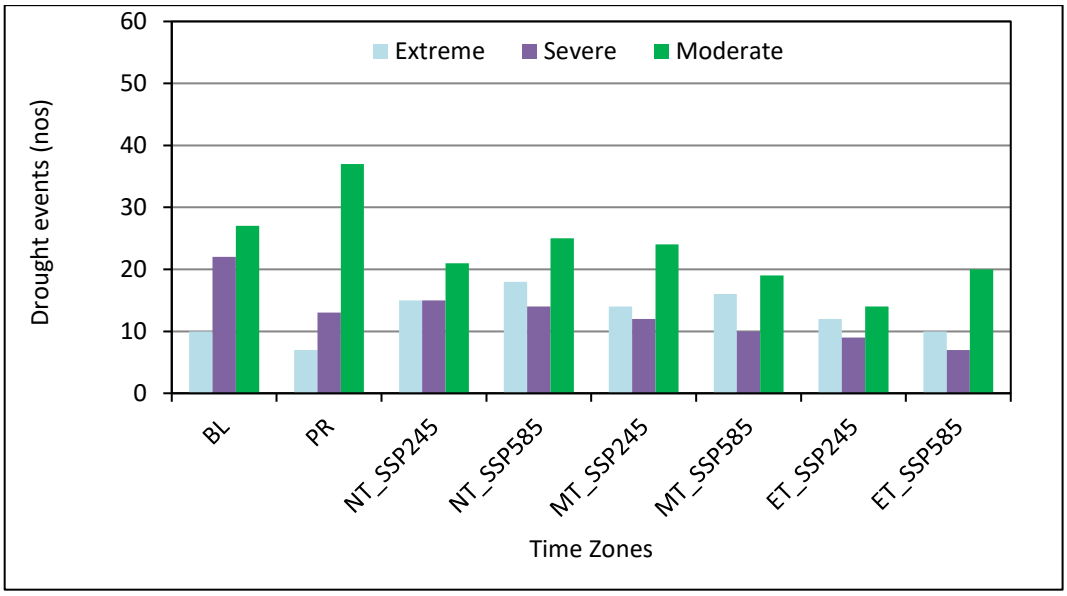

Figure 5.191: Comparison of all types of hydrological drought events at AB Road Crossing on R. Parvati under future climate scenarios

The comparison of hydrological drought events of various severities viz., extreme, severe, moderate and mild at Ujjain on River Shipra during various time periods are given in Table 5.57 and Figure 5.192. It can be observed that the extreme hydrological events are projected to decrease during the near-term, and then increase during the mid-term and thereafter decrease during end-term under both future climate scenarios whereas the severe hydrological events are projected to decrease during the near-term, and then increase during the mid-term and thereafter decrease during end-term under both future climate scenarios. The

moderate hydrological events are projected to decrease in the near-term, mid-term and end-term under both future climate scenarios. Similarly, the mild drought events are also projected to decrease noticeably during all future time periods under both future climate scenarios.

Table 5.57: Comparison of hydrological drought events at Ujjain on R. Shipra

Drought Events	BL	PR	NT_ SSP245	NT_ SSP585	MT_ SSP245	MT_ SSP585	ET_ SSP245	ET_ SSP585
Extreme	13	9	11.31	11.08	15.46	16.23	11.00	10.54
Severe	11	12	9.23	8.85	13.77	12.69	9.31	9.38
Moderate	32	32	15.15	15.92	22.54	20.77	15.00	15.16
Mild	110	97	66.85	66.77	88.77	83.46	71.62	66.31

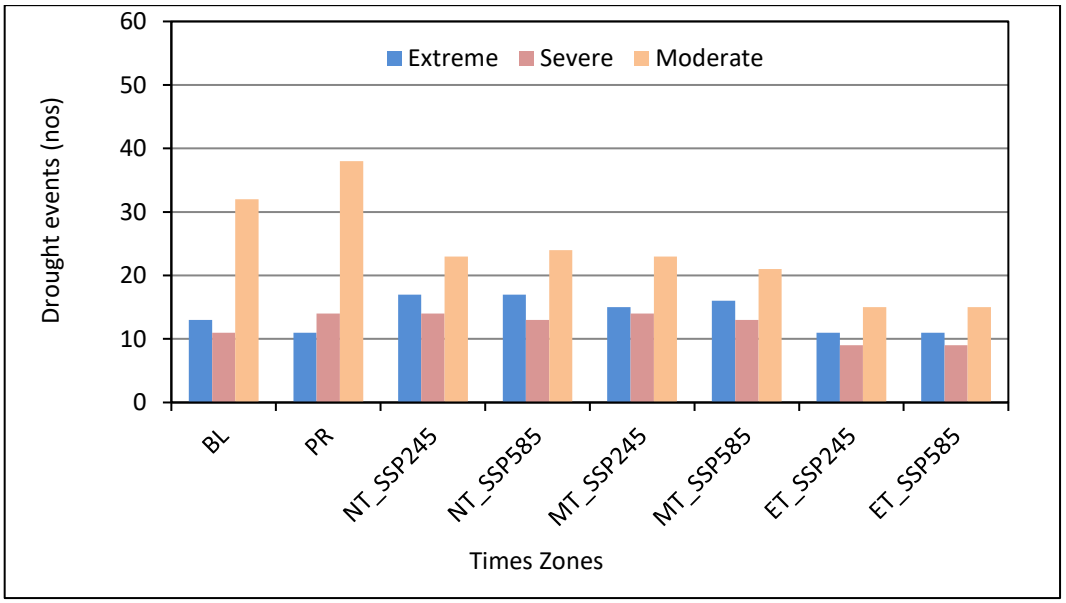

Figure 5.192: Comparison of all types of hydrological drought events at Ujjain on R. Shipra under future climate scenarios

The comparison of hydrological drought events of various severities viz., extreme, severe, moderate and mild at Sarangpur on River Kalisindh during various time periods are given in Table 5.58 and Figure 5.193. It can be observed that the extreme hydrological events are projected to increase during the near-term, mid-term and end-term under both future climate scenarios whereas the severe and moderate hydrological events are projected to decrease during the near-term, mid-

Table 5.58: Comparison of hydrological drought events at Sarangpur on R. Kalisindh

Drought Events	BL	PR	NT_ SSP245	NT_ SSP585	MT_ SSP245	MT_ SSP585	ET_ SSP245	ET_ SSP585
Extreme	9	11	11.62	11.85	12.85	15.54	11.15	10.46
Severe	15	4	8.69	9.85	13.46	13.85	9.31	7.92
Moderate	34	28	12.62	11.92	24.54	18.62	14.15	17.23
Mild	99	103	70.31	66.85	90.00	88.31	68.62	68.85

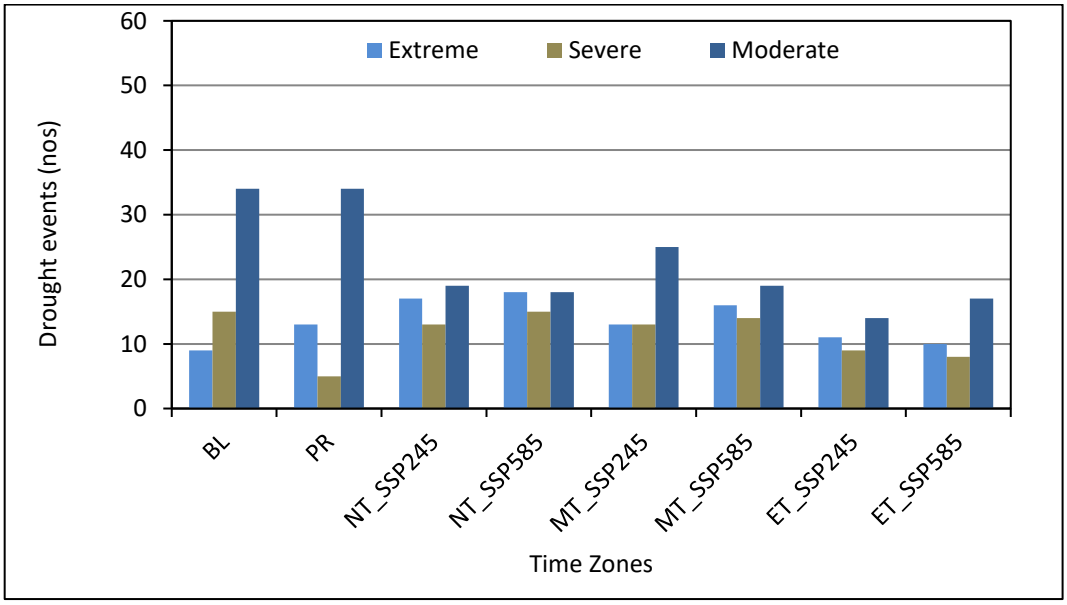

Figure 5.193: Comparison of all types of hydrological drought events at Sarangpur on R. Kalisindh under future climate scenarios

term and end-term under both future climate scenarios. Similarly, the mild drought events are also projected to decrease marginally during all future time periods under both future climate scenarios.

The comparison of hydrological drought events of various severities viz., extreme, severe, moderate and mild at Mahidpur on River Shipra during various time periods are given in Table 5.59 and Figure 5.194. It can be observed that the extreme hydrological events are projected to decrease during the near-term, mid-term and end-term under both future climate scenarios whereas the severe and moderate hydrological events are projected to increase during the near-term, mid-term and end-term under both future climate scenarios. Similarly, the mild drought events are also projected to decrease substantially during all future time periods under both future climate scenarios.

Table 5.59: Comparison of hydrological drought events at Mahidpur on R. Shipra

Drought Events	BL	PR	NT_ SSP245	NT_ SSP585	MT_ SSP245	MT_ SSP585	ET_ SSP245	ET_ SSP585
Extreme	15	10	8.92	9.54	13.00	12.54	8.85	8.69
Severe	8	7	11.15	8.23	14.92	13.92	9.15	9.38
Moderate	26	29	17.62	14.77	24.54	17.08	19.23	15.85
Mild	117	111	72.92	78.08	96.00	98.69	76.31	72.46

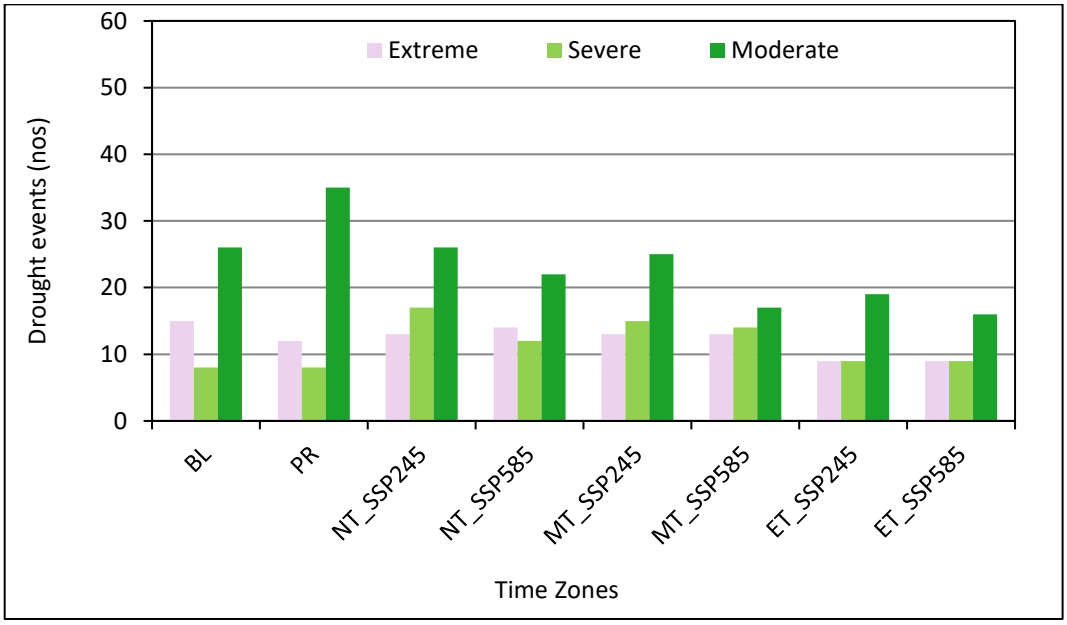

Figure 5.194: Comparison of all types of hydrological drought events at Mahidpur on R. Shipra under future climate scenarios

The comparison of hydrological drought events of various severities viz., extreme, severe, moderate and mild at Salavad on River Kalisindh during various time periods are given in Table 5.60 and Figure 5.195. It can be observed that the extreme hydrological events are projected to increase during the near-term, mid-term and end-term under both future climate scenarios whereas the severe and moderate hydrological events are projected to decrease during the near-term, mid-term and end-term under both future climate scenarios. Similarly, the mild drought events are also projected to decrease substantially during all future time periods under both future climate scenarios.

The comparison of hydrological drought events of various severities viz., extreme, severe, moderate and mild at Aklera on River Parwan during various time periods are given in Table 5.61 and Figure 5.196. It can be observed that the extreme

Table 5.60: Comparison of hydrological drought events at Salavad on R. Kalisindh

Drought Events	BL	PR	NT_ SSP245	NT_ SSP585	MT_ SSP245	MT_ SSP585	ET_ SSP245	ET_ SSP585
Extreme	12	13	14.08	12.69	15.62	16.23	11.85	10.08
Severe	19	10	5.46	6.85	10.08	13.00	7.77	8.00
Moderate	27	23	10.54	9.85	23.08	17.54	13.77	19.15
Mild	97	99	61.69	60.31	83.85	83.92	69.31	61.38

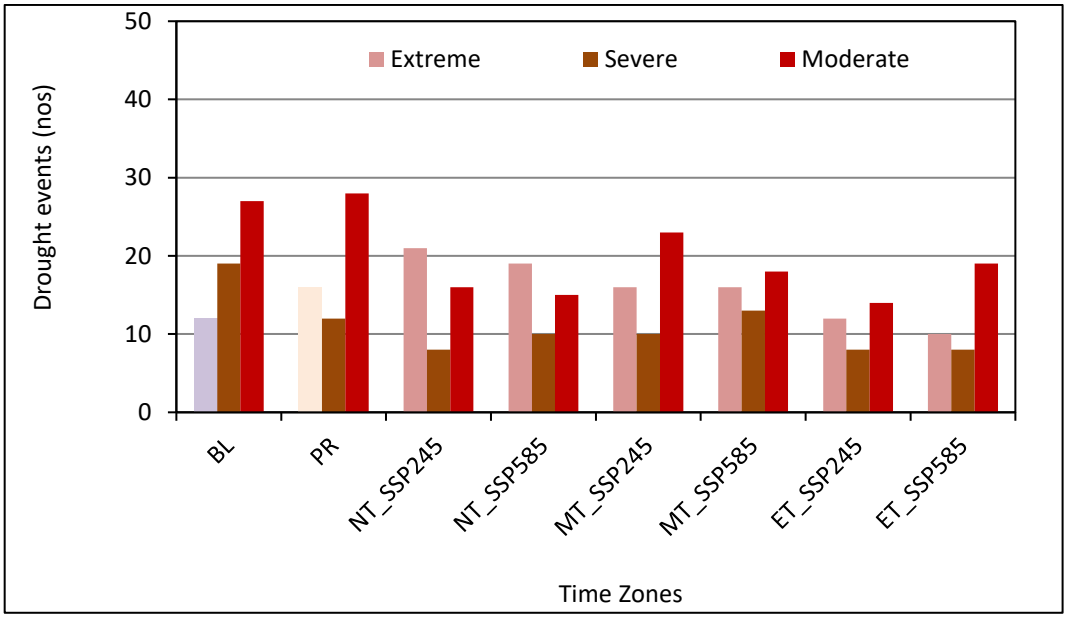

Figure 5.195: Comparison of all types of hydrological drought events at Salavad on R. Kalisindh under future climate scenarios

Table 5.61: Comparison of hydrological drought events at Aklera on R. Parwan

Drought Events	BL	PR	NT_ SSP245	NT_ SSP585	MT_ SSP245	MT_ SSP585	ET_ SSP245	ET_ SSP585
Extreme	12	13	9.38	11.23	15.77	15.92	11.31	10.77
Severe	19	10	10.62	10.15	12.15	13.46	8.15	8.31
Moderate	27	23	16.54	17.31	22.15	20.08	16.46	17.62
Mild	97	99	69.85	65.85	87.77	86.54	71.77	62.31

hydrological events are projected to decrease during the near-term, and then increase during the mid-term and decrease during the end-term under both future climate scenarios whereas the severe and moderate hydrological events are projected to decrease during the near-term, mid-term and end-term under both future climate scenarios. Similarly, the mild drought events are also projected to decrease substantially during all future time periods under both future climate scenarios.

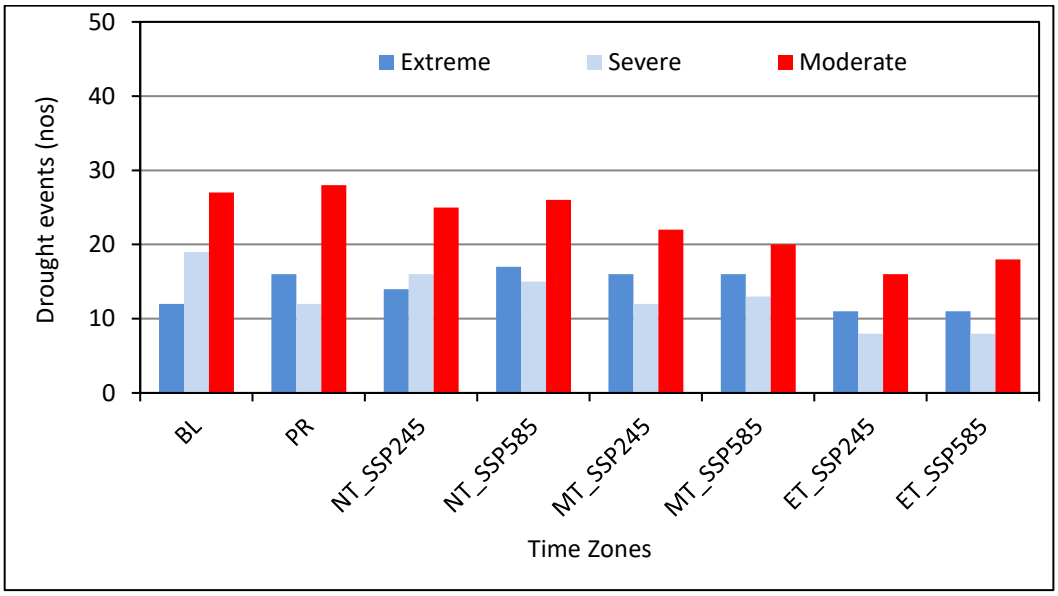

Figure 5.196: Comparison of all types of hydrological drought events at Aklera on R. Parwan under future climate scenarios

5.8 Impact of upcoming dams

Climate change, including variations of precipitation and stream flow, is real and undeniable. Since the agricultural lands are located in the command areas located below the dams, the effects of reductions rainfall resulting in the reduction in stream flow during drought years can be substantial. Reservoirs are key infrastructures for various water supplies and hydropower generation. The role of reservoirs is particularly relevant in regions that experience seasonal water scarcity due to seasonality, high inter-annual variability, and periodic floods and droughts. Reservoirs can also be used to control the river flow during extreme periods such as floods and droughts. During droughts, some of the stored water is released to maintain ecological flow, as well as meet basic water requirements. Construction of new reservoirs of increasing the number of reservoirs and water

storage capacity is a technique commonly used to ameliorate the effects of droughts on water availability Dams have a far-reaching impact on the prosperity of the region in the command areas, vicinity of the water spread areas and downstream of the reservoir, as it generally helps in the build-up of the groundwater levels and ground storage and also improves the biodiversity of the entire region.

Generally, most of the area under Mohanpura and Kundaliya projects is predominantly under agriculture, with urbanization and industrialization being witnessed in few pockets. Majority of the rural population have small land holdings of less than 5 ha (80%) and about 20-30% of the population fall below the poverty line. Nearly 10% of rural population falls under the category of land less formers mainly surviving on the work being generated in Kharif and Rabi crops in their areas. The area also supports a huge number of migratory industrial labors as well as agriculture sector-based laborers. These dams are located in the semi-arid climate with high rates of soil erosion with limited water storage structures to tap the runoff potential being generated from the catchment, which mostly flows down to River Yamuna. The soils are low in fertility due to loss of top soil and the agricultural productivity has also declined in these areas. The high intensity rainfall during the extreme rainfall events resulting in floods and the loss of soil moisture during water deficit years have aggravated the problem of land degradation and soil loss in the region.

The Kundaliya project is a major multipurpose project, which was proposed and now constructed on Kalisindh River in lower Chambal basin in Zirapur tehsil of Rajgarh district in Madhya Pradesh. The total catchment area upto the dam site is 4925 sq. km, which comprises of 3850 sq. km of Kundaliya catchment and 1075 sq. km of Lakhundar catchment. The gross storage capacity of the dam is 582.75 MCM with a dead storage of 30 MCM. Therefore, the live storage capacity of Kundaliya dam is 552.75 MCM. The average annual rainfall in the area is 966.75 mm.

The water availability comprises of the surface water availability and ground water availability. The surface water availability upto the dam site is 925.90

MCM (@ 0.188MCM/sq. km.) or *188.0 mm*. The groundwater availability is considered as 92.59 MCM (10% of available surface water). This translates to a total water availability upto dam site as 1018.49 MCM. However, few projects are being planned upstream of Kundaliya dam and the upstream surface water use is 385.11 MCM. Similarly, the groundwater is also being used upstream of dam for irrigation (30 MCM), domestic use (10 MCM) and industrial use (20 MCM) which amounts to 60 MCM. However, water will also be available from regeneration from agricultural areas (41.53 MCM) and also from domestic and industrial use (36 MCM). The total regeneration of water from the various uses is 77.53 MCM. After considering the major heads viz., total water availability of 1018.49 MCM, upstream surface water utilization of 385.11 MCM, upstream groundwater utilization of 60 MCM and regeneration of 77.53 MCM, the net water availability at Kundaliya dam is 650.71 MCM. However, few committed uses have been planned from the Kundaliya dam itself, which includes ecological flows of 30 MCM, drinking water including reservoir losses & supply losses of 10 MCM and water use for industrial purposes of 15 MCM. The balance water available at the Kundaliya dam after consideration of the planned committed uses from the dam itself works out to 595.71 MCM. The total irrigation requirement in the command area downstream of the Kundaliya dam is 473.96 MCM.

The impact of Kundaliya dam and Mohanpura dam on the irrigation in the command area during the drought years needs to assessed. A drought occurs when there is a deficit in rainfall during the principal rainy months of the monsoon season. When there was no dam, the irrigation was completely rain-fed in the command areas with some water being lifted directly from the rivers by the farmers located in the vicinity of the river. However, most of the runoff used to flow downstream without being fully utilized. Table 5.62 shows the rainfall deficit, corresponding live storage, and the unmet irrigation water demand after considering all the upstream demands and higher priority demands from the Kundaliya reservoir. The threshold rainfall at which there shall be no unmet demand (irrigation deficit) is 827.5 mm, which is a 14.4% deficit in the rainfall in the catchment. However, if the rainfall deficit exceeds beyond this threshold value (827.5mm), it will result in unmet demands. The graph showing the unmet demand corresponding to various quantum of rainfall deficit is given in Figure

5.197. It can be observed that upto a rainfall deficit of 139.3 mm, the planned irrigation demands can be met fully. An year is considered as a drought year if the rainfall deficit is 25% and more. The 75% average annual rainfall is 725.0 mm and the corresponding unmet demand is 107.94 MCM which is about 22.8% of

Table 5.62: Supply demand scenario in Kundaliya dam during rainfall deficit years

S. No	Annual rainfall	Rainfall Deficit (%)	Annual runoff (mm)	Annual runoff (MCM)	Ground water availability (MCM)	Total Water Availability	Total U/S SW Use (MCM)	U/S Use of GW upto	Regeneration (MCM)	Net water availability at	Commited use from Kundaliv	Balance available	Actual Gross Stora	Actual Live Storage (MCM)	Irrigation demand	Irrig water deficit	Irrig Water Deficit (%)
1	966.75		188.00	925.90	92.59	1018.49	385.31	60.00	77.53	650.71	55.00	595.71	582.75	552.75	473.96		
2	950	-1.7	184.74	909.86	90.99	1000.84	385.31	60.00	77.53	633.06	55.00	578.06	582.75	552.75	473.96		
3	925	-4.3	179.88	885.91	88.59	974.51	385.31	60.00	77.53	606.73	55.00	551.73	582.75	552.75	473.96		
4	900	-6.9	175.02	861.97	86.20	948.17	385.31	60.00	77.53	580.39	55.00	525.39	580.39	550.39	473.96		
5	875	-9.5	170.16	838.03	83.80	921.83	385.31	60.00	77.53	554.05	55.00	499.05	554.05	524.05	473.96		
6	850	-12.1	165.30	814.08	81.41	895.49	385.31	60.00	77.53	527.71	55.00	472.71	527.71	497.71	473.96		
7	827.5	-14.4	160.92	792.53	79.25	871.79	385.31	60.00	77.53	504.01	55.00	449.01	504.01	474.01	473.96		
8	825	-14.7	160.43	790.14	79.01	869.15	385.31	60.00	77.53	501.37	55.00	446.37	501.37	471.37	473.96	-2.59	-0.5
9	800	-17.2	155.57	766.20	76.62	842.82	385.31	60.00	77.53	475.04	55.00	420.04	475.04	445.04	473.96	-28.92	-6.1
10	775	-19.8	150.71	742.25	74.23	816.48	385.31	60.00	77.53	448.70	55.00	393.70	448.70	418.70	473.96	-55.26	-11.7
11	750	-22.4	145.85	718.31	71.83	790.14	385.31	60.00	77.53	422.36	55.00	367.36	422.36	392.36	473.96	-81.60	-17.2
12	725	-25.0	140.99	694.37	69.44	763.80	385.31	60.00	77.53	396.02	55.00	341.02	396.02	366.02	473.96	-107.94	-22.8
13	700	-27.6	136.13	670.42	67.04	737.46	385.31	60.00	77.53	369.68	55.00	314.68	369.68	339.68	473.96	-134.28	-28.3

the planned irrigation requirement. Therefore, it can be summarized that the Kundaliya project can cater to drought effectively as it can supply the full irrigation demand along with all other planned demands from the reservoir along with all the upstream demands when the rainfall deficit is 14.4%. Any rainfall deficit exceeding this threshold limit will result in irrigation deficits.

The Mohanpura project is a major multipurpose project, which was proposed and now constructed on Newaj River in lower Chambal basin in Biaora tehsil of Rajgarh district in Madhya Pradesh. The total catchment area upto the dam site is 3726 sq. km. The gross storage capacity of the dam is 539.42 MCM with a dead storage of 39.03 MCM. Therefore, the live storage capacity of Mohanpura is 500.39 MCM. The average annual rainfall in the area is 966.75 mm. The water availability comprises of the surface water availability and ground water availability. The surface water availability upto the dam site is 782.46 MCM (@ 0.21 MCM/sq. km.) or *210.0 mm*. The groundwater availability is considered as 78.25 MCM (10% of available surface water). This translates to a total water availability upto dam site as 860.71 MCM. However, few projects are being planned upstream of Mohanpura dam and the upstream surface water use is 293.04 MCM. Similarly, the groundwater is also being used upstream of dam for

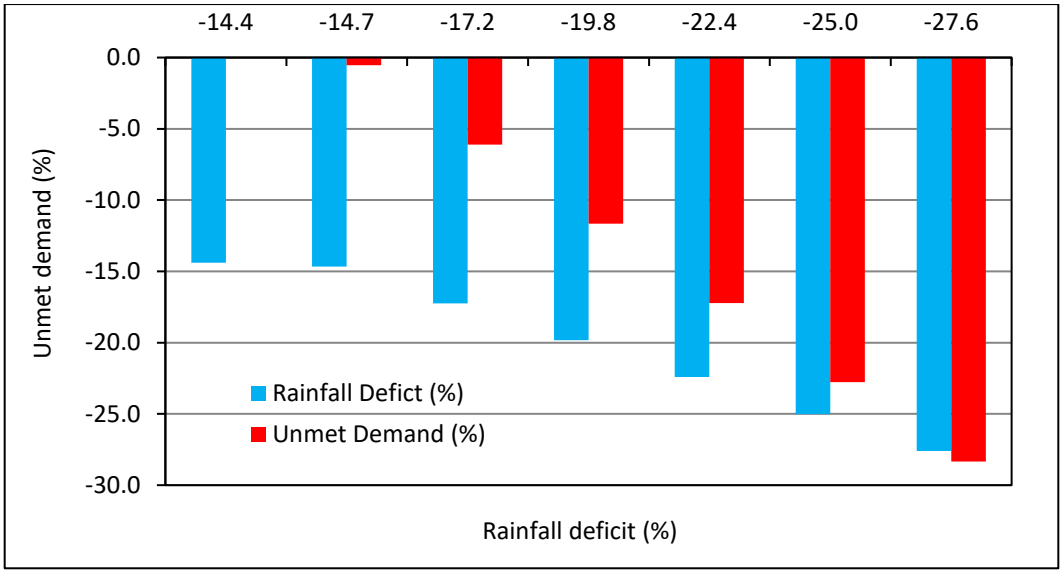

Figure 5.197: Rainfall deficit and unmet demand at Kundaliya dam

irrigation (30 MCM), domestic use (10 MCM) and industrial use (20 MCM) which amounts to 60 MCM. However, water will also be available from regeneration from agricultural areas (32.30 MCM) and also from domestic and industrial use (36 MCM). The total regeneration of water from the various uses is 68.30 MCM. After considering the major heads viz., total water availability of 860.71 MCM, upstream surface water utilization of 293.04 MCM, upstream groundwater utilization of 60 MCM and regeneration of 68.30 MCM, the net water availability at Mohanpura dam is 575.97 MCM.

Few committed uses have also been planned from the Mohanpura dam itself, which includes ecological flows of 52 MCM, drinking water including reservoir losses & supply losses of 20 MCM and water use for industrial purposes of 60 MCM. The balance water available at the Mohanpura dam after consideration of the planned committed uses from the dam itself works out to 443.97 MCM. The total irrigation requirement in the command area downstream of the Mohanpura dam is 350.37 MCM. Table 5.63, shows the rainfall deficit, corresponding live storage, and the unmet irrigation water demand after considering all the upstream demands and higher priority demands from the Mohanpura reservoir.

The threshold rainfall at which there shall be no unmet demand (irrigation deficit) is 757.25 mm, which is a 21.7 % deficit in the rainfall in the catchment. However,

Table 5.63: Supply demand scenario in Mohanpura dam during rainfall deficit years

Annual rainfall (mm)	Rainfall Defict (%)	Annual runoff (mm)	Annual runoff (MCM)	Ground water availability (MCM)	Total Water Availability at Mohanpurs Dam (MCM)	Total U/S SW Use (MCM)	U/S Use of Ground water upto Mohanpura dam (MCM)	Regeneration (MCM)	Net water availability at Mohanpura Dam (MCM)	Commited Use from the Mohanpura dam (MCM)	Balance available for irrigation at Mohanpura Dam (MCM)	Actual Gross Storage (MCM)	Actual Dead Storage (MCM)	Actual Live Storage (MCM)	Irrigation demand d/s of Mohanpura dam (MCM)	Irrig Water Deficit (MCM)	Irrig Water Deficit (%)
966.75	0	210.00	782.46	78.25	860.71	293.04	60.00	68.30	575.97	132.00	443.97	539.42	39.03	500.39	350.37		
950	-1.7	206.36	768.90	76.89	845.79	293.04	60.00	68.30	561.06	132.00	429.06	539.42	39.03	500.39	350.37		
925	-4.3	200.93	748.67	74.87	823.54	293.04	60.00	68.30	538.80	132.00	406.80	538.80	39.03	499.77	350.37		
900	-6.9	195.50	728.43	72.84	801.28	293.04	60.00	68.30	516.54	132.00	384.54	516.54	39.03	477.51	350.37		
875	-9.5	190.07	708.20	70.82	779.02	293.04	60.00	68.30	494.29	132.00	362.29	494.29	39.03	455.26	350.37		
850	-12.1	184.64	687.97	68.80	756.76	293.04	60.00	68.30	472.03	132.00	340.03	472.03	39.03	433.00	350.37		
825	-14.7	179.21	667.73	66.77	734.50	293.04	60.00	68.30	449.77	132.00	317.77	449.77	39.03	410.74	350.37		
800	-17.2	173.78	647.50	64.75	712.25	293.04	60.00	68.30	427.51	132.00	295.51	427.51	39.03	388.48	350.37		
775	-19.8	168.35	627.26	62.73	689.99	293.04	60.00	68.30	405.26	132.00	273.26	405.26	39.03	366.23	350.37		
757.25	-21.7	164.49	612.90	61.29	674.19	293.04	60.00	68.30	389.45	132.00	257.45	391.90	39.03	389.45	350.42		
750	-22.4	162.92	607.03	60.70	667.73	293.04	60.00	68.30	383.00	132.00	251.00	383.00	39.03	343.97	350.37	-6.40	-1.8
725	-25.0	157.49	586.79	58.68	645.47	293.04	60.00	68.30	360.74	132.00	228.74	360.74	39.03	321.71	350.37	-28.66	-8.2
700	-27.6	152.06	566.56	56.66	623.22	293.04	60.00	68.30	338.48	132.00	206.48	338.48	39.03	299.45	350.37	-50.92	-14.5
675	-30.2	146.63	546.33	54.63	600.96	293.04	60.00	68.30	316.22	132.00	184.22	316.22	39.03	277.19	350.37	-73.18	-20.9

if the rainfall deficit exceeds beyond this limit threshold value (757.25 mm), it will result in unmet demands. The graph showing the unmet demand corresponding to rainfall deficit is given in Figure 5.198. It can be observed that upto a rainfall deficit of 164.5 mm, the planned irrigation demands can be met fully. A year is considered as a drought year if the rainfall deficit is 25% and

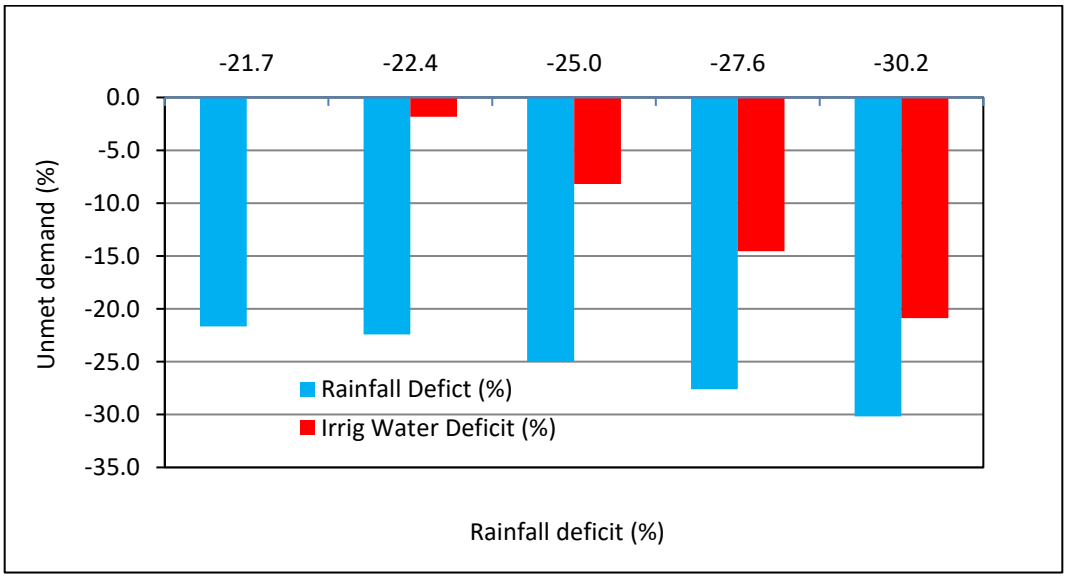

Figure 5.198: Comparison of rainfall deficit and unmet demand at Mohanpura dam

more. The 75% average annual rainfall is 725.0 mm and the corresponding unmet demand is 28.66 MCM which is about 8.20% of the planned irrigation requirement. Even if the rainfall deficit increases to the extent of 291.75 mm, the

corresponding unmet demand is limited to the extent of 20.9% only, which is manageable based on the suggestions given here. As such, the Mohanpura project can also cater to drought effectively as it can supply the full irrigation demand along with all other planned demands from the reservoir along with all the upstream demands when the rainfall deficit is upto 21.74%. Any rainfall deficit exceeding this threshold limit will result in irrigation deficits.

During drought years with higher severities, multiple options may be available including a) reduction in cropped area during both kharif and rabi season; b) adoption of less water intensive crops during rabi season such as gram, barely and peas; c) practice deficit irrigation during drought years and d) use of groundwater to meet the unmet demand based on its availability. The Kundaliya project and the Mohanpura project has been designed based on the pressurized irrigation system, which has very high efficiency. The extent of the command area and the irrigation water demands have also been planned accordingly. Based on the analysis of the supply-demand scenario for Kundaliya dam and the projects existing and being planned upstream, it can be seen that the Kundaliya reservoir is able to meet the ecological, domestic, industrial water demands along with full irrigation demands along with all upstream demands, during normal rainfall years as well as those years when the rainfall deficit is well within 14.4%. Similarly, based on the analysis of the supply-demand scenario for Mohanpura dam and the projects existing and being planned upstream, it can be seen that the Mohanpura reservoir is also able to meet the ecological, domestic, industrial water demands along with full irrigation demands after consideration of all upstream demands, during normal rainfall years as well as those years when the rainfall deficit is well within 21.7%. However, during drought years when the rainfall deficit exceeds 14.4%, the suggestions mentioned above may be implemented so that the irrigation can be continued without much hindrance in the command area.

Other than providing irrigation for the kharif and rabi crops, and also providing sufficient buffer during water shortages and droughts, there are multiple other benefits that gets accrued from these projects. The provision of ecological flows from dams will help to improve the biodiversity in the region whereas the irrigation activities in both kharif and rabi seasons will provide better livelihood

opportunities to the farming community and agriculturally based workforce. Another major advantage of the sustained irrigation activities will be in the form of availability of soil moisture in the command area, which will prevent erosion of fertile top soil from the agricultural fields. The continuous availability of soil moisture will result in improvement of microbial activity leading to increase in the type and number of micro-organisms in the soils responsible for good soil and crop health. The agricultural activities from the dams will also help to relieve the pressure on groundwater resources. It will also provide the much-needed fodder for the livestock and thereby reduce the livestock pressure on the existing forests. These continued agricultural activities with the increase in the vegetal cover will lead to improvement of organic matter which will ultimately lead to the increase in the soil fertility of the low-fertile soil encountered in the region and will lead to enhanced crop productivity. There will be additional reservoir-based livelihood options including fish farming and recreational activities. All these activities including higher crops yields from agricultural operations, income from livestock related activities, fish farming will provide better employment opportunities and scope for higher income generation to the people located in the command area.

5.9 Drought Vulnerability Assessment

The drought characteristics over Chambal basin have been evaluated using various drought indices including the frequency, intensity, duration and magnitude of various types of droughts including the meteorological, hydrological and groundwater drought. As the extent of drought varies from region to region, similar mitigation/adaptation strategies may not be adequate to combat drought. It is therefore important that vulnerability assessments of the region of interest are carried out in order to prepare a comprehensive adaptation plan that may be suited and applicable to the area. The drought vulnerability assessment helps to reveal the degree of exposure of an area to water stresses.

Drought in any particular region is dependent on many indicators (factors). The spatially varying indicators includes it geographical location, watershed characteristics, rainfall pattern, soil types, land use and land cover, slope, geomorphology, regional climatic factors and socio-economic factors. These factors considerably influence the water availability; hence it is important to

consider these factors. It is under this context drought vulnerability was assessed over Chambal basin in western Madhya Pradesh region for baseline, present and future time periods.

5.9.1 Spatial factors of drought vulnerability

5.9.1.1 Land use and land cover

Land use and land cover in any particular region is of utmost importance due to its direct influence on vulnerability to drought. Figure 5.199 shows the land use and land cover in Chambal basin in western Madhya Pradesh. The study area predominantly consists of agricultural land and some areas of range brushes and forests. Urban area, water bodies and barren area also prevails in small patches. Among the various land use classes, during a drought event, the agricultural area will be worst affected due to inadequate water availability and depleted soil moisture in the event of a drought. Since agricultural demands are very much higher as compared to any other demands, and the cropped are may be greatly affected due to long dry spells and droughts, therefore the agricultural area has been considered to be more vulnerable among various land use classes. Therefore,

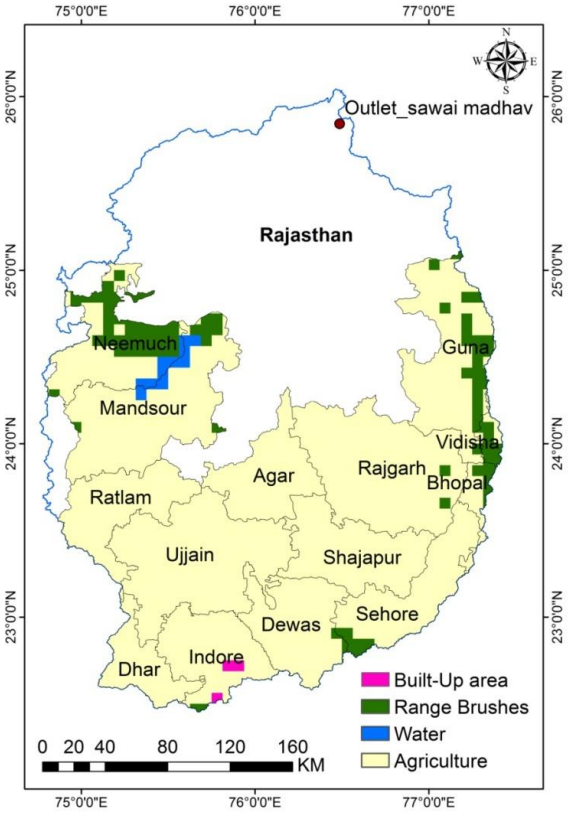

Figure 5.199: Land use and Land cover

higher weights have been assigned to agricultural land use. Similarly, as the barren area is unproductive, so it has the lowest priority among all classes.

5.9.1.2 Elevation

The elevation is another important factor that has to be considered for vulnerability assessments. The critical evaluation of elevation variations over the region is important to understand the movement, distribution and occurrence of water. The water availability is generally higher in the lower reaches due to accumulation of higher overland flows and as more stream's confluence in the lower reaches. Also, the lower reaches get more time for water retention as compared to upper and middle reaches of the basin and sufficient soil moisture is available for longer period in lower parts of the basin. Therefore, the upper reaches of the basin have been considered to be more vulnerable followed by middle and lower reaches of the basin. The elevation band map is prepared using SRTM satellite data obtained from USGS Earth Explorer. Figure 5.200 shows different elevation classes over Chambal basin. The study area has been classified into five elevation bands viz., < 300 m, 300-400 m, 400-500 m, 500-600 m and > 600 m.

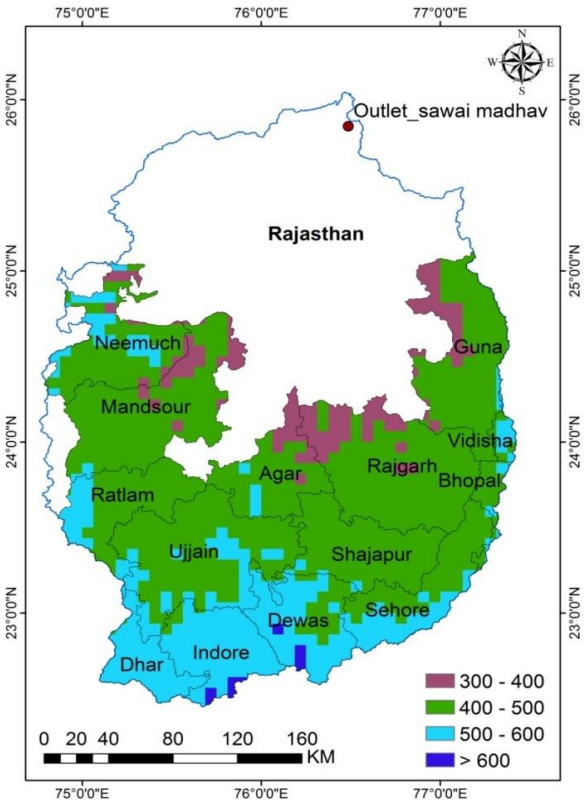

Figure 5.200: Elevation band

5.9.1.3 Soil type

The soil plays one of the most important functions as it stores moisture and supplies it to plants when there is need for water requirement by crops. The water holding capacity and water retention properties of the soil directly depend on the soil type, its texture and structure. The soil map of the study area is given in Figure 5.201. Soils in the Chambal basin is classified into four major textural classes, viz., clayey, coarse sandy clay, clay loam and sandy loam. Clay soil is considered as least vulnerable to drought as it can retain relatively more moisture as compared to other types of soils. On the other hand, coarse sandy clay is more vulnerable due to its lower water holding capacity.

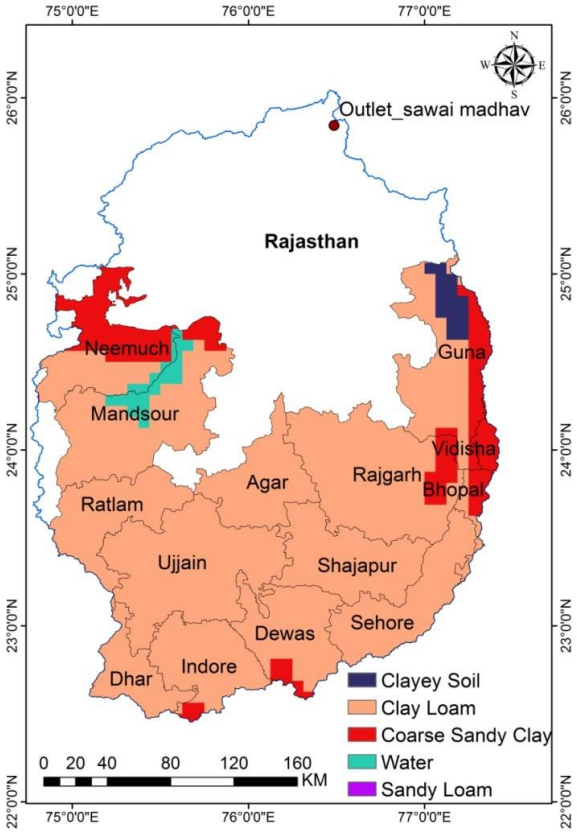

Figure 5.201: Soil types

5.9.2 Temporal factors of drought vulnerability

Drought is dynamic phenomenon and depends on various parameters that stimulate it. The spatio-temporal drought indicators represent different types of droughts viz., meteorological drought (rainfall departure), soil moisture drought (3m-SPI), surface water drought (SDI/6m-SPI) and groundwater drought

(GDI/12m-SPI). The indicators used for the drought vulnerability analysis include rainfall departure; the soil moisture, surface water and groundwater drought events evaluated by 3m-SPI, 6m-SPI/SDI and 12m-SPI respectively; and the drought severities pertaining to soil moisture, surface water and groundwater droughts evaluated by 3m-SPI, 6m-SPI/SDI and 12m-SPI respectively.

The rainfall departure helps to identify the rainfall anomaly and the rainwater deficit during drought years as the rainwater is a very crucial resources for irrigation in vast rainfed areas. Based on several studies and reviewed literature, the 3m-SPI has been used to evaluate soil moisture drought characteristics. The soil moisture drought may lead to delayed agricultural activities and reduced crop yields during droughts. Soil moisture reserve is critical for sustaining agriculture in the region during monsoon and non-monsoon periods and due to rainfall deficit during droughts, less quantum of water will be stored in the soil matrix. The spatial plots of the 3m-SPI have been prepared for the various months of the monsoon season. The 6m-SPI and 12m-SPI along with the analogous 6m-SDI, and 12m-SDI has also been evaluated for study area. Inter-relationships were developed between the 3m-SPI & 3m-SDI; 6m-SPI and 6m-SDI and 12m-SPI and 12m-SDI. Based on the strength of these developed relationships, the 6m-SPI best represents the surface water drought in the study area. Similarly, based on the relationships examined with 6m-SPI & GDI and 12m-SPI and GDI, the 12m-SPI best represents the groundwater drought in the study area. All these indicators have been used to evaluate the drought years, and number of drought events and the drought severities. The monthly rainfall departure for July, August and September months have been used for the assessment of vulnerability to drought. The spatial plot of rainfall departure during September 2002 is given in Figure 5.202. The spatial plot of 6m-SPI during July 2000 is given in Figure 5.203 whereas the spatial pot of GDI during May 2000 is given in Figure 5.204.

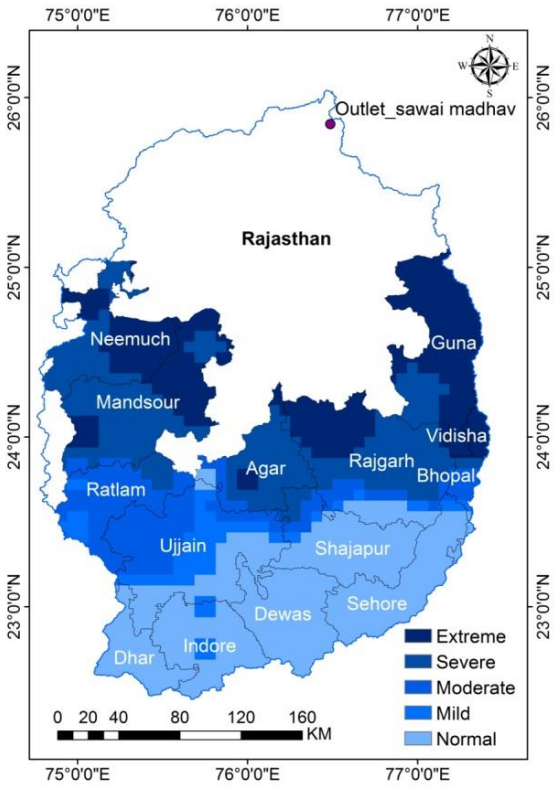

Figure 5.202: Rainfall departure during September 2002

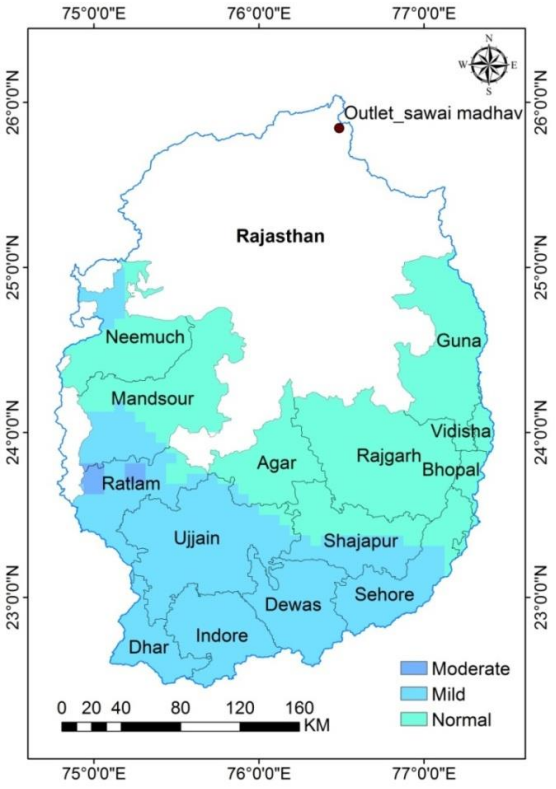

Figure 5.203: 6m-SPI during July 2000

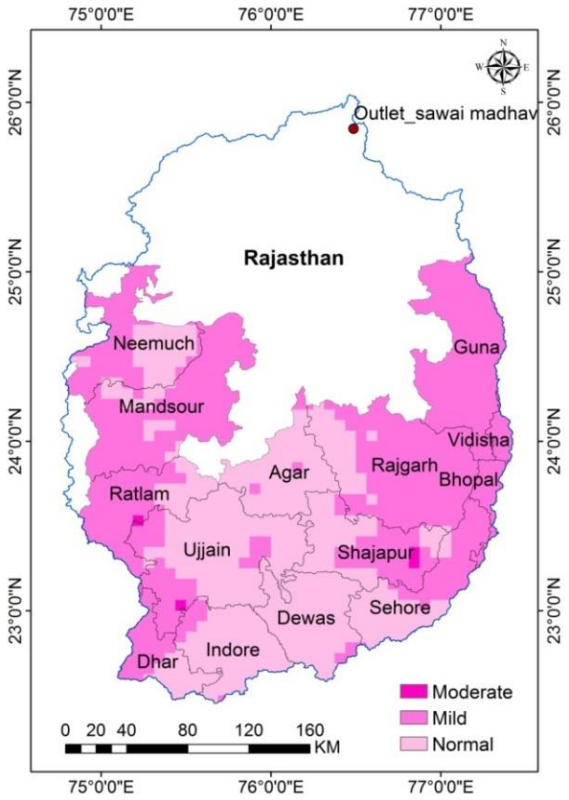

Figure 5.204: GDI during May (pre-monsoon) in 2000

The vulnerability has been derived on the basis of these spatial and temporal aspects. However, the drought vulnerability has to be compared during five time periods viz., baseline, present, near-term, mid-term and end-term periods. Also, for the future time periods, there are 13 GCMs and two future climate scenarios which will lead to different drought years and different vulnerable areas, which will be rather very difficult for comparison. Therefore, the vulnerability to drought, desertification and extreme climate has been evaluated based on the drought severities, drought events, rainfall departures that have been estimated for all the years in each of the five time periods and then average out for the respective duration. This will help to arrive at the vulnerability averaged over each of the time period. In deriving drought vulnerability, integration of various spatial and temporal factors was carried out using a weighing scheme based on the relative significance of various factors responsible for vulnerability to drought.

Table 5.64 shows the various indicators considered for the assessment of drought vulnerability and the weight assigned to the individual classes of each of these indicators. The assigned weights and the range of the weights for various factors are based on the relative degree of influence of various classes within each factor on overall vulnerability to drought. The spatio-temporal drought indicators represent different types of droughts viz., meteorological drought (rainfall departure), soil moisture drought (3m-SPI), surface water drought (SDI/6m-SPI) and groundwater drought (GDI/12m-SPI). Similarly, the various classes of the spatial indicators viz., land use, soil type and elevation bands also have different

Table 5.64: Weights of drought vulnerability indicators

S. No	Aspects	Indicators	Sub-classes	Weight
1.	Spatial	Land use and Land cover	1.Barren	0
			2.Water	1
			3. Range Brushes	3
			4.Built-Up area	4
			5. Agriculture	5
		Elevation band	1. 200-300	1
			2. 300-400	2
			3. 400-500	3
			4. 500-600	4
			5. >600	5
		Soil type	1. Clayey Soil	1
			2. Clay Loam	2
			3. Sandy Loam	3
			4. Coarse Sandy Clay	5
2.	Spatio-temporal	Rainfall departure (RD)	1. Mild drought (-20 to -25%)	1
			2. Moderate drought (-25 to -35%)	2
			3. Severe Drought (-35 to -50%)	3
			4. Extreme Drought (-50 to -65%)	4
			5. Excessive Drought (< -65%)	5
		Average Drought Events (DE) - Soil moisture, Surface water, Groundwater	1. 1 - 2	1
			2. 2 - 3	2
			3. 3 - 4	3
			4. 4 - 5	4
			5. > 5	5
		Average Drought Severity (DS) -	1. -2.50 – -4.00	1
			2. -4.00 – -6.00	2

		Soil moisture, Surface water, Groundwater	3. -6.00 – -8.00	3
			4. -8.00 – -9.50	4
			5. < -9.50	5

ranges of vulnerabilities which have been represented by a range of appropriate weights. The range of the numerical weights for the factors varies between 0 and 5. The weight of 0 indicates that, the sub-class of the given factor is causing no impact whereas weight of 1 cause least impact with respect to drought vulnerability. On the other hand, a higher weight indicates that the particular sub-class is having higher impacts. In order to understand the weights assigned to various factors let's consider an example, for say, soil. Various sub-classes of soil prevail in the region, but the soil with high water holding capacity have been assigned the least weight and the one with least water holding capacity have been assigned higher weight. Different layers of spatial and spatio-temporal maps have been prepared using ArcGIS and weights as proposed in Table 5.64 have been assigned to various sub-classes of factors. The weights assigned to various sub-classes of factors are integrated which provides composite weight for various aspects.

5.9.3 Drought Vulnerability Index (DVI)

In order to compute the Drought Vulnerability Index (DVI), the spatially varying and spatio-temporally varying indicators have been integrated based on the assigned weights. Simple summation of weights scheme and derivation of DVI from this has been used to evaluate vulnerability to drought. The DVI has been estimated and varies between 0 to 1. The DVI of higher value is more vulnerable to drought. The composite maps depicting DVI values have been divided into five vulnerability classes viz., not vulnerable (DVI: < 0.20), mildly vulnerable (DVI: 0.20 – 0.40), moderately vulnerable (DVI: 0.40 – 0.60), severely vulnerable (DVI: 0.60 – 0.80), extremely vulnerable (DVI: > 0.80). The drought vulnerability during the baseline, present, near-term, mid-term and end-term periods are given in Figure 5.205 to Figure 5.209 respectively.

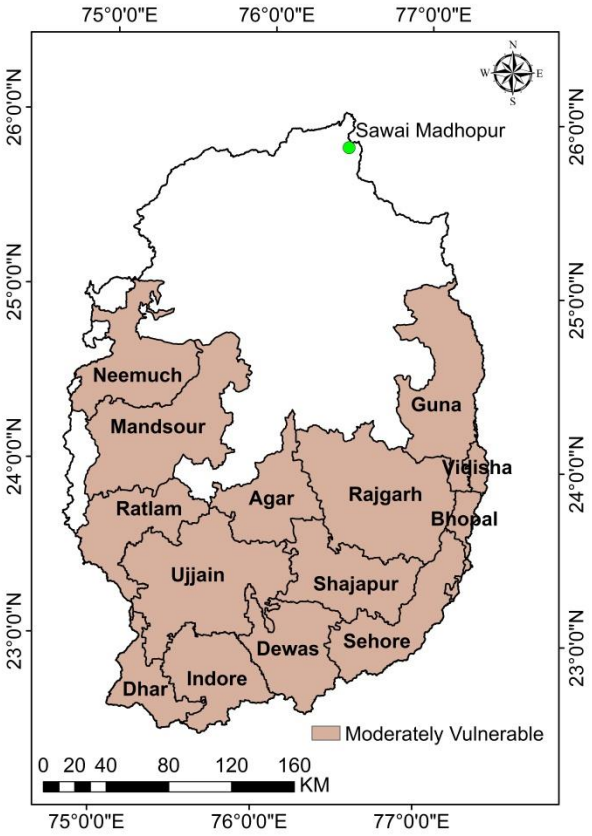

Figure 5.205: Drought vulnerability during the baseline period

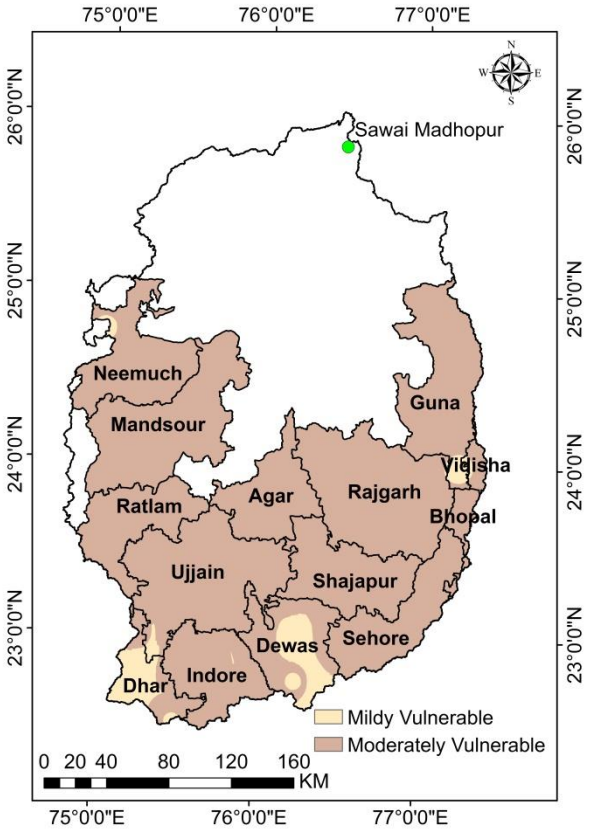

Figure 5.206: Drought vulnerability during the present period

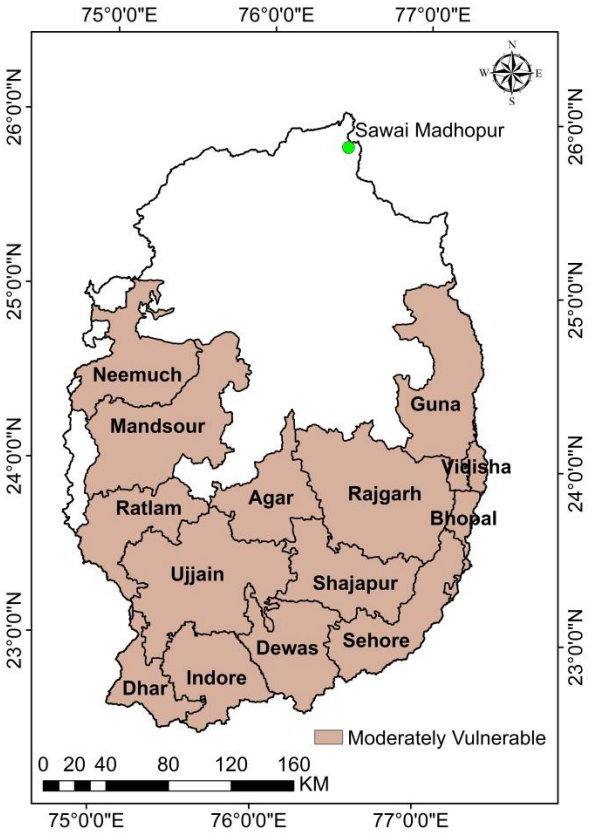

Figure 5.207: Drought vulnerability during the near-term period under SSP585 scenario

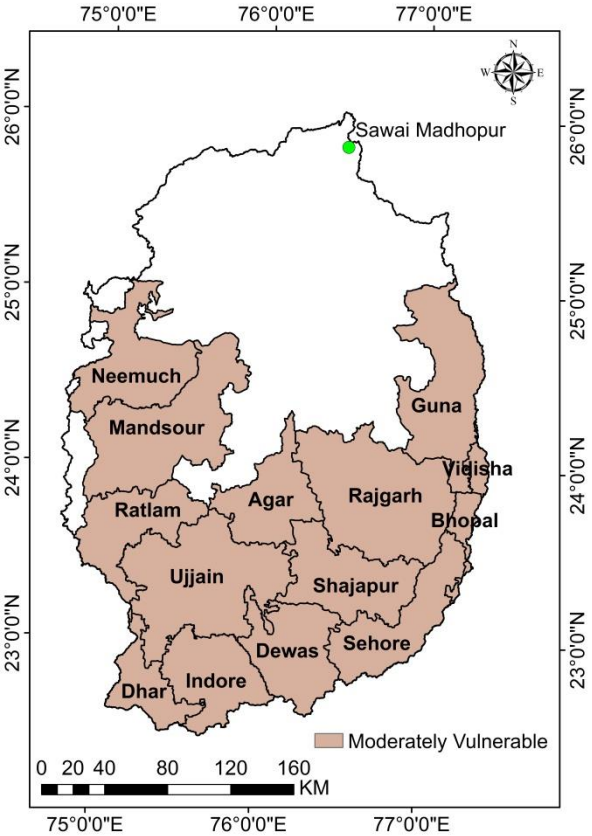

Figure 5.208: Drought vulnerability during the mid-term period under SSP245 scenario

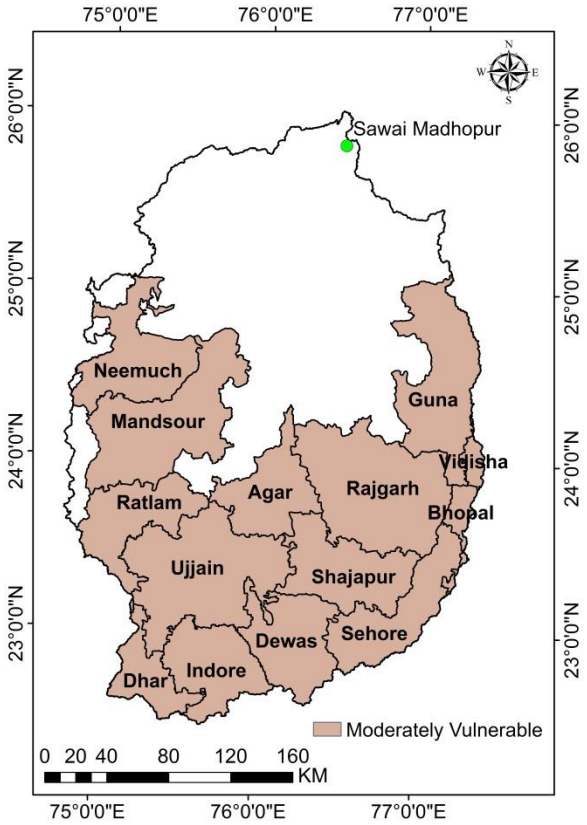

Figure 5.209: Drought vulnerability during the end-term period under SSP245 scenario

The area statistics of the vulnerability classes during the various time periods have been extracted from these vulnerability maps. As it is visible, the vulnerability of study area falls under the moderately vulnerable class during the baseline period and all future time periods, except during the present period. During the present period, the study area was under two vulnerability classes viz., mild vulnerability (5.3%) and moderately vulnerable (94.7%). As such, it can be seen that there is no increase in the average drought vulnerability in all the future time periods as compared to the baseline period. This may be due to the fact that higher annual and extreme rainfall along with higher annual, high and low flow has been projected during the future time periods. However, there will be dry spells during the monsoon months for which supplemental irrigation has been planned.

5.10 Desertification Vulnerability Assessment

The vulnerability to desertification has been evaluated based on various indicators discussed earlier. Only those desertification indicators that can be easily projected into the future have been used in the desertification vulnerability assessment. The

desertification indicators considered in the study include aridity index, annual average air temperature, and rainfall erosivity. The rainfall erosivity is a major factor responsible for soil erosion and has therefore been considered. The average annual air temperature in the region is projected to increase as compared to the baseline period which may lead to higher evaporation and evapotranspiration resulting in lower soil moisture. The capability to hold soil particle together will decrease due to inadequate soil moisture availability. Further increases in the temperature projected by the GCMs will make this indicator more relevant for comparing the changes in the desertification potential. The aridity index is another important indicator that can be assessed into the future and has therefore been used as an indicator in the desertification vulnerability analysis. The potential evapotranspiration is another important factor as the projected increase may lead to higher crop water requirement and soil moisture deficits in future. However, it has not been considered separately as it gets already accounted for in the aridity index. Also, the soil type, slope and land use and their relative weights is similar to that considered in the spatially varying indicator for drought vulnerability assessment. Table 5.65 shows the various indicators considered for the assessment

Table 5.65: Weights of desertification vulnerability indicators

S. No.	Aspects	Indicators	Sub-classes	Weight
1.	Spatial	Land use and Land cover	1.Barren	0
			2.Water	1
			3. Range Brushes	3
			4.Built-Up area	4
			5. Agriculture	5
		Elevation band	1. 200-300	1
			2. 300-400	2
			3. 400-500	3
			4. 500-600	4
			5. >600	5
		Soil type	1. Clayey Soil	1
			2. Clay Loam	2
			3. Sandy Loam	3
			4. Coarse Sandy Clay	5
2.	Spatio-temporal	Aridity Index (AI)	1. Humid	1
			2. Dry sub-humid	2
			3. Semi-arid	4
			4. Arid	5
		Average Annual	1. 24 - 25^{o}C	1

		Air Temperature (AAAT)	2. 25 - 26ºC	2
			3. 26 - 27ºC	3
			4. 27 - 28ºC	4
			5. > 28ºC	5
		Rainfall Erosivity (RE)	1. 350 - 400	1
			2. 400 - 450	2
			3. 450 - 500	3
			4. 500 - 550	4
			5. > 550	5

of desertification vulnerability and the weight assigned to the individual classes of each of these indicators. The desertification vulnerability assessment approach is similar to that adopted for the assessment of drought vulnerability; wherein appropriate weights have been assigned to the sub-classes of the indicators considered in the assessment.

The weights are based on the relative degree of influence of each sub-class on the desertification vulnerability. The range of the numerical weights for the factors varies between 0 and 5. The weight of 0 indicates that, the sub-class of the given factor is causing no impact whereas weight of 1 cause least impact with respect to drought vulnerability. On the other hand, a higher weight indicates that the particular sub-class is having higher impacts. The spatial plots of each of these desertification indicators have been prepared. The rainfall erosivity is much higher in the districts bordering Rajasthan with higher erosivity in the north-western parts of the study area covering the districts of Guna, Agar, Rajgarh and parts of Mandsaur and Neemuch.

5.10.1 Desertification Vulnerability Index (DSVI)

In order to compute the Desertification Vulnerability Index (DSVI), the spatially varying and spatio-temporally varying indicators have been integrated based on the assigned weights. Simple summation of weights scheme and derivation of DSVI been used to evaluate vulnerability to desertification. The DSVI has been estimated and varies between 0 to 1. The DSVI of higher value is more vulnerable to drought. The composite maps depicting DSVI values have been divided into five vulnerability classes viz., not vulnerable (DSVI: < 0.20), mildly vulnerable (DSVI: 0.20 – 0.40), moderately vulnerable (DSVI: 0.40 – 0.60), severely

vulnerable (DSVI: 0.60 – 0.80), extremely vulnerable (DSVI: > 0.80). The desertification vulnerability during the baseline, present, near-term, mid-term and end-term periods are given in Figure 5.210 to Figure 5.214 respectively. The area statistics of the desertification vulnerability classes during the various time periods have been extracted from these vulnerability maps.

The desertification vulnerability of study area generally falls under the mild and moderate vulnerable classes during the baseline present and all future time periods. The comparison of the area under different vulnerability classes during the various time periods is given in Figure 5.215. During the baseline period, the study area was under two vulnerability classes about 88.2% under mild vulnerability and 11.7% under moderately vulnerable classes, which has changed only marginally with 85.6% under mild vulnerability class and the remaining 14.3% under moderate vulnerability class during the present period. However, the desertification vulnerability is projected to increase in future time periods. The area under the moderate vulnerability class is projected to increase in the near-term to 26.2% and 30.3% under SSP245 and SSP585 scenario respectively with corresponding decreases in the mildly vulnerable class. The area under moderate

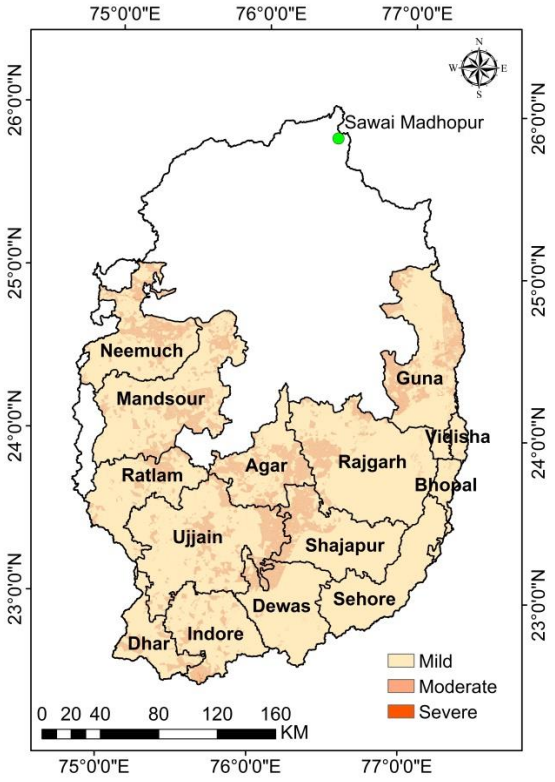

Figure 5.210: Desertification vulnerability during the baseline period

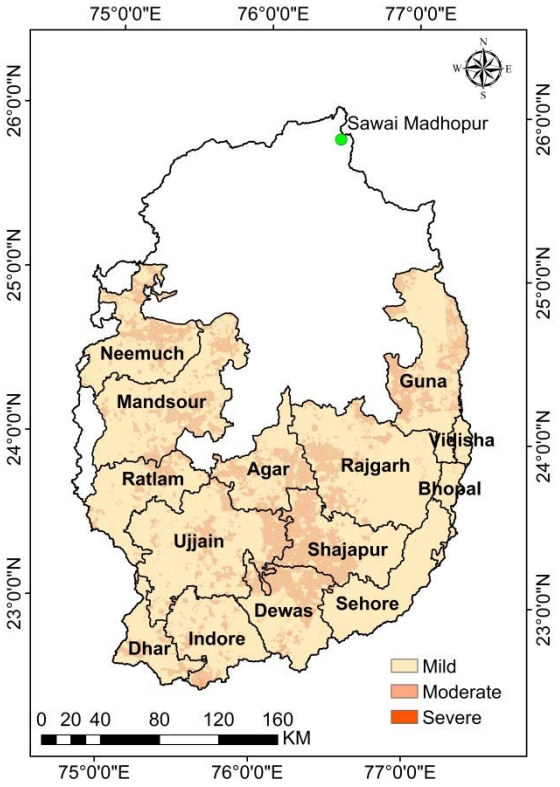

Figure 5.211: Desertification vulnerability during the present period

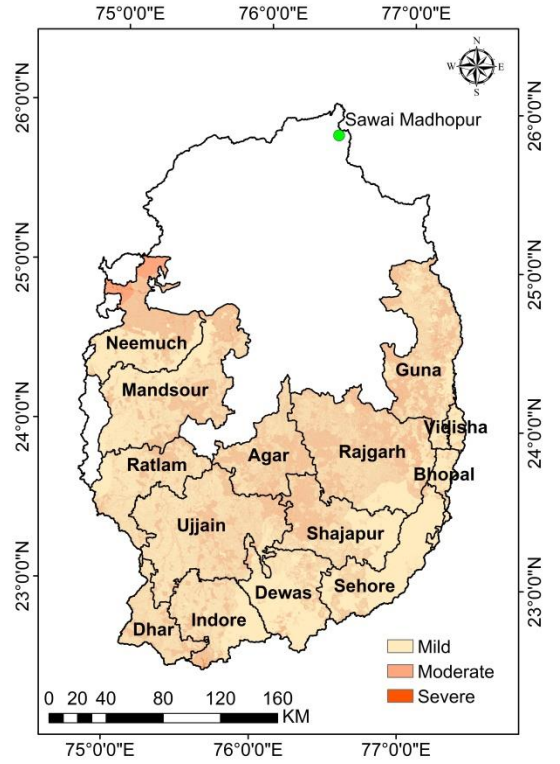

Figure 5.212: Desertification vulnerability during near-term period under SSP245 scenario

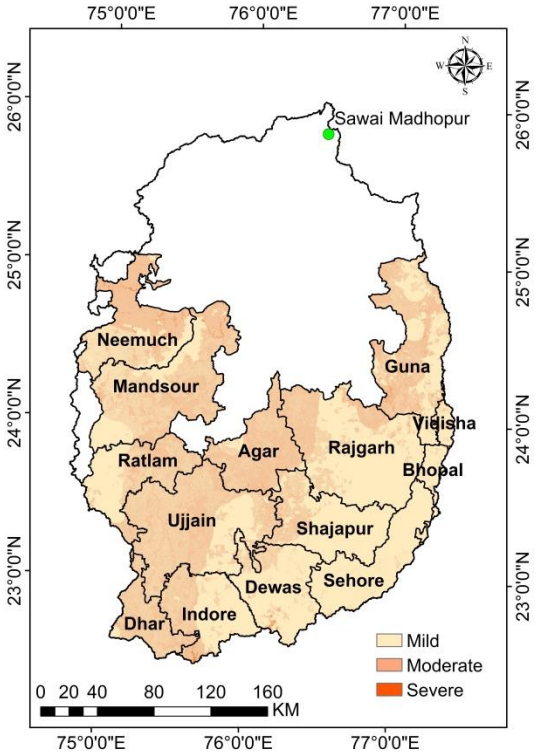

Figure 5.213: Desertification vulnerability during mid-term period under SSP245 scenario

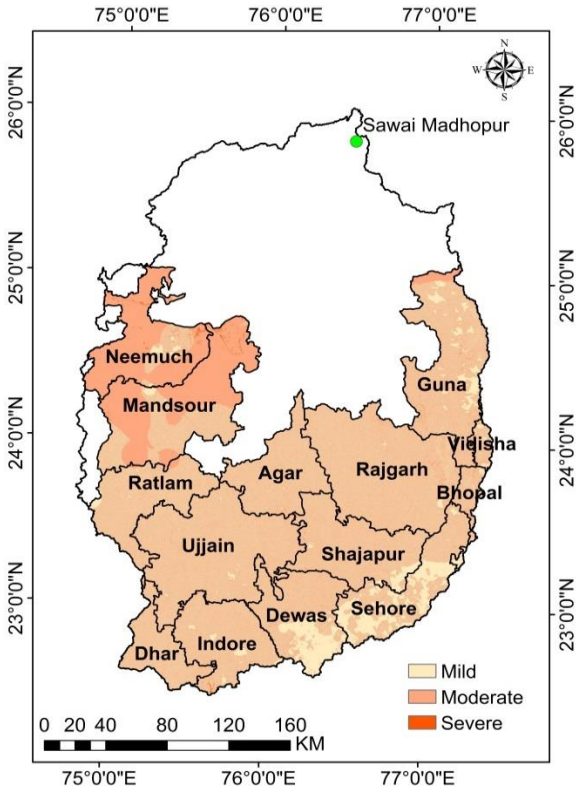

Figure 5.214: Desertification vulnerability during end-term period under SSP245 scenario

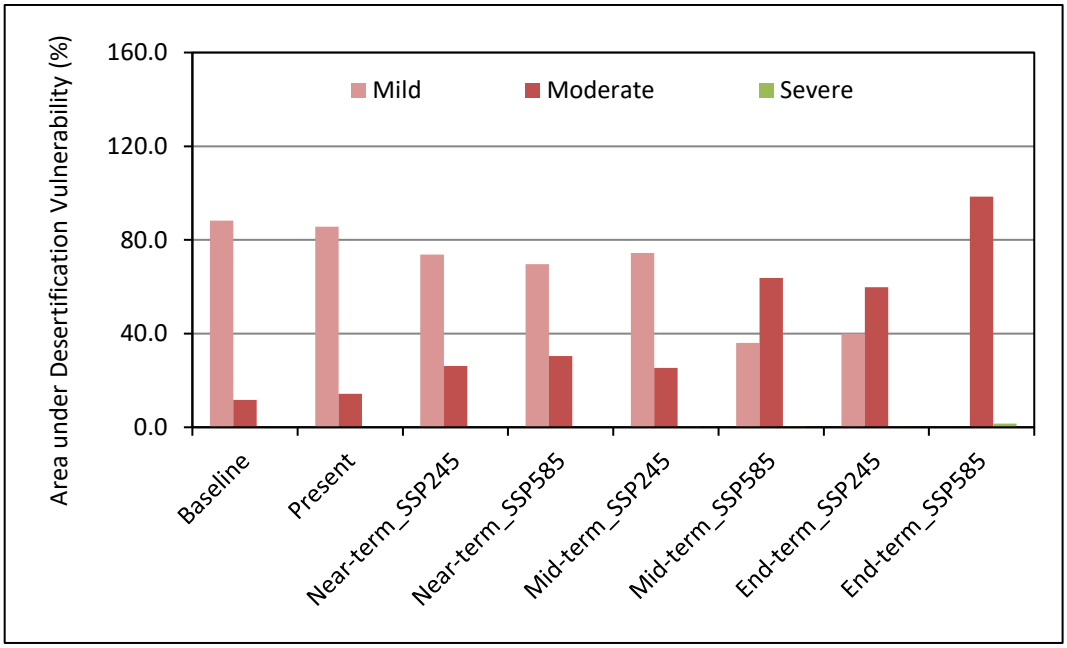

Figure 5.215: Comparison of areas under desertification vulnerability classes during various time periods

vulnerability class is projected to increase further during the mid-term to 25.4% and 63.7% under SSP245 and SSP585 scenario respectively with corresponding decreases in the mildly vulnerable class. It can be observed that the area under moderately vulnerable class is projected to increase significantly under SSP585 scenario during the mid-term (63.7%). During the end-term, the area under moderate vulnerability class is expected to increase further to 59.8% under SSP245 scenario. The situation can get aggravated further during the end-term under SSP585 scenario with 98.5% under moderate vulnerability class and remaining 1.5% under the severe vulnerability class. Therefore, it can be seen that the average desertification vulnerability is projected to increase in all future time periods which may lead to increase in the integrated vulnerability in the study area.

5.11 Extreme Climate Vulnerability Assessment

The vulnerability to extreme climate has been evaluated based on various indicators related to extreme precipitation and temperature. The extreme climate vulnerability indicators pertaining to rainfall include 1-day maximum rainfall, daily rainfall intensity, annual rainfall and number of rainy days whereas the extreme climate vulnerability indicators pertaining to temperature include 1-day max of maximum temperature, 1-day max of minimum temperature, very hot days and very hot nights. These extreme climate indicators are the stimulating factors that may be responsible for aggravating the intensification of drought and desertification. Table 5.66 shows the various indicators considered for the assessment of extreme climate vulnerability and the weight assigned to the individual classes of each of these indicators. The extreme climate vulnerability assessment approach is similar to that adopted for the assessment of drought vulnerability; wherein appropriate weights have been assigned to the sub-classes of the indicators considered in the assessment.

The weights are based on the relative degree of influence of each sub-class on the extreme climate vulnerability. The range of the numerical weights for the factors varies between 0 and 5. The weight of 0 indicates that, the sub-class of the given factor is causing no impact whereas weight of 1 cause least impact with respect to drought vulnerability. On the other hand, a higher weight indicates that the

particular sub-class is having higher impacts. The spatial plots of each of these extreme climate vulnerability indicators have been prepared. The 1-day maximum rainfall has already increased is highest in all the districts bordering Rajasthan covering Guna, Rajgarh, Agar, Ratlam and Mandsaur. It is projected to increase further in the study area. The average daily rainfall intensity is higher in Guna district and parts of Mandsaur, Neemuch, and Rajgarh districts all of which are bordering districts near to Rajasthan. Similarly, a smaller number of rainy days is seen in the bordering districts of Neemuch, Mandsaur, Ratlam, Rajgarh and Guna. The increase in the 1-day maximum rainfall magnitude and increase in the average daily rainfall intensity coupled with the lesser number of rainy days are a cause of concern as it may lead to higher soil erosion and land degradation. The projected increases in the very hot days, very hot nights coupled with the decreases in the cold nights particularly during the crop growth stages will affect the plant growth thereby leading to changes in crop yields as well. The increase in minimum temperature affects the night time respiration rates of the soybean crop and can reduce biomass accumulation. The projected increases of all these extreme climate indicators in all the future time periods are a cause of concern and may lead to higher vulnerability in future.

5.11.1 Extreme Climate Vulnerability Index (ECVI)

In order to compute the Extreme Climate Vulnerability Index (ECVI), these spatio-temporally varying indicators have been integrated based on the assigned weights. Simple summation of weights scheme and derivation of ECVI been used to evaluate vulnerability to desertification. The ECVI has been estimated and varies between 0 to 1. The ECVI of higher value is more vulnerable to drought. The composite maps depicting ECVI values have been divided into five vulnerability classes viz., not vulnerable (ECVI: < 0.20), mildly vulnerable (ECVI: 0.20 – 0.40), moderately vulnerable (ECVI: 0.40 – 0.60), severely vulnerable (ECVI: 0.60 – 0.80), extremely vulnerable (ECVI: > 0.80). The extreme climate vulnerability during the baseline, present, near-term, mid-term and end-term periods are given in Figure 5.216 to Figure 5.220 respectively. The area statistics of the extreme climate vulnerability classes during the various time periods have been extracted from these vulnerability maps.

Table 5.66: Weights of extreme climate vulnerability indicators

S.No.	Variable	Indicators	Sub-classes	Weights
1.	Rainfall	1-day Maximum rainfall (RF) (mm)	RF > 130	5
			110 < RF < 130	4
			90 < RF < 110	3
			70 < RF < 90	2
			50 < RF < 790	1
		Daily Rainfall Intensity (DRI)	DRI > 21	5
			18 < DRI < 21	4
			15 < DRI < 18	3
			12 < DRI < 15	2
			9 < DRI < 12	1
		Number of Rainy Days (NRD)	NRD> 65	5
			55 < NRD< 65	4
			45 < NRD< 55	3
			35 < NRD< 45	2
			25 < NRD< 35	1
		Annual Rainfall (ARF) (mm)	ARF < 800	5
			800 < RF < 900	4
			900 < RF < 1000	3
			1000 < RF < 1100	2
			1100 < RF < 1200	1
2.	Maximum and Minimum Temperature	1-day Max of Tmax (°C)	Tmax > 45°C	5
			44°C - 45°C	4
			43°C - 44°C	3
			42°C - 43°C	2
			41°C - 42°C	1
		1-day Min of Tmin (°C)	Tmin > 31°C	5
			30°C - 31°C	4
			29°C - 30°C	3
			28°C - 29°C	2
			27°C - 28°C	1
		Very hot day events (Tmax> 40°C)	> 60	5
			50 - 60	4
			40 – 50	3
			30 – 40	2
			20 - 30	1
		Very hot night events (Tmin> 25°C)	>105	5
			85 to 105	4
			65 to 85	3
			45 to 65	2
			25 to 45	1

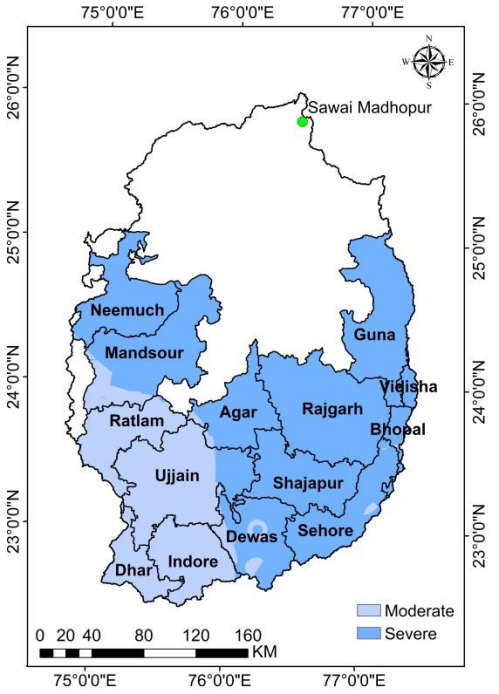

Figure 5.216: Extreme climate vulnerability during baseline period

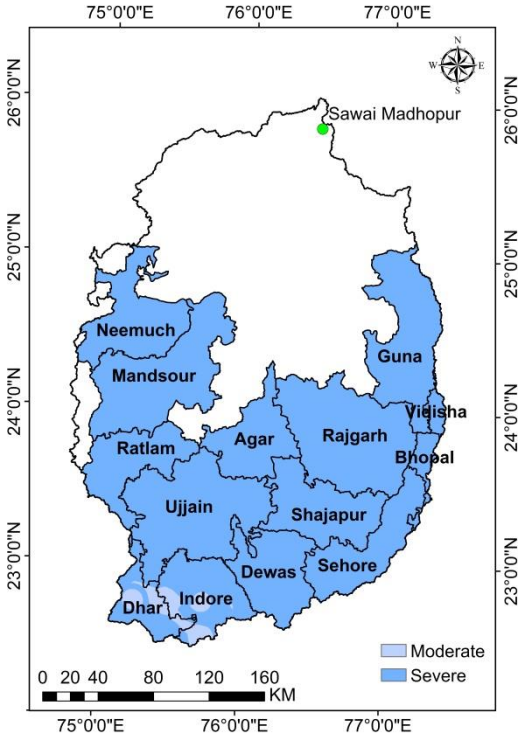

Figure 5.217: Extreme climate vulnerability during present period

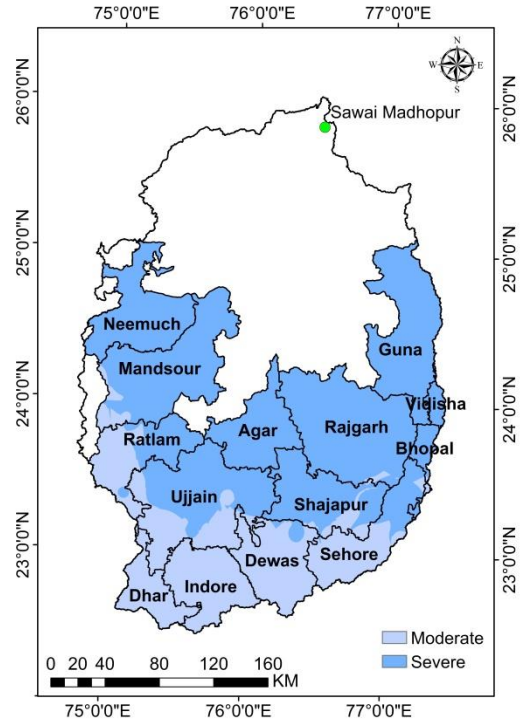

Figure 5.218: Extreme climate vulnerability during near-term period under SSP585 scenario

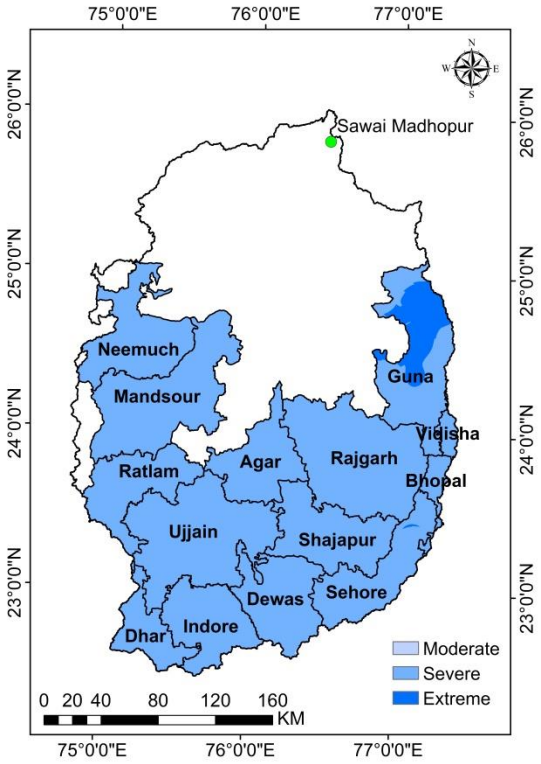

Figure 5.219: Extreme climate vulnerability during mid-term period under SSP585 scenario

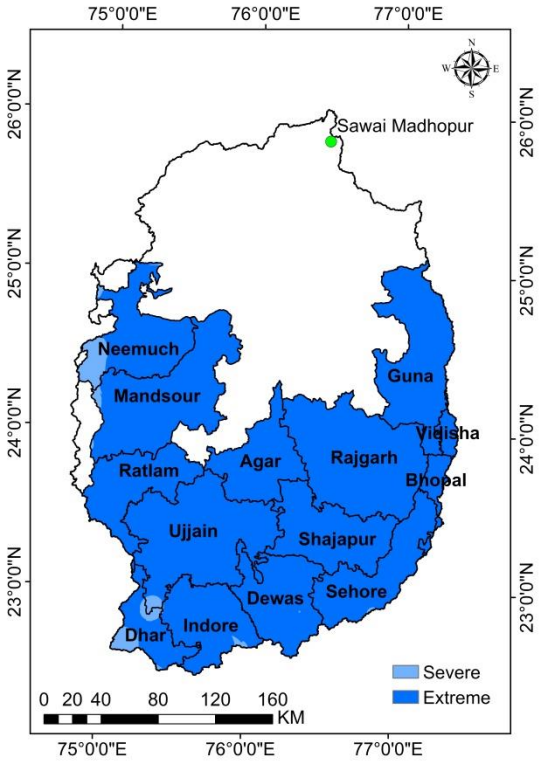

Figure 5.220: Extreme climate vulnerability during end-term period under SSP585 scenario

The extreme climate vulnerability of study area generally falls under the moderate and severely vulnerable classes during the baseline present and near-term time periods, whereas it varies between severe and extremely vulnerable classes during the mid-term and end-term. The comparison of the area falling under different extreme climate vulnerability classes during the various time periods is given in Figure 5.221. During the baseline period, the study area was under two vulnerability classes about 30.4% under moderate vulnerability and 69.6% under severely vulnerable classes, which has changed only considerably with only 2.3% under moderate vulnerability class and the remaining 97.7% under severe vulnerability class during the present period. However, the extreme climate vulnerability is projected to increase in future time periods.

However, during the near-term the area under the moderate and severe vulnerability is projected to be more or less similar to that during the baseline period with very slight changes under both scenarios. During mid-term, the vulnerability is projected to increase with almost the entire area falling under

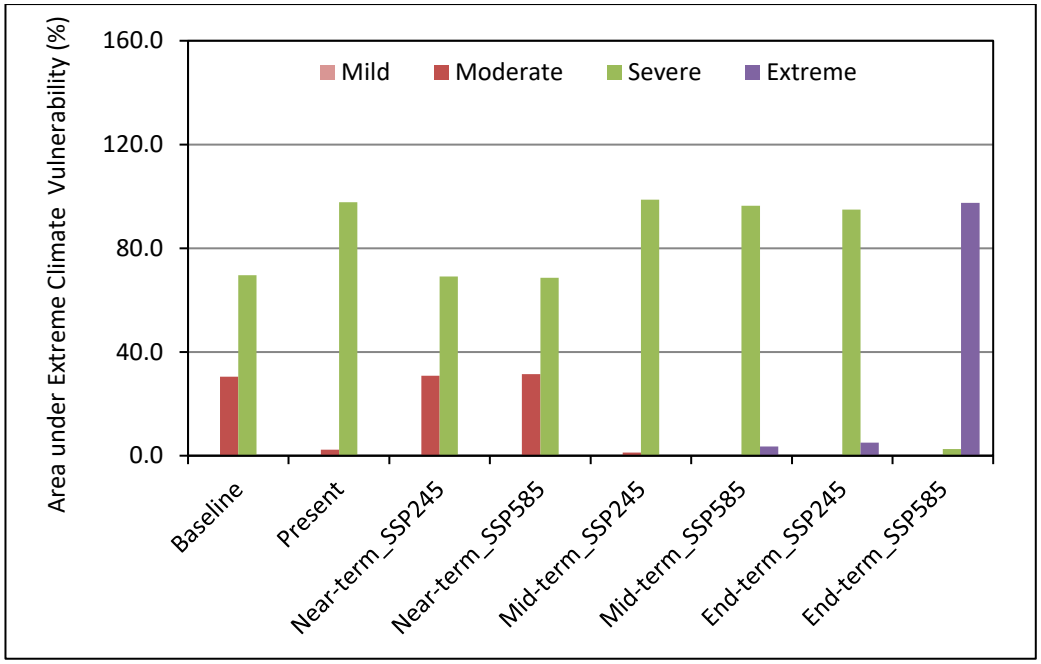

Figure 5.221: Comparison of areas under extreme climate vulnerability classes during various time periods

severe vulnerability class (98.7%) and the remaining 1.1% (moderate vulnerability) and 0.20% (extreme vulnerability) under SSP245 scenario.

However, under SSP585 scenario, the situation is projected to be more vulnerable with 96.4% under severe vulnerability class and 3.6% under extreme vulnerability class. The situation is projected to get aggravated further during the end-term under SSP585 scenario with only 2.6% under severe drought and the remaining 97.4% area falling under extreme vulnerability class. Therefore, it is amply clear that the extreme climate vulnerability is projected to increase in all future time periods which may contribute to intensification of the integrated vulnerability in the study area.

5.12 Integrated Vulnerability Assessment

The integrated vulnerability assessment framework is an exercise that has been carried out to derive the combined impacts of vulnerabilities to drought, desertification and climate change in the study area. From all the analysis carried out in this study, it is clear that the climate change will have considerable impact

on the precipitation and temperature, water availability, extreme runoff and dry spells with consequences on drought, desertification and extreme climate and their associated vulnerabilities. The drought, desertification and extreme climate vulnerabilities have been evaluated separately in the previous sections. Based on the analysis it can be observed that even though the projected future drought vulnerability is similar to that during the baseline period, but the area under desertification and extreme climate vulnerabilities are projected to be of higher severities in future. Therefore, it is interesting to study the overall vulnerability of the study area considering the combined changes in these three aspects. The integrated vulnerability has been evaluated based on the spatial indicators viz., soil type, slope and land use whereas the spatio-temporal indicators considered include soil moisture drought events and severity, surface water drought events and severity, groundwater drought events and severity, rainfall departure, annual air temperature, aridity index, rainfall erosivity, annual rainfall, number of rainy days, daily rainfall intensity, 1-day maximum rainfall, 1-day maximum of MaxT, 1-day maximum of MinT, very hot days and very hot nights. Table 5.67 shows the various indicators considered for the assessment of integrated vulnerability and the weight assigned to the individual classes of each of these indicators.

5.12.1 Integrated Vulnerability Index (INVI)

The Integrated Vulnerability Index (INVI) has been computed based on the spatially varying and spatio-temporally varying indicators which have been integrated based on the assigned weights. The INVI is indicative of the combined vulnerability to droughts, desertification and extreme climate. The INVI has been estimated and varies between 0 and 1. The INVI of higher value is more vulnerable to drought. The composite maps depicting INVI values have been divided into five vulnerability classes viz., not vulnerable (INVI: < 0.20), mildly vulnerable (INVI: 0.20 – 0.40), moderately vulnerable (INVI: 0.40 – 0.60), severely vulnerable (INVI: 0.60 – 0.80), extremely vulnerable (INVI: > 0.80). The extreme climate vulnerability during the baseline, present, near-term, mid-term and end-term periods are given in Figure 5.222 to Figure 5.223 respectively. The area statistics of the extreme climate vulnerability classes during the various time periods have been extracted from these vulnerability maps.

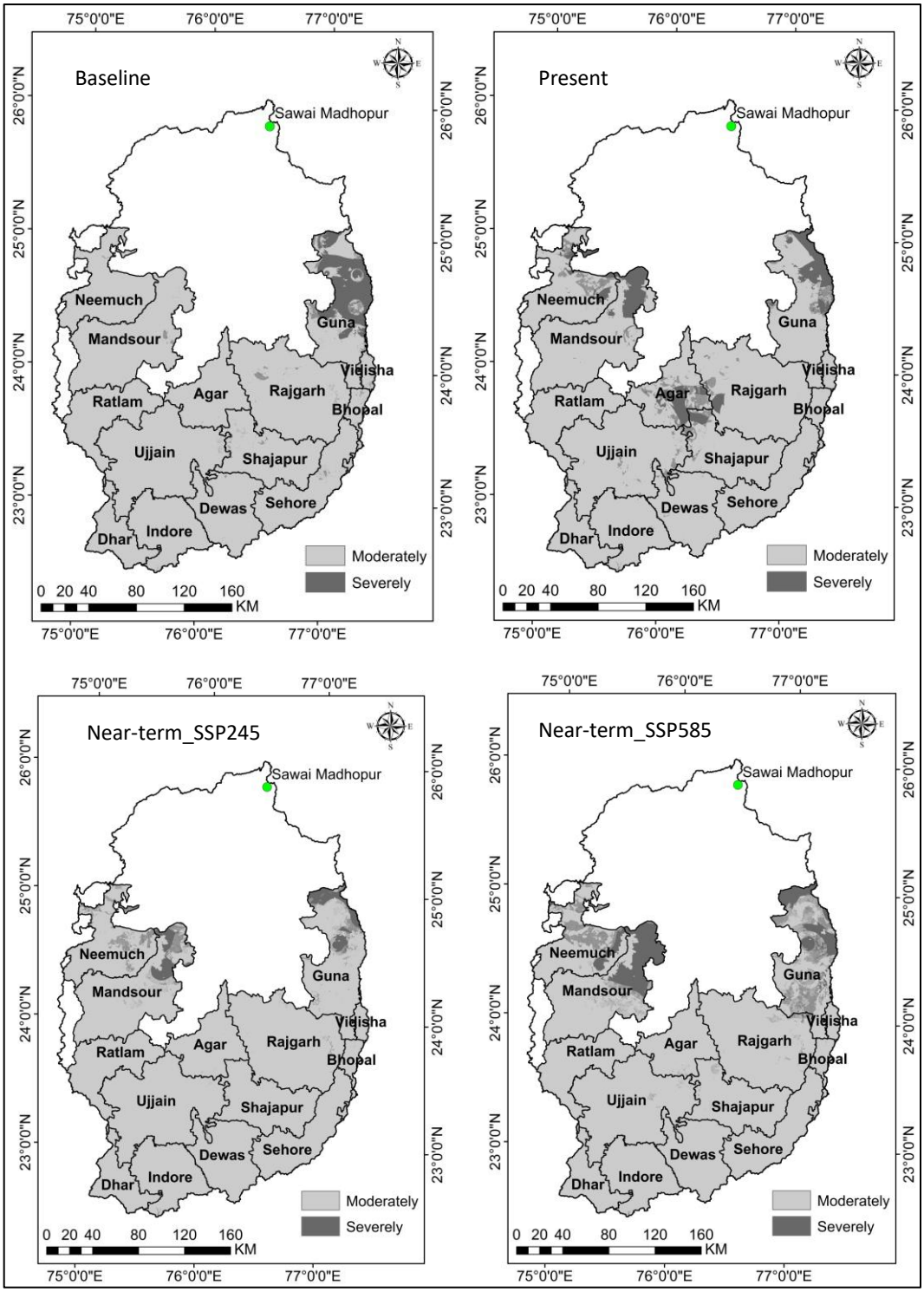

Figure 5.222: Integrated vulnerability during baseline, present, near-term (SSP245) and near-term (SSP585)

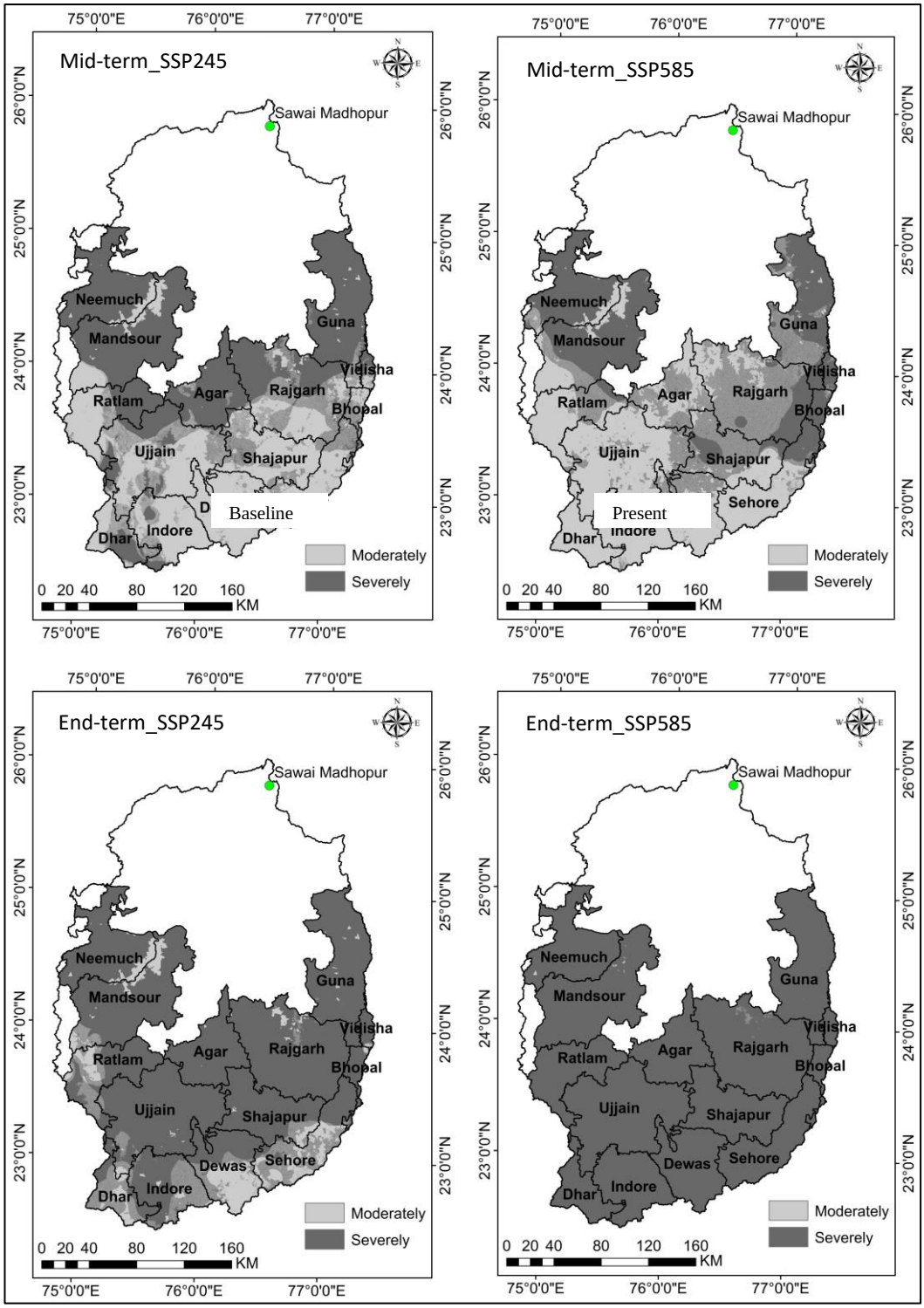

Figure 5.223: Integrated vulnerability during mid-term (SSP245), mid-term (SSP585), end-term (SSP245) and end-term (SSP585)

The integrated vulnerability of study area generally falls under the moderate and severely vulnerable classes during the baseline present and future time periods. The comparison of the area falling under various integrated vulnerability classes during the various time periods is given in Figure 5.224. During the baseline

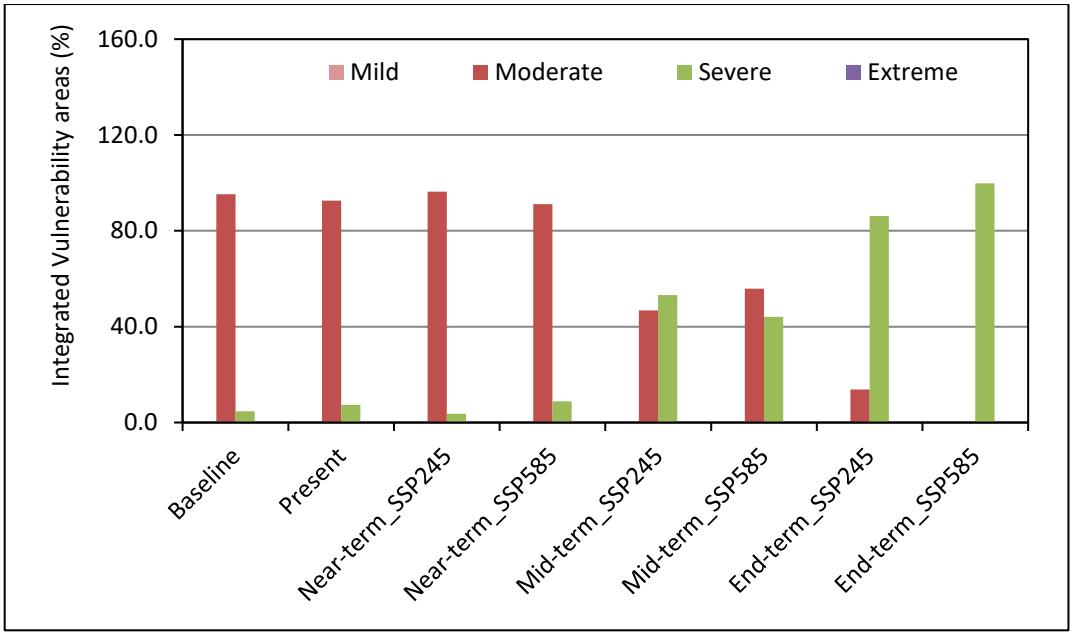

Figure 5.224: Comparison of areas under extreme climate vulnerability classes during various time periods

period, the study area was under two vulnerability classes with about 95.2% area under moderate vulnerability class and only 4.8% area under severely vulnerable classes, which has changed marginally to 92.6% area under moderate vulnerability class and the remaining 7.4% under severe vulnerability class during the present period. However, the integrated vulnerability scenario is projected to increase in future time periods.

A progressive increase in the area under severe vulnerability class is projected during the future time periods. As compared to the baseline period, the area under the moderate vulnerability class is projected to decrease to 91.2% whereas the area under severe vulnerability is projected to increase to 8.8% under SSP585 scenario. During mid-term, the integrated vulnerability is projected to increase with about 53.2% and 44.1% area falling under severe vulnerability class under SSP245 and SSP585 scenario respectively. The situation is projected to get worsened further during the end-term viz., 86.2% and 99.9% of the area falling under sever vulnerability class under SSP245 and SSP585 scenario respectively. Based on the integrated vulnerability it is clearly evident that the overall vulnerability in the study area is projected to be higher during future time periods, as more areas are projected to fall under the severe vulnerability class as compared to the baseline period when majority area was under the moderate

vulnerability class. The results obtained from the vulnerability analysis will help to the decision makers to plan for suitable adaptation strategies.

5.13 Climate Change Adaptation

As it is evident from the analysis, climate change will increase the variability of rainfall patterns and is likely to generate more extreme events, such as floods and droughts. This will translate into significant impacts on the water safety and security as a result of alteration in the patterns of water availability and its distribution. These changes are projected to escalate in future and therefore there is a high need for adaptation technologies. The water sector along with the agriculture sector is the critical area of focus for adaptation. The Fifth Assessment Report of Working Group 2 of the Intergovernmental Panel on Climate Change (IPCC WGII AR5) has emphasized the role of technology in supporting adaptation to changes in water (IPCC, 2014). However, water is a complex sector, due to the intrinsic linkage between freshwater resources and other sectors and ecosystems.

Adaptation technology use has been broadly defined as the application of technology in order to reduce the vulnerability, or enhance the resilience, of a natural or human system to the impacts of climate change (UNFCCC, 2005). Adaptation refers to anticipating the adverse effects of climate change and taking appropriate action to prevent or minimize the damages as well as taking advantages of the opportunities that may arise. In short, it is the process of adjusting to the current or projected impacts of climate change. However, poor planning and lack of regard for specific measures targeted for possible outcomes including emphasis only on short-term measures can result in maladaptation that does not succeed in reducing the vulnerability but in contrast increases it (IPCC, 2001: 378). In the water sector, site-specific solutions need to be considered within the broader context of integrated water management approaches.

Broadly there may be three major types of adaptation viz., a) structural and physical adaptation based on technological and engineering interventions, and ecosystem services, b) social adaptation which include educational, informational, behavioral aspects and c) Institutional adaptation brought into effect by economic

organizations, laws and regulation, government policies and programs. The adaptations measures for climate change impacts can be broadly divided into two aspects viz., a) adaptation for water sector and b) adaptation for agricultural sector. Since India is predominantly an agriculture-based economy, adaptation is necessary for both these sectors to tackle the diverse impacts of climate change on both these vital sectors.

The comprehensive analysis of the climate change impacts on water availability, drought and desertification along with the various vulnerability analysis including drought vulnerability, desertification vulnerability, extreme climate vulnerability, and the integrated vulnerability, reflected higher vulnerabilities of all these aspects in the future time periods, the highest impacts being projected during the end-term. The possible impacts of climate change related droughts may include crop failures and subsequent loss of livelihoods in the agriculture sector; reduced crop yields with declining income levels resulting in food security issues; fodder shortages for livestock leading to reduced productivity or even cattle death; disposal of cattle, jewelry and land in areas vulnerable to drought and out-migration of population in search of alternate livelihoods. Also, there shall be environmental impacts including decline in groundwater recharge, lowering of groundwater levels due to overexploitation of groundwater during periods of droughts and extended dry spells, and loss of agro-biodiversity and degeneration of forests due to overgrazing.

The possible impacts of climate change related enhanced desertification may include many of the impacts related to drought described above and in addition desertification may lead to land degradation and soil erosion, dwindling of agricultural activities, changes in the land use to shrubs and thorny plants, loss of soil fertility resulting in lower crop productivity, growth in demand of fertilizers to enhance the dwindling crop productivity, and increased pressure on groundwater aquifers. Therefore, appropriate adaptation measures required for the water sector may include,

a) ‘Increasing surface water storage capacity’ by constructing additional water resources infrastructure like dams, increasing the storage capacity of existing structures as the increased drought can reduce the safe yield of the

reservoirs. The storage can be increased by removing the accumulated sediment in the reservoirs, raising the dam height, or planning auxiliary reservoirs elsewhere for supplementing water to the main reservoir.

b) 'Water diversions' through interlinking of rivers for inter-basin water transfer from water-excess river basins to water-deficit basins.

c) 'Diversifying the options for water supply' which may include conjunctive use of surface and groundwater, and treatment of waste water for use during periods of water shortages.

d) improvement of the water conveyance systems like lining of canals to improve the water use efficiency and crop productivity.

e) adoption of pressurised irrigation systems in all upcoming water resources projects for increasing the system efficiency.

f) application of science and technology in water resources management viz., sensor-based irrigation water scheduling depending on the soil moisture availability and crop water needs, sensor-based reservoir gate operations for water release management during floods and normal operations; real-time weather monitoring, and real-time flood forecasting in major river systems in the study area.

g) water conservation measures including check dams, stop dams, farm ponds etc., which will minimise the risks to crop health during dry spells and short-term droughts.

h) soil conservation measures to arrest/reduce the soil erosion thereby preventing the reservoir sedimentation and loss of storage capacity. It also helps in preserving the top fertile soil thereby preventing land degradation and enhancing land productivity.

i) waste water reuse for agriculture and industries after proper treatment.

j) integrated water resources management (IWRM) based planning for water management for managing drought, water and livelihoods.

k) rainwater harvesting for storing the rainwater for later use in tanks and groundwater aquifers as a measure of climate resilience.

l) adoption of water use efficient technologies for domestic and industrial sectors as well.

m) efficient water use in industries by recycling water for use in its operations, rainwater harvesting within the industrial complex, limited or no groundwater use by industries, and adoption of innovative water saving technologies in water intensive industries like power plants, distilleries etc.

n) limiting the use of thermal energy in the industrial sector by shifting to renewable energy resources including solar and wind energy.

o) adoption of modern water saving technologies in the domestic sector including water efficient flushing systems, reuse of grey water from kitchens for toilet flushing and gardening.

p) modifying the water demands in the agriculture, domestic and industrial sectors through technological advancements

q) promoting groundwater recharge through percolation basins and injection wells thereby increasing the climate resilience for seasonal and extended periods of droughts.

Similarly, looking into the projected variability in the rainfall patterns resulting in variability in water availability in both space and time, the adaptation measures to sustain the agricultural operations in the study area without many hindrances may include,

a) Increasing the 'water use efficiency' through adoption of pressurised irrigation systems like drip and sprinkler irrigation, wherein the principle of '*more crop per drop*' can become a reality.

b) planning for 'life saving supplemental irrigation' during critical dry spells through use of existing water storage structures during kharrif season or by planning additional small surface water storage structures or by sustainable groundwater use depending on groundwater availability.

c) adoption of changes in 'cropping pattern' through cultivation of less water intensive crops in both kharif and rabi seasons, e.g. millets etc.

d) adoption of '*gram and mustard*' instead of wheat during rabi season in the event of water scarcity/drought encountered during the monsoon season.

e) changing the '*harvest period*' in accordance with the perceived shifts of season.

f) avoiding water intensive crops including rice, sugarcane and banana by importing these products from water rich region, which is basically '*virtual water transfer*'.

g) introduction of 'high yielding crop varieties' with low crop water requirement will help to increase the crop yields and farm incomes.

h) 'biotechnologies' to improve water-use efficiency of crops.

i) 'rainwater harvesting' and adoption of improved farm ponds for field water storage will help in creating favourable micro-environment and build-up of soil moisture in the vicinity of the farm pond. It can also be used to provide minimal supplemental irrigation during dry spell epochs.

j) 'reuse' of treated wastewater for irrigation will provide the much-needed water resources particularly during dry spells and drought years and prevent land being left fallow.

k) rational use of fertilisers and pesticides or adopting organic farming in a phased manner i.e. 'integrated nutrient management' comprising of organic, inorganic, bio-fertilizer and compost.

l) creation of conducive markets for organic produce for enhancing farm incomes.

m) crop insurance to farmers to protect them during crop failures.

n) creation of additional sources of livelihood like dairy farming, fish farming, handicrafts etc.

o) livestock management for health and diseases and livestock insurance.

p) composting of agricultural waste at farm and household level instead of burning. This will reduce the air pollution and GHGs emissions and also increase the soil fertility and crop yields.

q) use of physical control measures and bio-control agents/ bio-pesticide and crop management through ‘integrated pest and disease management’.

r) land use change based on ‘land capability classification’ to reduce further land degradation.

s) combating land degradation by ‘soil conservation measures.

t) improved agro-meteorological information network for weather forecasting and early warning system;

u) issuance of crop advisory in accordance with the weather forecasts.

6.0 CONCLUSIONS AND SCOPE OF FUTURE WORK

Water availability is most vital indicator needed for the socio-economic development of the agriculture based Indian economy where majority of the rural population is dependent on agriculture. Soil health is another important indicator for the sustained crop yields and farm incomes. However, the unplanned and overexploitation of both land and water resources has resulted in its degeneration. These anthropogenic activities coupled with the adverse effects of climate change may further exacerbate the already precarious situation in water stressed areas.

The comprehensive study carried out in Chambal basin falling in Madhya Pradesh, focused mainly on the investigation of the climate change signals, identification of the critical dry spell characteristics, supplemental irrigation planning during dry spells, evaluation of drought characteristics, investigation of possible desertification, climate change impact assessments on water availability and extreme events through hydrological modelling, drought vulnerability assessment, desertification vulnerability assessment, extreme climate vulnerability assessment and assessment of integrated vulnerability to combined effects of drought, desertification and extreme climate vulnerabilities. These investigations have been carried out for five time zones viz., baseline (1961-1990), present (1991-2015), near-term (2021-2040), mid-term (2041-2070) and end-term (2071-2100). The changes during the various time periods are given below,

- The average annual rainfall decreases from east to west with 1000-1100 mm in parts of Dewas, Vidisha, Sehore, Shajapur and Guna districts; 900-1000 mm in Agar, Indore, Ujjain, and parts of Dhar, Dewas and Shajapur districts; and 800-900 mm Neemuch, Mandsaur, Ratlam and parts of Ujjain, and Dhar districts. The average annual rainfall has been decreasing steadily during the last few decades. Very high variability of 23.4% has been observed in the seasonal rainfall, which may be responsible for the water stress in the region.
- The extreme events including the extreme rainfall (>200mm/day), very heavy rainfall (>100mm/day) heavy rainfall (>50mm/day) have increased in the study area substantially. The 1-day maximum rainfall varied between 104.0 mm to 520.0 mm, but not significant trends have been detected. The average daily rainfall intensity in the study area is 18.82 mm/day and varied between 18.83 mm/day during 1951 and 41.18 in 2015.
- The 5-day AMC has increased in majority of the study area comprising of Dhar, Indore, Dewas, Ujjain, Ratlam, Rajgarh, Bhopal, Vidisha, parts of Dewas, Agar, Mandsaur, Neemuch and Guna districts. There are 50 rainy days in a year and it varies between 30 and 83 days. There has been a decrease in the number of rainy days in the present period in 47 blocks out of 53 blocks.
- The mean temperature has also increased in the study area. The average increase in maximum temperature is at the rate of 1.05^{o}C/100 years, which is significant and in tune with IPCC projections. The very hot days (MaxT>40^{o}C) and hot days (MaxT>35^{o}C) have increased whereas the number of cold nights (MinT<10^{o}C) has decreased. The increase in the very hot night and hot night events are more pronounced in the districts bordering Rajasthan. Also, the decrease in the cold night events is highest again in the districts bordering Rajasthan.
- The ‘agricultural area’ and ‘land not suitable for agriculture’ has indicated a progressive decline in land availability for agricultural operations. The area under paddy cultivation and pulses has decreased substantially in

Mandsaur, Neemuch, Ratlam and Rajgarh districts. The number of macro-farmers (land holding>10 ha) and medium farmers (land holding of 4-10 ha) have decreased substantially whereas the number of marginal farmers (land holding < 1ha), small farmers (land holding of 1-2 ha) and semi-medium farmers (land holding of 2-4 ha) have increased considerably.

- The species distribution under the livestock population has changed considerably wherein the goat and sheep population has increased substantially in most of the districts. The barren areas have increased in Neemuch district along with barren patches in Mandsaur, Agar, Shajhapur and Rajgarh districts.
- More than 50% of the blocks are drought prone based on the probability analysis of annual rainfall. During the baseline period, 5 drought years identified include 1965, 1966, 1972, 1979 and 1989 during which more than 50% of the area was under drought whereas during the present period, only 2 drought years have been identified viz., 2000 and 2002.
- The number of extreme, severe and moderate soil moisture drought events is projected to increase in all future time periods, the highest being during the mid-term and end-term. Similarly, the soil moisture drought severity is projected to increase both during the mid-term and end-term periods. The soil moisture drought severity is projected to be higher under SSP585 scenario.
- The extreme surface water drought events are projected to increase substantially during the mid-term and end-term, with higher events during the mid-term under both scenarios in all the major river systems except for R. Shipra at Mahidpur. However, the severe surface water drought events are projected to decrease considerably during the near-term, mid-term and end-term in all the major river systems except for R. Shipra at Mahidpur where it is projected to increase in all future time periods.
- As compared to the baseline period, the number of groundwater droughts is expected to decrease during the near-term and thereafter increase during the mid-term and end-term time periods as observed during the baseline period. The groundwater drought severity is projected to increase both

during the mid-term and end-term periods as compared to the baseline period. The groundwater drought severity is projected to be higher under the SSP585 scenario.

- Generally, two CDS are observed in most of the years for which planning and provision of supplemental irrigation is necessary to prevent the crops from water stress during the crop growth period, which otherwise may lead to reduced crop yields. The total CDS events, as compared to the baseline period (44), are projected to increase substantially during mid-term (51) & end-term (51) under SSP245 scenario and 53 and 50 events during the mid-term and end-term under SSP585 scenario. The mean duration of CDS events is projected to increase from 17 days during the baseline period to 25 and 26 days during the near-term; 25 days during the mid-term; and 24 and 25 days during the end-term under SSP245 and SSP585 scenario respectively.
- The net supplemental irrigation requirement at Dhar for soyabean is projected to decrease under all future time zones. Similarly, the net supplemental irrigation requirement at Ujjain for maize is projected to decrease under all future time zones. This may be attributed to the higher water availability projected for future.
- The average annual stream flow is projected to increase substantially under all future time periods for all the major rivers including R. Chambal, R. Chambal, R. Shipra, R. Kalisindh, and R. Parwan. As compared to SSP245 scenario, average stream flow is projected to be higher under SSP585 scenario.
- The high flows are projected to increase substantially under all future time periods for all the major rivers in the study area, with the largest high flows during end-term. The high flows are projected to be higher under SSP585 scenario. Similarly, the low flows are projected to increase substantially under all future time periods for all the major rivers in the study area with the largest low flows during the mid-term.
- The Mohanpura dam shall be able to fulfil all water demands even if the rainfall deficit is 21.7% (757.25 mm). For a drought year, when rainfall

deficit is 25%, the unmet irrigation demand is limited to 8.2% only, which can be taken care of by appropriate supply-demand management. Similarly, Kundaliya dam shall be able to fulfil all water demands even if the rainfall deficit is 14.4% (827.50 mm). For a drought year, when rainfall deficit is 25%, the unmet irrigation demand is limited to 22.8% only, which can be taken care of by appropriate management measures.

- The management options during drought years include reduction in cropped area during rabi season based on storage available in dams; adoption of less water intensive crops during rabi season such as gram, barely and peas; deficit irrigation; and use of groundwater to meet the unmet demand.
- The study area has been under moderate drought vulnerability during the baseline and present periods and no considerable changes have been projected for the future. The area will continue to remain under the moderate vulnerability class as evaluated by DVI based on the spatial and spatio-temporal indicators.
- The desertification vulnerability in the study area falls under mild, moderate and severe vulnerability classes during all time periods. However, the vulnerability is projected to increase substantially in future time periods progressively, with more areas falling under the moderate vulnerability class. During the end-term, most of the area is under moderate vulnerability class with large patches under severe vulnerability in the districts of Neemuch and Mandsaur.
- The extreme climate vulnerability in the study area was under mild, moderate and severe vulnerability classes during the baseline, present and near-term periods. However, the extreme climate vulnerability is projected to increase with considerable area falling under the extreme vulnerability class. During the end-term, most of the study area is falling under extreme vulnerability class
- The integrated vulnerability based on the integration of the drought, desertification and extreme climate vulnerability is projected to increase substantially during the mid-term and end-term. During the end-term, most

of the study area is projected to be severely vulnerable under both future climate scenarios.

Based on the findings of this study appropriate adaptation and mitigation measures are required to adapt to the changing scenario and enhancing the climate resilience. The measures suggested for climate change adaptation and resilience in the water sector which is the primary driving resources for all other water related sectors include, increasing surface water storage capacity by provision of additional water infrastructure, removal of sediments from existing reservoirs, water diversions, diversifying the options for water supply, lining of canals, adoption of pressurized irrigation systems, sensor based irrigation water scheduling and reservoir gate operations, real-time weather monitoring, real-time flood forecasting, integrated water resources management, adoption of water use efficient technologies for domestic and industrial sectors, recycle and reuse of water and promoting groundwater recharge for increasing the climate resilience.

Similarly, the climate change adaptation measures suggested in the agriculture sector include, increasing the water use and application efficiency through drip and sprinkler irrigation systems, provision of life saving supplemental irrigation, cropping pattern change by cultivation of less water intensive crops like gram, mustard, millets etc., high yielding crop varieties' with low crop water requirement, rainwater harvesting and provision of farm ponds, reuse' of treated wastewater, 'integrated nutrient management through use of organic, inorganic, bio-fertilizer and compost, creation of additional sources of livelihood like dairy farming, fish farming, handicrafts, integrated pest and disease management, soil conservation measures to arrest and prevent further land degradation, improved agro-meteorological information network for weather forecasting and early warning system and issuance of crop advisory in accordance with the weather forecasts.

The future scope of work can include the impact of climate change on the future groundwater availability through groundwater modeling studies; field studies to assess the water use efficiency of pressurized irrigation systems adopted in the command areas of Mohanpura and Kundaliya dams; impact of climate change on the crop growth and crop yield of major crops like soyabean, wheat and gram; and

planning and design of alternative livelihoods, value addition and market linkages in non-command areas.

REFERENCES

1. Abbaspour, K. C., Vejdani, M. and Haghighat, S. (2007). SWATCUP calibration and uncertainty programs for SWAT. In Proc. Intl. Congress on Modelling and Simulation (MODSIM'07), 1603-1609. L. Oxley and D. Kulasiri, eds. Melbourne, Australia: Modelling and Simulation Society of Australia and New Zealand.
2. Abbaspour, K. C., Vejdani, M. and Haghighat, S. (2007). SWATCUP calibration and uncertainty programs for SWAT. In Proc. Intl. Congress on Modelling and Simulation (MODSIM'07), 1603-1609. L. Oxley and D. Kulasiri, eds. Melbourne, Australia: Modelling and Simulation Society of Australia and New Zealand.
3. Abramowitz. M. and Stegun, I. A. (1965). Handbook of mathematical functions: with formulas, graphs, and mathematical tables, Courier Corporation, 55.
4. Abramowitz. M. and Stegun, I. A. (1965). Handbook of mathematical functions: with formulas, graphs, and mathematical tables, Courier Corporation, 55.
5. Accepting the Standardized Precipitation Index: a calculation algorithm, Journal of American Water Resources Association, 35(2): 311-322. https://doi.org/10.1111/j.1752-1688.1999.tb03592.x
6. Adhikary, S. K., Das, S. K., Saha, G. C. and Chaki, T. (2013). Groundwater drought assessment for barind irrigation project in Northwestern Bangladesh, 20th International Congress on modelling and simulation. adelaide, Australia, 1–6, December 2013.
7. Adhikary, S. K., Das, S. K., Saha, G. C. and Chaki, T. (2013). Groundwater drought assessment for barind irrigation project in Northwestern Bangladesh, 20th International Congress on modelling and simulation. Adelaide, Australia, 1–6, December 2013.
8. Ahmadi, H. (2014). Examination of factors contributing to desertification. Forest and Grassland J., 62: 66-70.
9. Ahmadi, H., Azarnivand, H., Ekhtesasei, M. R. and Tazeh, M. (2009). A research on technogenic desertification indices (Case Study: Yazd). Desert., 17(3): 211-214.
10. Ahmed, K., Sachindra, D. A., Shahid, S., Iqbal, Z., Nawaz, N. and Khan, N. (2020). Multi-model ensemble predictions of precipitation and temperature using machine learning algorithms. Atmos. Res., 236, 1-20.
11. Akhtar-Schuster, M., Thomas, R. J., Stringer, L. C., Chasek, P. and Seely, M. (2011). Improving the enabling environment to combat land degradation: institutional, financial, legal and science-policy challenges and solutions. Land Degrad. Dev., 22: 299-312. doi: 10.1002/ldr.1058.

12. Alexander, L. V., Zhang, X., Peterson, T. C., Caesar, J., Gleason, B., Klein Tank, A. M. G., Haylock, M., Collins, D., Trewin, B., Rahimzadeh, F., Tagipour, A., Kumar, K. R., Revadekar, J., Griffiths, G., Vincent, L., Stephenson, D. B., Burn, J., Aguilar, E., Brunet, M., Taylor, M., New, M., Zhai, P., Rusticucci, M. and Vazquez-Aguirre, J. L. (2006). Global observed changes in daily climate extremes of temperature and precipitation. Journal of Geophysical Research – Atmospheres., 111.

13. Al-Faraj, F. A. M., Scholz, M. and Tigkas, D. (2014). Sensitivity of surface runoff to drought and climate change: application for shared river basins, water, 6: 3033-3048. doi:10.3390/w6103033.

14. Anctil, F., Larouche, W., Viau, A. A. and Parent, L. E. (2002). Exploration of the standardized precipitation index (SPI) with regional analysis. Canadian Journal of Soil Science, 82: 527-538.

15. Angelidis, P., Maris, F., Kotsovinos, N. and Hrissanthou, V. (2012). Computation of drought index SPI with alternative distribution functions. Water resources management., 26(9): 2453-2473.

16. Arabzadeh, R. S. M., Kholoosi, M. M. and Bazrafshan, J. (2016). Regional hydrological drought monitoring using principal components analysis. ASCE J. Irrig. Drain. Eng., 142(1): 04015029. DOI: 10.1061/(ASCE)IR.1943-4774.0000925.

17. Arnold, J. G. and Allen. P. M. (1999). Automated methods for estimating baseflow and groundwater recharge from streamflow records, J. American Water Resour. Assoc., 35(2): 411-424.

18. Arnold, J. G., Moriasi, D. N., Gassman, P. W., Abbaspour, K. C., White, M. J., Srinivasan, R., Santhi, C., Harmel, R. D., van Griensven, A., Van Liew, M. W., Kannan, N. and Jha M. K. (2012). SWAT: model use, calibration, and validation, Transactions of the ASABE, American Society of Agricultural and Biological Engineers, 55(4): 1491-1508.

19. Aufhammer, M., Ramanathan, V. and Vincent, J. R. (2012). Climate change, the monsoon, and rice yield in India. Clim. Change., 111:411-424. https://doi.org/10.1007/s10584-011-0208-4.

20. Baig, I. A., Chandio, A. A., Ozturk, I., Kumar, P., Khan, Z. A. and Salam, M. A. (2022). Assessing the long- and short-run asymmetrical effects of climate change on rice production: empirical evidence from India. Environ. Sci. Pollut. Res., 29: 34209-34230. https://doi.org/10.1007/ s11356-021-18014-z.

21. Basamma, K. A., Purohit, R. C., Bhakar, S. R., Kothari, M., Joshi, R. R., Sharma, D., Singh, P. K. and. Mittal, H. K (2017). Analysis of short-term droughts in the Mewar Region of Rajasthan by standard precipitation index. Int. J. Curr. Microbiol.App.Sci., (2017) 6(6): 182-192. https://doi.org/10.20546/ijcmas.2017.606.022.

22. Basharin, D., Polonsky, A. and Stankūnavičius, G. (2016). Projected precipitation and air temperature over Europe using a performance-based selection method of CMIP5 GCMs. J. Water Clim. Change., 7, 103-113.

23. Belal, A. A., El–Ramady, H. R., Mohamed, E. S. and Saleh, A. M. (2014). Drought risk assessment using remote sensing and GIS techniques, Arabian Journal of Geosciences, 7, 35-53, doi:10.1007/s12517-012-0707-2.

24. Benitez, J. B. and Domecq, R. M. (2014). Analysis of meteorological drought episodes in Paraguay. Climatic Change 127, 15-25 https://doi.org/10.1007/s10584-014-1260-7.

25. Bera, S. (2017). Trend analysis of rainfall in Ganga Basin, India during 1901-2000. Am. J. Clim. Chang., 6:116–131. https://doi.org/10.4236/ajcc.2017.61007.

26. Bhan, S. C. (2010). Climate change: an overview of observed trends in rainfall and temperature over India. Haryana J. Hortic. Sci., 39(1&2):42-47.

27. Bhardwaj, M., Kumar, P., Kumar, S., Dagar, V. and Kumar, A. (2022). A district level analysis for measuring the effects of climate change on production of agricultural crops, i.e., wheat and paddy: evidence from India. Environ Sci. Pollut. Res., 29:31861–31885. https://doi.org/10.1007/s11356-021-17994-2.

28. Bhatt, S., Pandit, B. A., Khan, J. N. Kumar, R. and Rehana, J. (2017). Water requirements and irrigation scheduling of Maize Crop using CROPWAT Model. Int. J. Curr. Microbiol. App. Sci., 6(11): 1662-1670. doi: https://doi.org/10.20546/ijcmas.2017.611.199.

29. Bhuniya, P., Das, P. and Maiti, R. (2020). Meteorological drought Study through SPI in three drought prone districts of West Bengal, India. Earth Systems and Environment, 4(3) DOI:10.1007/s41748-019-00137-6.

30. Bisaro, A., Kirk, M., Zdruli, P. and Zimmermann, W. (2014). Global drivers setting desertification research priorities: Insights from a stakeholder consultation forum. Land Degrad. Dev., 25: 5-16. https://doi.org/10.1002/ldr.2220.

31. Bouraima, Z., Weihua, W. and Chaofu (2015). Irrigation water requirements of rice using CROPWAT model in Northern Benin, Int. J. Agric. & Biol. Eng., 8(2): 58-64.

32. Bridges, E. M. and Oldeman, L. R. (1999). Global assessment of human-induced soil degradation. Arid Soil Research and Rehabilitation, 13:4, 319-325, DOI: 10.1080/089030699263212.

33. Brown, J. F., Wardlow, B. D., Tadesse, T., Hayes, M. J. and Reed, B. C. (2008). The Vegetation Drought Response Index (VegDRI): A new integrated approach for monitoring drought stress in vegetation. GIS Science and Remote Sensing., 45 (1): 16–46.

34. Burke, E. J. and Brown, S. J. (2008). Evaluating uncertainties in the projection of future drought. Journal of Hydrometeorology, 9: 292-299, doi: 10.1175/2007JHM929.1.

35. Burn, D. H. (1994). Hydrologic effects of climatic change in West Central Canada. J. Hydrology., 160, 53-70.

36. Calow, R., Robins, N., Macdonald, A. and Nicol, A. (1999). Planning for groundwater drought in Africa. In Proceedings of international conference on integrate drought management: lessons for Sub-Saharan Africa. IHP-V, Technical Documents in Hydrology, 35: 255-270.

37. Central Water Commission (1982). Report on identification of drought prone areas of 99-districts, New Delhi.

38. Chaudhari, K. N. and Dadhwal, V. K. (2004). Assessment of impact of drought 2002 on the production of major kharif and rabi crops using standardized precipitation index. Journal of Agrometeorology, 6: 10-15.

39. D'Odoricoa, P., Bhattachan, A., Davis, K. F., Ravi, S. and Runyan, C. W. (2013). Global desertification: drivers and feedbacks. Advances in Water Resources, 51: 326-344. https://doi.org/10.1016/j.advwatres.2012.01.013

40. Dash, S. and Maity, R. (2019). Temporal evolution of precipitation-based climate change indices across India: contrast between pre- and post-1975 features, Theor. Appl. Climatol., 138: 1667-1678. https://doi.org/10.1007/s00704-019-02923-8.

41. Dash, S. K. and Hunt, J. C. R. (2007). Variability of climate change in India. Curr. Sci., 93(6):782-788.

42. Dash, S. K. Saraswat, V., Panda, S. K. and Sharma, N. (2013). A study of changes in rainfall and temperature patterns at four cities and corresponding meteorological subdivisions over coastal regions of India, Glob. Planet. Change, 108: 175-194. http://dx.doi.org/10.1016/j.gloplacha.2013.06.004.

43. Dash, S. K., Pattnayak, K. C., Panda, S. K., Vaddi, D. and Mamgain, A. (2015). Impact of domain size on the simulation of Indian summer monsoon in RegCM4 using mixed convection scheme and driven by HadGEM2. Clim. Dyn., 44, 961-975. doi: 10.1007/s00382-014-2420-1

44. Diwakar, S. K., Kaur, S., Patel, N., (2014). Hydrologic assessment in middle narmada basin, India using SWAT Model. International Journal of Engineering Technology and Computer Research, 2(6): 10-25.

45. Domonkos, P. (2003). Recent precipitation trends in hungary in the context of larger scale climatic changes. Natural Hazards, 29: 255-271.

46. Douglas, E. M., Vodel, R. M. and Knoll, C. N. (2000). Trends in flood and low flows in United States: impact of spatial correlation., J. Hydrol., 240: 90-105.

47. Dutta, D. and Das, D. K. (2001). Water requirement of some crops grown under shallow perched water-table at Indira Gandhi Canal Command, Western Rajasthan. Journal of the Indian Society of Soil Science, 49(1): 1-6.

48. Dutta, D., Kundu, A., Patel, N. R., Saha, S. K. and Siddiqui, A. R. (2015). Assessment of agricultural drought in Rajasthan (India) using remote sensing derived vegetation condition index (VCI) and standardized precipitation index (SPI). The Egyptian Journal of Remote Sensing and Space Science, 18: 53-63. https://doi.org/10.1016/j.ejrs.2015.03.006.

49. Easterling, D. R., Alexander, L. V., Mokssit, A. and Detemmerman, V. (2003). CCI/CLIVAR workshop to develop priority climate indices. Bulletin of the American Meteorological Society, 84(10): 1403-1407.

50. Edwards, D. C. and McKee, T. B. (1997). Characteristics of 20th century drought in the United States at multiple time 15 scales. Climatology Report Number 97-2, Colorado State University, Fort Collins, Colorado.

51. Engel, B., Storm, D., White, M., Arnold, J. and Arabi, M. (2007). A hydrologic/water quality model application protocol. J. American Water Resour. Assoc. 43(5): 1223-1236.

52. FAO. (2000). Land resource potential and constraints at regional and country levels, World Soil Resources Report 90, FAO, Land and Water Development Division. Rome, 114.

53. FA.O. (2002). Land degradation assessment in dry lands: LADA, FAO, Rome.

54. Farokhnia, A., Morid, S. and Byun, H. R. (2010). Application of global SST and SLP data for drought forecasting on Tehran plain using data mining and ANFIS techniques. Theoretical and applied climatology, 104(1-2): 71-81.

55. Fitsume, D., Michael B. and Lijalem, K. (2015). Crop water requirement determination of chickpea in the central vertisol areas of Ethiopia using FAO CROPWAT model, Afr. J. Agric. Res., 10(7): 685-689.

56. Fitsume, D., Michael B. and Lijalem, K. (2015). Crop water requirement determination of chickpea in the central vertisol areas of Ethiopia using FAO CROPWAT model, Afr. J. Agric. Res., 10(7): 685-689.

57. Fleskens, L. and Stringer, L. C. (2014). Land management and policy responses to mitigate desertification and land degradation. Land Degrad. Dev., 25: 1-4.

58. Fowler, H. J., Blenkinsop, S. and Tebaldi, C. (2007). Linking climate change modelling to impacts studies: recent advances in downscaling techniques for hydrological modelling. Int. J. Climatol., 27: 1547-1578.

59. Frich, P., L. Alexander, P. Della-Marta, B. Gleason, M. Haylock, A. Tank, K. and Peterson, T. (2002). Observed coherent changes in climate extremes during the second half of the twentieth century. Clim. Res., 19: 193–212.

60. Gebrehiwot, T. Van der Veena, A. and Maathuis, B. (2011). Spatial and temporal assessment of drought in the Northern highlands of Ethiopia. International Journal of Applied Earth Observation and Geoinformation, 13(3): 309-321. https://doi.org/10.1016/j.jag.2010.12.002.

61. Ghosh, S. and Dutta, S. (2012). Impact of climate change on flood characteristics in Brahmaputra basin using a macro-scale distributed hydrological model. Journal of Earth System Sciences 121 (3), 637-657. DOI:10.2166/wcc.2020.186

62. Ghosh, S., Das, D., Kao, S. C. and Ganguly, A. R. (2012). Lack of uniform trends but increasing spatial variability in observed Indian rainfall extremes. Nat Clim Chang 2:86–91. https://doi.org/10.1038/NCLIMATE1327.

63. Gidey, E., Dikinya, O. and Sebego, R. et al. (2018). Analysis of the long-term agricultural drought onset, cessation, duration, frequency, severity and spatial extent using vegetation health index (VHI) in Raya and its environs, Northern Ethiopia. Environ. Syst. Res., 7 13 https://doi.org/10.1186/s40068-018-0115-z

64. Gogoi, B. and Lahon, D. (2022). Impact of climate change on Biodiversity of Northeast India: An overview, Indian. J. Appl. Pure. Bio., 37(2):322–331.

65. Golian, S., Mazdiyasni, O. and AghaKouchak, A. (2014), Trends in meteorological and agricultural droughts in Iran. Theor Appl Climatol., 119(3-4): 679-688. doi 10.1007/s00704-014-1139-6.

66. Guhathakurta, P. and Rajeevan, M. (2008). Trends in the rainfall pattern over India. Int. J. Climatol., 28:1453-1469.

67. Guhathakurta, P., Sreejith, O. P. and Menon, P. A. (2011). Impact of climate change on extreme rainfall events and food risk in India. J. Earth Syst. Sci., 120:359-373. https://doi.org/10.1007/s12040-011-0082-5.

68. Guttman, N. B. (1991). A sensitivity analysis of the palmer hydrologic drought index. Water Resources Bulletin., 27: 797-807.

69. Guttman, N. B. (1998). Comparing the palmer drought index and the standardised precipitation index. American Water Resources Association, 34: 113-121.

70. Guttman, N. B. (2007). Accepting the Standardized Precipitation Index: a calculation algorithm, Journal of American Water Resources Association, 35(2): 311-322. https://doi.org/10.1111/j.1752-1688.1999.tb03592.x

71. Hargreaves, G. H. and Samani, Z. A. (1982). Estimating potential evapotranspiration. Journal of Irrigation and Drainage Engineering, 108, 223-230.

72. Hatmoko, W., Radhika, Raharja, B., Tollenaar, D. and Vernimmen, R. (2015). Monitoring and prediction of hydrological drought using a drought early warning system in Pemali Comal river basin, Indonesia. Procedia Environmental Sciences, 24, 56-64. https://doi.org/10.1016/j.proenv.2015.03.009.

73. Hatmokoa, W., Radhika, Raharja, B., Tollenar, D. and Vernimmen, R. (2015). Monitoring and prediction of hydrological drought using a drought early warning system in Pemali-Comal River Basin, Indonesia, Procedia Environmental Sciences, 24: 56-64. https://doi.org/10.1016/j.proenv.2015.03.009.

74. Hatmokoa, W., Seizarwati , W. and Vernimmen, R. (2016). Comparison of TRMM satellite rainfall and APHRODITE for drought analysis in the

Pemali-comal River Basin, Procedia Environmental Sciences, 33: 187-195. https://doi.org/10.1016/j.proenv.2016.03.069.

75. Hayes, M. J., Svoboda, M. D., Wilhite, D. A. and Vanyarkho, O. V. (1999). Monitoring the 1996 drought using the standardized precipitation index. Bulletin of the American Meteorological Society. 80(3): 429-438.

76. Hayes, M. (2000). Revisiting the SPI: clarifying the process. Drought Network News., 12(1): 13-14.

77. Hayes, M. J., Alvord, C. and Lowrey, J. (2007). Drought indices. Feature Article, Intermountain West Climate Summary. 3(6): 2-6.

78. Helen, H. and Tobias, A. O. (1996). Grassroots indicators for desertification: experience and perspectives from Eastern and Southern Africa. IDRC, e-ISBN: 1552502864

79. Helsel, D. R. and Hirsch, R. M. (1992). Statistical methods in water resources, Vol. 49., Elsevier.

80. Higginbottom, T. P. and Symeonakis, E. (2014). Assessing land degradation and desertification using vegetation index data: current frameworks and future directions, Remote Sens.-Basel., 6: 9552- 9575.

81. Himanshu, S. K., Pandey, A. and Shrestha, P. (2017). Application of SWAT in an Indian river basin for modeling runoff, sediment and water balance, Environ. Earth Sci., 76:3. DOI 10.1007/s12665-016-6316-8.

82. Hirsch, R.M. and Slack, J.R., 1984. A nonparametric trend test for seasonal data with serial dependence. Water Resource Research, 20 (6), 727–732. doi:10.1029/WR020i006p00727

83. Horridge, M., Madden, J. and Wittwer, G. (2005). The impact of the 2002–2003 drought on Australia. Journal of Policy Modeling., 27(3): 285-308.

84. Huang, J., Zhang, G., Zhang, Y., Guan, X., Wei, Y. and Guo, R. (2020). Global desertification vulnerability to climate change and human activities, Land Degrad Dev., 1-12. DOI: 10.1002/ldr.3556.

85. Hughes, D. A., Kingston, D. G. and Todd, M. C. (2011). Uncertainty in water resources availability in the Okavango River Basin as a result of climate change. Hydrol. Earth Syst. Sci., 15, 931-941.

86. Hughes, D. A., Mantel, S. and Mohobane, T. (2014). An assessment of the skill of downscaled GCM outputs in simulating historical patterns of rainfall variability in South Africa. Hydrol. Res., 45, 134-147.

87. IPCC (2007). Climate change 2007: synthesis report. Contribution of working groups I, II and III to the fourth assessment report of the Intergovernmental Panel on Climate Change (IPCC). Geneva, Switzerland., 104.

88. IPCC (2014). Climate change 2014: synthesis report. Contribution of working groups I, II and III to the fifth assessment report of the Intergovernmental Panel on Climate Change (IPCC), Geneva, Switzerland, 151.

89. IPCC Climate Change 2021: The Physical Science Basis. Contribution of Working Group I to the Sixth Assessment Report of IPCC by Lee, J. Y., Marotzke, J., Bala, G., Cao, L., Corti, S., Dunne, J. P., Engelbrecht, F., Fischer, E., Fyfe, J. C., Jones, C., Maycock, A., Mutemi, J., Ndiaye, O., Panickal, S. and Zhou, T. (2021). Future Global Climate: Scenario-Based Projections and NearTerm Information. In Climate Change 2021: The Physical Science Basis. Contribution of Working Group I to the Sixth Assessment Report of the Intergovernmental Panel on Climate Change [Masson-Delmotte, V., Zhai, P., Pirani, A., Connors, S. L., Péan, C., Berger, S., Caud, N., Chen, Y., Goldfarb, L., Gomis, M. I., Huang, M., Leitzell, K., Lonnoy E., Matthews, J. B. R., Maycock, T. K., Waterfield, T., Yelekçi, O., Yu, R. and Zhou B. (eds.)]. Cambridge University Press, Cambridge, United Kingdom and New York, NY, USA, pp. 553-672, doi:10.1017/9781009157896.006.

90. Jafari, M., Ahmadi, H. and Abbasi, H. R. (2011). Evaluation of the effects of soil properties on desertification (Case study: Segzi Pediment of Isfahan, Iran). Desert., 16(1): 1-4.

91. Jain, S. K. and Kumar, V. (2012). Trend analysis of rainfall and temperature data for India, Current Science, 102 (1): 37-49.

92. Jain, M. and Sharma, S. T. (2014). Hydrological Modeling of Vamsadhara River Basin, India, Using SWAT. International Conference on Emerging Trends in Computer and Image Processing (ICETCIP 2014), Paltaya, 15-16 December 2014, 82-86.

93. Jain, S. K., Keshri, R., Goswami, A. and Sarkar, A. (2010). Application of meteorological and vegetation indices for evaluation of drought impact: a case study for Rajasthan, India. Nat. Hazards, 54: 643-656. https://doi.org/10.1007/s11069-009-9493-x.

94. Jain, S., Salunke, P., Mishra, S. K. and Sahany, S. (2019). Performance of CMIP5 models in the simulation of Indian summer monsoon. Theor. Appl. Climatol., 137, 1429-1447.

95. Jha, M., Gassman, P. W., Arnold, J. G., Secchi, S. S., Campbell, T. and King, C. L. (2004). Hydrologic modeling of upper mississippi river basin using SWAT, The Canadian Society for Engineering in Agricultural, Food and Biological Systems, Paper No. 042069

96. Kar, S. K., Nema, A. K., Singh, A., Sinham B. L. and Mishra, C. D. (2016). Comparative study of reference evapotranspiration estimation methods including artificial neural network for dry sub-humid agro-ecological region. Journal of Soil and Water Conservation, 15(3): 233-241

97. Kermen, E. and Gül, O. (2018). Comparing two streamflow-based drought indices. In proceedings of the 4th international conference water resources and wetlands. Tulcea, Romania, 5-9 September 2018, 190-195.

98. Keyantash, J. A. and Dracup, J. A. (2004). An aggregate drought index: Assessing drought severity based on fluctuations in the hydrologic cycle and surface water storage. Water Resour. Res., 40(9).

99. Khaladkar, R. M., Mahajan, P. N. and Kulkarni, J. R. (2009). Alarming rise in the number and intensity of extreme point rainfall events over the indian region under climate change scenario. RR 123, Indian Institute of Tropical Meteorology, ISSN 0252-1075. http://www.imdpune.gov.in/Clim_Pred_LRF_New/Reports. html.

100. Khan, F., Ali, S., Mayer, C., Ullah, H. and Muhammad, S. (2022). Climate change and spatio-temporal trend analysis of climate extremes in the homogeneous climatic zones of Pakistan during 1962-2019. PLOS ONE 17(7): e0271626. https:// doi.org/10.1371/journal.pone.0271626.

101. Khandelwal, S. S. and Dhiman, S. D. (2015). Irrigation water requirements of different crops in Limbasi branch canal command area of Gujarat, Journal of Agrometeorology, 17(1): 114-117.

102. Khare, D., Singh, R. and Shukla, R. (2014). Hydrological modeling of Barinallah watershed using ArcSWAT model. International Journal of Geology, Earth & Environmental Sciences, 4(1): 224-235.

103. Kharin, N., Tateishi, R. and Harahsheh, H. (2000). A new desertification map of Asia. Desertification Control Bulletin., 36: 5-17.

104. Khosravi, H., Zehtabian, G., Ahmadi, H. and Azarnivand, H. (2014). Hazard assessment of desertification as a result of soil and water recourse degradation in Kashan Region, Iran. Desert., 19 (1): 45-55.

105. Kjellstrom, T., Briggs, D., Freyberg, C., Lemke, B., Otto, M. and Hyatt, O. (2016). Heat, human performance, and occupational health: A key issue for the assessment of global climate change impacts. Annual Review of Public Health., 37, 97-112. https://doi.org/10.1146/annurev-publhealth-032315-021740

106. Komuscu, A. U. (1999). Using the SPI to analyze spatial and temporal patterns of drought in Turkey. Drought Network News, 11, 7-13.

107. Kosmas, C., Kairis, O., Karavitis, C., Ritsema, C., Salvati, L., Acikalin, S. and Belgacem, A. (2013). Evaluation and selection of indicators for land degradation and desertification monitoring: methodological approach. Environmental Management, 54(5): 951-970.

108. Kothyari, U. C. and Singh, V. P. (1996). Rainfall and temperature trends in India. Hydrol. Process., 10:357-372.

109. Krishnakumar, K. N., Rao, G. S. and Gopakumar, C. S. (2009). Rainfall trends in twentieth century over Kerala, India. Atmos. Environ., 43:1940-1944. https://doi.org/10.1016/j.atmosenv.2008.12.053.

110. Krishnamurthy, C. K. B., Lall, U. and Kwon, H. H. (2009). Changing frequency and intensity of rainfall extremes over India from 1951 to 2003. J. Clim., 22:4737-4746, https://doi.org/10.1175/2009JCL.

111. Kulanthaivelu, R. K., Iyyanar. S. and Ramakrishnan, S. (2022). Climate change and agricultural losses in India. Am. J. Econ. Sociol., 81(2): 339-358. https://doi.org/10.1111/ajes.12461.

112. Kumar, K. R., Sahai, A. K., Kumar, K.K., Patwardhan, S. K., Mishra, P. K., Revadekar, J. V., Kamala, K. and Pant, G. B. (2006). High-resolution

climate change scenarios for India for the 21st century. Curr. Sci., 90(3): 334-345.

113. Kumar, R., Musuuza J. L. VanLoon, A. F., Teuling, A. J., Barthel, R., TenBroek, J. Mai, J., Samaniego, L. and Attinger, S. (2016). Multiscale evaluation of the standardized precipitation index as a groundwater drought indicator. Hydrol. Earth Syst. Sci., 20: 1117-1131.

114. Kundu, S., Khare, D. and Mondal, A, (2017). Interrelationship of rainfall, temperature and reference evapotranspiration trends and their net response to the climate change in Central India. Theoret. Appl. Climatol., 130:879–900. https://doi.org/10.1007/ s00704-016-1924-5.

115. Kundzewicz, Z. W. and Robson, A. J. (2004). Change detection in hydrological records - a review of the methodology. Hydrol. Sci. J., 49(1): 7-19.

116. Ladisa, G., Todorovic, M. and Liuzzi, G. T. (2012). A GIS-based approach for desertification risk assessment in Apulia region, SE Italy. Physics and Chemistry of the Earth, Parts A/B/C., 49: 103-113.

117. Lal, R., Hall, G. F. and Miller, F. P. (1989). Soil degradation: I. Basic processes. Land Degrad. Dev. 11, 51–69. doi:10.1002/ldr.3400010106.

118. Lal, M. and Singh, S. K. (2001). Global warming and monsoon climate. Mausam, 52(1): 245-262.

119. Lana, X., Serra, C. and Burgue˜no, A. (2001). Patterns of monthly rainfall shortage and excess in terms of the standardized precipitation index for Catalonia (NE Spain). International Journal of Climatology 21: 1669-1691.

120. Lavado Contador, J. F., Schnabel, S., Gómez Gutiérrez, A. and Pulido Fernández, M. (2009). Mapping sensitivity to land degradation in Extremadura, SW Spain. Land Degrad. Dev., 20: 129-144.

121. Lin, N. F. and Tang, J. (2002). Geological environment and causes for desertification in arid-semiarid regions in China. Env. Geol., 41: 806-815. https://doi.org/10.1007/s00254-001-0456-0.

122. Lindstrom, G. and Bergstrom, S. (2004). Runoff trends in Sweden 1807-2002. Hydrological Sciences Journal, 49: 69-83.

123. Liu, W. T. and Kogan, F. N. (1996): Monitoring regional drought using the vegetation condition Index. International Journal of Remote Sensing, 17(14): 2761-2782. DOI: 10.1080/01431169608949106.

124. Lloyd-Hughes, B. and Saunders, M. A. (2002). A drought climatology for Europe. International Journal of Climatology, 22: 1571-1592. https://doi.org/10.1002/joc.846.

125. Lloyd-Hughes, B. and Saunders, M. A. (2002). Seasonal prediction of European spring precipitation from El Ni˜no-Southern Oscillation and local sea-surface temperatures. International Journal of Climatology, 22: 1-14.

126. Low, P. S. (2013). Economic and social impacts of desertification, land degradation and drought. White Paper I. UNCCD 2nd Scientific

Conference, prepared with the contributions of an international group of scientists. http://2sc.unccd.int.

127. Mahmood, R., Jia, S. and Zhu, W. (2019). Analysis of climate variability, trends, and prediction in the most active parts of the Lake Chad basin, Africa. Sci. Rep., 9, 6317 (2019). https://doi.org/10.1038/s41598-019-42811-9

128. Maraun, D., Wetterhall, F., Ireson, A. M., Chandler, R. E., Kendon, E. J., Widmann, M., Brienen, S., Rust, H. W., Sauter, T., Venema, V. K. C., Chun, K. P., Goodess, C. M., Jones, R. G., Onof, C., Vrac, M. and Thiele-Eich, I. (2010). Precipitation downscaling under climate change. Recent developments to bridge the gap between dynamical models and the end user. Rev. Geophys., 48(3).

129. Marengo, J. A., Torres, R. R. and Alves, L. M. (2017). Drought in Northeast Brazil-past, present, and future. Theoretical and Applied Climatology., 129(3-4): 1189-1200.

130. Mavromatis, T. (2007). Drought index evaluation for assessing future wheat production in Greece. International Journal of Climatology., 27(7): 911-924.

131. McKee, T. B. (1995). Drought monitoring with multiple time scales. In: Proceedings of 9th Conference on Applied Climatology. Boston., 1995.

132. McKee, T. B., Doesken, N. J. and Kleist, J. (1993). The relationship of drought frequency and duration to time scales. In: Proceedings of the 8th Conference on Applied Climatology. Boston, MA: American Meteorological Society.

133. McLeod, A. I., Hipel, K. W. and Bodo, B. A. (1991). Trend assessment of water quality time series, Water Resour. Bull., 19, 537-547.

134. Mehrotra, D. and Mehrotra, R. (1995). Climate change and hydrology with emphasis on the Indian subcontinent. Hydrol. Sci., J., 40(2):231-242. https://doi.org/10.1080/02626669509491406

135. Min, S. K., Kwon, W. T., Park, E. H. and Choi, Y. (2003). Spatial and temporal comparisons of droughts over Korea with East Asia. International Journal of Climatology, 23: 223-233.

136. Mishra, A. K. and Singh, V. P. (2010). A review of drought concepts. J. Hydrol., 391(1-2): 202-216.

137. Mishra, V., Bhatia, U. and Tiwari, A. D. (2020). Bias-corrected climate projections for South Asia from Coupled Model Intercomparison Project-6. Sci. Data., 7, 338. https://doi.org/10.1038/s41597-020-00681-1.

138. Misra, S., Sarkar, S., Mitra, P. and Shastri, H. K. (2022). Statistical downscaling of high resolution precipitation in India using convolutional long short term memory networks, research square, 1-24. doi: https://doi.org/10.21203/rs.3.rs-867282/v1.

139. Misra, V., Jayasankar, C. B., Mishra, A. K., Mitra, A. and Murugavel, P. (2022). Dynamic downscaling the South Asian Summer monsoon from a

global reanalysis using a Regional Coupled Ocean-Atmosphere Model, JGR. Atmospheres., https://doi.org/10.1029/2022JD037490.

140. Mondal, A., Khare, D. and Kundu, S. (2015). Spatial and temporal analysis of rainfall and temperature trend of India. Theoret. Appl. Climatol., 122:143–158. https://doi.org/10.1007/s00704-014-1283-z.

141. Morid, S., Smakhtin, V. and Bagherzadeh, K. (2007). Drought forecasting using artificial neural networks and time series of drought indices. Int. J. Climatol., 27(15): 2103-2111.

142. Murthy, C. S., SeshaSai, M. V. R., Prabir K. D., Naresh Kumar, M., Abhishek, C. and Dwivedi, R. S. (2010). Assessing agricultural drought vulnerability using time series rainfall and NDVI. NNRMS Bulletin, pp. 63-72.

143. Mustafa, S. T., Abdollahi, K., Verbeiren, B. and Huysmans, M. (2017). Identification of the influencing factors on groundwater drought and depletion in north-western Bangladesh. Hydrogeology Journal, 25(5): 1357-1375.

144. Nagireddy, N. R., Keesara, V. R., Venkata Rao, G., Sridhar, V., Srinivasan, R., (2023). Assessment of the impact of climate change on streamflow and sediment in the Nagavali and Vamsadhara Watersheds in India. Appl. Sci. 2023, 13, 7554. https://doi.org/10.3390/ app13137554.

145. Naidu, C. V., Rao, B. R. S. and Rao, D.V.B. (1999). Climatic trends and periodicities of annual rainfall over India. Meteorol. Appl., 6:395-404.

146. Nakicenovic, N. (2000). Greenhouse gas emissions scenarios. Technological Forecasting & Social Change., 65(3).

147. Nalbantis, I. and Tsakiris, G. (2009). Assessment of hydrological drought revisited. Water Resour. Manage., 23 (5): 881-897. https://doi.org/10.1007/s11269-008-9305-1.

148. Nandagiri, L. and Kovoor, G. M. (2006). Performance evaluation of reference evapotranspiration equations across a range of Indian climates. J. Irrig. Drain Eng., 132(3): 238-249.

149. Nasrollah, A., Pahlavanravi, A., Basirani, N., Ebrahimi, M. and Kharazmi, R. (2014). Assessment of land degradation and desertification with Use of IMDPA Model (Case Study; Chah-hashm Plain, Iran). International Journal of Advanced Biological and Biomedical Research., 2(10): 2644-2650.

150. Natasha L. D. (2011). Desertification extreme climatic indices analysis: case study-Southeast Africa. Centre for Natural Resources and the Environment., Lisbon.

151. National Drought Mitigation Center (NDMC), (2006). Monitoring drought. The Standardized Precipitation Index - Interpretation of SPI Maps, National Climatic Data Center. http://www.drought.unl.edu/monitor/interp.htm

152. Neitsch, S. L., Arnold, J. G., Kiniry J. R., Srinivasan, R. and Williams. J. R. (2002). Soil and water assessment tool, user manual, version 2000. Temple, Tex.: Grassland, Soil and Water Research Laboratory.

153. Nikoo S. (2011). The impact assessment of temporal variation of climatological and groundwater condition on desertification intensity in Garmsar Plain. J. Desert Manage.., 2: 39-48.

154. Nilawar, A. P. and Waikar M. L. (2019). Impacts of climate change on stream flow and sediment concentration under RCP 4.5 and 8.5: A case study in Purna river basin. India, Sci. Total Environ. 650(2): 2685-2696. doi: 10.1016/j.scitotenv.2018.09.334.

155. Odorico, P., Bhattachan, A., Davis, K. F., Ravi, S. and Runyan, C. W. (2013). Global desertification: Drivers and feedbacks. Adv. Water Resource., 51: 326-344.

156. OFDA (Office of U.S. Foreign Disaster Assistance).(2012). Annual report 2012, Office of U.S. Foreign Disaster Assistance, Washington D. C.

157. Oldeman, L. R. (1992). The global extent of soil degradation, ISRIC Bi-Annual Report., 19-36.

158. Oliveira A. S. E et al., (2021). Impacts of land use and land cover changes on hydrological processes and sediment ~ yield determined using the SWAT model, International Journal of Sediment Research, https://doi.org/10.1016/j.ijsrc.2021.04.002

159. Osman, M. A. A., Abdel-Rahman, E. M., Onono, J. O., Olaka, L. A., Elhag, M. M., Adan, M., Tonnang, H. E. Z. (2023). Mapping, intensities and future prediction of land use/land cover dynamics using google earth engine and CA- artificial neural network model. PLoS One, 18(7):e0288694. doi: 10.1371/journal.pone.0288694.

160. Owrangi, M. A., Adamowski, J., Rahnemaei, M., Mohammadzadeh, A. and Sharifan, R. A. (2011). Drought monitoring methodology based on AVHRR images and SPOT vegetation maps. J. Water Resour. Prot., 3(5), 325-334.

161. Pachauri, R. K., Meyer, L., Plattner, G. K. and Stocker, T. (2015). IPCC, 2014: Climate Change 2014: Synthesis Report. Contribution of Working Groups I, II and III to the Fifth Assessment Report of the Intergovernmental Panel on Climate Change., IPCC.

162. Pal, I. and Al-Tabbaa, A. (2009). Trends in seasonal precipitation extremes – an indicator of 'climate change' in Kerala, India. J. Hydrol., 367:62– 69. https://doi.org/10.1016/j.jhydrol.2008.12.025 Pal I, Al-Tabbaa A (2010) Regional changes in extreme monsoon rainfall defcit and excess in India. Dyn Atmos Oceans 49: 206-214. https://doi.org/10.1016/j.dynatmoce.2009.07.

163. Palmer, W. C. (1965). Meteorological drought. U.S. department of commerce. Weather Bureau, 58.

164. Panda, A. and Sahu, N. (2019). Trend analysis of seasonal rainfall and temperature pattern in Kalahandi, Bolangir and Koraput districts of Odisha, India. Atmos. Sci. Lett., https://doi.org/10.1002/asl.932.

165. Pandey, B. K., Khare, D., Kawasaki, A. and Meshesha, T. W. (2021). Integrated approach to simulate hydrological responses to land use dynamics and climate change scenarios employing scoring method in upper Narmada basin, India, J. Hydrol., 598: 123629. https://doi.org/10.1016/j.jhydrol.2021.126429.

166. Partal, T. and Kahya, E. (2006). Trend analysis in Turkish precipitation data. Hydrologic Process. 20, 2011-2026.

167. Patel, N. R., Chopra, P. and Dadhwal, V. K. (2007. Analyzing spatial patterns of meteorological drought using standardized precipitation index. Meteorological Applications, 14(4): 329 - 336.

168. Patra, J. P., Mishra, A., Singh, R. and Raghuwanshi, N. S. (2012). Detecting rainfall trends in twentieth century (1871–2006) over Orissa State, India. Clim. Change., 111:801–817. https://doi.org/10.1007/s10584-011-0215-5.

169. Pattnayak, K. C., Panda, S. K. and Dash, S. K. (2013). Comparative study of regional rainfall characteristics simulated by RegCM3 and recorded by IMD. Glob. Planet Change, 106: 111-122. doi: 10.1016/j.gloplacha.2013.03.006.

170. Pettorelli, N, Vik J. O., Mysterud, A., Gaillard, J. M., Tucker, C. J. and Stenseth, N. C. (2005). Using the satellite-derived NDVI to assess ecological responses to environmental change. Trends Ecol. Evol., 20(9): 503-10. doi: 10.1016/j.tree.2005.05.011.

171. Pichuka, S., Prasad R. R., Maity, R. and Kunstmann, H. (2017). Development of a method to identify change in the pattern of extreme streamflow events in future climate: Application on the Bhadra reservoir inflow in India, J. Hydrol.: Regional Studies., 9: 236-246.

172. Prajapati, V. K., Khanna, M. and Singh, M. (2022). PCA-based composite drought index for drought assessment in Marathwada region of Maharashtra state, India. Theor. Appl. Climatol. 149: 207-220 https://doi.org/10.1007/s00704-022-04044-1

173. Priyanka and Nagraj S. Patil (2016). Runoff modelling for Malaprabha Sub basin using SWAT hydrological model, Int. J. Res. Engg. Tech., 5(7): 35–38.

174. Quiring, S. M. and Ganesh, S. (2010). Evaluating the utility of the vegetation condition index (VCI) for monitoring meteorological drought in Texas. Agricultural and Forest Meteorology 150(3): 330-339. https://doi.org/10.1016/j.agrformet.2009.11.015.

175. Radhakrishnan, K., Sivaraman, I., Jena, S. K., Sarkar, S. and Adhikary, S. (2017). A climate trend analysis of temperature and rainfall in India. Clim Chang Environ Sustain 5(2):146-153. https://doi.org/10.5958/2320-642X.2017.00014.X.

176. Rahman, G., et al. (2018). Spatial and temporal variation of rainfall and drought in Khyber Pakhtunkhwa Province of Pakistan during 1971-2015. Arabian Journal of Geosciences, 11, Article No. 46. https://doi.org/10.1007/s12517-018-3396-7.

177. Rahman, A. M. A. E. (2023). An overview of land degradation, desertification and sustainable land management using GIS and remote sensing applications, Rend. Fis. Acc. Lincei., 34: 767–808. https://doi.org/10.1007/s12210-023-01155-3.

178. Rai, P. K., Singh, G. P. and Dash, S. K. (2020). Projected change and variability assessment of indian summer monsoon precipitation in South Asia CORDEX Domain Under High-Emission pathway. Pure Appl. Geophys., 177: 3475-3499. https://doi.org/10.1007/ s00024-019-02373-3.

179. Rehana, S., Yeleswarapu, P., Basha, G. and Munoz-Arriola, F. (2022). Precipitation and temperature extremes and association with large-scale climate indices: An observational evidence over India, J. Earth Syst. Sci., 131: 170. https://doi.org/10.1007/s12040-022-01911-3.

180. Reynolds, J. F., Smith, D. M., Lambin, E. F., Turner, B. L., Mortimore, M., Batterbury, S. P., Downing, T. E., Dowlatabadi, H., Fernandez, R. J., Herrick, J. E., Huber Sannwald, E., Jiang, H., Leemans, R., Lynam, T., Maestre, F. T., Ayarza, M. and Walker, B. (2007). Global Desertification: Building a science for dry land development. Sci., 316: 847- 851.

181. Rimkus, E., Stonevicius, E., Kilpys, J., Maciulyte, V., and Valiukas, D. (2017). Drought identification in the eastern Baltic region using NDVI. Earth Syst. Dynam., 8: 627-637. https://doi.org/10.5194/esd-8-627-2017.

182. Roxy, M. K., Ghosh, S., Pathak, A., Athulya, R,. Mujumdar, M., Murtugudde, R., Terray, P. and Rajeevan, M. (2017). A threefold rise in widespread extreme rain events over central India, Nature Communications., 1-11. doi: 10.1038/s41467-017-00744-9.

183. Rubio, J. L. and Recatala, L. (2005). The relevance and consequences of Mediterranean desertification including security aspects. 1-21.

184. Sahoo, R. N., Dutta, D., Khanna, M. et al. (2015). Drought assessment in the Dhar and Mewat Districts of India using meteorological, hydrological and remote-sensing derived indices. Nat. Hazards 77: 733-751 https://doi.org/10.1007/s11069-015-1623-z.

185. Sahu, M., Lahari, S., Gosain, A. K. and Ohri A. (2016). Hydrological modeling of Mahi Basin Using SWAT, Journal of Water Resource and Hydraulic Engineering, 5(3): 68-79.

186. Saini, D., Singh, O. and Bhardwaj, P. (2020). Standardized precipitation index based dry and wet conditions over a dry land ecosystem of north western India. Geol., Ecol. Landscapes, 1-13, 10.1080/24749508.2020.1833614.

187. Sakcali, M. S., Bahadir, H. and Ozturk, M. (2008). Eco-physiology of capparis spinosa L. A plant suitable for combating desertification. Pak. J. Bot., 40(4): 1481-1486.

188. Salas, J. D. (1993). Analysis and modeling of hydrologic time series. In Handbook of Hydrology (ed. Maidment, D. R.), McGraw-Hill, New York, 19.1-19.72.

189. Salavati, L., Zitti, M. and Ceccarelli, T. (2007). Integrating economic and environmental indicators in the assessment of desertification risk: a case study. Applied Ecology and Environmental Research, 6(1): 129-138.

190. Saleh, A. M., Elsharkawy, M. M., AbdelRahman, M. A. E. and Arafat, S. M. (2021). Evaluation of soil quality in arid Western Fringes of the Nile Delta for sustainable agriculture, Hindawi. Applied and Environmental Soil Science, Article ID 1434692: 1-17. https://doi.org/10.1155/2021/1434692

191. Salunke, P., Keshri, N. P., Mishra, S. M. and Dash, S. K. (2023). Future projections of seasonal temperature and precipitation for India. Front. Clim., 5: 1-9. DOI 10.3389/fclim.2023.1069994

192. Salunkhe, S. S., Bera, A. K., Rao, S. S., Venkataraman, V. R., Raj, U. and Murthy, Y. V. N .K. (2018). Evaluation of indicators for desertification risk assessment in part of Thar Desert Region of Rajasthan using geospatial techniques. J. Earth Syst. Sci., 127:116. https://doi.org/10.1007/s12040-018-1016-2.

193. Salvati, L., Zitti, M. and Perini, L. (2013). Fifty years on: long-term patterns of land sensitivity to desertification in Italy, land degrad. Dev., 27(2): 97-107.

194. Sarparast, M., Ownegh, M., Najafinejad, A. and Sepehr, A. (2018). An applied statistical method to identify desertification indicators in northeastern Iran. Geoenvironmental Disasters., 5(1): 3.

195. Satriagasa, M.C., Tongdeenok, P. and Kaewjampa, N. (2023). Assessing the implication of climate change to forecast future flood using SWAT and HEC-RAS Model under CMIP5 Climate Projection in Upper Nan Watershed, Thailand. Sustainability, 15: 5276. https:// doi.org/10.3390/su15065276

196. Schmidt, G. A., Ruedy, R., Hansen, J. E., Aleinov, I., Bell, N., Bauer, M., Bauer, S., Cairns, B., Canuto, V., Cheng, Y., Genio, A. D., Faluvegi, G., Friend, A. D., Hall, T. M., Hu, Y., Kelley, M., Kiang, N. Y., Koch, D., Lacis, A. A., Lerner, J., Lo, K. K., Miller, R. L., Nazarenko, L., Oinas, V., Perlwitz, J., Rind, D., Romanou, A., Russell, G. L., Sato, M., Shindell, D. T., Stone, P. H., Sun, S., Tausnev, N., Thresher, D. and Yao, M. S. Present-day atmospheric simulations using GISS model: comparison to in situ, satellite and reanalysis data. J. Climate, 19: 153-192.

197. Seiler, R. A., Hayes, M. E. and Bressan, L. (2002). Using the standardized precipitation index for flood risk monitoring. In: International Journal of Climatology, 22: 1365-1376.

198. Senatore, A., Hejabi, S., Mendicino, G., Bazrafshan, J. and Irannejad, P. (2018). Climate conditions and drought assessment with the palmer drought severity Index in Iran: evaluation of CORDEX South Asia climate projections (2070–2099). Climate Dynamics, 1-27.

199. Seneviratne, S. I., Nicholls, N., Easterling, D., Goodess, C. M., Kanae, S., Kossin, J., Luo, Y., Marengo, J., McInnes, K., Rahimi, M., Reichstein, M., Sorteberg, A., Vera, C. and Zhang, X. (2012). Changes in climate extremes and their impacts on the natural physical environment. In: Managing the Risks of Extreme Events and Disasters to Advance Climate Change Adaptation A Special Report of Working Groups I and II of the Intergovernmental Panel on Climate Change (IPCC). Cambridge University Press., Cambridge, UK, and New York, NY, USA, 109-230.

200. Shabbar, A. and Bonsal, B. (2003). An assessment of changes in winter cold and warm spells over Canada. Nat. Hazards, 19: 173-188.

201. Shafer, B. and Dezman, L. (1982). Development of a Surface water supply index (SWSI) to assess the severity of drought conditions in snowpack runoff areas. Proceedings of the Western Snow Conference. 164-175.

202. Shah, R., Manekar, V. L., Christian, R. A. and Mistry, N. J. (2013). Estimation of reconnaissance drought index (RDI) for Bhavnagar District, Gujarat, India. Int. J. Environ Ecol. Eng., 7(7): 507-510. http://schol ar.waset.org/1307-6892/16568.

203. Shahid, S. and Hazarika, M. K. (2010). Groundwater droughts in Nort-Western districts of Bangladesh, Water Resources Management, 24(10): 1989-2006.

204. Shakerian, N., Zehtabian, G. R., Azarnivand, H. and Khosravi, H. (2011). Evaluation of desertification intensity based on soil and water criteria in Jarghooyeh region. Desert, 16(1): 23-32.

205. Shewale, M. P. and Shravan, K. (2005). Climatological features of drought incidences in India, Meteorological Department Report, National climate centre, Office of the additional director general of meteorology (Research)., India Meteorological Department, Pune.

206. Shivhare, V., Goel, M. K., Singh, C. K. (2014). Simulation of surface runoff for upper Tapi sub catchment area (Burhanpur watershed) using SWAT. Int. Arch. Photogramm Remote Sens. Spatial In.. Sci., 40(8): 391. https://doi.org/10.5194/isprsarchives-XL-8-391-2014.

207. Shukla, S. and Wood, A. W. (2008). Use of a standardized runoff index for characterizing hydrologic drought. Geophysical research letters, 35(2).

208. Singh, M. (2012). Challenges and opportunities for sustainable viability of marginal and small farmers in India. Agric. Situat. India., 3:1 33–142.

209. Singh, R., Arya, D. S., Taxak A. K. and Vojinovic, Z. (2016). Potential impact of climate change on rainfall intensity-duration-frequency curves in Roorkee, India. Water Resour. Manage., 30(13): 4603-4616. doi: 10.1007/s11269-016-1441-4.

210. Singh, R. P. Roy, S. and Kogan, F. N. (2003). Vegetation and temperature condition indices from NOAA AVHRR data for drought monitoring over India. Int. J. Remote Sens., 24: 4393-4402. https://doi.org/10.1080/0143116031000084323.

211. Sonmez, F. K., Komuscu, A. U. and Erkan, A. (2005). An analysis of spatial and temporal dimension of drought vulnerability in turkey using the standardized precipitation index. Nat. Hazards, 35, 243-264. https://doi.org/10.1007/s11069-004-5704-7

212. Sood, A. and Smakhtin, V. (2015). Global hydrological models: a review. Hydrol. Sci. J., 60, 549-565.

213. Spinoni, J., Naumann, G., Carrao, H., Barbosa, P. and Vogt, J. (2013). World drought frequency, duration, and severity for 1951-2010. Int. J. Climatol., 34(8): 2792-2804.

214. Stephenson, D. B., Douville, H. and Rupakumar, K. (2001). Searching for a fngerprint of global warming in the Asian summer monsoon. Mausam, 52(1): 213-220.

215. Stute, M., Clement, A. and Lohmann, G. (2001). Global climate models: past, present, and future. Proc. Natl. Acad. Sci., USA., doi: 10.1073/pnas.191366098.

216. Svoboda, M., Lecomte, D. G., Hayes, M., Heim, R. D., Gleason, K. N., Angel, J., Rippey, B. D., Tinker, R. H., Palecki, M., Stooksbury, D. D., Miskus, D. D. and Stephens, S. T. (2002). The Drought monitor. Bulletin of American Meteorological Society, 83(8): 1181-1190. doi:10.1175/1520-0477-83.8.1181.

217. Svoboda Mark, D. (2013). National drought mitigation centre, University of Nebraska-Lincoln, U.S. Drought monitor.

218. Swain, S., Mishra, S. K., Pandey, A., Pandey, A. C., Jain, A., Chauhan, S. K. and Badoni, A. K. (2022). Hydrological modelling through SWAT over a Himalayan catchment using high-resolution geospatial inputs, Environmental Challenges, 8: 100579. https://doi.org/10.1016/j.envc.2022.100579

219. Swain, S., Taloor, A. K., Dhal, L., Sahoo, S. and Al-Ansari, N. (2022). Impact of climate change on groundwater hydrology: a comprehensive review and current status of the Indian hydrogeology. Appl. Water. Sci., 12:120. https://doi.org/10.1007/s13201-022-01652-0.

220. Swetalina, N. and Thomas, T. (2016). Evaluation of hydrological drought characteristics for Bearma Basin in Bundelkhand Region of Central India, Procedia Technology, 24: 85 - 92. https://doi.org/10.1016/j.protcy.2016.05.013.

221. Sylwia, T. and Schnarr, E. (2014). A review of downscaling methods for climate change projections. Technical Report, US Agency for International Development.

222. Tabari, H., Nikbakht, J. and Hosseinzadeh Talaee, P. (2013). Hydrological drought assessment in Northwestern iran based on streamflow drought index (SDI). Water Resour. Manage. 27: 137-151 (2013). https://doi.org/10.1007/s11269-012-0173-3.

223. Tabari, H., Paz, S. M., Buekenhout, D. and Willems, P. (2021). Comparison of statistical downscaling methods for climate change

impact analysis on precipitation-driven drought. Hydrol. Earth Syst. Sci., 25: 3493–3517, https://doi.org/10.5194/hess-25-3493-2021.

224. Tallaksen, L. M. and Van Lanen, H. A. J. (2004). Hydrological drought: processes and estimation methods for streamflow and groundwater. developments in water Science. 48, Elsevier Science B.V., 579.

225. Taskiris, G., Nalbantis, I., Vangelis, H., Verbeiren, B., Huysmans, M., Tychon, B., Jacquemin, I., Canters, F., Vanderhaegen, S., Engelen, G., Poelmans, L., Becker, P. and Batelaan, O. (2013). A system-based paradigm of drought analysis for operational management. Water Resour, Manage., 27 (15): 5281-5297. https://doi.org/10.1016/j.jhydrol.2014.10.059

226. Tavares, J. (2012). Assessment and mapping of desertification sensitivity in an insular sahelian mountain region-case study of the Ribeira Seca Watershed, Cape Verde. In EGU. General Assembly Conference Abstracts., 14: 7742.

227. Taylor, C. H. and Loftis, J. C. (1989). Testing for trend in lake and groundwater quality time series. Water Resour. Bull., 25 (4): 715-726.

228. Tebaldi, C. and Knutti, R. (2007). The use of the multi-model ensemble in probabilistic climate projections. Phil. Trans. Roy. Soc. A, Math. Phys. Eng. Sci., 365: 2053-2075.

229. Temesgen, B., Eching, S., Davidoff, B. and Frame, K. (2005). Comparison of some reference evapotranspiration equations for California. J. Irrig. Drain Eng., 131(1):73–84.

230. Thomas, T., Gunthe, S. S. and Sudheer, K. P. (2014). Analysis of monsoon rainfall variability over Narmada basin in central India: Implication of climate change, Journal of Water and Climate Change, 6(3): 615-627.

231. Thomas, T., Gunthe, S. S., Ghosh, N. C. and Sudheer, K. P. (2015). Analysis of monsoon rainfall variability over Narmada basin in central India: Implication of climate change. J. Water, Clim. Chang., 6(3): 615-627. https://doi.org/10.2166/wcc.2014.041.

232. Tigkas, D., Vangelis, H. and Tsakiris, G. (2012). Drought and climate change impact on streamflow in small watersheds. Sci Total Environ 440: 33-41. https://doi.org/10.1016/j.scitotenv.2012.08.035.

233. Townshend, J. and Justice, C. (1995). Analysis of the dynamics of African vegetation using normalised difference vegetation index, Int. J. Remote Sens., 7(11): 1435-1445. DOI:10.1080/01431168608948976.

234. Trzaska, S. and Schnarr, E. (2014). A review of downscaling methods for climate change projections. United States Agency for International Development by Tetra Tech ARD., 1-42.

235. Tsakiris, G., Pangalou, D. and Vangelis, H. (2007). Regional drought assessment based on the reconnaissance drought index (RDI). Water Resour. Manage., 21(5): 821-833.

236. UNISDR (United Nations International Strategy for Disaster Reduction Secretariat). (2011). Global assessment report on disaster risk reduction. Geneva, Switzerland.

237. Uniyal, B, Jha, M. K. and Verma, A. K. (2015). Assessing climate change impact on water balance components of a river basin using SWAT model. Water Resour. Manage., 29: 4767-4785.

238. Van Griensven, A. and Bauwens. W. (2003). Multi objective auto calibration for semi distributed water quality models. Water Resour. Res., 39(12): 1348-1356.

239. Van Lanen, H. A. J. and Peters, E. (2000). Definition, effects and assessment of groundwater droughts. In drought and drought mitigation in Europe; Vogt, J. V., Somma, F., Eds.; Advances in Natural and Technological Hazards Research; Springer: Dordrecht, The Netherlands, 49-61.

240. Van Liew, M. W., Arnold J. G. and Bosch. D. D. (2005). Problems and potential of auto calibrating a hydrologic model. Trans. ASAE 48(3): 1025-1040.

241. Van Lynden, G. W. J. and Oldeman, L. R. (1997). Assessment of the status of human-induced soil degradation in south and southeast Asia (ASSOD), International Soil Reference and Information Centre.

242. VanLanen, H. A. J. and Peters, E. (2000). Definition, effects and assessment of groundwater droughts. In Drought and Drought Mitigation in Europe, JV Vogt, F Somma (eds). Kluwer Academic Publishers: Dordrecht, 49-61.

243. Vicente-Serrano, S. M. (2006). Differences in spatial patterns of drought on different time scales: An Analysis of the Iberian Peninsula. Water Resour. Manage. (20): 37-60 https://doi.org/10.1007/s11269-006-2974-8.

244. Vicente-Serrano, S. M., Beguería, S. and López-Moreno, J. I. (2010). A multi scalar drought index sensitive to global warming: the standardized precipitation evapotranspiration index. Journal of Climate., 23(7): 1696-1718.

245. Vogt, J., Barbosa, P., Hofer, B., Magni, D., Jager, A. D., Singleton, A., Horion, S., Sepulcre, G., Micale, F., Sokolova, E., Calcagni, L., Marioni, M. and Antofie, T. E. (2011). Developing a european drought observatory for monitoring, assessing and forecasting droughts across the European continent. In AGU Fall Meeting Abstracts.

246. Von Storch, H. and Navarra, A. (1995). Analysis of climate variability – applications of statistical techniques, springer-verlag, New York.

247. Wang, X. M., Zhang, C. X., Hasi, E. and Dong, Z. B. (2010). Has the three norths forest shelterbelt program solved the desertification and dust storm problems in arid and semiarid China. J. Arid Environ., 74: 13-22.

248. Wang, X., Song, J., Xiao, Z., Wang, J. and Hu, F. (2022). Desertification in the Mu Us sandy land in China: response to climate change and human activity from 2000 to 2020. Geography and

Sustainability, 3(2): 177-189. https://doi.org/10.1016/j.geosus.2022.06.001.

249. Wilhite, D. A. and Glantz, M. H. (1985). Understanding: the drought phenomenon: the role of definitions. Water International., 10(3): 111-120.

250. Wilhite, D. A. (1992). Drought. Encyclopedia of earth system science, vol. 2, edited by William A. Nierenberg., 81-92.

251. Wilhite, D. A. (2000). Drought as a natural hazard: concepts and definitions. Published in Drought: A Global Assessment, Vol. I, edited by Donald A. Wilhite., 3-18.

252. Wilhite, D. A. (2005). Drought and water crises: science, technology and management issues. CRC Press.

253. Wilhite, D. A. and Pulwarty, R. S. (2005). Drought and water crises: science, technology, and management issues, 389-398. CRC Press, Boca Raton, Florida

254. Wilk, J. and Hughes, D. A. (2002). Simulating the impacts of land-use and climate change on water resource availability for a large south Indian catchment. Hydrol. Sci. J., 47(1): 19-30. https://doi.org/10.1080/02626660209492904.

255. World Meteorological Organization (WMO) (2006). United States. Office of Mission to Planet Earth. Scientific assessment of ozone depletion.

256. Wu, H., Hayes, M. J., Wilhite, D. A. and Svoboda, M. D. (2005). The effect of the length of record on the standardized precipitation index calculation. International Journal of Climatology, 25: 505-520

257. Wu, H., Svoboda, M. D., Hayes, M. J., Wilhite, D. A. and Wen, F. (2007). Appropriate application of the standardized precipitation index in arid locations and dry seasons. Int. J. Climatol., 27(1): 65-79.

258. Xie, Y., Mei, Y., Guangjin, T. and Xuerong, X. (2005). Socio-economic driving forces of arable land conversion: A case study of Wuxian City, China. Global Environmental Change, 15(3): 238-252.

259. Xiong, L. and Guo, S. (2004). Trend test and change-point detection for the annual discharge series of the Yangtze River at the Yichang hydrological station, Hydrological Sciences Journal, 49(1): 99-112

260. Yaduvanshi, A., Nkemelang, T., Bendapudi, R. and New, M. (2021). Temperature and rainfall extremes change under current and future global warming levels across Indian climate zones, Weather and Climate Extremes, 31, ISSN 2212-0947, https://doi.org/10.1016/j.wace.2020.100291.

261. Yang, J., Tian, H., Pan, S., Chen, G., Zhang, B. and Dangal, S. (2018). Amazon drought and forest response: Largely reduced forest photosynthesis but slightly increased canopy greenness during the extreme drought of 2015/2016. Global Change Biology, 24(5): 1919-1934.

262. Yu, Y. S., Zou, S. and Whittemore, D. (1993). Non-parametric trend analysis of water quality data of river in Kansas, J. Hydrol., 150: 61-80.

263. Yue, S., Pilon, P. J., Phinney, B. and Cavadias, G. (2002). Patterns of trend in Canadian stream flow. Proceedings of 58th Annual Eastern Snow Conference, CGU, 14-17 May, Ottawa, Ontario, Canada.

264. Zehtabian, G., Karimi, K., Fard, S. N. N., Mirdashtvan, M. and Khosravi, H. (2013). Comparability analyses of the SPI and RDI meteorological drought indices in South Khorasan province in Iran. International journal of Advanced Biological and Biomedical Research, 1(9): 981-992

265. Zhang, D. Liu, X. and Bai, P. (2019). Assessment of hydrological drought and its recovery time for eight tributaries of the Yangtze River (China) based on downscaled GRACE data. J. Hydrol., 568: 592-603.

266. Zhang, X., Alexander, L., Hegerl, G. C., Jones, P., Tank, A. K., Peterson, T. C., Trewin, B. and Zwiers F. W. (2011). Indices for monitoring changes in extremes based on daily temperature and precipitation data. Clim. Change., 2: 851-870.

267. Zhang, X., Vincent, L. A., Hogg, W. D. and Niitsoo, A. (2000). Temperature and precipitation trends in Canada during the 20th century, Atmosphere-Ocean., 38 (3): 395-429. doi: 10.1080/07055900.2000.9649654.

268. Zhu, Y., Liu, Y., Ma, X., Ren, L. and Singh, V.P. (2018). Drought analysis in the yellow river basin based on a short-scalar palmer drought severity index. Water, 10: 1526.

269. Zhu, Z., Yang, C., Cao, M., Liu, K. and Yang, L. (2007). Analysis on the soil factor and physiological response of the plants in the process of sandy desertification on grassland. Acta. Ecologica Sinica., 27(1): 48-57.

270. Zolfaghari, F., Khosravi, H., Shahriyari, A., Jabbari, M. and Abolhasani, A. (2019). Hierarchical cluster analysis to identify the homogeneous desertification management units. PLoS ONE, 14(12): e0226355. https://doi.org/10.1371/journal. pone.0226355.

APPENDIX-A Project summary

Table A.1: Summary

Project objectives			
Objectives as per project document		Revised objective	Reasons for revision
i) Assessment of climate change signals in Chambal basin. ii) Evaluation of drought characteristics and investigation of the desertification. iii) Hydrologic modeling for simulation of the hydrological processes in the basin. iv) Assessment the impact of climate change under projected climate scenarios on the future water availability, drought and desertification. v) Evaluation of the impacts of upcoming irrigation projects on the drought and desertification. vi) Integrated assessment of vulnerability to drought, desertification and climate change.		None	None
***Manpower* deployed (against sanctioned manpower)**			
Sanctioned		Deployed	
Designation	Person months	Designation	Person months
JRF	48	JRF	42
Infrastructure/ equipment			
Planned (as per project proposal)		Developed/ procured	Reasons for deviation
i) Laptop- ZBook Mobile Workstation ii) Desktop & Accessories iii) Camera iv) Software/Portable hard disks/Pen drives/Accessories		Not procured Procured Not procured Procured XLSTAT for 1 year – Online license & pen drives	Administrative delays and no approvals for rest of the listed items
Field work			
Planned (as per project proposal)		Completed	Reasons for deviation
Soil sampling, infiltration and hydraulic conductivity tests		Completed	
Workshop/ Capacity building/ technology transfer			
Planned (as per project proposal)		Organized	Reasons for deviation
Stakeholder Workshops - 4		Organized - 2	Could not be organized due to Covid & non-availability of officials in monsoon season
Study area			
Planned		Extended	
Chambal basin in Western M.P.		None	
New data generated in the project			
Planned (as per project proposal)		Achievement	Reasons for deviation
None			

Envisaged contribution of the project		
Planned (as per project proposal)	Contribution made	Reasons for deviation
1) The results of the analysis will be helpful for the planning development of both rain-fed and irrigated agriculture and focusing more resources in the hotspots to be identified by the vulnerability analysis. 2) This study shall address the issues related to future climate change impacts on water availability, the likely scenario under extreme events, investigate for any desertification aspects and shall suggest measures to address these impacts through various adaptation mechanisms.	All	None
How research outcome benefited the end user department and society		
Planned (as per project proposal)	Benefit derived	Reasons for deviation
1) The research outcome shall benefit the various stakeholders, decision makers, and the scientific community by helping them to understand the issues of climate change and help in developing water resources management strategies under changing climate, droughts and the likely possibilities of desertification. 2) The outcomes of the study shall be published in International Conferences and Journals which will be helpful to the scientific community in addressing similar type of issues in other parts of the country and the world. 3) The recommendations of the study will help the State to harness and develop the water resources in a sustainable manner by having a foresight into the water availability and occurrence of extreme events under the future scenarios of climate change.	All; Publications in three international conferences and one more submitted in an upcoming international conference. Communication to reputed high impact factor journals to be imitated soon after the final report submission. State can plan to harness and utilize the water resources based on the climate change impacts assessments, vulnerability assessments and the suggested adaptation strategies.	None
End-of-project deliverables		
Planned (as per project proposal)	Achieved	Reasons for deviation
1) A comprehensive methodology for the integrated assessment of climate change, vulnerability due to climate change and desertification 2) Impact of climate change on the water resources in Chambal basin. 3) Integrated drought vulnerability map for the study area based on multiple indicator approach.	All	None

4) Suggestion of adaptation measures					
Outsourcing (>1 lakh)/ consultancy (All)					
Consultant (name and qualifications), organization / outsource agency		Work assigned		Estimated cost Rs	Actual cost Rs
None		None			
Financial achievement					
S No	Head	Approved budget	Approved revised budget	Final expenditure	Reasons for deviation
1	Remuneration/Emoluments for Manpower etc.	1526400	NA	1202187	
2	Travelling Expenditure	785000	NA	176513	
3	Infrastructure/Equipment	615000	NA	109634	
4	Experimental Charges/Field work/Consumables	400000	NA	129149	
5	Capacity building/Technology transfer	500000	NA		
6	Contingency	211320	NA	22443	
7	Outsourcing/ consultancy	400000	NA		
	Total	**4440000**	**NA**	**1639926**	

Table A.2: Quantitative outcome

i. Research papers published/ submitted		
S No	Research paper (National/ International Journal/ conferences/ symposium/ workshop/ seminar)	Impact factor for Journal
1.	Development of a Framework for Integrated Assessment of Drought Vulnerability in Chambal basin in Western Madhya Pradesh, India in International Conference on Water and Environmental Management (WEM-2022), CWRDM, Kozhikode, 22-24 June 2022.	
2.	Evaluation of Critical Dry Spells and Supplemental Irrigation Planning for Chambal basin in Western Madhya Pradesh, India, Roorkee Water Conclave (RWC-2022), 2-4 March, 2022.	
3.	Detection of Climate Change Signals in the Historical Climate Datasets for Chambal basin in Madhya Pradesh, 2nd International Conference on Sustainable Water Management, Pune, Maharashtra, 6-8 November 2019.	

Reports/Monographs/Internal publications brought out	
S. No.	Reports/Monographs/Internal publications
1	One Status Report and Three Interim Reports at the end of each completed year. Final Report is being submitted now.

ii. New techniques/models/ software/ knowledge developed, if any

Developed a framework for integrated assessment of drought vulnerability, desertification vulnerability and extreme climate vulnerability.

iii. Web site/ application developed

Name	Web address	Server location	Launch date	Details of information available
None				

iv. Patents filed/awarded, if any

Workshop/ conferences/ seminars/capacity building programmes organised

S. No.	Topic	Dates, duration, No. of participants	Report published (Y/N)
	None		

v. Stake holders feedback and action taken on constructive feed back

S No.	Feedback received	Action taken
Stake holder meet (Topic and date)		
1.	Stakeholders Workshop on "Impact Assessment of the Upcoming Irrigation Projects and Climate Change on the Drought and Desertification Scenario for Chambal Basin in Western Madhya Pradesh" on 27.03.2019	The stakeholders from various line departments, and field organizations appreciated the work done in the study which was initiated based on the requirement of WRD, M.P. for such study in the region. The member suggested investigating the groundwater droughts in the region which has been conducted. The Status Report and the progress of the study were showcased.
2.	Stakeholders Workshop on "Impact Assessment of the Upcoming Irrigation Projects and Climate Change on the Drought and Desertification Scenario for Chambal Basin in Western Madhya Pradesh" on 08.01.2021	The stakeholders were satisfied with the progress of the study and the thrust towards developing a framework for assessment of integrated vulnerability as well as drought vulnerability, desertification vulnerability and extreme climate vulnerability. The Interim Reports and the progress of the study were showcased and appreciated by the participants.

vi. Field observations obtained, thematic maps generated (water quality and

salinity, isotope, soil moisture, stage and discharge, sediment, water level, river cross sections, geophysical/ resistivity survey, hydrogeological investigations etc.)

S No	Parameter, frequency, period, groundwater/ river/ tank/ hand pump/ spring/ sea-water	Number (planned)	Numbers (measured)
	Thematic maps of land use land cover, soil type, DEM have been prepared	NA	NA

vii. Field installations (piezometers, river stage/ discharge, soil moisture etc.)

S. No	Name, make/ model	Unit price, total price, quantity	Date of installation	% utilization	Remarks regarding maintenance/ breakdown
	None				

viii. Equipment/ software purchased

a. Equipment purchased

S. No	Name, make/ model	Unit price, total price, quantity	Date of installation	% utilization	Remarks regarding maintenance/ breakdown
1.	One HP Desktop with monitor	52198/-	11.12.2019	100%	None

b. Software purchased

S. No	Name, version, license	Unit price, total price, quantity	Date of installation	% utilization	Remarks regarding maintenance/ breakdown
1.	Software - Procured XLSTAT for 1 year – online license	650 USD	10.09.2020	100%	License exhausted after one year

ix. Plans for utilizing the equipment facilities in future

S. No.	Installation/ equipment	Planned future use
1.	One HP Desktop with monitor	For writing papers to be published in high IF Journals and Conferences

x. Data dissemination policy for data generated in the project

No new data has been generated in the project. The findings obtained from the study shall be disseminated through reports and publications in journals and conferences.

xi. Number of post-graduate/doctoral candidates completed their courses

1. Sh. Gaurav Sharma, M. Tech Dissertation
2. Sh. Anoop Dongre, M. Tech Dissertation

xii. Foreign deputation/visit of PI/Co-PIs/students, if any

None

A.3 Activity chart

S. No.	Items of work	Year 1				Year 2				Year 3				Year 4			
		Q1	Q2	Q3	Q4	Q1	Q2	Q3	Q4	Q1	Q2	Q3	Q4	Q1	Q2	Q3	Q4
1.	Field visit to the basin and areas prone to desertification for interaction with the decision makers and the stakeholders.																
2.	Inception Workshop to gather the issues and expectations from the project.																
3.	Collection of hydro-meteorological data including precipitation and weather datasets from Superintendent Land Records, Water Resources Department, Agriculture Department and India Meteorological Department.																
4.	Collection of literature pertaining to studies already carried out by the line departments related to droughts, floods, desertification.																
5.	Collection of hydrological data including the gauge, discharge, silt, water quality data at all the gauging sites in the basin from Water Resources Department and Central Water Commission.																
6.	Collection of data pertaining to population and other human indicators.																
7.	Procurement of high resolution satellite digital datasets pertaining to land use/ land cover, soil, topography and DEM.																
8.	Field experiments for evaluation of hydrologic soil properties including infiltration and hydraulic conductivity of soils and collection of soil samples for related laboratory analysis to ascertain other soil properties.																
9.	Preparation of maps on soil type/texture, land use/cover, topography, contour, settlements, roads, geology, hydrogeology, etc. in GIS environment.																
10.	Preparation of Status Report																
11.	First Stakeholders Workshop to showcase the progress and address related issues.																
12.	Assessment of climate change signals in the basin based on the historical datasets of precipitation and temperature during the baseline period.																
13.	Evaluation of meteorological drought characteristics in the basin through departure analysis, probability analysis and drought indicators viz., Standardized Precipitation Index (SPI)/Reconnaissance Drought Index (RDI)/Effective EDI.																
14.	Evaluation of surface drought characteristics in the basin using truncation level approach and Surface Water Drought Index (SDI).																
15.	Evaluation of groundwater drought characteristics in the basin using Groundwater Drought Index (GDI)/Groundwater Resource Index (GRI).																
16.	Evaluation of agricultural drought characteristics using Normalized Difference Vegetation Index based Vegetation Condition Index (VCI).																
17.	Dry spell analysis for evaluation of dry spells and planning of supplemental lifesaving irrigation.																
18.	Drought vulnerability analysis based on the indicator based approach considering the spatially and temporally varying aspects.																
19.	Preparation of First Interim Report.																
20.	Second Stakeholders Workshop.																
21.	Hydrologic model setup, calibration based on the observed datasets and validation based on the independent datasets.																
22.	Application of global datasets GCM/RCM for simulation of the future hydrology in the basin under various emission scenarios and models.																
23.	Evaluation of future water availability in the near-term, mid-term and end of the century and comparison with the present availability.																
24.	Evaluation of future flood characteristics including the frequency and magnitude during various time horizons.																
25.	Evaluation of low flow characteristics including the frequency and magnitude during various time horizons.																
26.	Evaluation of future drought characteristics including the severity, intensity and duration during various time horizons.																
27.	Preparation of Second Interim Report.																
28.	Third Stakeholders Workshop.																
29.	Investigation into the desertification aspects based on the indicator based approaches under present conditions.																
30.	Evaluation of desertification aspects under alternate climate and land use scenarios.																
31.	Assessment of impact of upcoming dams on the drought scenario																
32.	Integrated assessment of vulnerability under climate change, drought and desertification in the basin.																
33.	Mitigation and adaptation mechanisms based on the vulnerability assessment and impact assessments.																
34.	Preparation of Final Report covering all the above aspects.																

All the items as planned have been completed except for one Stakeholder Workshop due to the cited reasons. A short extension was sought for three months to compete remaining work elements which was granted.

Appendix B Supplementary results

None